RIDGE MODELLING: MODEL SCALE SIMULATION OF RAMMING TESTS CONDUCTED WITH THE USCGC POLAR STAR

Volume I - Main Report

TP 9496E

Prepared for:

Transport Canada
The Policy and Coordination Group
Transportation Development Centre

CA1
DTC 800
88
R35
v.1
c.2

Prepared by:

FLEET TECHNOLOGY NEWFOUNDLAND LIMITED

89-04036/

Date Due

SEP 5	1989		

BRODART, INC Cat No. 23 233 Printed in U.S.A.

mm

CA1
DTC 800
88
R35
V. 1
C. 2

FTNL 3208C

RIDGE MODELLING: MODEL SCALE SIMULATION OF RAMMING TESTS CONDUCTED WITH THE USCGC POLAR STAR
VOLUME I - MAIN REPORT

TP 9496E

Prepared for Transport Canada
The Policy and Coordination Group
Transportation Development Centre

Guy Favreau Complex,
200 René Lévesque Blvd. West,
Suite 601, West Tower,
Montreal, Quebec.
H2Z 1X4

Library and Information Centre /
Centre de Documentation (GSLA)
RECEIVED - REÇU LE
JAN 24 1989
Transport Canada / Transports Canada

BY

G. COMFORT

Prepared by:

FLEET TECHNOLOGY NEWFOUNDLAND LIMITED,
P.O. Box 5040,
St.John's, Newfoundland.
A1C 5V3

SEPTEMBER 1988

407177

403713

PROJECT TEAM:

The project team included:

Fleet Technology Newfoundland Limited: Razek Abdelnour

Fleet Technology Limited: George Comfort
Rick Brown
Darlene Bourne
Andre Lemieux
Christine Genge

AKAC Consultants Limited: Dr. A. Keinonen

Institute of Marine Dynamics: Don Spencer

DISCLAIMER:

The contents of this report reflect the views of Fleet Technology Newfoundland Limited and not necessarily the official views or policies of Transport Canada.

Un sommaire en français de ce rapport est inclus avant la Table des matières.

Approved by:
I.F. Glen, President.
Fleet Technology Limited.

Transport Canada Transports Canada
Development Développement

REPORT DOCUMENTATION FORM

1. Transport Canada Report No. **TP 9496E**	2. TDC Project No. 7000	3. Recipient's Catalogue No.

4. Title and Subtitle **RIDGE MODELLING: Model Scale Simulation of Ramming Tests Conducted with the USCGC POLAR STAR** (Two Volumes)	5. Report Date September 1988 6. Performing Organization Report No. 3208C
7 Author(s) **G. Comfort**	8. Transport Canada File No. D1460-257
9. Performing Organization Name and Address Fleet Technology Newfoundland Limited 65A Lemarchant Road, P.O. Box 5040 St. John's, Newfoundland A1C 5V3	10. DSS File No. 12SD.T8200-7-7540 11. DSS or Transport Canada Contract No T8200-7-7540/01-SD
12 Sponsoring Agency Name and Address Transportation Development Centre (TDC) 200 René-Lévesque Blvd. West Suite 601, West Tower Montreal, Quebec H2Z 1X4	13. Type of Report and Period Covered Final 14. Sponsoring Agency Code
15 Supplementary Notes Appendices separately bound.	16. TDC Project Officer **T. Peirce**

17 Abstract

A project was undertaken to improve present knowledge of ridge modelling and to investigate preferred techniques for the production of model ice ridges. The general approach used for the project was to attempt to simulate, at model scale, a small number of field ridge ramming events that were relatively well documented. After a review of the available full scale data, it was decided to use field data collected during ramming tests with the USCGC POLAR STAR in 1982 in the Bering Sea in partially consolidated first-year ridges as the reference event(s) for this study. Preliminary model tests were first conducted by Fleet Technology Limited's ice tank in Kanata. More extensive tests were then conducted at the Institute for Marine Dynamics in St. John's, Nfld. Tests were conducted at a scale factor of 19.1. Two ridge modelling techniques were used: i.e. the production of a single ridge with both a consolidated and an unconsolidated portion; and the production of ridges which separately modelled the unconsolidated and consolidated portions of the ridge. Parameters that were varied during the tests included the ice-model friction factor, the size of the ridge, and the size and strength of the consolidated layer of the ridge. Conclusions are drawn and recommendations are made regarding the accuracy of ridge modelling techniques and the preferred techniques for the production of model ice ridges.

18 Key Words Ship, Icebreaking, Ice Modelling, Ice Ridges	19. Distribution Statement Limited number of copies available from the Transportation Development Centre.

20 Security Classification (of this report) Unclassified	21. Security Classification (of this page) Unclassified	22. No. of Pages 523	23. Price Nil

TDC CD1 [illegible]
Rev 86

Canada

Transports Canada Transport Canada
Développement Development

FORMULE DOCUMENTAIRE DU RAPPORT

1 Nº du rapport Transports Canada
TP 9496E

2. Nº de l'étude — CDT
7000

3. Nº de catalogue du destinataire

4. Titre et sous-titre
RIDGE MODELLING: Model Scale Simulation of Ramming Tests Conducted with the USCGC POLAR STAR
(Deux Volumes)

5. Date du rapport
Septembre 1988

6. Nº du rapport de l'organisme exécutant
3208C

7. Auteur(s)
G. Comfort

8. Nº de dossier Transports Canada
D1460-257

9. Nom et adresse de l'organisme exécutant
Fleet Technology Newfoundland Limited
65A Lemarchant Road, P.O. Box 5040
St. John's (Terre-Neuve)
A1C 5V3

10. Nº de dossier — ASC
12SD.T8200-7-7540

11. Nº de contrat — ASC ou Transports Canada
T8200-7-7540/01-SD

12. Nom et adresse de l'organisme parrain
Centre de développement des transports (CDT)
200 ouest, boul. René-Lévesque
Suite 601, tour ouest
Montréal (Québec) H2Z 1X4

13. Genre de rapport et période visée
Final

14. Code de l'organisme parrain

15. Remarques additionnelles
Annexes reliées séparément.

16. Agent de projet — CDT
T. Peirce

17 Résumé

Le projet dont il est rendu compte ici vise à développer les connaissances actuelles en modélisation physique des crêtes de pression ainsi qu'à dégager les techniques de modélisation à privilégier. L'approche générale retenue a été de tenter de simuler, à échelle réduite, un petit nombre de cas réels de charge de crêtes de pression relativement bien documentés. Après avoir étudié toutes les données vraie grandeur disponibles, il a été décidé de se servir, pour les fins de la présente étude, de celles concernant les essais de charge de crêtes partiellement consolidées de première année, faits par le USCGC Polar Star, en 1982, dans la mer de Béring. Les essais préliminaires de modélisation ont eu lieu dans le bassin des glaces de Fleet Technology Limited, à Kanata. Des essais plus poussés ont ensuite été faits à l'Institut de dynamique marine à St. John's, Terre-Neuve. Le facteur de réduction d'échelle retenu à cette occasion a été de 19,1. Deux techniques de modélisation des crêtes ont été utilisées: 1) production d'une crête comportant une partie consolidée et une autre non consolidée, et 2) production de deux crêtes distinctes, l'une consolidée, l'autre non consolidée. Parmi les paramètres que les chercheurs ont fait varier lors des essais, figuraient: le coefficient de frottement glace-maquette, la taille de la crête de pression ainsi que l'épaisseur et la résistance de la couche consolidée. Le rapport présente des conclusions concernant la justesse des résultats livrés par les différentes techniques de modélisation ainsi que des recommandations quant aux techniques à privilégier.

18 Mots-clés
Navire, déglaçage, modélisation des glaces, crêtes de pression.

19. Diffusion
Nombre limité d'exemplaires disponibles au Centre de développement des transports.

20. Classification de sécurité (de ce rapport)
non classifié

21. Classification de sécurité (de cette page)
non classifiée

22. Nombre de pages
523

23. Prix
aucun

CDT TDC 79-005
Rev 86

Canada

ACKNOWLEDGEMENTS

This project was partially funded by the National Research Council of Canada through the Institute for Marine Dynamices (IMD).

The technical staff of the IMD who performed the tests have contributed greatly to the success of this project. They were cooperative throughout the program and maintained a keen interest in the project while working long hours to maintain the project schedule.

As well, the support of the United States Coast Guard, who kindly loaned us a 19.1:1 scale model of the USCGC POLAR STAR for testing during this project, is gratefully acknowledged.

Finally, we wish to acknowledge the assistance of R. Voelker of NKF Engineering Limited with whom we had several discussions regarding the 1982 field ramming tests with the USCGC POLAR STAR that were used as a full scale reference for this study.

EXECUTIVE SUMMARY

Objectives:

A project has been undertaken to improve present knowledge of: (a) the accuracy of physical model results for ice ridges; and (b) preferred techniques for the production of ice ridges in the model basin.

General Approach and Scope:

The general approach used was to attempt to simulate, at model scale, a small number of field ridge ramming tests that were relatively well documented. The study comprised three main tasks, as follows:

1. Review of available full scale data and selection of field ridge ramming event(s) for modelling.
2. Preliminary ridge modelling tests at Fleet Technology Limited's (FTL) ice tank in Kanata and development of test plan.
3. Detailed ridge modelling tests at the Institute for Marine Dynamics (IMD).

Selection of Field Ridge Ramming Event(s) for Modelling:

Tests conducted in 1982 in the Bering Sea with the USCGC POLAR STAR (Geisel et al, 1982) were selected as the reference field event(s) for this study. These ramming tests were conducted in partially consolidated first-year riges. Ramming tests done for ridges 17 and 18 during the trials were selected as the field reference event(s) for this study as the ridge profile was documented best for these ridges.

Ridge Modelling Tests:

Ridge modelling tests at FTL and IMD were conducted at a scale of 1:19.1 as this was the scale of the available model of the USCGC POLAR STAR. Efforts were made to duplicate the ice environmental condition tested in the field (which was a partially consolidated first year ridge embedded in a first-year ice sheet).

Two general approaches were used to model the field ridge(s):

(a) produce ridges that consisted of both consolidated and unconsolidated material. This models the general composition of the field ridge(s).

(b) produce ridges that separately modelled the consolidated and unconsolidated portions of the field ridge(s) and conduct separate ramming tests.

Several parameters were varied during the model tests including the ice-model friction factor, the speed of the model, and the size, consolidation depth and the strength of the model ridges.

Tests Results and Conclusions:

(i) Ridge modelling techniques

The tests have indicated that the approach of separately modelling the consolidated and unconsolidated portions of the ridge (i.e. (b) above) provided comparable accuracy for the prediction of ridge penetration energy to that of producing partially consolidated ridges (i.e. (a) above) in the basin.

Practical methods for the production of partially consolidated ridges in the basin were developed. The tests have indicated that the cross-sectional area of the ridge and the mean depth of consolidation can be controlled relatively well. This can be accomplished by controlling: a) the volume of ice initially put into the ridge; and b) the thickness of intact ice which is initially pushed over the unconsolidated material in the ridge; and c) the placement and subsequent removal of insulation mats on the ridge surface.

However, the flexural strength of the consolidated layer of the ridge was found to be a difficult property to control.

In general, the measurement of ridge properties was found to be difficult and time-consuming. At present, techniques for the characterization of ridge properties are not standardized. This is one area where further research is believed to be warranted.

(ii) Quantitative prediction of ridge penetration energy

The model test results have indicated the following dependence of ridge penetration energy on the test parameters:

a) ridge cross-sectional area - a clear trend was not observed as this parameter was not varied over a wide range. The effect of this parameter was masked by variations in other properties,
b) mean depth of consolidation - the ridge penetration energy was found to increase (in an approximately linear manner) with an increased mean depth of consolidation,
c) ice-model friction - the ridge penetration energy was found to double (approximately) when the ice-model friction factor was increased from 0.04 to 0.16,
d) speed - this parameter was found to have a negligible effect on the ridge penetration energy over the range of speeds tested (i.e. 0.65 m/s to 1.0 m/s model scale).

e) flexural strength of ridge consolidated layer - the ridge penetration energy was found to be weakly dependent on the flexural strength. The ridge penetration energy increased by about 30% for an approximate variation in flexural strength of 0 kPa to 1500 kPa. This relationship is highly scattered as other variables which affect the ridge penetration energy more significantly (such as the mean depth of consolidation) were also varied.

The model test results have been compared to the full scale data and to the results of a numerical predictor of ridge penetration energy recently developed by Stubbs et al, 1986 (Stubbs, J., et al, 1986, "Development of a Method for Estimating Ship Performance Capabilities and Identifying Limiting Conditions When Transiting Ice Ridges", Transport Canada report **TP 8275E**). Froude scaling laws were used throughout to compare model scale data with full scale results and the scale factor was taken as the geometric scale factor of the model (i.e. 19.1). This scaling practice is presently common in ice model-testing.

The model test results obtained at the low and high friction factors bracket the numerical predictions of Stubbs et al, 1986 for the penetration energy of the unconsolidated material within about ±30%.

If the field data are accepted at face value, then the following conclusions are indicated:

a) Tests with partially consolidated ridges - the model tests results underpredict the ridge penetration energy. The model tests results at the low and high friction factor indicated ridge penetration energies that were about 30% and 60% respectively of the measured field data. It should be noted that the flexural strength of the consolidated layer was too strong (by a factor of about 2-5) for these ridges. Thus, despite the fact the ridges were too strong, the ridge penetration energy was underpredicted by the model tests.

b) Tests with purely consolidated and purely unconsolidated ridges - the total penetration energy measured in the field was compared to the sum of the penetration energies obtained from model tests conducted in purely consolidated and purely unconsolidated ridges.

For the model tests done at a high friction factor (i.e. 0.16), this sum bracketed the field data within ±20%.

For the model tests done at a low friction factor (i.e. 0.04), this sum was about 40% of the field data.

Unfortunately, the strength of the conclusions that can be obtained from the study is limited by uncertainties in the field data, including:

a) discrepancies between the horizontal force measured before the ship contacted the ridge (while it transitted level ice) and the predicted level ice resistance of the ship. The measured forces exceed the predicted level ice resistance by a factor in excess of 2. A bias of this amount would cause the field data to overestimate the ridge penetration energy by about 35%. This amount is significant in relation to the observed discrepancies between the model test and field test data.

b) uncertainties in the field ice-hull friction factor. Two different apparata (i.e. a sliding arm and a rotating arm tribometer) were used to measure the ice-hull friction factor. One major difference between these apparata is that the sliding arm tribometer slides the ice past the hull without causing crushing while the rotating arm tribometer both crushes and slides the ice sample. The mean ice-hull friction factors measured by these apparata were 0.045 and 0.20, respectively. In an effort to bound this uncertainty, we have conducted the model tests at two friction factors (i.e. 0.04 and 0.16). It should be remembered that the technique used to measure the ice-hull friction factor in the model tests was similar to the sliding arm tribometer tests as an ice sample was slid over the surface without causing the ice to crush.

c) anomalies in the ridge profiles. For ridge 18, the measured keel area was too small in relation to the measured total area to maintain isostatic equilibrium. For ridge 17, the consolidated layer was measured to be very thick over the 15 m to 25 m horizontal baseline. It is hypothesized that this mass may represent a local incusion of multi-year ice.

As stated on the previous page, a direct comparison of the field and model scale data indicates that the model test results underpredict the ridge penetration energy. Both items (a) and (c) above introduce uncertainties in scaling and comparison which are in this direction. Clearly, a better match could be obtained between the field and model test data if the field penetration resistance data were "corrected" to account for the observed discrepancy in level ice resistance (i.e. item (a) above). Item (c) above also contributes to an underprediction of the field data by the model test results as the model tests, and subsequent model scale vs. full scale comparisons, were based on field data that appear to underestimate the ridge cross-sectional area.

Recommendations:

This project represents the first time (to our knowledge) that efforts have been made to duplicate a field ramming event in partially consolidated ridges in the model basin. It is a first step towards understanding the accuracy of ice model tests in ridges and preferred techniques for the production and testing of model ice ridges.

We recommend that this initial project be followed with additional studies, including:

a) further model basin tests aimed at developing a standard technique for modelling the resistance of ridges. This would be performed by using the POLAR STAR model to determine the energies needed to penetrate a parametric series of model ridges in which shape, area and strength are varied systematically. The resulting scale of ridge penetration energies, when compared to the energies measured during full-scale ridge events for the POLAR STAR, would then permit the model ridges to be identified which best simulated the resistance of the corresponding field ridges. The results would thus provide a scientific basis for modelling ridges for use in standardized model tests.

b) similar ridge modelling tests with other ships. Field ramming tests that were relatively well documented have also been carried out with the MV KIGORIAK and MV POLAR STERN.

It is recognized that the KIGORIAK field data are proprietary (to Dome Petroleum Limited). Therefore, it may not be possible to conduct a similar study for that ship.

c) ridge modelling tests should be conducted using MOD-ICE (non-refrigerated solidified wax) and/or BEADS-ICE (refrigerated mixture of water, dopant and plastic beads). These modelling materials provide better scaling of the ice density. The tests conducted in this program should be repeated with these other modelling materials, or alternatively, the additional ridge modelling tests recommended above in (a) should be repeated in these materials.

d) field ridge-ramming tests with the specific objective of producing a very well documented set of field data for the purpose of providing a full scale reference for subsequent model scale vs. full scale comparisons.

e) basic laboratory and analytical studies of the ridge-ship interaction. We note that this is one of the major objectives of the planned Joint Research Project Agreement (JRPA). Therefore, future ridge modelling efforts should be planned such that they augment the results of this program.

SOMMAIRE

Objectifs

Ce projet a été entrepris dans le but de développer les connaissances actuelles concernant la justesse des résultats obtenus par modélisation physique des crêtes de pression et de dégager les techniques à privilégier pour la modélisation des crêtes de pression en bassin des carènes.

Approche générale et portée de l'étude

L'approche générale retenue a été de tenter de simuler, à échelle réduite, un petit nombre de cas réels de charge de crêtes de pression relativement bien documentés. Il s'agissait principalement de:

1. Faire un tour d'horizon en vue de la modélisation, des données disponibles concernant des essais de charge de crêtes de pression en conditions réelles.

2. Procéder à des essais préliminaires de modélisation de crêtes de pression au bassin des glaces de Fleet Technology Limited (FTL) à Kanata et à l'élaboration d'un plan d'expérimentation.

3. Procéder à des essais de modélisation plus poussés à l'Institut de dynamique marine (IDM).

Sélection des essais de charge à reproduire à échelle réduite

Les essais faits en 1982 dans la mer de Béring par le USCGC POLAR STAR (Geisel et al, 1982) ont été retenus comme base de référence de la modélisation envisagée, plus précisément les essais de charge des crêtes de première année partiellement consolidées numéros 17 et 18, pour lesquels les chercheurs bénéficiaient de données de caractérisation en profil des plus complètes.

Essais de modélisation des crêtes de pression

Ces essais ont été réalisés à l'échelle 1/19,1 aux installations de FTL et de l'IDM puisqu'il s'agissait de l'échelle de réduction de la maquette du POLAR STAR dont les chercheurs disposaient. Ces derniers ont tenté de reproduire en bassin les conditions glacielles rencontrées en vraie grandeur (soit une crête de première année partiellement consolidée prise dans une couche de glace de première année).

Deux approches générales de modélisation ont été adoptées:

(a) modélisation de crêtes formées à la fois de glace consolidée et de glace non consolidée, comme cela se rencontre dans la réalité.

(b) modélisation de crêtes consolidées à côté de crêtes non consolidées en vue d'essais de charge séparés.

Plusieurs paramètres ont été variés au cours des essais en bassin, parmi lesquels: le coefficient de frottement glace-maquette, la vitesse de la maquette et la taille, la profondeur de consolidation et la résistance des crêtes simulées.

Résultats et conclusions

(i) Techniques de modélisation des crêtes

Les essais ont permis de constater que la modélisation séparée de portions consolidées et non consolidées d'une crête (technique b ci-dessus) livrait, en ce qui concerne l'énergie de pénétration de la crête, des approximations comparables en justesse à celles obtenues par l'autre technique, soit la modélisation de crêtes partiellement consolidées (technique a ci-dessus).

Les chercheurs ont mis au point des méthodes pratiques de réalisation de crêtes partiellement consolidées en bassin. Les essais ont montré que la section transversale et la profondeur moyenne de consolidation de la crête pouvaient être assez bien maîtrisées en réglant: a) la quantité de glace utilisée pour constituer la crête de pression, b) l'épaisseur de la couche de glace intacte qui est poussée en début d'essai par-dessus la glace non consolidée de la crête, et c) les temps de mise en place et d'enlèvement des matelas isolants servant à maintenir la température de la glace formant la crête à la valeur souhaitée.

Toutefois, la résistance en flexion de la couche consolidée était une propriété plus difficile à maîtriser.

En général, le mesurage des paramètres caractérisant une crête de pression s'avérait ardu et long à réaliser. A l'heure actuelle, les techniques de caractérisation de crêtes ne sont pas normalisées. Il s'agit d'un domaine où la recherche mériterait d'être poussée plus loin.

(ii) Appréciation quantitative de l'énergie de pénétration d'une crête

Les essais en bassin ont révélé les relations suivantes entre l'énergie de pénétration des crêtes et les paramètres d'essai:

a) section transversale de la crête - aucune relation nette n'a pu être observée étant donné que la plage de variation de ce paramètre n'a pas été très étendue, les effets de ce paramètre ayant été masqués par les variations d'autres paramètres.
b) profondeur moyenne de consolidation - l'énergie de pénétration d'une crête augmentait (à peu près proportionnellement) avec la profondeur moyenne de consolidation.
c) coefficient de frottement glace-maquette - l'énergie de pénétration doublait presque lorsque l'on faisait passer ce coefficient de 0,04 à 0,16.

d) vitesse - ce paramètre a exercé une influence négligeable sur la valeur de l'énergie de pénétration, du moins dans la plage de variation vérifiée (soit entre 0,65 m/s et 1,0 m/s, échelle réduite).

e) résistance en flexion de la couche consolidée - l'énergie de pénétration n'était que faiblement liée à la résistance en flexion de la crête. Ainsi, elle a augmenté d'approximativement 30 %, pendant que la résistance en flexion de la crête passait de 0 à 1500 kPa environ. Cette relation est influencée par d'autres variables dont l'effet sur l'énergie de pénétration est beaucoup plus marqué (exemple, la profondeur moyenne de consolidation).

Les résultats des essais sur maquette ont été comparés à ceux des essais en vraie grandeur ainsi qu'aux valeurs d'énergie de pénétration calculées à l'aide du modèle numérique mis au point en 1986 par Stubbs et al (Stubbs, J., et al, 1986, "Development of a Method for Estimating Ship Performance Capabilities and Identifying Limiting Conditions When Transiting Ice Ridges", rapport **TP 8275E** de Transports Canada). Les lois de similitude de Froude ont été appliquées à l'ensemble des données de la comparaison, le facteur d'échelle retenu ayant été le facteur de réduction d'échelle géométrique de la maquette utilisée, soit 19,1. Cette façon de procéder est présentement courante en modélisation dans les glaces.

En ce qui concerne l'énergie de pénétration des couches non consolidées, les résultats des essais sur maquette obtenus aux valeurs extrêmes de la plage des coefficients de frottement encadrent les valeurs théoriques calculées par Stubbs et al en 1986 à plus ou moins 30 % près.

Si l'on accepte telles quelles toutes les données des essais en vraie grandeur, les conclusions suivantes s'imposent:

a) Essais de pénétration de crêtes partiellement consolidées - les essais sur maquette sous-estiment l'énergie de pénétration des crêtes. Les résultats des essais sur maquette, obtenus aux valeurs extrêmes de la plage des coefficients de frottement testés, s'établissaient respectivement à environ 30 et 60 % des valeurs mesurées en vraie grandeur. À noter que la résistance en flexion de la couche consolidée était trop élevée: elle dépassait de 2 à 5 fois celle des crêtes témoins. Or, malgré le fait que cette résistance ait été trop élevée, les essais sur maquette ont abouti à des valeurs d'énergie de pénétration sous-estimées.

b) Essais de pénétration de crêtes consolidées et de crêtes non consolidées - l'énergie totale de pénétration mesurée en vraie grandeur a été comparée à la somme des énergies de pénétration mesurée aux essais sur maquette concernant tour à tour des crêtes consolidées et non consolidées.

Les essais sur maquette à coefficient de frottement élevé (0,16) ont donné une gamme de résultats dont les sommes encadraient les valeurs en vraie grandeur à plus ou moins 20 % près.

Aux essais réalisés à coefficient de frottement faible (0,04), la somme des énergies de pénétration s'est établie à environ 40 % des valeurs en vraie grandeur.

Malheureusement, la valeur des conclusions que l'on peut tirer de la présente étude est grevée par les incertitudes dont souffrent les données des essais en vraie grandeur, notamment:

a) écarts entre la force horizontale mesurée avant que la proue du navire ne heurte la crête de pression (c'est-à-dire pendant que celui-ci avançait dans une glace uniforme) et la résistance à la marche théorique du navire dans une glace uniforme. En effet, les forces mesurées dépassent cette valeur théorique par un facteur supérieur à 2. En principe, un écart de cette amplitude devrait avoir pour effet que les données en vraie grandeur conduisent à une surestimation de l'énergie de pénétration des crêtes par environ 35 %. Or, ce dépassement est loin d'être négligeable devant les écarts observés entre les valeurs dégagées par les essais sur maquette et celles des essais en vraie grandeur.

b) incertitudes concernant le coefficient de frottement glace-coque. Deux dispositifs différents ont servi à mesurer ce coefficient: un tribomètre à bras coulissant et un autre à bras rotatif. Les deux se différencient principalement par le fait que le premier agit en frottement pur, alors que l'autre exerce une force à la fois de translation et d'écrasement. Les coefficients de frottement moyens obtenus par ces deux appareils s'établissaient à 0,045 et 0,20 respectivement. Voulant circonscrire l'étendue de l'incertitude liée à ce facteur, les chercheurs ont réalisé des essais sur maquette aux deux valeurs extrêmes du coefficient de frottement (0,04 et 0,16). Il convient de rappeler que la technique tribométrique appliquée relativement à la maquette est assimilable aux mesures tribométriques par appareil à bras coulissant en ceci que l'éprouvette de glace a été frottée contre la coque sans aucun effort de compression.

c) anomalies dans les profils de crête. La crête 18 présentait une superficie de crête sous glace trop faible par rapport à la superficie totale de la crête pour maintenir un équilibre isostatique. Quant à la crête 17, sa couche consolidée était très épaisse sur toute la largeur de la crête qui variait entre 15 et 25 mètres. Selon toute hypothèse, cette masse pourrait être de la glace de plusieurs années.

Comme il a été mentionné à la page précédente, une comparaison directe des résultats des essais en vraie grandeur et sur maquette révèle que ces derniers aboutissent à une sous-estimation de l'énergie de pénétration des crêtes de pression. Les facteurs indiqués en a) et b) ci-dessus rendent incertains les rapports de similitude adoptés pour les fins des essais sur maquette ainsi que toute comparaison fondée sur ces rapports. De toute évidence, une meilleure similitude entre les données des essais en vraie grandeur et celles de la modélisation pourrait être atteinte si les résultats des essais de prénétration de crête in situ étaient "corrigés" à la lumière de l'écart constaté au niveau de la résistance à la marche dans une glace uniforme (facteur (a) ci-dessus). Le facteur c) ci-dessus contribue également à la sous-estimation dénoncée, étant donné que la modélisation et les comparaisons subséquentes des résultats étaient fondées sur des données en vraie grandeur qui semblent aboutir à une section transversale de crête inférieure à la réalité.

Recommandations

Ce projet représente, autant que nous puissions en juger, la première tentative de reproduire en bassin des glaces, donc à échelle réduite, un cas réel de charge d'une crête de pression partiellement consolidée. Il s'agit d'un premier pas vers l'appréciation de la justesse des résultats tirés des essais sur maquette et vers la détermination des techniques à privilégier en vue de la réalisation et de la caractérisation des crêtes de pression simulées.

Nous recommandons de lancer des études complémentaires à cette première recherche, notamment de procéder:

a) à d'autres essais en bassin des glaces visant à mettre au point une technique standard de modélisation de la résistance des crêtes de pression. Cette nouvelle série d'essais, qui serait réalisé à l'aide de la maquette du Polar Star, servirait à déterminer l'énergie de pénétration d'une crête de pression simulée dont la forme, la section et la résistance seraient systématiquement variées. La comparaison des énergies de pénétration mesurées lors de cette série d'essais paramétriques et des énergies mesurées en vraie grandeur à bord du Polar Star devraient alors permettre d'identifier les crêtes de pression qui simulent le mieux la résistance des crêtes réelles correspondantes. De cette manière, le choix d'une technique normalisée de modélisation d'une crête de pression reposerait sur une base scientifique.

b) à la modélisation physique de la charge des crêtes de pression, à l'aide de maquettes d'autres navires. Des essais en vraie grandeur relativement bien documentés ont déjà été réalisés par le NM KIGORIAK et le NM POLAR STERN.

Il est vrai que les données inhérentes au KIGORIAK sont la propriété exclusive de Dome Petroleum Limited et qu'il ne sera peut-être pas possible de procéder à une modélisation du navire.

c) à des essais en bassin mettant en oeuvre les glaces synthétiques MOD-ICE (cire solidifiée non réfrigérée) ou BEADS-ICE (mélange réfrigéré d'eau, de dopant et de billes de plastique): ces matériaux permettent de mieux respecter les lois de similitude concernant le paramètre densité de la glace. Les essais du présent programme devraient être repris dans les matériaux précités ou, à défaut, les nouveaux essais préconisés en a) ci-dessus.

d) à des essais de charge en vraie grandeur dans le but spécifique de produire des données exhaustives y afférentes et susceptibles de servir de référence aux futurs essais sur maquette.

e) à des études de laboratoire et analytiques fondamentales sur les interactions crête de pression-navire. Nous avons noté que ces études représentent également l'un des objectifs principaux du projet de recherche conjoint envisagé. Aussi, conviendrait-il que les prochain travaux de modélisation soient délimités afin qu'ils apportent un complément aux études dudit projet conjoint.

TABLE OF CONTENTS

VOLUME I - MAIN REPORT

1.0 INTRODUCTION AND GENERAL APPROACH..............................1

2.0 REVIEW OF AVAILABLE FULL SCALE DATA AND SELECTION OF EVENTS FOR MODELLING..............................2
2.1 Background..............................2
2.2 Available Full Scale Data..............................4
2.3 Selection of Events for Modelling..............................11
2.4 Summary of Model Scale Target Ridge Properties..............................33

3.0 TESTS CONDUCTED AT FLEET TECHNOLOGY LIMITED'S ICE TANK......36
3.1 Test Description..............................36
3.2 Ice and Ridge Properties..............................41
3.3 Test Results..............................50

4.0 TESTS CONDUCTED AT THE INSTITUTE OF MARINE DYNAMICS.........56
4.1 Test Setup and Matrix..............................56
4.2 Ice and Ridge Properties..............................80
4.3 Data Reduction Procedures and Results for Ridge Modelling Tests..............................94
4.4 Results of Model Test of Level Ice Resistance of the USCGC POLAR STAR..............................109

5.0 ANALYSIS AND DISCUSSION OF TEST RESULTS..............................110
5.1 Ridge Building and Testing Tech. from Model Tests.....110
5.2 Prediction of Ridge Penetration Force from Model Tests..............................120
5.3 Prediction of Ridge Penetration Energy from Model Tests..............................121

6.0 CONCLUSIONS AND RECOMMENDATIONS..............................136
6.1 Ridge Building and Testing Techniques..............................136
6.2 Quantitative Prediction of Ridge Penetration Energy from Model Tests..............................138
6.3 Recommendations..............................144

7.0 REFERENCES..............................145

VOLUME II - APPENDICES

APPENDIX A - RAW DATA FROM SHEET #1 TESTS AT FLEET TECHNOLOGY LIMITED
APPENDIX B - RAW DATA FROM SHEET #2 TESTS AT FLEET TECHNOLOGY LIMITED
APPENDIX C - RAW DATA FROM SHEET #1 TESTS AT THE IMD
APPENDIX D - RAW DATA FROM SHEET #2 TESTS AT THE IMD
APPENDIX E - RAW DATA FROM SHEET #3 TESTS AT THE IMD
APPENDIX F - RAW DATA PLOTS FOR TEST T2R1 FOR A RANGE OF FILTERING RATES
APPENDIX G - RAW DATA PLOTS FOR TEST T1R1 FOR A RANGE OF FILTERING RATES
APPENDIX H - SUMMARY OF AVAILABLE FIELD DATA FOR RIDGES 17 AND 18

LIST OF TABLES

NO. TITLE PAGE

2.1 Partial List of Parameters Which Were Considered Significant....3
2.2 Summary of Full Scale Penetration Forces and Energies for Ridges 17 and 18....19
2.3 Comparison of Cumulative Penetration Energies Per Unit Thickness for the Unconsolidated and Consolidated Portions of the Ridge....22
2.4 Comparison of Predicted and Measured Level Ice Resistance....25
2.5 Scaling Laws....34
2.6 Model Scale Ridge and Level Ice Properties....35

3.1 Summary of Key Model Setup Parameters....39
3.2 Matrix of Tests Done at FTL....40
3.3 Summary of Ice and Ridge Properties....47

4.1 Key Model Setup Parameters....57
4.2 Test Matrix....74
4.3 Parameters Varied During Each Test....75
4.4 Base Cases Used to Develop Table 4.3....76
4.5 Summary of Tests Conducted in Open Water....70
4.6 Summary of Model Scale Level Ice Properties....84
4.7 Summary of Ridge Cross-sectional Geometry Data....90
4.8 Summary of Model Scale Measured Flexural Strengths of Ridge Consolidated Layer....91
4.9 Summary of Measured Ridge Bulk Densities....91
4.10 Summary of Ridge Penetration Force....107
4.11 Cumulative Penetration Energy Summary....108

5.1 Summary of Model Scale Ridge Cross-sectional Areas....113
5.2 Average Model Scale Thickness of Consolidated Layer....115
5.3 Summary of Model Scale Measured Flexural Strengths of Ridge Consolidated Layer....118

LIST OF FIGURES

NO. TITLE PAGE

2.1 Empirical Predictor of Cross-Sectional Area of First Year Ridges....5
2.2 Principle Features of a Polar Class Icebreaker....12
2.3 Full Scale Penetration Energy for Ridge 17....14
2.4 Smoothed Velocity and Force Time Histories for Ramming Test of Ridge 17....15
2.5 Smoothed Velocity and Force Time Histories for Ramming Test of Ridge 18....17

2.6 Full Scale Penetration Energy for Ridge 18................18
2.7 Level Ice Resistance of the USCGC POLAR STAR..............24
2.8 Pressure Ridge No. 17.....................................27
2.9 Pressure Ridge No. 18.....................................28
2.10 Comparison of Computed and Measured Profiles for Ridge 18...32

3.1 Comparison of Ridge Mold Shape and Cross-Sectional Profile of Ridge 18..37
3.2 Basin Setup...38
3.3 Thermocouple Locations....................................42
3.4 Raw Friction Factor Measurements..........................48
3.5 Typical Ridge Temperature Time History....................49
3.6 Full Scale Comparison of Cumulative Ridge Penetration Energy from Field Tests and Model Tests...................54

4.1 Force at Model Attachment to Towpost Resulting from Impulsive Load on Model....................................59
4.2 Schematic Description of Approach Used to Form the Ridges for Sheet No. 1 Tests......................................62
4.3 Schematic Description of Approach Used to Form the Ridges for Sheet No. 2 and No.3 Tests............................65
4.4 Basin Layout for Sheet No. 1 Tests........................71
4.5 Basin Layout for Sheet No. 2 Tests........................72
4.6 Basin Layout for Sheet No. 3 Tests........................73
4.7 Instrumentation System Schematic..........................78
4.8 Schematic of Locations on the Model Where Forces and Motions were Measured.......................................79
4.9 Sample Ridge Cross-sectional Profiles: Sheet No. 2.......88
4.10 Sample Ridge Cross-sectional Profiles: Sheet No. 3.......89
4.11 Thermocouple Locations for Sheet No. 2....................93
4.12 Sample Plot of Raw Measured Time Histories................95
4.13 Sample Plot of Computed Vessel Motions Time Histories.....96
4.14 Sample Force and Velocity Time Histories for Ridge 2-1N: Test Data Filtered at 2 Hz.................................98
4.15 Model Scale Penetration Force and Energy for Ridge 2-1N: Test Data Filtered at 100 Hz...............................99
4.16 Model Scale Penetration Force and Energy for Ridge 2-1N: Test Data Filtered at 2 Hz.................................100
4.17 Model Scale Penetration Force and Energy for Ridge 3-1N: Test Data Filtered at 2 Hz.................................101
4.18 Model Scale Penetration Force and Energy for Ridge 3-1N: Test Data Filtered at 100 Hz...............................102

5.1 Penetration Energy vs. Ridge Cross-Sectional Area: Ship Penetration Distance = 0.33 LWL.........................122
5.2 Penetration Energy vs. Ridge Cross-Sectional Area: Ship Penetration Distance = 0.67 LWL.........................122
5.3 Penetration Energy vs. Mean Thickness of Consolidated Layer: Ship Penetration Distance = 0.33 LWL..............123
5.4 Penetration Energy vs. Mean Thickness of Consolidated Layer: Ship Penetration Distance = 0.67 LWL..............123

5.5 Area Normalized Penetration Energy Vs. Mean Thickness of Consolidated Layer....................................125
5.6 Relationship of Full Scale Penetration Energy to Flexural Strength of Consolidated Layer Ship Penetration Distance = 0.33 LWL....................................126
5.7 Relationship of Full scale Ridge Penetration Energy to Flexural Strength of Consolidated Layer Ship Penetration Distance = 0.67 LWL....................................126
5.8 Ridge Penetration Energy as a Function of the Penetration Distance: Ice Model Friction Factor = 0.04...............128
5.9 Ridge Penetration Energy as a Function of the Penetration Distance: Ice Model Friction Factor = 0.16...............128
5.10 Schematic Representation of Analysis Technique Used to Develop the Stubbs et al, 1986 Predictor.................132
5.11 Penetration Energy for Unconsolidated Material Only......132

1.0 INTRODUCTION AND GENERAL APPROACH

Ridges are important features of the ice environment which can greatly effect the performance of icebreaking vessels. The performance of ships in ridges is an area that is not well understood at present as the work to date has generally been focussed on the performance of ships in level ice.

This study has been undertaken to improve present knowledge of:

a) the ability of physical model tests to simulate the interaction of a ship with a first year ridge.

b) preferred techniques for the production of first year ridges for testing in the ice model basin.

The general approach adopted for this study was to attempt to simulate at model scale, a small number of field ridge ramming events that were relatively well-documented. Accordingly, the project was generally comprised of the following three tasks:

a) Review of available literature and selection of field ridge ramming events for modelling.

b) Preliminary ridge modelling tests at Fleet Technology Limited's ice tank in Kanata and development of test plan.

c) Detailed ridge modelling tests at the Institute of Marine Dynamics.

2.0 REVIEW OF AVAILABLE FULL SCALE DATA AND SELECTION OF EVENTS FOR MODELLING

2.1 Background

2.1.1 Project Data Requirements

To meet the project requirements, it was necessary to identify well-documented events in which ridge ramming tests were carried out in the field. Field data are required to describe both the ship performance during the ramming event and the ice environment. Table 2.1 provides a partial list of the parameters which were considered significant, and hence, necessary to characterize.

As described in section 2.1.2, ice ridges may generally be classified as first year and multi-year based on their age. Multi-year ridges are totally consolidated whereas first year ridges have partial to nil consolidation. This difference greatly affects the resistance of the ridge to a ship.

It was decided to focus on the modelling of first year ridge ramming events during this study. This represents a more common scenario for a ship operating in ice (as the ship will generally attempt to avoid transiting heavily-consolidated multi-year ridges).

2.1.2 Overview Description of Ice Ridges

Ice ridges are formed in nature when ice sheets are driven together due to the action of environmental forces (eg. winds, currents, adjacent pack ice).

Upon formation, ridges consist of an unconsolidated accumulation of ice blocks. With the passage of time, the consolidation of the ridge increases. This process is important for icebreaking ships as the consolidation of the ridge affects its resistance.

For the arctic environment, ridges may be generally categorized by age as:

a) **first year ridges** which are partially consolidated. The above-water portion of these ridges (ie. the sail) can be expected to be almost totally unconsolidated. The below-water portion of these ridges (i.e. the keel) typically consists of a consolidated zone near the waterline with an unconsolidated zone comprised of loose ice blocks beneath it.

b) **multi-year ridges** which are ridges that have survived more than one melt season. Both the sail and the keel of the ridges are totally consolidated.

Both multi-year and first year ridges are common in the arctic. In marginal ice zones, only first year ridges are present. The consolidation of the ridge (relative to the total area of the ridge) is one parameter that can be expected to vary from one geographic region to another (as it is related to the number of freezing degree-days to which the ridge has been exposed.

TABLE 2.1

PARTIAL LIST OF PARAMETERS WHICH WERE CONSIDERED SIGNIFICANT

ICE ENVIRONMENTAL PARAMETERS:

- **Ice Ridge**
  - cross-sectional geometry (eg. shape, width, and depth)
  - consolidated layer profile
  - porosity and distribution of block sizes
  - strength of ice in the ridge
  - snow cover
  - longitudinal variation of the above properties over the beam of the ship and beyond
- **Level Ice Adjacent to the Ridge**
  - thickness
  - strength
  - snow cover

SHIP-RELATED PARAMETERS:

- **Velocity as a function of penetration distance into the ridge and as a function of time**
- **Penetration as a function of time**
- **Forces acting on the ship and the resulting ship motions as a function of penetration distance and time**
- **Icebreaking pattern**
- **Orientation of the ramming direction with respect to the ridge centreline**
- **Ice-hull friction**
- **Ship draft and ballast conditions**
- **Ship hull and bow geometry**

Numerous field studies have been undertaken to document multi-year ridges (eg. Kovacs, 1983; Dickens and Wetzel, 1981; Wright et al, 1979, Kovacs, 1973) and first year ridges (eg. Geisel et al, 1982; Danielewicz and Pilkington, 1982; Dome Petroleum Ltd., 1980; Comfort and Edwards, 1978; Gladwell, 1975).

Typically these studies have provided data on the cross-sectional profile of the ridge sail (determined by surveying) and of the ridge keel (determined by drilling and/or surveying using an echo-sounder). In addition, some detailed studies of the structure of first year ice ridges in the Baltic have been undertaken by careful excavation of the ridge sail (eg. Keinonen, 1973).

These studies, and others, have provided data to assist the general characterization of ice ridges. Numerous investigators (eg. Kovacs, 1973; Keinonen, 1973; Comfort and Edwards, 1978) have investigated the functional relationship of key ridge parameters (eg. sail area, keel area, sail height, keel depth, ridge consolidation). Most recently, Stubbs et al, 1986 have developed an empirical predictor of the cross-sectional area of first year ridges. (See Figure 2.1).

Figure 2.1 also shows the ridges which were selected as a full scale reference for this study. These ridges are discussed further in section 2.3.

2.2 Available Full Scale Data

After an initial survey of the literature, the following field tests were selected for detailed investigation:

SHIP	TEST DATE	TEST LOCATION	SOURCE
CCGS LOUIS S. ST. LAURENT	1977	Baffin Bay	Nawwar, 1980
MV KIGORIAK	1979-80	Southern Beaufort Sea	° Data confidential (Dome Petroleum Ltd. 1980) ° Tests referenced in Keinonen,1983 a,b
MV ARCTIC	1981	Admiralty Inlet and Baffin Bay	Nawwar et al 1984
USCGC POLAR STAR	1982	Bering Sea	Geisel et al, 1982
MV ROBERT LEMEUR	1982-83	Southern Beaufort Sea	Results of winter 1982 trials are confidential to Dome Petrol. Ltd.
POLAR STERN	1984	Labrador Shelf	Schwarz, et al, 1986
USCGC POLAR SEA	1985	Barrow, Alaska	Glen et al, 1987
MV ARCTIC	1986	Admiralty Inlet	Canarctic, 1987

Each of the above field test programs are discussed briefly in the following section.

Empirical Predictor (units as indicated):

$$CSA = 1310 * \tanh(hs) * \left(\frac{\mathrm{Tanh}(hs)}{500 * (1 - \tanh^2(hs))}\right)^{(150 * (\frac{hr}{Wr} - .02)^2)}$$

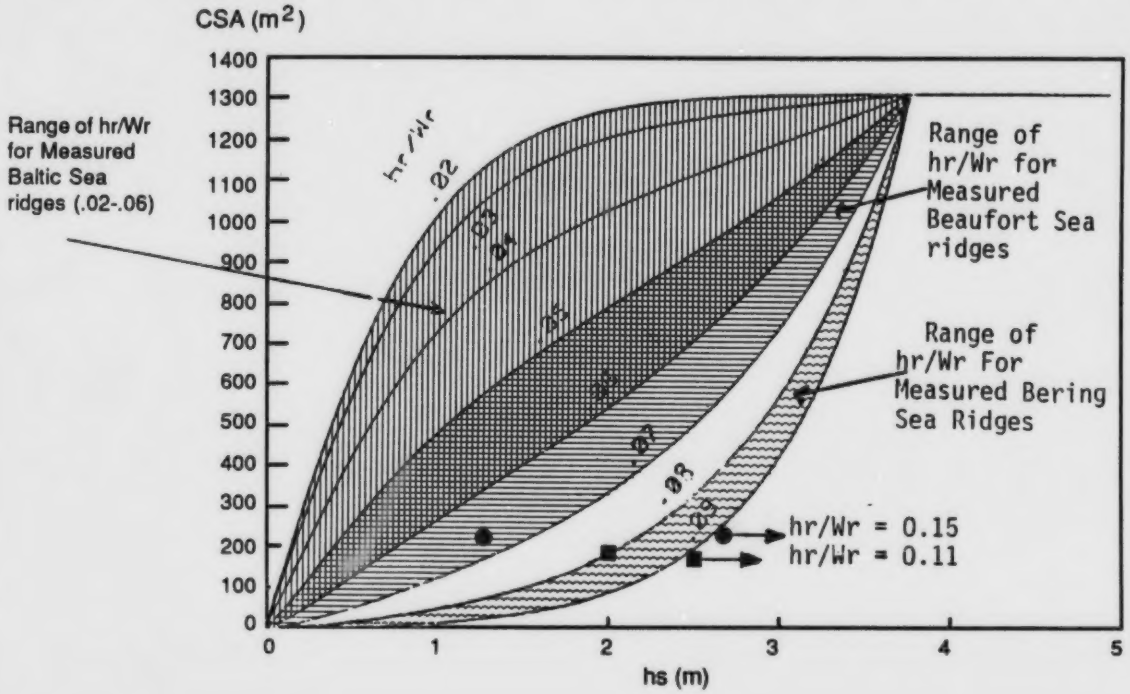

Nomenclature

CSA: Ridge cross-sectional area
hs: Ridge sail height
hr: Average ridge thickness
Wr: Ridge width

Reference Ridges Used in This Study

Ridge #	Based on Measured CSA & hs	Based on Measured CSA & hr/Wr
17	●	●→
18	■	■→

Figure 2.1
Empirical Predictor of Cross-Sectional Area of First Year Ridges

(After Stubbs et al, 1986)

2.2.1 Evaluation of Available Full Scale Data Sets

(i) Ship: CCGS LOUIS S. ST. LAURENT

Trials Date and Location: 1977 - Baffin Bay

Summary: Performance data were collected while the ship transited Baffin Bay enroute to Lancaster Sound. Dedicated ramming tests of first year ridges were not conducted during these trials.

Masthead video records have been analyzed to determine the deceleration of the ship and the ridge penetration force. Estimates of the ridge sail height and width were also made from the video records. A total of 109 ridges were analyzed. Empirical relationships between the ridge penetration force and the ridge properties were derived. However, the data are highly scattered.

Evaluation: These tests were not conducted with the objective of studying the resistance of first year ridges. These data are not considered usable as a full scale reference for this project as many of the requisite ship and ice parameters have not been documented. However, these results are useful for a gross verification of the results of this study.

ii) Ship: MV KIGORIAK

Trials Date and Location: 1979-80 Southern Beaufort Sea

Summary: An extensive series of field tests were carried out by Dome Petroleum Limited to evaluate the KIGORIAK. Some tests were carried out to evaluate its performance in first year ridges by conducting dedicated ramming trials in which both the ice ridge and ship performance parameters were documented.

These test data are confidential and consequently, the test results could not be reviewed. Sample plots of the ridge data that were collected and the measured trends in ridge penetration resistance are presented in Keinonen, 1983.

Evaluation: These ramming tests were carried out with the objective of evaluating the KIGORIAK's performance in first year ridges. The sample data that have been released indicate that the tests were documented relatively well. Consequently, it is expected that this data set would be valuable as a full scale reference.

Unfortunately, these test data are confidential and cannot be used for this study.

iii) Ship: MV ARCTIC (with original bow)

Trials Date and Location: 1981 - Admiralty Inlet and Baffin Bay

Summary: Ship performance data collected during operational voyages has been analyzed to investigate optimum ramming cycles. These results are useful for statistical analyses.

No information is available to describe the ridges that were transited.

Evaluation: This data set is not usable for this ridge modelling test program.

iv) Ship: USCGC POLAR STAR

Trials Date and Location: 1982 - Bering Sea, Alaska

Summary: The objective of these tests was to measure penetration forces and energies for first year ridges. These data were collected for input to a trafficability analysis of the Polar Class vessels.

Six ridges were penetrated. The ship transited the ridge without stopping in all cases except for one ridge which required two rams for penetration.

Time histories of the horizontal force on the ship and of the ship's horizontal velocity are available for each test. The force on the ship was determined from measurements of the ship's motions.

A centreline profile of the ridge cross-section and consolidated layer is available for each ridge. In several cases, there are gaps in the available data as the ridge was not fully drilled or profiled. Also, measurements were made of the thickness of the adjacent level ice and of the ice salinity and temperature (from which the ice flexural strength was inferred).

Evaluation: The main problem with this data set is that it only includes relatively small ridges. Furthermore, only one of the ridges is fully-profiled and there are significant gaps in the remaining ridge profiles.

Nevertheless, this data set represents a good resource for the project as a full scale reference. Furthermore, a 19.1:1 scale model of the USCGC POLAR STAR could be obtained on loan from the USCG for this project.

(v) Ship: MV ROBERT LEMEUR

Trials Date and Location: 1982-83 - Southern Beaufort Sea

Summary: The main objective of the winter, 1982 trials was to obtain ship performance data. As part of these trials, rams were conducted in first year ridges. However, the results of these tests are confidential to Dome Petroleum Limited.

Further ramming tests were conducted in the summer of 1983. The objective of these tests was to measure the total vertical force and bending response of the ship during ramming. The horizontal thrust of the ship was not measured.

Evaluation: The results of the winter, 1982 tests have the potential to provide the required full scale reference data for this project. However, these data are proprietary and could not be reviewed.

The summer, 1983 tests were not conducted with the objective of obtaining ship performance data in first year ridges. The horizontal thrust of the ship was not measured and these data are not considered to be usable for this project.

(vi) Ship: POLAR STERN

Trials Date and Location: 1984 - Labrador Sea

Summary: The objectives of these test were to obtain overall performance data for the POLAR STERN in level ice and in first year ridges.

Ramming tests were conducted for four first year ridges.

The ice environment was well-documented. Ridge cross-sectional profiles were measured at three locations corresponding to the centreline of the ship and the edge of the ship on the port and starboard sides.

Relevant ship parameters were also well-documented.

Model tests were conducted by HSVA and these results are compared with the full scale data.

Evaluation: This is a well-documented set of field data.

The main problem with these tests for this study is that all of the field ridges had no consolidation. Therefore, they are only representative of unconsolidated first year ridges. As arctic first year ridges typically have some consolidation, the ridges tested during this field program only represent a special case.

Furthermore, the modelling of partially-consolidated ridges is more difficult than that of a totally-unconsolidated ridge. Therefore, the project objective (of developing improved ridge modelling techniques) will be better served by focusing on the modelling of partially-consolidated ridges.

Other problems of lesser concern include:

a) Ridge #4 was not drilled completely. It was only drilled to a depth of 3.4 metres (11 ft.). This is unfortunate as this was the largest ridge and several rams were necessary to penetrate the ridge.

b) The published reports do not contain all of the required raw data.

c) The relevant part of the report is written in German.

(viii) Ship: USCGC POLAR SEA

Trials Date and Location: 1985 - Barrow, Alaska

Summary: The objective of these tests was to obtain global vertical force and pressure/area data resulting from impacts of the bow with multi-year ice.

A total of 40 rams were conducted in multi-year ridges. In most cases, the ridge did not fail as a result of the ram. (The ridge only failed during one of the rams).

A good data set was obtained to describe the ridge geometry and properties. However, these data are confidential to the participating oil companies until 1991.

With regard to the ship parameters, the vertical global force on the ship was measured. The horizontal force was not measured and would have to be inferred for the present ridge modelling program. The ship's velocity time history was measured for each ram. However, there are gaps in these data.

Evaluation: These data are not readily usable for the present ridge modelling program.

(ix) Ship: MV ARCTIC (with new bow)

Trials Date and Location: 1986 - Admiralty Inlet and Baffin Bay

Summary: As the reports for this project were under editorial review at the time when our survey was conducted, we did not review the data. However, we obtained some understanding of the scope and nature of this project through discussions with A. Sneyd of Canarctic Shipping Limited.

The objective of the tests was to obtain ship performance data. The data set only includes one ram in a first year ridge that was a total of 3 m deep. This ridge provided very little resistance to the ship and it was easily penetrated by the ship in one ram.

Evaluation: This data set is not considered to be usable for the present project as the ridge that was rammed was very small.

2.3 Selection of Events for Modelling

2.3.1 General Description of Selected Field Reference Data

After a review of the available full scale data, it was decided to use the data collected during the 1982 trials of the USCGC POLAR STAR in the Bering Sea. Figure 2.2 describes the condition of the ship for these trials. Test results and additional data are reported in Geisel et al, 1982.

For these tests, the ice cover consisted of partially-consolidated first year ridges that were embedded in a level ice sheet. From visual inspections, the ridges appeared to be well-bonded to the ice sheet and the ridge was not observed to separate from the ice sheet during the ramming test (R. Voelker, NKF, personal communication).

A level ice sheet was present on both sides of the ridges and tests were conducted by:

a) accelerating the ship to a steady speed in the level ice forward of the ridge

b) transiting the level ice and penetrating the ridge

c) transiting in level ice beyond the ridge

Thus, the ship transited a sequence of level ice, ridged ice, and level ice over the period that the penetration forces and the ship velocity was measured.

A low friction coating (i.e. Inerta 160) was present on the ship during these trials. This coating was generally uniform and in good condition. Patches of bare steel or of severe wear were not observed (R. Voelker, NKF, personal communication). The Inerta 160 coating was highly polished near the stem at the waterline.

The ice-hull friction factor was measured during these trials using both a sliding arm tribometer and a rotating arm tribometer. One difference between these two test methods is that the former slides the ice past the hull without causing crushing while the latter simultaneously crushes and slides the ice past the hull. These test methods and test results are described in Geisel et al, 1982.

The friction factor was measured about 0.5 m and 1 m above the waterline for the tests done with the sliding arm and rotating arm tribometers, respectively. The coating in these areas had not been subjected to ice abrasion and wear.

Ridges #17 and #18 were selected for modelling as the ridge cross-sectional profile was documented best for these ridges. For each ridge test, the following data are available in Geisel et al, 1982:

a) Ship Parameters - Horizontal force time history
- Velocity time history

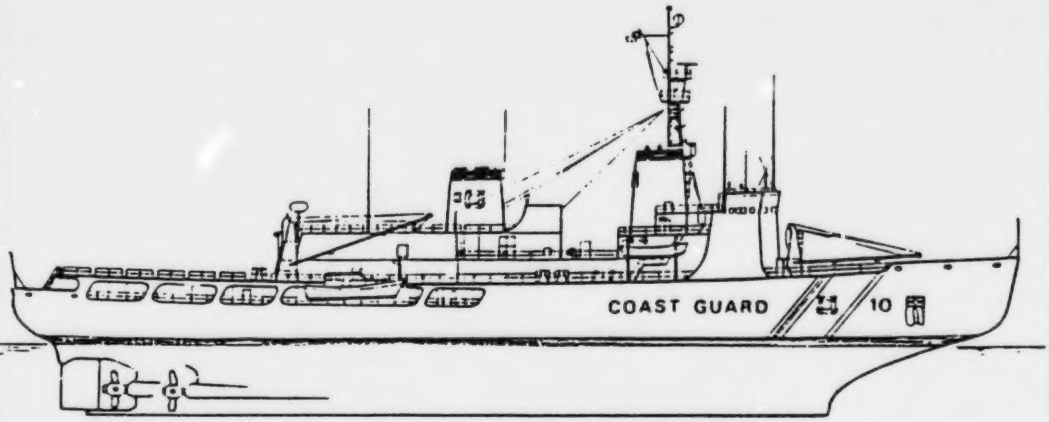

SHIP STATISTICS:

LENGTH OVERALL	399 FEET
LENGTH AT WATERLINE	352 FEET
BEAM	83.5 FEET
DRAFT	31.8 FEET
DISPLACEMENT, CAPACITY LOAD	13,190 TONS
RANGE (MAXIMUM)	28,274 MILES
SUSTAINED SPEED (OPEN WATER)	17 KNOTS
PROPULSION	DIESEL ELECTRIC OR GAS TURBINE
SHP	18,000 D-E 60,000 G-T
NUMBER OF SCREWS	3
COMPLEMENT	14 OFFICERS 126 ENLISTED
SCIENTIST ACCOMODATIONS	10
HEIGHT OF BRIDGE ABOVE WATERLINE	55 FEET
HEIGHT OF ALOFT CONN ABOVE WATERLINE	104 FEET

FIGURE 2.2

PRINCIPLE FEATURES OF A POLAR CLASS ICEBREAKER
(after Geisel, 1982)

b) Ice Parameters
   - One centreline transverse profile to describe the ridge geometry and consolidation
   - Level ice thickness
   - Baseline measurements of the ice temperature and salinity (from which the ice flexural strength was inferred).

The velocity time history was determined from direct measurements of the ship speed using a Doppler speed log. The force time history was determined from measurements of the ship's thrust and from measurements of the motions of the ship in the six degrees of freedom. Efforts were made to account for the hydrodynamic added mass in these computations. For further description of the analysis techniques used, the reader is referred to Geisel et al, 1982. Raw data are not presented in the report and are no longer available (R. Voelker, NKF, personal communication).

2.3.2 Ridge Penetration Energy

(i) Reduction and Analysis of Field Data

The field data were analyzed as follows:

a) the velocity time history was numerically integrated to determine the penetration time history of the ship.

b) the force-displacement relationship was determined.

c) the cumulative penetration energy was computed by numerically integrating the force-displacement curve. The cumulative penetration energy was then plotted as a function of the penetration distance.

Figure 2.3 shows the cumulative penetration energy computed for ridge 17. For these computations, the velocity and force time histories were smoothed as shown on Figure 2.4.

As the time scales of the force and velocity time histories were not synchronized with the distance baseline used for the ridge profile, the cumulative penetration energy was determined for two start points, as follows:

a) the ship was assumed to first contact the ridge when the velocity starts to reduce. This point is shown on Figure 2.4 as case **A**.

b) the ship was assumed to first contact the ridge when the force begins to rise. This point is shown on Figure 2.4 as case **B**.

The computed penetration energy was generally similar for both of these cases. See Figure 2.3.

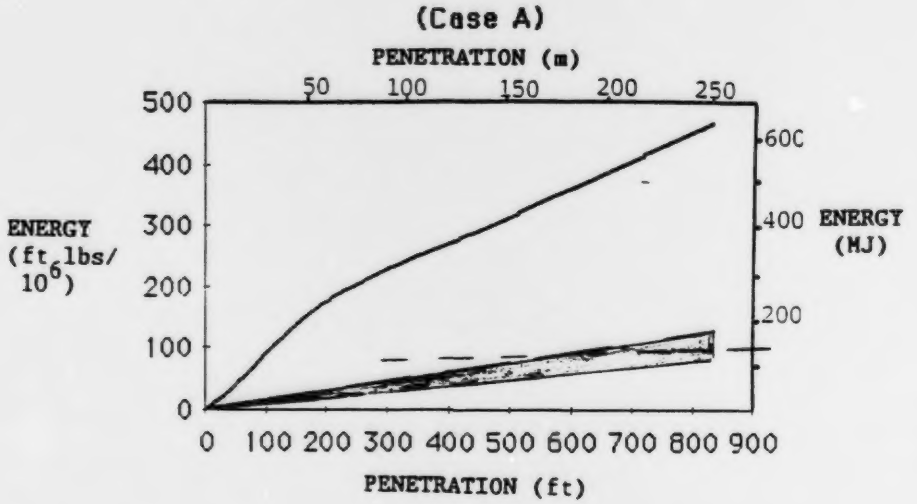

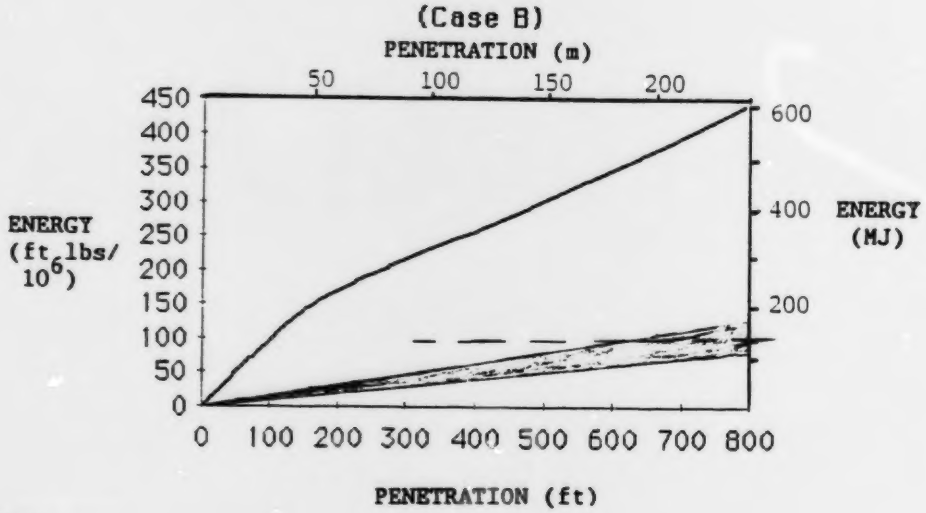

LEGEND:

———	Total Cumulative Penetration Energy Measured During Field Tests
- - - -	Total Penetration Energy Predicted by Stubbs et al, 1986 for the "pure ridge" (i.e. the unconsolidated material)
■	Range of Cumulative Penetration Energy Predicted for Consolidated Layer Only for Range of Ship Speeds Which Occurred During the Ramming Event. See Section 2.3.2 (ii).

FIGURE 2.3

FULL SCALE PENETRATION ENERGY FOR RIDGE 17

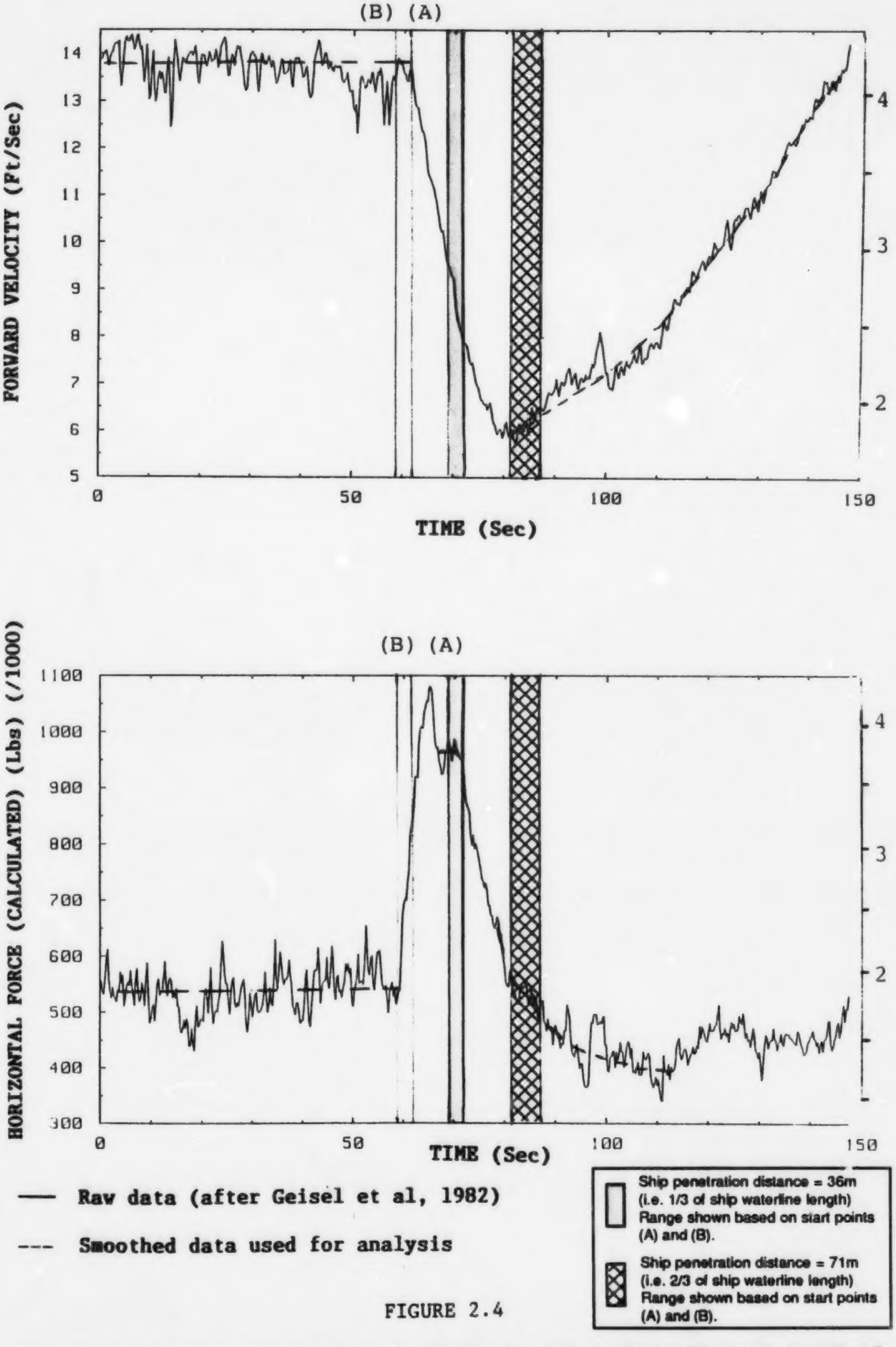

FIGURE 2.4

SMOOTHED VELOCITY AND FORCE TIME HISTORIES FOR RAMMING TEST OF RIDGE 17

The full scale data for ridge 18 was analyzed to determine the penetration energy. For these calculations, the velocity and force time histories were smoothed as shown in Figure 2.5. As the time scales of the force and velocity time histories were not synchronized with the distance baseline used for the ridge profile, three analyses of cumulative penetration energy versus penetration distance were done. These are believed to cover the range of possible cases as follows:

a) The start of the ridge profile corresponds in time to the point where the force on the ship starts to rise. This occurs at about +4 seconds. (This is noted as (1) on Figure 2.5).

b) The start of the ridge profile corresponds in time to the point where the force on the ship starts to rise steeply. This occurs at about +7 seconds. (This is noted as (2) on Figure 2.5).

c) The start of the ridge profile corresponds in time to the point where the velocity of the ship starts to reduce. This occurs at about +8.5 seconds. (This is noted as (3) on Figure 2.5).

Figure 2.6 shows the relationship of the cumulative penetration energy to the penetration distance for each of these cases. This relationship is generally similar for each case.

Cases (2) and (3) are considered to be more representative of the "startpoint" of ridge 18. Thus, subsequent analyses have been based on the range of penetration energies represented by cases (2) and (3).

Table 2.2 summarizes the full scale penetration forces and energies for ridges 17 and 18.

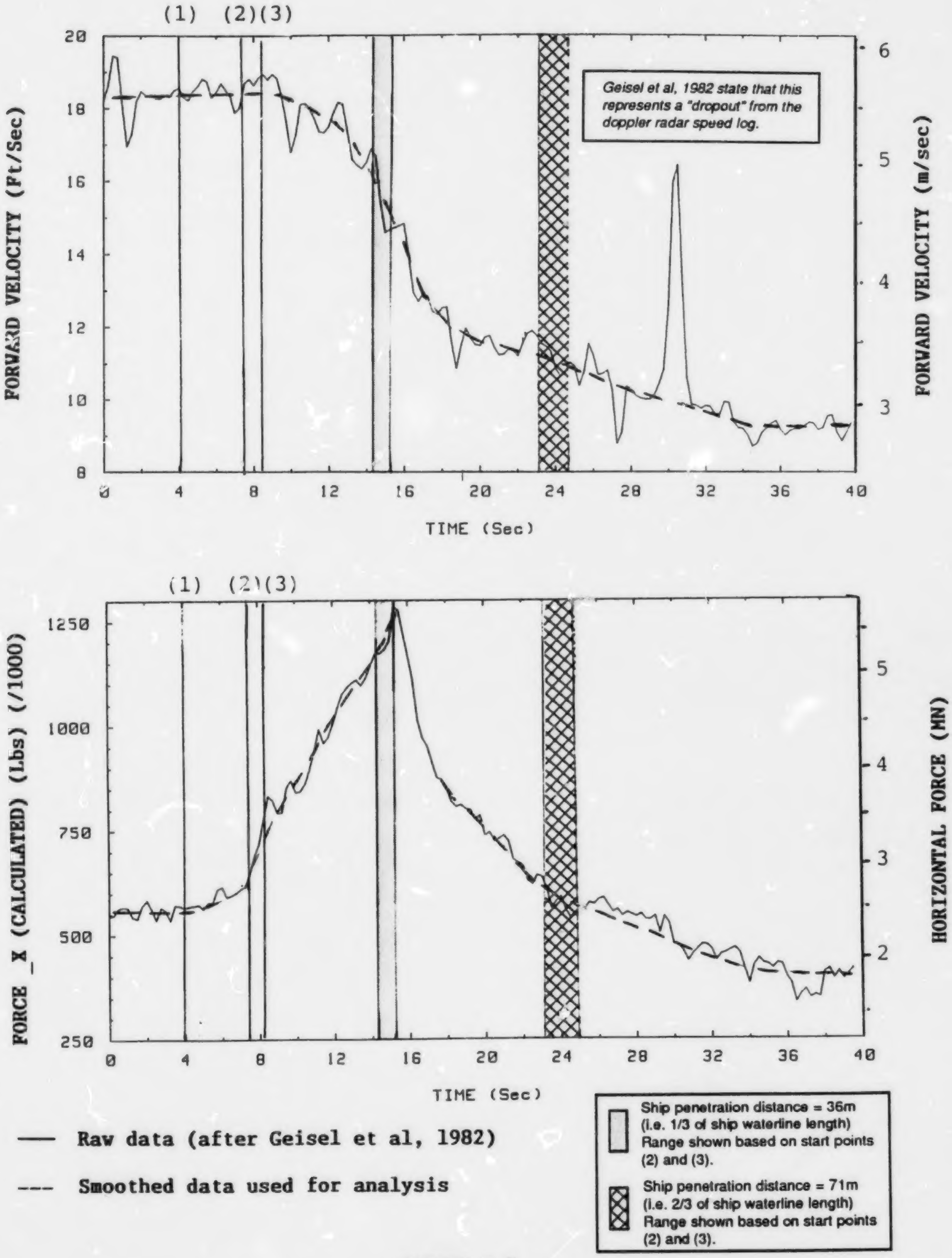

FIGURE 2.5

SMOOTHED VELOCITY AND FORCE TIME HISTORIES FOR RAMMING TEST OF RIDGE 18

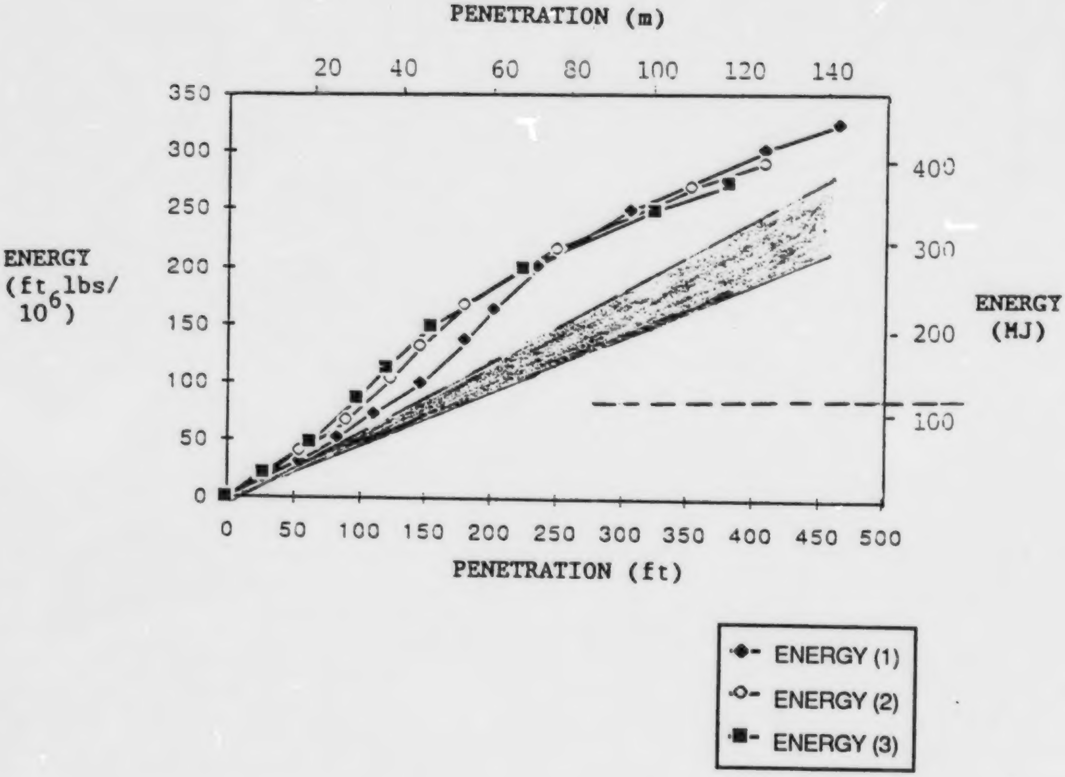

LEGEND:

———	Total Cumulative Penetration Energy Measured During Field Tests
– – – –	Total Penetration Energy Predicted by Stubbs et al, 1986 for the "pure ridge" (i.e. the unconsolidated material)
■	Range of Cumulative Penetration Energy Predicted for Consolidated Layer Only for Range of Ship Speeds Which Occurred During the Ramming Event. See Section 2.3.2 (ii).

FIGURE 2.6

FULL SCALE PENETRATION ENERGY FOR RIDGE 18

Table 2.2

Summary of Full Scale Penetration Forces and Energies for Ridges 17 and 18

Ridge Penetration Energy (MJ)

Penetration Distance (m)	Ridge 17	Ridge 18
26.8 (0.25 LWL)	106 - 117	85 - 93
35.4 (0.33 LWL)	142 - 157	127 - 153
71.9 (0.67 LWL)	260 - 263	273 - 277
80.5 (0.75 LWL)	271 - 283	301 - 306

Maximum Ridge Penetration Force

Ridge #	Max. Penetration Force (MN)	Penetration (m) at which max. force occurred
17	4.8	15 to 26 (.14 to .24 LWL)
18	5.7	37 to 45 (.34 to .42 LWL)

Notes:

1. LWL taken as 107.3 m (352 ft.) See Figure 2.2.
2. The above values for ridges 17 and 18 cover the range of cases where the bow was considered first to contact the ridge. The above penetration energies for ridge 18 are the range for cases (2) and (3). See Section 2.3.

(ii) Relative Contribution of Unconsolidated and Consolidated Portions of Ridge to Total Ridge Penetration Energy

The relative contribution of the consolidated and unconsolidated portions of the ridge to the total penetration energy is of interest as this provides some guidance towards the areas where ridge modelling efforts need to be focussed.

The cumulative energy that would be required for the ship to penetrate an ice sheet equal in thickness to the mean thickness of the consolidated layer has been predicted for the range of ship speeds which occurred during the ramming of ridges 17 and 18. These computations are based on predictions of the level ice resistance of the USCGC POLAR STAR for the ice thicknesses and ship speeds of interest. A semi-empirical predictor of level ice resistance for the USCGC POLAR STAR (which is based on field data collected in the Bering Sea in 1982 and in Antarctica in 1984) was used to make these predictions. This predictor is described in Glen et al, 1985.

The table below summarizes these computations:

Ridge	Basis of Level Ice Resistance Predictor Used (1)	Ship Speed		Avg. Thickness (m) of Consolidated Layer of Ridge (2)	Range of Level Ice Resistance (MN) Predicted for Range of Ship Speeds
		Entering Ridge (m/s)	Minimum During Ramming Event (m/s)		
17	Coefficients Based on 1982 Test Data Only	4.1	1.8	0.4	0.46 - 0.73
17	Coefficients Based on combination of 1982 and 1984 Test Data	4.1	1.8	0.4	0.40 - 0.72
18	Coefficients Based on 1982 Test Data Only	5.6	2.9	0.9	2.0 - 2.7
18	Coefficients Based on combination of 1982 and 1984 Test Data	5.6	2.9	0.9	1.7 - 2.5

Notes: (1) Coefficients based on the regression of level ice resistance data collected during 1982 trials in the Bering Sea, 1984 trials in Antarctica and the combined 1982 and 1984 data are presented in Glen et al, 1985.

(2) See section 2.3.3 for values.

Figures 2.3 and 2.6 compare the computed penetration energies with the total cumulative penetration measured in the field for ridges 17 and 18, respectively.

Recently, a semi-empirical predictor of ridge resistance, and penetration energy, has been developed by Stubbs et al, 1986. The energy required to penetrate the unconsolidated material only (i.e. the "pure ridge" penetration energy as defined by Stubbs et al, 1986) predicted by this relation for ridges 17 and 18 is also shown on Figures 2.3 and 2.6 respectively.

For ridge 18, the sum of the penetration energies predicted for the consolidated layer only (using a predictor of level ice resistance) and for the unconsolidated material only (using the Stubbs et al, 1986 predictor) agrees well with the total penetration energy measured in the field. See Figure 2.6.

For ridge 17, the sum of these two components is significantly less than the total measured in the field. See figure 2.3.

Efforts have been made to further understand the relative contributions of the consolidated and unconsolidated portions of the ridge by estimating the cumulative penetration energy per unit thickness for each portion. This analysis normalizes the penetration energy to the thickness (as the thickness of the consolidated layer was significantly less than that of the unconsolidated material for ridges 17 and 18).

Table 2.3 summarizes these computations. As would be expected, they indicate that the consolidated layer contributes a significantly greater proportion of the total penetration energy.

It should be recognized that these comparisons are tentative for several reasons. The use of algorithms developed to predict level ice resistance as predictors of the resistance of the consolidated layer is unproven. Furthermore, it is expected that some interaction will occur between the unconsolidated and consolidated portions of the ridge during penetration of the ship.

Nevertheless, the preliminary calculations done in this section are valuable in that they provide some preliminary understanding of the relative significance of the consolidated and unconsolidated portions of the ridge.

Table 2.3
Comparison of Cumulative Penetration Energies Per Unit Thickness for the Unconsolidated and Consolidated Portions of the Ridge

Ridge	Ship Penet. Dist.	Mean Total[1] Thickness of Ridge (m)	Mean Thick.[2] of Cons. Layer (m)	Total[3] Meas. Cum. Pen.Energy (MJ)	Predicted[4] Cum.Penet. Energy for Cons.Layer Only (MJ)	Cum.Penet.Energy/Unit Thickness(MJ/m)		
						Unconsol.[5] Material	Cons.[6] Layer	Ratio of Unit Penet. Energies for: Cons.layer/ Uncons. Material
17	36m (i.e.0.33 LWL)	5.8	0.4	142 - 157	14 - 26	21 - 26	35 - 65	1.3 - 3.0
17	71m (i.e.0.67 LWL)	5.8	0.4	260 - 263	28 - 52	39 - 43	70 - 130	1.6 - 3.3
18	36m (i.e.0.33 LWL)	4.4	0.9	127 - 153	61 - 97	8 - 26	68 - 108	2.6 - 13.5
18	71m (i.e.0.67 LWL)	4.4	0.9	273 - 277	121 - 192	24 - 44	134 - 213	3.0 - 8.9

Notes:

1. Mean Thickness of ridge computed as: total ridge area/ridge width. See section 2.3.3(i) for values.

2. Mean thickness of consolidated layer computed as: total area of cons. layer/ridge width. See Section 2.3.3(i) for values.

3. This range spans the range of ridge "startpoints" that were considered. See Table 2.2 and previous section.

4. The range of cumulative penetration energies predicted for the consolidated layer only is based on predictions of the level ice resistance of the USCGC POLAR STAR for the range of speeds which occurred during the ramming event. See previous text in this section and figures 2.3 and 2.6.

5. The cumulative penetration energy/unit thickness for the unconsolidated material was computed as follows:

$$\frac{\textbf{Total Meas. Cum. Penet. Energy - Predicted Cum. Penet. Energy for Consolidated Layer Only}}{\textbf{Mean Total Thickness of Ridge - Mean Thickness of Consolidated Layer}}$$

6. The cumulative penetration energy/unit thickness for the consolidated layer was computed as follows:

$$\frac{\textbf{Predicted Cumulative Penet. Energy for Cons. Layer Only}}{\textbf{Mean Thickness of Consolidated Layer}}$$

(iii) Comparison of Horizontal Force with Level Ice Resistance of the USCGC POLAR STAR

It is of interest to compare the measured forces in level ice on the forward side of the ridge with the level ice resistance of the USCGC POLAR STAR predicted by Glen et al, 1985. See Figure 2.7 and Table 2.4.

The measured resistances are significantly higher (by a factor of about 2.3) than the predicted values.

For ridge 17, the ship travelled about 200 m before the horizontal force increased significantly (See Figure 2.3). This distance represents about two ship lengths. Thus, it can be reasonably assumed that the ship was travelling in level ice only over this portion of the data record.

For ridge 18, the data record is much shorter and the initial portion (before the force starts to rise and the velocity starts to reduce) represents an approximate ship travel distance of only 30 m. See Figure 2.5. Thus, it may be that the ship was transitting ridged ice at the bow and level ice further aft during this part of the record. Therefore, a direct comparison of the measured forces and the predicted level ice resistance for the initial portion of the data record for ridge 18 may not be fair.

If the ice near the ridge was thicker, it would help to explain the discrepancy between the predicted and measured forces. For example, if the ice thickness near the ridge was twice the level ice thickness (reflecting the effects of rafting, perhaps), the predicted resistances would match the measured data within about 10%.

In the field, efforts were made to profile the ice beyond the region affected by the ridge and the ridge profiles (shown in Figures 2.8 and 2.9) indicate that the ice thickness near the ridge was close to the "adjacent level ice thickness".

Measurements of the "adjacent level ice thickness" were made in areas which were well-separated from the ridge and are believed to be reliable (R. Voelker, NKF, personal communication).

This issue is of great concern as it may indicate a large error in the measured horizontal force, and hence, the computed ridge penetration energy. To obtain some understanding of its potential significance, let us assume that the field data overestimate the horizontal force by 1.4 MN (i.e. 315 kips) which is the approximate discrepancy between each measured and predicted resistance. (See Table 2.3). An average force of 1.4 MN over a penetration distance of 71 m (i.e. 0.67 LWL) represents an energy of 99 MJ. This value is about 35% of the total penetration energy for ridge 18 (which was 273 - 277 MJ for a penetration distance of 71 m).

Unfortunately, additional data are not available to resolve this issue. (R. Voelker, NKF, personal communication).

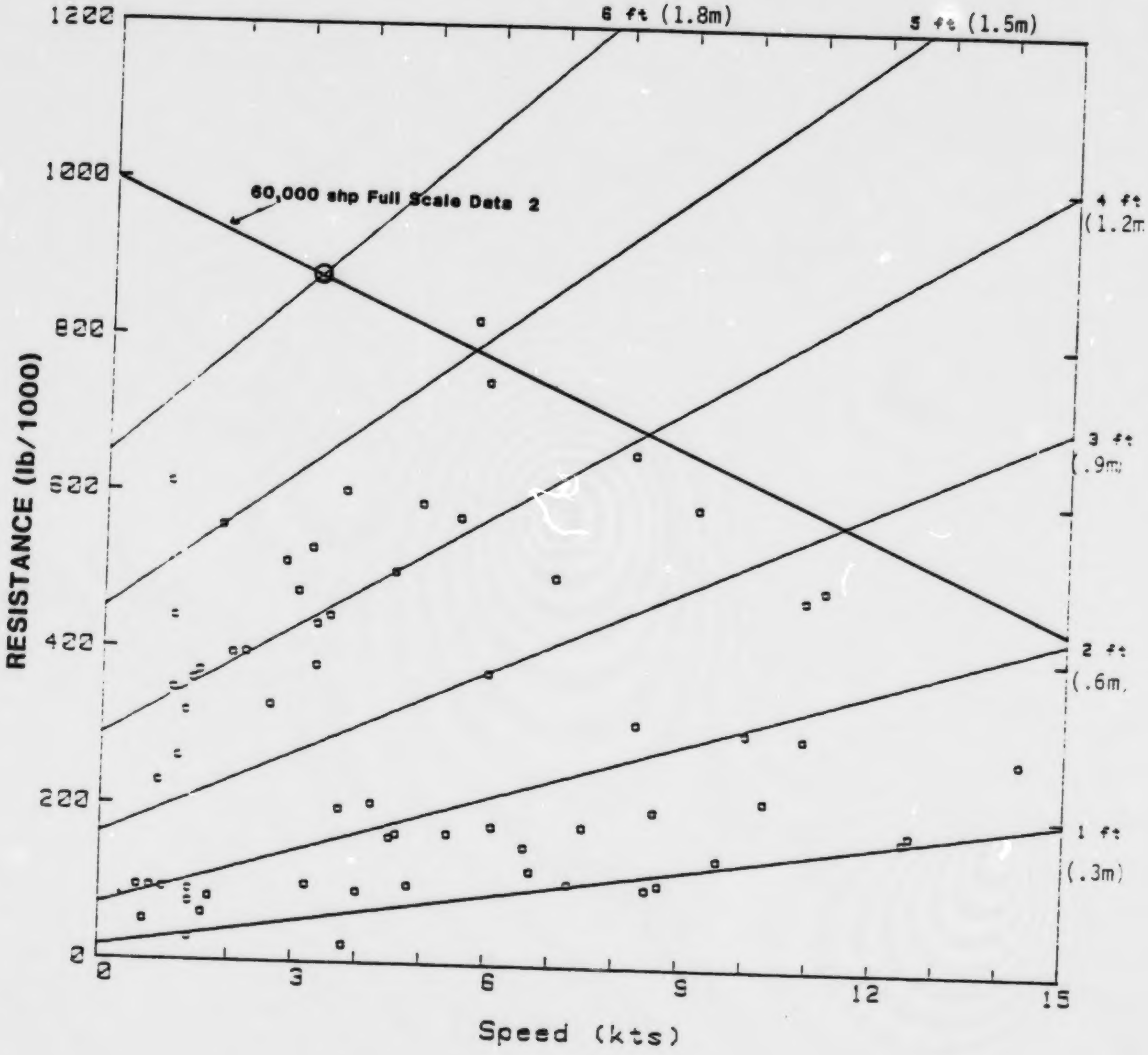

FIGURE 2.7

LEVEL ICE RESISTANCE OF THE USCGC POLAR STAR
(after Glen et al)

Table 2.4

Comparison of Predicted and Measured Level Ice Resistance

Ridge	Thick.(m) of Adj. Level ice	Approx.Steady Ship Speed (m/s) Before Entering Ridge	Approx. Mean Measured Horizontal Force (MN) Before Entering Ridge	Predicted Resistance (MN) of Adjacent Level Ice (See Note 1)
17	0.51	4.1	2.3	0.97 (1.0)
18	0.46	5.6	2.5	1.1 (1.1)

Notes: 1. The level ice resistance was predicted using the semi-empirical predictor developed by Glen et al, 1985. This predictor is based on field measurements of the level ice resistance of the POLAR STAR in 1982 in the Bering Sea (34 data points) and of the level ice resistance of the POLAR SEA in 1984 in Antarctica (30 data points). Regression coefficients based on the 1982 data, the 1984 data, and the combined 1982 and 1984 data are presented in Glen et al, 1985. The resistance has been predicted using the coefficients obtained from both the combined data sets and from the 1982 data. The latter predictions are shown in parenthesis.

2.3.3 Ice and Ridge Properties

(i) Summary and Analysis of Field Data

The cross-sectional profiles for ridges 17 and 18 were analyzed. As there were gaps in both of these profiles, it was necessary to complete these profiles using interpolation. Figures 2.8 and 2.9 show the measured profiles and indicate how the profiles were interpolated.

The table below summarizes the measured ridge areas:

Parameter	Ridge 17	Ridge 18
Ridge width	39.3 m (129 ft)	40 m (131 ft)
Total ridge cross-sectional area	227 m^2 (2450 ft^2)	175 m^2 (1880 ft^2)
Area of consolidated layer (Note: Only areas below the waterline were included as the sail was assumed to be unconsolidated).	58 m^2 (622 ft^2)	35 m^2 (380 ft^2)
Total keel area	208 m^2 (2240 ft^2)	146 m^2 (1570 ft^2)
Sail area	19 m^2 (202 ft^2)	30 m^2 (320 ft^2)
Mean depth of consolidated layer (computed as: area of cons. layer/ridge width)	0.4 m (1.5 ft)	0.9 m (2.9 ft)
Mean depth of keel (computed as: keel area/ ridge width)	5.3 m (17.4 ft)	3.7 m (12.0 ft)
Mean height of sail (computed as: sail area/ ridge width)	0.5 m (1.6 ft)	0.7 m (2.4 ft)

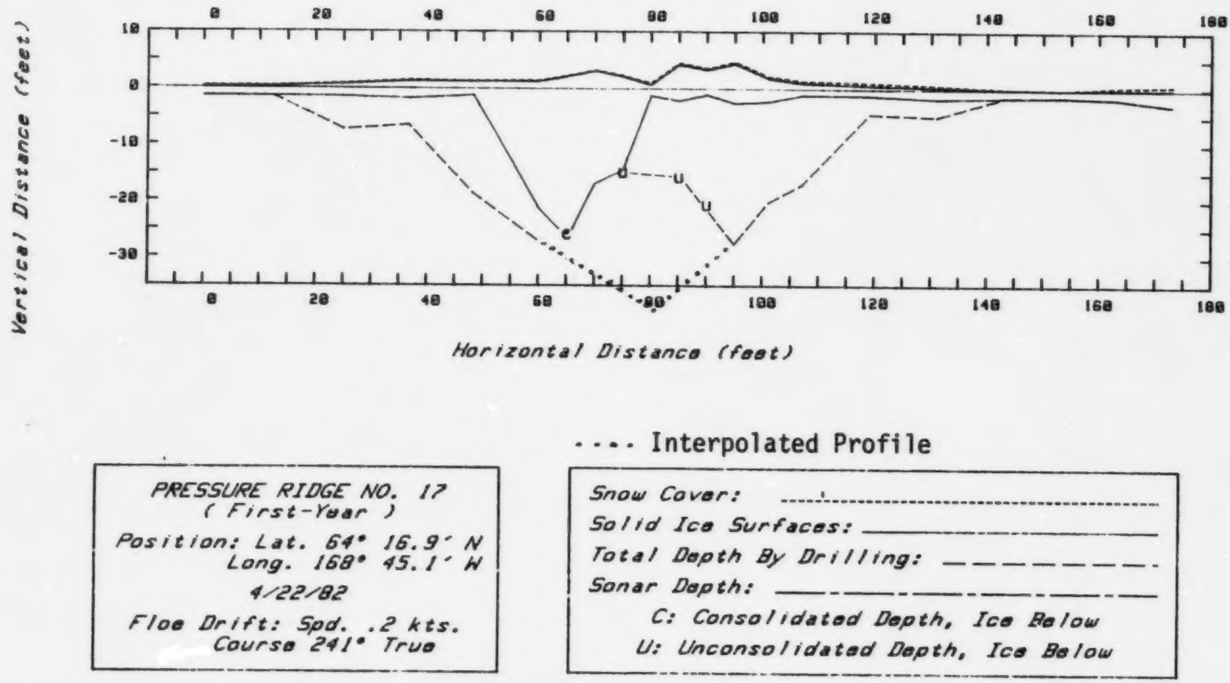

PRESSURE RIDGE NO. 17

SUMMARY OF PHYSICAL CHARACTERISTICS

Adjacent Floe Thicknesses	1.7 ft
Maximum Sail Height	4.3 ft
Maximum Keel Depth	27.7 ft
Maximum Depth of Consolidation	26.0 ft

SUMMARY OF DIMENSIONAL RATIOS

Maximum Keel Depth/Maximum Sail Height	6.4
Maximum Consolidated Depth/Maximum Sail Height	6.0
Maximum Consolidated Depth/Adjacent Level Ice Thickness	15.3

FIGURE 2.8

PRESSURE RIDGE NO. 17
(after Geisel et al, 1982)

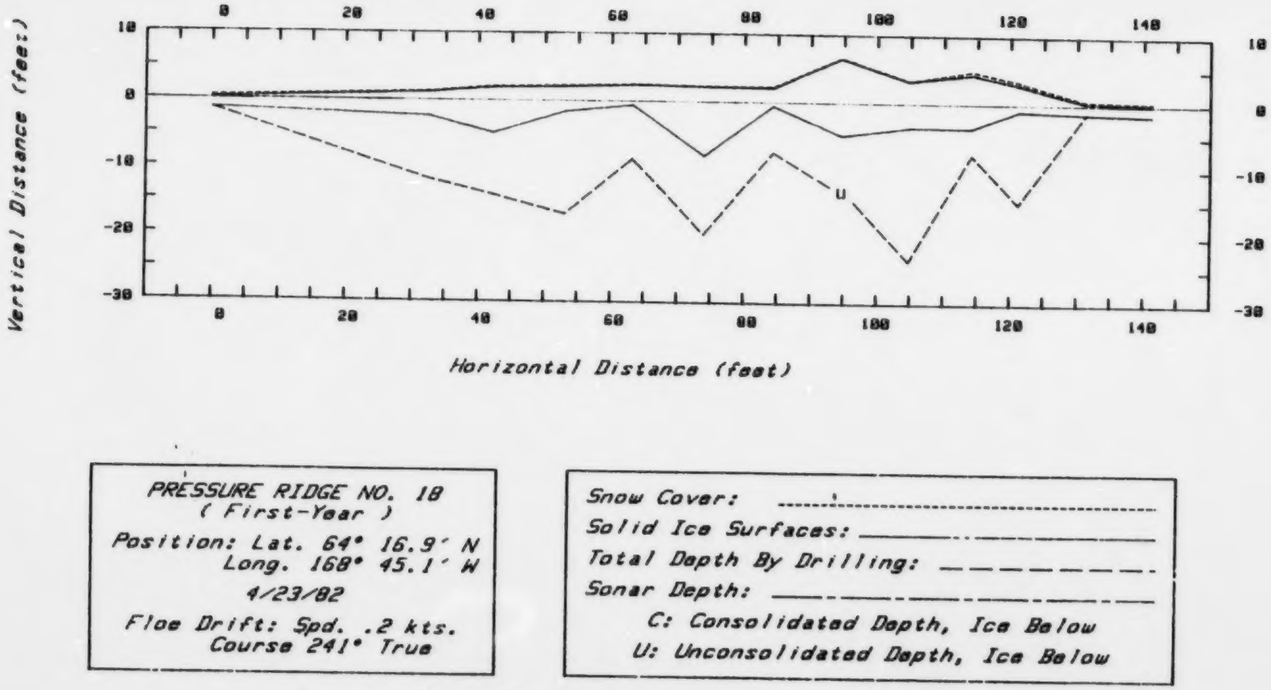

PRESSURE RIDGE NO. 18

SUMMARY OF PHYSICAL CHARACTERISTICS

Adjacent Floe Thicknesses	1.5 ft
Maximum Sail Height	6.5 ft
Sail Width (83'-131')	48.0 ft
Maximum Keel Depth	23.6 ft
Keel Width (0'-131.3')	131.3 ft
Maximum Depth of Consolidation	8.2 ft

SUMMARY OF DIMENSIONAL RATIOS

Maximum Keel Depth/Maximum Sail Height	3.6
Maximum Consolidated Depth/Maximum Sail Height	1.3
Maximum Consolidated Depth/Adjacent Level Ice Thickness	5.5

FIGURE 2.9

PRESSURE RIDGE NO. 18
(after Geisel et al, 1982)

In addition, the following basic ice properties were measured during the trials:

Ice Property	Average Value			
Ice-hull friction factor	Sliding tribometer tests: Rotating arm tribometer tests: (see Note 1)	0.045 0.20		
		Lane Formula	Vaudrey Formula	Weeks et al Formula
Ice salinity and temperature (which were used to estimate the ice flexural strength)	Flexural strength (KPa) of level ice:	320	440	260
	Flexural strength (KPa) of ridged ice:	280	390	290
	(See Notes 2 and 3)			

Notes: 1. The sliding arm tribometer slides an ice sample along the hull without causing crushing while the rotating arm tribometer simultaneously crushes and slides the ice past the hull. See Geisel et al, 1982 for a description of these test methods.

2. Geisel et al, 1982 calculated the ice flexural strength using the relations of Lane, 1980, Vaudrey, 1977 and Weeks and Assur, 1967. The average values given by these relations are listed above.

3. Appendix H lists all of the computed flexural strengths. The values above are the average flexural strengths over the April 9 to 23 period. The ramming tests for ridges 17 and 18 were conducted on April 22 and 23 respectively.

(ii) Discussion of Measured Ridge Profiles

Consolidated Layer for Ridge 17 - The consolidated layer for ridge 17 is very unusual. Over the horizontal baseline from 15 m to 25 m (i.e. 50 to 80 ft.), the consolidated layer is very thick (i.e. a maximum of 7.9 m) and generally triangular in shape. See Figure 2.8. It is unlikely that the ridge would be locally consolidated to this depth.

It may be that this represents a local inclusion of multi-year ice. However, the occurrence of multi-year ice in the Bering Sea is rare and a distinct change in freeboard was not observed at this point in the ridge (R. Voelker, NKF, personal communication).

Another possible explanation is that the boreholes used to establish the consolidated layer profile happened to be drilled through ice blocks that were rotated to near-vertical, or through layers of rafted ice. However, the measured profile for the ridge indicates at least four boreholes over a horizontal baseline of about 4.6 m (i.e. 15 ft) where the consolidated layer exceeded 4.6 m (i.e. (15 ft) in depth.

Unfortunately, additional data are not available to resolve this issue (R. Voelker, NKF, personal communication).

As only one ridge profile was done, the longitudinal extent of this mass is not known. If this mass were extensive, one would expect large forces during the ramming event. However, as the extent of this mass is unknown, an assessment can not be made of the degree to which the penetration force, and hence the penetration energy, has been affected.

For the establishment of target ridge properties at model scale, the mean thickness of the consolidated layer has been computed including the area of this mass. See section 2.4. Subsequent comparisons of model test results and field data for this ridge have been made based on the total cross-sectional area of the ridge and the mean thickness of the consolidated layer, with this mass included. See Section 5.

If this mass was not sufficiently extensive to significantly affect the penetration force, the above modelling technique and method of comparison is expected to cause the model tests to overpredict the field data.

Comparison of Measured Areas for Sail and Keel of Ridges 17 and 18 - A general check on the field data can be made by comparing the measured sail and keel areas. Numerous investigators (eg. Keinonen, 1973; Comfort and Edwards, 1978, Dickins and Wetzel, 1981) have found a good correlation between the keel area and the total area of the ridge, reflecting isostatic principles.

The table below lists the ratios of these areas that were measured for ridges 17 and 18. (See previous section for values).

Ratio	Ridge 17	Ridge 18
$\frac{\text{Total Keel Area}}{\text{Total Ridge Area}}$	0.91	0.84
$\frac{\text{Total Sail Area}}{\text{Total Keel Area}}$	0.09	0.20

The ratio of the keel area to the total area is close to, and less than, the specific gravity of sea ice for ridges 17 and 18, respectively.

For a fully-consolidated multi-year ridge, the ratio of these two areas has generally been found to be near the specific gravity of sea ice (eg. Dickins and Wetzel, 1981).

For partially-consolidated ridges, this ratio is expected to exceed the specific gravity of sea ice (as the keel is not fully consolidated).

To obtain further understanding, we have computed the keel profile from the measured sail profile for ridge 18. The model used to compute the ridge profile is based on the principle of isostatic equilibrium and is described by Keinonen, 1973.

The keel profile for ridge 18 was computed and is compared with the measured profile on Figure 2.10. The following values were assumed in making these calculations:

- Mass density of seawater: 1025 kg/m^3
- Mass density of sea ice in the sail, keel and consolidated layer: 900 kg/m^3
- Porosity of sail and keel: 35%

Figure 2.10 shows that the computed keel profile is significantly larger than the profile measured in the field. The computed ridge cross-sectional area is greater than the measured area by about 33 per cent.

These comparisons suggest that the field data underestimate the keel area, especially for ridge 18.

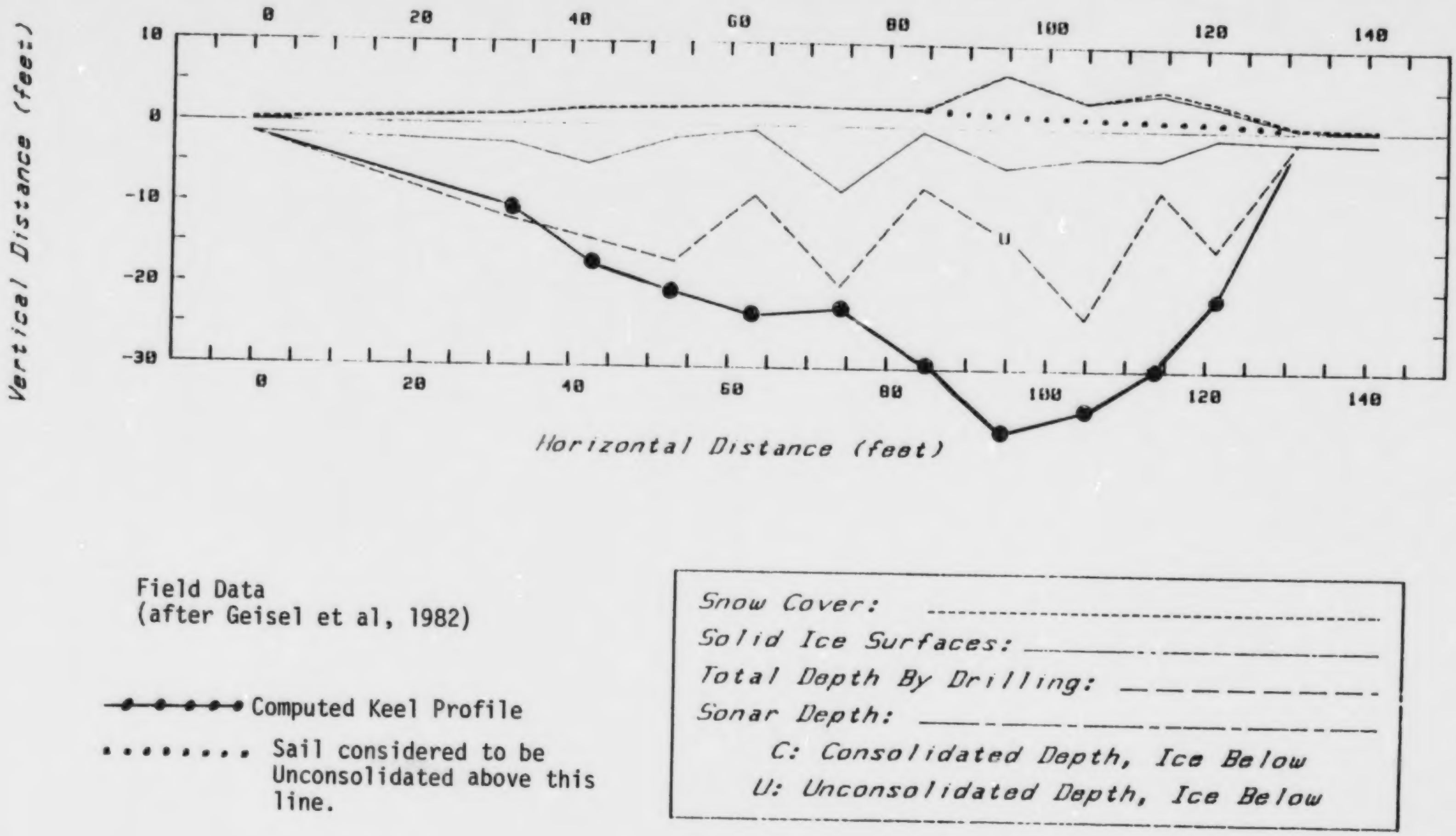

FIGURE 2.10 COMPARISON OF COMPUTED AND MEASURED PROFILES FOR RIDGE 18

2.4 Summary of Model Scale Target Ridge Properties

As outlined in Section 2.3, the 1982 ridge ramming tests conducted with the USCGC POLAR STAR in the Bering Sea were selected as the full scale reference event for this project. As a 19.1:1 scale model of this ship was already available (on loan from the United States Coast Guard), it was decided to conduct the model test program at this scale.

Table 2.5 summarizes key scaling relationships based on Froude scaling laws (which have been commonly used in ice model testing to date). These scaling laws were used to define the target ridges for the model tests, as listed in Table 2.6.

It was originally intended to reproduce both ridge 17 and 18 at model scale in the IMD ice tank. The general shape of these ridges is triangular and trapezoidal, respectively. This would have allowed an evaluation of the influence of ridge shape on the ridge penetration energy and force.

However, as will be discussed in Section 4, difficulties were encountered in the basin in shaping the ridge keels to match the above profiles.

For the preliminary tests done at FTL's ice tank, a ridge mold was used to achieve the target shape for ridge #18.

This system was impractical at the IMD as the ridge mold would have interfered with the IMD's underwater carriage. A diver and ridge profiling stick were used to shape the keel profile of one of the ridges in the sheet #1 tests. However, this proved to be very time-consuming and efforts to match the target ridge shape were discontinued. For the remainder of the tests done at the IMD, efforts were concentrated on modelling the width, the consolidated layer thickness and the cross-sectional area of the ridge.

Table 2.5

Scaling Laws

Length	L	$L_p = \lambda L_m$
Beam	B	$B_p = \lambda B_m$
Ice thickness	h	$h_p = \lambda h_m$
Ice flexural strength	σ_f	$\sigma f_p = \lambda \sigma f_m$
Ice elastic modulus	E	$E_p = \lambda E_m$
Velocity	V	$V_p = \sqrt{\lambda}\ V_m$
Time	t	$t_p = \sqrt{\lambda}\ t_m$
Force	F	$F_p = \lambda^3\ F_m$
Mass	m	$m_p = \lambda^3\ m_m$
Mass Density of Water and Ice	ρ	$\rho_p = \rho_m$
Coefficient of Kinetic Friction	μ	$\mu_p = \mu_m$

Where, λ = geometric scale factor

Subscript p = prototype

Subscript m = model

Note: In this case, $\lambda = 19.1$

Table 2.6

Model Scale Ridge and Level Ice Properties

Property	Ridge 17	Ridge 18
Level Ice:		
Thickness (mm)	27	24
Flexural Strength (kpa)	17.8 (see Note 1)	17.8 (see Note 1)
Ice-model friction factor	0.045 to 0.20	0.045 to 0.20
Ridges:		
Flexural Strength of Consolidated Layer (kpa)	16.8 (see Note 1)	16.8 (see Note 1)
Width (m)	2.1	2.1
Cross-sectional area (m^2)	0.62	0.48
Area of consol. layer (m^2)	0.16	0.10
Avg. thickness of consol. layer (mm)	24	46
General Ridge shape	Triangular	Trapezoidal

Note: 1. The average flexural strength predicted by the Lane, Vaudrey, and Weeks and Assur formulae (see Section 2.3) were averaged to obtain the above values.

3.0 TESTS CONDUCTED AT FLEET TECHNOLOGY LIMITED'S ICE TANK

Preliminary testing was carried out in advance of the tests done at the IMD. This was done to assist in defining the test plan for the project and to provide the project team with basic experience in the model testing of ridges before conducting tests at the IMD (which constituted the bulk of the project budget).

3.1 Test Description

3.1.1 Test Setup and Matrix

For these tests, ridge #18 (from the 1982 USCGC POLAR STAR trials - Geisel et al, 1982) was selected as the ridge ramming event to be modelled. Ridge #18 was approximated as a trapezoid as shown in Figure 3.1. This form scaled the total cross-sectional area and surface width of ridge 18. These tests were done at 19.1:1 scale as this was the scale of the available POLAR STAR model.

As these tests were preliminary in nature, a relatively simple test setup was used. The model was restrained in the surge, sway and yaw directions. Pitch, roll and heave motions were allowed. These tests were conducted at a constant velocity of 0.98 m/sec which corresponds to a full scale value of 4.3 m/sec. (14 ft/sec) using Froude scaling laws. This full scale velocity is near the mid-range ship velocity for the field data for ridge 18. (During this test, the ship velocity reduced from approximately 18.5 ft/sec to 9.5 ft/sec).

Table 3.1 summarizes key model setup parameters for these tests.

Figure 3.2 schematically shows the basin setup used for these tests. Two ice sheets were tested as follows:

Sheet #	Test Date	Field Event Simulated	Ice Modelling Material
1	March 28	Penetration of Ridge 18	EGAD Ice
2	March 31	Penetration of Ridge 18	Matrix of plastic beads in EGAD ice (termed BEADS-ICE)

Table 3.2 describes the test matrix.

Tests were done using both EGAD ice and BEADS-ICE to investigate the influence of the model material density on the test results. The measured densities for these two materials were 0.93 and 0.89 g/cc respectively. This material is described further in section 3.2 (i.e. Ice and Ridge Properties).

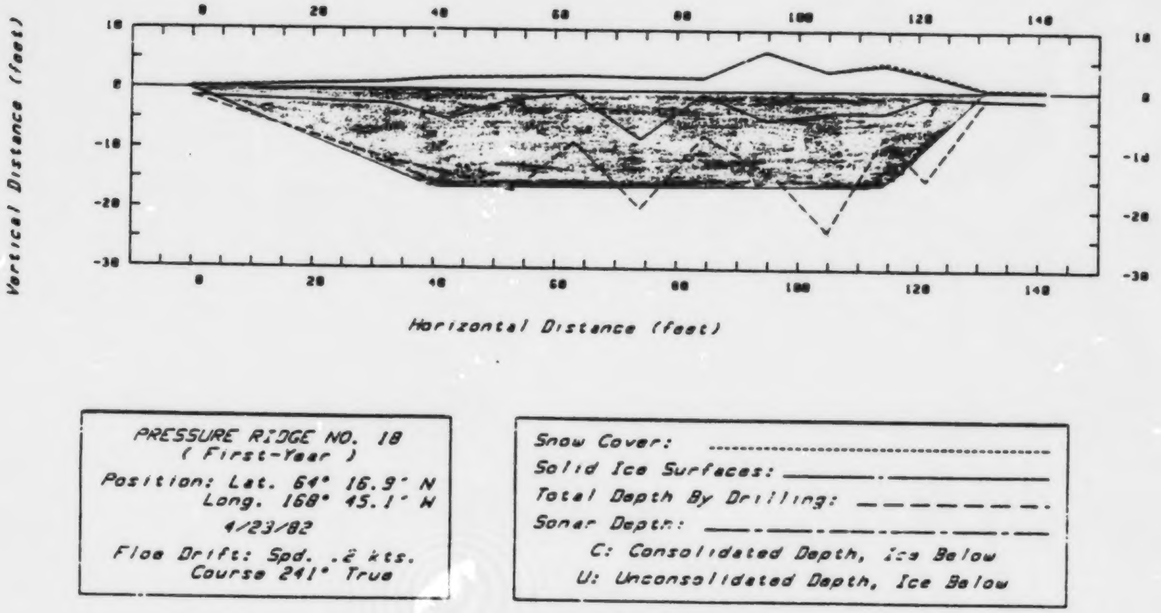

▨ Shape of ridge mold used to approximate ridge 18 for the model tests

RIDGE MOLD CROSS-SECTIONAL PROFILE

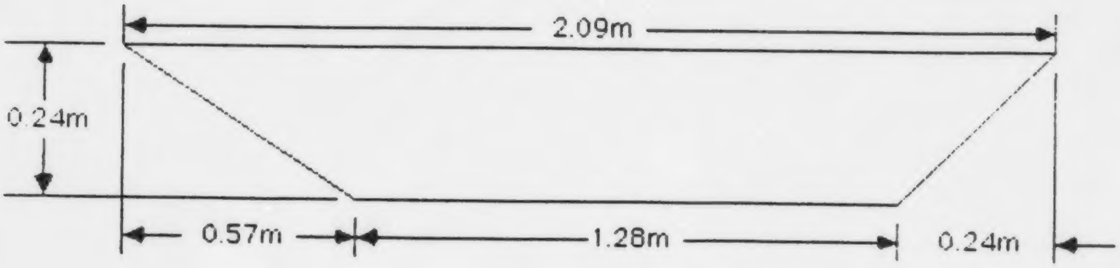
2.09m
0.24m
0.57m
1.28m
0.24m

FIGURE 3.1

COMPARISON OF RIDGE MOLD SHAPE AND CROSS-SECTIONAL PROFILE OF RIDGE 18

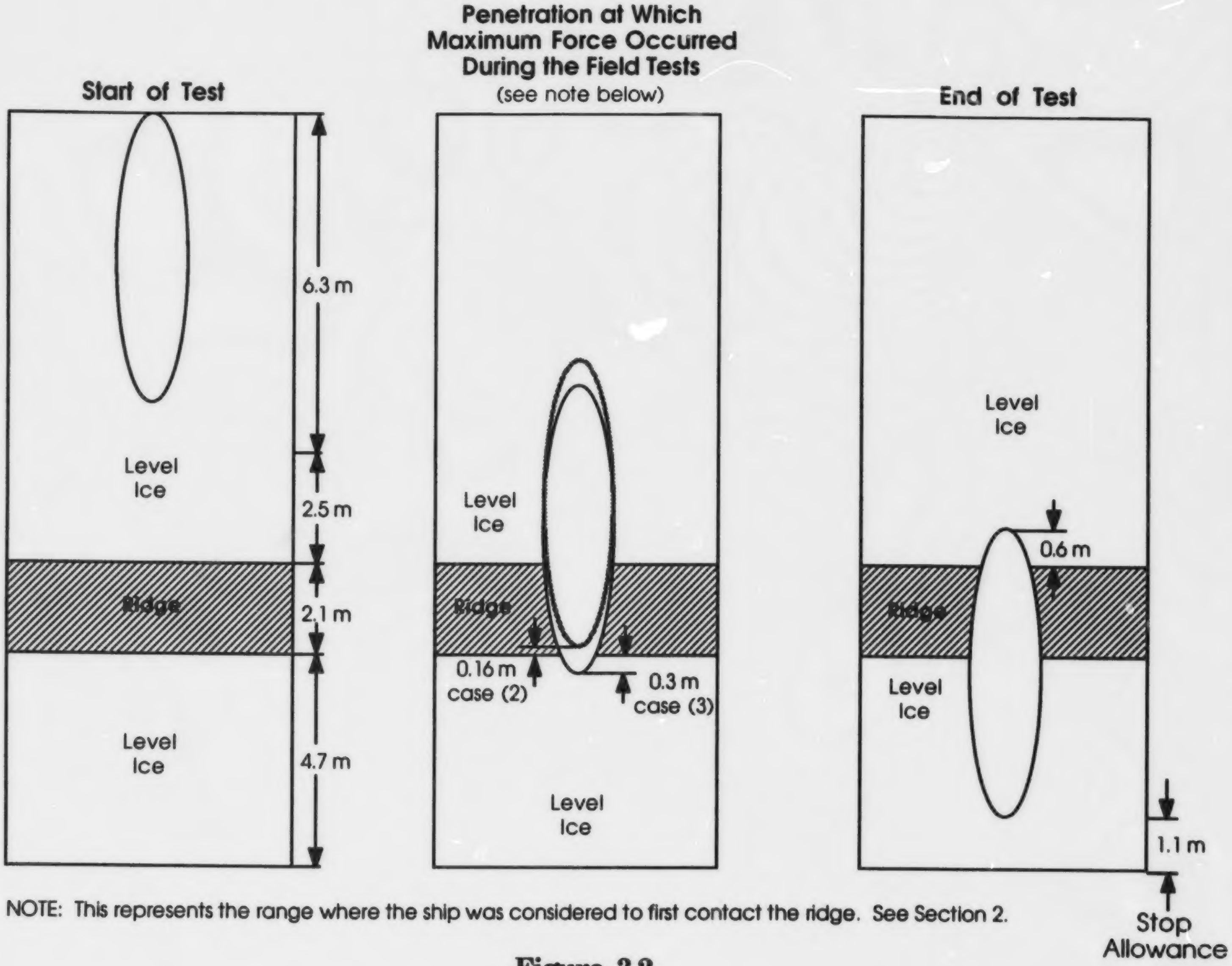
Start of Test
Penetration at Which Maximum Force Occurred During the Field Tests
(see note below)
End of Test
6.3 m
2.5 m
2.1 m
4.7 m
Level Ice
Ridge
Level Ice
Level Ice
Ridge
0.16 m case (2)
0.3 m case (3)
Level Ice
Level Ice
0.6 m
Ridge
Level Ice
1.1 m
Stop Allowance

NOTE: This represents the range where the ship was considered to first contact the ridge. See Section 2.

Figure 3.2

BASIN SETUP

Table 3.1

Summary of Key Model Setup Parameters

Parameter		Model Test Setup M.S. Value	 F.S. Value	Target F.S. Value
Model Ballasting:	Draft	0.51 m	9.7 m	9.7 m (31.8 ft)
	Pitch gyradius	0.24 LWL	0.24 LWL	No data (see note 1)
	Roll Period	2.5 sec	10.9 sec	11.9 sec (see note 2)
Ice Model Friction Factor:	EGADS Ice	0.05	0.05	0.045 to 0.20
	BEADS Ice	0.10	0.10	(see note 3)
Ship Velocity:		Held constant at 0.98 m/s	4.3 m/s (14.0 ft/s)	5.6 m/s to 2.9 m/s (see note 4)

Notes:

1. Data for the full scale pitch gyradius could not be located (D. Middleton, USCG, personal communication). The value adopted for these tests is the same used by Arctec Inc., who conducted 1:48 scale model tests of this vessel (Coburn et al, 1981).

2. Value obtained from Stability booklet for USCGC Polar Star.

3. The average ice-hull friction factors that were measured during the field trials were 0.045 (for tests done with a sliding arm tribometer) and 0.20 (for tests done with a rotating arm tribometer). See Geisel et al, 1982 for a description of these test methods.

4. The ship velocity reduced from about 5.6 m/s to 2.9 m/s (18.5 ft/sec. to 9.5 ft/sec) while penetrating ridge 18.

Table 3.2

Matrix of Tests Done at FTL

Sheet #	Ice Modelling Material	Test Name (see Note 1)	Model Speed (m/s)	Test Description
1	EGAD-ICE	PENETRATION TEST 1	0.98	Model penetrated ridge and stopped. (See Note 2)
1	EGAD-ICE	PENETRATION TEST 2	0.5	Immediate continuation of 'Penetration Test 2'. (See Note 2).
1	EGAD-ICE	EXTRACTION TEST	0.5	Model pulled back through broken ridge
2	BEADS-ICE	PENET	1.0	Model penetrated ridge
2	BEADS-ICE	EXT	0.5	Model pulled back through broken ridge

Notes: 1. Refer to plots of raw data in appendices A and B by test name.

2. The carriage was inadvertently stopped after the model had partially penetrated the ridge. Test "Penetration Test 2" is an immediate continuation of test "Penetration Test 1".

3.1.2 Test Documentation

The following parameters were recorded during the tests:

a) the total horizontal force on the model
b) the horizontal displacement of the model
c) the temperatures in and near the ridge during the freeze and the tempering process

The horizontal force and displacement of the model were recorded at 30 Hz/channel using a laboratory-standard digital data acquisition system. This system consisted of a Hewlett Packard 9816 computer and an Analogue Devices AD200 digitizing card. These test data were not filtered.

Temperatures were recorded by locating a total of 18 Type T thermocouples in the ridge, the water, the air and the parent ice sheet. Figure 3.3 shows the locations were temperatures were measured. These temperatures were logged manually at several points during the freeze and warmup process.

As well, the tests were photographed using 35 mm still cameras and video cameras.

3.2 Ice and Ridge Properties

3.2.1 Ice Modelling Materials and Ridge Formation Techniques

Tests were done using two ice modelling materials, as follows:

a) EGAD-ice
b) BEADS-ice

EGAD-ice was prepared by adding dopants to the water according to the recommendations of G. Timco (of the National Research Council).

BEADS-ice is a new material proposed for ice modelling that has been under development at Fleet Technology Limited. It is prepared by spreading a layer of polypropylene beads (of about 3mm diameter) over EGAD-doped water and conducting a freeze. Sufficient beads are added to the water so that beads extend to the depth of the target ice thickness. The resulting BEADS-ice material consists of a matrix of plastic beads and EGAD-ice. As the results of small scale laboratory tests with this material were promising (El-Tahan 1988), it was decided to conduct one ridge-ramming test with this material.

One of the principal differences between EGAD-ice and BEADS-ice is the ice density. The density of BEADS-ice was 0.89 g/cc whereas the density of the EGAD-ice was 0.93 g/cc. Thus, it can be seen that the BEADS-ice provides better scaling of the full scale density of cold ice (which is about 0.9 g/cc).

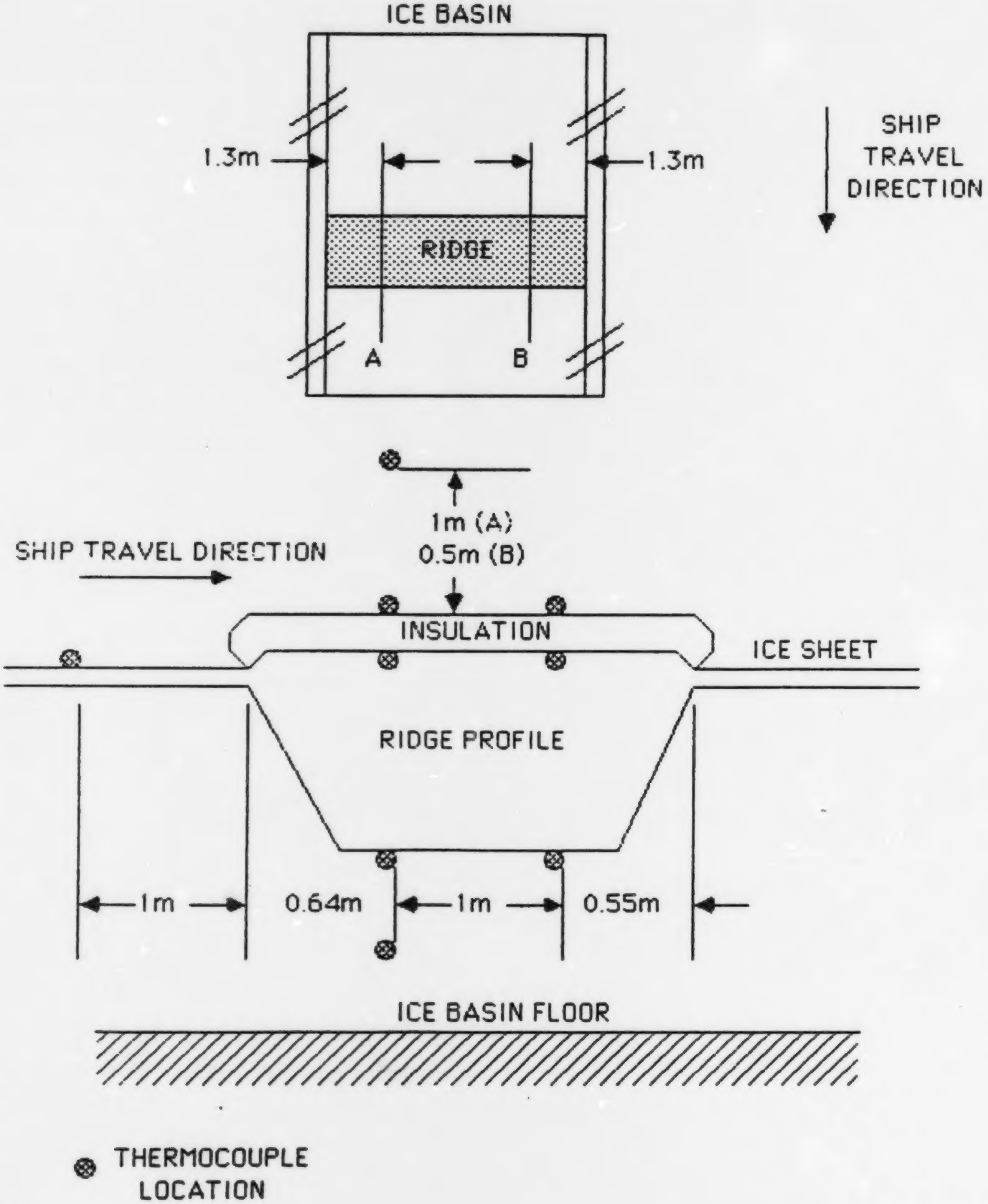
ICE BASIN
1.3m
1.3m
SHIP TRAVEL DIRECTION
RIDGE
A
B
1m (A)
0.5m (B)
SHIP TRAVEL DIRECTION
INSULATION
ICE SHEET
RIDGE PROFILE
1m
0.64m
1m
0.55m
ICE BASIN FLOOR
THERMOCOUPLE LOCATION

FIGURE 3.3

THERMOCOUPLE LOCATIONS

Ridges were built during these tests, as follows:

- **Sheet #1 - EGAD-ice:**

  a) Grow ice sheet of 25 mm thickness

  b) Break ice sheet into pieces with a maximum linear dimension of about five times the ice thickness. Push broken pieces into the ridge mold.

  c) Cover ridge surface with a layer of R12 Fiberglas insulation

  d) Grow second ice sheet around the ridge

  e) Temper sheet and ridge for testing

- **Sheet #2 - BEADS-ice:**

  a) Grow ice sheet of 25 mm thickness

  b) break ice sheet into pieces with a maximum linear dimension of about five times the ice thickness

  c) Make ridge as follows:

    - consolidated layer - slide two sheets over each other

    - unconsolidated layer - put broken ice pieces in ridge mold

    - combination of consolidated and unconsolidated layers - slide consolidated layer over unconsolidated rubble in mold.

  d) Cover ridge surface with one layer of R12 Fiberglas insulation

  e) Grow second ice sheet around the ridge

  f) Temper sheet and ridge for testing

Plates 3.1 to 3.3 show some of the above steps in the ridgebuilding processes.

Plate 3.1

Insulation Mats on Ridge for Test Done In EGAD-Ice at FTL

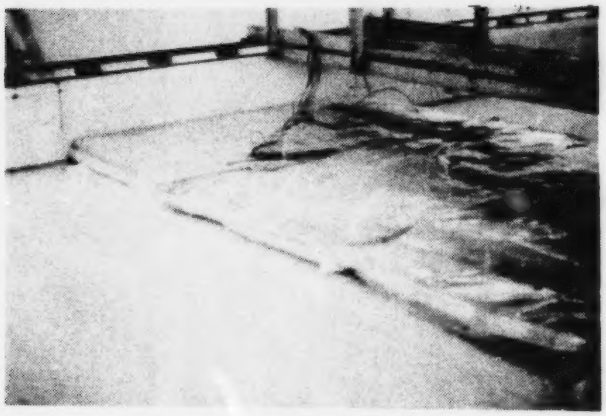

Plate 3.2

Insulation Mats On Ridge for Test Done in BEADS-Ice at FTL

Plate 3.3

Ridge in BEADS-Ice at FTL (Thermocouple wires seen extending from ridge).

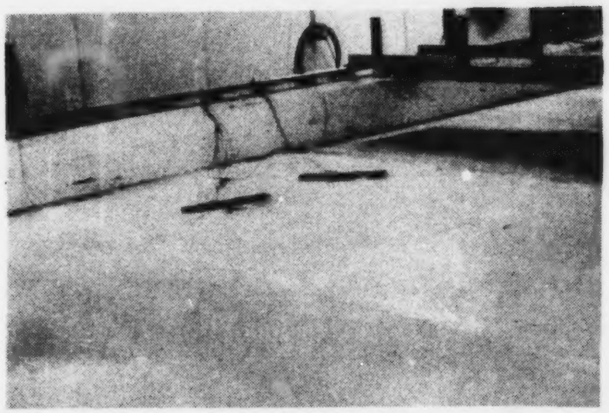

3.2.2 Ice and Ridge Properties

i) Measurement Techniques

The following properties of the level ice and the ridges were measured:

PROPERTY		MEASUREMENT TECHNIQUE
Level ice:	thickness	Vernier caliper
	flexural strength	In-situ cantilever beam tests
	elastic modulus	Measurements of the deflections of the ice sheet for a range of point loads.
	ice density	Measurements of the weight and volume of small ice blocks removed from the ice sheet.
	ice-model friction	Measurements of the force required to pull an ice sample loaded with known weights over the surface of the model.
Ridge:	flexural strength of consolidated layer	In-situ cantilever beam tests
	bulk density	Measurement of the force required to submerge a vertical column in the ridge and of the volume of the ridge.
	temperature	A total of 18 Type T thermocouples were embedded in the ridge and were logged manually.

These techniques are similar to those used subsequently during the tests done at the IMD and are described further in Section 4.2.1.

Plates 3.4 and 3.5 show a submergence test in progress and sites where the ridge bulk density and flexural strength were measured, respectively.

ii) Summary of Ice and Ridge Properties

Table 3.3 summarizes the measured ice and ridge properties.

Figure 3.4 describes the friction factor measurements that were carried out.

Figure 3.3 shows the locations where temperatures were measured. Temperature data have been plotted as a function of the tempering time. Figure 3.5 shows a typical plot. A complete set of plots is included in Appendix A and B for the EGAD-ice and BEADS-ice tests, respectively.

Plate 3.4

Submergence Test to Measure the Bulk Density of the Ridge at FTL

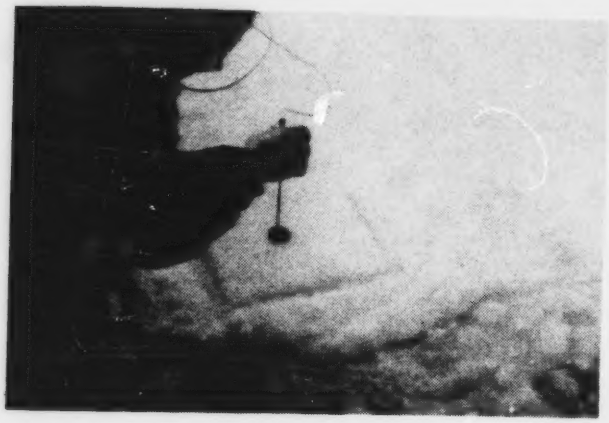

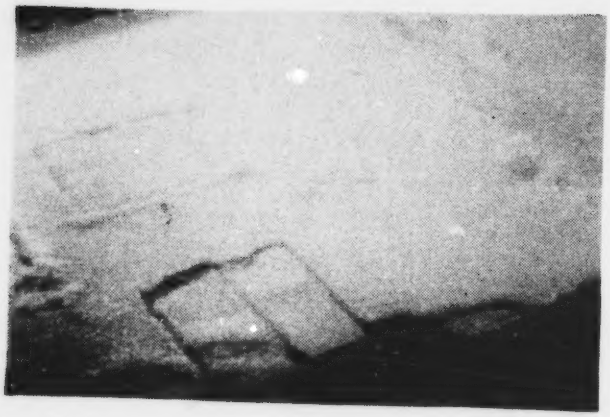

Plate 3.5

Submergence Tests and Cantilever Beam Test Sites for BEADS-Ice Ridge at FTL

Plate 3.6

Vertical Cross-section of BEADS-Ice Ridge at FTL

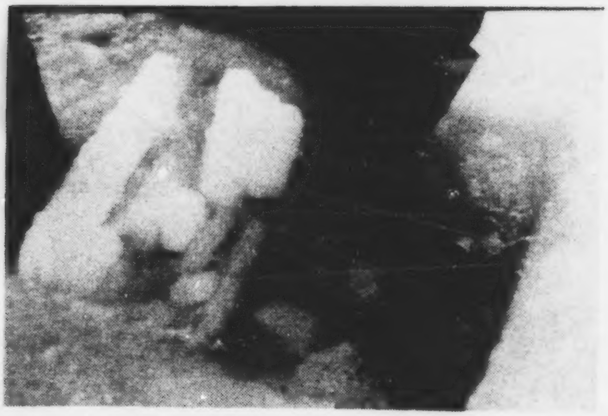

Table 3.3

Summary of Ice and Ridge Properties

	Sheet #1		Sheet #2	
	Measured Model Scale Value	Extrapolated Full Scale Value	Measured Model Scale Value	Extrapolated Full Scale Value
Material	EGAD-ice	n/a	BEADS-ice	n/a
Ice Density (g/cc)	0.93	0.93	0.89	0.89
Level ice flexural strength (kPa)	19.9 ± 1.9	380 ± 36	23.1 ± 2.0	440 ± 38
Level ice elastic modulus (MPa)	6.2 ± 1.3	118 ± 25	27.3 ± 1.5	520 ± 29
Level ice thickness (mm)	25.8 ± 1.8	490 ± 34	29.1 ± 1.5	560 ± 29
Ridge shape	Trapezoidal	(See Fig.3.1)	Trapezoidal	(See Fig.3.1)
Ridge flexural strength (kPa)	6.6 ± 0.9	126 ± 17	3.9 ± 0.7	74 ± 13
Ridge bulk density (N/m^3)	8900	8900	7000	7000
Mean Ridge consolidated layer depth (m)	.340 ±.003	6.5 ± .06	.149 ± .003	2.85 ± .06
Ridge Keel Description	Keel consisted almost entirely of soft, weak ice which was bonded together.		Keel in two distinct layers. Upper layer consisted of two solid ice sheets which were not well-bonded to each layer. Lower layer consisted of loose blocks.	

Note: Model scale values have been extrapolated to full scale values using Froude scaling laws, as described in Section 2.

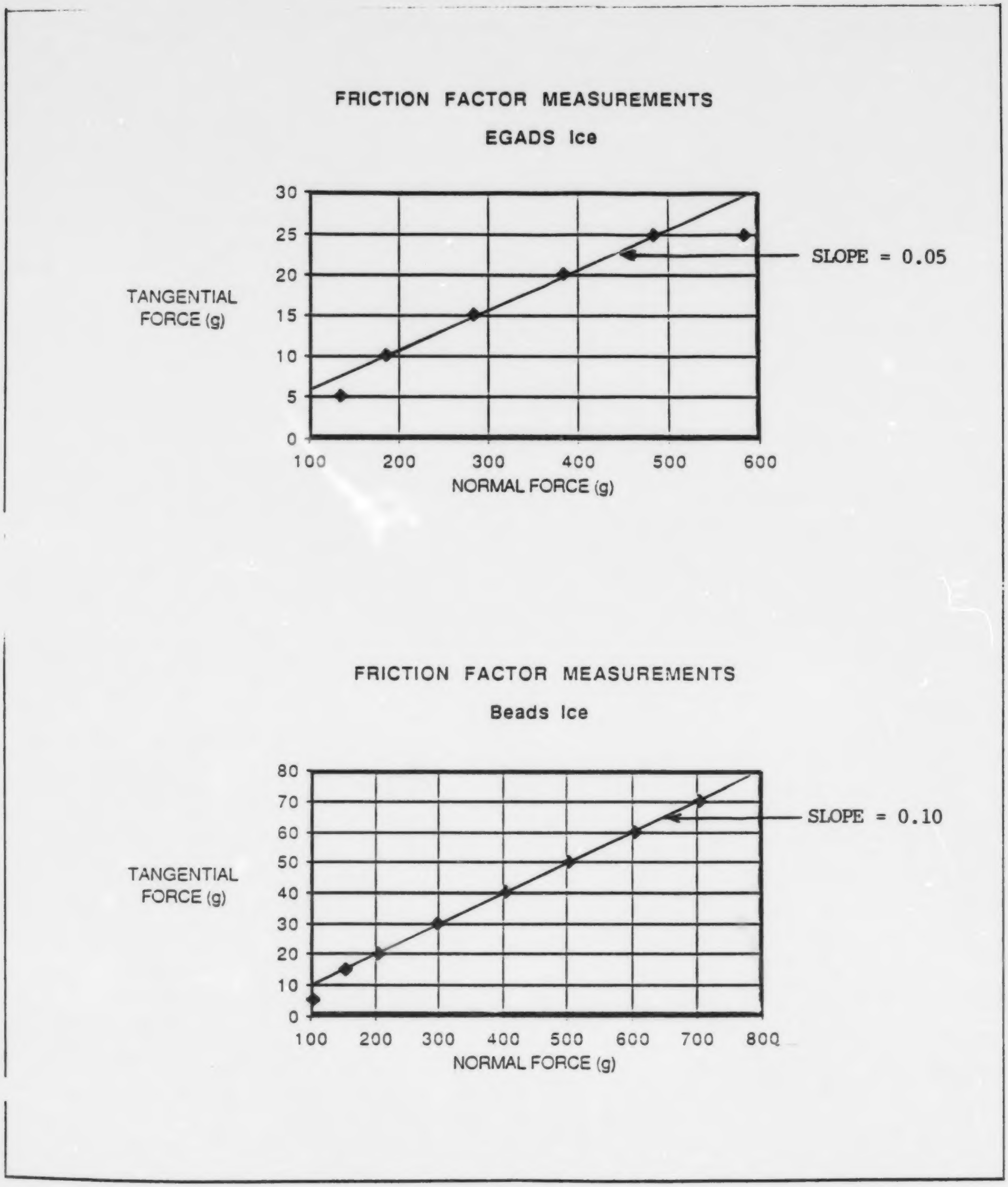

FRICTION FACTOR MEASUREMENTS

EGADS Ice

FRICTION FACTOR MEASUREMENTS

Beads Ice

FIGURE 3.4

RAW FRICTION FACTOR MEASUREMENTS

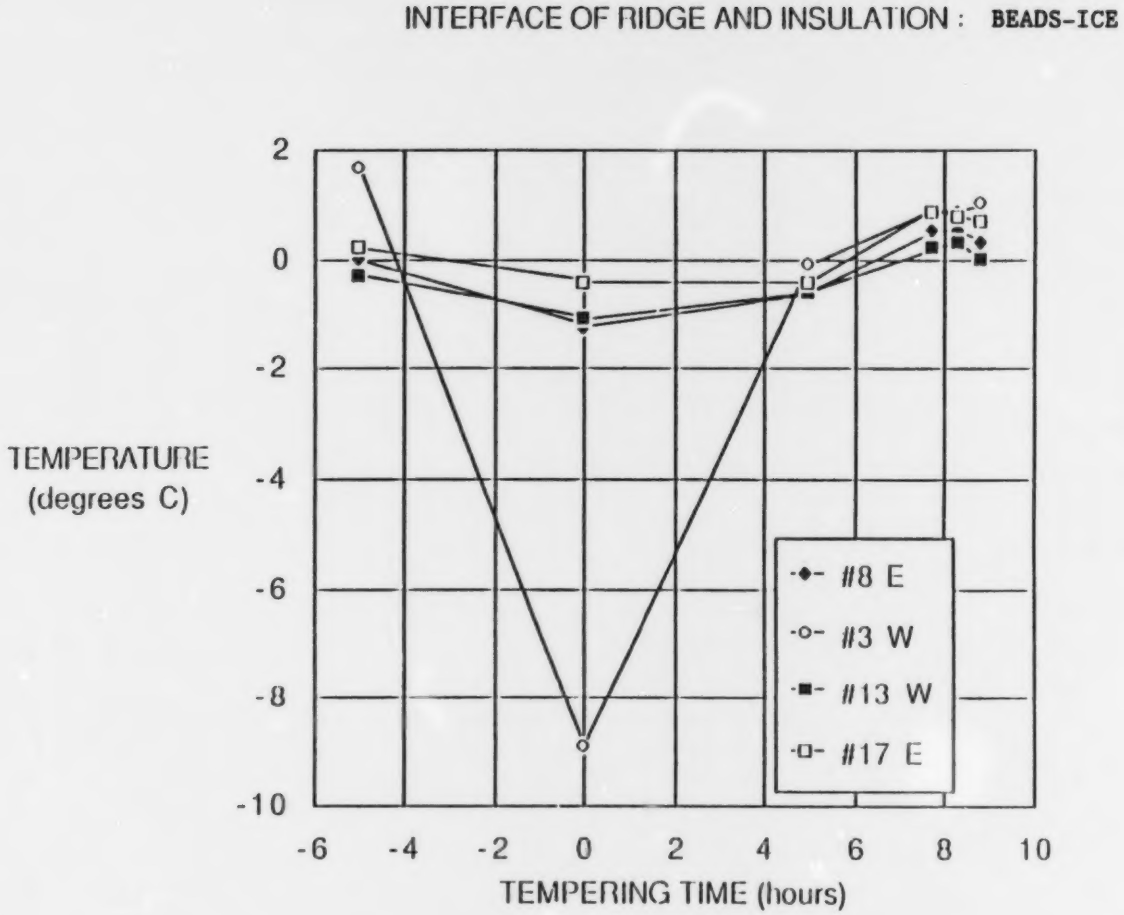

FIGURE 3.5

TYPICAL RIDGE TEMPERATURE TIME HISTORY

The ridge keel produced during the first test (with EGAD-Ice) was very soft and consisted almost totally of soft, slushy material that was weakly bonded together. It was very difficult to distinguish the consolidated layer from the unconsolidated material beneath. This is reflected by the low value measured for the flexural strength of the consolidated layer and by the high value for the thickness of the consolidated layer. See Table 3.3

The ridge produced during the second test (with BEADS-Ice) provided better modelling of a partially-consolidated ridge. In this case, the ridge keel consisted of two distinct layers. The upper layer was consolidated while loose blocks were present beneath it. Plates 3.6 and 3.7 show vertical cross-sections of the ridge. Plate 3.8 shows the distribution of ice piece sizes in the ridge. Plate 3.9 shows the broken ice in the channel after transit by the model and the distribution of ice piece sizes in the level ice adjacent to the ridge for the BEADS-Ice.

3.3 Test Results

Plates 3.10 to 3.13 and 3.14 to 3.15 show the tests conducted in EGADS-Ice, and BEADS-Ice, respectively.

Test data were reduced as follows:

a) time histories were plotted for each transducer for each test.
b) the model scale force-displacement relationship was computed for each test run and the model scale cumulative penetration energy was determined as a function of the penetration distance.
c) the computed model scale cumulative penetration energies were extrapolated to full scale values.

Time histories of the raw data are plotted in Appendices A and B for sheets 1 and 2 respectively. Figure 3.6 shows the cumulative penetration energy as a function of the penetration distances for sheets 1 and 2 and compares these results to the full scale data.

The table below also compares the cumulative penetration energy measured during the model tests with the field data:

Test	Cumulative Penetration Energy (MJ)	
	Penetration Distance = 36 m (i.e. 0.33 LWL)	Penetration Distance = 72 m (i.e. 0.67 LWL)
Field Data for Ridge 18	127 - 153	273 - 277
Model Test 1 (EGAD-ice)	62	No Data (See Note 1)
Model Test 2 (BEADS-ice)	62	116

Note: 1. This ridge was penetrated in two runs as the carriage was inadvertently stopped.

Plate 3.7

Vertical Cross-Section of BEADS-Ice Ridge at FTL

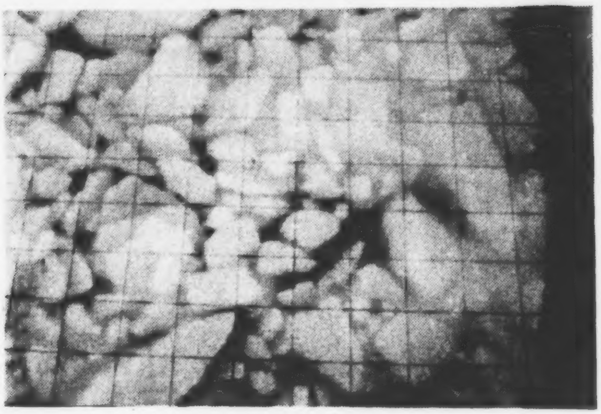

Plate 3.8

Distribution of Ice Piece Sizes in BEADS-Ice Ridge at FTL. Grid Size: 10 cm x 10 cm

Plate 3.9

Distribution of Ice Piece Size in Level Ice Adjacent to Ridge for BEADS-Ice at FTL
Grid Size: 10 cm x 10 cm

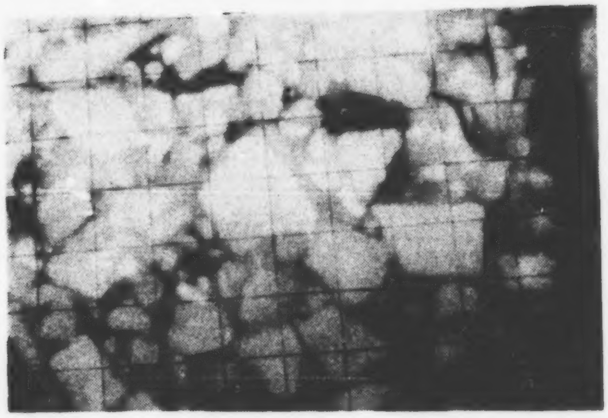

Plate 3.10

Penetration of Ship in Ridge in EGAD-Ice ridge at FTL

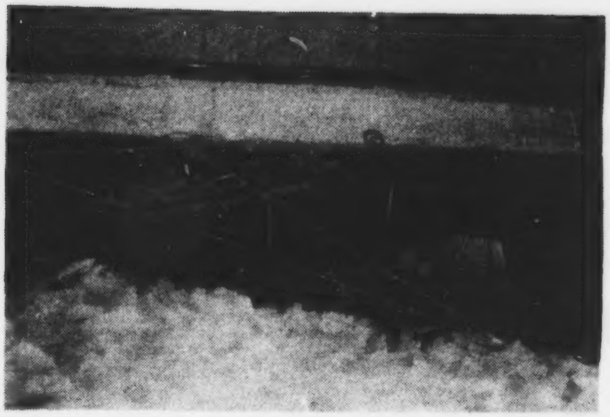

Plate 3.11

Penetration of Ship in Ridge in EGAD-Ice ridge at FTL

Plate 3.12

Penetration of Ship in Ridge in EGAD-Ice ridge at FTL

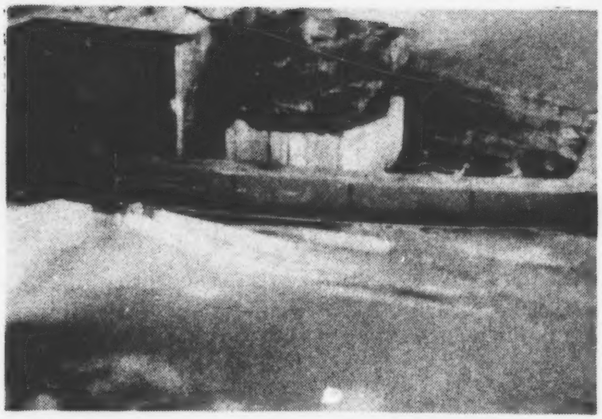

Plate 3.13

View of Basin After Tests in EGAD-Ice at FTL

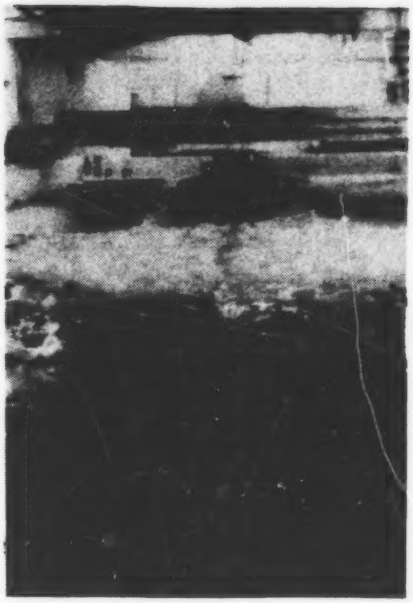

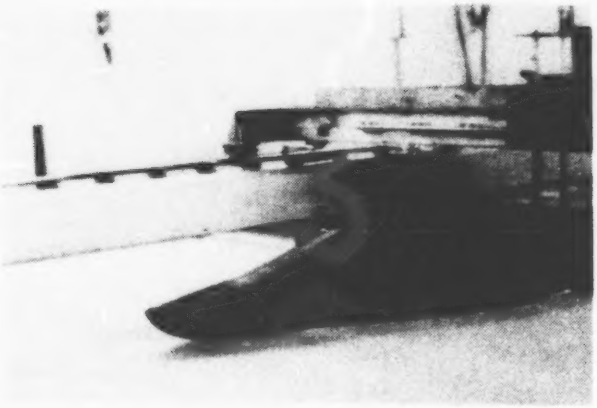

Plate 3.14

Penetration of Ship in Ridge in BEADS-Ice at FTL

Plate 3.15

Icebreaking Behind Ship in Test in BEADS-Ice at FTL

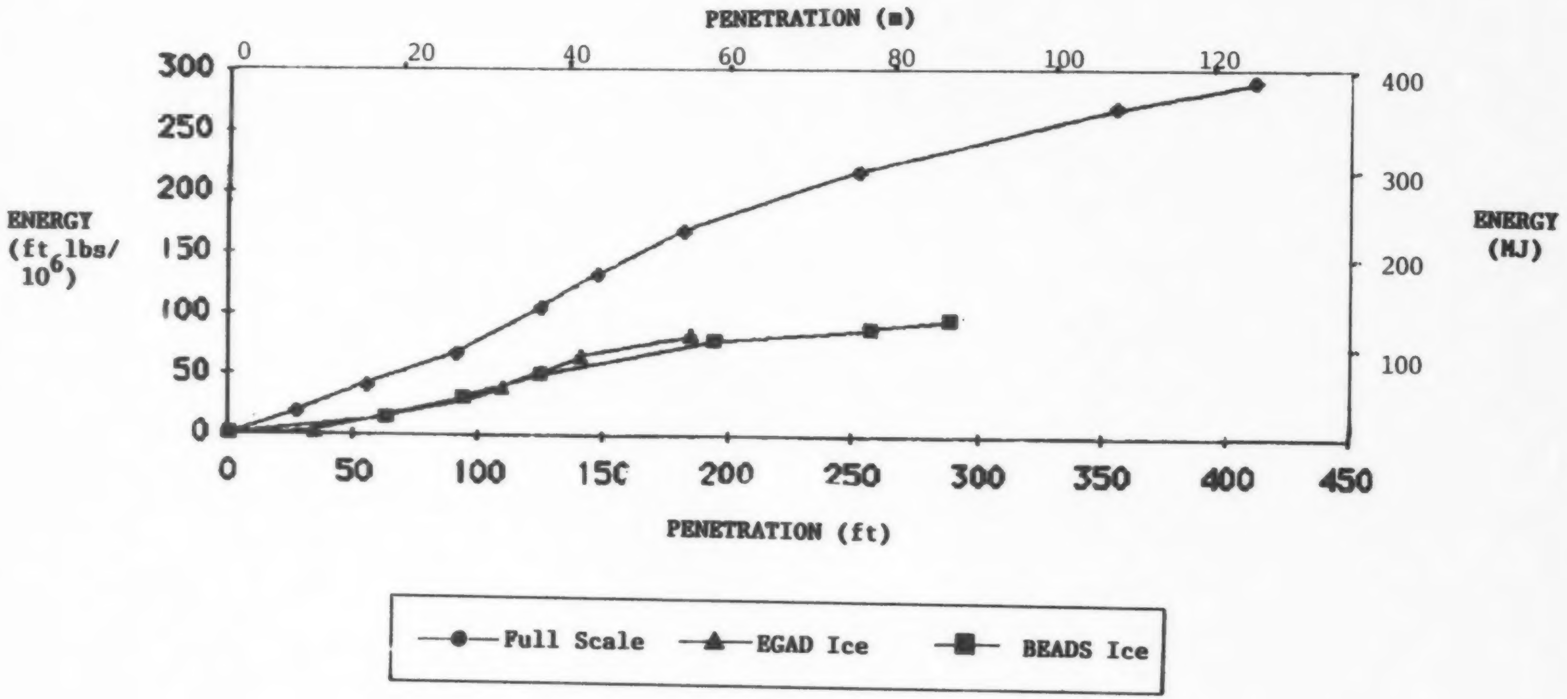

FIGURE 3.6

FULL SCALE COMPARISON OF CUMULATIVE RIDGE PENETRATION ENERGY FROM FIELD TESTS AND MODEL TESTS

3.3.2 Summary

The FTL ice tests were conducted to provide the project team with basic experience in ridge modelling prior to conducting the tests at the IMD. Therefore, they were preliminary in nature.

The FTL ice tests have indicated that:

Ridge Formation Techniques:

a) the general three step approach (i.e. conduct freeze #1; form ridges; and conduct freeze #2) is a practical method of producing a model ice ridge in a model ice sheet.

b) the ridge was well-bonded to the ice sheet for each method and the ridge did not tear out of the ice sheet during the tests.

c) both ridge-building methods produced ridges that were very weak in relation to the target field ridge.

d) both ridge-building methods produced depths of consolidation that were too large in relation to the field data. Method #2 provided better control of the consolidated layer depth than did method #1.

Prediction of Ridge Penetration Energy from Model Tests:

a) The ridge penetration energies predicted by the model tests appear to be significantly lower than the field data. This may result from a number of factors. The consolidated layer of the model scale ridge was very weak and more closely resembled slush than ice.

b) Definitive comparisons between BEADS-ice and EGAD-ice are not possible. The depth of consolidation for the EGAD-ice ridge was more than twice that of the BEADS-ice ridge. Also, the flexural strength of the consolidated layer for the EGAD-ice ridge was approximately twice that of the BEADS-ice ridge. Both of these effects would be expected to produce a higher penetration force, and hence penetration energy, for the EGAD-ice ridge. However, the ridge penetration energy predicted by the model tests with each of these materials were nearly equal. This may reflect the difference in density between these two modelling materials.

   The icebreaking pattern was significantly different for these two materials as may be seen by comparing plates 3.13 and 3.15. The piece sizes were significantly smaller for the BEADS-ice test. See plate 3.9.

4.0 TESTS CONDUCTED AT THE INSTITUTE OF MARINE DYNAMICS

4.1 Test Set-up and Matrix

4.1.1 Test Set-up

Tests were conducted using a 19.1:1 scale model of the USCGC POLAR STAR. Table 4.1 summarizes key ballasting and surfacing preparation parameters for the model. Three model set-ups were used during the project, as summarized below:

Test Date	Ice Sheet Number	Ridge Number	Summary Description
April 29	1	2;3	Model attached to carriage using constant tow force apparatus available at the IMD. This apparatus used a relatively slender towpost of about 25 mm diameter.
April 29	1	1;4	Model towpost clamped to frame of constant tow force apparatus. Slender towpost used.
May 3; May 5	2;3	All ridges	Model attached directly to carriage using relatively large and stiff towpost.

For all model test setups, the model was free in the pitch, roll and heave directions of motion and the model was restrained in the yaw and sway directions of motion.

Initially, it was planned to use a constant tow force apparatus available at the IMD to simulate the reduction in ship velocity that occurs during field ridge ramming events. With this set-up, the model was attached through a relatively slender towpost of about 25 mm diameter to a frame mounted on roller bearings and attached to the main carriage. A constant towforce was applied to the model using a system of deadweights and pulleys and the intermediate frame was free to travel independently of the main carriage. Closed-loop, positional control was provided to the intermediate frame to regulate the speed of the main carriage to ensure that the intermediate frame did not contact the end stops on the bearing rails.

For the tests done using this apparatus, deadweights were added to the towforce mechanism based on a review of the level ice resistance measured for the USCGC POLAR SEA in the Bering Sea and in Antarctica (Glen et al, 1985). Figure 2.7 summarizes the measured and predicted full scale level ice resistances during those trials.

TABLE 4.1

KEY MODEL SETUP PARAMETERS

PARAMETER		TARGET FULL SCALE VALUE	MODEL TEST SET-UP	
			MEAS. M.S. VALUE	EXTRAP. F.S. VALUE
Ballasting:	Draft	9.70 m (31.8 ft)	0.51 m (1.66 ft)	9.7 m
	Pitch Period	No data found (See Note 1)	1.6 sec. (See Note 2)	7 sec.
	Roll Period	11.9 sec. (See Note 4)	2.6 sec.	11.4 sec.
Surface Preparation:	Ice-Hull Friction Factor	Avg. of Sliding Tribometer Tests = 0.045 Avg. of Rotating Arm Tribometer Tests= 0.20 (See Note 3)	Sheets #1&#2: 0.04 Sheet #3: 0.16	0.04 0.16

Notes:

1. Data for the full scale pitch period could not be located (D. Middleton, USCG, personal communication). For these tests, the model was ballasted to maintain the same pitch gyradius (i.e. 0.24 LWL) that was used by Arctec Incorporated who conducted 1:48 scale model tests of this vessel (Coburn et al, 1981).

2. These values were measured by pitching and rolling the model in the water. See test T3R7 for plots of test data.

3. The full scale ice-hull friction factor was measured using both a rotating arm tribometer and a sliding tribometer. The rotating arm tribometer simultaneously crushes and slides the ice past the hull while the sliding tribometer slides the ice past the hull without causing crushing failure. These test methods and results are described in Geisel et al, 1982.

4. This value was obtained from the stability booklet for the USCGC POLAR STAR. The corresponding model scale value is 2.7 sec.

It was hoped that the use of this apparatus would allow the model:

a) to impact the ridge at a steady speed of 1.26 m/s (i.e. 18 ft/sec full scale) which simulates the reference field ramming event. (See section 2).

b) to decelerate as the ship penetrated the ridge, and thus simulate the velocity time history of the ship during the reference field ramming event.

Unfortunately, difficulties were experienced with this apparatus and a steady model speed was not achieved. Consequently, the measured towpost resistance showed large fluctuations, reflecting inertial loads.

It was decided to conduct the remainder of the tests at a constant velocity by fixing the model directly to the main carriage using a towpost.

For the sheet #1 tests, a relatively slender towpost (of about 25 mm diameter) was used as the constant tow force apparatus had been built to accept this size of towpost. Vibrations occurred during the sheet #1 tests and the measured towpost resistance fluctuated at a frequency of about 1 Hz.

For the remaining ice sheets (i.e. sheets #2 and #3), a much larger and stiffer towpost was used.

An effort was made to measure the in-situ natural frequency of the system comprised of the model and the large towpost, the carriage structure and the transport wheels. A single impulsive load was applied to the model. Figure 4.1 shows the time history of the horizontal force at the model-towpost attachment point. A natural frequency of 5 Hz for the system is indicated by this test.

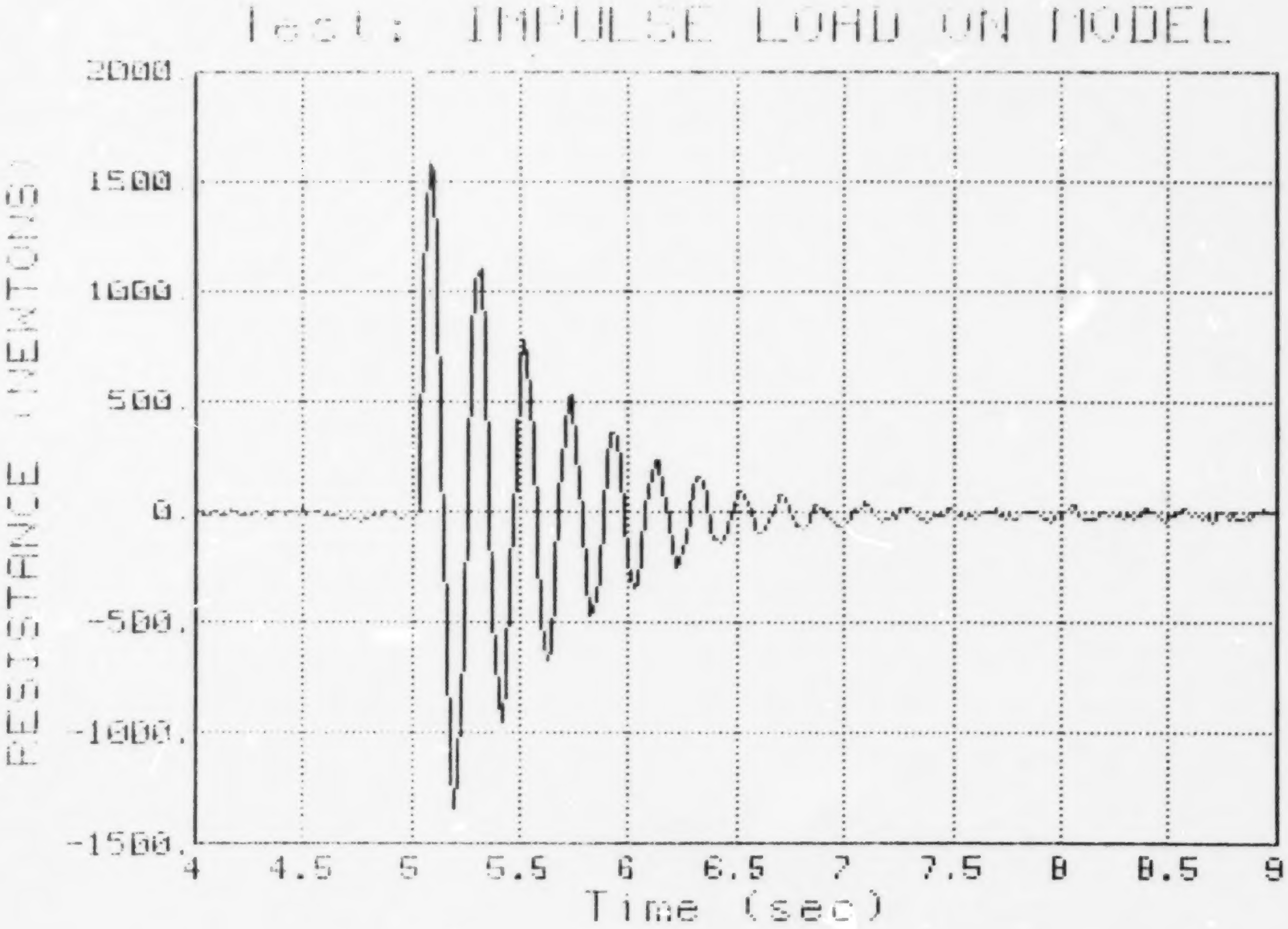

FIGURE 4.1

FORCE AT MODEL ATTACHMENT TO TOWPOST RESULTING FROM IMPULSIVE LOAD ON MODEL

4.1.2 Ridge Formation Techniques

The reference field event involved the ramming of a first year ridge that was embedded in a first year ice sheet (see Section 2). Therefore, efforts were focussed on reproducing this environmental condition in the basin.

Two ridge formation techniques were used during the project. In general, a three-step process was used, as follows:

a) grow a level ice sheet,

b) form ridges using the ice in the first level ice sheet

c) perform a second freeze to grow level ice around the ridges and to partially consolidate the ridges.

Figure 4.2 schematically describes the approach used to produce ridges for the sheet #1 tests. Plates 4.1 to 4.4 also describe this process.

In general, this approach was effective. However, a number of difficulties were encountered and the ridge formation technique was altered for the sheet #2 and #3 tests.

The difficulties that were encountered with the approach used for sheet #1 included:

a) The process presented safety hazards. It was necessary for staff to spend a significant portion of time at locations where a fall into the basin was likely. This was brought about by the necessity to conduct several operations in the basin (eg. deployment and retrieval of ridge restraint strips, positioning of floating boom). This condition worsened at the end of the ridge-building process as surfaces became progressively icy.

b) It was difficult to accurately control the volume of ice that was put into each ridge. The floating boom had to be repositioned at the start of each ridge-building sequence. This had to be done by moving the boom in the water as the floating boom could not be lifted and moved by the work carriage. This repositioning process redistributed the broken ice pieces with the result the volume of ice put into the ridge was not well-known.

   It is believed that this problem could have been resolved with a purpose-built boom structure. (The floating boom that was used was already on hand at the start of the test program).

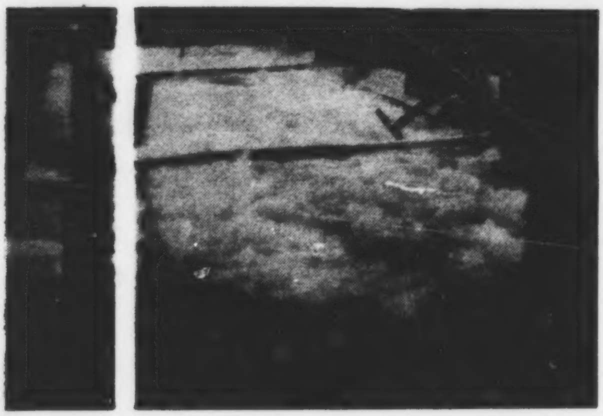

Plate 4.1

Ice Pieces Tamped to Provide Even Distribution for Method #1

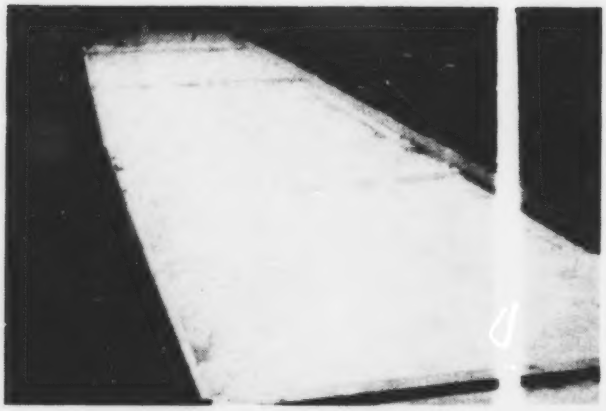

Plate 4.2

Ice Ridge Between Ridge Restraint Strips Prior to Freeze #2 for Method #1

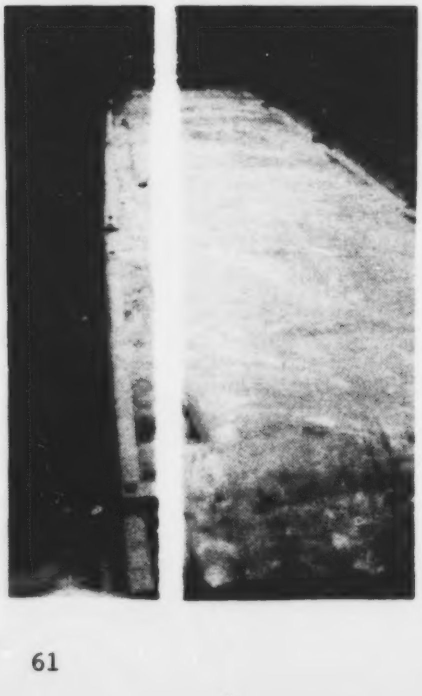

Plate 4.3

Insulation Mats On Ice Ridge. Ridge Restraint Strips Removed Prior to Start of Freeze #2 for Method #1

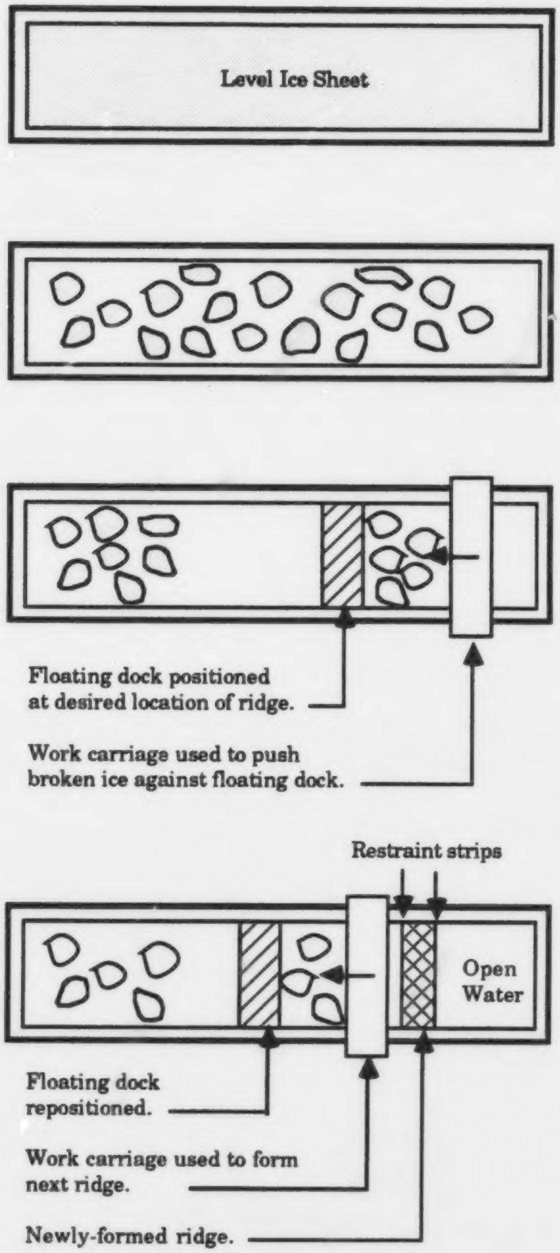

1. Grow A Level Ice Sheet

2. Form Ridges

(a) Break up ice sheet into pieces with a maximum linear dimension of approximately 5 times the ice thickness.

(b) Form each ridge using the required amount of broken ice.

Floating dock positioned at desired location of ridge.

Work carriage used to push broken ice against floating dock.

(c) Install wooden restraining strips for ridge and proceed to next ridge location.

Floating dock repositioned.

Work carriage used to form next ridge.

Newly-formed ridge.

Figure 4.2
Schematic Description of Approach Used To Form The Ridges For Sheet No. 1 Tests

(d) Shape ridges underwater using cross-sectional profile jig. (Note: This was only done for one ridge)

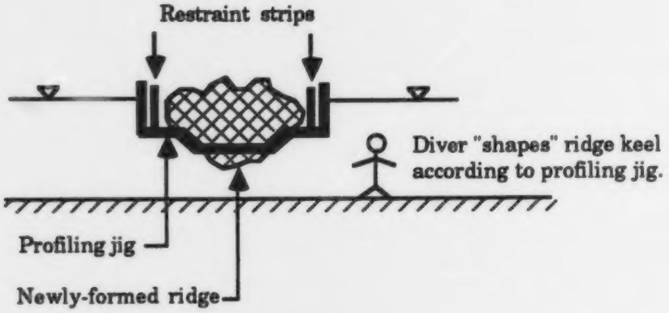
Restraint strips
Diver "shapes" ridge keel according to profiling jig.
Profiling jig
Newly-formed ridge

(e) Remove ridge restraint strips. Cover selected ridges with insulation mats.

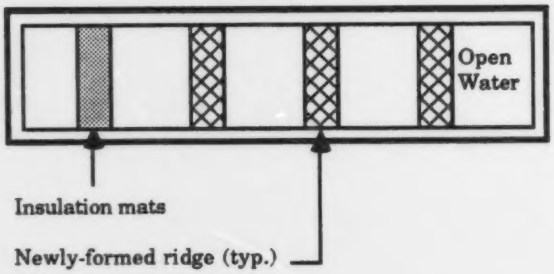
Open Water
Insulation mats
Newly-formed ridge (typ.)

3. Seed Basin and Grow Second Ice Sheet. Commence Warm-up as Appropriate. Remove Insulation Mats Prior to Testing.

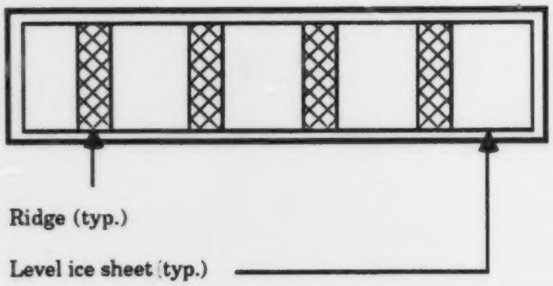
Ridge (typ.)
Level ice sheet (typ.)

Figure 4.2 (cont.)

Schematic Description of Approach Used To Form The Ridges For Sheet No. 1 Tests

c) The ridge-building process took about eight hours to complete and the open water areas were self-seeded by the moisture in the room. Efforts were made to skim the newly-formed ice prior to commencing the second freeze. This proved to be very difficult and time-consuming. The ice could not be easily cleared (as the ridges obstructed the basin). As well, numerous cases occurred where the cleared ice dropped into the basin in patches which made it impossible to produce a uniform level ice sheet around the ridge.

d) The consolidated layer was very hard for some ridges. This is believed to have resulted from the fact that the ice blocks in this layer were bonded together by unseeded ice (as the layer began to consolidate almost immediately after the ice pieces had been piled together). This problem was most pronounced for the last ridge that was built (i.e. ridge 1-4).

e) A diver was deployed in the water to ensure that the shape of the ridge keel matched the field reference ridge. This operation was very time-consuming and was not judged to be required as the profile of newly-formed ridge generally matched the target shape. Therefore, this operation was discontinued after the first ridge.

After the sheet #1 tests, debriefing sessions were held with IMD staff and a revised method for building ridges was developed. Figure 4.3 schematically describes the method that was used to build the ridges in sheets #2 and #3. Plates 4.5 to 4.9 also describe the process.

This approach generally worked well and resolved many of the difficulties associated with the approach used for the sheet #1 ridges. This approach offered many advantages, including:

a) improved safety,

b) improved control of the thickness of the consolidated layer,

c) improved efficiency. The total time required for the ridge-building operation was reduced to 3-4 hours.

d) improved control of the volume of ice placed in each ridge.

e) better uniformity of the level ice sheet around the ridges.

1. Grow A Level Ice Sheet

2. Form Ridges

(a) Cut ice sheet and break into pieces with a maximum linear dimension of approximately 5 times the ice thickness.

(b) Transport broken ice pieces from elsewhere in the ice sheet to the ridge location using the work carriage.

(c) Level ice sheet pushed over top of rubble to assist the formation of the consolidated layer. In most cases only one level ice sheet was pushed over the newly-formed rubble. However, in some cases two ice sheets were pushed over the rubble.

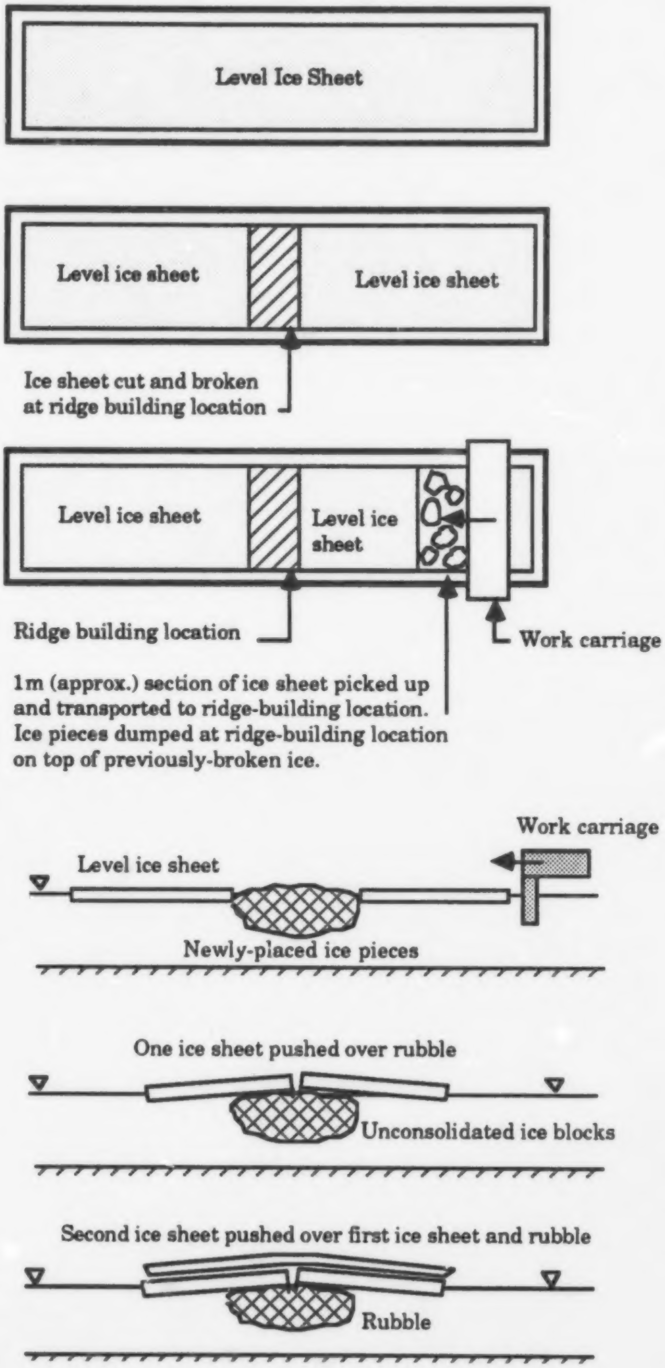
Level Ice Sheet
Level ice sheet
Level ice sheet
Ice sheet cut and broken at ridge building location
Level ice sheet
Level ice sheet
Ridge building location
Work carriage
1m (approx.) section of ice sheet picked up and transported to ridge-building location. Ice pieces dumped at ridge-building location on top of previously-broken ice.
Work carriage
Level ice sheet
Newly-placed ice pieces
One ice sheet pushed over rubble
Unconsolidated ice blocks
Second ice sheet pushed over first ice sheet and rubble
Rubble

Figure 4.3

Schematic Description of Approach Used To Form The Ridges For The Sheet No. 2 and No. 3 Tests

(a) Move ridge to desired ridge location in the basin and repeat steps 2(a) to 2(c).

(e) Cover ridges with insulation mats as desired.

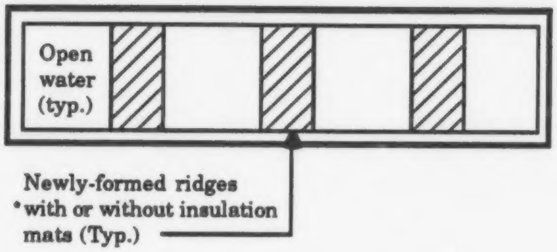
Open
water
(typ.)
Newly-formed ridges
*with or without insulation
mats (Typ.)

3. Commence Growth of Second Ice Sheet Without Seeding.
Commence Warm-up As Appropriate.
Remove Insulation Mats Prior To Testing.

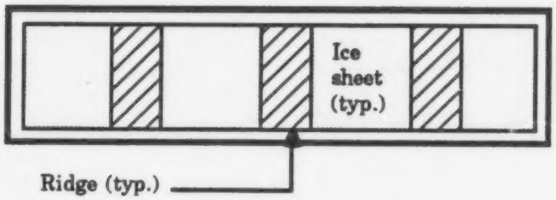
Ice
sheet
(typ.)
Ridge (typ.)

Figure 4.3 (cont.)
Schematic Description of Approach Used To Form The Ridges For The Sheet No. 2 and No. 3 Tests

Plate 4.4

Ridges in Level Ice Sheet Prior to Testing for Method #1

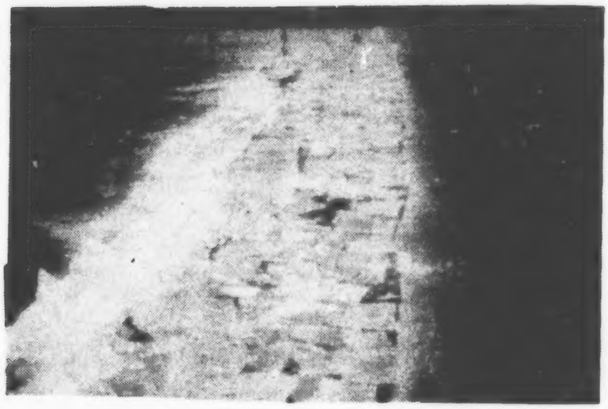

Plate 4.5

Ice Cover Cut and Broken at Ridgebuilding Location for Ridgebuilding Method #2

Plate 4.6

Ice Pieces Physically Transported and Dumped at Ridge Site During Ridgebuilding Method #2

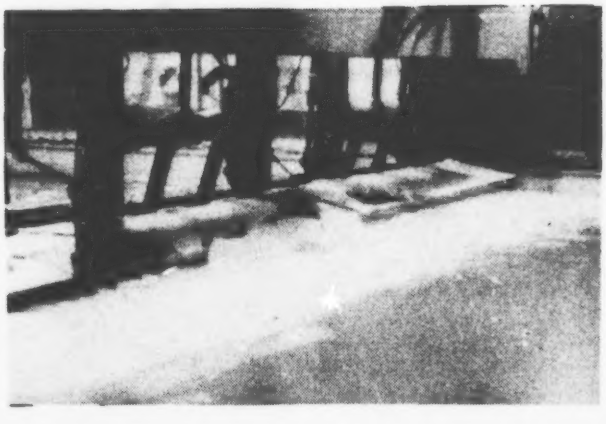

Plate 4.7

Ice Sheet Pushed Over Rubble During Ridgebuilding Method #2

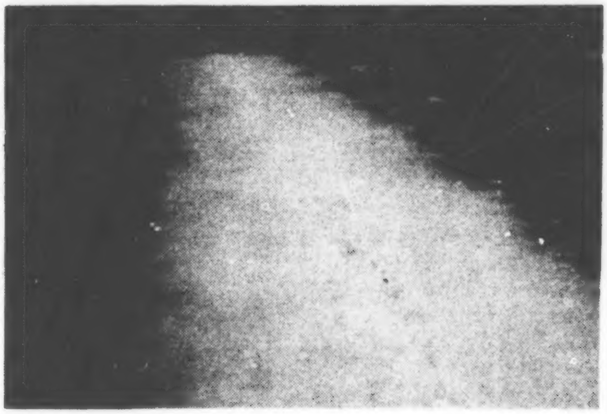

Plate 4.8

Ice Sheet Pushed Over Rubble During Ridge-building Method #2

Plate 4.9

Ridges in Level Ice Sheet Prior to Testing for Ridge-Building Method #2

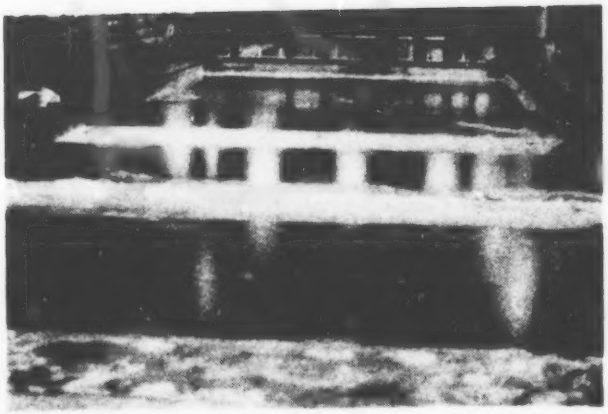

4.1.3 Test Matrix

A basic test program was conducted with the overall objective of improving the present state-of-the-art in ridge modelling. As discussed in Section 2, a field ramming event was chosen as a reference case for comparison with the model scale results.

The following parameters were parametrically varied:

a) ice-hull friction - The ice-model friction factor was 0.04 for sheets #1 and #2. For the sheet #3 tests, the model surface was roughened to a friction factor of 0.16.

b) ridge size - For most tests, the ridge cross-sectional area and width were selected to scale ridge #18 (as this was the selected field reference event). One test was conducted with a ridge that was approximately twice this size.

c) ship velocity - It was initially intended to conduct both constant speed tests and tests in which the ship was allowed to decelerate as it penetrated the ridge. However, problems were encountered with the constant tow force mechanism (that was intended to be used for reducing velocity tests). Consequently, only constant speed tests were carried out. To obtain some understanding of the significance of ship velocity, constant speed tests were carried out at speeds of 1.0 m/s and 0.65 m/s. These values scale the mid-range and the minimum ship velocity during the field reference event, respectively.

d) ridge structure - The field reference ridge consisted of a consolidated layer with an unconsolidated portion beneath. Most tests simulated this ridge structure. Some tests were conducted with ridges consisting of unconsolidated and consolidated material only to assess the relative contribution of each portion to the penetration energy and resistance of the ridge.

e) thickness of consolidated layer - The thickness of the consolidated layer was controlled by the number of ice sheets pushed over the rubble and by the amount of insulation, and its time of removal, put on the ridge surface.

f) strength of consolidated layer - A basic test was conducted in which the consolidated layer was pre-cut into pieces with a maximum linear dimension of about five times the ice thickness. This was done to simulate a layer of zero strength.

g) ridge formation technique - As discussed in 4.1.2, a variety of ridge formation techniques were used. Key parameters that were varied included the number of ice sheets pushed over the rubble, the amount of surface insulation on the ridge, and the time at which the surface insulation was removed.

In addition, a number of tests were duplicated to provide information on the repeatability of the test results.

Figures 4.4 to 4.6 show the basin layout that was used for sheets #1, 2 and 3 respectively.

Table 4.2 summarizes the tests that were conducted. Table 4.3 shows the principal parameters that were varied during each test. The "base cases" that have been assumed for Table 4.3 are described in Table 4.4.

A number of open water tests were also carried out as summarized in Table 4.5 below:

TABLE 4.5

SUMMARY OF TESTS CONDUCTED IN OPEN WATER

TEST DATE	TEST #	TYPE OF TEST	MODEL SCALE SHIP SPEED SHIP SPEED (m/s)
MAY 5	T3R4	Open Water Resistance	1.0
MAY 5	T3R5	Open Water Resistance	1.0
MAY 5	T3R6	Open Water Resistance	0.65
MAY 5	T3R7	Measurement of Pitch and Roll Period	n/a

Note: Refer to Appendix E for plots of test data by test number.

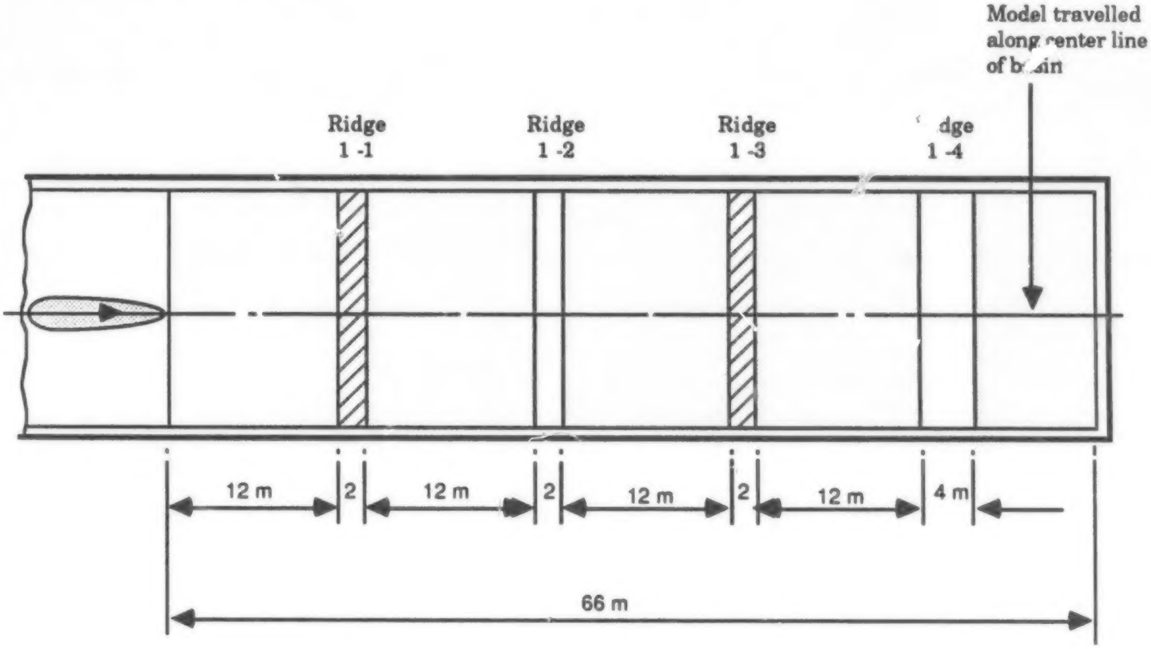
Model travelled along center line of basin
Ridge 1 -1
Ridge 1 -2
Ridge 1 -3
Ridge 1 -4
12 m
2
12 m
2
12 m
2
12 m
4 m
66 m

Legend:

▨ Ridge surface insulated with R8

☐ Ridge surface not insulated

Note: All distances are approximate.

Figure 4.4
Basin Layout For Sheet No. 1 Tests

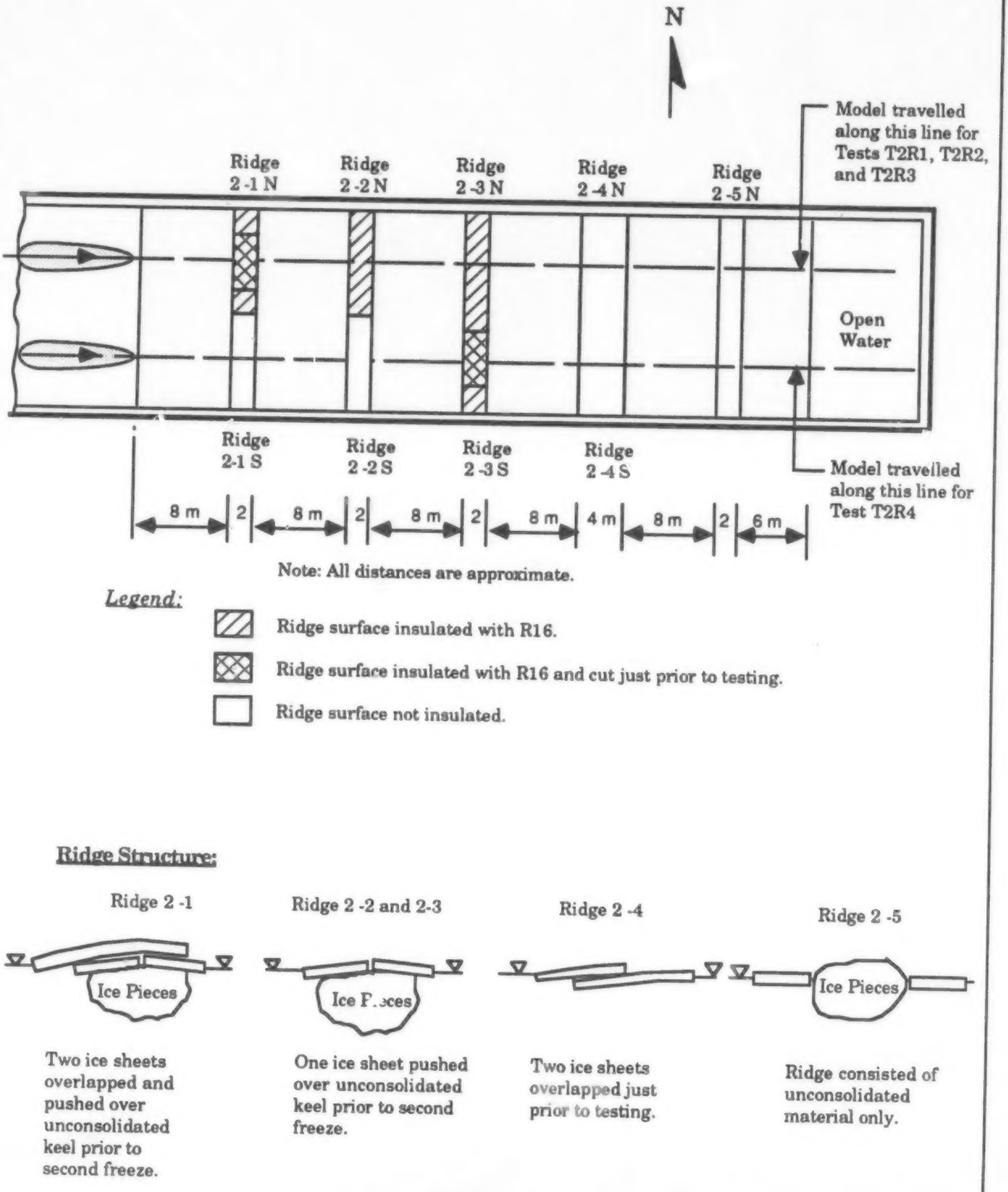
N
Model travelled along this line for Tests T2R1, T2R2, and T2R3
Ridge 2-1 N
Ridge 2-2 N
Ridge 2-3 N
Ridge 2-4 N
Ridge 2-5 N
Open Water
Ridge 2-1 S
Ridge 2-2 S
Ridge 2-3 S
Ridge 2-4 S
Model travelled along this line for Test T2R4
8 m
2
8 m
2
8 m
2
8 m
4 m
8 m
2
6 m
Ridge Structure:
Ridge 2-1
Ice Pieces
Ridge 2-2 and 2-3
Ice Pieces
Ridge 2-4
Ridge 2-5
Ice Pieces

Note: All distances are approximate.

Legend:

- ▨ Ridge surface insulated with R16.
- ▩ Ridge surface insulated with R16 and cut just prior to testing.
- ☐ Ridge surface not insulated.

Ridge 2-1: Two ice sheets overlapped and pushed over unconsolidated keel prior to second freeze.

Ridge 2-2 and 2-3: One ice sheet pushed over unconsolidated keel prior to second freeze.

Ridge 2-4: Two ice sheets overlapped just prior to testing.

Ridge 2-5: Ridge consisted of unconsolidated material only.

Figure 4.5

Basin Layout For Sheet No. 2 Tests

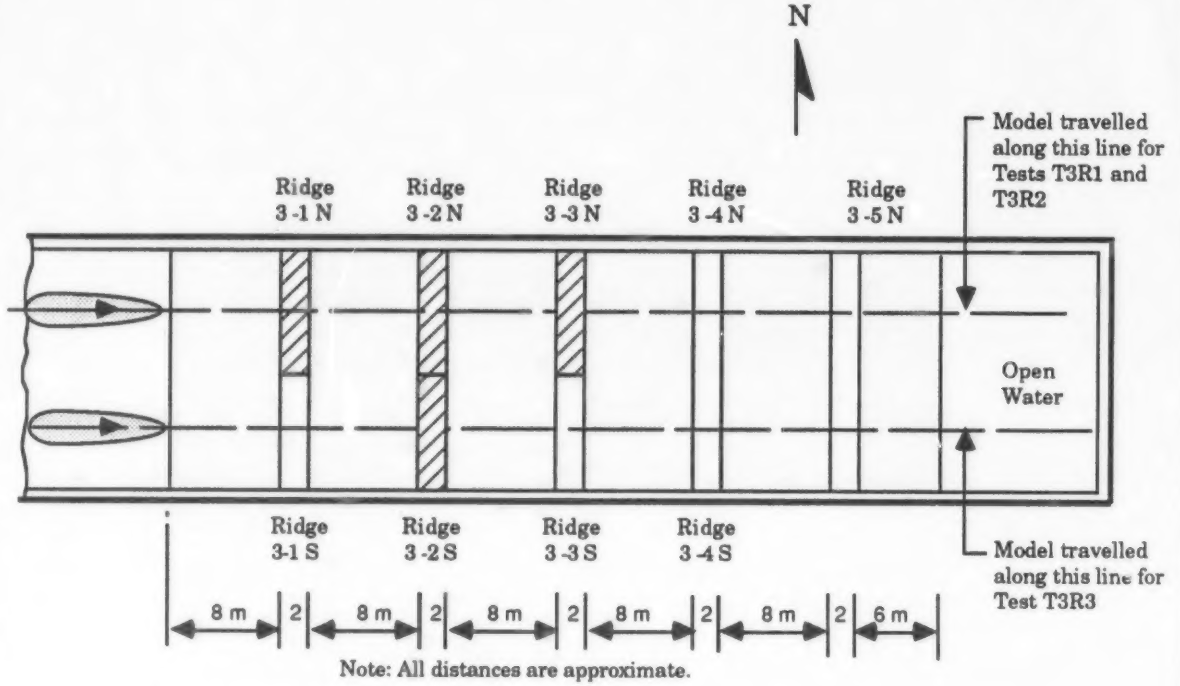
N
Model travelled along this line for Tests T3R1 and T3R2
Ridge 3-1 N
Ridge 3-2 N
Ridge 3-3 N
Ridge 3-4 N
Ridge 3-5 N
Open Water
Ridge 3-1 S
Ridge 3-2 S
Ridge 3-3 S
Ridge 3-4 S
Model travelled along this line for Test T3R3
8 m
2
8 m
2
8 m
2
8 m
2
8 m
2
6 m
Note: All distances are approximate.

Legend:

▨ Ridge surface insulated with R8.

☐ Ridge surface not insulated.

Ridge Structure:

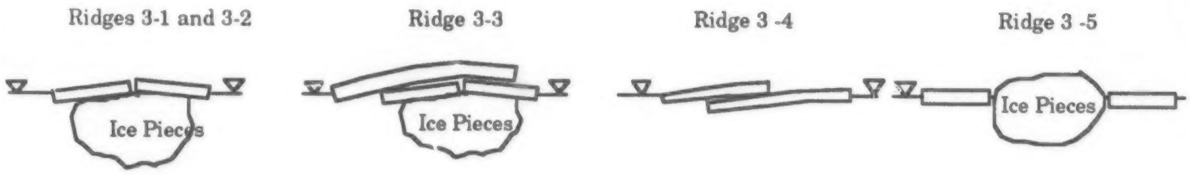
Ridges 3-1 and 3-2
Ridge 3-3
Ridge 3-4
Ridge 3-5
Ice Pieces
Ice Pieces
Ice Pieces

Ridges 3-1 and 3-2: One ice sheet pushed over unconsolidated keel prior to second freeze.

Ridge 3-3: Two ice sheets overlapped and pushed over unconsolidated keel prior to second freeze.

Ridge 3-4: Two ice sheets overlapped prior to start of second freeze.

Ridge 3-5: Ridge consisted of unconsolidated material only.

Figure 4.6

Basin Layout For Sheet No. 3 Tests

Table 4.2
Test Matrix

Sheet No.	Test No.	Ridge No.	Ice-Model Friction Factor	Model Scale Ship Speed (m/s)	Formation Technique for Ridge Consolidated Layer	Ridge Insulation	Tempering Time (hrs) Before Ins. was Removed	Comments
1	1	1	0.04	1.0	Rubble allowed to consolidate during second freeze	R8	5.0	
1	2	2	0.04	Var.	Rubble allowed to consolidate during second freeze	None	n/a	IMD constant tow force apparatus used
1	3	3	0.04	Var.	Rubble allowed to consolidate during second freeze	R8	5.0	IMD constant tow force apparatus used
1	4	4	0.04	1.0	Rubble allowed to consolidate during second freeze	None	n/a	
2	T2R1	2-1N	0.04	1.0	Two ice sheets overlapped & placed over rubble	R16	0	Ridge partially cut
2	T2R2	2-2N	0.04	0.65	One ice sheet placed over rubble	R16	0	
2	T2R3	2-3N	0.04	1.0	One ice sheet placed over rubble	R16	0	
2	T2R3	2-4N	0.04	1.0	Two ice sheets overlapped - no rubble beneath	None	n/a	Ridge formed just prior to testing
2	T2R3	2-5N	0.04	1.0	Ridge comprised of unconsolidated material only	None	n/a	Ridge formed just prior to testing
2	T2R4	2-1S	0.04	1.0	Two ice sheets overlapped and placed over rubble	None	n/a	
2	T2R4	2-2S	0.04	1.0	One ice sheet placed over rubble	None	n/a	
2	T2R4	2-3S	0.04	1.0	One ice sheet placed over rubble	R16	0	Ridge consolidated layer cut prior to testing
2	T2R4	2-4S	0.04	1.0	Two ice sheets overlapped - no rubble beneath	None	n/a	Ridge formed just prior to testing
3	T3R1	3-1N	0.16	1.0	One ice sheet placed over rubble	R8	4.5	
3	T3R2	3-2N	0.16	0.65	One ice sheet placed over rubble	R8	4.5	
3	T3R2	3-3N	0.16	1.0	Two ice sheets overlapped and placed over rubble	R8	4.5	
3	T3R2	3-4N	0.16	1.0	Two ice sheets overlapped - no rubble beneath	None	n/a	Ridge formed before second freeze
3	T3R2	3-5N	0.16	1.0	Ridge comprised of unconsolidated material only	None	n/a	Ridge formed just prior to testing
3	T3R3	3-1S	0.16	1.0	One ice sheet placed over rubble	None	n/a	
3	T3R3	3-2S	0.16	1.0	One ice sheet placed over rubble	R8	4.5	
3	T3R3	3-3S	0.16	1.0	Two ice sheets overlapped and placed over rubble	None	n/a	
3	T3R3	3-4S	0.16	1.0	Two ice sheets overlapped - no rubble beneath	None	n/a	Ridge formed before second freeze

Notes:

1. Plots of test data for sheets 1, 2, and 3 are provided in Appendices C, D, and E respectively. Refer to plots of test data by above test numbers.
2. See Figures 4.4, 4.5, and 4.6 for basin layouts for sheets 1, 2, and 3 respectively and for locations of the above ridges.

Table 4.3
Parameters Varied During Each Test

Sheet No.	Test No.	Ridge No.	Variation From Base Case
1	1	1-1	**Base Case**
1	2	1-2	See Note 1 - Ship velocity: reduced during test; ridge insulation: reduced to nil
1	3	1-3	See Note 1 - Ship velocity: reduced during test
1	4	1-4	Ride cross-sectional area: doubled
2	T2R1	2-1N	Consolidated layer thickness: increased; ridge consolidated layer strength: partially cut
2	T2R2	2-2N	Ship velocity: held constant at reduced value of 0.65 m/s
2	T2R3	2-3N	**Base Case**
2	T2R3	2-4N	Ridge structure: ridge only comprised of a consolidated layer
2	T2R3	2-5N	Ridge structure: ridge only comprised of unconsolidated material
2	T2R4	2-1S	Consolidated layer thickness: increased; ridge surface insulation: reduced to nil
2	T2R4	2-2S	Ridge surface insulation: reduced to nil
2	T2R4	2-3S	Ridge consolidated layer strength: reduced to zero by fully cutting the ridge
2	T2R4	2-4S	Ridge structure: ridge only comprised of a consolidated layer
NOTE: ICE-HULL FRICTION INCREASED TO 0.16 **FOR SHEET #3 FROM 0.04 FOR SHEET #2**			
3	T3R1	3-1N	**Base Case**
3	T3R2	3-2N	Ship velocity: held constant at reduced value of 0.65 m/s
3	T3R2	3-3N	Consolidated layer thickness: increased
3	T3R2	3-4N	Ridge structure: ridge only comprised of a consolidated layer
3	T3R2	3-5N	Ridge structure: ridge only comprised of an unconsolidated layer
3	T3R3	3-1S	Ridge surface insulation: reduced to nil
3	T3R3	3-2S	Repetition of base case
3	T3R3	3-3S	Ridge surface insulation: reduced to nil
3	T3R3	3-4S	Ridge structure: ridge only comprised of a consolidated layer

Notes:

1. For ridges 1-2 and 1-3, the model was attached to the carriage using a constant tow force mechanism. Problems were encountered with this apparatus and these test results are not considered useable.

2. See Table 4.4 for a description of the above base cases.

TABLE 4.4

BASE CASES USED TO DEVELOP TABLE 4.3

	SHEET #1	SHEET #2	SHEET #3
Ice-model friction factor	0.04	0.04	0.16
Ship speed	Constant at 1 m/s	Constant at 1 m/s	Constant at 1 m/s
Ridge characteristics:	Ridge area, width, and consolidated layer thickness were intended to scale ridge #18 (i.e. the field reference ridge).		
Consolidated Layer	Formed by allowing the rubble to freeze	Formed by pushing one ice sheet over the rubble and then conducting a second freeze.	
Ridge Surface Insulation	R8	R16	R8
Time of Removal of Surface Insulation	5 hours after commencement of warmup	Start of warmup period	4.5 hrs after commencement of warmup period

4.1.4 Test Documentation

For each test, the following ship performance parameters were documented:

a) force in the horizontal direction at the attachment between the model and the towpost.

b) ship and carriage speed

c) transverse load on the model at the yaw restraint,

d) the pitch, roll, and heave motions of the model.

Figure 4.7 summarizes the parameters that were measured and the instrumentation system that was used.

For the Sheet #1 tests, a gyro-stabilized platform was used to measure the pitch, roll, and heave motions of the model. For the sheet #2 tests, these motions were measured using Linear Variable Differential Transformers (LVDT's) fixed at three locations on the model.

Figure 4.8 shows the locations on the model where forces and motions were measured.

The model was photographed using four video cameras for each test. Two cameras provided underwater views while the others provided above water views. In addition, several still photographs were taken during each test using a 35 mm camera.

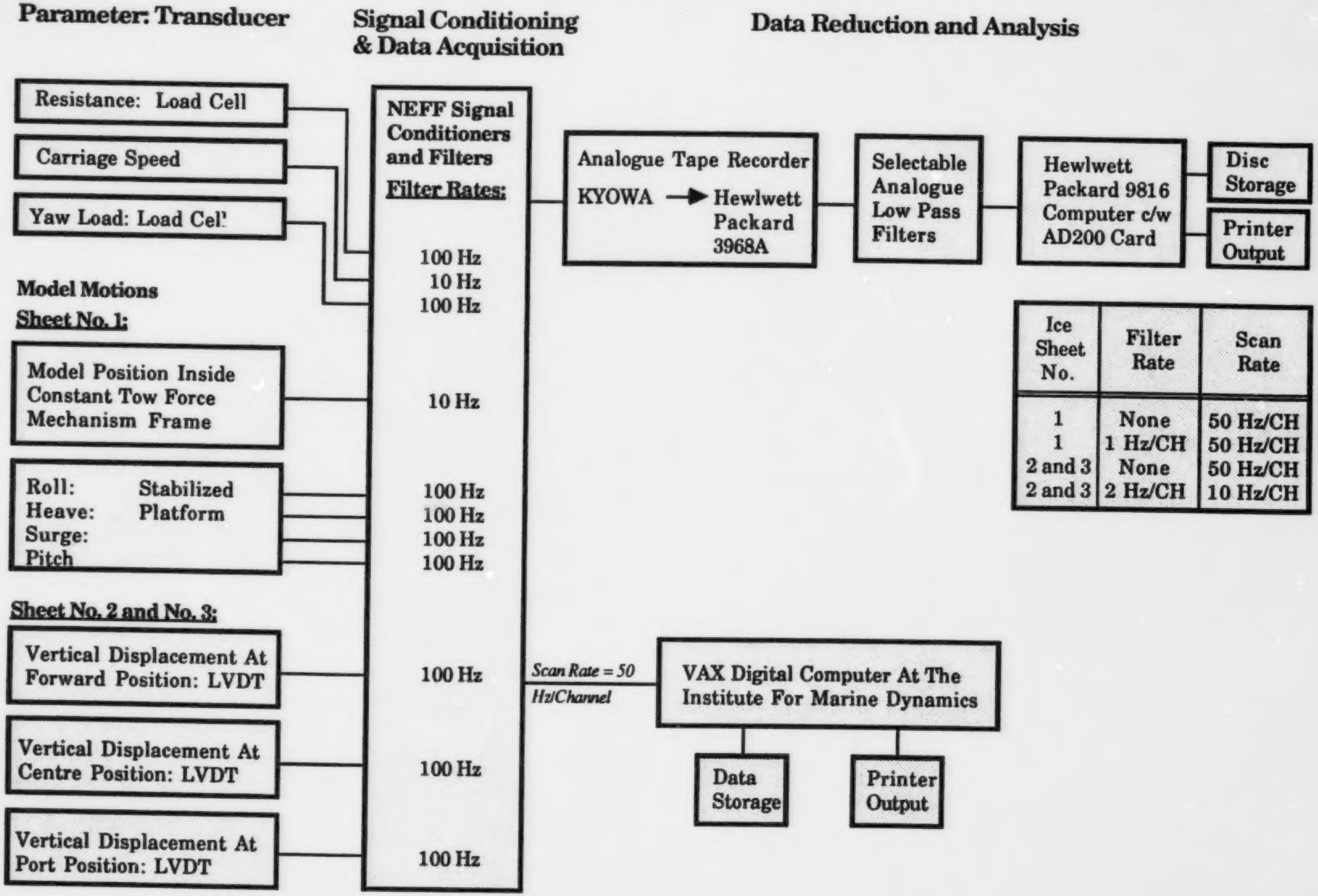
Parameter: Transducer
Signal Conditioning & Data Acquisition
Data Reduction and Analysis
Resistance: Load Cell
Carriage Speed
Yaw Load: Load Cel!
Model Motions
Sheet No. 1:
Model Position Inside Constant Tow Force Mechanism Frame
Roll: Heave: Surge: Pitch
Stabilized Platform
Sheet No. 2 and No. 3:
Vertical Displacement At Forward Position: LVDT
Vertical Displacement At Centre Position: LVDT
Vertical Displacement At Port Position: LVDT
NEFF Signal Conditioners and Filters
Filter Rates:
100 Hz
10 Hz
100 Hz
10 Hz
100 Hz
100 Hz
100 Hz
100 Hz
100 Hz
100 Hz
100 Hz
Analogue Tape Recorder
KYOWA → Hewlwett Packard 3968A
Selectable Analogue Low Pass Filters
Hewlwett Packard 9816 Computer c/w AD200 Card
Disc Storage
Printer Output
Ice Sheet No.
Filter Rate
Scan Rate
1 None 50 Hz/CH
1 1 Hz/CH 50 Hz/CH
2 and 3 None 50 Hz/CH
2 and 3 2 Hz/CH 10 Hz/CH
Scan Rate = 50 Hz/Channel
VAX Digital Computer At The Institute For Marine Dynamics
Data Storage
Printer Output

Figure 4.7 Instrumentation System Schematic

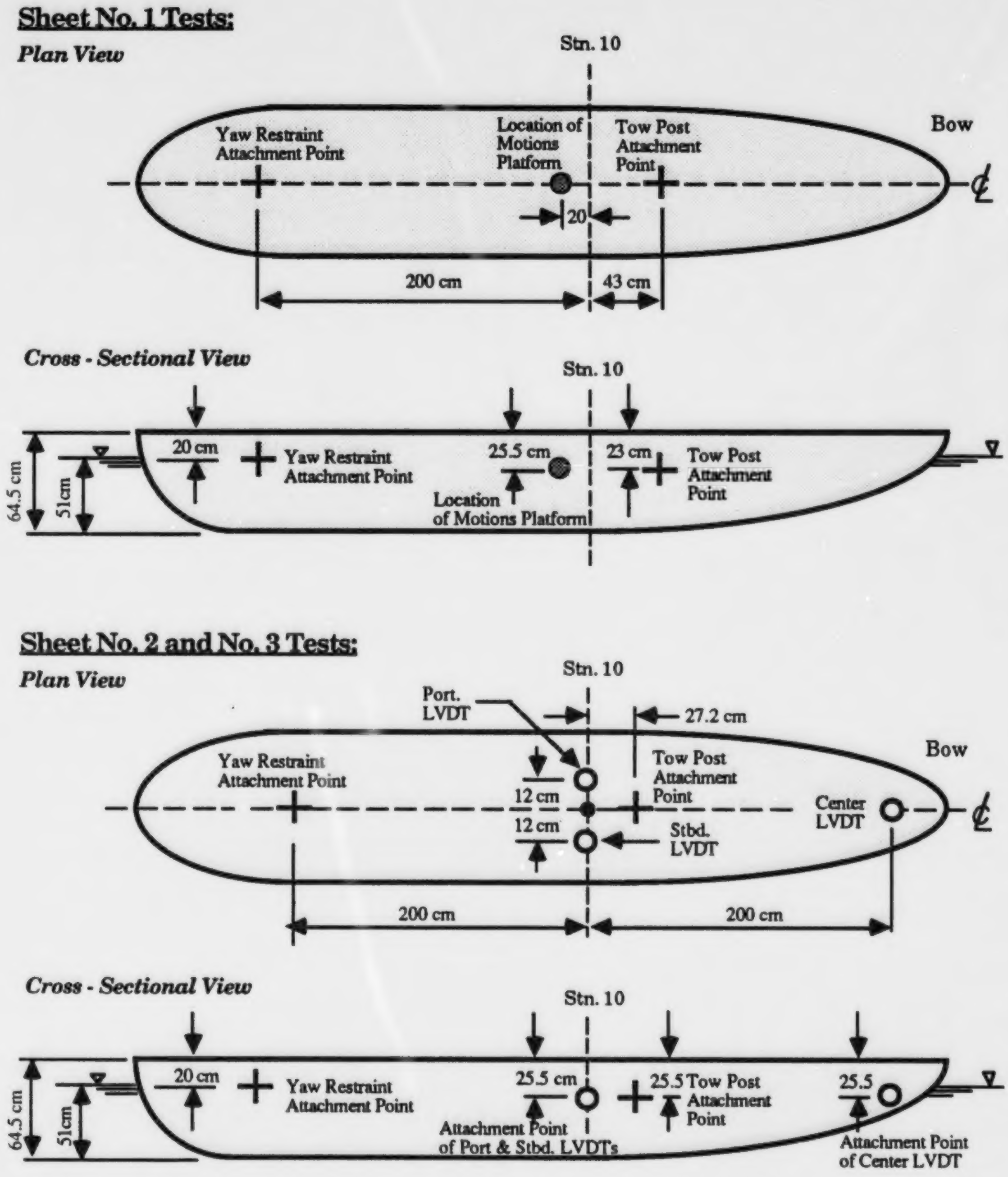
Sheet No. 1 Tests:
Plan View
Stn. 10
Yaw Restraint Attachment Point
Location of Motions Platform
Tow Post Attachment Point
Bow
20
200 cm
43 cm
Cross - Sectional View
Stn. 10
20 cm
Yaw Restraint Attachment Point
25.5 cm
Location of Motions Platform
23 cm
Tow Post Attachment Point
64.5 cm
51cm
Sheet No. 2 and No. 3 Tests:
Plan View
Stn. 10
Port. LVDT
27.2 cm
Yaw Restraint Attachment Point
Tow Post Attachment Point
Bow
12 cm
12 cm
Stbd. LVDT
Center LVDT
200 cm
200 cm
Cross - Sectional View
Stn. 10
20 cm
Yaw Restraint Attachment Point
25.5 cm
Attachment Point of Port & Stbd. LVDTs
25.5
Tow Post Attachment Point
25.5
Attachment Point of Center LVDT
64.5 cm
51cm

Note: Heave calculated at tow post attachment point

Not to scale

Sign Conventions: +ve Roll: Stbd down
+ve Pitch: Bow up
+ve Heave: Upwards

Figure 4.8

Schematic of Locations On the Model Where Forces and Motions Were Measured

4.2 Ice and Ridge Properties

4.2.1 Measurement Techniques

The following properties of the level ice and ridges were measured:

PROPERTY		MEASUREMENT TECHNIQUE
Level ice:	thickness	vernier caliper
	flexural strength	in-situ cantilever beams
	elastic modulus	measurements of deflections due to point loads
	ice density	measurements of weight and volume of small ice blocks removed from the sheet
	ice-model friction factor	measurements of the force required to pull an ice sample loaded with known weights over a surface that was prepared in a similar manner to that of the model
Ridges:	cross-sectional profile	rods with fiduciary markings and L-shaped profiling rod
	thickness of consolidated layer	vernier caliper
	flexural strength of consolidated layer	in-situ cantilever beams cut in consolidated layer
	compressive and shear strength of consolidated layer	Small ice blocks were removed from the ridge and were loaded in compression, or double shear, using a hand-operated lever apparatus at the IMD. (Note: These tests were only done once during the warmup period for comparison with the flexural strength data that were collected).
	bulk density of ridge	Measurements of the force required to submerge a known volume or weight of ice. Estimated from measurements of volume of ice used to build the ridge.
	temperature	Thermocouples embedded in ridge.

The properties of the level ice were measured using standard techniques and equipment at the IMD. The ice thickness was measured using a vernier caliper while the ice flexural strength was measured by conducting in-situ cantilever beam tests. The elastic modulus of the ice sheet was determined by measuring the deflection of the sheet for known applied loads.

The ice density was measured by: a) removing small ice blocks from the ice sheet and; b) measuring their weight with a balance beam and their volume with a linear scale.

For the ridges in sheets #2 and #3, the cross-sectional profile was measured by inserting rods with fiduciary markings through the ridge at known spacings. These fiduciary rods were visible on the video record obtained by the underwater cameras and were scaled to determine the cross-sectional profile of the ridge.

The cross-sectional profile of the ridges in sheet #1 were measured using a profiling apparatus available at the IMD. This consisted of an L-shaped rod with fiduciary markings. Measurements were made by inserting the rod under the ridge at known horizontal distances and pulling it up until it contacted the bottom of the ridge.

For the measurement of flexural strength, cantilever beams were cut in the consolidated layer. These beams were cut according to the same conventions used for level ice and the length and width of the beams were approximately five and two times the thickness, respectively. Care was taken to remove most of the unconsolidated material beneath the beam before conducting the tests. This was difficult as the beam was relatively fragile and several beams were broken during the cutting operation. The beams were loaded manually using a spring scale for these tests.

The flexural strength was determined by the following relation (which assumes the ice to be an elastic material with properties that are uniform through its thickness):

$$\sigma_f = \frac{6PL}{bh^2}$$

where σ_f = ice flexural strength

P = beam failure load

L = length of beam

b = width of beam

h = thickness of beam

The compressive and shear strength of the consolidated layer was measured using a hand-operated, lever apparatus already on hand at the IMD. This apparatus is regularly used by the IMD to measure these properties for level ice sheets. Small ice blocks (about 0.1 x 0.2 m in area) were cut out of the consolidated layer and removed from the water for insertion into this apparatus. Only a limited number of these tests were performed as they were done to provide index values for comparison with the measured flexural strengths during the warmup period for the sheet #2 tests.

Two methods were used to determine the bulk density of the ridge, as follows:

a) a vertical column was cut free in the ridge and the force required to submerge it was measured. The overall volume of the ice column was determined from measurements of the surface area and the depth. The bulk density, γb, was calculated as:

$$\gamma_b = \frac{\gamma_w \cdot Vol_r - F}{Vol_r}$$

where γ_w = weight density of water

F = submergence force

Vol_r = overall volume of ice column

In practice, the depth, and hence the volume of the ice column was very difficult to measure accurately as the loose blocks were very easily disturbed. In many cases, the depth of the ice column was estimated by using the average depth of the ridge cross-sectional profile for the middle portion of the ridge (where the submergence tests were carried out).

A second difficulty with this method was the fact that the cutting operation (which was necessary to isolate a vertical ridge column) disturbed the loose blocks. When this was observed to occur, the measurement site was abandoned and a new site was selected.

b) The second method that was used also involved cutting a vertical ice column in the ridge and submerging it. The in-air weight of the ice column was measured by collecting it in a pail with a perforated bottom and lifting it out of the water. The weight of the pail was monitored over time as the water drained. Water drained from both between the ice blocks and from inside the ice structure (as the ice was in a saturated state).

It was hoped that these two effects could be separated by analyzing the weight time history. It was expected that the inter-block water would drain more quickly than the interstitial water and that the weight time history would follow a general bilinear trend. In practice, this did not occur as the water drained very rapidly. It is expected that this performance could be improved by using a pail with a fewer number of drainage holes.

For these tests, the in-air weight of the ice column was considered to be the weight measured at the point where the slope change of the weight time history was greatest.

The bulk density γ_b, of the ridge was computed by solving the following two equations:

$$F = \gamma_w \, Vol_r - Wt \text{ in air}$$

$$Wt \text{ in air} = \gamma_b \, Vol_r$$

where Vol_r = volume of ice column

γ_w = weight density of water

F = force to submerge the ice column

Finally, measurements were made of the temperature distribution for two ridges in each ice sheet. A total of 18 Type T thermocouples were embedded in the ridges. These thermocouples were manually logged at several points during the ridge formation process.

4.2.2 Level Ice Properties

Table 4.6 below summarizes the measured level ice properties. Summary data describing the growth, and tempering time history of the sheet, along with the measured mechanical properties are provided in Appendices C, D and E for ice sheets 1, 2 and 3 respectively.

Table 4.6

Summary of Model Scale Level ice Properties

Sheet No.	Period When Ridge Penetration Tests Were Carried Out	Avg. Ice Thickness (mm)	Avg. Flexural Strength (kPa)	Ice Elastic Modulus (mpa)	Ice Weight Density (kN/m^3)
1	1330-1430 April 29	22.7	12.5 (1310)	13.4 (1110)	9.4 (1318)
2	1230-1400 May 3	20.8	25.5 (1000) 12.0 (1410)	No data	9.7 (1239)
3	1300-1430 May 5	22.4	17.5 (1130) 8.0 (1440)	16.6 (1110)	No data

Notes:

1. The above ice thicknesses were measured at the locations where cantilever beam tests were done. The above values are the mean of the average thicknesses measured at each beam test location. See Appendices C, D and E for test data.
2. The time of measurement is shown above in parentheses for the collected flexural strengths, elastic modulus and ice density data.
3. Where flexural strengths were measured at two locations at about the same time, the mean flexural strengths measured at each location were averaged and are listed above.

4.2.3 Ridge Properties

This section summarizes the ridge properties data that were collected. Raw data describing the ridges in sheets 1, 2 and 3 are included in Appendices C, D and E.

(i) Ridge structure and composition: Most ridges consisted of a consolidated layer above an accumulation of ice blocks which were unconsolidated. Ridges 2-4S, 2-4N, 3-4S and 3-4N were exceptions as they were comprised of a consolidated layer only. Also, ridges 2-5N and 3-5N were exceptions as they consisted of unconsolidated material only.

Plates 4.10 to 4.12, and 4.13 to 4.15 show typical vertical cross-sections of the partially-consolidated ridges in sheet #1 and sheets #2 and #3, respectively. In general, the consolidated layer consisted of two or more ice sheet layers that were well-bonded. In some cases, it was difficult to define a clear demarcation between the consolidated layer and the loose blocks beneath as the blocks were lightly bonded to the bottom of the consolidated layer. In general, the rotation of a vertical column of the ridge to horizontal was sufficient to break these bonds.

(ii) Cross-sectional geometry: Figure 4.9 to 4.10 show typical cross-sectional profiles for the ridges in sheets 1, 2 and 3 respectively. Table 4.7 summarizes the measured ridge cross-sectional areas and thicknesses of the consolidated layer.

(iii) Flexural strength of consolidated layer: Table 4.8 summarizes the measured values.

(iv) Ridge bulk density: Table 4.9 summarizes the ridge bulk densities that were measured using both of the methods described in Section 4.2.1.

In general, the bulk densities determined from measurements of the submergence force and ice column volume are higher than those determined from measurements of the submergence force and in-air weight of the ice column.

The bulk densities determined by the former method are considered to be more reliable as they fall between the measured weight densities for a level ice sheet (i.e. 9.4 kN/m^3) and that of water (i.e. about 10 kN/m^3).

The bulk densities determined using the latter method are below that measured for the ice sheet (see Table 4.9).

Plate 4.10

Typical Vertical Cross-Section of Ridge During Sheet #1 Tests

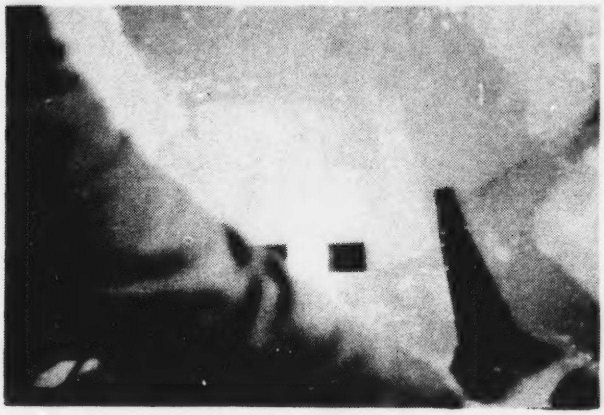

Plate 4.11

Typical Vertical Cross-Section of Ridge During Sheet #1 Tests

Plate 4.12

Typical Vertical Cross-Section of Ridge During Sheet #1 Tests

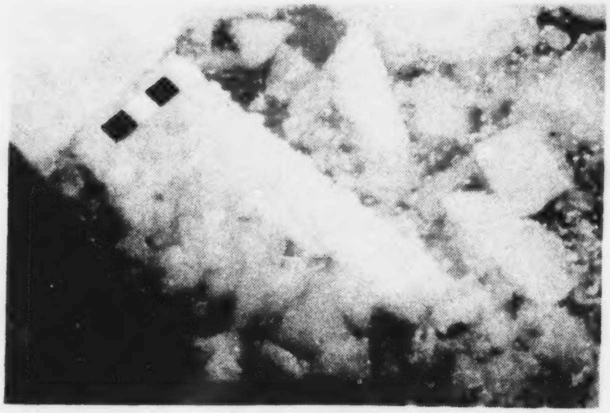

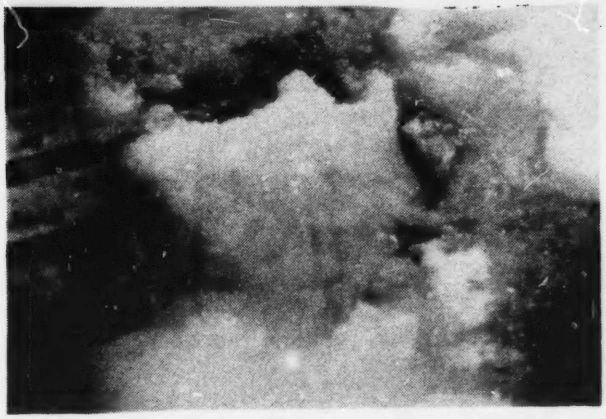

Plate 4.13

Typical Vertical Cross-Section of Ridge During Sheet #2 and Sheet #3 Tests

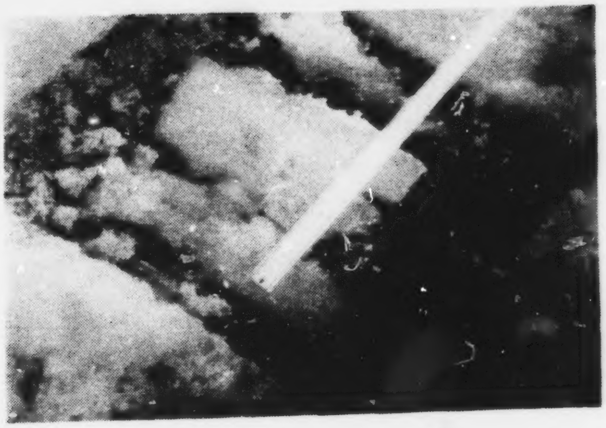

Plate 4.14

Typical Vertical Cross-Section of Ridge During Sheet #2 and Sheet #3 Tests

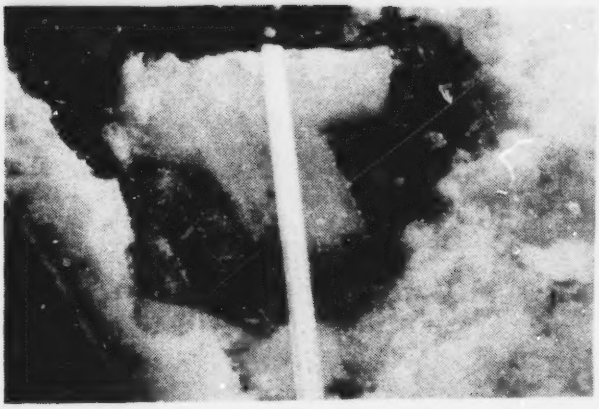

Plate 4.15

Typical Vertical Cross-Section of Ridge During Sheet #2 and Sheet #3 Tests

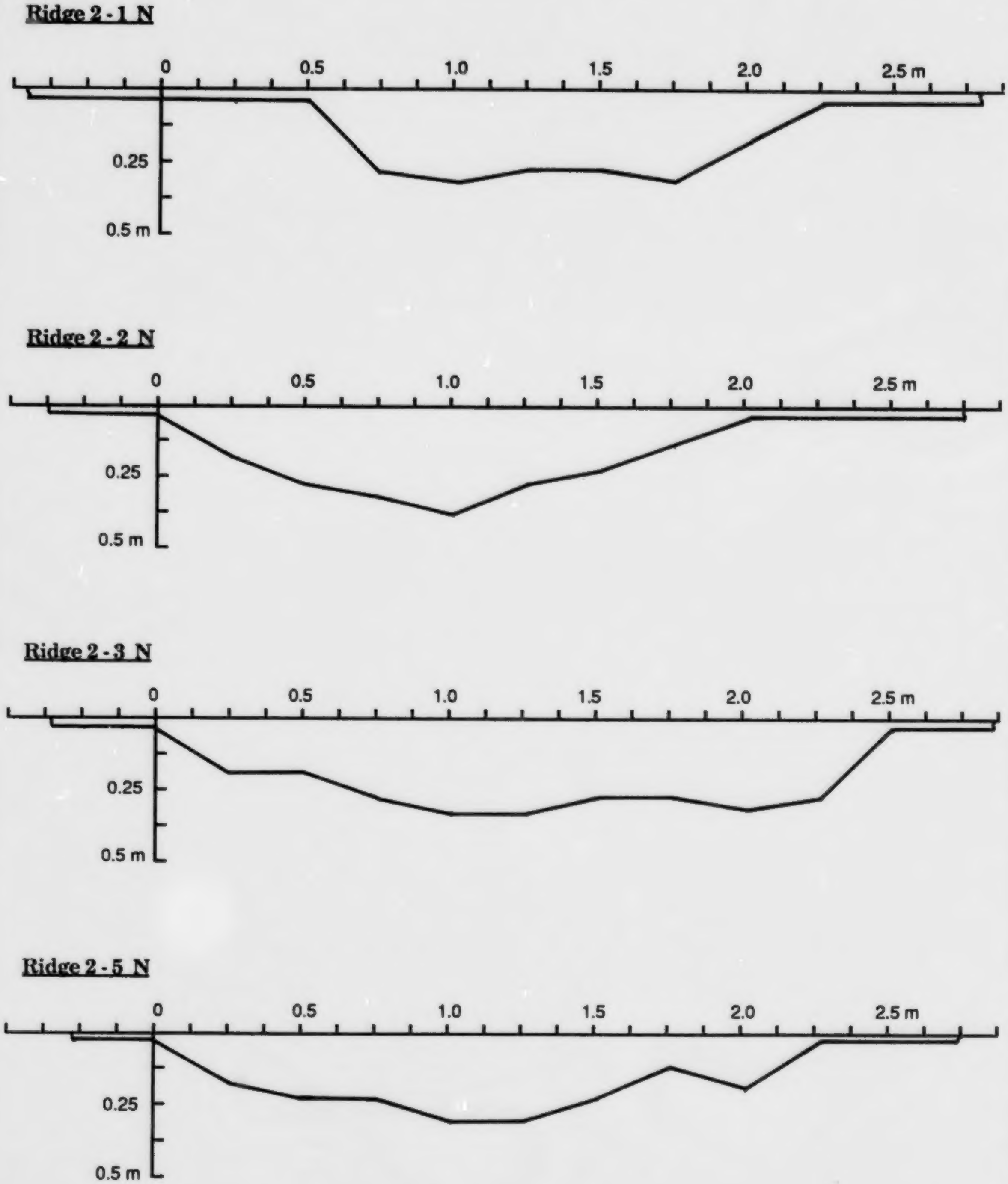

Figure 4.9

Sample Ridge Cross-Sectional Profiles: Sheet No. 2

Ridge 3 - 1 N

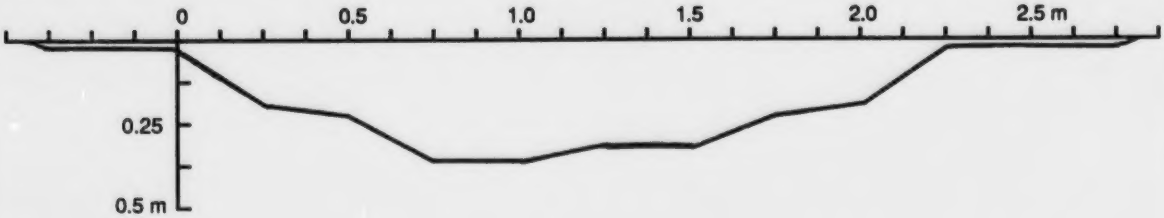

Ridge 3 - 2 N

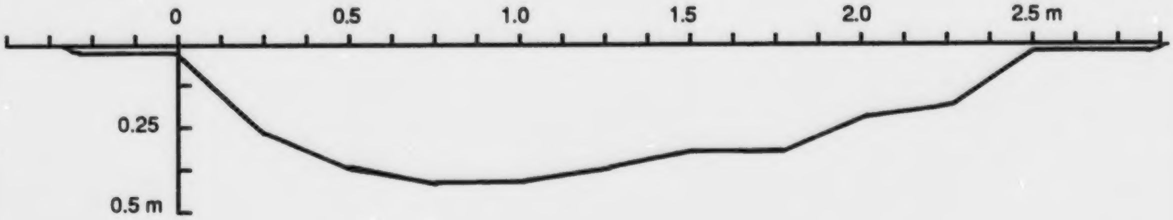

Ridge 3 -1 S

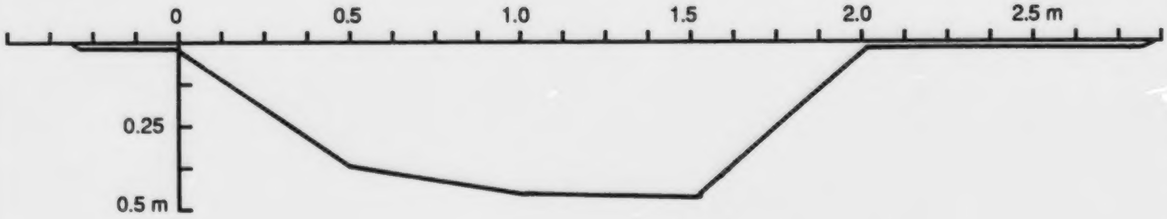

Ridge 3 - 2 S

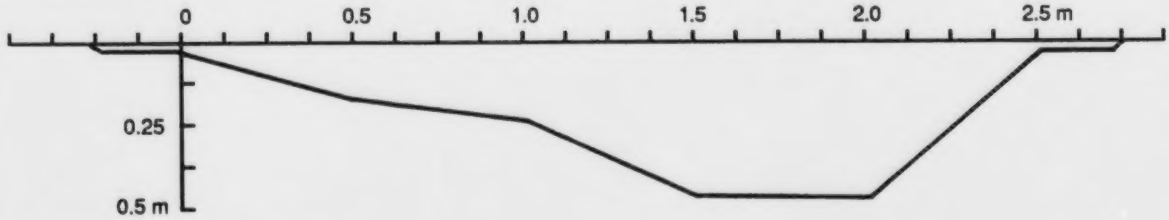

Figure 4.10
Sample Ridge Cross-Sectional Profiles: Sheet No. 3

Table 4.7
Summary of Ridge Cross-Sectional Geometry Data

Sheet No.	Ridge No.	Avg.Consol. Layer Thick (mm)	Ridge Width (m)	Computed[4] Area of Consol. Layer(m^2)	Measured Total Area of Ridge(m^2)	Average Depth (m) of Ridge[9]	Avg.Consol.Layer Thickness / Thickness of Level Ice
1	1-1	80	2.1	0.17	0.56[7]	0.27[8]	3.5
1	1-2	Not Meas.	2.1	0.22[5]	0.26[7]	0.12[8]	No data
1	1-3	Not Meas.	2.1	0.17[6]	0.34[7]	0.16[8]	No data
1	1-4	107	4.0	0.43	0.77[7]	0.19[8]	4.7
2	2-1N	65	1.8	0.11	0.42	0.23	3.1
2	2-2N	59	2.0	0.11	0.46	0.23	2.8
2	2-3N	69	2.5	0.17	0.61	0.24	3.3
2	2-4N	42[1]	4.0	0.17[1]	n/a[1]	0.042[1]	2.0
2	2-5N	Nil[2]	2.2	n/a[2]	0.46	0.21[2]	n/a[2]
2	2-1S	69	1.8[3]	0.12	Not Meas.	No Data	3.3
2	2-2S	50	2.0[3]	0.10	Not Meas.	No Data	2.4
2	2-3S	53	2.5[3]	0.13	Not Meas.	No Data	2.5
2	2-4S	42[1]	4.0	0.17	n/a[1]	0.042[1]	2.0
3	3-1N	47	2.2	0.10	0.56	0.25	2.1
3	3-2N	44	2.5	0.11	0.74	0.30	2.0
3	3-3N	63	2.0	0.13	0.70	0.35	2.8
3	3-4N	45[1]	2.0	0.09	n/a[1]	0.45[1]	2.0
3	3-5N	Nil[2]	2.0	n/a	Not Meas.	No Data	n/a[2]
3	3-1S	84	2.0	0.17	0.66	0.33	3.8
3	3-2S	56	2.5	0.14	0.67	0.27	2.5
3	3-3S	93	2.0	0.19	0.68	0.34	4.2
3	3-4S	45[1]	2.0	0.09	n/a[1]	0.045[1]	2.

Notes:
1. This ridge was comprised of a consolidated layer only.
2. This ridge was comprised of unconsolidated material only.
3. Ridge widths inferred from widths measured for ridges on north side of basin.
4. Area of consolidated layer computed as:
   Avg. thickness of consol. layer X ridge width
5. The area of the consolidated layer for ridge 1-2 was computed using the average thickness of the consolidated layer for ridge 1-4. neither of these ridges were insulated.
6. The area of the consolidated layer for ridge 1-3 was computed using the average thickness of the consolidated layer for ridge 1-3. Both of these ridges were insulated.
7. These data represent the total keel area and not the total area of the ridge.
8. These data represent the average keel depth and not the average total depth of the ridge.
9. Average depth of ridge computed as: total area of ridge/ridge width.

Table 4.8

Summary of Model Scale Measured Flexural Strengths of Ridge Consolidated Layer

Sheet No.	Ridge No.	Average Flexural Strength (kPa)	Ridge Insulated ?
1	1-1	22.5 (post-test value)	Yes
1	1-4	41.8 (post-test value)	No
2	2-2N	93.0 (pre-test value)	Yes
2	2-3N	65.0 (post-test value)	Yes
2	2-1N	62.0 (post-test value)	Yes
2	2-1S	76.0 (post-test value)	No
3	3-3S	77.0 (post-test value)	No
3	3-3N	43.0 (post-test value)	Yes
3	3-2S	79.0 (post-test value)	Yes

Table 4.9

Summary of Measured Ridge Bulk Densities

Sheet No.	Ridge No.	Average Bulk Density (kN/m^3)	Data From Which the Bulk Density Was Computed
1	1-4	8.8	Submergence Force and Volume of Ice Column
2	2-3N	8.9	Submergence Force and In-Air Wt. of Ice Column
2	2-3N	9.5	Submergence Force and Estimates of Volume of Ice Column[1]
2	2-1N	9.5	Submergence Force and Estimates of Volume of Ice Column[1]
3	3-1S	9.4	Submergence Force and Estimated Volume of Ice Column[1]
3	3-1N	9.3	Submergence Force and Estimated Volume of Ice Column[1]
3	3-2N	8.6	Submergence Force and In-Air Wt. of Ice Column
3	3-2N	9.1	Submergence Force and Volume of Ice Column

Note: 1. The depth of the ice column was taken as the average depth of the ridge shown on the ridge cross-sectional profiles over the centre portion of the ridge.

(v) Ridge temperatures: Thermocouples were positioned to determine the vertical temperature profile for ridges that were insulated and non-insulated. Temperatures were measured in the air, at the ridge surface (both above and below the insulation where applicable), inside the ridge, and in the water. See Figure 4.11 for a description of the positions where temperatures were measured. Temperature data were logged manually and were collected at several points during the ridge formation process (e.g. initial formation of ridges at start of second freeze, before and after the insulation mats were removed, and when the tempering process was nearing completion).

Raw temperature data for the ridges in sheets 1, 2 and 3 are included in Appendices C, D and E respectively.

The table below compares the range of ridge surface and internal temperatures close to testing for insulated and non-insulated ridges.

Ridge Surface	Sheet #1		Sheet #2		Sheet #3	
Insulated ?	Yes	No	Yes	No	Yes	No
Approx. Elapsed Time (hrs) before testing	1	1	1	1	1	1
Range of ridge surface and internal temperatures (°C)	-0.4 to -1.4	-0.5 to -1.0	-1.2 to -1.4	-0.9 to -1.1	-1.1 to -2.2	-0.7 to -1.3

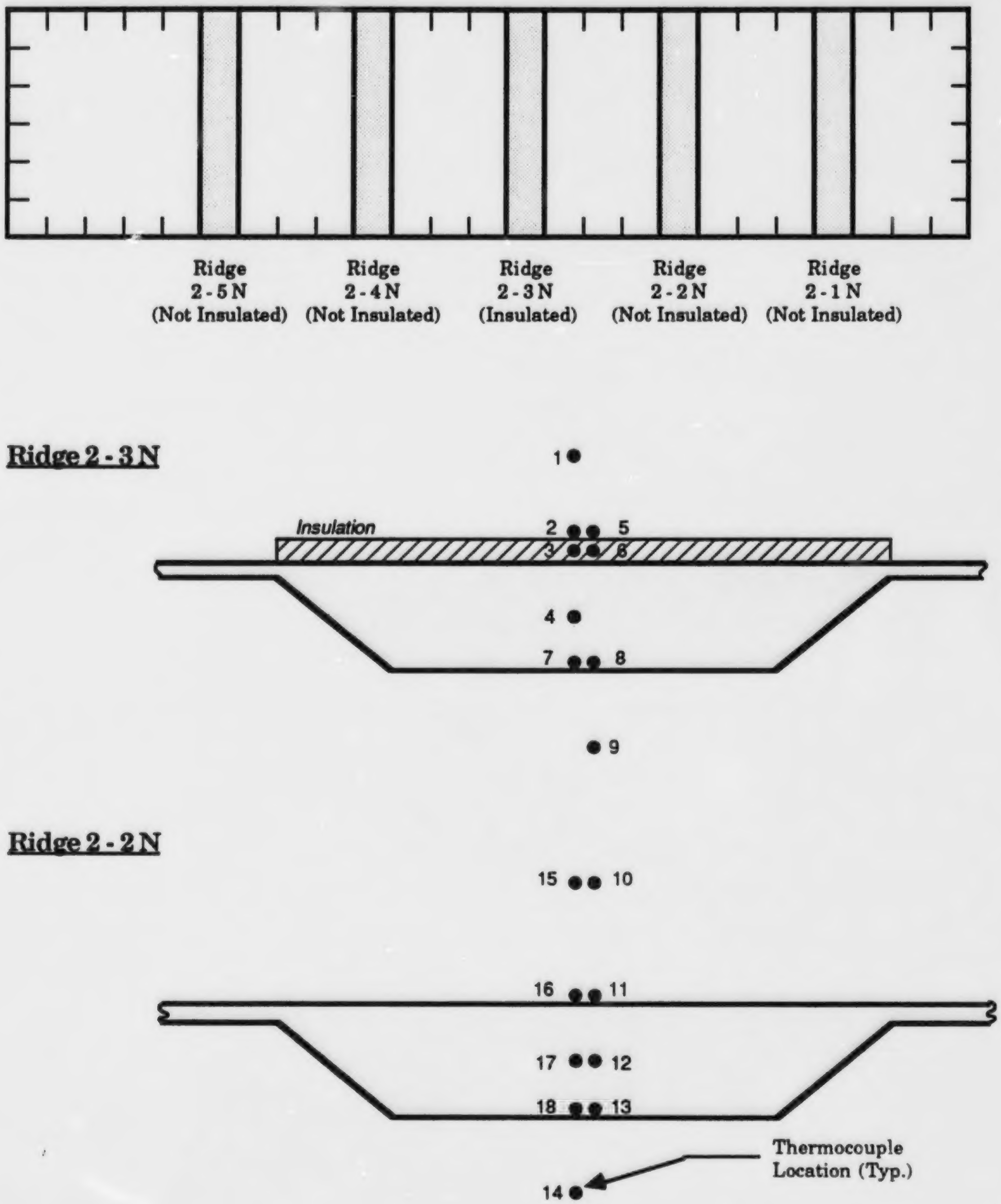
Ridge 2-5N (Not Insulated)
Ridge 2-4N (Not Insulated)
Ridge 2-3N (Insulated)
Ridge 2-2N (Not Insulated)
Ridge 2-1N (Not Insulated)
Ridge 2-3N
1
Insulation
2
5
3
6
4
7
8
9
Ridge 2-2N
15
10
16
11
17
12
18
13
Thermocouple Location (Typ.)
14

Figure 4.11
Thermocouple Locations For Sheet No. 2

4.3 Data Reduction Procedures and Results for Ridge Modelling Tests

4.3.1 Data Reduction

As outlined in Section 4.1, the test data were collected in both digital and analogue format.

Initially, the data that were in digital format were analyzed using hardware and software available at the IMD.

Time histories were plotted for the raw data in model scale units. This was done for all data channels for each test excepting the measurements of the vertical model displacements at the port, centre, and starboard locations made during the sheet #2 and #3 tests.

These data were used to compute the pitch, roll and heave motions of the model. These computations were made taking into account the positions of the individual displacement transducers, as shown in Figure 4.8, using software available at the IMD. Thus, it should be recognized that these plots reflect reduced data, as opposed to raw data.

Figures 4.12 to 4.13 show the measured and computed time histories for a typical test.

Further analysis was subsequently done using the analogue data at Fleet Technology Limited's offices in Kanata. For this analysis, the analogue data were filtered and digitized as shown schematically in Figure 4.7.

Figure 4.12 shows a typical force time history for a ridge penetration test. This time history shows significant force fluctuations that are periodic in nature.

The analogue test data were filtered using analogue low-pass filters in an effort to remove this ringing. A filtering rate of 2 Hz was used for the sheet #2 and #3 test data. This rate was selected by progressively filtering the force time history for test T2R1. Plots of the filtered time histories are included in Appendix F.

A lower filtering rate of 1 Hz was found to be necessary to eliminate most of the ringing for the sheet #1 tests (see Appendix G). This reflects the fact that the towpost used for the sheet #2 and #3 tests was significantly stiffer than that used for the sheet #1 tests.

The analogue test data were also digitized without filtering, as shown in Figure 4.7. This provided a digital data record which could be analyzed and compared to the filtered record.

Both the filtered and the unfiltered data were analyzed to determine and plot the:

(a) force versus displacement record for each ridge; and

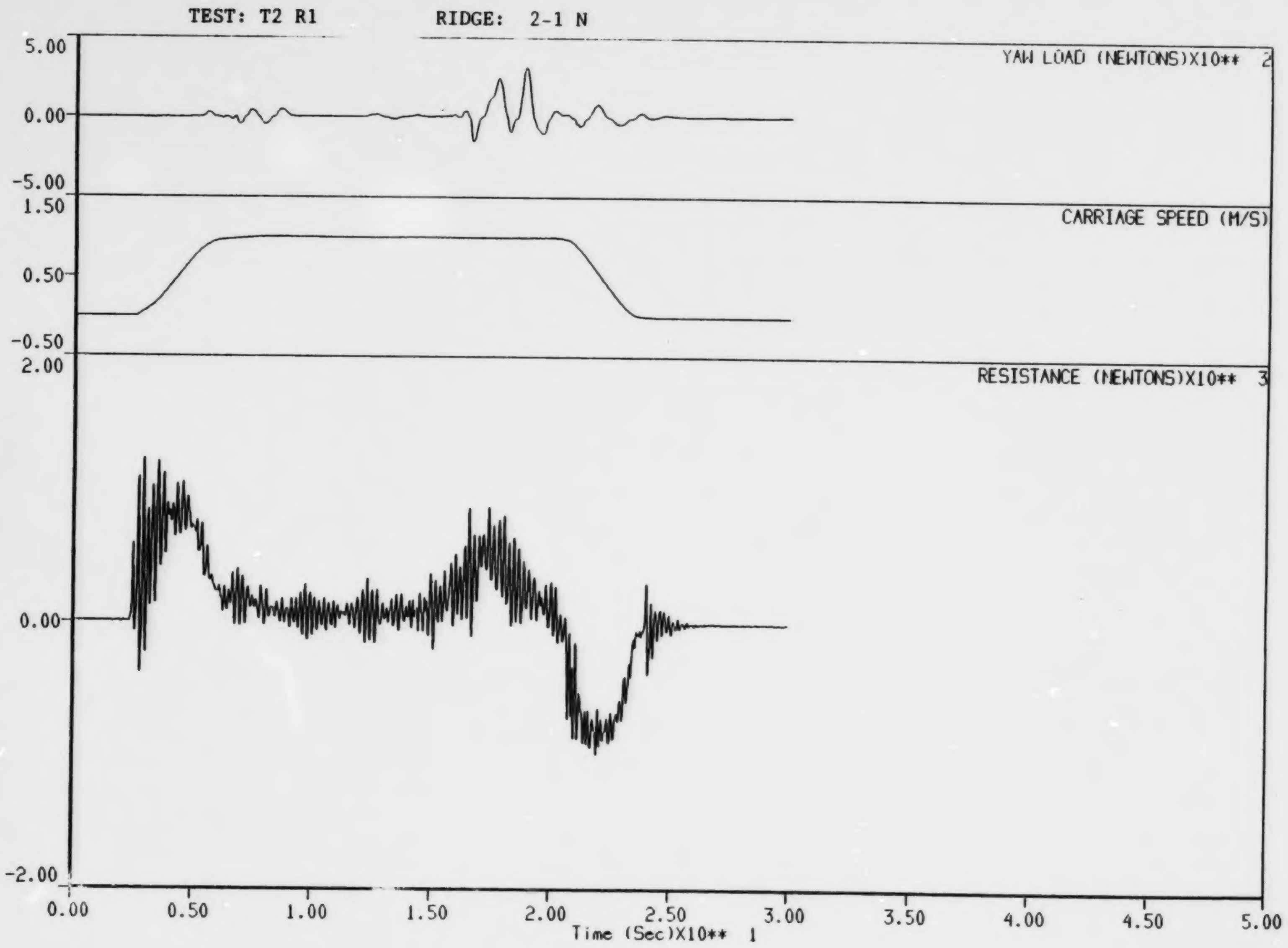

FIGURE 4.12

SAMPLE PLOT OF RAW MEASURED TIME HISTORIES

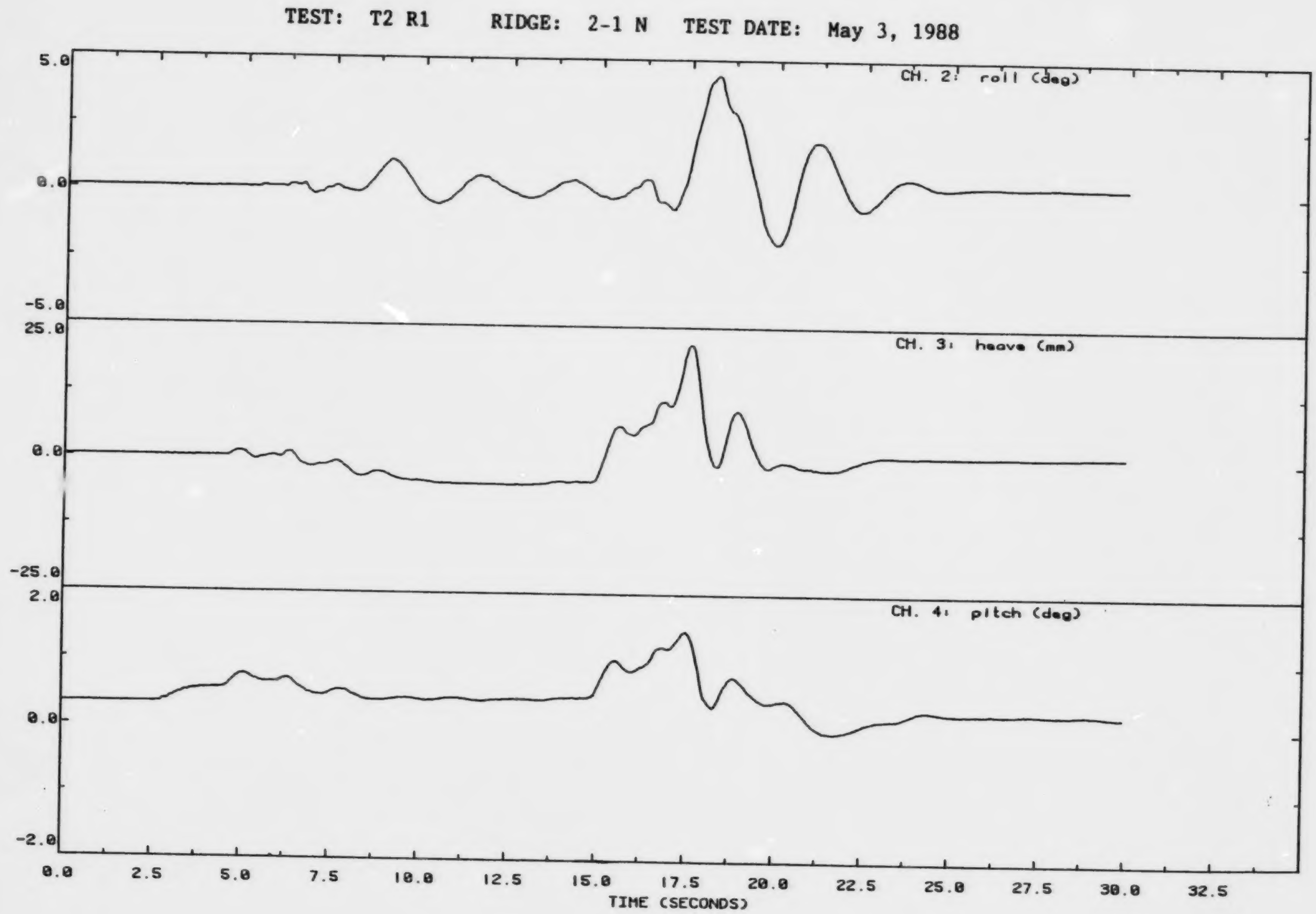

FIGURE 4.13

SAMPLE PLOT OF COMPUTED VESSEL MOTIONS TIME HISTORIES

(b) cumulative penetration energy for each ridge as a function of the total penetration distance.

Figures 4.15 to 4.18 show sample plots. The limits of integration used for the plots of force vs. displacement and cumulative penetration energy are shown in Figure 4.14 as dotted lines.

All raw and reduced data plots for the tests done in Sheets #1, 2 and 3 are included in appendices C, D and E respectively. Each of these appendices contains:

a) raw measured time histories for all transducers (except for the plotted ship motion time histories which have been computed from the measured model displacements).

b) plots of the model scale force vs. penetration and the model scale cumulative penetration energy vs. distance for all tests. These plots have been provided for both unfiltered and filtered data.

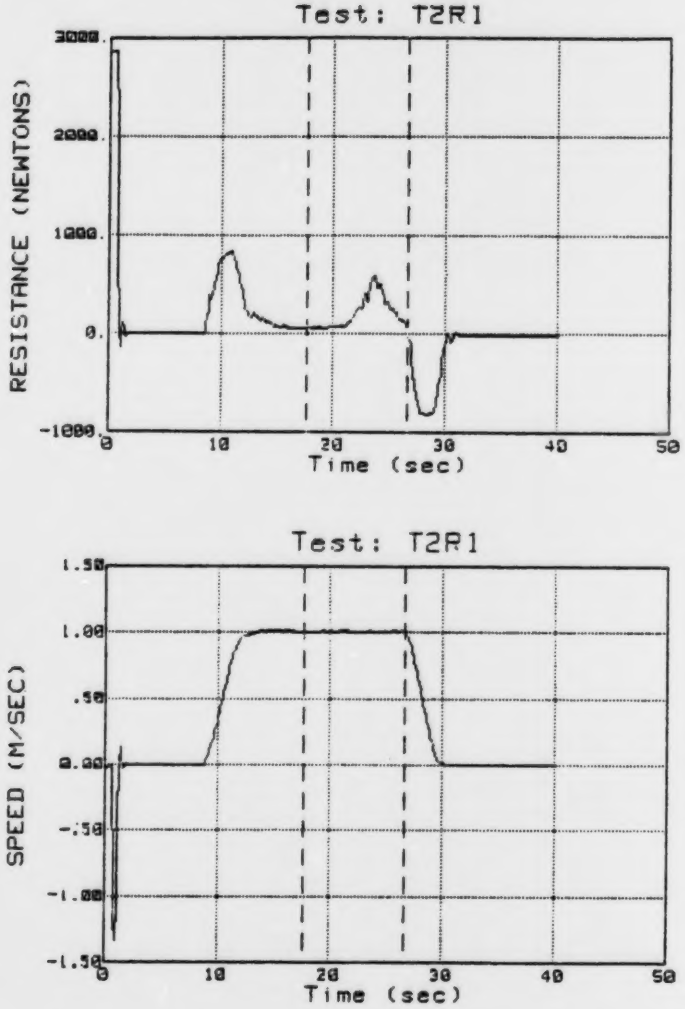

FIGURE 4.14

SAMPLE FORCE AND VELOCITY TIME HISTORIES
FOR RIDGE 2-1 N: TEST DATA FILTERED AT 2 HZ

MODEL SCALE PENETRATION FORCE
TEST: T2R1H   RIDGE: 2-1N

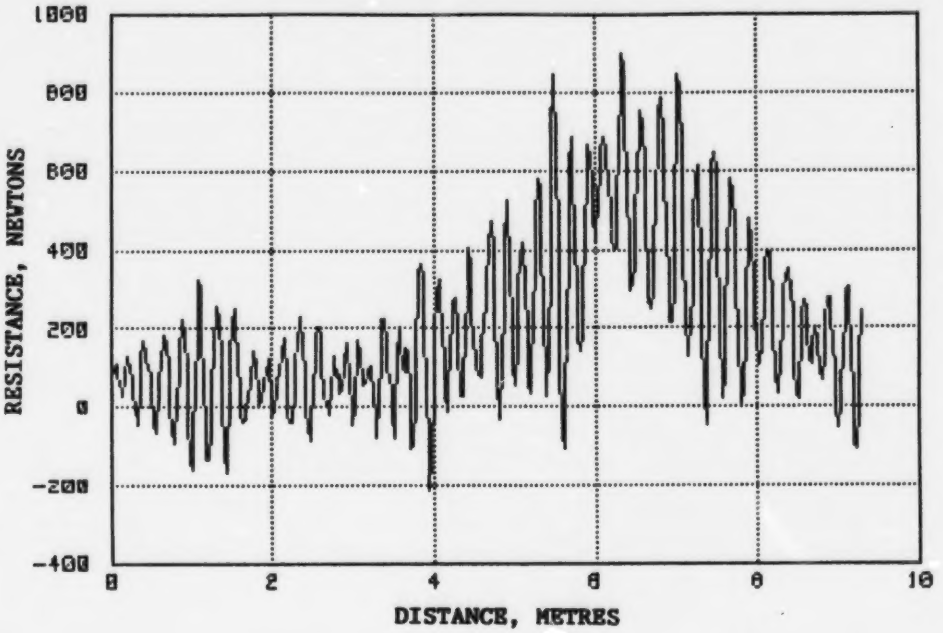

MODEL SCALE PENETRATION ENERGY
TEST: T2R1H   RIDGE: 2-1N

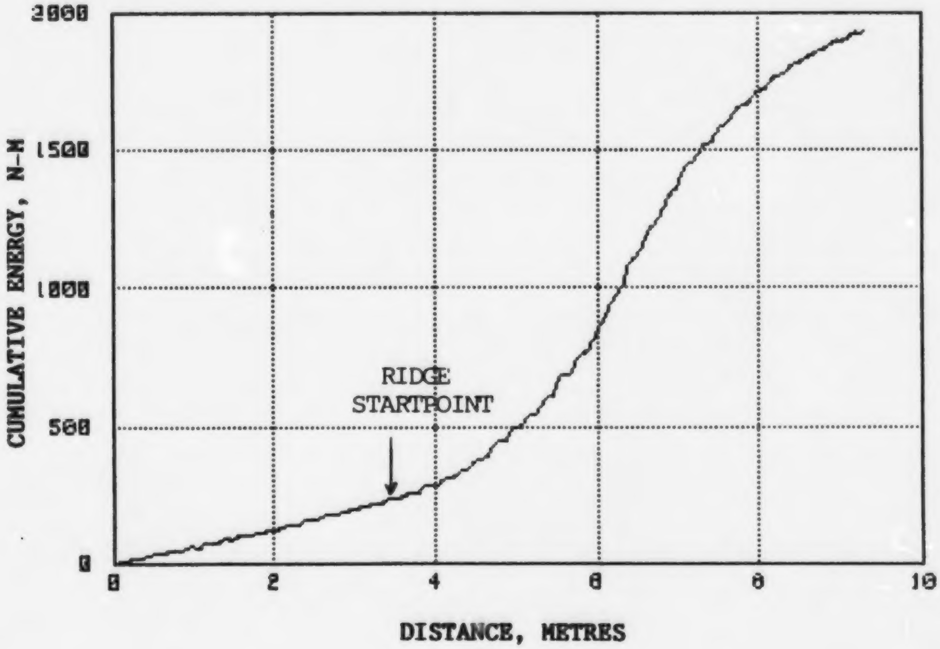

FIGURE 4.15

MODEL SCALE PENETRATION FORCE AND ENERGY FOR
RIDGE 2-1 N: TEST DATA FILTERED AT 100 HZ

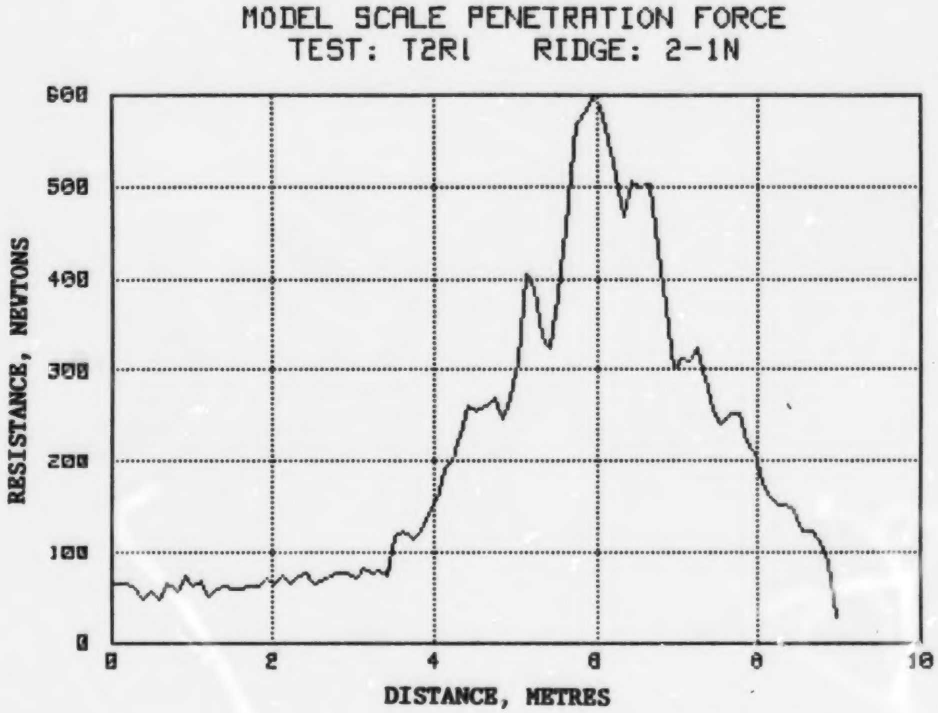

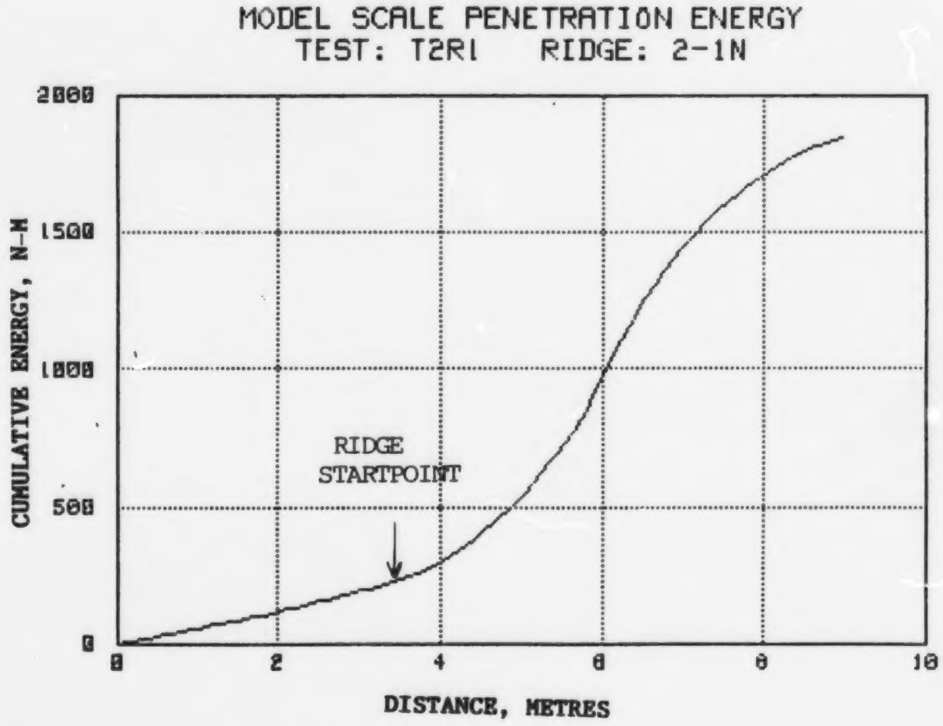

FIGURE 4.16

MODEL SCALE PENETRATION FORCE AND ENERGY FOR RIDGE 2-1 N: TEST DATA FILTERED AT 2 HZ

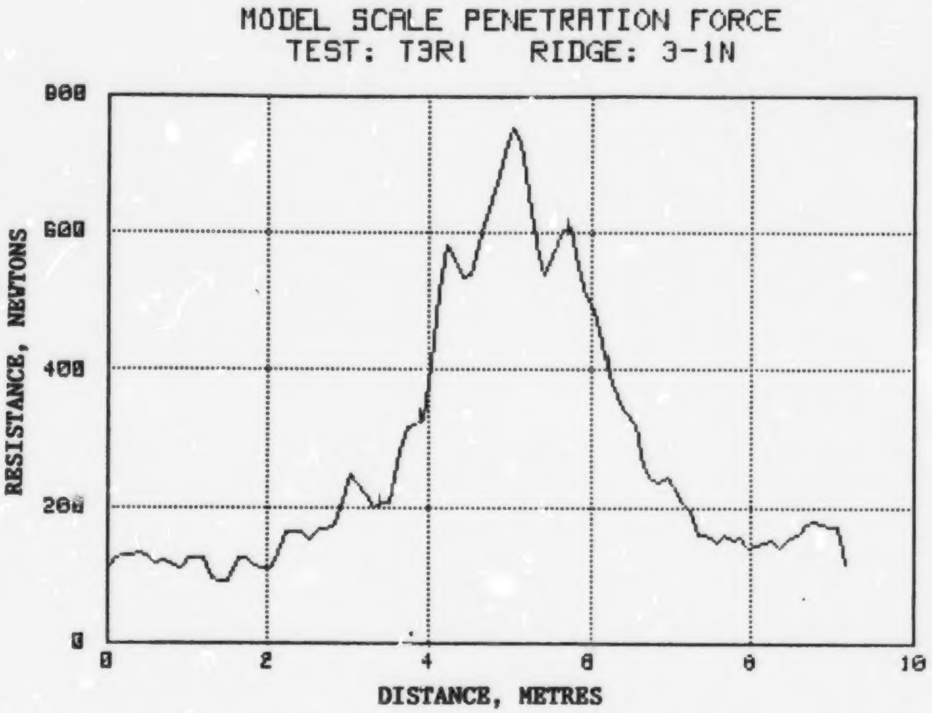
MODEL SCALE PENETRATION FORCE
TEST: T3R1 RIDGE: 3-1N

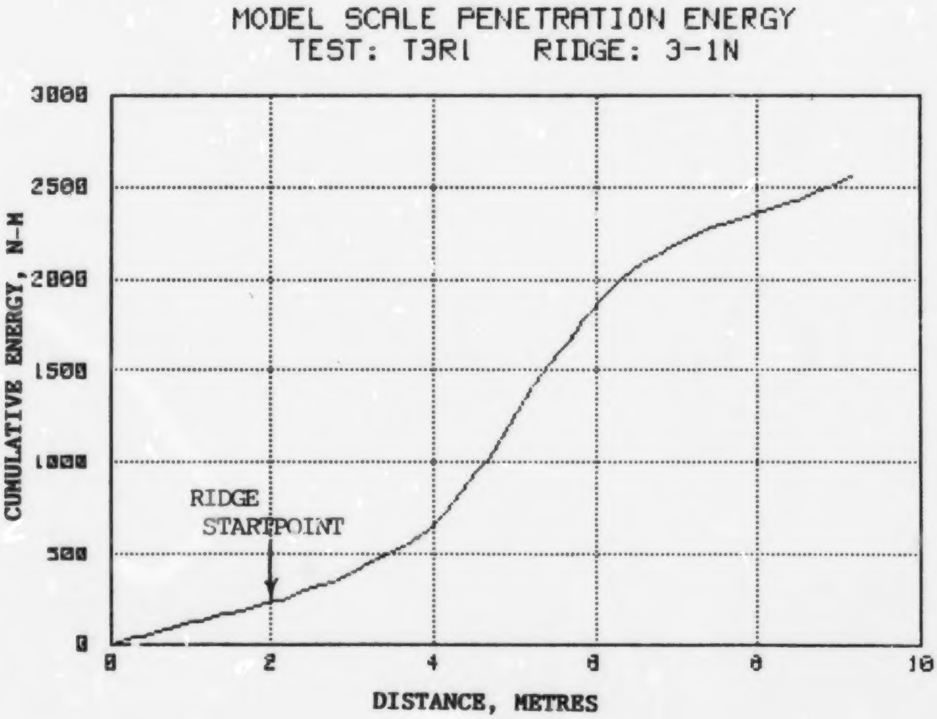
MODEL SCALE PENETRATION ENERGY
TEST: T3R1 RIDGE: 3-1N

FIGURE 4.17

MODEL SCALE PENETRATION FORCE AND ENERGY FOR RIDGE 3-1 N: TEST DATA FILTERED AT 2 HZ

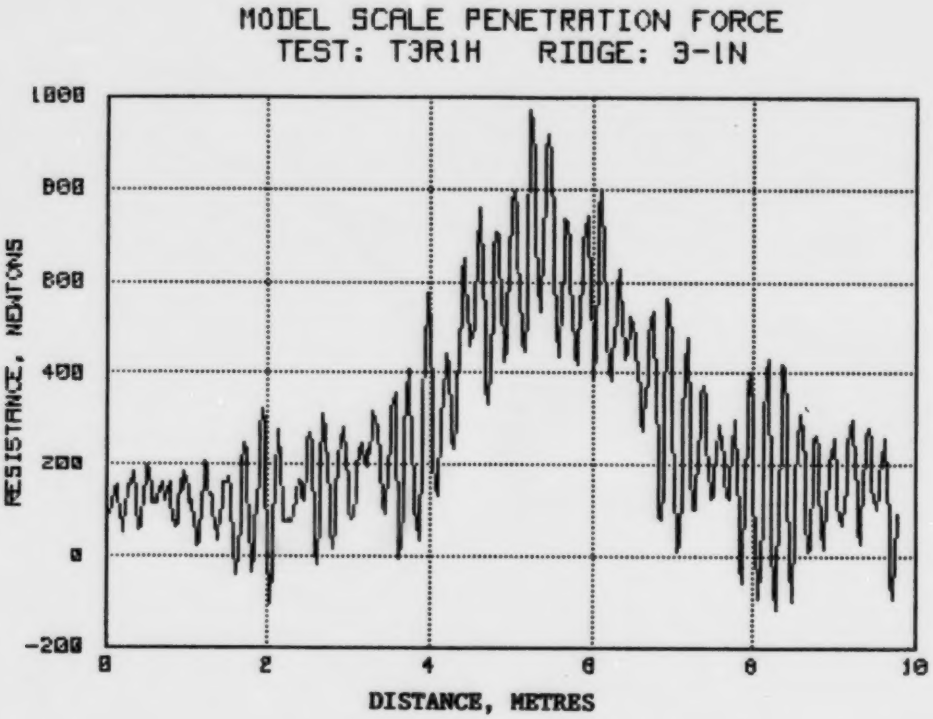

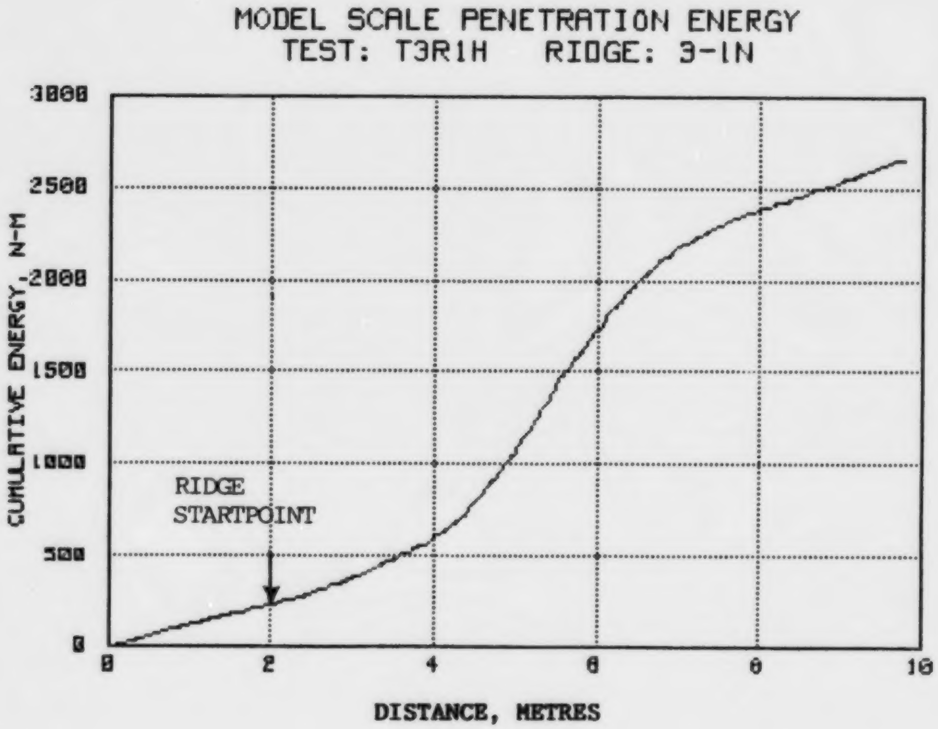

FIGURE 4.18

MODEL SCALE PENETRATION FORCE AND ENERGY FOR
RIDGE 3-1 N: TEST DATA FILTERED AT 100 HZ

4.3.2 Test Results

Plates 4.16 to 4.24 show the tests conducted.

In order to compare the model test results with the field data, it was necessary to establish the 'start point' of the ridge on the plots of force vs. penetration and of cumulative penetration energy vs. penetration. The same general approach used to analyze the field data was used for the model data.

During the initial portion of the test segment shown on the plots of model scale force and energy, the model transited level ice. The point at which the bow was considered to first contact the ridge (i.e. the "start point") was determined by reviewing the force-displacement plot. The start point was selected as the point at which the mean force started to increase. The start points used for ridges 2-1 N and 3-1 N are shown on Figures 4.15 to 4.18. The start point penetration distances used for each ridge in sheets 1, 2 and 3 are listed in appendices C, D and E respectively.

To provide a standard basis for comparing the cumulative penetration energies measured during each test and for comparison with the field data, the full scale penetration energy was determined for the following full scale penetration distances:

a) 27 m which corresponds to one quarter of the waterline length (LWL) of the USCGC POLAR STAR.

b) 36 m which corresponds to one third of the waterline length of the USCGC POLAR STAR.

c) 71 m which corresponds to two thirds of the waterline length (LWL) of the USCGC POLAR STAR.

d) 80 m which corresponds to three quarters of the waterline length of the USCGC POLAR STAR.

These penetration distances bracket the maximum ridge penetration forces. (The maximum ridge penetration force typically occurred at a penetration of about 0.25 to 0.5 LWL). Furthermore, these distances correspond approximately to the forebody and midbody of the ship.

The penetration energy was determined by subtracting the cumulative penetration energy at the ridge start point from the cumulative penetration energy that was measured at the penetration distance of interest.

Froude scaling laws (as listed in Table 2.2) were used to extrapolate the model scale results to full scale values.

Tables 4.10 and 4.11 summarize the measured ridge penetration forces and energies in both model scale and full scale units.

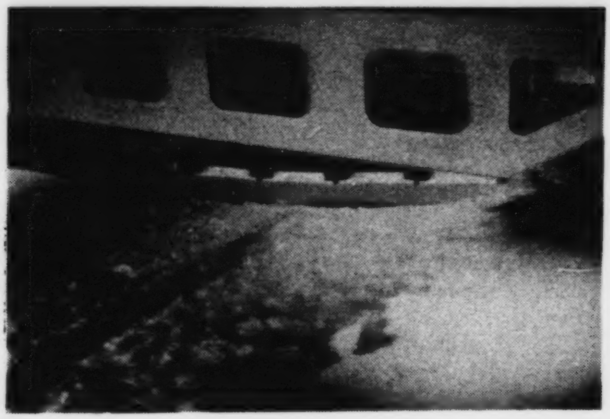

Plate 4.16

Typical Penetration of Ship in Ridge in Sheet #1

Plate 4.17

Typical Penetration of Ship In Ridge in Sheet #1

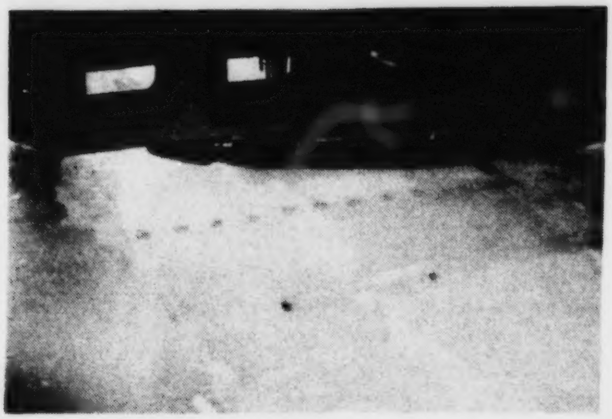

Plate 4.18

Typical Penetration of Ship in Ridge in Sheet #2. Yellow fiduciary rods used to profile ridge seen in foreground

Plate 4.19

Typical Penetration of Ship In Ridge in Sheet #2. Yellow fiduciary rods used to profile ridge seen in foreground

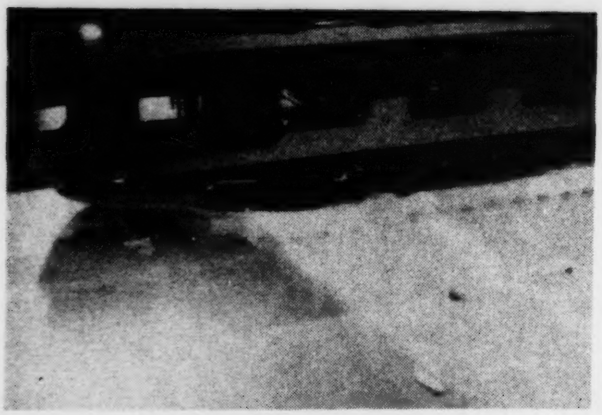

Plate 4.20

Penetration of Ships in Unconsolidated Rubble During Sheet #3 Tests

Plate 4.21

Penetration of Ships in Unconsolidated Rubble During Sheet #3 Tests

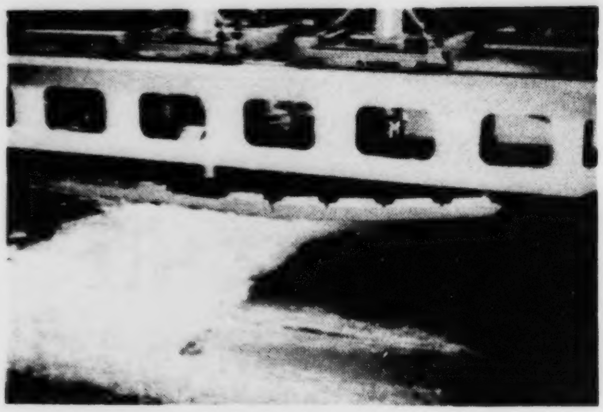

Plate 4.22

View of Ridge 3-2 after Penetration By Ship
Approx. Width of Channel: 1 m

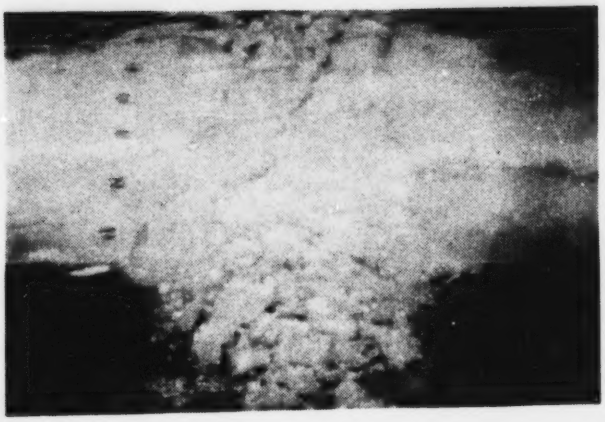

Plate 4.23

View of Ridge 3-3 after Penetration By Ship
Approx. Width of Channel: 1 m

Plate 4.24

Typical Distribution of Ice Piece Sizes in Ridge for Sheet #2 Tests
Approx. Width of Broken Ice in Photo: 1 m

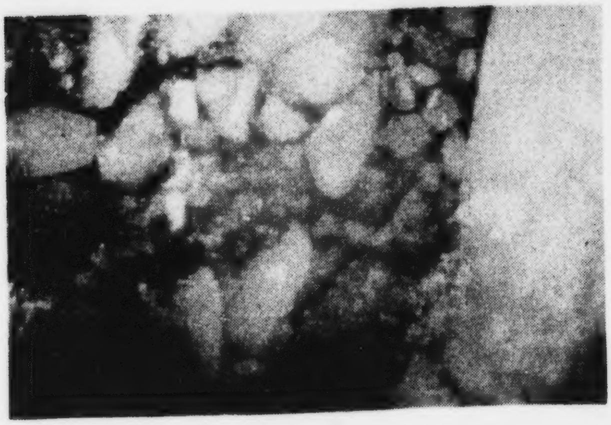

Table 4.10

Summary of Ridge Penetration Force

Sheet No.	Test No.	Ridge No.	Ridge Penetration Force									
			Penet.=0.25 LWL		Penet.=0.33 LWL		Penet.=0.67 LWL		Penet.=0.75 LWL		Max.Penet.Force	
			M.S. Value	F.S. Value	M.S. Value	F.S. Value	M.S. Value	F.S. Value	M.S. Value	F.S. Value	M.S. Value	F.S. Value
1	1	1-1	255N	1.78MN	303N	2.11MN	500N	3.48MN	600N	4.18MN	623N	4.34MN
1	4	1-4	520N	3.62MN	670N	4.67MN	1130N	7.87MN	1170N	8.15MN	1252N	8.72MN
2	T2R1	2-1N	260N	1.81MN	375N	2.61MN	319N	2.22MN	250N	1.74MN	596N	4.15MN
2	T2R2	2-2N	171N	1.19MN	254N	1.77MN	301N	2.10MN	118N	0.82MN	452N	3.15MN
2	T2R3	2-3N	324N	2.26MN	416N	2.90MN	130N	0.91MN	116N	0.81MN	431N	3.00MN
2	T2R3	2-4N	96N	0.67MN	83N	0.58MN	72N	0.50MN	62N	0.43MN	102N	0.71MN
2	T2R3	2-5N	198N	1.38MN	207N	1.44MN	100N	0.70MN	91N	0.63MN	210N	1.46MN
2	T2R4	2-1S	335N	2.33MN	393N	2.74MN	306N	2.13MN	156N	1.09MN	818N	5.70MN
2	T2R4	2-2S	197N	1.37MN	247N	1.72MN	344N	2.40MN	263N	1.83MN	573N	4.00MN
2	T2R4	2-3S	275N	1.92MN	310N	2.16MN	155N	1.08MN	120N	0.84MN	337N	2.35MN
2	T2R4	2-4S	105N	0.73MN	112N	0.78MN	105N	0.73MN	105N	0.73MN	115N	0.80MN
3	T3R1	3-1N	200N	1.39MN	330N	2.30MN	610N	4.25MN	400N	2.79MN	752N	5.24MN
3	T3R2	3-2N	400N	2.79MN	542N	3.78MN	No Data		No Data		542N	3.78MN
3	T3R2	3-3N	610N	4.25MN	723N	5.04MN	734N	5.11MN	526N	3.67MN	962N	6.70MN
3	T3R2	3-4N	457N	3.18MN	538N	3.75MN	303N	2.11MN	162N	1.13MN	652N	4.54MN
3	T3R2	3-5N	296N	2.06MN	340N	2.37MN	164N	1.14MN	134N	0.93MN	344N	2.40MN
3	T3R3	3-1S	505N	3.52MN	758N	5.28MN	527N	3.67MN	398N	2.77MN	756N	5.27MN
3	T3R3	3-2S	245N	1.71MN	444N	3.09MN	490N	3.41MN	393N	2.74MN	694N	4.84MN
3	T3R3	3-3S	534N	3.72MN	624N	4.35MN	978N	6.81MN	791N	5.51MN	1179N	8.22MN
3	T3R3	3-4S	154N	1.07MN	190N	1.32MN	482N	3.36MN	498n	3.47MN	652N	4.54MN

Note: This table is based on test data that were filtered at 2 Hz for the sheet #2 and #3 tests and at 1 Hz for the sheet #1 tests.

Table 4.11

Cumulative Penetration Energy Summary

Sheet No.	Test No.	Ridge No.	Cumulative Penetration Energy							
			Penet.=0.25 LWL		Penet.=0.33 LWL		Penet.=0.67 LWL		Penet.=0.75 LWL	
			M.S. Value	F.S. Value	M.S. Value	F.S. Value	M.S. Value	F.S. Value	M.S. Value	F.S. Value
1	1	1-1	324N·m	43.1MJ	433N·m	57.6MJ	1140N·m	151.7MJ	1400N·m	186.3MJ
1	4	1-4	416N·m	55.4MJ	740N·m	98.5MJ	2312N·m	307.7MJ	2913N·m	387.7MJ
2	T2R1	2-1N	243N·m	32.3MJ	353N·m	47.0MJ	1272N·m	169.3MJ	1411N·m	187.8MJ
2	T2R2	2-2N	152N·m	20.2MJ	256N·m	34.1MJ	860N·m	114.5MJ	957N·m	127.4MJ
2	T2R3	2-3N	260N·m	34.6MJ	451N·m	60.0MJ	1023N·m	136.1MJ	1075N·m	143.1MJ
2	T2R3	2-4N	84N·m	11.2MJ	138N·m	18.4MJ	251N·m	33.4MJ	283N·m	37.7MJ
2	T2R3	2-5N	157N·m	20.9MJ	272N·m	36.2MJ	499N·m	66.4MJ	527N·m	70.1MJ
2	T2R4	2-1S	274N·m	36.5MJ	447N·m	59.5MJ	1459N·m	194.2MJ	1575N·m	209.6MJ
2	T2R4	2-2S	150N·m	20.0MJ	243N·m	32.3MJ	936N·m	124.6MJ	1075N·m	143.1MJ
2	T2R4	2-3S	210N·m	27.9MJ	360N·m	47.9MJ	797N·m	106.1MJ	867N·m	115.4MJ
2	T2R4	2-4S	130N·m	17.3MJ	162N·m	21.6MJ	347N·m	46.2MJ	403N·m	53.6MJ
3	T3R1	3-1N	278N·m	37.0MJ	417N·m	55.5MJ	1474N·m	196.2MJ	1735N·m	230.9MJ
3	T3R2	3-2N	448N·m	59.6MJ	701N·m	93.3MJ	No Data		No Data	
3	T3R2	3-3N	486N·m	64.7MJ	809N·m	107.7MJ	2317N·m	308.4MJ	2636N·m	350.8MJ
3	T3R2	3-4N	347N·m	46.2MJ	607N·m	80.8MJ	1301N·m	173.1MJ	1518N·m	202.0MJ
3	T3R2	3-5N	256N·m	34.1MJ	395N·m	52.6MJ	895N·m	119.1MJ	965N·m	128.4MJ
3	T3R3	3-1S	436N·m	58.0MJ	628N·m	83.6MJ	1727N·m	229.8MJ	2024N·m	269.4MJ
3	T3R3	3-2S	260N·m	34.6MJ	451N·m	60.0MJ	1491N·m	198.4MJ	1717N·m	228.5MJ
3	T3R3	3-3S	434N·m	57.8MJ	665N·m	88.5MJ	2370N·m	315.4MJ	2833N·m	377.0MJ
3	T3R3	3-4S	150N·m	20.0MJ	231N·m	30.7MJ	798N·m	106.2MJ	994N·m	132.3MJ

Note: This table is based on test data that were filtered at 2 Hz for the sheet #2 and #3 tests and at 1 Hz for the sheet #1 tests.

4.4 Results of Model Test of Level Ice Resistance of the USCGC POLAR STAR

Although the main focus of the project was on the conduct of ridge modelling tests, one model test data point of level ice resistance was obtained during the first penetration test conducted in sheet #1. For this test (i.e. test T1R1) the model transitted about two ship lengths at constant speed in level ice before contacting the ridge. The results of this test are summarized below:

		Model Scale Value	Extrapolated Full Scale Value (see Table 2.5 for scaling laws)
Ice Mechanical Properties: (See Table 4.6 for values)	Thickness	22.7 mm	0.43 m
	Flexural Strength	12.5 kPa	240 kPa
	Elastic Modulus	13.4 MPa	260 MPa
Ice-ship friction factor		0.04	0.04
Ship speed		1 m/s	4.4 m/s
Mean Resistance (See Initial Portion of Test T1R1 in Appendix C for data record)		75 N	0.52 MN

Plate 4.25 below shows the icebreaking pattern which occurred during this test.

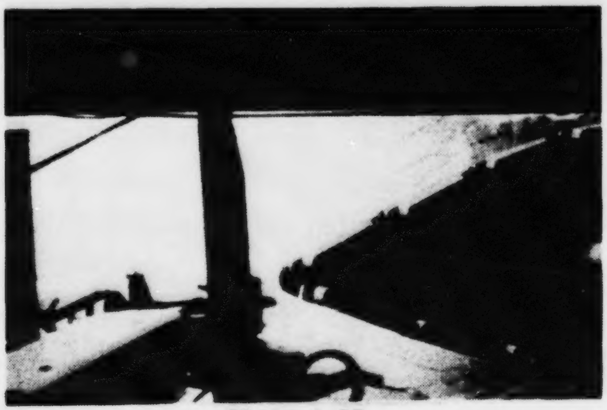

Plate 4.25
Breaking Pattern in Level Ice

The level ice resistance predicted by this model test is less than the level ice resistance predicted by a semi-empirical relation developed by Glen et al, 1985. This numerical relation predicts a level ice resistance of 0.83 MN for the above test conditions.

5.0 ANALYSIS AND DISCUSSION OF TEST RESULTS

5.1 Ridge-building and Testing Techniques

Three ridge-building and testing techniques have been tried during this project, as follows:

Method Number	Sheet Number	Summary Description
1	1	Use a two-freeze process. Construct ridges by creating a rubble pile (from the ice produced during the first freeze). Produce a consolidated layer by allowing the rubble to freeze. (This method was used to produce the ridges in sheet #1 and is shown schematically in Figure 4.2).
2	2;3	Use a two-freeze process. Construct ridges by physically transporting broken ice pieces (from the first ice sheet) to the ridge location and produce a consolidated layer by rafting one or two ice sheet layers as desired over the rubble. Conduct a second freeze to grow an adjacent ice sheet and to partially consolidate the ridge. (This method was used to produce partially-consolidated ridges in sheets 2 and 3 and is shown schematically in Figure 4.3).
3	2;3	Produce ridges in the basin that consist of consolidated and unconsolidated ice only. Conduct separate tests. (This modelling method was used for some ridges in sheets 2 and 3. See Figures 4.5 and 4.6).

5.1.1 Logistical and Practical Ridge-Building Considerations

Methods #1 and #2 involved a two-freeze process whereas method #3 may be used with a single freeze. Also, method #3 was simple to perform with existing equipment at the IMD. Thus, method #3 offers clear advantages in this respect. The principal question with method #3 is whether the total resistance of a partially-consolidated ridge can be reliably predicted by conducting separate tests in ridges that scale the unconsolidated and consolidated portions only of the target ridge. This question is addressed in section 5.2.

Method #1 had the greatest manpower and ridge-building time requirements. This partly reflects the fact that this was the first method attempted and the equipment used (eg. floating boom, ridge restraint strips) were prototypes.

As a result there were safety hazards with this method. It is believed that some of these problems could be overcome with custom-built equipment. As well, some of the problems encountered with this method reflected a lack of experience. For example, significant difficulties were encountered in seeding the adjacent ice sheet (which would be produced during the second freeze). For subsequent ridge-building operations, the ice-seeding step was omitted as it was found there was sufficient moisture in the laboratory to 'self-seed' the ice sheet. This produced an ice sheet that was considered to have adequate ice properties.

Thus, it is believed that refinements are possible with method #1. Nevertheless, method #2 had fewer manpower requirements and could be applied relatively easily with existing equipment at the IMD. Furthermore, it produced ridges that were considered to provide better scaling of the target ridge (as will be discussed subsequently). Consequently, method #2 is considered to be preferable to method #1.

However, both methods #1 and #2 required significantly more labour and equipment resources (eg. basin time) than did method #3.

5.1.2 Ridge Properties and Control

(i) Shape and Size of Ridges:

Initially it was planned to control the size and shape of the ridges by:

a) controlling the ridge surface width.
b) controlling the volume and distribution of ice used to make the ridge
c) using a diver, along with a cross-sectional ridge profile standard, to shape the ridge.

This approach was generally followed. However, the use of a diver proved to be very time-consuming and was discontinued after the first ridge.

Subsequently, the shape of the ridges was not controlled although efforts were made to distribute ice blocks in the ridge evenly. This was done by dumping ice blocks over the full width of the ridge and by tamping the ice blocks.

Cross-sectional profiles of the ridges in sheets 1, 2 and 3 are presented in appendices C, D and E respectively. In general, the ridge shape is bounded by a triangle and a trapezoid. This range is similar to the field data (as the shape of ridges 17 and 18 closely resembled a triangle and a trapezoid, respectively).

Table 5.1 summarizes the measured ridge cross-sectional areas and compares them to the target values.

In general, the areas of the ridges in the basin show reasonable agreement with the target values. The total area of ridges 17 and 18 in model scale units were 0.62 and 0.48 m^2 respectively. The total area of the ridges in the basin ranged from 0.42 m^2 to 0.74 m^2. (This range excludes ridge 1-4 which was intended to be larger than the target ridges).

Tests were also conducted with some ridges that were comprised of unconsolidated material only (i.e. ridges 2-5 N and 3-5 N) and of consolidated material only (i.e. ridges 2-4 S, 2-4 N, 3-4 S, and 3-4 N). The areas of these ridges also show reasonable agreement with the respective individual portions of the target ridges.

It is interesting to compare the total area of ridge 2-5 (i.e. 0.46 m^2) with the unit volume of ice put into the ridge (i.e. 0.3 m^3/m width of the basin). As this ridge was comprised of unconsolidated material only, the above areas may be used to obtain a measure of the bulk porosity of the ridge. A bulk porosity of 35% is indicated.

TABLE 5.1
SUMMARY OF MODEL SCALE RIDGE CROSS-SECTIONAL AREAS

Target Full Scale Ridges (in model scale units):

Ridge	Cons. Layer	Total Area
17	0.16 m^2	0.62 m^2
18	0.10 m^2	0.48 m^2

Ridges In IMD Basin:

Ridge	Vol. (m^3/m of basin width) of Ice Used to Make the Ridge			Vol. (m^3/m of basin width) of Ridge Measured During Tests	
	Cons. Layer	Uncons. Layer	Total	Cons. Layer (Computed as per Table 4.7)	Total
1-1	Not measured			0.17	0.56[2]
1-4	Not measured			0.43[1]	0.77[1,2]
2-1 N	0.09	0.21	0.3	0.12	0.42
2-2 N	0.045	0.26	0.3	0.12	0.46
2-3 N	0.045	0.26	0.3	0.17	0.61
2-4 N	0.17[3,6]	0[3,6]	0.17[3,6]	0.17[3,6]	0.17[3,6]
2-5 N	0[4]	0.3[4]	0.3[4]	0[4]	0.46[4]
2-1 S	0.07	0.21	0.3	Not Measured	
2-2 S	0.045	0.26	0.3	Not Measured	
2-3 S	0.045	0.26	0.3	Not Measured	
2-4 S	0.17[3,6]	0[3,6]	0.17[3,6]	0.17[3,6]	0.17[3,6]
3-1 N	0.045	0.26	0.3	0.10	0.56
3-2 N	0.045	0.26	0.3	0.11	0.74
3-3 N	0.09	0.21	0.3	0.13	0.70
3-4 N	0.04[5]	0[5]	0.04[5]	0.09[5]	0.09[5]
3-5 N	0[4]	0.3[4]	0.3[4]	0[4]	Not Meas.[4] But Expected to be Equal to that of 2-5N
3-1 S	0.045	0.26	0.3	0.17	0.66
3-2 S	0.045	0.26	0.3	0.14	0.67
3-3 S	0.09	0.21	0.3	0.19	0.68
3-4 S	0.04[5]	0[5]	0.04[5]	0.09[5]	0.09[5]

Notes:
1. The width of ridge 1-4 was approximately twice that of the target ridge. See Tables 4.7 and 2.4.
2. The total area was not measured for ridges 1-1 and 1-4. These values are the area of the keel only.
3. This ridge was comprised of consolidated material only and was formed by rafting two sheets about two hours prior to testing.
4. This ridge was comprised of unconsolidated material only and was formed about two hours prior to testing.
5. This ridge was comprised of consolidated material only and was formed by rafting two sheets prior to the second freeze.
6. The width of ridges 2-4 S and 2-4 N was inadvertently made to be approximately double the target value. See Table 4.7.

It is interesting to compare the total areas measured for ridges 3-2 S and 3-2 N. As these ridges were both insulated, these measurements provide an indication of the variation in ridge area that can be expected over the width of the basin. The variation in area for these two ridges is approximately 10%.

(ii) Thickness of Consolidated Layer:

Table 5.2 summarizes the mean thickness of the consolidated layer that was measured for each ridge. The mean thickness of the consolidated layer ranged from 44 mm to 107 mm. As listed in section 2.4, the target model scale thickness of the consolidated layer for ridges 17 and 18 was 24 mm and 47 mm respectively.

The factors affecting the thickness of the consolidated layer include:

a) the thickness and number of ice sheets used to form the consolidated layer (for method #2).

b) the presence of insulation on the ridge surface and the time at which it is removed.

Table 5.2 clearly shows that the former factor is very significant. For ridges which were insulated, the final consolidated layer thickness, C_f, can be predicted as follows:

$$C_f = C_i + C_{New}$$

where C_i = total thickness of ice sheet placed over rubble at time of formation of ridge

C_{New} = thickness added to consolidated layer during the second freeze

The thickness that was added to the consolidated layer during the second freeze (i.e. C_{New}) ranged from 23 mm to 49 mm for the sheet #2 ridges and from 23 mm to 36 mm for the sheet #3 ridges. The mean thickness of the level ice adjacent to the ridges in sheets 2 and 3 was 21 mm and 22 mm respectively. Thus, for first order predictions of the final consolidated layer thickness, it is suggested that C_{New} be taken as the target thickness of the adjacent ice sheet.

TABLE 5.2

AVERAGE MODEL SCALE THICKNESS OF CONSOLIDATED LAYER

RIDGE	FORMATION OF CONSOL. LAYER AT TIME OF RIDGE BUILDING			INSULATION ON RIDGE SURFACE		MEAN THICKNESS OF CONSOL. LAYER (mm)
	THICKNESS OF ICE SHEET (mm)	NO. OF ICE SHEETS USED	THICK. OF CONSOL. LAYER AT TIME OF FORMATION (mm)	R-VALUE	TIME OF REMOVAL (SEE NOTE 1)	
1-1	20	0 (Method #1 Used)		R8	+5 hrs.	80
1-4	20	0 (Method #1 Used)		0	n/a	107
2-1 N	20	2	40	R16	0	65
2-2 N	20	1	20	R16	0	59
2-3 N	20	1	20	R16	0	69
2-1 S	20	2	40	0	n/a	69
2-2 S	20	1	20	0	n/a	50
2-3 S	20	1	20	R16	0	53
3-1 N	20	1	20	R8	+4.5	47
3-2 N	20	1	20	R8	+4.5	44
3-3 N	20	2	40	R8	+4.5	63
3-1 S	20	1	20	0	n/a	84
3-2 S	20	1	20	R8	+4.5	56
3-3 S	20	2	40	0	n/a	93

Notes: 1. The above times of removal represent the time elapsed after the warmup period was commenced.

Generally, C_{Nev} was greater for sheet #2 than for sheet #3. This is believed to reflect the fact that the insulation mats were removed at the commencement of the warmup period for sheet #2 while they were removed 4.5 hours into the warmup period for sheet #3. Thus, it is believed that some additional ice growth occurred during the warmup period for sheet 2 while the insulation mats reduced this growth for sheet 3.

The presence of insulation mats on the ridge surface also affects the thickness of the consolidated layer. The ridges in sheet #1 and #3 follow the expected trend in that the consolidated layer is significantly thicker for non-insulated ridges. The ridges in sheet #2 are anomalous in that the thickness of the consolidated layer of non-insulated ridges is approximately equal, (or in one case, less) than that of insulated ridges. This is believed to reflect the fact that the insulation mats were removed at the commencement of the warmup period for sheet 2.

The R value of the insulation was varied from R8 to R16. A clear relationship between the thickness of the consolidated layer and the R value of the insulation is not evident in Table 5.2. This indicates that the other parameters that were varied (i.e. the ridge-building method and the time at which the insulation mats were removed) are more significant.

(iii) Strength of consolidated layer:

This is a difficult issue to quantify as full scale data are not available to define the bulk strength of the consolidated layer. Numerous investigators have conducted small scale tests both in-situ and on ice samples that were removed from the ridge. During the 1982 trials of the USCGC POLAR STAR (i.e. the reference event for this study) the ice salinity and temperature were measured and the flexural strength was inferred.

This paucity of data makes it difficult to define properties tests for model scale ridges that are meaningful.

Nevertheless, the strength of the consolidated layer is expected to be an important issue affecting the penetration energy and force. Therefore, some quantification of this parameter is necessary.

For this study, we elected to measure the flexural strength of the consolidated layer by conducting in-situ cantilever beam tests (as described in section 4). This test method has been used in the field for level ice and is commonly used in ice model-testing for level ice. It also has the practical advantages of being relatively simple and quick to perform. Furthermore, it is an in-situ test and thus disturbance of the model ice material is minimized.

During the warmup period for the sheet #2 tests, the compressive and shear strength of small ice blocks removed from the consolidated layer was measured using a hand-operated lever apparatus at the IMD. The ratio of the measured compressive and shear strengths to the measured flexural strength of the consolidated layer was similar to that which is typical for these index strengths in level ice. (D. Spencer, IMD, personal communication.)

It was hoped the Ice Strength Indexer (which was designed and tested by Melville Shipping Ltd., Baker et al, 1987) would be available for this test program. Unfortunately, this apparatus was too small for direct use (as it had been designed for use in level ice) and there was insufficient time within the IMD's schedule to modify it for use in this project.

The measured flexural strengths have been summarized in Table 4.8. This table is reproduced as Table 5.3. The average model scale, post-test, flexural strength ranged from 22.5 kPa to 79 kPa. These values represent a range of full scale strengths (using Froude scaling laws) from 430 kPa to 1500 kPa. These strengths are significantly higher than the strengths predicted by Geisel et al, 1982 for the field ridges (which are approximately 300 kPa). See section 2.3.

This indicates that the consolidated layer of the model scale ridges was too strong.

From visual observations, it was clear that the consolidated layer of the ridges was stronger than the adjacent level ice. However, the flexural strength of the adjacent level ice was typically low in relation to the predicted field values. The flexural strength of the level ice in the basin during the ridge penetration test period is considered to be about 10-15 kPa (which corresponds to an approximate full scale strength of 200-300 kPa). See section 4.2 for values. These values are somewhat below the range of average full scale level ice strengths (i.e. 260 to 440 kPa) predicted by Geisel et al, 1982. See section 2.3 for values.

The flexural strength of the consolidated layer was affected by the placement of insulation on the ridge surface. See Table 5.3.

For sheet #1, the flexural strength of a non-insulated ridge was measured to be approximately twice that of an insulated ridge (i.e. 42 kPa vs 23 kPa). This trend is repeated in the results from the sheet #2 tests although the difference in flexural strength between non-insulated and insulated ridges is not as large. See Table 5.3. This probably reflects the fact that the insulation mats were removed at the commencement of the warmup period and thus, all ridges were exposed to the same thermal conditions over a relatively long time period (i.e. about 10 hours).

Table 5.3
Summary of Model Scale Measured Flexural Strengths of Ridge Consolidated Layer

Sheet No.	Ridge No.	Average Flexural Strength (kPa)	Ridge Insulated ?
1	1-1	22.5 (post-test value)	Yes
1	1-4	41.8 (post-test value)	No
2	2-2N	93.0 (pre-test value)	Yes
2	2-3N	65.0 (post-test value)	Yes
2	2-1N	62.0 (post-test value)	Yes
2	2-1S	76.0 (post-test value)	No
3	3-3S	77.0 (post-test value)	No
3	3-3N	43.0 (post-test value)	Yes
3	3-2S	79.0 (post-test value)	Yes

Summary of Average Full Scale Ridge Flexural Strengths Used for Subsequent Analysis

Ridge No.	Ridge Insulated?	Ridge Flexural Strength (kPa)	Data Source
1-4	Yes	430	In-situ tests on ridge 1-1
1-4	No	800	In-situ tests on ridge 1-4
2-1N	Ridge consolidated layer partially cut in centre.		
2-2N	Yes	1210	Avg. of in-situ tests on ridge 2-1N and 2-3N
2-3N	Yes	1210	Avg. of in-situ tests on ridge 2-1N and 2-3N
2-4N	Ridge comprised of consolidated material only.		
2-5N	Ridge comprised of unconsolidated material only.		
2-1S	No	1450	In-situ tests on ridge 2-1S
2-2S	No	1450	In-situ tests on ridge 2-1S
2-3S	Ridge consolidated layer fully cut.		
2-4S	Ridge comprised of consolidated material only.		
3-1N	Yes	1170	Avg. of in-situ tests on ridges 3-3N and 3-2S
3-2N	Yes	1170	Avg. of in-situ tests on ridges 3-3N and 3-2S
3-3N	Yes	1170	Avg. of in-situ tests on ridges 3-3N and 3-2S
3-4N	Ridge comprised of consolidated material only.		
3-5N	Ridge comprised of unconsolidated material only.		
3-1S	No	1470	In-situ tests on ridge 3-3S
3-2S	Yes	1170	Avg. of in-situ tests on ridges 3-3N and 3-2S
3-3S	No	1470	1470 In-situ tests on ridge 3-3S
3-4S	Ridge comprised of consolidated material only.		

For sheet #3, this trend is less clear. The average flexural strengths were measured as 43 kPa and 79 kPa for insulated ridges (two separate ridges) and 77 kPa for a non-insulated ridge (one ridge only). Thus, it can be seen that the average strength of the insulated ridges was less than that of the non-insulated ridge. However, the data are highly scattered.

From visual inspection, it was clear that the consolidated layer of ridge 1-4 was significantly harder than that of ridge 1-1 and that of all the ridges in sheets 2 and 3. The consolidated layer of ridge 1-4 was formed by allowing loose ice rubble to consolidate during the second freeze. It is believed that these ice blocks were bonded together with ice that was primarily unseeded. This would help to explain the hardness of ridge 1-4. One of the reasons for the change in ridge-building method for the ridges in sheets 2 and 3 (from method #1 to method #2) was to reduce the hardness of the ridge's consolidation layer.

It is interesting to note that the measured flexural strength of ridge 1-4 was less than that for the sheet #2 and #3 ridges. This indicates that the flexural strength is not a reliable index of the hardness of the consolidated layer.

5.2 Prediction of Ridge Penetration Force From Model Tests

The maximum full scale ridge penetration force was 4.8 MN and 5.7 MN for ridges 17 and 18 respectively. See Table 2.2. The respective maximum ridge penetration forces in model scale units (using Froude scaling laws) are 689 N and 818 N.

Table 4.10 has summarized the maximum ridge penetration forces that were measured during the model tests. The maximum ridge penetration force measured during the model tests varied from 337 N to 1179 N for tests in partially-consolidated ridges. This range excludes ridge 1-4 (for which a maximum penetration force of 1252 N was measured) as the consolidated layer of ridge 1-4 was very hard.

Thus, it can be seen that the ridge penetration forces measured in the laboratory bracket the values expected from the field data (using Froude scaling laws).

Direct comparisons are not possible, however. The model tests were conducted at constant speed whereas the ship decelerated in the field. This would be expected to cause the model tests to overpredict the ridge penetration force.

Furthermore, the consolidated layer of many of the ridges in the laboratory was too thick and too strong (in flexure) in relation to the field ridge. This would also be expected to cause the model tests to overpredict the ridge penetration force.

5.3 Prediction of Ridge Penetration Energy From Model Tests

Two general ridge modelling methods have been tried as follows:

(a) **Partially-consolidated ridges** have been produced and penetrated by the ship. Each of these ridges consisted of a consolidated and an unconsolidated portion.

(b) **Segmented ridges** have been produced which were comprised of unconsolidated and consolidated material only. Separate ramming tests were conducted for each portion of the ridge.

The test results obtained from both of these test types are discussed separately in the following sections. Froude scaling laws have been used throughout to compare model scale values and full scale data. Furthermore, the geometric scale of the model (i.e. 19.1:1) has been used to establish the scale factor. (This practice is presently common in ice model-testing). Therefore, the following discussion is specific to this scaling procedure.

5.3.1 Partially-consolidated Ridges

(i) Effect of ridge cross-sectional area:

Figures 5.1 and 5.2 compare the ridge penetration energy predicted from the model tests with the field data for ship penetration distances of 0.33 LWL and 0.67 LWL respectively.

A clear trend is not evident and the data are highly scattered. This reflects the facts that the ridge cross-sectional area was not varied over a wide range, and that other factors (e.g. ice-model friction factor, and the thickness of the consolidated layer) were also varied.

The full scale penetration energy predicted for ridge 1-4 is significantly higher than that for other ridge tests with the same ice-model friction factor. This is believed to reflect the fact that the consolidated layer of this ridge was very hard. Therefore, this data point is considered to be anomalous.

(ii) Effect of the mean thickness of the consolidated layer:

Figures 5.3 and 5.4 show the relationship of the ridge penetration energy to this parameter for ship penetration distances of 0.33 LWL and 0.67 LWL.

As would be expected, the ridge penetration energies predicted by the model tests generally increase with the mean thickness of the consolidated layer. This trend is evident for the tests done at both ice-model friction factors and for both ship penetration distances that were considered (i.e. 0.33 LWL and 0.67 LWL).

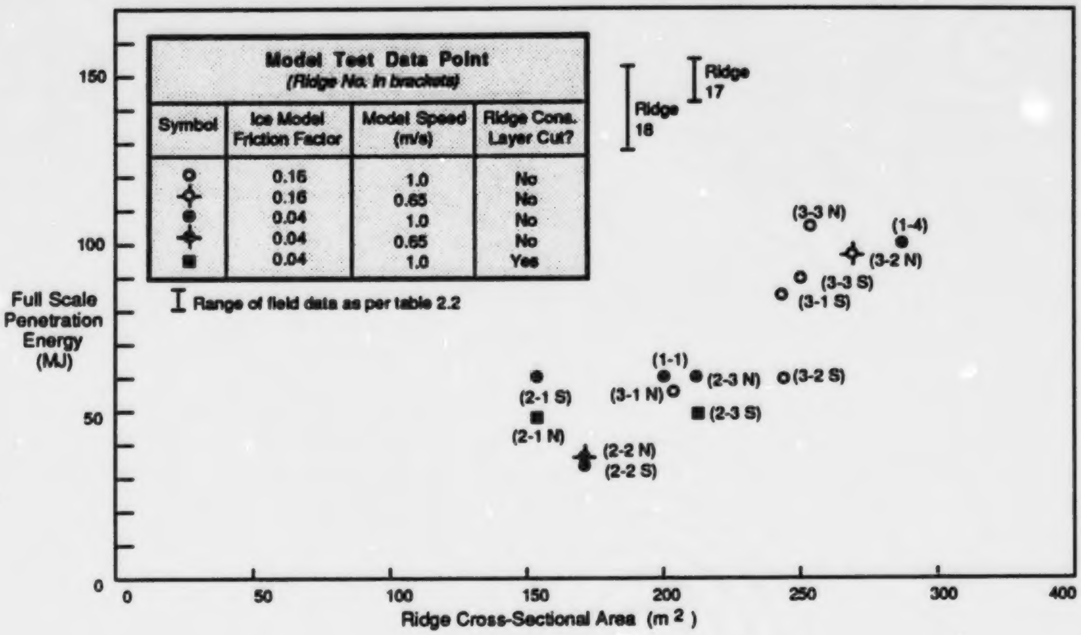

Figure 5.1

Penetration Energy vs. Ridge Cross-Sectional Area: Ship Penetration Distance = 0.33 LWL

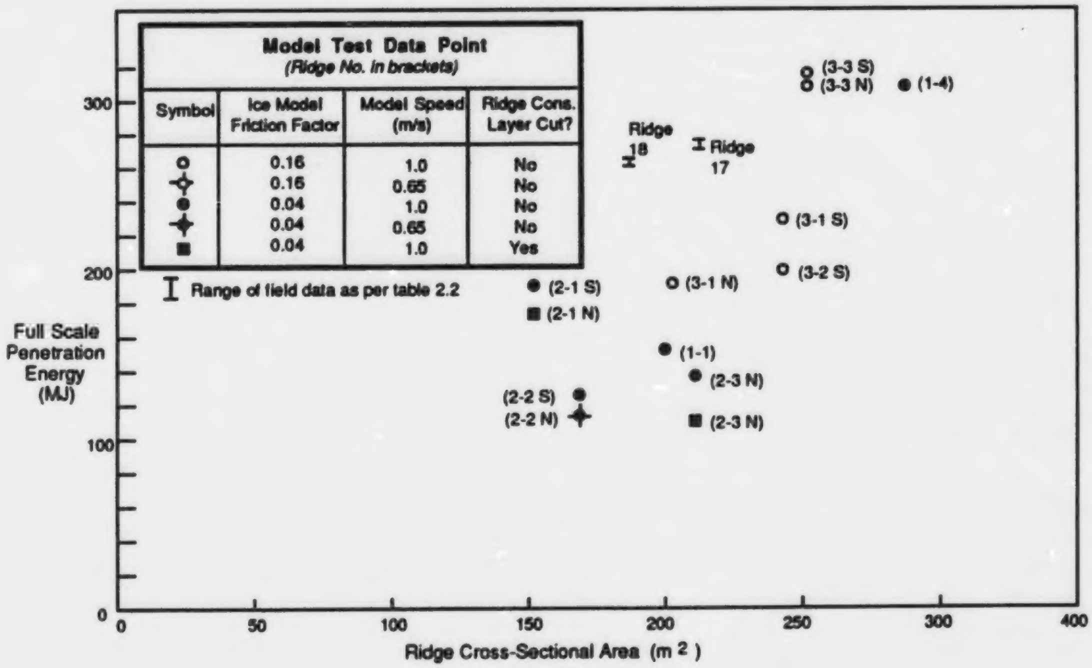

Figure 5.2

Penetration Energy vs. Ridge Cross-Sectional Area: Ship Penetration Distance = 0.67 LWL

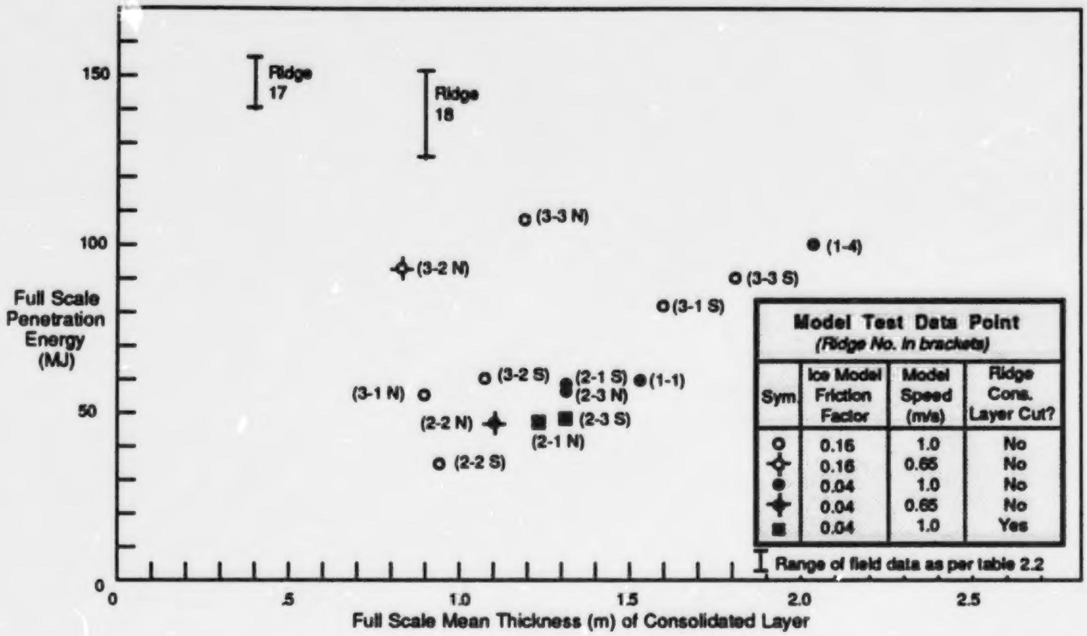

Figure 5.3

Penetration Energy vs. Mean Thickness of Consolidated Layer: Ship Penetration Distance = 0.33 LWL

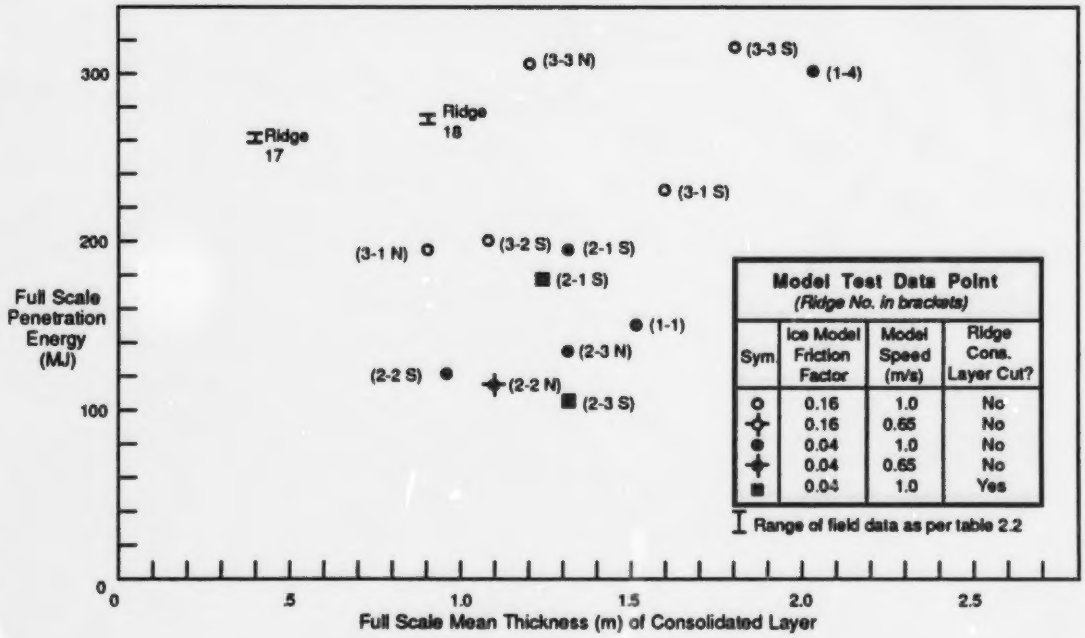

Figure 5.4

Penetration Energy vs. Mean Thickness of Consolidated Layer: Ship Penetration Distance = 0.67 LWL

It is difficult to make direct comparisons between the penetration energy and the mean thickness of the consolidated layer as the total cross-sectional area of the ridge was also varied during the model tests. To gain further understanding, the penetration energies measured during the model tests have been normalized to the cross-sectional area of ridge 18. The procedure used to normalize the model test data is summarized below:

Full scale area - normalized penetration energy = Full scale penetration energy predicted from model tests

$$x \; \frac{\textbf{Extrapolated full scale cross-sectional area of model scale ridge}}{\textbf{Measured full scale cross-sectional area of ridge 18}}$$

This analysis procedure implicitly assumes that the penetration energy is linearly related to the cross-sectional area of the ridge.

Figure 5.5 shows the relationship of the area-normalized penetration energy to the mean thickness of the consolidated layer. For each ice-model friction factor that was tested, the model test data indicate a clear trend of increasing penetration energy with increasing mean thickness of the consolidated layer.

(iii) Effect of model speed:

Most of the tests were conducted at a constant model speed of 1 m/s (i.e. 4.4 m/s full scale). For two ridges (i.e. ridges 2-2N and 3-2N), the ship speed was reduced to 0.65 m/s (i.e. 2.8 m/s full scale).

The predicted penetration energies for these ridges are plotted on Figures 5.1 to 5.4 for comparison with the other tests that were done at higher speed. There does not appear to be a significant difference between the data obtained for the high speed and the low speed tests.

This indicates that the ridge penetration energy does not depend greatly on the model speed over the range of model speeds that were tested.

(iv) Effect of the flexural strength of the ridge's consolidated layer:

Figures 5.6 and 5.7 show the relationship of the full scale penetration energy predicted by the model tests to this parameter for ship penetration distances of 0.33 LWL and 0.67 LWL respectively.

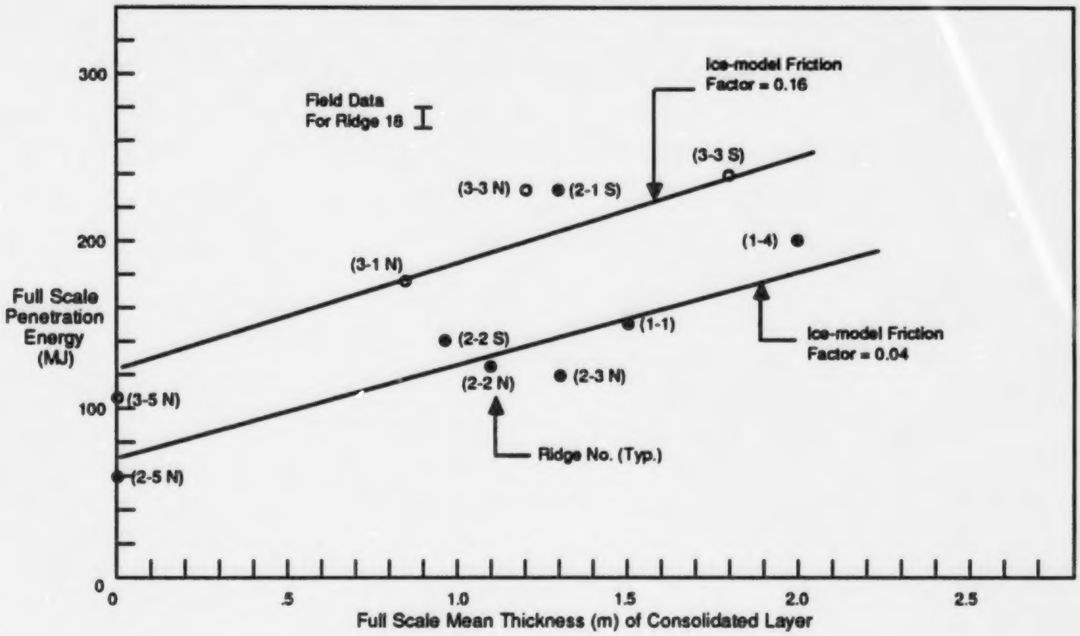

Notes:

1. Model speed = 1 m/s for all tests.
2. See text for normalizing procedure

Figure 5.5

Area-Normalized Penetration Energy Vs. Mean Thickness of Consolidated Layer: Ship Penetration Distance = 0.67 LWL

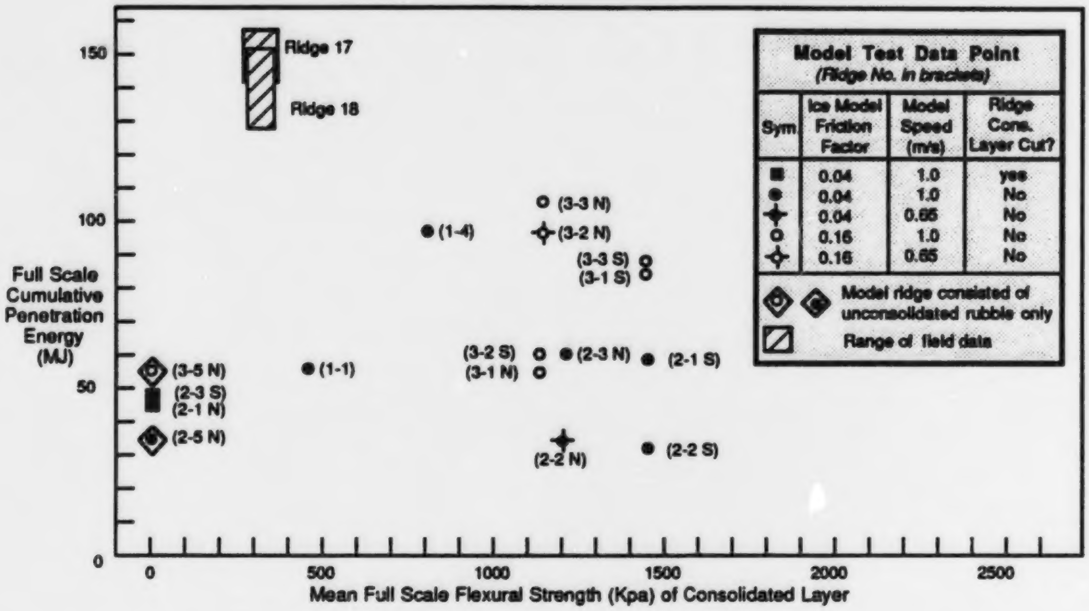

Figure 5.6

Relationship of Full Scale Ridge Penetration Energy To Flexural Strength of Consolidated Layer
Ship Penetration Distance = 0.33 LWL

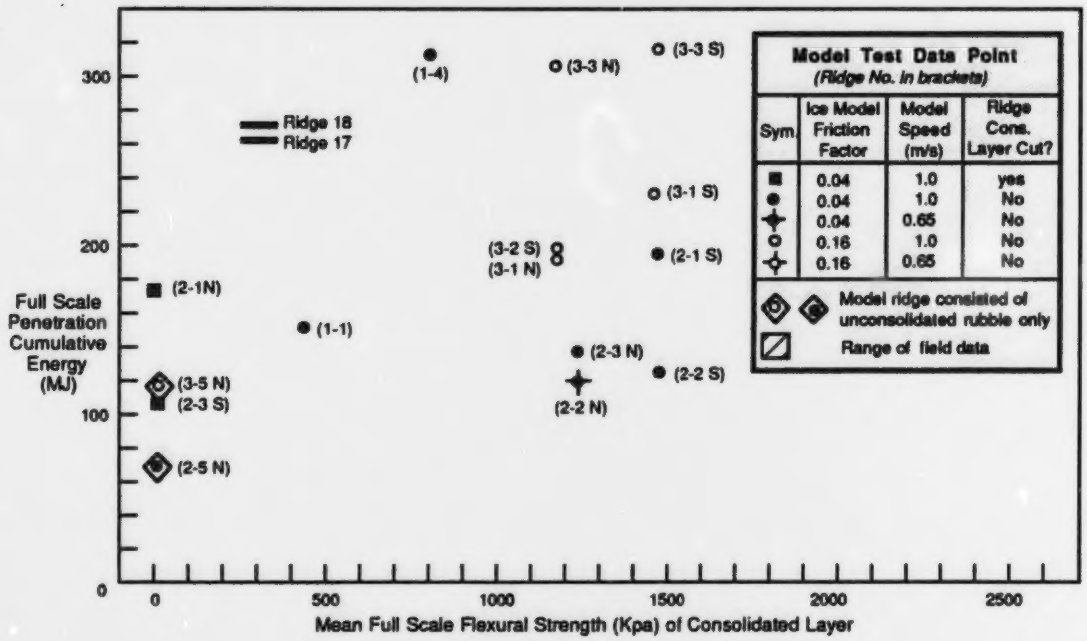

Figure 5.7

Relationship of Full Scale Ridge Penetration Energy To Flexural Strength of Consolidated Layer
Ship Penetration Distance = 0.67 LWL

A clear trend is not evident and the data are highly scattered. These data suggest that the ridge penetration energy is independent of the flexural strength of the consolidated layer.

This indicates that the influence of other parameters that were varied for these tests (i.e. ice-model friction, total area of the ridge, and the mean thickness of the consolidated layer) are more significant.

(v) Effect of ice-model friction:

The ice-model friction factor was 0.04 and 0.16 for tests done in sheet #1 and sheet #2, and for tests done in sheet #3, respectively.

Figures 5.1 to 5.7 show that the ridge penetration predicted by these tests is highly dependent on the ice-model friction factor. In each figure, the test data are clearly grouped by the ice-model friction factor. As would be expected, higher ridge penetration energies are predicted by the model tests done with a higher ice-model friction factor.

The effect of the ice-model friction factor on the penetration energy is also evident from a review of Figures 5.8 and 5.9. (These figures depict the results of the tests done in segmented ridges and are discussed in the next section).

The model test data indicate that the ridge penetration energy increased by a factor of about 1.5 to 2 when the ice-model friction factor was increased from 0.04 to 0.16.

5.3.2 Segmented Ridges

Tests were conducted in which the two components (i.e. the consolidated and unconsolidated portions) of the target field ridge (which was partially consolidated) were modelled and penetrated separately.

Figures 5.8 and 5.9 plot the full scale cumulative penetration energy predicted by these tests for ice-model friction factors of 0.04 and 0.19 respectively. The field data for ridge 18 are also plotted in this figure for comparison.

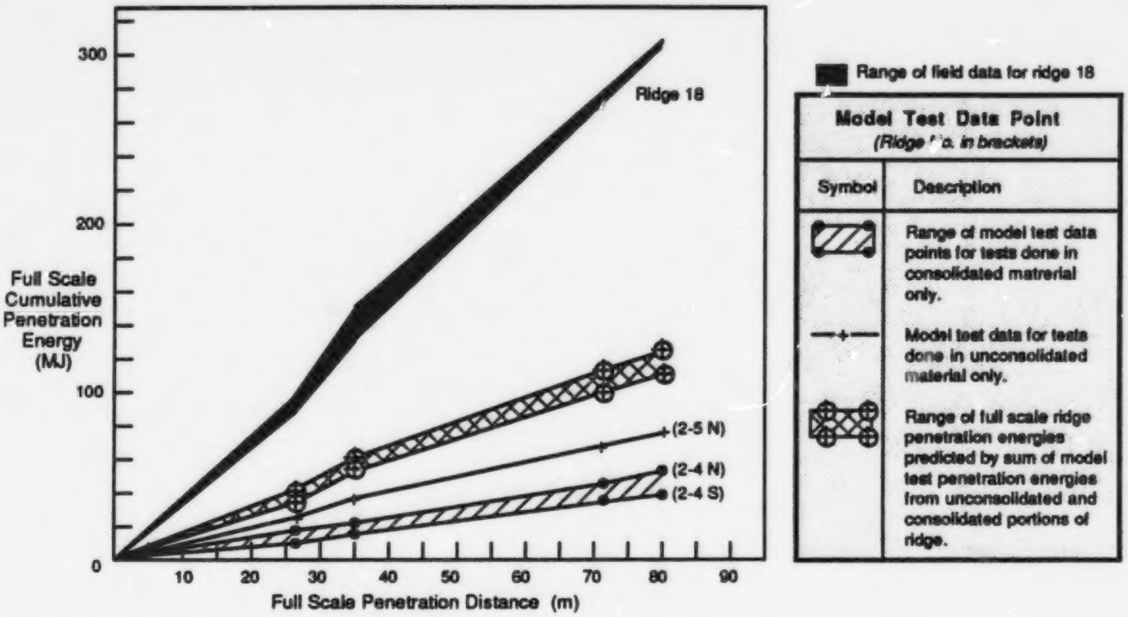

Figure 5.8
Ridge Penetration Energy As a Function of the Penetration Distance:
Ice Model Friction Factor = 0.04

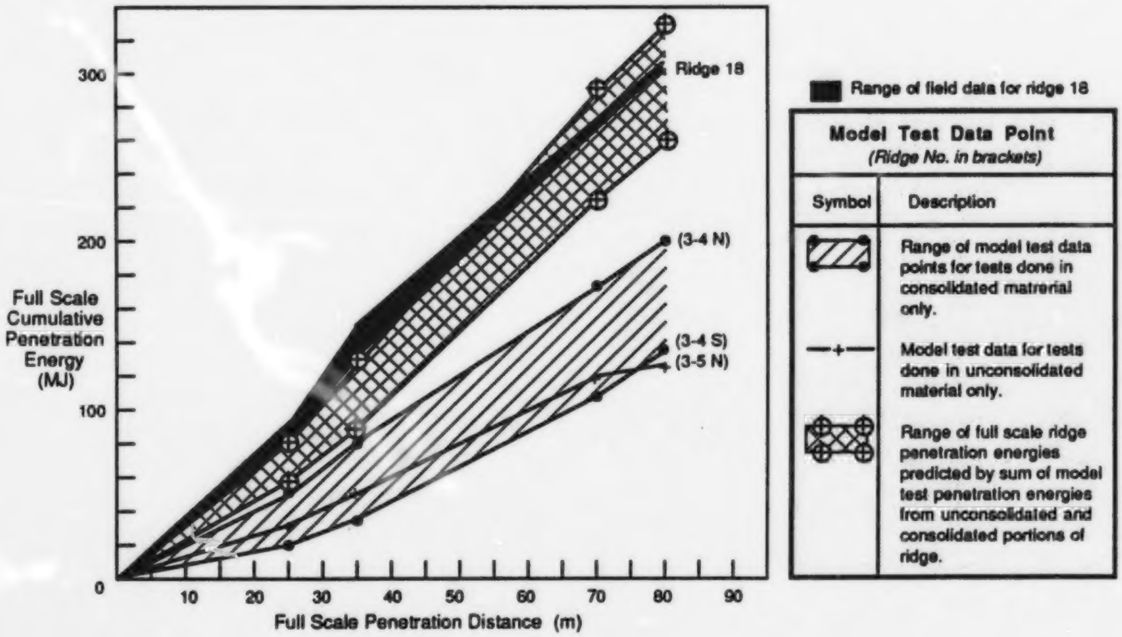

Figure 5.9
Ridge Penetration Energy As a Function of the Penetration Distance:
Ice Model Friction Factor = 0.16

The table below also compares the penetration energies predicted by these model tests with the field data:

Ice-Model Friction Factor	Ship Penetration Distance	Ratio of Penetration Energies Predicted by Model Tests To The Field Data for Ridge 18		
		Penet.Energy For Consol.Layer From Model Tests	Penet.Energy For Unconsol. Layer From Model Tests	Sum of Penet. Energy For Unconsol & Consol.Ridges in Basin
		Total Penet. Energy for Field Ridge	Total Penet. Energy for Field Ridge	Total Penet.Energy for Field Ridge
0.04	0.33 LWL	0.12 - 0.17	0.24 - 0.28	0.36 - 0.46
0.04	0.67 LWL	0.12 - 0.17	0.24	0.36 - 0.41
0.16	0.33 LWL	0.24 - 0.53	0.35 - 0.42	0.54 - 1.05
0.16	0.67 LWL	0.39 - 0.62	0.44	0.81 - 1.07

The above values span the range of ridge startpoints that were assumed in reducing the field data (see Section 2.3) and the range of penetration energies measured during the model tests for the two purely-consolidated ridges that were penetrated (see Figures 5.8 and 5.9).

The penetration energies measured during the model tests for ridges 3-4N and 2-4N were higher than those measured for ridges 3-4S and 2-4S, respectively. This reflects the fact that the former ridges were tested before the latter (by as much as an hour) and thus, the latter ridges were more deteriorated.

This difference is most pronounced for the ridges in sheet #3. The purely-consolidated ridge in sheet #2 was formed about two hours prior to testing, and thus the ice was well-tempered when the ridge was formed. On the other hand, the purely-consolidated ridge in sheet #3 was formed prior to the second freeze. Thus, it is unlikely that the ice in this ridge was tempered to the same degree as for the sheet #2 ridge.

It was noted visually that the two ice sheets comprising these purely-consolidated ridges were bonded together more strongly for the ridge in sheet #3. This is to be expected as the ridge in sheet #3 had been subjected to a freeze and tempering process whereas the ridge in sheet #2 had not.

It is believed that this difference has contributed to the greatly increased resistance, and hence penetration energy, that was measured for ridges 3-4N and 3-4S in comparison to ridges 2-4N and 2-4S (see Figures 5.8 and 5.9).

5.3.3 Comparison of Test Results With Numerical Prediction of Ridge Penetration Energy Predictor Done by Stubbs et al, 1986

Recently, a simple, semi-empirical numerical predictor of ridge penetration force has been developed by Stubbs et al, 1986. This predictor is based on regression analyses of full scale ridge penetration tests for several icebreaking ships. The 1982 ramming tests conducted with the USCGC POLAR STAR (which were selected as the full scale reference data set for this study) were one of the sets of full scale data that were included in the regression. This predictor has the following form:

$$R_{TOT} = R_{OW} + R_{CONS} + R_{UNCONS}$$

where R_{TOT} = total resistance of ridge

R_{OW} = open water resistance

R_{CONS} = resistance of consolidated layer of ridge

R_{UNCONS} = resistance of unconsolidated layer of ridge

The open water resistance was neglected by Stubbs et al, 1986 in making their predictions.

The resistance of the consolidated layer was predicted by considering it to be equal to the pure level ice resistance of the ship for an ice sheet equal in thickness to the average thickness of the consolidated layer. This was done for a ship speed equal to that at which the ship contacted the ridge. For reduction and analysis of the 1982 USCGC POLAR STAR data, the level ice resistance data measured during those same field trials were used to determine the resistance of the consolidated layer of the ridge (J. Stubbs, Wartsila, personal communication).

The resistance of the unconsolidated material was then determined, as follows:

R_{UNCONS} = Measured total resistance of ship during field tests (i.e. R_{TOT})

- Predicted resistance of ship in level ice of equal thickness to the mean thickness of the consolidated layer at a ship speed equal to the speed at which the ship contacted the ridge (i.e. R_{CONS}).

The ridge penetration energy was determined by numerically integrating the force-displacement curves, as shown schematically on Figure 5.9.

The penetration energies measured during the model tests done in ridges comprised of unconsolidated material only (i.e. ridges 2-5N and 3-5N) have been compared to the prediction of "pure ridge" penetration energy to Stubbs et al, 1986. (These predictions were intended to quantify the penetration energy of the unconsolidated material only of the full scale ridges).

For these comparisons, the penetration energies measured during the model tests have been computed using the same approach as Stubbs et al, 1986 to define the region of the force-displacement curve over which the ridge was penetrated. See Figure 5.10.

The table below summarizes these model scale data and extrapolates them to full scale values using Froude scaling laws.

Ridge	Model Scale Penetration Energy (N.m)	Extrapolated Full Scale Penetration Energy (MJ)
2-5N	536	71
3-5N	1023	136

Figure 5.11 compares the extrapolated model scale results with the predictions of Stubbs et al, 1986.

The agreement between the model test results and the predicted values is encouraging. The model test results for the two ice-model friction factors that were tested bracket the predicted value and the discrepancy is approximately ± 30%.

5.3.4 Comparison of Model Test Results with Field Data

Figures 5.1 to 5.9 compare the model test results with the field data.

The following discussion is based on an acceptance of the model test and field test data at face value.

(i) Model tests with partially-consolidated ridges:

The model test results generally underpredict the field data.

For ridges which approximated the cross-sectional area and the mean thickness of the consolidated layer of the target field ridges, the penetration energy predicted by the model tests was about 30% and 60% of the field value for the model tests done at low and high friction factors, respectively. See Figures 5.1 to 5.5. It should be remembered that the flexural strength of the consolidated layer of these model ridges was too strong in relation to the predicted strength of the field ridges (by a factor of about 2 to 5). See section 4 for discussion.

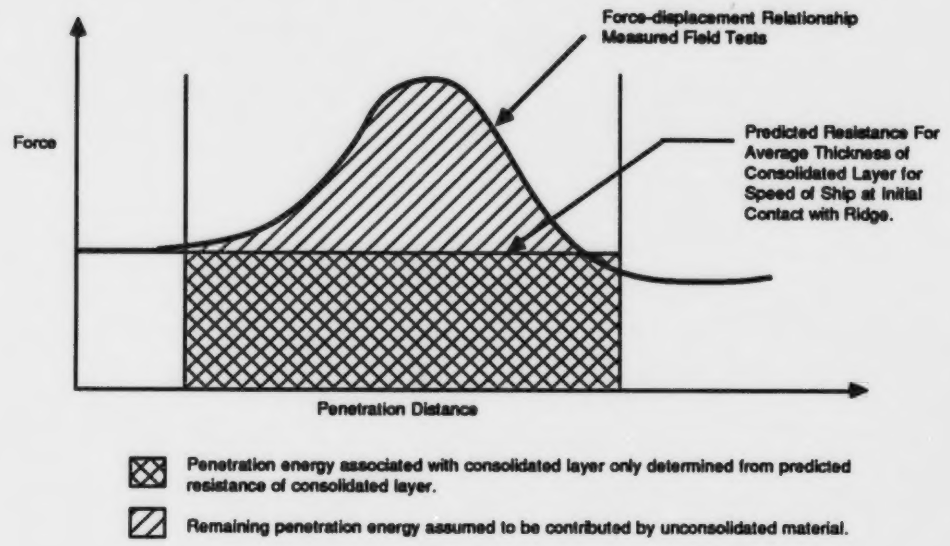
Force-displacement Relationship
Measured Field Tests
Predicted Resistance For
Average Thickness of
Consolidated Layer for
Speed of Ship at Initial
Contact with Ridge.
Force
Penetration Distance
Penetration energy associated with consolidated layer only determined from predicted resistance of consolidated layer.
Remaining penetration energy assumed to be contributed by unconsolidated material.

Figure 5.10

Schematic Representation of Analysis Technique Used To Develop The Stubbs et al, 1986 Predictor

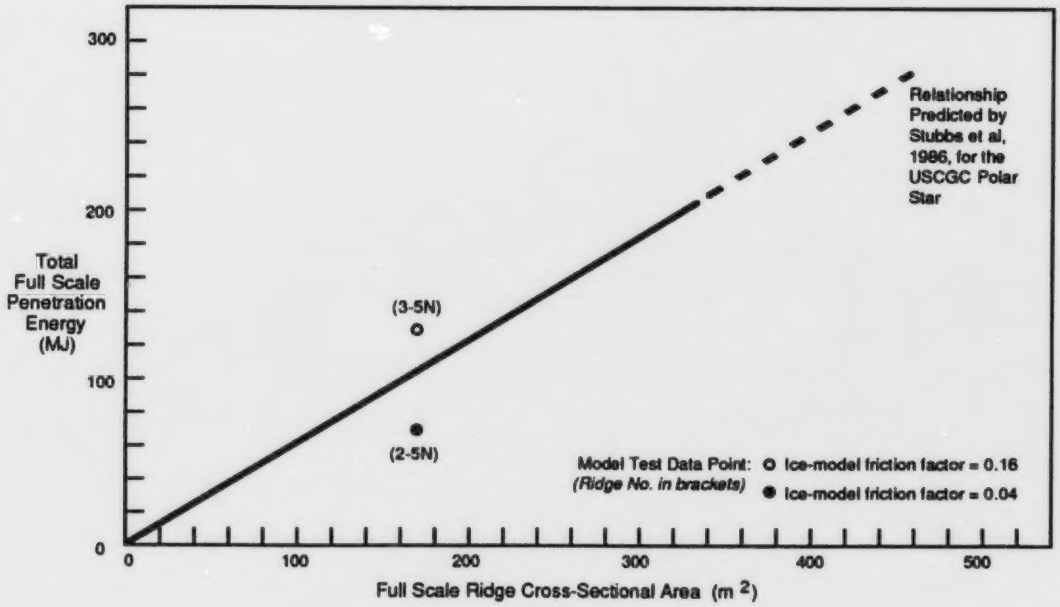

Figure 5.11

Penetration Energy for Unconsolidated Material Only

This modelling inaccuracy would tend to cause the model test results to overpredict the penetration force, and hence, energy. Thus, despite the fact that the ridges were too strong, the ridge penetration energy measured in the field was significantly underpredicted by the model tests.

Better agreement between the model test and field results was obtained for the model tests done in ridges with cross-sectional areas, and consolidated layer thicknesses, that exceeded those of the target field ridges. This is to be expected as each of these factors would increase the force, and hence the energy, necessary to penetrate the ridge in the model tests.

(ii) Model Tests in segmented ridges:

The total penetration energy predicted by the model tests (i.e. the sum of the penetration energies for the purely consolidated and purely unconsolidated model ridges) agreed with the measured field data within about ±20% for the model tests done at a high friction factor (i.e. 0.16). For the model tests done at a low friction factor (i.e. 0.04), the total penetration energy predicted by the model tests was about 50% of the measured field data. See Figures 5.8 and 5.9.

The relative contribution of the unconsolidated and consolidated portions of the ridge to the total penetration energy is also of interest. The measured field data, and predictions of the resistance of the consolidated layer based on predictions of level ice resistance, suggest that the consolidated layer of ridge 18 (which was the field ridge simulated during these model tests) contributed about 75% of the total penetration energy of the ridge. See Figure 2.6.

The model test results indicate that the unconsolidated material contributed a greater proportion of the total penetration energy. The energies required to penetrate the unconsolidated and consolidated ridges were about equal in the model tests.

It should be recognized that it is very difficult to make firm comparisons. Analytical techniques to predict the penetration force and energy of the consolidated layer of the ridge and of the composite ridge, are still at an early stage of development and have not been verified. The use of theories intended to predict the level ice resistance of the ship to predict the resistance of the consolidated layer can only be considered to be a first-order solution to the problem.

(iii) Effect of uncertainties in the field data;

Numerous uncertainties inherent in the field data used as a reference for this study are described in section 2. These include:

a) discrepancies between the horizontal force measured during the field tests before the ship contacted the ridge (while it was transitting level ice) and the predicted level ice resistance of the ship. The measured horizontal force is greater than the predicted level ice resistance by a factor in excess of 2.

   As described in section 2, this discrepancy is sufficient to account potentially for about 35% of the penetration energy measured during the field tests.

   This is a large amount in relation to the observed differences between the model test and field test results (The ridge penetration energies predicted by the model tests were about 30% and 60% of the measured field data for the model tests done at low and high friction factors, respectively).

b) uncertainties in the ice-hull friction factor. The average friction factors measured by tests conducted with a sliding arm and rotating arm tribometer were 0.045 and 0.20 respectively. The method used in the model tests to measure the friction factor more closely resembled the field sliding arm tribometer (as the ice was slid along the surface without causing it to crush).

   In an effort to bound this uncertainty, model tests were conducted at two friction factors (i.e. 0.04 and 0.16).

   Generally, the model tests conducted at the higher friction factor provided better agreement with the ridge penetration energy measured during the field tests.

c) an imbalance between the sail and keel areas measured for ridge 18 in relation to that required for isostatic equilibrium. Computations based on this principle and the measured sail area suggest that a keel area about 30% greater than the measured value would have been required to maintain isostatic equilibrium.

   This effect would tend to cause model tests conducted with the scaled field ridge to underpredict the measured field penetration energy.

d) The presence of an anomaly in the consolidated layer of ridge 17. Over the 15 to 25 m (i.e. 50 to 80 ft) baseline, the consolidated layer is very thick and triangular in shape. The longitudinal extent of the consolidated mass is not known. It may be that the measured area of consolidated ice overestimates that effectively "seen" by the ship. If this were the case, then model tests which scaled the overall area of the consolidated layer would be expected to overpredict the ridge penetration energy.

The net effect of these uncertainties on the observations presented in the previous discussion is unclear. Unfortunately, they limit the strength of the conclusions that can be drawn from the study.

6.0 CONCLUSIONS AND RECOMMENDATIONS

6.1 Ridge Building and Testing Techniques

The following conclusions may be drawn from the test program and the following recommendations are made:

(a) The approach of separately determining the penetration energy of the consolidated and unconsolidated portions of a partially-consolidated ridge appears to provide comparable accuracy to that of modelling and testing both of these portions of the ridge together. It should be recognized that this conclusion is specific to the tests conducted in this program and that the strength of this conclusion is limited by uncertainties in the field data. It is recommended additional field data be obtained and additional model tests be conducted.

(b) Both method #1 and method #2 (see Sections 4 and 5 for description) are practical means for building partially-consolidated ridges in the basin.

(c) For the formation of partially-consolidated ridges in the basin, method #2 is considered to be preferable to method #1. Method #2 produced ridges that provided better scaling of the target ridges and provided better control of the ridge properties.

(d) The natural cross-sectional shape of model scale ridges is bounded by a trapezoid and a triangle. This is the same range found in the field. The cross-sectional profile of field ridges varies significantly both from ridge to ridge and over the length of an individual ridge. Thus, operations to shape the profile of ridges in the basin are not considered to be necessary unless the objective of the model tests is to duplicate exactly a field event that is very well-documented.

(e) The cross-sectional area of ridges produced in the basin may be predicted with reasonable accuracy based on measurements of the unit volume (i.e. volume of ice per unit width of the basin) of ice initially put into the ridge and an assumed porosity of about 40%.

(f) The variation in ridge cross-sectional area over the width of the basin was about 10% based on the results of two profiles for one ridge.

(g) The thickness of the consolidated layer can be controlled to a reasonable degree of accuracy by controlling the thickness of ice which is placed over the rubble and by the placement of insulation mats on the ridge surface. The time of removal of the insulation mats, in relation to the commencement of the warmup period, is another factor that affects the thickness of the consolidated layer. The thickness of the consolidated layer was not affected significantly by the R-value of the insulation (which was varied from R8 to R16 during the test program).

(h) The flexural strength of the consolidated layer of the ridges was significantly greater than that of the adjacent level ice. Typically, the consolidated layer was too strong (by a factor of about 2 to 5) in relation to the target field ridge while the adjacent level ice was too weak (by a factor of about 1.5) in relation to the target field case.

(i) The flexural strength of the consolidated layer may be controlled somewhat by the placement of insulation mats on the ridge surface. However, the control of this property is difficult.

(j) The flexural strength is not considered to be a reliable index of the hardness of the consolidated layer.

(k) The measurement of ridge properties is a difficult issue. Further work is required both at full scale and at model scale to develop tests that provide reliable and simple descriptors of the ridge properties that are meaningful to ship transit.

During this project, emphasis was placed on measuring basic ridge properties. The size and shape of the ridges along with the thickness of the consolidated layer were given highest priority. Tests were also conducted to measure the flexural strength of the consolidated layer and to measure the bulk density of the ridge.

It may also be valuable to characterize the piece size distribution in the ridge and the shear strength of the unconsolidated layer.

On the other hand, it should be recognized that the measurement of ridge properties is time-consuming and the properties of the ridges change greatly with time. Therefore, the reliability of ridge properties tests is questionable unless they are performed soon after the ridge has been penetrated by the ship.

This is an area where further research is warranted.

(l) The tests have indicated that the penetration energy is not affected significantly by the ship speed over a range of model scale speeds from 0.65 to 1.0 m/s. This suggests that it may not be necessary to conduct reducing-velocity tests to model ridge ramming events.

This conclusion is tentative and it is recommended that further tests be conducted before constant-speed tests be adopted as standard practice for ridge modelling work.

6.2 Quantitative Prediction of Ridge Penetration Energy From Model Tests

Froude scaling laws have been used throughout to compare model test data with full scale data. Furthermore, the geometric scale of the model (i.e. 19.1:1) has been used to establish the scale factor. Therefore, the conclusions below are specific to this scaling procedure.

6.2.1 Relationship of Ridge Penetration Energy to Test Parameters Observed from Model Test Results in Partially-Consolidated Ridges

(a) Cross-sectional area - A clear trend was not observed. This is believed to reflect the fact that the ridge area was not varied over a wide range and other parameters (eg. size and strength of the consolidated layer) were also varied during the tests.

(b) Mean thickness of consolidated layer - The ridge penetration energy increased significantly with the mean thickness of the consolidated layer.

(c) Friction - The ridge penetration energy is greatly dependent on the ice-model friction factor.

(d) Ship Speed - The effect of ship speed on ridge penetration energy was insignificant over the range of ship speeds tested (i.e. 2.8 to 4.4 m/s full scale).

(e) Flexural strength of the consolidated layer - the model test data indicates that the penetration energy is weakly dependent on the flexural strength of the consolidated layer. However, this relationship is highly scattered reflecting the variations in other properties (thickness of consolidated layer) that occurred.

In summary, the parameters that had the greatest effect on the ridge penetration energy were:

a) the ice-model friction factor
b) the mean thickness of the consolidated layer

It is also believed that the cross-sectional area of the ridge is an important parameter. However, this parameter was not varied over a large range during the project. Therefore, firm conclusions can not be drawn regarding the significance of this parameter.

6.2.2 Comparison of Model Tests Results with Numerical Predictions by Stubbs et al, 1986 of the Penetration Energy for Unconsolidated Material

The model tests results obtained for the two ice-model friction factors that were tested bracket the numerical predictions by approximately ±30%.

6.2.3 Results of Model Tests In Segmented Ridges and Relative Penetration Energies for Purely Consolidated and Unconsolidated Ridges

The model test results indicated that:

a) for the field event that was simulated (i.e. the ramming of ridge 18), the energies required to penetrate purely consolidated and purely unconsolidated ridges, which scaled the respective portions of ridge 18, are approximately equal.

The measured field data, and computations of the energy required to penetrate the consolidated layer only based on the predicted level ice resistance of the ship, suggest that the energy required to penetrate the consolidated layer was approximately three times that required to penetrate the unconsolidated material.

Thus, the model test results suggest that the unconsolidated material appear to contribute a significantly greater proportion of the total penetration energy than do the field data of ridge 18.

It should be recognized that this conclusion is tentative as the use of a predictor of level ice resistance to predict the penetration energy of the consolidated portion of the ridge is unproven.

b) the correlation observed between the total penetration energy measured in the field for ridge 18 and the sum of the penetration energies predicted by model tests in purely consolidated and purely unconsolidated ridges is greatly dependent on the ice-model friction factor.

For the tests done at a low friction factor of 0.04, the sum of the model test results is approximately 40% of the total penetration energy measured during the field tests.

For the tests done at a higher friction factor of 0.16, the sum of the model tests results bracket the total penetration energy measured in the field by about ±20%.

6.2.4 Quantitative Comparison of Model Test Results with Field Data

If the field data are accepted at face value, then the following conclusions may be drawn:

(i) Model-testing in partially-consolidated ridges

a) the model tests results underpredict the penetration energy.

For model tests which provided reasonable scaling of the ridge cross-sectional area, and of the mean thickness of the consolidated layer the results of model tests done at low and high friction factors of 0.04 and 0.16 predict ridge penetration energies that are approximately 30% and 60% respectively of the value measured in the field.

b) As would be expected, the model tests conducted with ridges that were larger than the scaled field ridges, and with ridges that had a thicker mean consolidated layer than the scaled field ridges provided better prediction of the penetration energy measured in the field.

Each of these effects would be expected to produce increased ridge penetration energies in the model tests.

c) The consolidated layer of the ridge was too strong in flexure in relation to the predicted field values for many of the model tests conducted. However, some tests were conducted in which the consolidated layer was pre-cut, or non-existent. The penetration energies predicted by these tests was less than that predicted for ridges with a strong consolidated layer.

In all cases, the model test data underpredicted the field measurements. As would be expected, the agreement between the field and model data was best for the model tests done with a high ice-model friction factor and for ridges with higher flexural strength.

In summary, the model test data underpredict the field data by a significant amount (i.e. 40 to 70% depending on the ice-model friction factor) for tests done in model ridges which provided reasonable scaling of the cross-sectional area and consolidated layer thickness of the field ridges. It should be noted that the flexural strength of the consolidated layer was too large (by a factor of about 2-5) for the above ridges.

As would be expected, closer agreement was observed between the model tests and field data for tests done with ridges that were too large in cross-sectional area or that had a consolidated layer which was too thick.

However, in all cases, the model test data underpredicted the field measurements of ridge penetration energy.

(ii) Model-testing in segmented ridges

a) See item (b) of section 6.2.3 for a comparison of the field and model test data.

b) The results of model tests in segmented ridges appear to provide comparable accuracy for the prediction of ridge penetration energy to that obtained from the conduct of model tests in partially-consolidated ridges.

Unfortunately, the strength of the above conclusions is limited by uncertainties in the field data, including:

a) the level ice resistance of the POLAR STAR is predicted to be significantly less (by a factor in excess of 2) than the horizontal force measured during the ramming tests before the ship contacted the ridge. This may indicate that the field data overpredict the ridge penetration energy.

b) the field data indicate a wide variation in the ice-hull friction factor depending on the technique used to measure this parameter.

c) the keel area measured for ridge 18 is too small in relation to the total ridge cross-sectional area to maintain isostatic equilibrium. Based on the measured profile of the sail and the consolidated layer, the computed keel area is approximately 30% greater than the measured area.

d) the consolidated layer of ridge 17 is unusual in that it is very thick and triangular over the 5 m to 25 m baseline. This may represent a local inclusion of multi-year ice. This raises questions regarding the proper procedure for scaling of the consolidated layer of this ridge.

The net effect of the above uncertainties is unclear, as summarized below:

Uncertainty	Trend Expected to Result from Uncertainty
a) discrepancy in level ice resistance and measurement of horizontal force	Will reduce the measured ridge penetration energy for the field tests which would contribute to better agreement between the model test and field test data.
b) Uncertainty in ice-hull friction factor	Unclear. Model tests conducted at two ice-model friction factors in an effort to bracket the field data.
c) Keel area for ridge 18	Model tests conducted with ridges that provided exact scaling of the measured field ridge cross-sectional profile will underpredict the field ridge penetration energy (as the actual field ridge was larger than the measured ridge).
d) Anomalies in consolidated layer of ridge 17	Model tests were conducted with ridges that had a mean consolidated layer thickness computed from the total area of consolidated ice in the profile. If not all of the consolidated ice was "seen" by the ship during the field ramming event (reflecting the fact that this mass might have been a local inclusion of multi-year ice), then the model tests are expected to underpredict the penetration energy measured in the field.

6.3 Recommendations

The work undertaken in this project represents the first time (to our knowledge) that efforts have been made to duplicate a field ramming event in partially-consolidated ridges in the ice model basin. The project has made a contribution towards understanding the accuracy of physical model tests in ice ridges and towards identifying preferred techniques for the construction of and testing of model ice ridges.

This project is a first step towards these objectives. We recommend that the following be undertaken to continue this work:

a) further model basin tests aimed at developing a standard technique for modelling the resistance of ridges. This would be performed by using the POLAR STAR model to determine the energies needed to penetrate a parametric series of model ridges in which shape, area and strength are varied systematically. The resulting scale of ridge penetration energies, when compared to the energies measured during full-scale ridge events for the POLAR STAR, would then permit the model ridges to be identified which best simulated the resistance of the corresponding field ridges. The results would thus provide a scientific basis for modelling ridges for use in standardized model tests.

b) similar ridge modelling tests to duplicate field ramming events for other ships. Field ridge ramming data have been collected for the MV KIGORIAK and the MV POLAR STERN. Unfortunately, the former data are confidential to Dome Petroleum Limited while the latter data were collected in ridges that were totally unconsolidated. Nevertheless, each of these data sets are relatively complete and have been documented relatively well. Thus they have the potential to provide reference data for a similar series of ridge modelling tests. Further ridge modelling tests would extend the results of the present study to other ships. This would be valuable and is recommended.

c) ridge modelling tests should be conducted using MOD-ICE and/or BEADS-ICE. These modelling materials provide better scaling of the ice density. The tests conducted in this program should be repeated with these other modelling materials, or alternatively, the additional ridge modelling tests recommended above in (a) should be repeated in these materials.

d) the collection of a dedicated set of field data for ridge ramming with the objective of providing a good reference data set for future model scale - full scale correlations.

e) basic laboratory and analytical studies to model ridge resistance and penetration energy. Work is required to improve present understanding of the ridge-ship interaction process and to develop methods to characterize ridges in a manner that is meaningful to ship transit.

    We note that this is one of the overall objectives of a Joint Research Project Agreement (JRPA) between Canada and Finland which is currently at the planning stage.

    Therefore, we recommend that future ridge modeling efforts be planned such that they augment the results of the JRPA.

7.0 REFERENCES

Canarctic Shipping Limited, 1987, Transport Canada reports TP 8134, TP 835 and TP 8137.

Coburn, J.L., et al, 1981, Winter 1981 Trafficability Tests of the USCGC POLAR SEA, Arctec Inc., report 583 submitted to the U.S. Maritime Administration.

Comfort G., and Edwards, R.Y., 1978, Ice Conditions in Viscount Melville Sound and Barrow Strait West, Arctec Canada Report 315 submitted to Environment Canada.

Danielewicz, B.W., and Pilkington, G.R., 1982, Selected Environmental Characteristics of Beaufort Sea Ice, distributed by Pallister Resource Management Limited.

Dickins, D. and Wetzel, V., 1981, Multi-year Pressure Ridge Study - Queen Elizabeth Islands, proc. POAC, Quebec City.

Dome Petroleum Ltd., 1980, Summary Compilation and Analysis of Ice Data Collected During KIGORIAK Research Tests 1979-80. Report #21, The KIGORIAK Research Series, proprietary report to Dome Petroleum Ltd.

Dome Petroleum Ltd., 1980, 1979-80 Full Scale Tests of the CANMAR KIGORIAK, Report 22, The KIGORIAK Research Series, proprietary report to Dome Petroleum Ltd.

El-Tahan, H., 1988, Results of Small Scale Laboratory Tests With Beads-ice, Fleet Technology Newfoundland Ltd. report to IRAP, report under preparation.

Geisel, F., Voelker, R.P., and Dane, K., 1982, Arctic Deployment of USCGC POLAR STAR - Winter 1982, contractor report 730 submitted by Arctec Inc. to U.S. Dept. of Transportation.

Gladwell, R.W., 1976, Field Studies of Eight First Year Sea Ice Pressure Ridges in the Southern Beaufort Sea, APOA, Project 75.

Glen, I., et al, 1985, POLAR Class Antarctic 1984 Level Ice Resistance Tests, Transport Canada report 7183E.

Keinonen, A.J., 1973, The Shape and Size of Ice Ridges in the Baltic According to Measurements and Calculations, Report 17, the Winter Research Navigation Board, Helsinki, Finland.

Keinonen, A.J., 1983, Ship Performance and Resistance in Ice Ridges, proc. WEGEMT conference.

Keinonen, A.J., and Duff, J., 1983, CANMAR KIGORIAK - Demonstration of Arctic Capabilities, proc. 7th POAC Conference, Helsinki.

Kovacs, A., 1973, Structure of a Multi-year Pressure Ridge, ARCTIC, Vol. 26, no. 1.

Kovacs, A., 1983, Characteristics of Multi-year Pressure Ridges, proc. POAC, Helsinki, Finland.

Nawwar, A., 1980, Development of Reference Data base for First Year Ridge Resistance and Penetration Characteristics, Arctec Canada Limited Report 383, submitted to the APOA.

Nawwar, A. et al, 1984, MV ARCTIC: Ice Transiting Performance to the Ramming Model, Transport Canada report TP 5320E.

Schwarz, J., Frederking, R., and Flehmke, A., 1986, Erste Eisbrechtechnische Expedition mit F.S. POLARSTERN Bd.1-3 Hamburgische Schiffbau Versuchsanstalt Abteilungeistechnik (HSVA) BMFT-MTK 310-311, BMFT-MTK 312-313.

Stubbs, J., et al, 1986, Development of a Method for Estimating Ship Performance Capabilities and Identifying Limiting Conditions When Transiting Ice Ridges, Transport Canada report TP8275E.

Wright, B., Hnatiuk, J., and Kovacs, A., 1979, Multi-year Pressure Ridges in the Canadian Beaufort Sea, proc. POAC, Trondheim, Norway.

Volume

2

Ridge Modelling: Model Scale Simulation of Ramming Tests Conducted with the USCGC POLAR STAR

Volume II - Appendices

TP 9496E

Prepared for:

Transport Canada
The Policy and Coordination Group
Transportation Development Centre

Prepared by:

FLEET TECHNOLOGY NEWFOUNDLAND LIMITED

CA1
DTC 800
88
R35
v.2
c.2

Date Due

SEP 5 1989

BRODART, INC. Cat. No. 23 233 Printed in U.S.A.

mm

CA1
DTC800
88
R35
V.2
C.2

FTNL 3208C

RIDGE MODELLING: MODEL SCALE SIMULATION OF RAMMING TESTS CONDUCTED WITH THE USCGC POLAR STAR

VOLUME II - APPENDICES

TP 9496E

Prepared for Transport Canada
The Policy and Coordination Group
Transportation Development Centre

Guy Favreau Complex,
200 Rene Levesque Blvd. West,
Suite 601, West Tower,
Montreal, Quebec.
H2Z 1X4

Library and Information Centre /
Centre de Documentation (GSLA)
RECEIVED - REÇU LE
JAN 24 1989
Transport Canada / Transports Canada

BY

G. COMFORT

Prepared by:

FLEET TECHNOLOGY NEWFOUNDLAND LIMITED,
P.O. Box 5040,
St.John's, Newfoundland.
A1C 5V3

SEPTEMBER 1988

407177

403[illegible]

PROJECT TEAM:

The project team included:

Fleet Technology Newfoundland Limited: Razek Abdelnour

Fleet Technology Limited: George Comfort
Rick Brown
Darlene Bourne
Andre Lemieux
Christine Genge

AKAC Consultants Limited: Dr. A. Keinonen

Institute of Marine Dynamics: Don Spencer

DISCLAIMER:

The contents of this report reflect the views of Fleet Technology Newfoundland Limited and not necessarily the official views or policies of Transport Canada.

Un sommaire en français de ce rapport est inclus dans le volume I.

Approved by:
I.F. Glen, President.
Fleet Technology Limited.

Transport Canada Transports Canada
Development Développement

REPORT DOCUMENTATION FORM

1. Transport Canada Report No.
TP 9496E

2. TDC Project No.
7000

3. Recipient's Catalogue No.

4. Title and Subtitle
RIDGE MODELLING: Model Scale Simulation of Ramming Tests Conducted with the USCGC POLAR STAR (Two Volumes)

5. Report Date
September 1988

6. Performing Organization Report No.
3208C

7. Author(s)
G. Comfort

8. Transport Canada File No.
D1460-257

9. Performing Organization Name and Address
Fleet Technology Newfoundland Limited
65A Lemarchant Road, P.O. Box 5040
St. John's, Newfoundland
A1C 5V3

10. DSS File No.
12SD.T8200-7-7540

11. DSS or Transport Canada Contract No.
T8200-7-7540/01-SD

12. Sponsoring Agency Name and Address
Transportation Development Centre (TDC)
200 René-Lévesque Blvd. West
Suite 601, West Tower
Montreal, Quebec H2Z 1X4

13. Type of Report and Period Covered
Final

14. Sponsoring Agency Code

15. Supplementary Notes
Appendices separately bound.

16. TDC Project Officer
T. Peirce

17. Abstract

A project was undertaken to improve present knowledge of ridge modelling and to investigate preferred techniques for the production of model ice ridges. The general approach used for the project was to attempt to simulate, at model scale, a small number of field ridge ramming events that were relatively well documented. After a review of the available full scale data, it was decided to use field data collected during ramming tests with the USCGC POLAR STAR in 1982 in the Bering Sea in partially consolidated first-year ridges as the reference event(s) for this study. Preliminary model tests were first conducted by Fleet Technology Limited's ice tank in Kanata. More extensive tests were then conducted at the Institute for Marine Dynamics in St. John's, Nfld. Tests were conducted at a scale factor of 19.1. Two ridge modelling techniques were used: i.e. the production of a single ridge with both a consolidated and an unconsolidated portion; and the production of ridges which separately modelled the unconsolidated and consolidated portions of the ridge. Parameters that were varied during the tests included the ice-model friction factor, the size of the ridge, and the size and strength of the consolidated layer of the ridge. Conclusions are drawn and recommendations are made regarding the accuracy of ridge modelling techniques and the preferred techniques for the production of model ice ridges.

18. Key Words
Ship, Icebreaking, Ice Modelling, Ice Ridges

19. Distribution Statement
Limited number of copies available from the Transportation Development Centre.

20. Security Classification (of this report)
Unclassified

21. Security Classification (of this page)
Unclassified

22. No. of Pages
523

23. Price
Nil

TDC CDT 79-005
Rev 86

Canada

Transports Canada Transport Canada
Développement Development

FORMULE DOCUMENTAIRE DU RAPPORT

1. N° du rapport Transports Canada
TP 9496E

2. N° de l'étude — CDT
7000

3. N° de catalogue du destinataire

4. Titre et sous-titre
RIDGE MODELLING: Model Scale Simulation of Ramming Tests Conducted with the USCGC POLAR STAR
(Deux Volumes)

5. Date du rapport
Septembre 1988

6. N° du rapport de l'organisme exécutant
3208C

7. Auteur(s)
G. Comfort

8. N° de dossier Transports Canada
D1460-257

9. Nom et adresse de l'organisme exécutant
Fleet Technology Newfoundland Limited
65A Lemarchant Road, P.O. Box 5040
St. John's (Terre-Neuve)
A1C 5V3

10. N° de dossier — ASC
12SD.T8200-7-7540

11. N° de contrat — ASC ou Transports Canada
T8200-7-7540/01-SD

12. Nom et adresse de l'organisme parrain
Centre de développement des transports (CDT)
200 ouest, boul. René-Lévesque
Suite 601, tour ouest
Montréal (Québec) H2Z 1X4

13. Genre de rapport et période visée
Final

14. Code de l'organisme parrain

15. Remarques additionnelles
Annexes reliées séparément.

16. Agent de projet — CDT
T. Peirce

17. Résumé

Le projet dont il est rendu compte ici vise à développer les connaissances actuelles en modélisation physique des crêtes de pression ainsi qu'à dégager les techniques de modélisation à privilégier. L'approche générale retenue a été de tenter de simuler, à échelle réduite, un petit nombre de cas réels de charge de crêtes de pression relativement bien documentés. Après avoir étudié toutes les données vraie grandeur disponibles, il a été décidé de se servir, pour les fins de la présente étude, de celles concernant les essais de charge de crêtes partiellement consolidées de première année, faits par le USCGC Polar Star, en 1982, dans la mer de Béring. Les essais préliminaires de modélisation ont eu lieu dans le bassin des glaces de Fleet Technology Limited, à Kanata. Des essais plus poussés ont ensuite été faits à l'Institut de dynamique marine à St. John's, Terre-Neuve. Le facteur de réduction d'échelle retenu à cette occasion a été de 19,1. Deux techniques de modélisation des crêtes ont été utilisées: 1) production d'une crête comportant une partie consolidée et une autre non consolidée, et 2) production de deux crêtes distinctes, l'une consolidée, l'autre non consolidée. Parmi les paramètres que les chercheurs ont fait varier lors des essais, figuraient: le coefficient de frottement glace-maquette, la taille de la crête de pression ainsi que l'épaisseur et la résistance de la couche consolidée. Le rapport présente des conclusions concernant la justesse des résultats livrés par les différentes techniques de modélisation ainsi que des recommandations quant aux techniques à privilégier.

18. Mots-clés
Navire, déglaçage, modélisation des glaces, crêtes de pression.

19. Diffusion
Nombre limité d'exemplaires disponibles au Centre de développement des transports.

20. Classification de sécurité (de ce rapport)
non classifié

21. Classification de sécurité (de cette page)
non classifiée

22. Nombre de pages
523

23. Prix
aucun

CDT/TDC 79-005
Rev 86

Canada

ACKNOWLEDGEMENTS

This project was partially funded by the National Research Council of Canada through the Institute for Marine Dynamices (IMD).

The technical staff of the IMD who performed the tests have contributed greatly to the success of this project. They were cooperative throughout the program and maintained a keen interest in the project while working long hours to maintain the project schedule.

As well, the support of the United States Coast Guard, who kindly loaned us a 19.1:1 scale model of the USCGC POLAR STAR for testing during this project, is gratefully acknowledged.

Finally, we wish to acknowledge the assistance of R. Voelker of NKF Engineering Limited with whom we had several discussions regarding the 1982 field ramming tests with the USCGC POLAR STAR that were used as a full scale reference for this study.

EXECUTIVE SUMMARY

Objectives:

A project has been undertaken to improve present knowledge of: (a) the accuracy of physical model results for ice ridges; and (b) preferred techniques for the production of ice ridges in the model basin.

General Approach and Scope:

The general approach used was to attempt to simulate, at model scale, a small number of field ridge ramming tests that were relatively well documented. The study comprised three main tasks, as follows:

1. Review of available full scale data and selection of field ridge ramming event(s) for modelling.
2. Preliminary ridge modelling tests at Fleet Technology Limited's (FTL) ice tank in Kanata and development of test plan.
3. Detailed ridge modelling tests at the Institute for Marine Dynamics (IMD).

Selection of Field Ridge Ramming Event(s) for Modelling:

Tests conducted in 1982 in the Bering Sea with the USCGC POLAR STAR (Geisel et al, 1982) were selected as the reference field event(s) for this study. These ramming tests were conducted in partially consolidated first-year riges. Ramming tests done for ridges 17 and 18 during the trials were selected as the field reference event(s) for this study as the ridge profile was documented best for these ridges.

Ridge Modelling Tests:

Ridge modelling tests at FTL and IMD were conducted at a scale of 1:19.1 as this was the scale of the available model of the USCGC POLAR STAR. Efforts were made to duplicate the ice environmental condition tested in the field (which was a partially consolidated first year ridge embedded in a first-year ice sheet).

Two general approaches were used to model the field ridge(s):

(a) produce ridges that consisted of both consolidated and unconsolidated material. This models the general composition of the field ridge(s).

(b) produce ridges that separately modelled the consolidated and unconsolidated portions of the field ridge(s) and conduct separate ramming tests.

Several parameters were varied during the model tests including the ice-model friction factor, the speed of the model, and the size, consolidation depth and the strength of the model ridges.

Tests Results and Conclusions:

(i) Ridge modelling techniques

The tests have indicated that the approach of separately modelling the consolidated and unconsolidated portions of the ridge (i.e. (b) above) provided comparable accuracy for the prediction of ridge penetration energy to that of producing partially consolidated ridges (i.e. (a) above) in the basin.

Practical methods for the production of partially consolidated ridges in the basin were developed. The tests have indicated that the cross-sectional area of the ridge and the mean depth of consolidation can be controlled relatively well. This can be accomplished by controlling: a) the volume of ice initially put into the ridge; and b) the thickness of intact ice which is initially pushed over the unconsolidated material in the ridge; and c) the placement and subsequent removal of insulation mats on the ridge surface.

However, the flexural strength of the consolidated layer of the ridge was found to be a difficult property to control.

In general, the measurement of ridge properties was found to be difficult and time-consuming. At present, techniques for the characterization of ridge properties are not standardized. This is one area where further research is believed to be warranted.

(ii) Quantitative prediction of ridge penetration energy

The model test results have indicated the following dependence of ridge penetration energy on the test parameters:

a) ridge cross-sectional area - a clear trend was not observed as this parameter was not varied over a wide range. The effect of this parameter was masked by variations in other properties,
b) mean depth of consolidation - the ridge penetration energy was found to increase (in an approximately linear manner) with an increased mean depth of consolidation,
c) ice-model friction - the ridge penetration energy was found to double (approximately) when the ice-model friction factor was increased from 0.04 to 0.16,
d) speed - this parameter was found to have a negligible effect on the ridge penetration energy over the range of speeds tested (i.e. 0.65 m/s to 1.0 m/s model scale).

e) flexural strength of ridge consolidated layer - the ridge penetration energy was found to be weakly dependent on the flexural strength. The ridge penetration energy increased by about 30% for an approximate variation in flexural strength of 0 kPa to 1500 kPa. This relationship is highly scattered as other variables which affect the ridge penetration energy more significantly (such as the mean depth of consolidation) were also varied.

The model test results have been compared to the full scale data and to the results of a numerical predictor of ridge penetration energy recently developed by Stubbs et al, 1986 (Stubbs, J., et al, 1986, "Development of a Method for Estimating Ship Performance Capabilities and Identifying Limiting Conditions When Transiting Ice Ridges", Transport Canada report **TP 8275E**). Froude scaling laws were used throughout to compare model scale data with full scale results and the scale factor was taken as the geometric scale factor of the model (i.e. 19.1). This scaling practice is presently common in ice model-testing.

The model test results obtained at the low and high friction factors bracket the numerical predictions of Stubbs et al, 1986 for the penetration energy of the unconsolidated material within about ±30%.

If the field data are accepted at face value, then the following conclusions are indicated:

a) Tests with partially consolidated ridges - the model tests results underpredict the ridge penetration energy. The model tests results at the low and high friction factor indicated ridge penetration energies that were about 30% and 60% respectively of the measured field data. It should be noted that the flexural strength of the consolidated layer was too strong (by a factor of about 2-5) for these ridges. Thus, despite the fact the ridges were too strong, the ridge penetration energy was underpredicted by the model tests.

b) Tests with purely consolidated and purely unconsolidated ridges - the total penetration energy measured in the field was compared to the sum of the penetration energies obtained from model tests conducted in purely consolidated and purely unconsolidated ridges.

   For the model tests done at a high friction factor (i.e. 0.16), this sum bracketed the field data within ±20%.

   For the model tests done at a low friction factor (i.e. 0.04), this sum was about 40% of the field data.

Unfortunately, the strength of the conclusions that can be obtained from the study is limited by uncertainties in the field data, including:

a) discrepancies between the horizontal force measured before the ship contacted the ridge (while it transitted level ice) and the predicted level ice resistance of the ship. The measured forces exceed the predicted level ice resistance by a factor in excess of 2. A bias of this amount would cause the field data to overestimate the ridge penetration energy by about 35%. This amount is significant in relation to the observed discrepancies between the model test and field test data.

b) uncertainties in the field ice-hull friction factor. Two different apparata (i.e. a sliding arm and a rotating arm tribometer) were used to measure the ice-hull friction factor. One major difference between these apparata is that the sliding arm tribometer slides the ice past the hull without causing crushing while the rotating arm tribometer both crushes and slides the ice sample. The mean ice-hull friction factors measured by these apparata were 0.045 and 0.20, respectively. In an effort to bound this uncertainty, we have conducted the model tests at two friction factors (i.e. 0.04 and 0.16). It should be remembered that the technique used to measure the ice-hull friction factor in the model tests was similar to the sliding arm tribometer tests as an ice sample was slid over the surface without causing the ice to crush.

c) anomalies in the ridge profiles. For ridge 18, the measured keel area was too small in relation to the measured total area to maintain isostatic equilibrium. For ridge 17, the consolidated layer was measured to be very thick over the 15 m to 25 m horizontal baseline. It is hypothesized that this mass may represent a local incusion of multi-year ice.

As stated on the previous page, a direct comparison of the field and model scale data indicates that the model test results underpredict the ridge penetration energy. Both items (a) and (c) above introduce uncertainties in scaling and comparison which are in this direction. Clearly, a better match could be obtained between the field and model test data if the field penetration resistance data were "corrected" to account for the observed discrepancy in level ice resistance (i.e. item (a) above). Item (c) above also contributes to an underprediction of the field data by the model test results as the model tests, and subsequent model scale vs. full scale comparisons, were based on field data that appear to underestimate the ridge cross-sectional area.

Recommendations:

This project represents the first time (to our knowledge) that efforts have been made to duplicate a field ramming event in partially consolidated ridges in the model basin. It is a first step towards understanding the accuracy of ice model tests in ridges and preferred techniques for the production and testing of model ice ridges.

We recommend that this initial project be followed with additional studies, including:

a) further model basin tests aimed at developing a standard technique for modelling the resistance of ridges. This would be performed by using the POLAR STAR model to determine the energies needed to penetrate a parametric series of model ridges in which shape, area and strength are varied systematically. The resulting scale of ridge penetration energies, when compared to the energies measured during full-scale ridge events for the POLAR STAR, would then permit the model ridges to be identified which best simulated the resistance of the corresponding field ridges. The results would thus provide a scientific basis for modelling ridges for use in standardized model tests.

b) similar ridge modelling tests with other ships. Field ramming tests that were relatively well documented have also been carried out with the MV KIGORIAK and MV POLAR STERN.

   It is recognized that the KIGORIAK field data are proprietary (to Dome Petroleum Limited). Therefore, it may not be possible to conduct a similar study for that ship.

c) ridge modelling tests should be conducted using MOD-ICE (non-refrigerated solidified wax) and/or BEADS-ICE (refrigerated mixture of water, dopant and plastic beads). These modelling materials provide better scaling of the ice density. The tests conducted in this program should be repeated with these other modelling materials, or alternatively, the additional ridge modelling tests recommended above in (a) should be repeated in these materials.

d) field ridge-ramming tests with the specific objective of producing a very well documented set of field data for the purpose of providing a full scale reference for subsequent model scale vs. full scale comparisons.

e) basic laboratory and analytical studies of the ridge-ship interaction. We note that this is one of the major objectives of the planned Joint Research Project Agreement (JRPA). Therefore, future ridge modelling efforts should be planned such that they augment the results of this program.

SOMMAIRE

Objectifs

Ce projet a été entrepris dans le but de développer les connaissances actuelles concernant la justesse des résultats obtenus par modélisation physique des crêtes de pression et de dégager les techniques à privilégier pour la modélisation des crêtes de pression en bassin des carènes.

Approche générale et portée de l'étude

L'approche générale retenue a été de tenter de simuler, à échelle réduite, un petit nombre de cas réels de charge de crêtes de pression relativement bien documentés. Il s'agissait principalement de:

1. Faire un tour d'horizon en vue de la modélisation, des données disponibles concernant des essais de charge de crêtes de pression en conditions réelles.
2. Procéder à des essais préliminaires de modélisation de crêtes de pression au bassin des glaces de Fleet Technology Limited (FTL) à Kanata et à l'élaboration d'un plan d'expérimentation.
3. Procéder à des essais de modélisation plus poussés à l'Institut de dynamique marine (IDM).

Sélection des essais de charge à reproduire à échelle réduite

Les essais faits en 1982 dans la mer de Béring par le USCGC POLAR STAR (Geisel et al, 1982) ont été retenus comme base de référence de la modélisation envisagée, plus précisément les essais de charge des crêtes de première année partiellement consolidées numéros 17 et 18, pour lesquels les chercheurs bénéficiaient de données de caractérisation en profil des plus complètes.

Essais de modélisation des crêtes de pression

Ces essais ont été réalisés à l'échelle 1/19,1 aux installations de FTL et de l'IDM puisqu'il s'agissait de l'échelle de réduction de la maquette du POLAR STAR dont les chercheurs disposaient. Ces derniers ont tenté de reproduire en bassin les conditions glacielles rencontrées en vraie grandeur (soit une crête de première année partiellement consolidée prise dans une couche de glace de première année).

Deux approches générales de modélisation ont été adoptées:

(a) modélisation de crêtes formées à la fois de glace consolidée et de glace non consolidée, comme cela se rencontre dans la réalité.

(b) modélisation de crêtes consolidées à côté de crêtes non consolidées en vue d'essais de charge séparés.

Plusieurs paramètres ont été variés au cours des essais en bassin, parmi lesquels: le coefficient de frottement glace-maquette, la vitesse de la maquette et la taille, la profondeur de consolidation et la résistance des crêtes simulées.

Résultats et conclusions

(i) Techniques de modélisation des crêtes

Les essais ont permis de constater que la modélisation séparée de portions consolidées et non consolidées d'une crête (technique b ci-dessus) livrait, en ce qui concerne l'énergie de pénétration de la crête, des approximations comparables en justesse à celles obtenues par l'autre technique, soit la modélisation de crêtes partiellement consolidées (technique a ci-dessus).

Les chercheurs ont mis au point des méthodes pratiques de réalisation de crêtes partiellement consolidées en bassin. Les essais ont montré que la section transversale et la profondeur moyenne de consolidation de la crête pouvaient être assez bien maîtrisées en réglant: a) la quantité de glace utilisée pour constituer la crête de pression, b) l'épaisseur de la couche de glace intacte qui est poussée en début d'essai par-dessus la glace non consolidée de la crête, et c) les temps de mise en place et d'enlèvement des matelas isolants servant à maintenir la température de la glace formant la crête à la valeur souhaitée.

Toutefois, la résistance en flexion de la couche consolidée était une propriété plus difficile à maîtriser.

En général, le mesurage des paramètres caractérisant une crête de pression s'avérait ardu et long à réaliser. A l'heure actuelle, les techniques de caractérisation de crêtes ne sont pas normalisées. Il s'agit d'un domaine où la recherche mériterait d'être poussée plus loin.

(ii) Appréciation quantitative de l'énergie de pénétration d'une crête

Les essais en bassin ont révélé les relations suivantes entre l'énergie de pénétration des crêtes et les paramètres d'essai:

a) section transversale de la crête - aucune relation nette n'a pu être observée étant donné que la plage de variation de ce paramètre n'a pas été très étendue, les effets de ce paramètre ayant été masqués par les variations d'autres paramètres.
b) profondeur moyenne de consolidation - l'énergie de pénétration d'une crête augmentait (à peu près proportionnellement) avec la profondeur moyenne de consolidation.
c) coefficient de frottement glace-maquette - l'énergie de pénétration doublait presque lorsque l'on faisait passer ce coefficient de 0,04 à 0,16.

d) vitesse - ce paramètre a exercé une influence négligeable sur la valeur de l'énergie de pénétration, du moins dans la plage de variation vérifiée (soit entre 0,65 m/s et 1,0 m/s, échelle réduite).

e) résistance en flexion de la couche consolidée - l'énergie de pénétration n'était que faiblement liée à la résistance en flexion de la crête. Ainsi, elle a augmenté d'approximativement 30 %, pendant que la résistance en flexion de la crête passait de 0 à 1500 kPa environ. Cette relation est influencée par d'autres variables dont l'effet sur l'énergie de pénétration est beaucoup plus marqué (exemple, la profondeur moyenne de consolidation).

Les résultats des essais sur maquette ont été comparés à ceux des essais en vraie grandeur ainsi qu'aux valeurs d'énergie de pénétration calculées à l'aide du modèle numérique mis au point en 1986 par Stubbs et al (Stubbs, J., et al, 1986, "Development of a Method for Estimating Ship Performance Capabilities and Identifying Limiting Conditions When Transiting Ice Ridges", rapport **TP 8275E** de Transports Canada). Les lois de similitude de Froude ont été appliquées à l'ensemble des données de la comparaison, le facteur d'échelle retenu ayant été le facteur de réduction d'échelle géométrique de la maquette utilisée, soit 19,1. Cette façon de procéder est présentement courante en modélisation dans les glaces.

En ce qui concerne l'énergie de pénétration des couches non consolidées, les résultats des essais sur maquette obtenus aux valeurs extrêmes de la plage des coefficients de frottement encadrent les valeurs théoriques calculées par Stubbs et al en 1986 à plus ou moins 30 % près.

Si l'on accepte telles quelles toutes les données des essais en vraie grandeur, les conclusions suivantes s'imposent:

a) Essais de pénétration de crêtes partiellement consolidées - les essais sur maquette sous-estiment l'énergie de pénétration des crêtes. Les résultats des essais sur maquette, obtenus aux valeurs extrêmes de la plage des coefficients de frottement testés, s'établissaient respectivement à environ 30 et 60 % des valeurs mesurées en vraie grandeur. À noter que la résistance en flexion de la couche consolidée était trop élevée: elle dépassait de 2 à 5 fois celle des crêtes témoins. Or, malgré le fait que cette résistance ait été trop élevée, les essais sur maquette ont abouti à des valeurs d'énergie de pénétration sous-estimées.

b) Essais de pénétration de crêtes consolidées et de crêtes non consolidées - l'énergie totale de pénétration mesurée en vraie grandeur a été comparée à la somme des énergies de pénétration mesurée aux essais sur maquette concernant tour à tour des crêtes consolidées et non consolidées.

Les essais sur maquette à coefficient de frottement élevé (0,16) ont donné une gamme de résultats dont les sommes encadraient les valeurs en vraie grandeur à plus ou moins 20 % près.

Aux essais réalisés à coefficient de frottement faible (0,04), la somme des énergies de pénétration s'est établie à environ 40 % des valeurs en vraie grandeur.

Malheureusement, la valeur des conclusions que l'on peut tirer de la présente étude est grevée par les incertitudes dont souffrent les données des essais en vraie grandeur, notamment:

a) écarts entre la force horizontale mesurée avant que la proue du navire ne heurte la crête de pression (c'est-à-dire pendant que celui-ci avançait dans une glace uniforme) et la résistance à la marche théorique du navire dans une glace uniforme. En effet, les forces mesurées dépassent cette valeur théorique par un facteur supérieur à 2. En principe, un écart de cette amplitude devrait avoir pour effet que les données en vraie grandeur conduisent à une surestimation de l'énergie de pénétration des crêtes par environ 35 %. Or, ce dépassement est loin d'être négligeable devant les écarts observés entre les valeurs dégagées par les essais sur maquette et celles des essais en vraie grandeur.

b) incertitudes concernant le coefficient de frottement glace-coque. Deux dispositifs différents ont servi à mesurer ce coefficient: un tribomètre à bras coulissant et un autre à bras rotatif. Les deux se différencient principalement par le fait que le premier agit en frottement pur, alors que l'autre exerce une force à la fois de translation et d'écrasement. Les coefficients de frottement moyens obtenus par ces deux appareils s'établissaient à 0,045 et 0,20 respectivement. Voulant circonscrire l'étendue de l'incertitude liée à ce facteur, les chercheurs ont réalisé des essais sur maquette aux deux valeurs extrêmes du coefficient de frottement (0,04 et 0,16). Il convient de rappeler que la technique tribométrique appliquée relativement à la maquette est assimilable aux mesures tribométriques par appareil à bras coulissant en ceci que l'éprouvette de glace a été frottée contre la coque sans aucun effort de compression.

c) anomalies dans les profils de crête. La crête 18 présentait une superficie de crête sous glace trop faible par rapport à la superficie totale de la crête pour maintenir un équilibre isostatique. Quant à la crête 17, sa couche consolidée était très épaisse sur toute la largeur de la crête qui variait entre 15 et 25 mètres. Selon toute hypothèse, cette masse pourrait être de la glace de plusieurs années.

Comme il a été mentionné à la page précédente, une comparaison directe des résultats des essais en vraie grandeur et sur maquette révèle que ces derniers aboutissent à une sous-estimation de l'énergie de pénétration des crêtes de pression. Les facteurs indiqués en a) et b) ci-dessus rendent incertains les rapports de similitude adoptés pour les fins des essais sur maquette ainsi que toute comparaison fondée sur ces rapports. De toute évidence, une meilleure similitude entre les données des essais en vraie grandeur et celles de la modélisation pourrait être atteinte si les résultats des essais de prénétration de crête in situ étaient "corrigés" à la lumière de l'écart constaté au niveau de la résistance à la marche dans une glace uniforme (facteur (a) ci-dessus). Le facteur c) ci-dessus contribue également à la sous-estimation dénoncée, étant donné que la modélisation et les comparaisons subséquentes des résultats étaient fondées sur des données en vraie grandeur qui semblent aboutir à une section transversale de crête inférieure à la réalité.

Recommandations

Ce projet représente, autant que nous puissions en juger, la première tentative de reproduire en bassin des glaces, donc à échelle réduite, un cas réel de charge d'une crête de pression partiellement consolidée. Il s'agit d'un premier pas vers l'appréciation de la justesse des résultats tirés des essais sur maquette et vers la détermination des techniques à privilégier en vue de la réalisation et de la caractérisation des crêtes de pression simulées.

Nous recommandons de lancer des études complémentaires à cette première recherche, notamment de procéder:

a) à d'autres essais en bassin des glaces visant à mettre au point une technique standard de modélisation de la résistance des crêtes de pression. Cette nouvelle série d'essais, qui serait réalisé à l'aide de la maquette du Polar Star, servirait à déterminer l'énergie de pénétration d'une crête de pression simulée dont la forme, la section et la résistance seraient systématiquement variées. La comparaison des énergies de pénétration mesurées lors de cette série d'essais paramétriques et des énergies mesurées en vraie grandeur à bord du Polar Star devraient alors permettre d'identifier les crêtes de pression qui simulent le mieux la résistance des crêtes réelles correspondantes. De cette manière, le choix d'une technique normalisée de modélisation d'une crête de pression reposerait sur une base scientifique.

b) à la modélisation physique de la charge des crêtes de pression, à l'aide de maquettes d'autres navires. Des essais en vraie grandeur relativement bien documentés ont déjà été réalisés par le NM KIGORIAK et le NM POLAR STERN.

   Il est vrai que les données inhérentes au KIGORIAK sont la propriété exclusive de Dome Petroleum Limited et qu'il ne sera peut-être pas possible de procéder à une modélisation du navire.

c) à des essais en bassin mettant en oeuvre les glaces synthétiques MOD-ICE (cire solidifiée non réfrigérée) ou BEADS-ICE (mélange réfrigéré d'eau, de dopant et de billes de plastique): ces matériaux permettent de mieux respecter les lois de similitude concernant le paramètre densité de la glace. Les essais du présent programme devraient être repris dans les matériaux précités ou, à défaut, les nouveaux essais préconisés en a) ci-dessus.

d) à des essais de charge en vraie grandeur dans le but spécifique de produire des données exhaustives y afférentes et susceptibles de servir de référence aux futurs essais sur maquette.

e) à des études de laboratoire et analytiques fondamentales sur les interactions crête de pression-navire. Nous avons noté que ces études représentent également l'un des objectifs principaux du projet de recherche conjoint envisagé. Aussi, conviendrait-il que les prochain travaux de modélisation soient délimités afin qu'ils apportent un complément aux études dudit projet conjoint.

TABLE OF CONTENTS

VOLUME II - APPENDICES

APPENDIX A - RAW DATA FROM SHEET #1 TESTS AT FLEET TECHNOLOGY LIMITED
APPENDIX B - RAW DATA FROM SHEET #2 TESTS AT FLEET TECHNOLOGY LIMITED
APPENDIX C - RAW DATA FROM SHEET #1 TESTS AT THE IMD
APPENDIX D - RAW DATA FROM SHEET #2 TESTS AT THE IMD
APPENDIX E - RAW DATA FROM SHEET #3 TESTS AT THE IMD
APPENDIX F - RAW DATA PLOTS FOR TEST T2R1 FOR A RANGE OF FILTERING RATES
APPENDIX G - RAW DATA PLOTS FOR TEST T1R1 FOR A RANGE OF FILTERING RATES
APPENDIX H - SUMMARY OF AVAILABLE FIELD DATA FOR RIDGES 17 AND 18

APPENDIX A

RAW DATA FROM SHEET #1 TESTS AT FLEET TECHNOLOGY LIMITED

CONTENTS:

- A.1 Raw Time Histories for All Data Channels
- A.2 Ice Properties and Temperature Data

APPENDIX A.1

RAW TIME HISTORIES FOR ALL DATA CHANNELS

March 27
3208

TEST LAYOUT

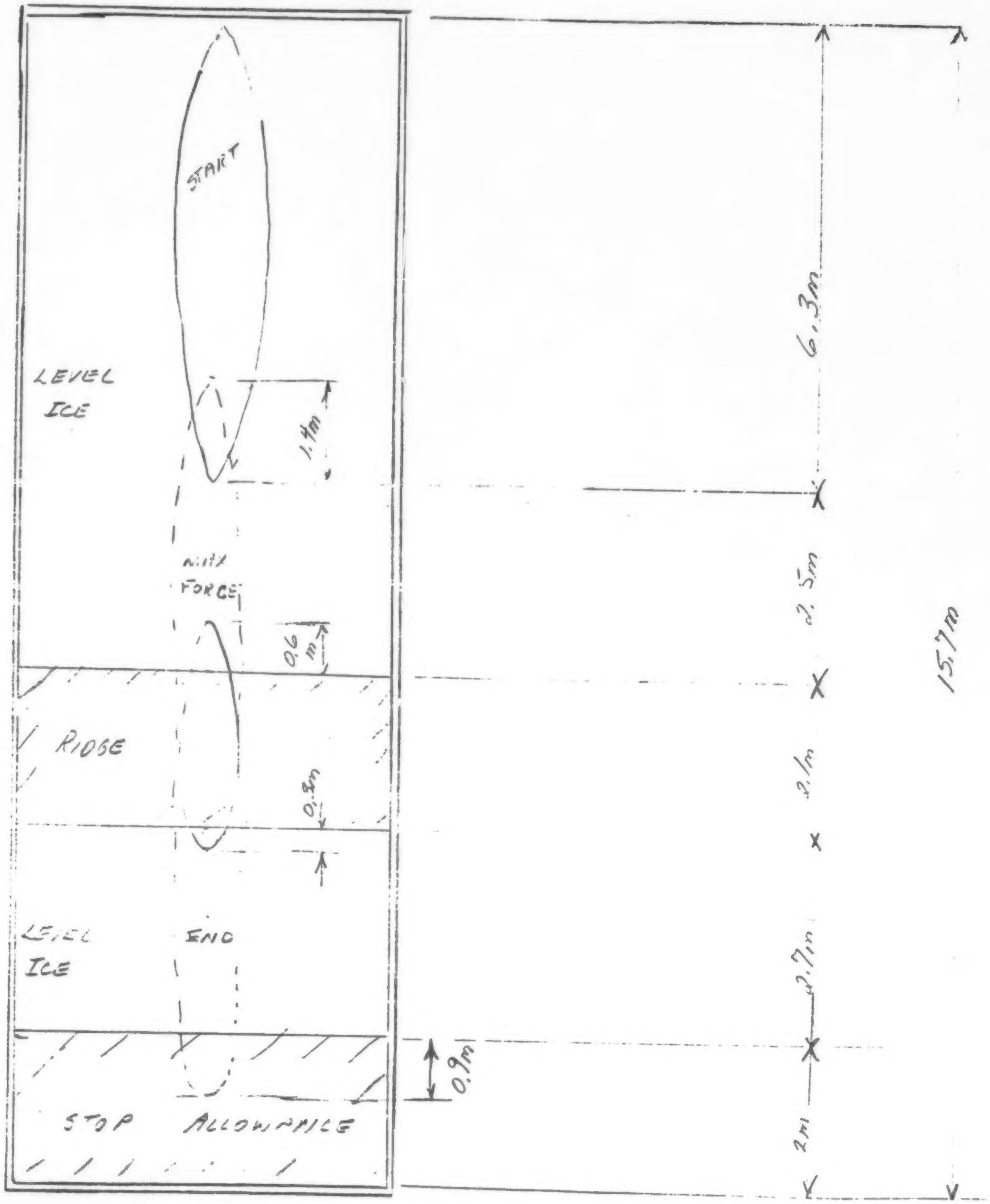
START
LEVEL ICE
1.4m
MAX FORCE
0.6 m
RIDGE
0.3m
LEVEL ICE
END
0.9m
STOP ALLOWANCE
6.3m
2.5m
2.1m
2.7m
2m
15.7m

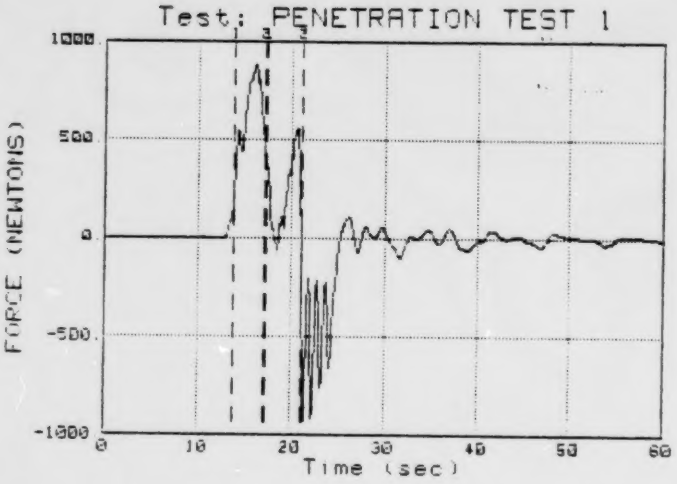
Test: PENETRATION TEST 1
1
3
2
1000.
500.
0.
-500.
-1000.
FORCE (NEWTONS)
0
10
20
30
40
50
60
Time (sec)

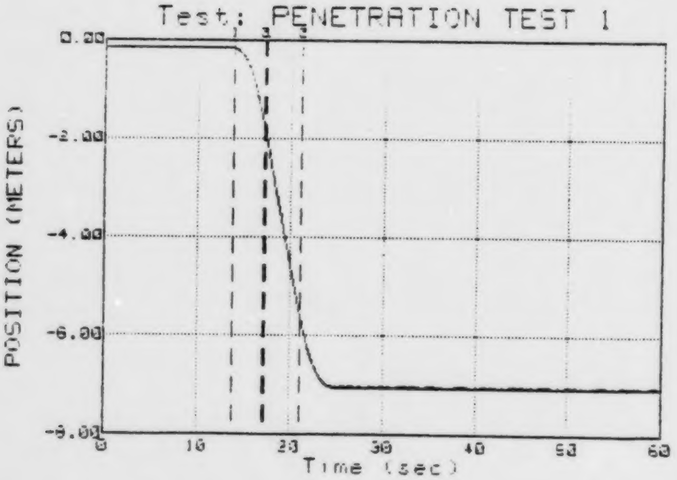
Test: PENETRATION TEST 1
1
3
2
0.00
-2.00
-4.00
-6.00
-8.00
POSITION (METERS)
0
10
20
30
40
50
60
Time (sec)

```
                              STATISTICS SUMMARY

                              Project Number 3208C
                                RIDGE MODELLING

                   Test Name:              PENETRATION TEST 1
                   Date:                          28 Mar 1988
                   Start Time:                       18:55:09
                   Scanning Rate                        30 Hz
                   Test Duration                60.0000 seconds

               Interval  1 beginning at:         13.8000 seconds
               Interval  1 ending at:            17.3000 seconds

CHANNEL     NAME       UNITS      MAXIMUM     MINIMUM        MEAN  STD DEVIATION
   1        FORCE     NEWTONS      886.42      208.57      626.87      175.84

   3      POSITION    METERS       -.1585     -1.9746      -.7648       .5470

               Interval  2 beginning at:         17.0000 seconds
               Interval  2 ending at:            21.0000 seconds

CHANNEL     NAME       UNITS      MAXIMUM     MINIMUM        MEAN  STD DEVIATION
   1        FORCE     NEWTONS      561.72      -66.35      241.65      194.93

   3      POSITION    METERS      -1.6827     -5.5887     -3.6649      1.1439
```

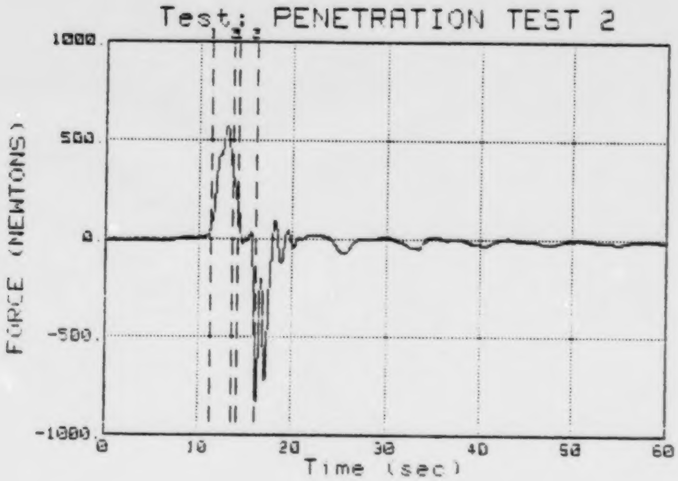
Test: PENETRATION TEST 2
1 2 2
FORCE (NEWTONS)
1000.
500.
0.
-500.
-1000.
0
10
20
30
40
50
60
Time (sec)

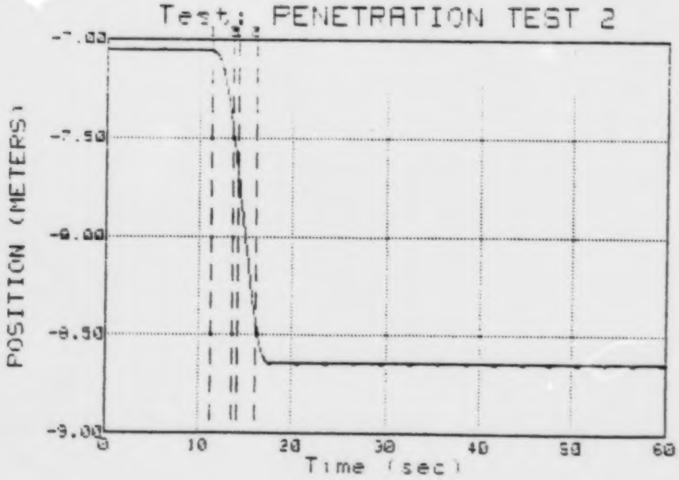
Test: PENETRATION TEST 2
1 2 2
POSITION (METERS)
-7.00
-7.50
-8.00
-8.50
-9.00
0
10
20
30
40
50
60
Time (sec)

```
                         STATISTICS SUMMARY


                        Project Number 3208C
                          RIDGE MODELLING

                 Test Name:              PENETRATION TEST 2
                 Date:                          28 Mar 1988
                 Start Time:                       18:57:41
                 Scanning Rate                        30 Hz
                 Test Duration               60.0000 seconds


             Interval  1 beginning at:         11.3000 seconds
             Interval  1 ending at:            14.1000 seconds

CHANNEL     NAME        UNITS      MAXIMUM    MINIMUM      MEAN  STD DEVIATION
   1        FORCE      NEWTONS      573.57      56.88    354.79      148.38

   3      POSITION     METERS      -7.0552    -7.6353   -7.2407       .1776

             Interval  2 beginning at:         13.6000 seconds
             Interval  2 ending at:            16.0000 seconds

CHANNEL     NAME        UNITS      MAXIMUM    MINIMUM      MEAN  STD DEVIATION
   1        FORCE      NEWTONS      343.67    -535.65     45.78      167.41

   3      POSITION     METERS      -7.4408    -8.4064   -7.9298       .2925
```

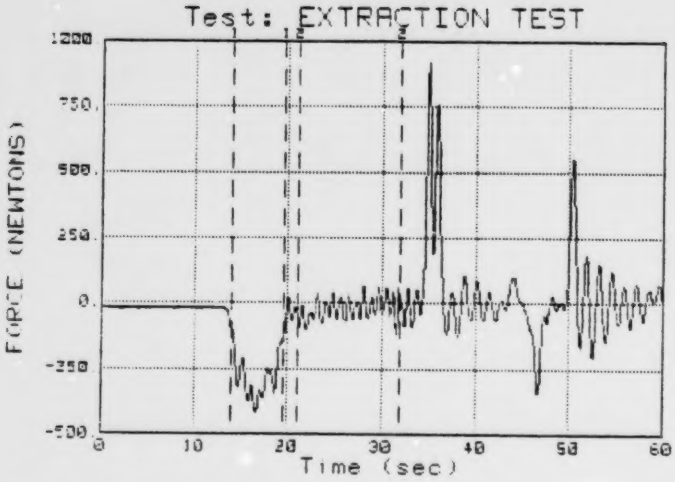
Test: EXTRACTION TEST
1
1
2
3
1200
750.
500.
250.
0.
-250
-500
FORCE (NEWTONS)
0
10
20
30
40
50
60
Time (sec)

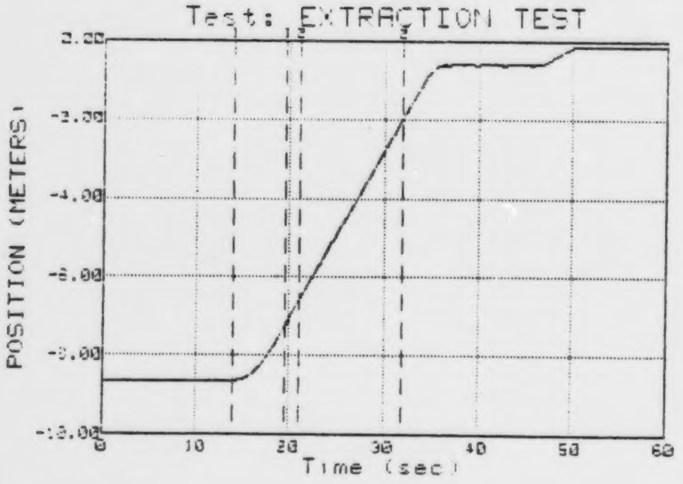
Test: EXTRACTION TEST
1
1
2
3
2.00
-2.00
-4.00
-6.00
-8.00
-10.00
POSITION (METERS)
0
10
20
30
40
50
60
Time (sec)

```
                         STATISTICS SUMMARY

                         Project Number 3209C
                           RIDGE MODELLING

                 Test Name:                 EXTRACTION TEST
                 Date:                          28 Mar 1988
                 Start Time:                       19:00:58
                 Scanning Rate                        30 Hz
                 Test Duration              60.0000 seconds

               Interval  1 beginning at:        14.0000 seconds
               Interval  1 ending at:           19.5000 seconds

CHANNEL     NAME       UNITS     MAXIMUM     MINIMUM       MEAN  STD DEVIATION
   1        FORCE     NEWTONS    -101.92     -417.14    -280.93       80.92

   3      POSITION    METERS     -7.2390     -8.6406    -8.1620        .4342

               Interval  2 beginning at:        21.0000 seconds
               Interval  2 ending at:           31.9000 seconds

CHANNEL     NAME       UNITS     MAXIMUM     MINIMUM       MEAN  STD DEVIATION
   1        FORCE     NEWTONS      63.99     -120.88     -20.94       39.24

   3      POSITION    METERS     -2.0106     -6.5832    -4.2984      1.3272
```

APPENDIX A.2

ICE PROPERTIES AND TEMPERATURE DATA

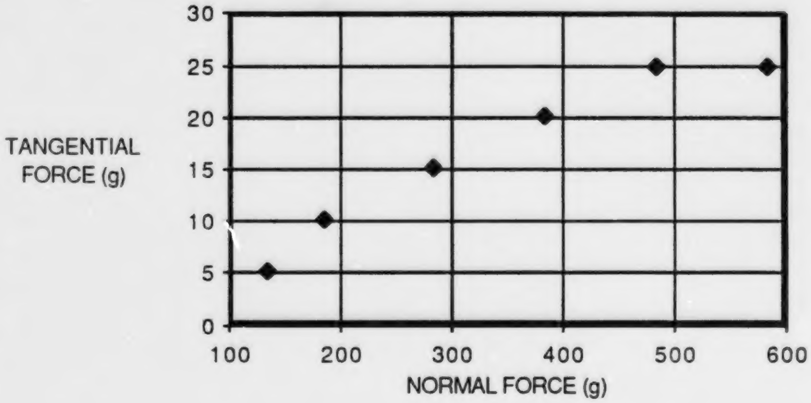

FRICTION FACTOR MEASUREMENTS

EGADS Ice

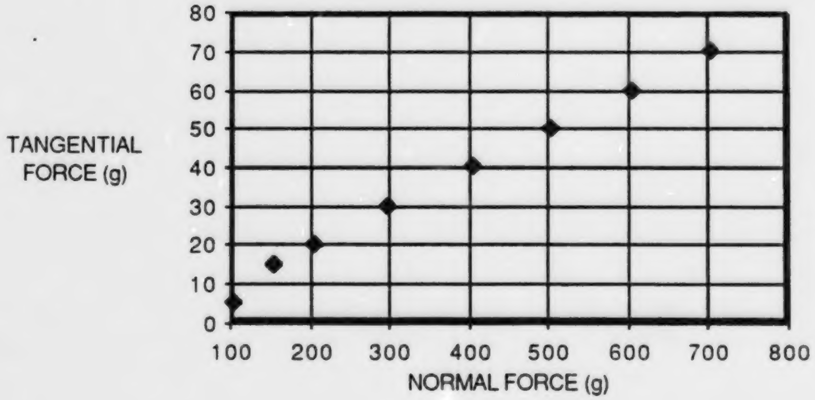

FRICTION FACTOR MEASUREMENTS

Beads Ice

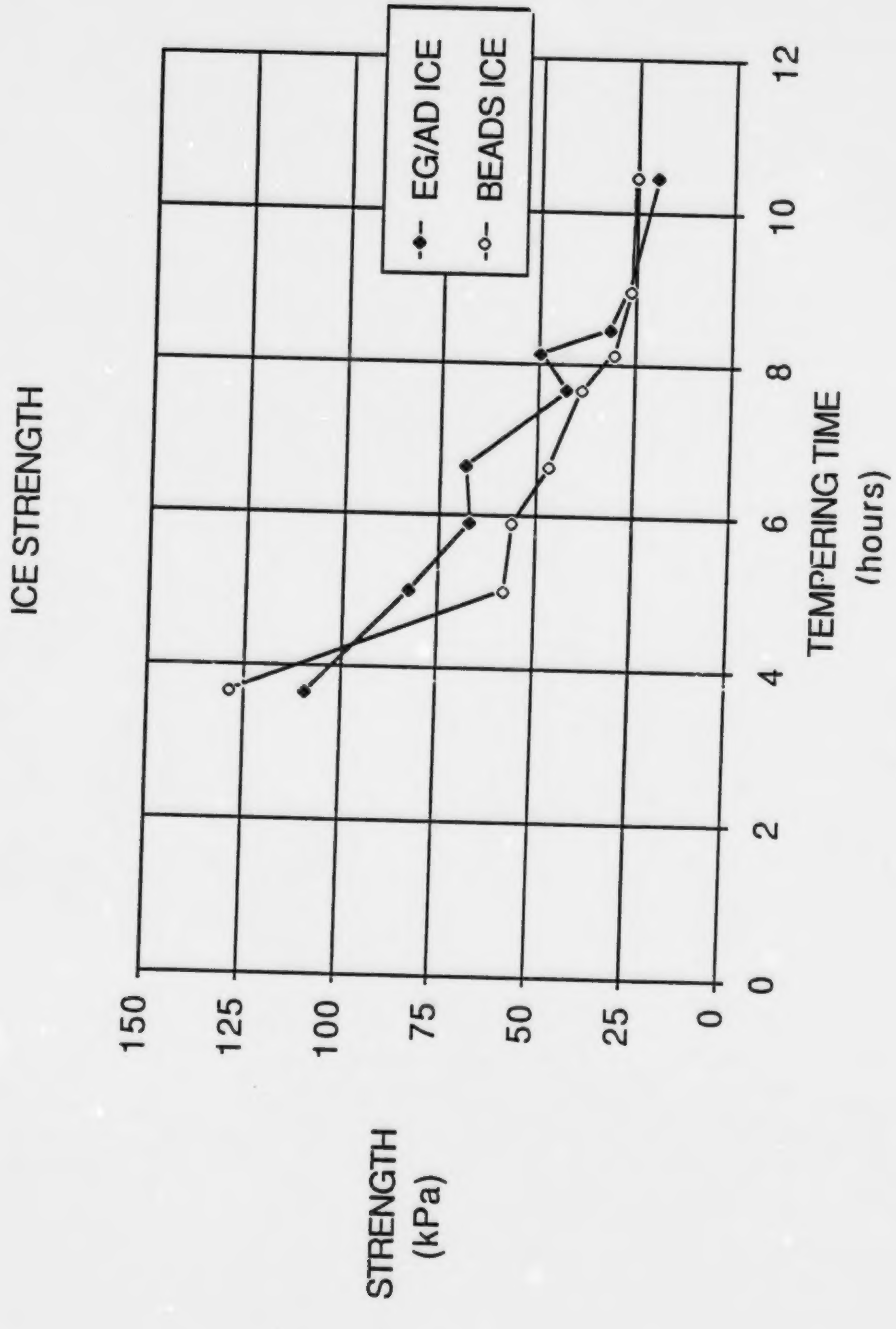
ICE STRENGTH
STRENGTH (kPa)
150
125
100
75
50
25
0
0
2
4
6
8
10
12
TEMPERING TIME (hours)
EG/AD ICE
BEADS ICE

ICE STRENGTH

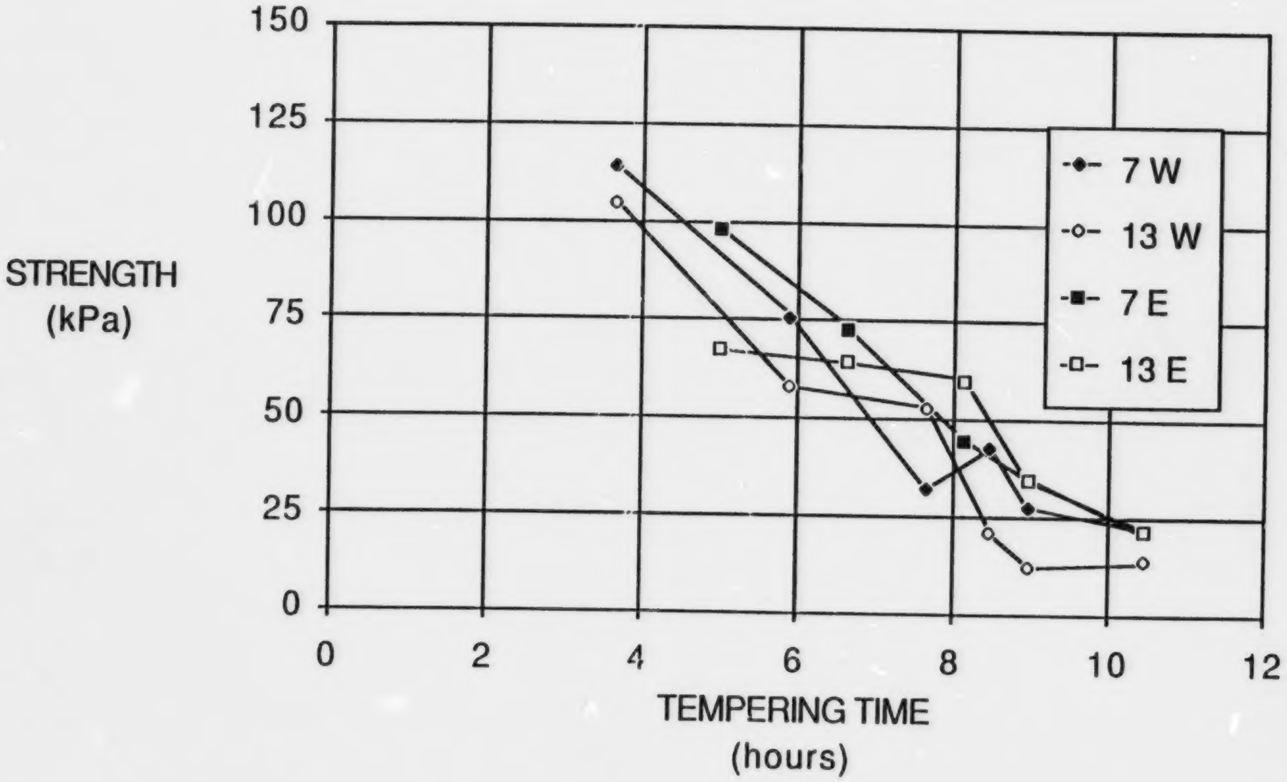

Figure 3.4. THERMOCOUPLE LAYOUT

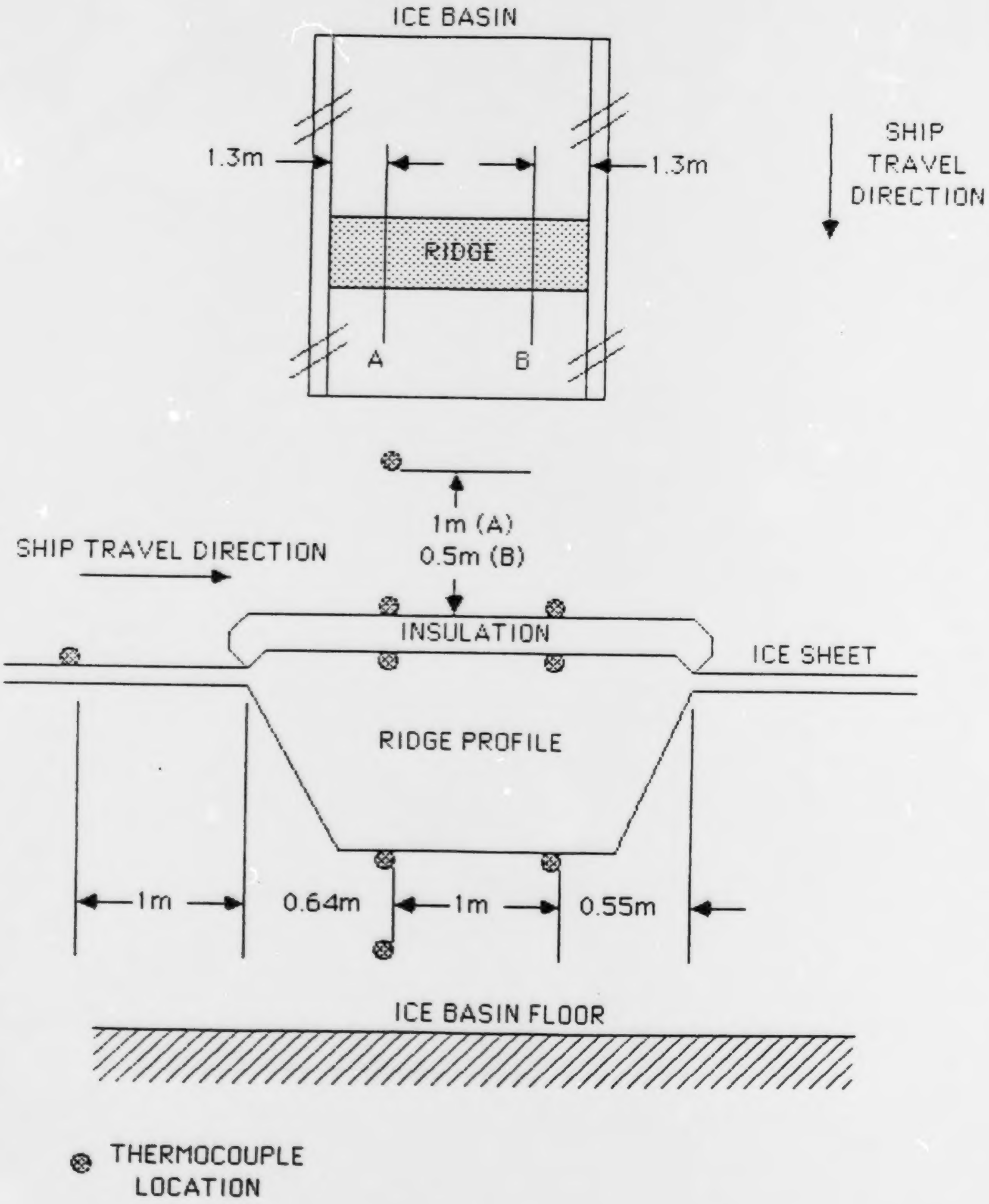
ICE BASIN
1.3m
1.3m
SHIP
TRAVEL
DIRECTION
RIDGE
A
B
1m (A)
0.5m (B)
SHIP TRAVEL DIRECTION
INSULATION
ICE SHEET
RIDGE PROFILE
1m
0.64m
1m
0.55m
ICE BASIN FLOOR
THERMOCOUPLE
LOCATION

AIR TEMPERATURE

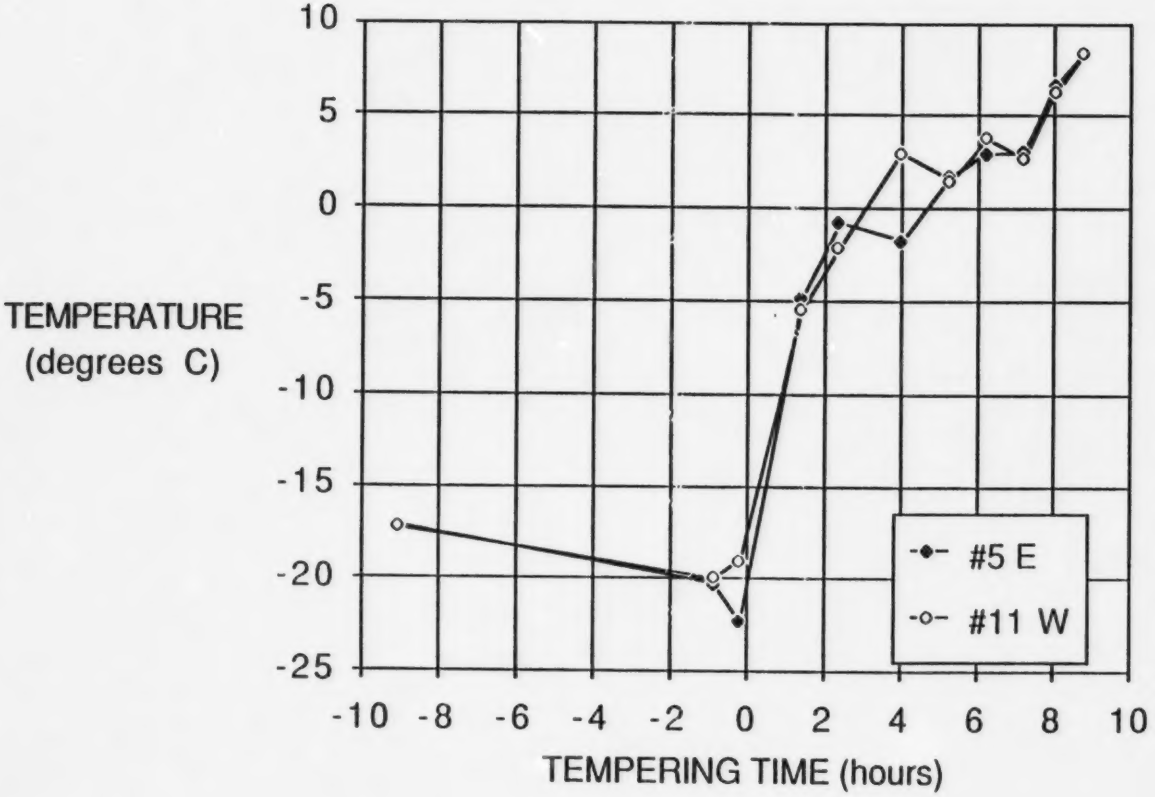

INTERFACE OF RIDGE
AND INSULATION

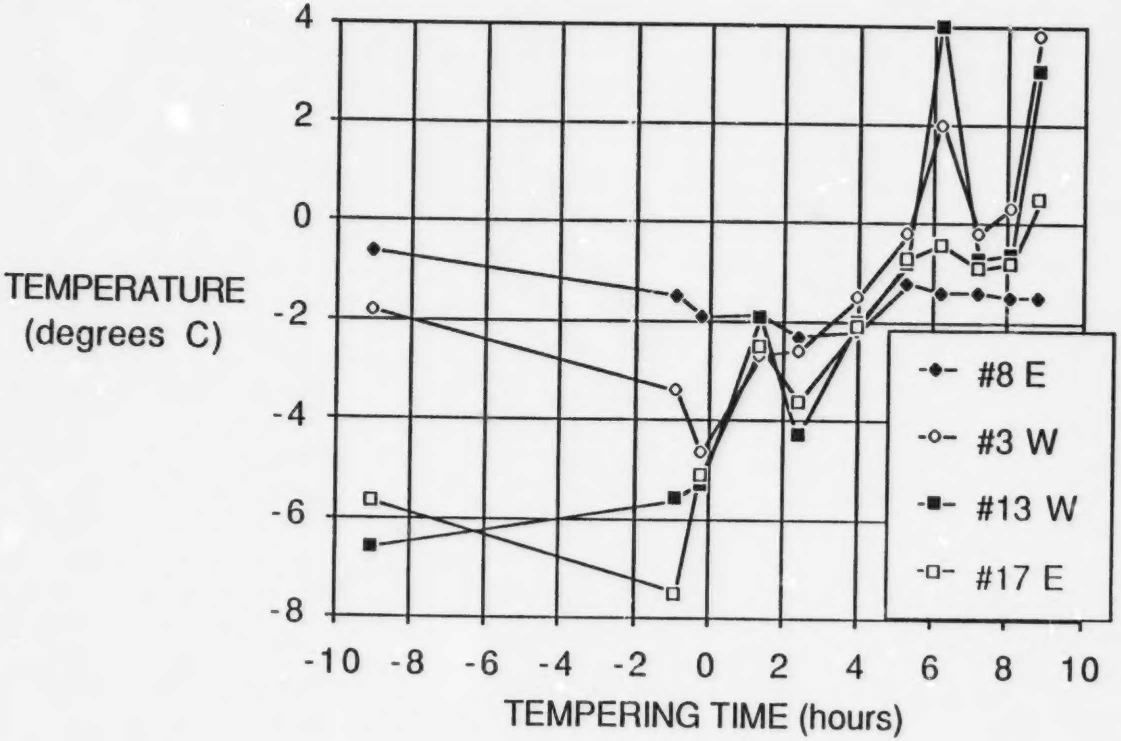

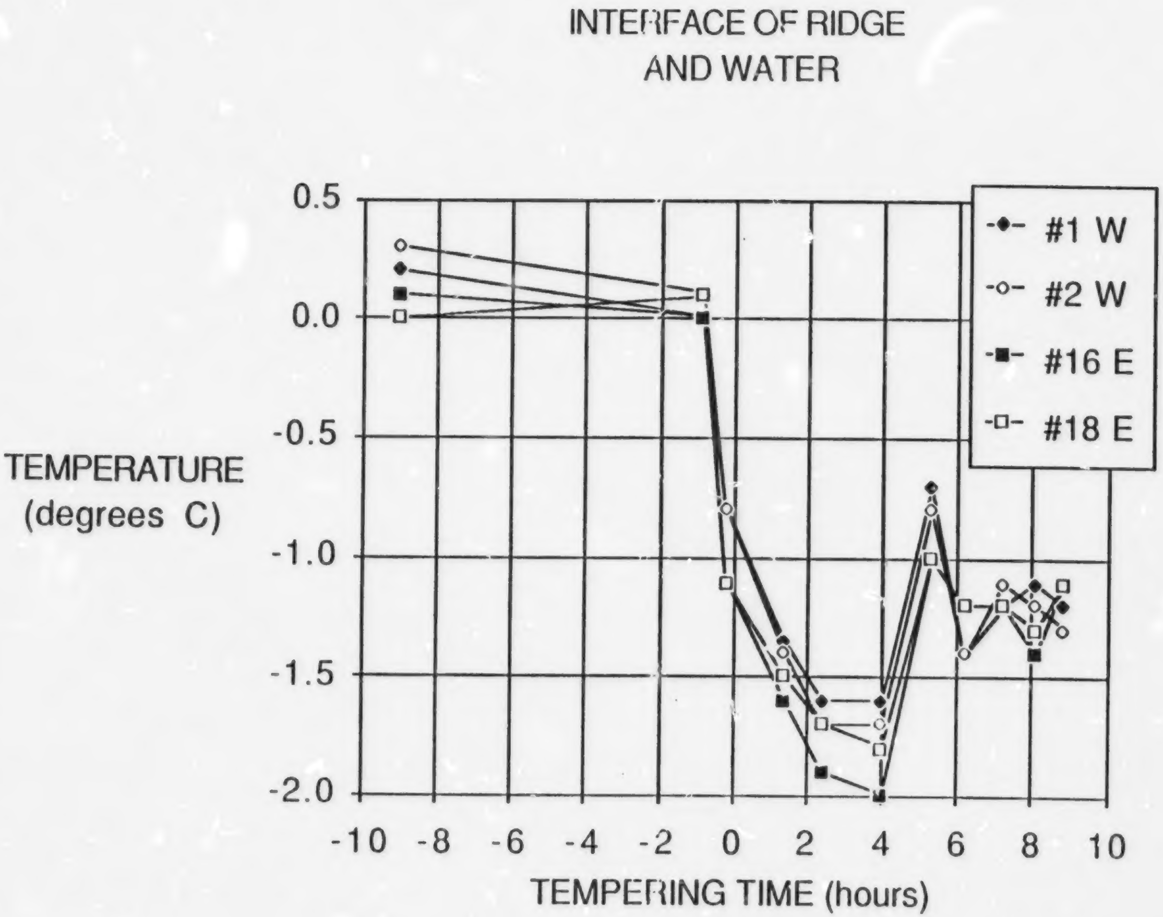
INTERFACE OF RIDGE AND WATER

ICE SHEET TEMPERATURE

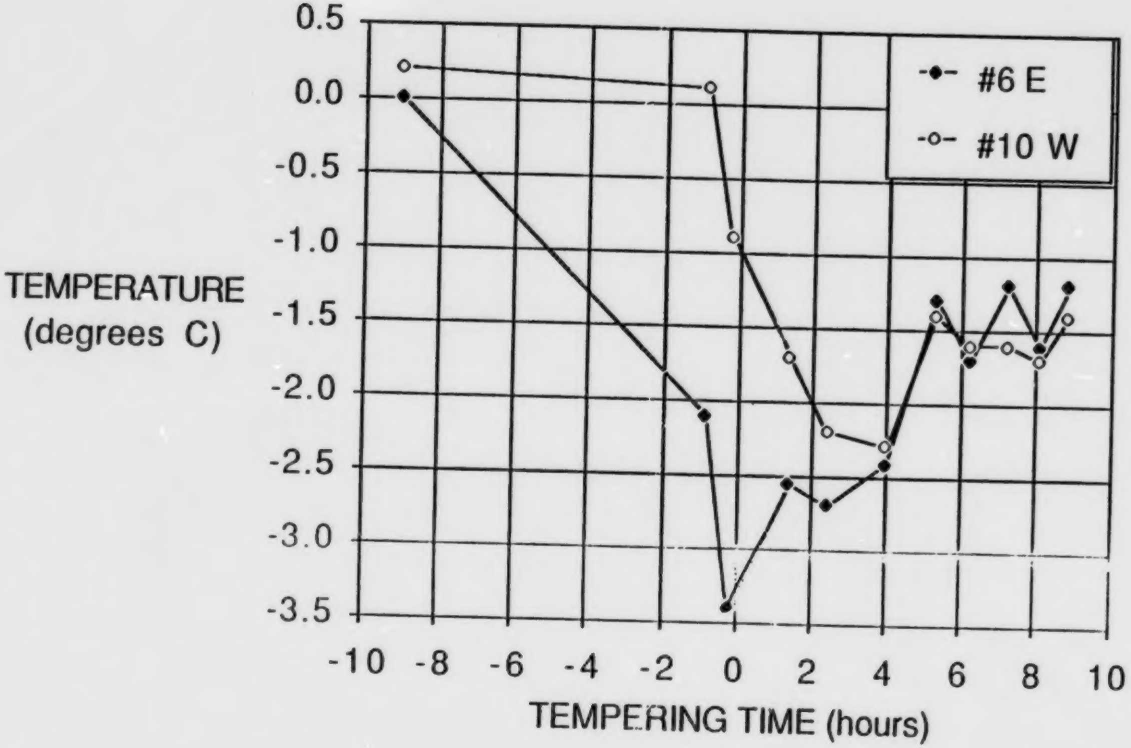

INTERFACE OF AIR
AND INSULATION

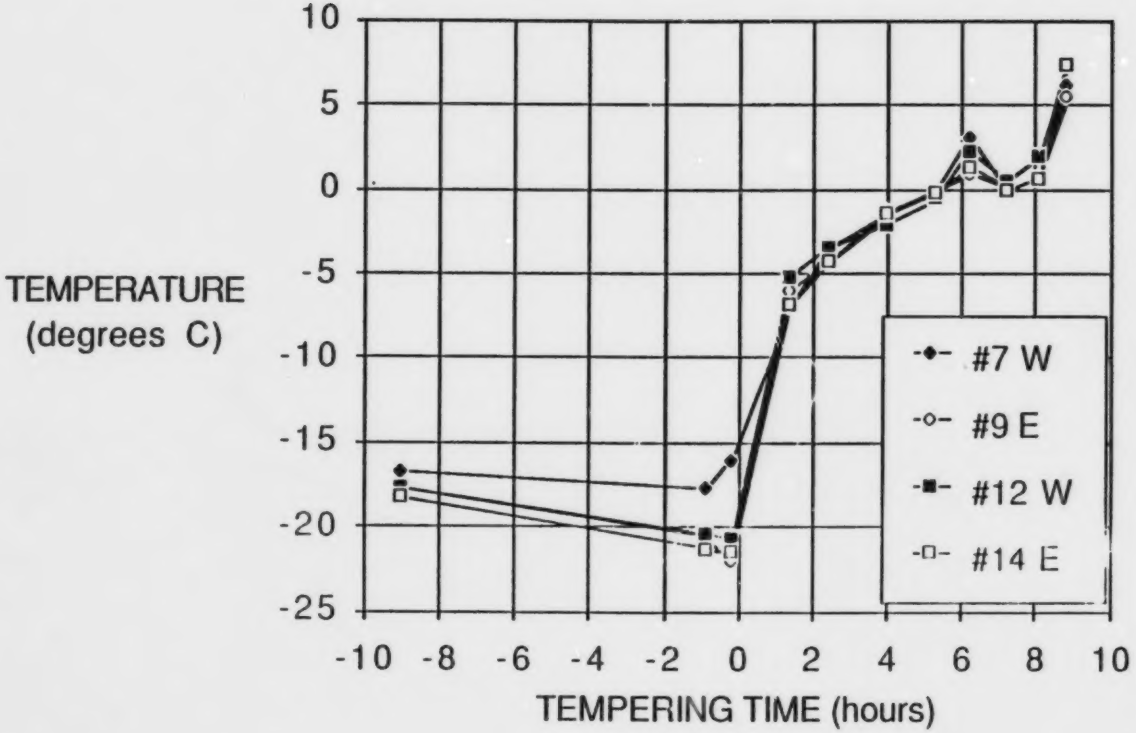

APPENDIX B

RAW DATA FROM SHEET #2 TESTS AT FLEET TECHNOLOGY LIMITED

CONTENTS:

B.1 Raw Time Histories for All Data Channels

B.2 Temperature Data

APPENDIX B.1

RAW TIME HISTORIES FOR ALL DATA CHANNELS

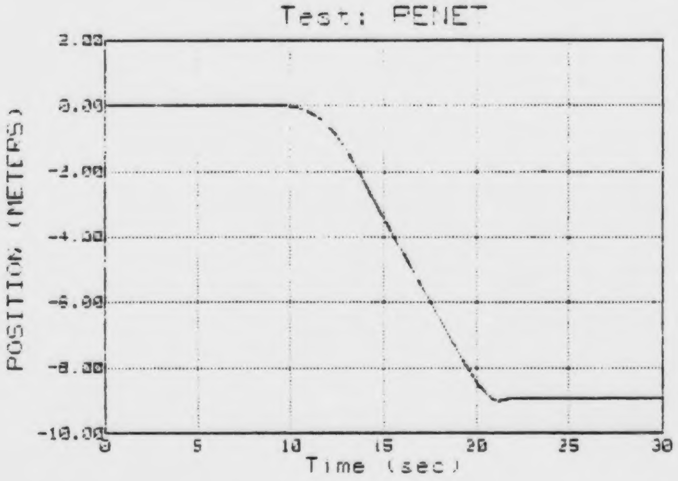
Test: PENET
2.00
0.00
-2.00
-4.00
-6.00
-8.00
-10.00
POSITION (METERS)
0
5
10
15
20
25
30
Time (sec)

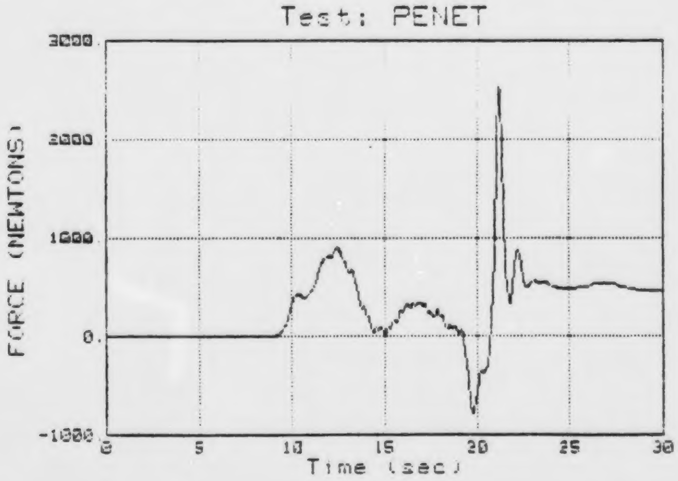
Test: PENET
3000
2000
1000
0.
-1000
FORCE (NEWTONS)
0
5
10
15
20
25
30
Time (sec)

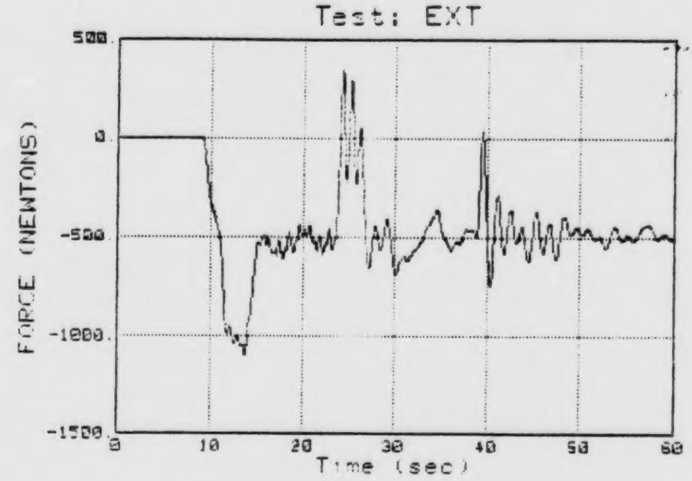
Test: EXT
FORCE (NEWTONS)
500.
0.
-500.
-1000.
-1500.
0
10
20
30
40
50
60
Time (sec)

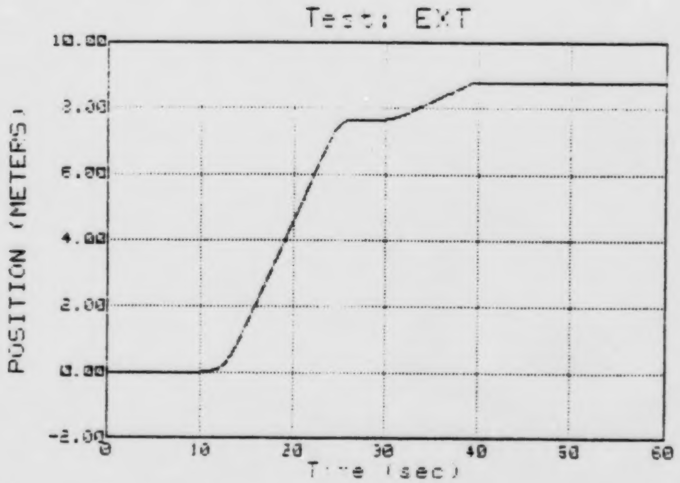
Test: EXT
POSITION (METERS)
10.00
8.00
6.00
4.00
2.00
0.00
-2.00
0
10
20
30
40
50
60
Time (sec)

APPENDIX B.2

TEMPERATURE DATA

Figure 3.4. THERMOCOUPLE LAYOUT

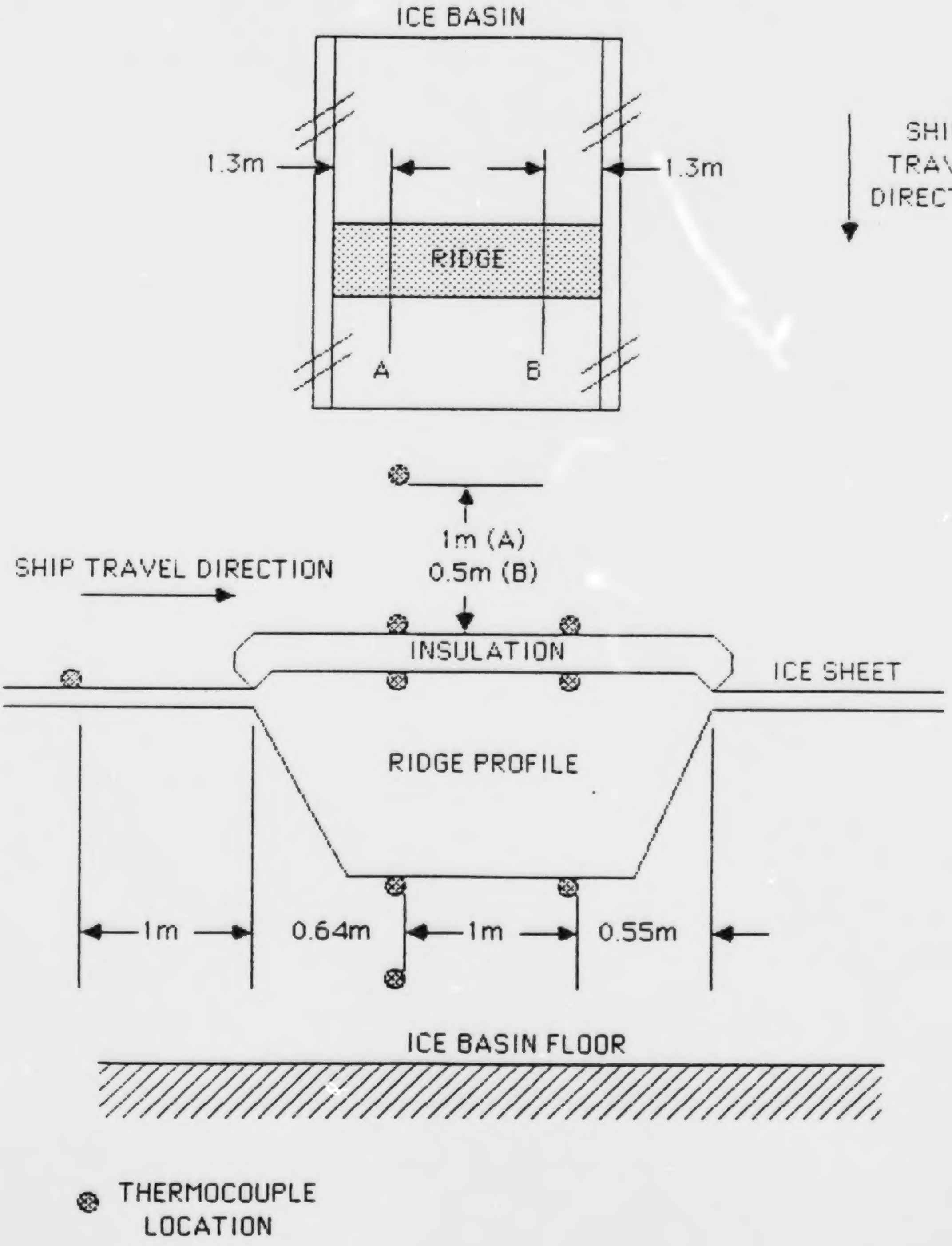
ICE BASIN
1.3m
1.3m
SHIP TRAVEL DIRECTION
RIDGE
A
B
1m (A)
0.5m (B)
SHIP TRAVEL DIRECTION
INSULATION
ICE SHEET
RIDGE PROFILE
1m
0.64m
1m
0.55m
ICE BASIN FLOOR
THERMOCOUPLE LOCATION

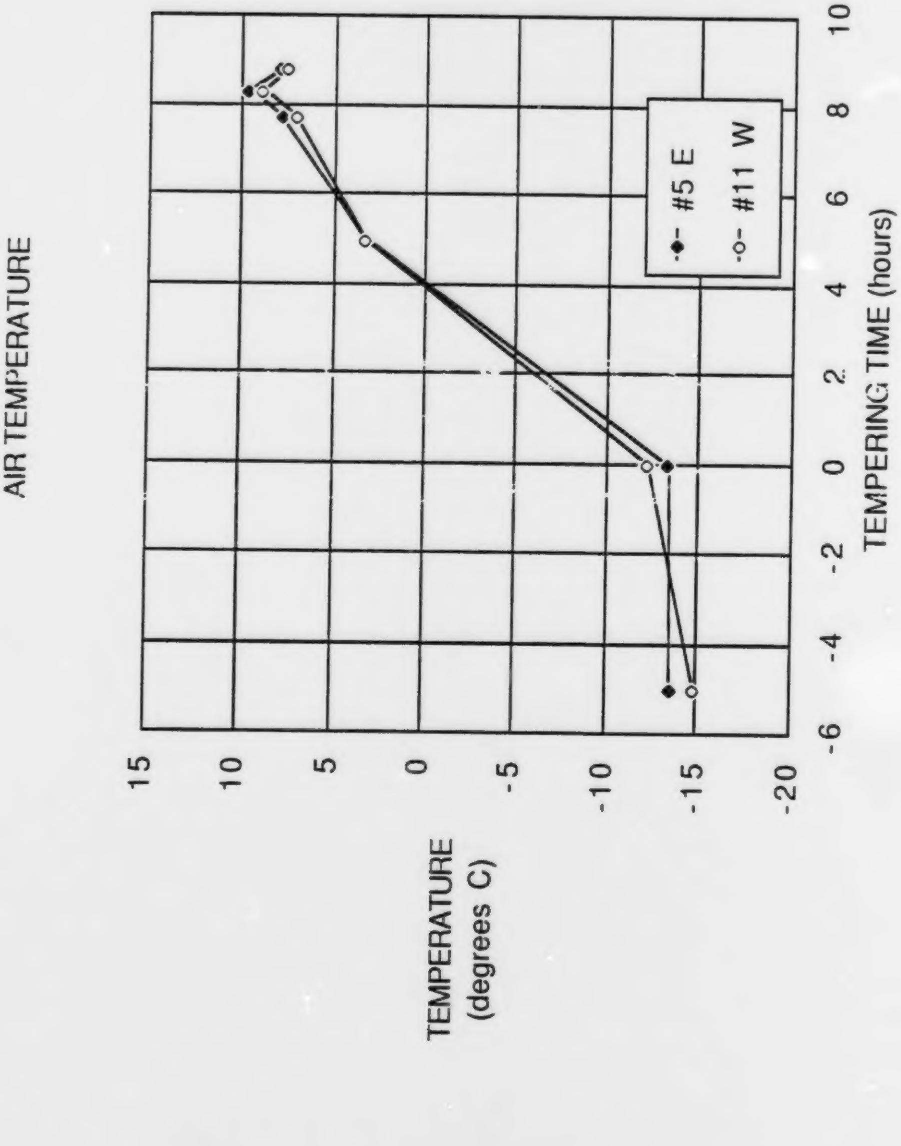
AIR TEMPERATURE
TEMPERATURE
(degrees C)
15
10
5
0
-5
-10
-15
-20
-6
-4
-2
0
2
4
6
8
10
TEMPERING TIME (hours)
#5 E
#11 W

INTERFACE OF RIDGE AND INSULATION

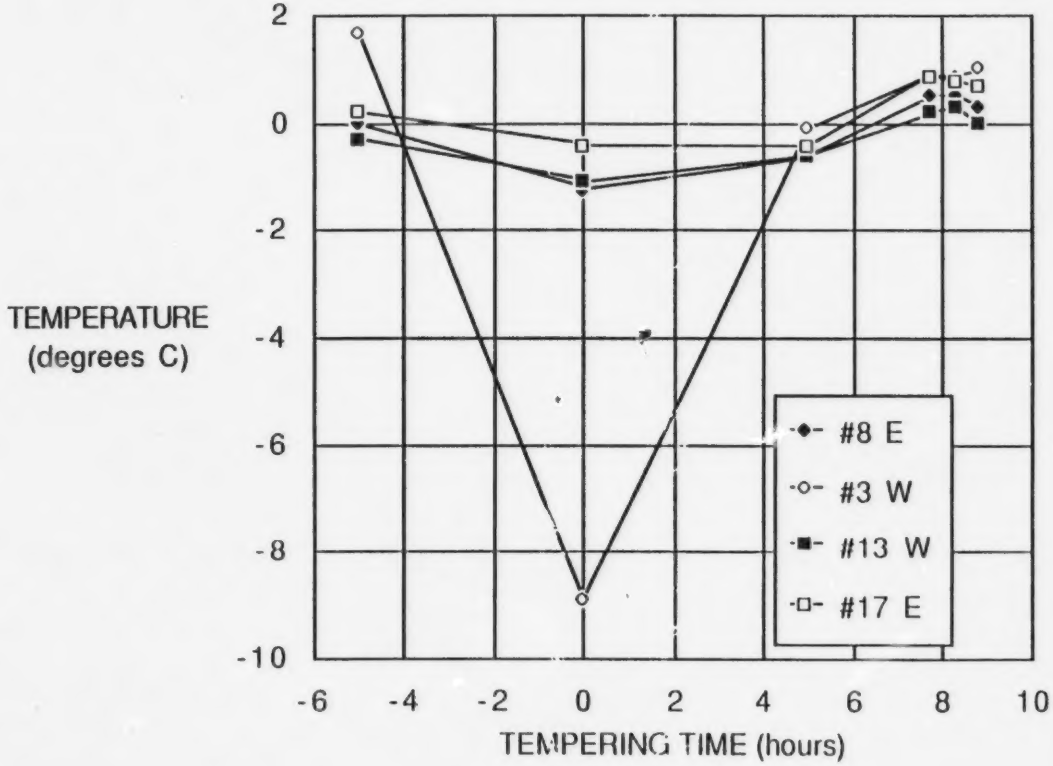

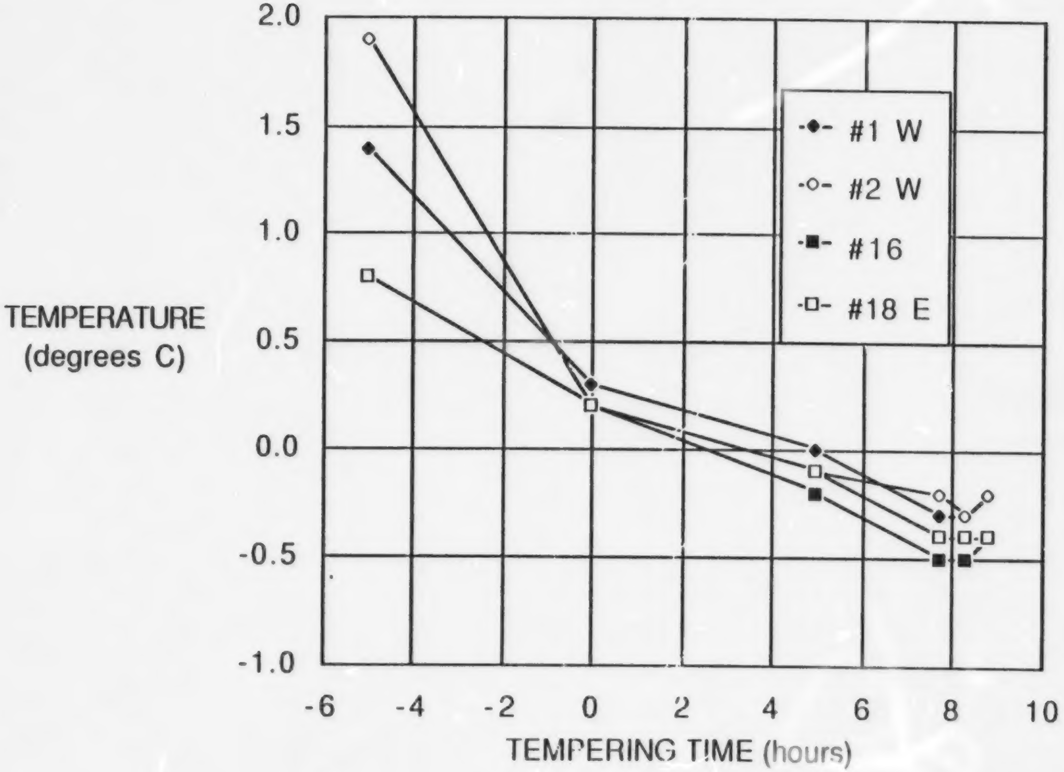

INTERFACE OF RIDGE AND WATER

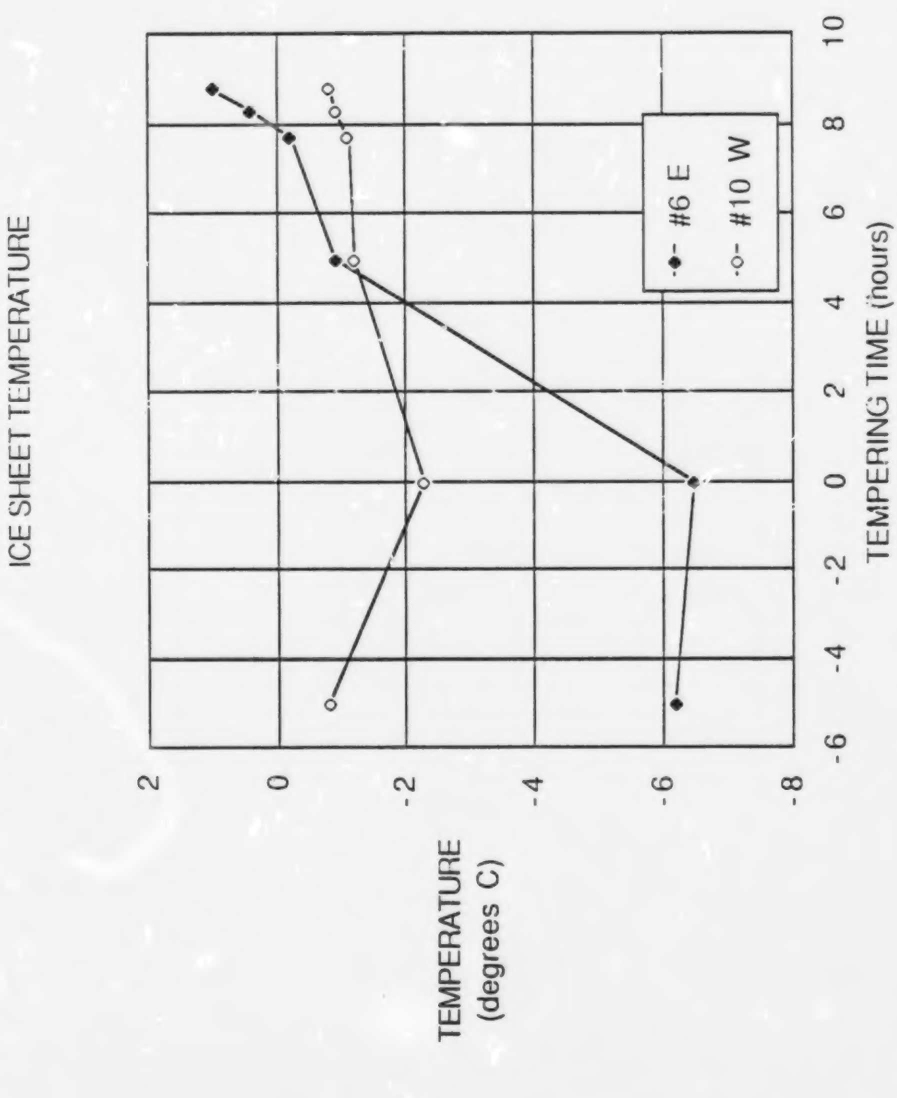
ICE SHEET TEMPERATURE
TEMPERATURE (degrees C)
2
0
-2
-4
-6
-8
TEMPERING TIME (hours)
-6
-4
-2
0
2
4
6
8
10
#6 E
#10 W

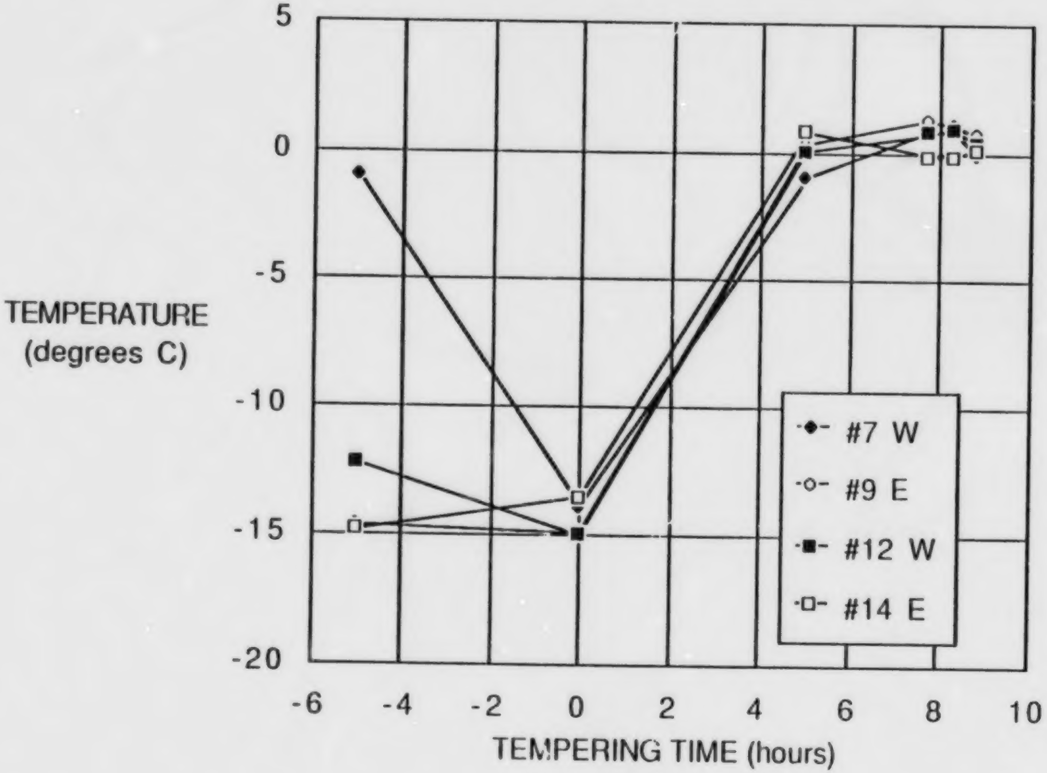

INTERFACE OF AIR AND INSULATION

APPENDIX C

RAW DATA FROM SHEET #1 TESTS AT THE IMD

CONTENTS:

C.1 Raw Time Histories For All Data Channels

C.2 Reduced Plots of Force Vs. Penetration and Cumulative Penetration Energy - Test Data Filtered at 1 Hz

C.3 Reduced Plots of Force Vs. Penetration and Cumulative Penetration Energy - Test Data Unfiltered

C.4 Ice and Ridge Properties

C.5 Temperature Data

APPENDIX C.1

RAW TIME HISTORIES FOR ALL DATA CHANNELS

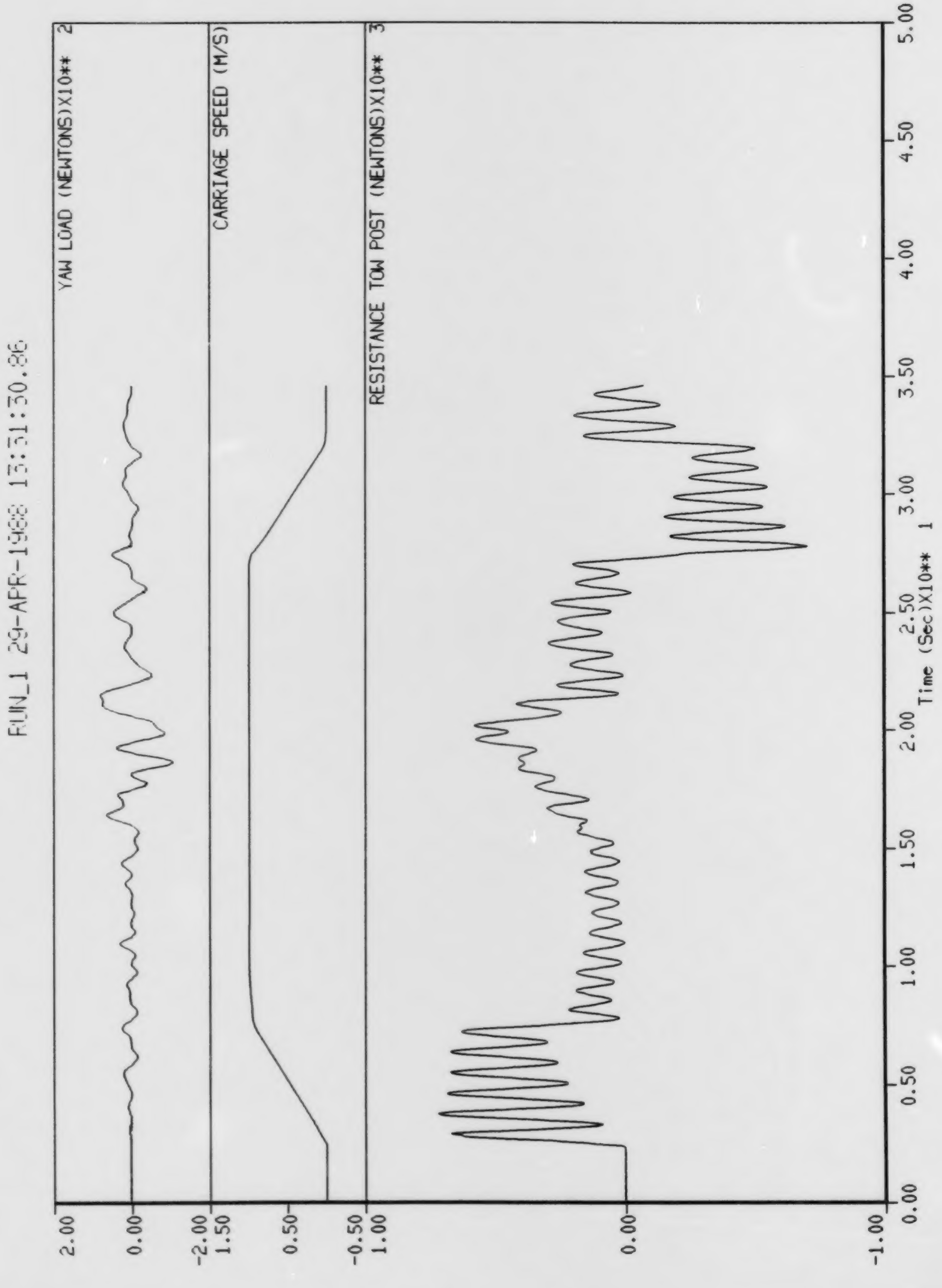
RUN_1 29-APR-1988 13:31:30.86
YAW LOAD (NEWTONS)X10** 2
CARRIAGE SPEED (M/S)
RESISTANCE TOW POST (NEWTONS)X10** 3
2.00
0.00
-2.00
1.50
0.50
-0.50
1.00
0.00
-1.00
0.00
0.50
1.00
1.50
2.00
2.50
3.00
3.50
4.00
4.50
5.00
Time (Sec)X10** 1

RUN_1 29-APR-1988 13:31:30.86

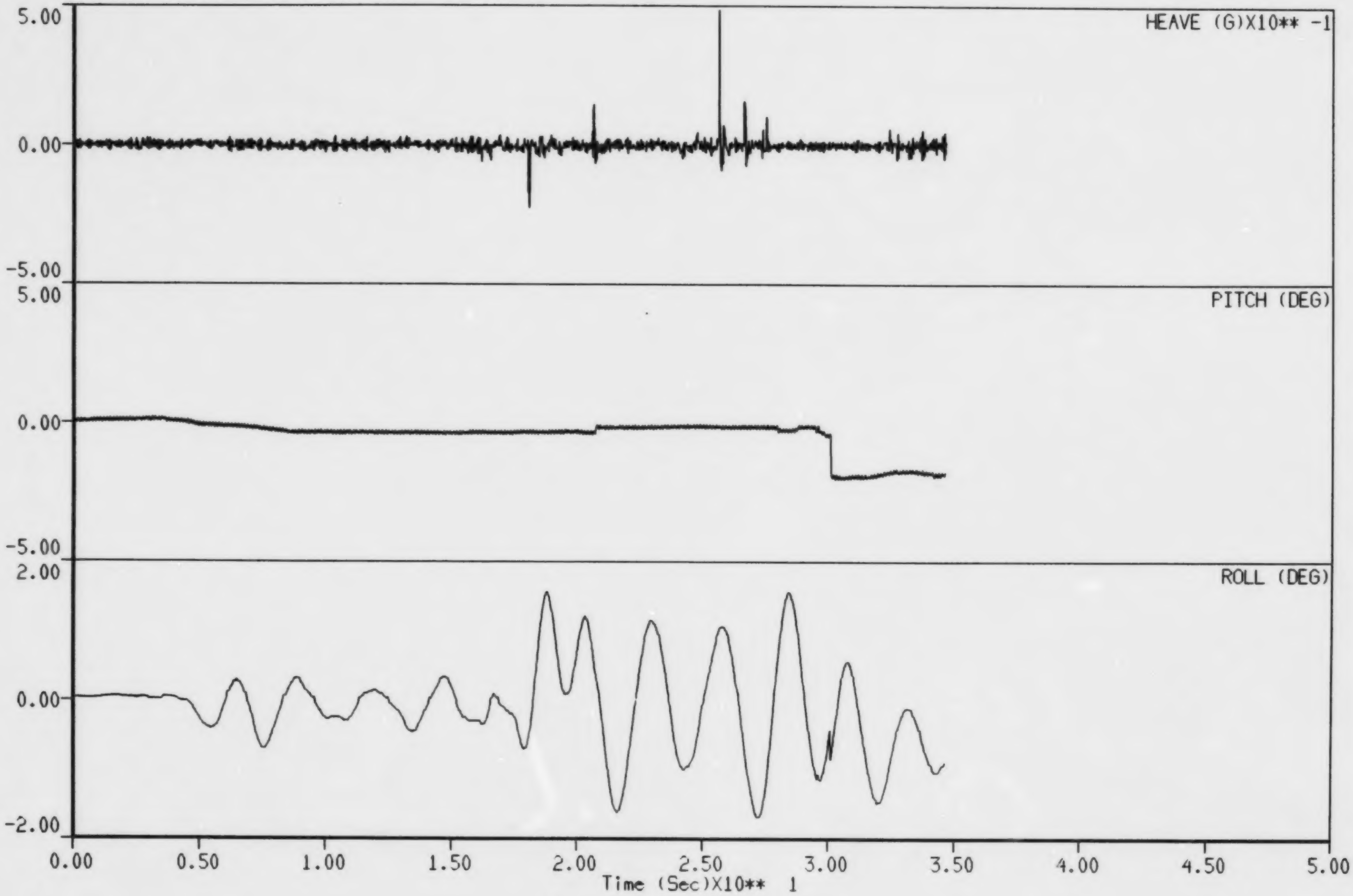

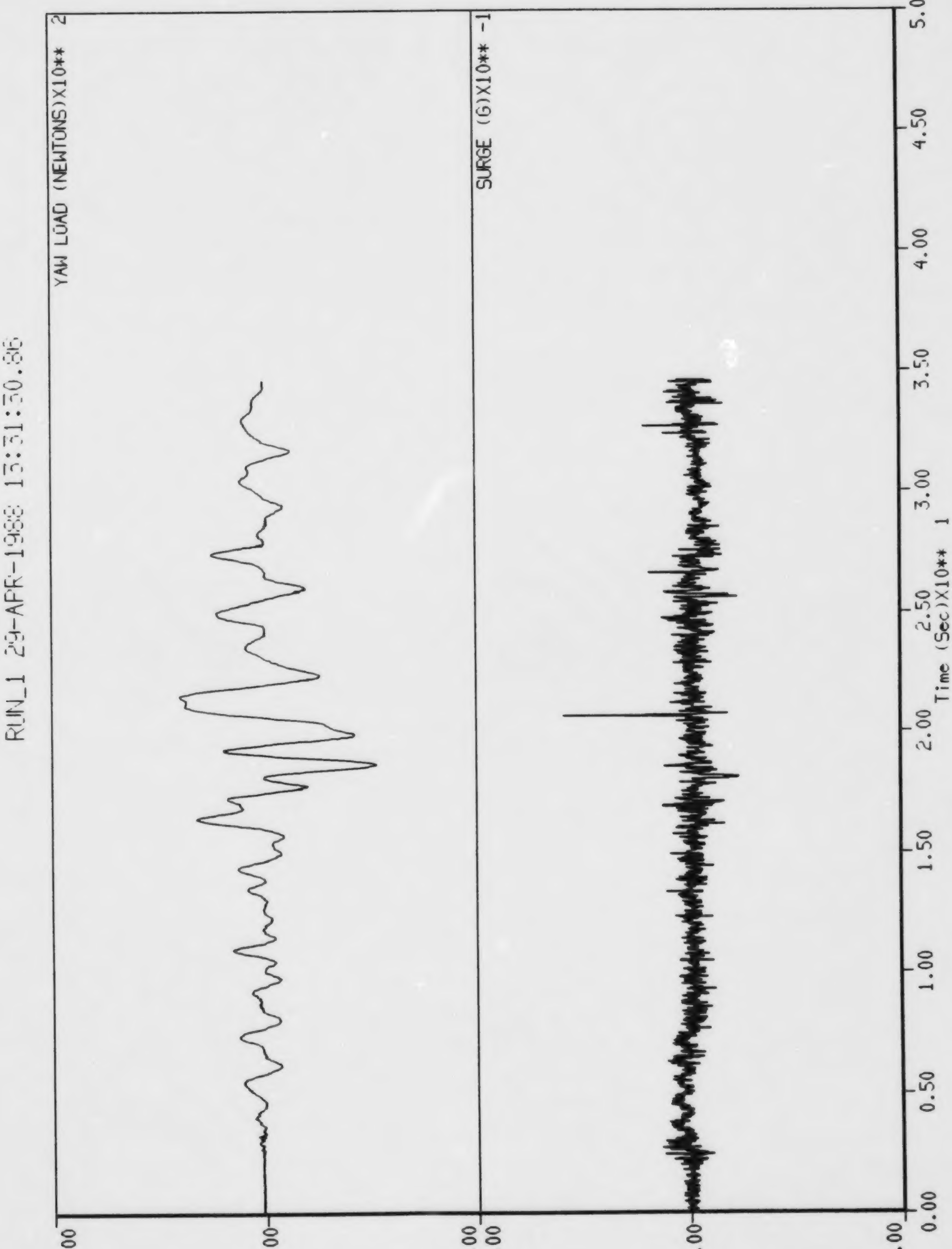
RUN_1 29-APR-1988 13:31:30.86
YAW LOAD (NEWTONS)X10** 2
SURGE (G)X10** -1
2.00
0.00
-2.00
5.00
0.00
-5.00
0.00
0.50
1.00
1.50
2.00
2.50
3.00
3.50
4.00
4.50
5.00
Time (Sec)X10** 1

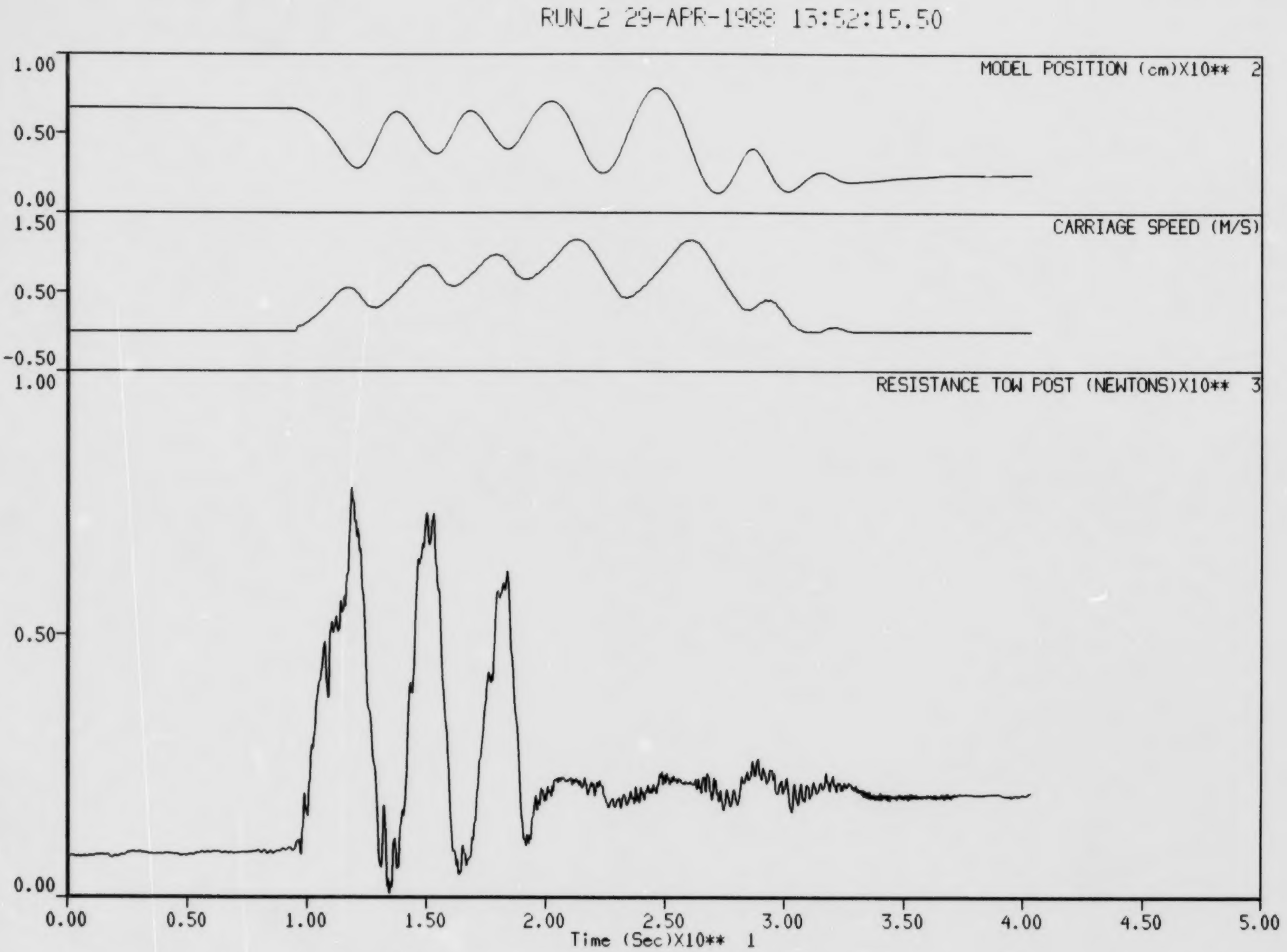
RUN_2 29-APR-1988 13:52:15.50
MODEL POSITION (cm)X10** 2
1.00
0.50
0.00
CARRIAGE SPEED (M/S)
1.50
0.50
-0.50
RESISTANCE TOW POST (NEWTONS)X10** 3
1.00
0.50
0.00
0.00
0.50
1.00
1.50
2.00
2.50
3.00
3.50
4.00
4.50
5.00
Time (Sec)X10** 1

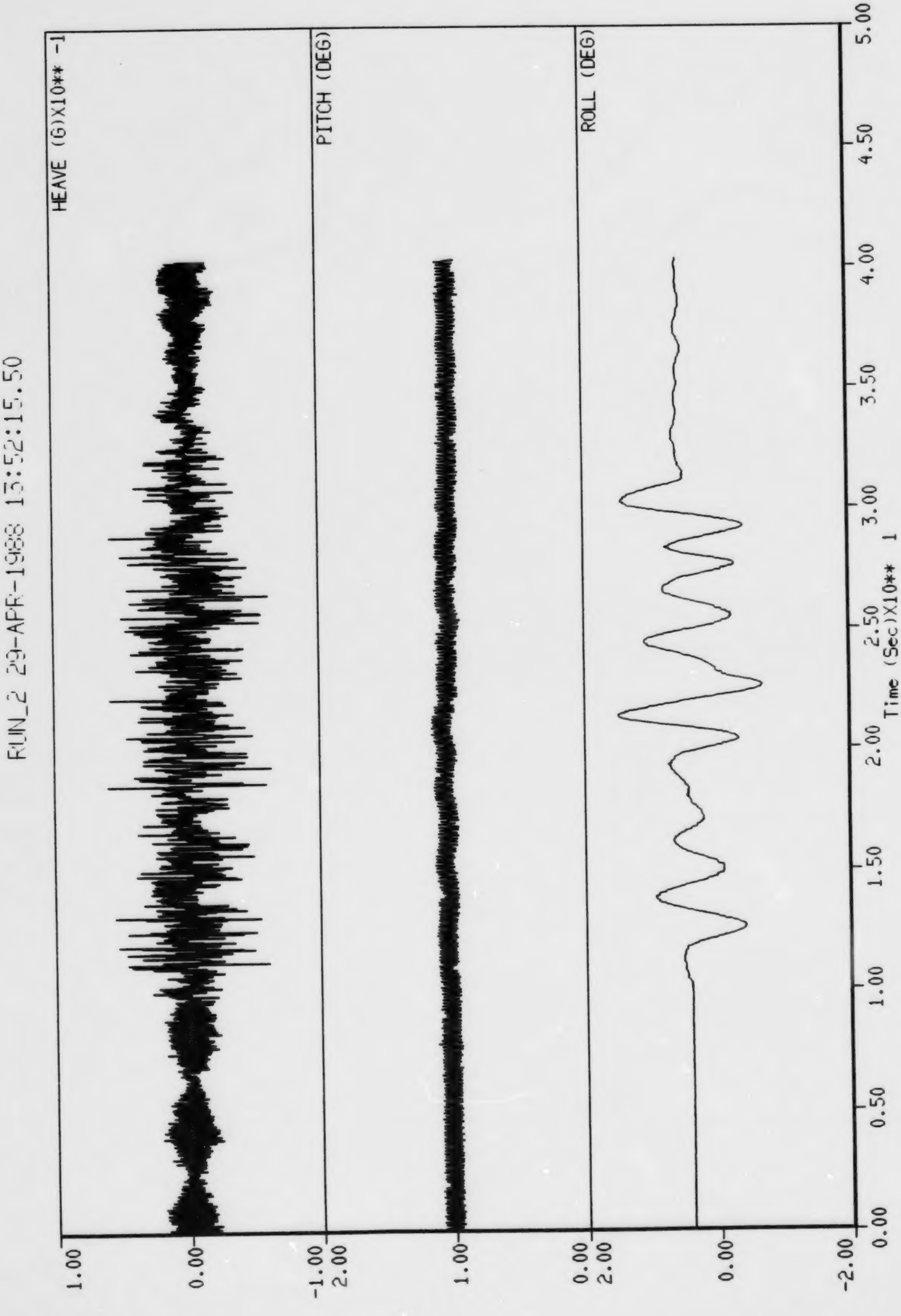
RUN_2 29-APR-1988 13:52:15.50
HEAVE (G)X10** -1
PITCH (DEG)
ROLL (DEG)
1.00
0.00
-1.00
2.00
1.00
0.00
2.00
0.00
-2.00
0.00
0.50
1.00
1.50
2.00
2.50
3.00
3.50
4.00
4.50
5.00
Time (Sec)X10** 1

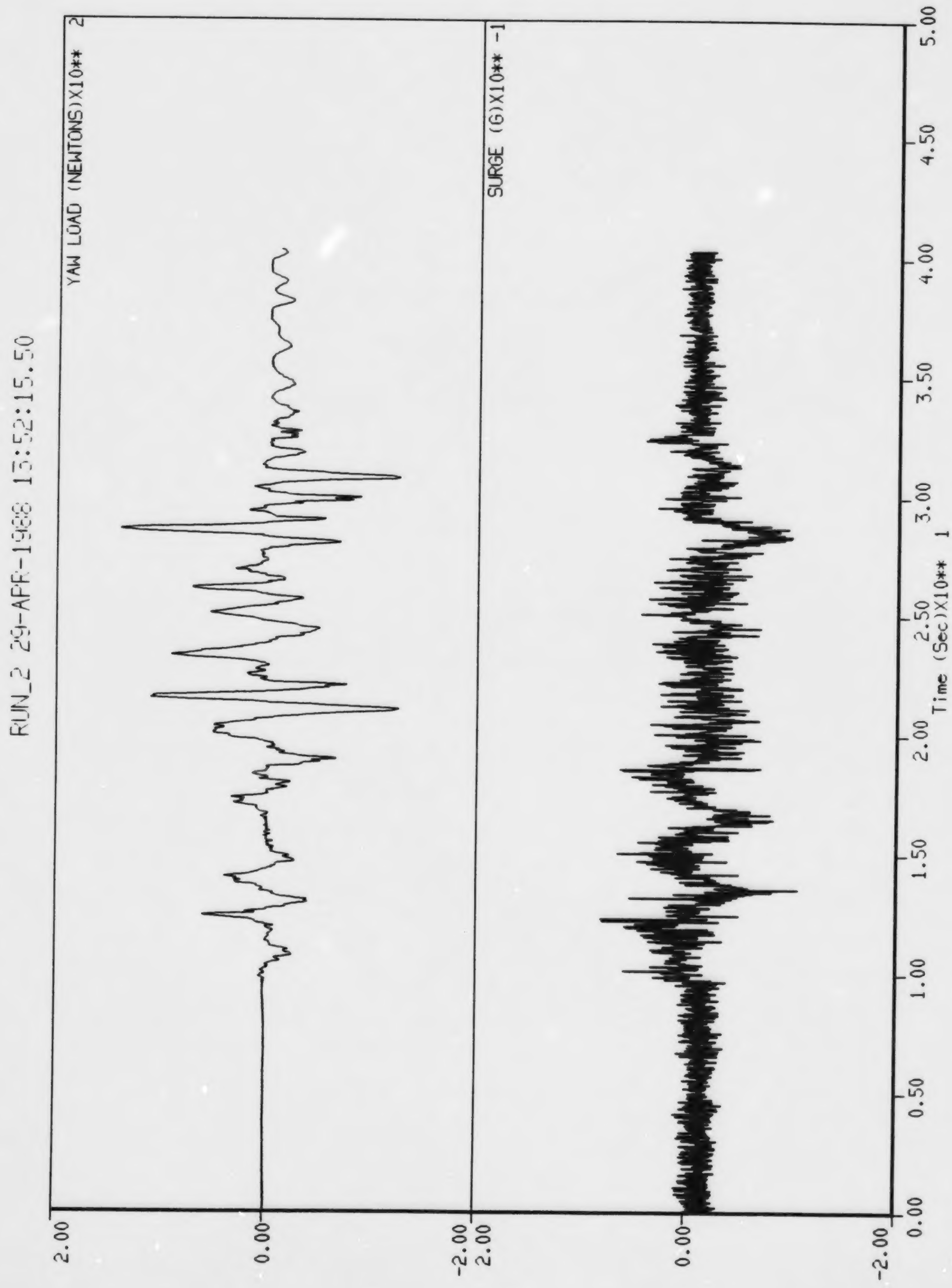
RUN_2 29-APR-1988 13:52:15.50
YAW LOAD (NEWTONS)X10** 2
SURGE (G)X10** -1
2.00
0.00
-2.00
2.00
0.00
-2.00
0.00
0.50
1.00
1.50
2.00
2.50
3.00
3.50
4.00
4.50
5.00
Time (Sec)X10** 1

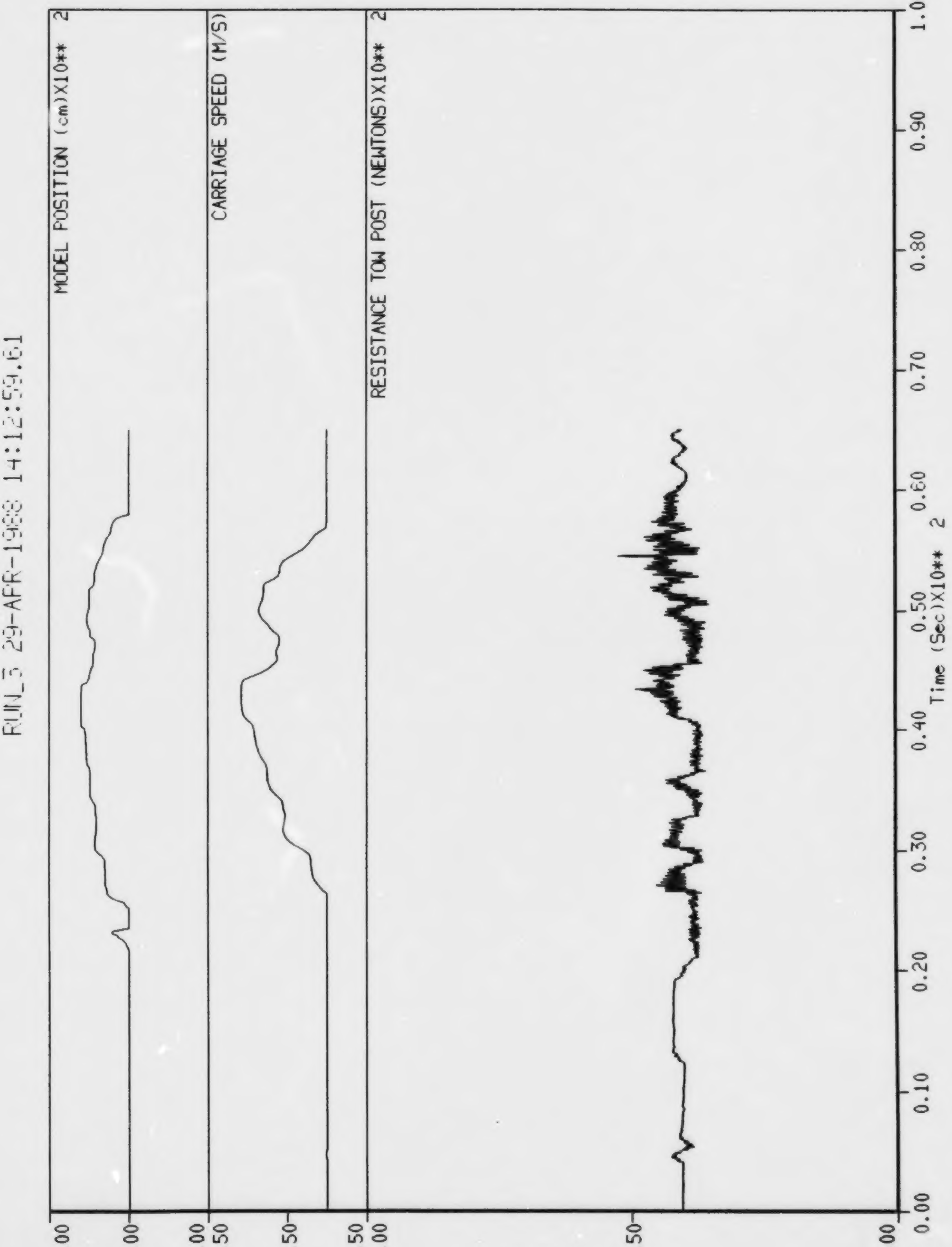
RUN_3 29-APR-1988 14:12:59.61
MODEL POSITION (cm)X10** 2
CARRIAGE SPEED (M/S)
RESISTANCE TOW POST (NEWTONS)X10** 2
1.00
0.00
-1.00
1.50
0.50
-0.50
5.00
2.50
0.00
0.00
0.10
0.20
0.30
0.40
0.50
0.60
0.70
0.80
0.90
1.00
Time (Sec)X10** 2

RUN_3 29-APR-1988 14:12:59.61

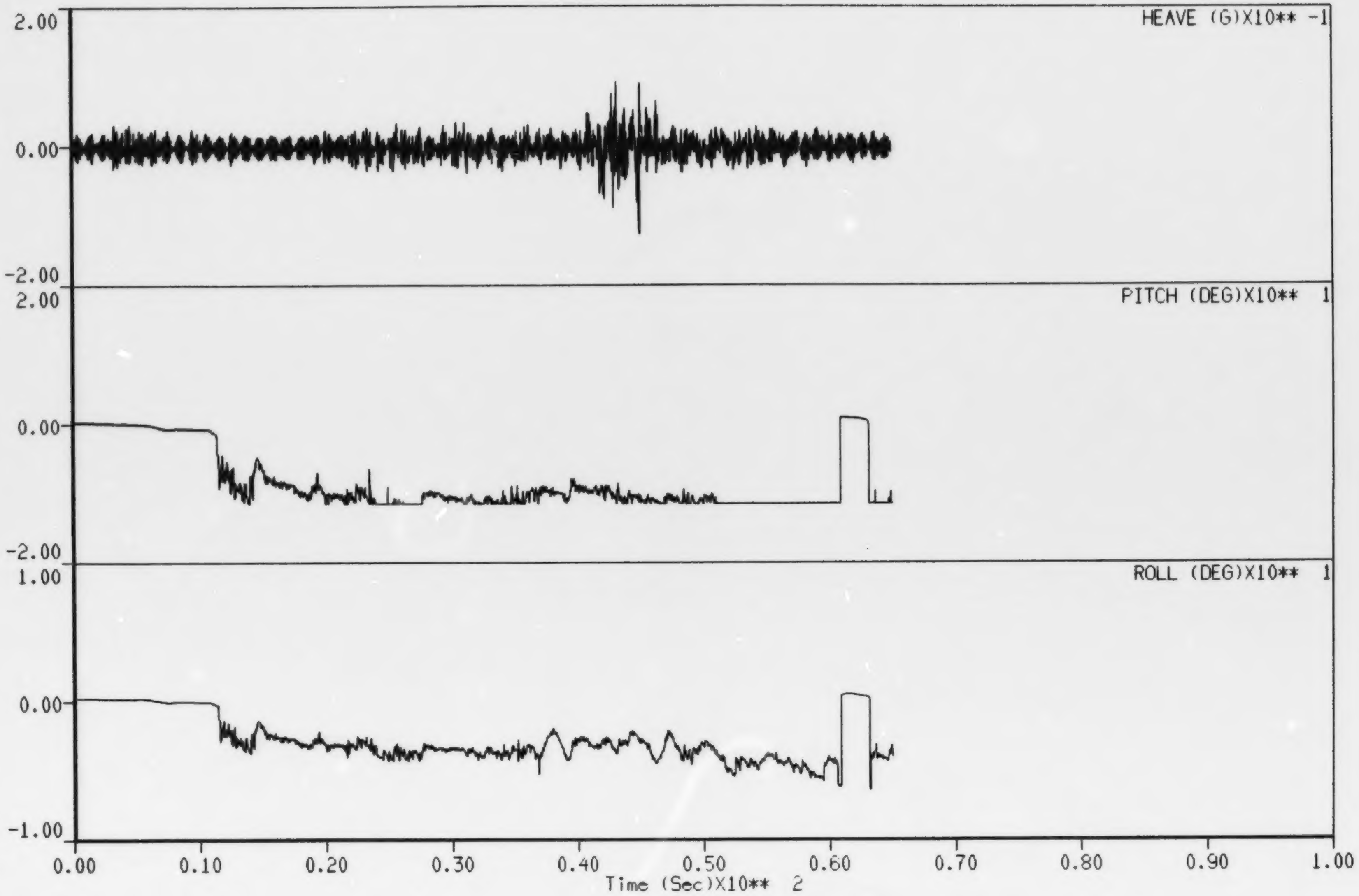

RUN_3 29-APR-1988 14:12:59.61

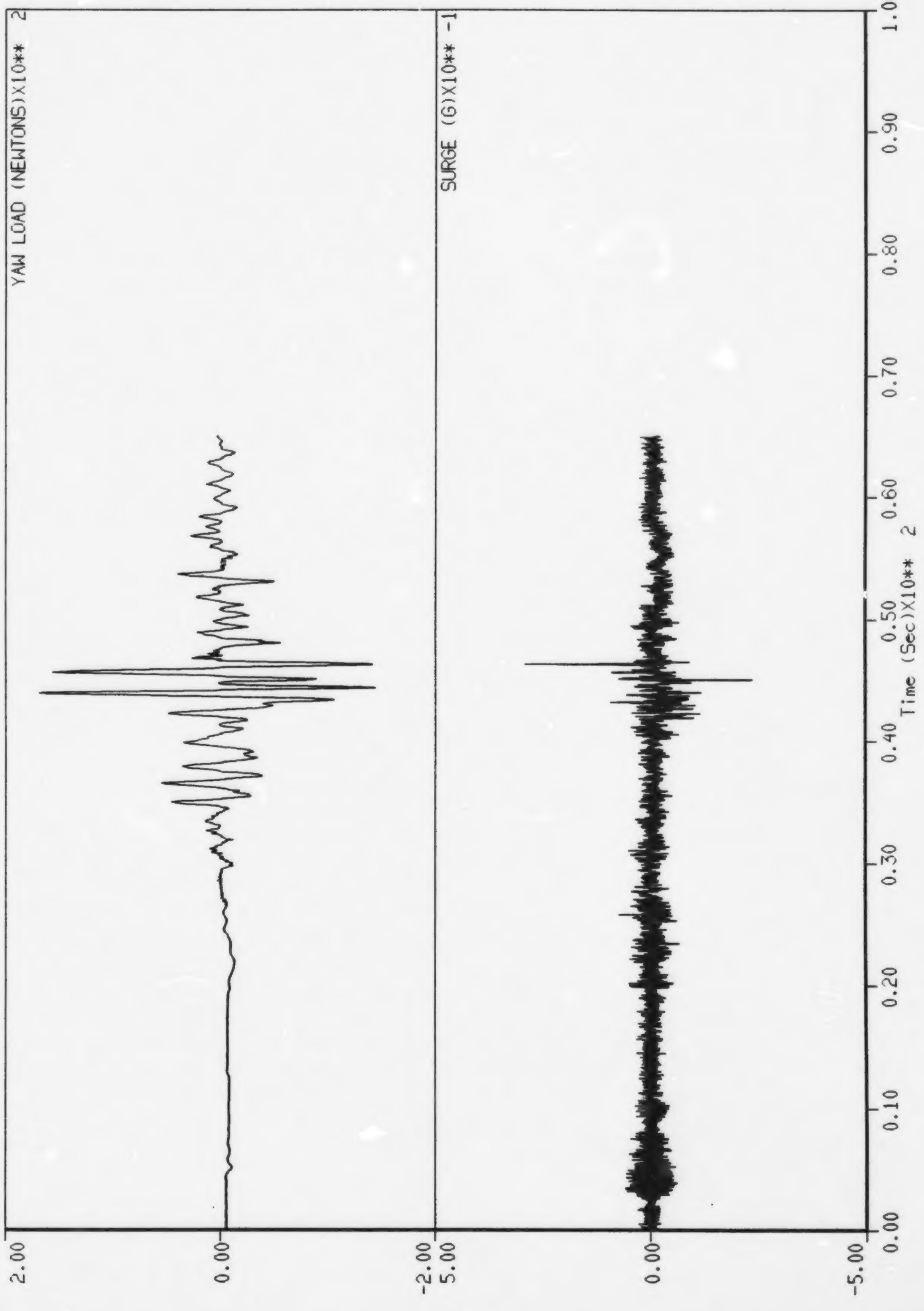

RUN_4 29-APR-1988 14:24:06.93

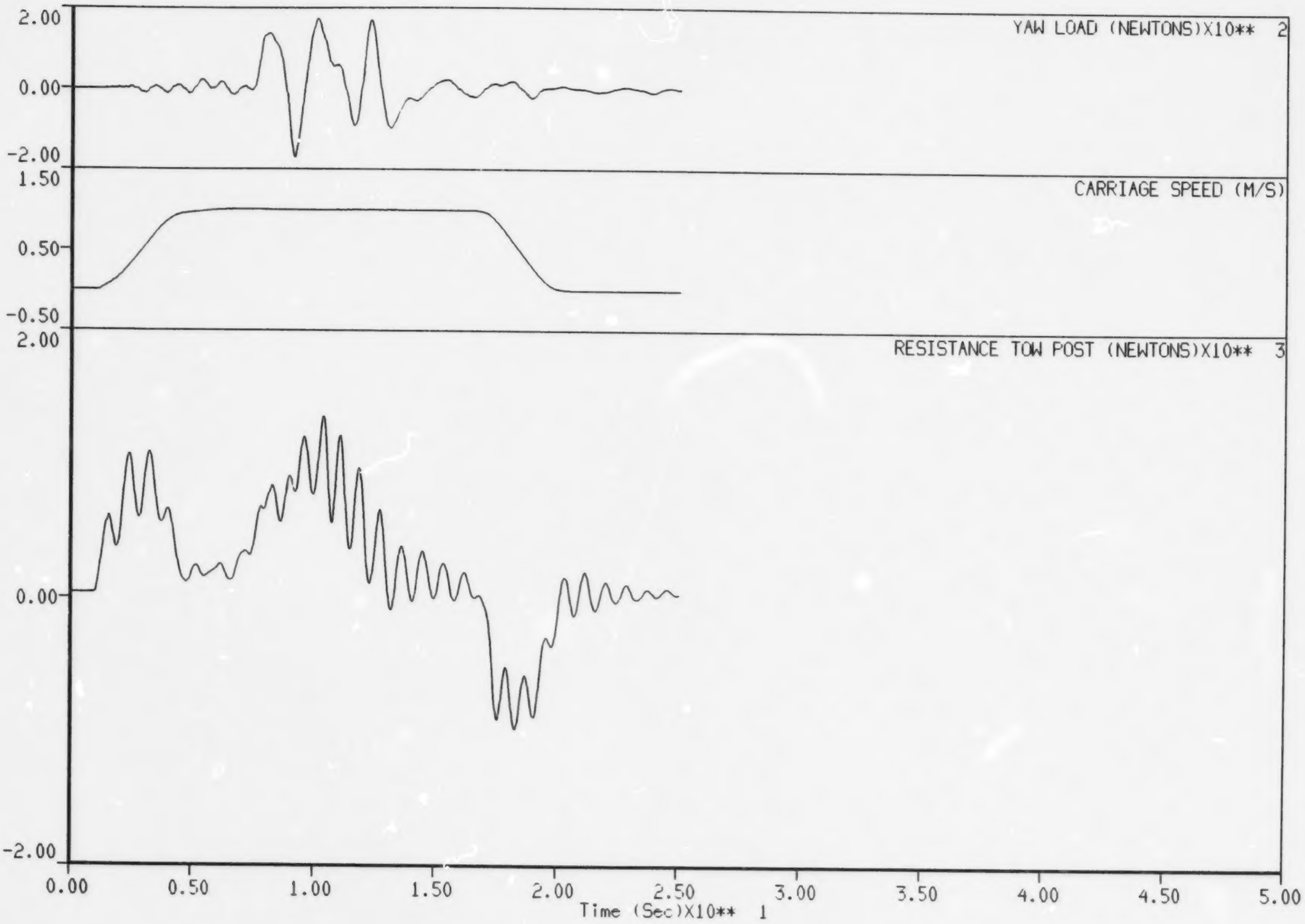

RUN_4 29-APR-1988 14:24:06.93

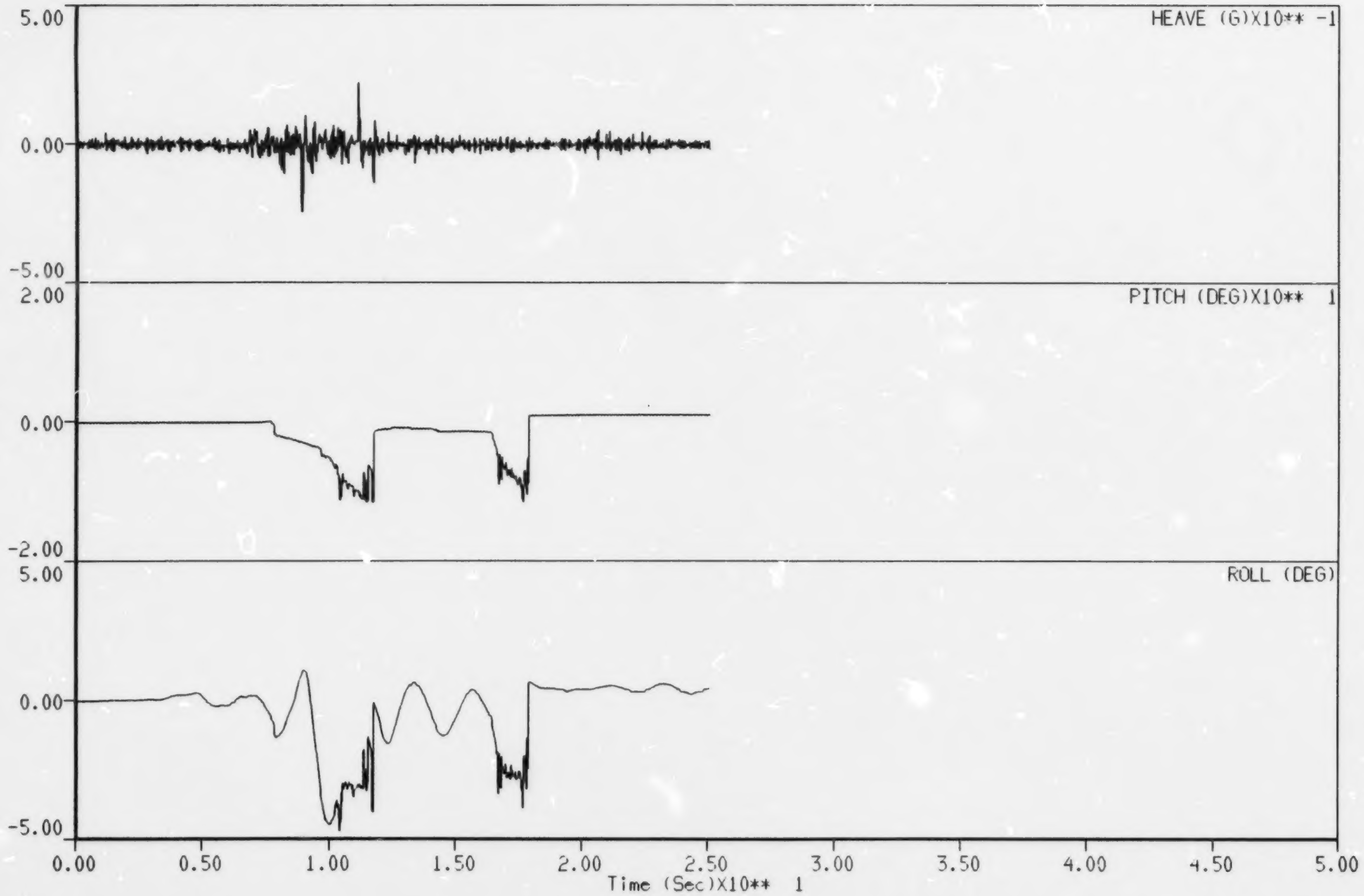

RUN_4 29-APR-1988 14:24:06.93

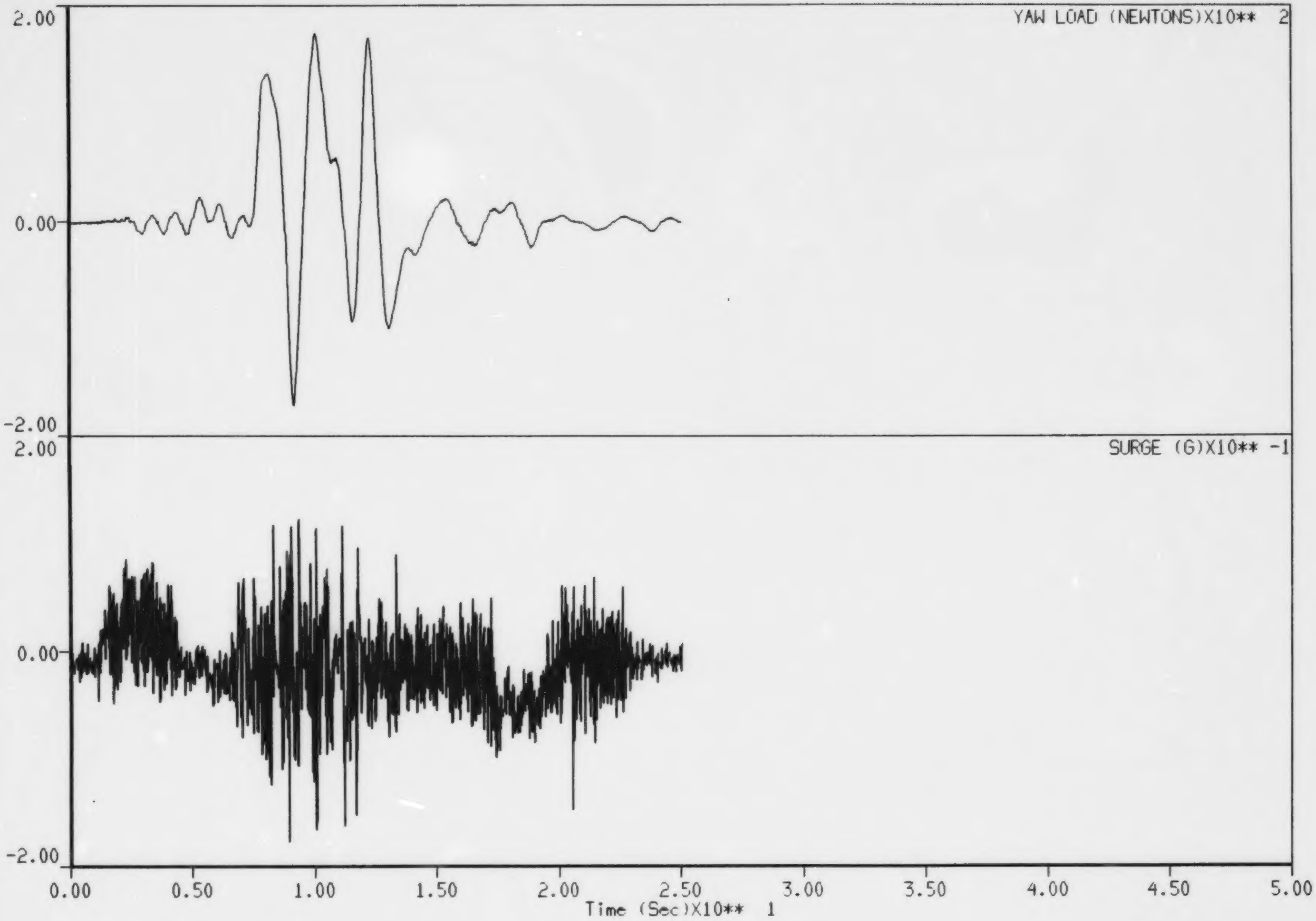

APPENDIX C.2

REDUCED PLOTS OF FORCE VS. PENETRATION AND CUMULATIVE PENETRATION ENERGY - TEST DATA FILTERED AT 1 HZ

MODEL SCALE RIDGE START POINT PENETRATION DISTANCES USED FOR REDUCTION OF PLOTS OF CUMULATIVE PENETRATION ENERGY VS. PENETRATION DISTANCE

RIDGE	PENETRATION (m) AT WHICH THE BOW WAS CONSIDERED TO FIRST CONTACT THE RIDGE
1-1	1.7
1-4	0.7
2-1 N	3.4
2-2 N	2.4
2-3 N	1.4
2-4 N	2.2
2-5 N	3.3
2-1 S	2.1
2-2 S	2.0
2-3 S	2.0
2-4 S	2.0
3-1 N	2.0
3-2 N	3.8
3-3 N	1.3
3-4 N	3.4
3-5 N	2.8
3-1 S	2.0
3-2 S	2.0
3-3 S	2.0
3-4 S	0

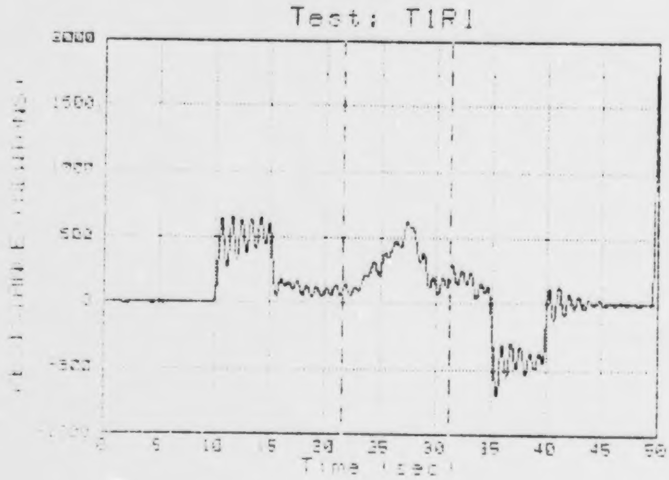

Test: T1R1

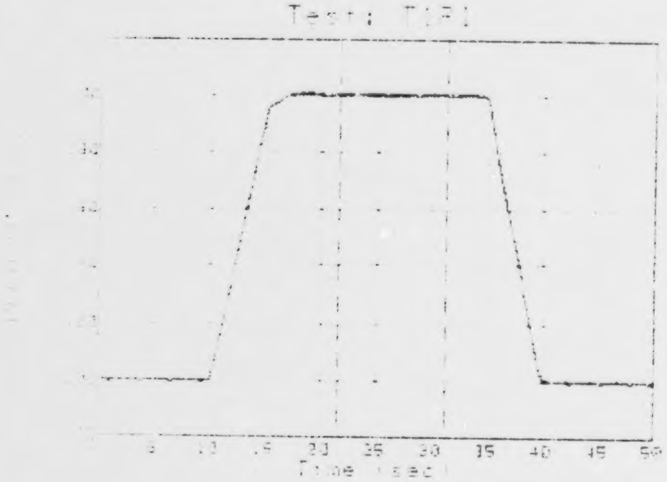

Test: T1R1

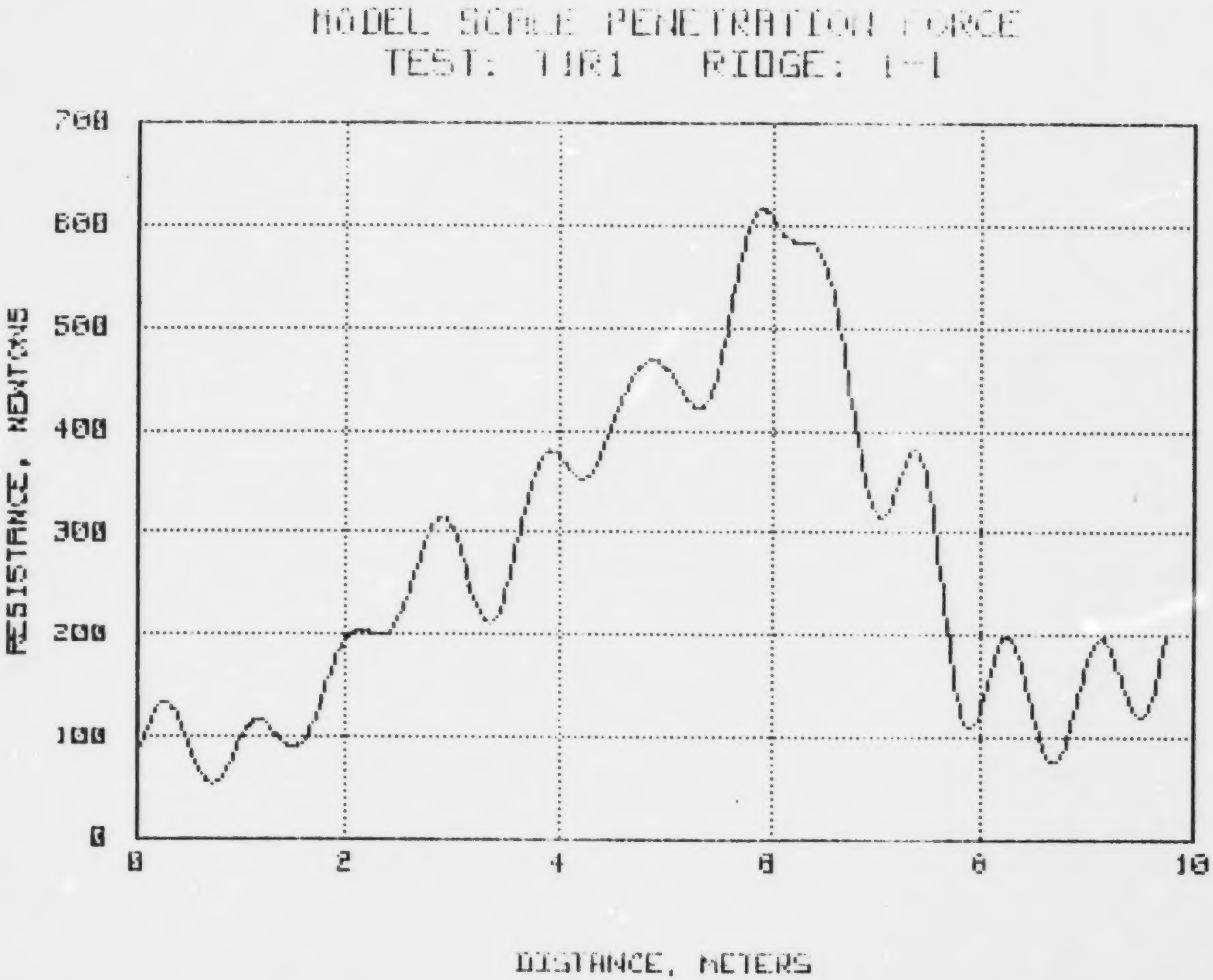
MODEL SCALE PENETRATION FORCE
TEST: TIR1 RIDGE: 1-1
RESISTANCE, NEWTONS
0
100
200
300
400
500
600
700
0
2
4
6
8
10
DISTANCE, METERS

MODEL SCALE PENETRATION ENERGY
TEST: T1R1   RIDGE: 1-1

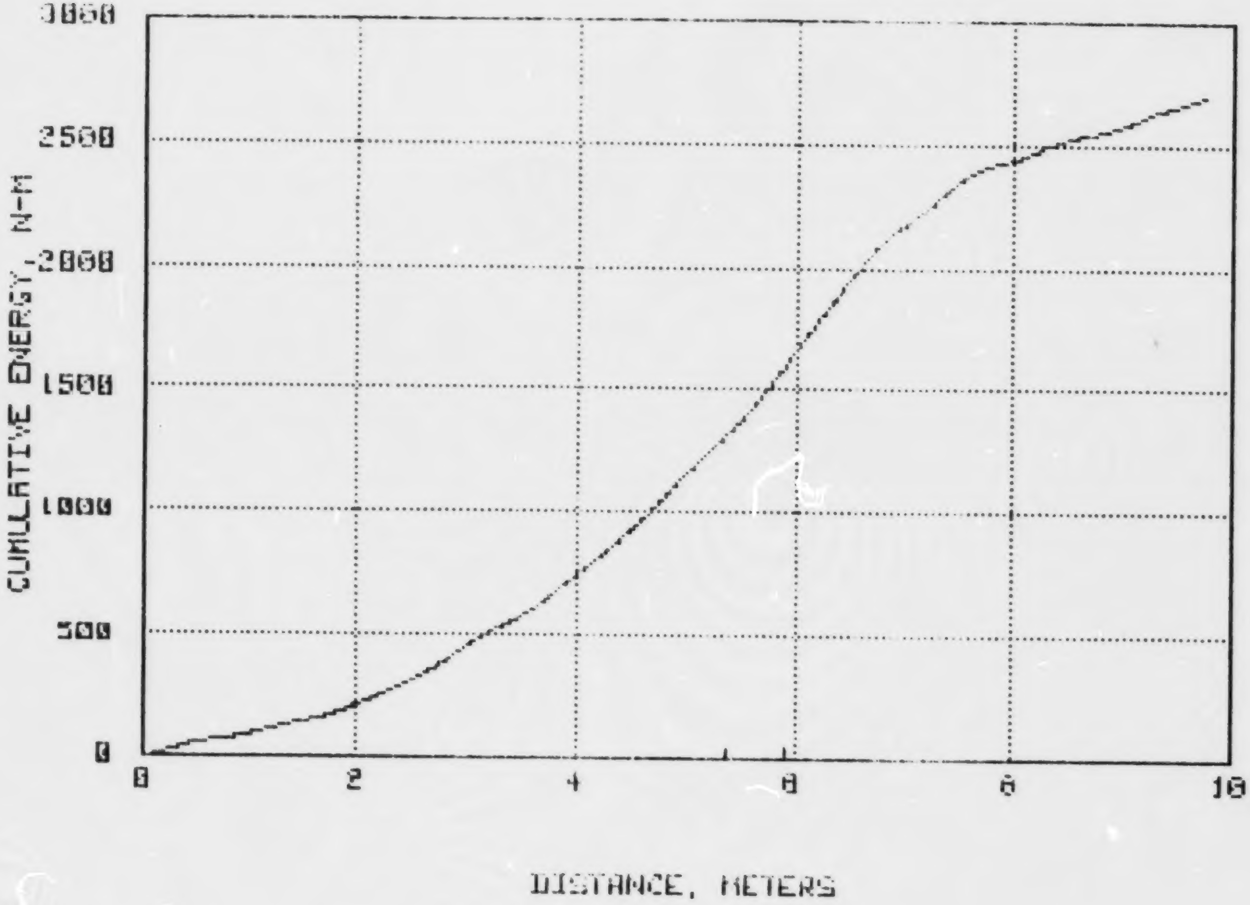

Test: T1R4

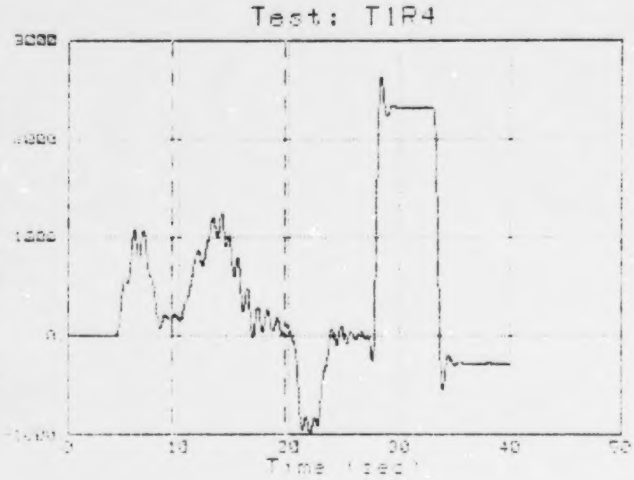

Test: T1R4

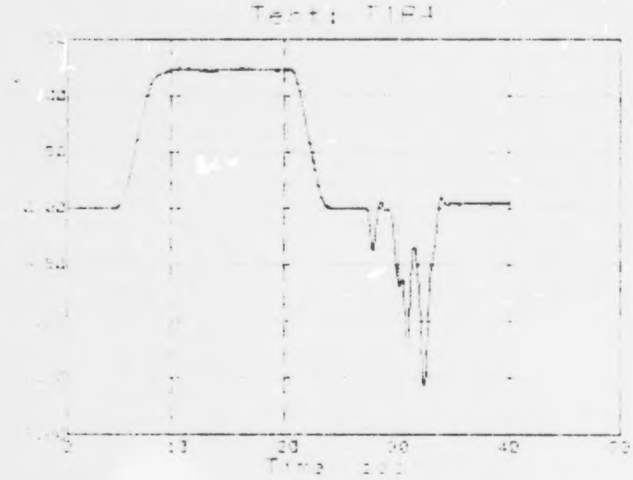

TEST: T1R4 RIDGE:4

DISTANCE,M	FORCE,N	CUM. ENERGY,N-M
0.00	177	0
1.26	237	235
2.52	744	799
3.77	846	1796
5.02	1010	3121
6.28	979	4464
7.54	727	5466
8.81	221	5975
10.06	73	6158
11.32	44	6334

PENETRATION OF 5.57 M AT MAX FORCE OF 1252 N
PENETRATION OF 12.55 M AT MAX ENERGY OF 6438 N-M

MODEL SCALE PENETRATION FORCE
TEST: T1R4 RIDGE: 4

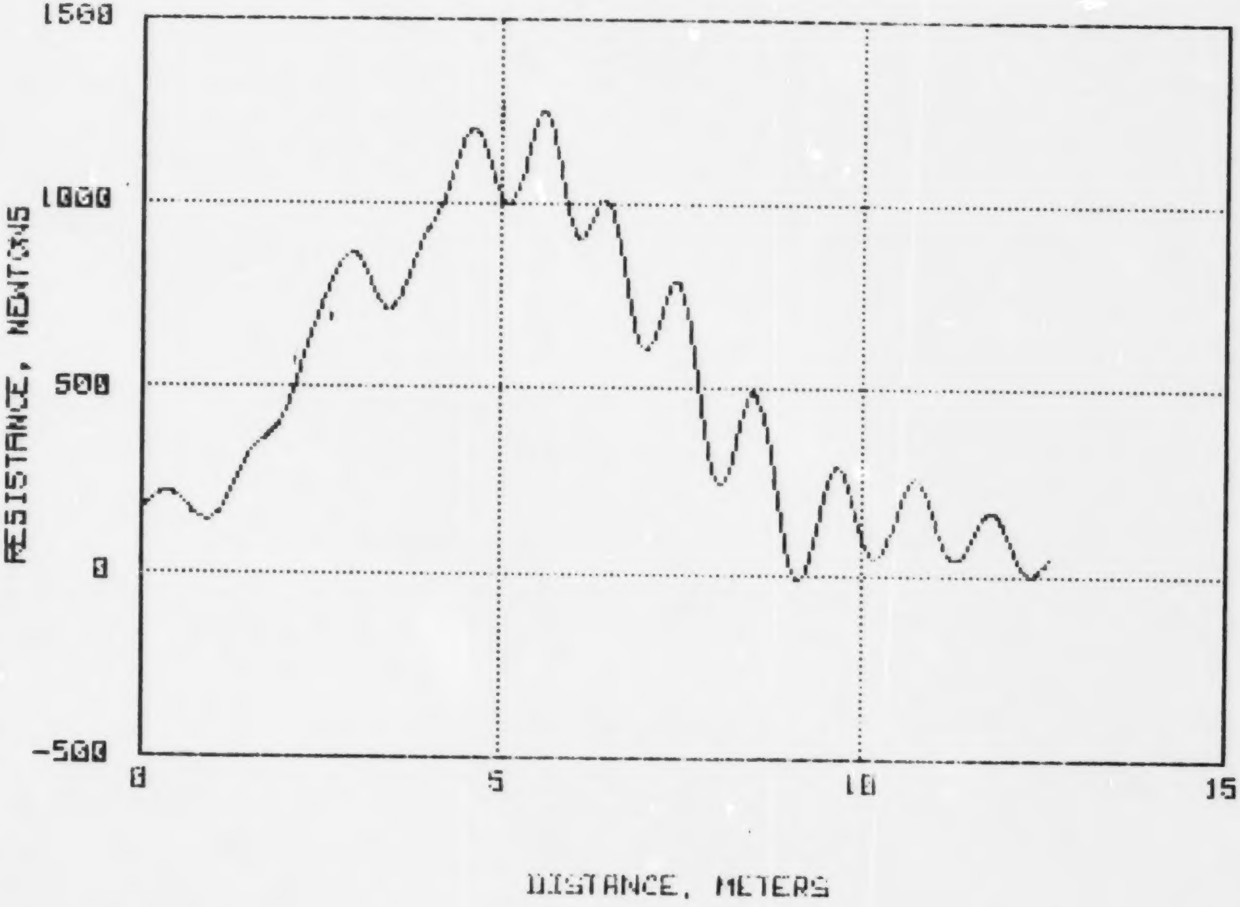

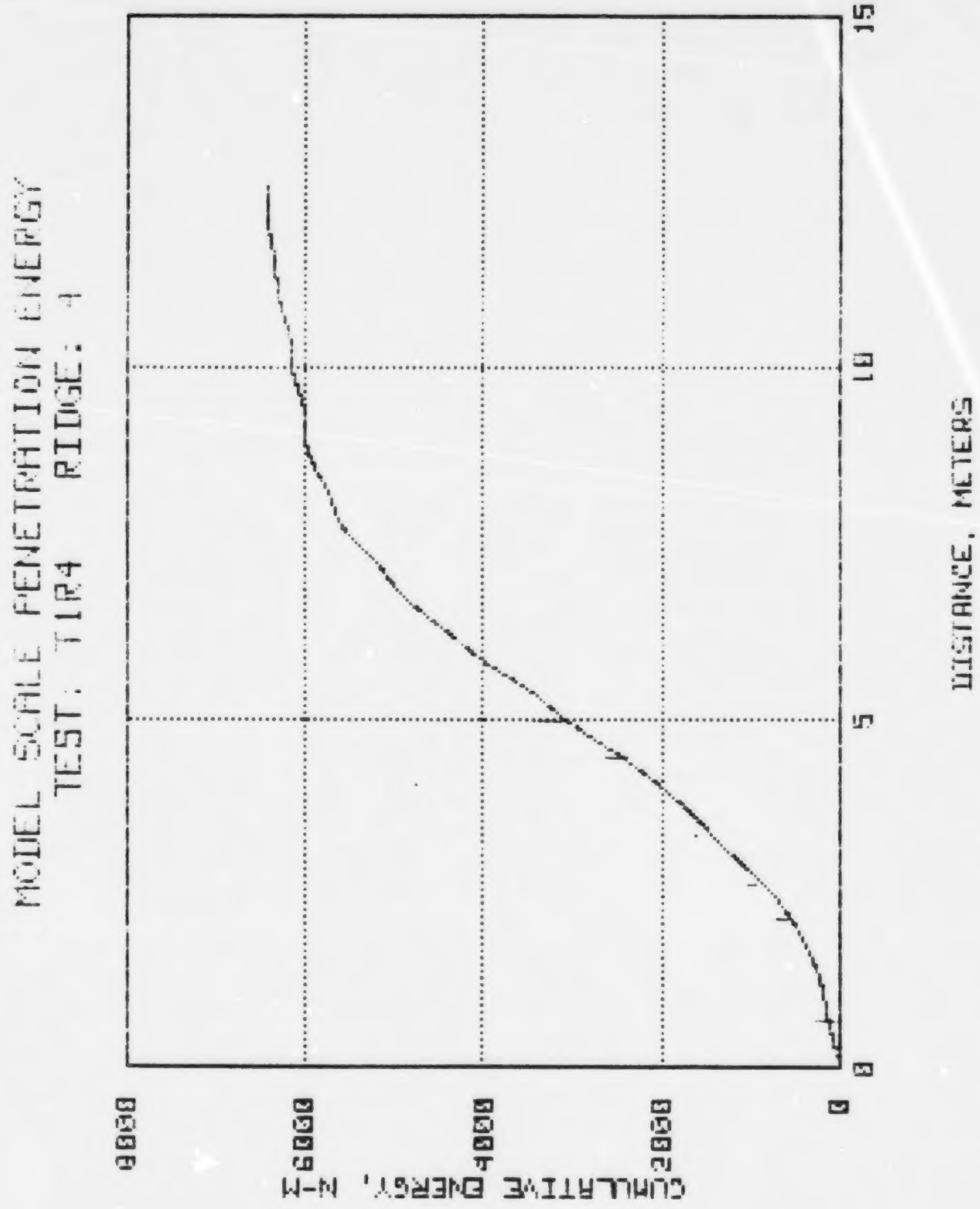
MODEL SCALE PENETRATION ENERGY
TEST: T1R4   RIDGE: 4
CUMULATIVE ENERGY, N-M
8000
6000
4000
2000
0
0
5
10
15
DISTANCE, METERS

APPENDIX C.3

REDUCED PLOTS OF FORCE VS. PENETRATION AND CUMULATIVE PENETRATION ENERGY - TEST DATA UNFILTERED

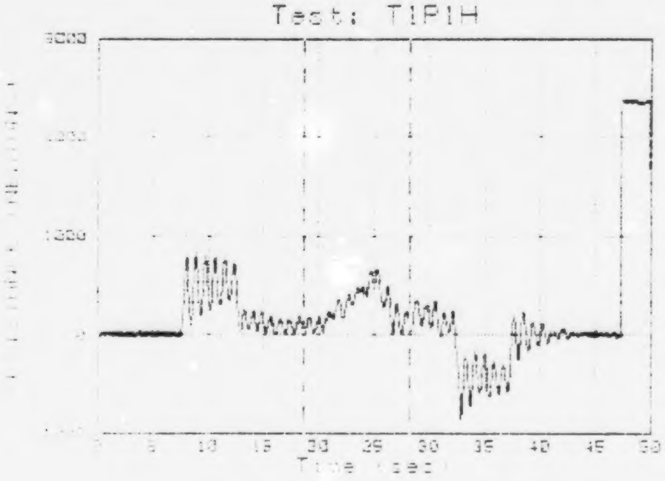
Test: T1P1H

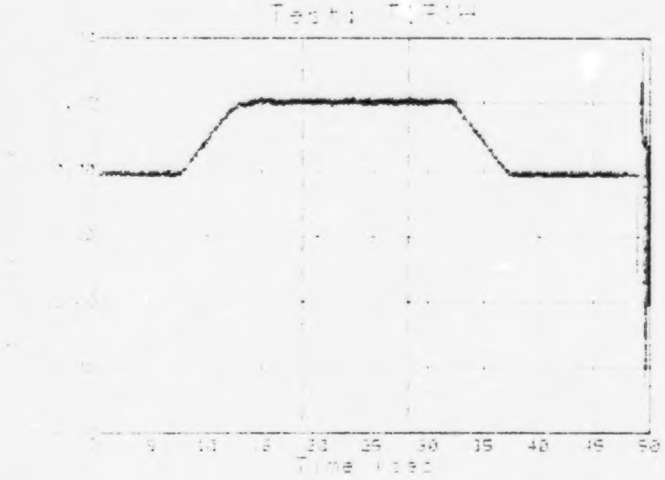
Test: T1P1H

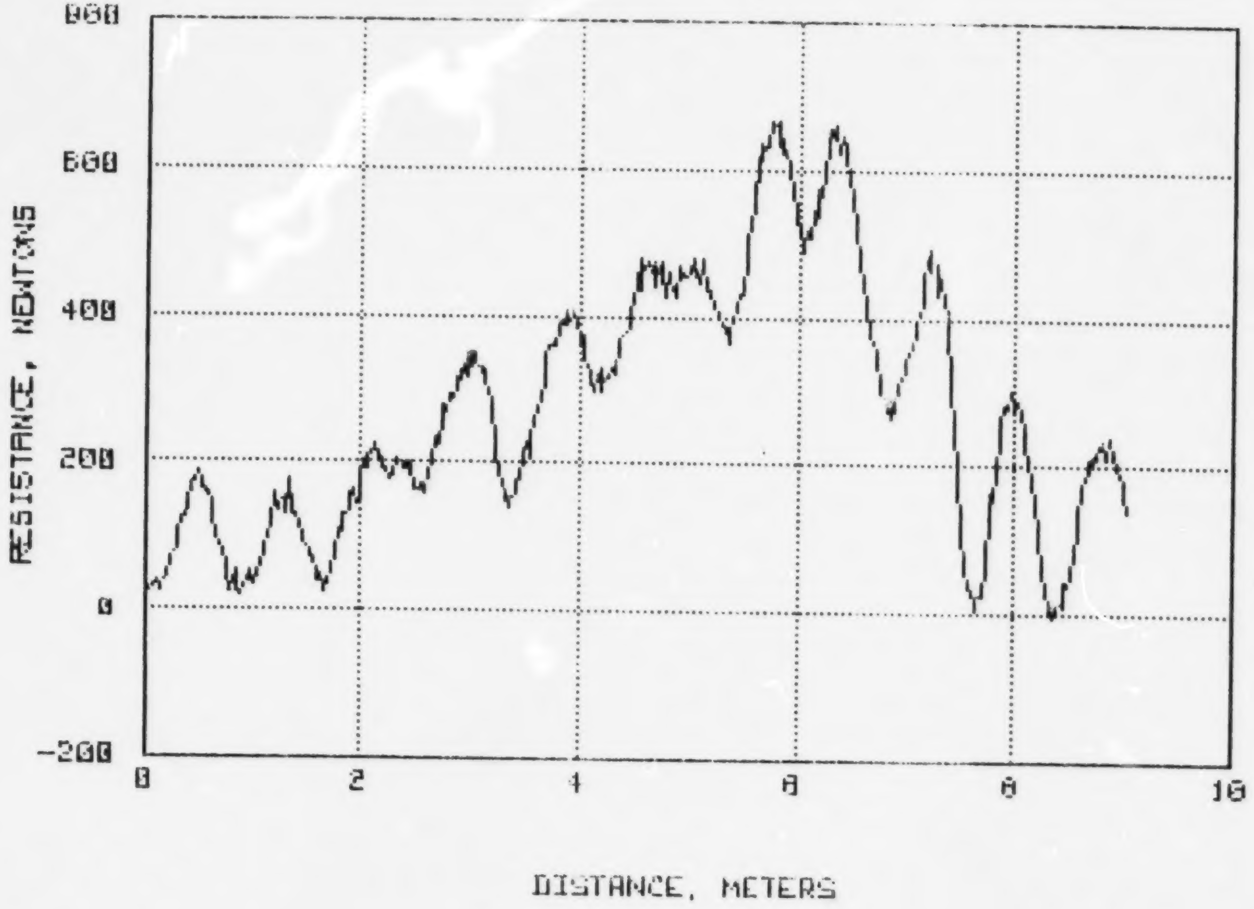

MODEL SCALE PENETRATION FORCE
TEST: T1R1H RIDGE: 1-1

MODEL SCALE PENETRATION ENERGY
TEST: T1R1H RIDGE: 1-1

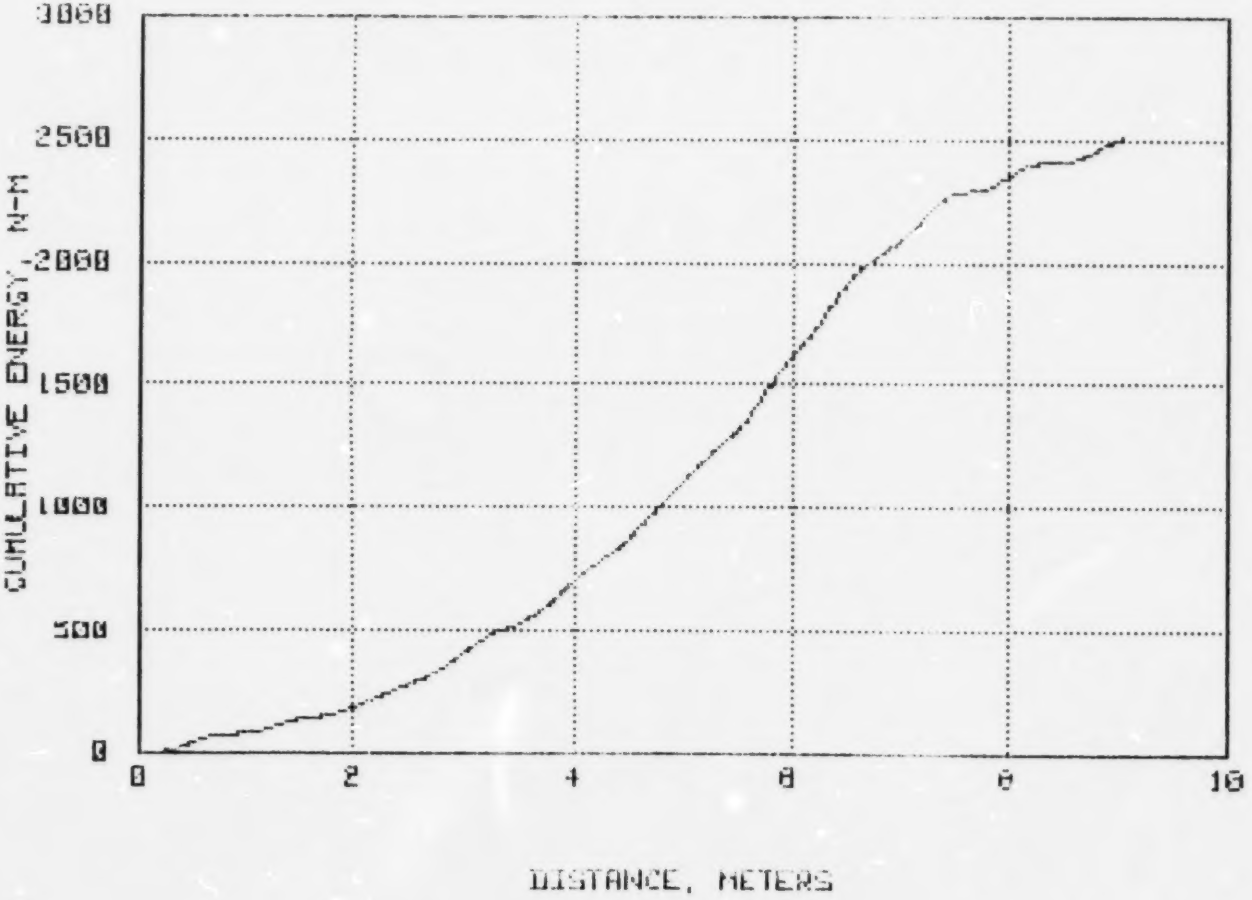

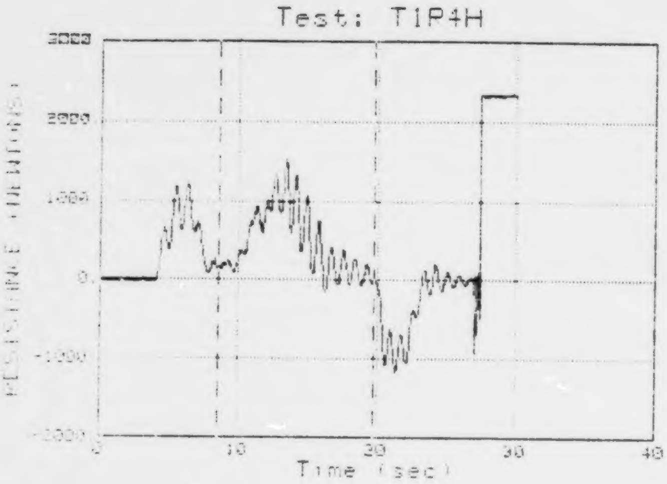

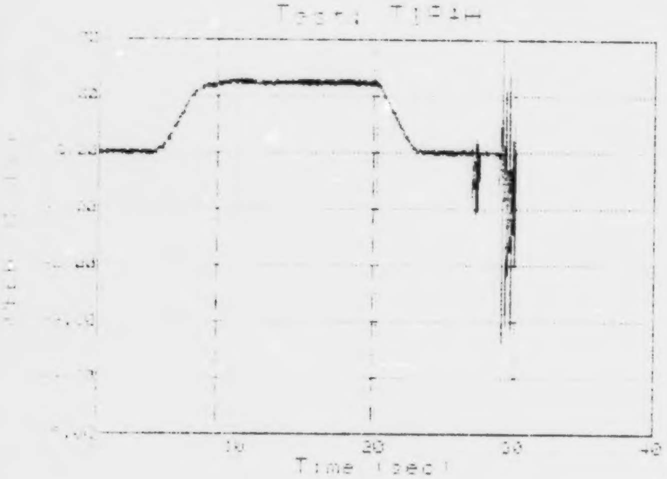

```
TEST:      T1R4H           RIDGE:4

DISTANCE,M                 FORCE,N       CUM. ENERGY,N-M
     0.00                    123                0
     1.33                    110              250
     2.73                    677              723
     4.17                    856             1780
     5.54                    937             3214
     6.92                   1316             4710
     8.32                    129             5732
     9.70                     46             6084
      .08                    383             6344
     [illegible].48                    100             6565
     [illegible].86                    -36             6625

PENETRATION OF   6.06 M AT MAX FORCE OF  1527 N
PENETRATION OF  13.53 M AT MAX ENERGY OF  6632 N-M
```

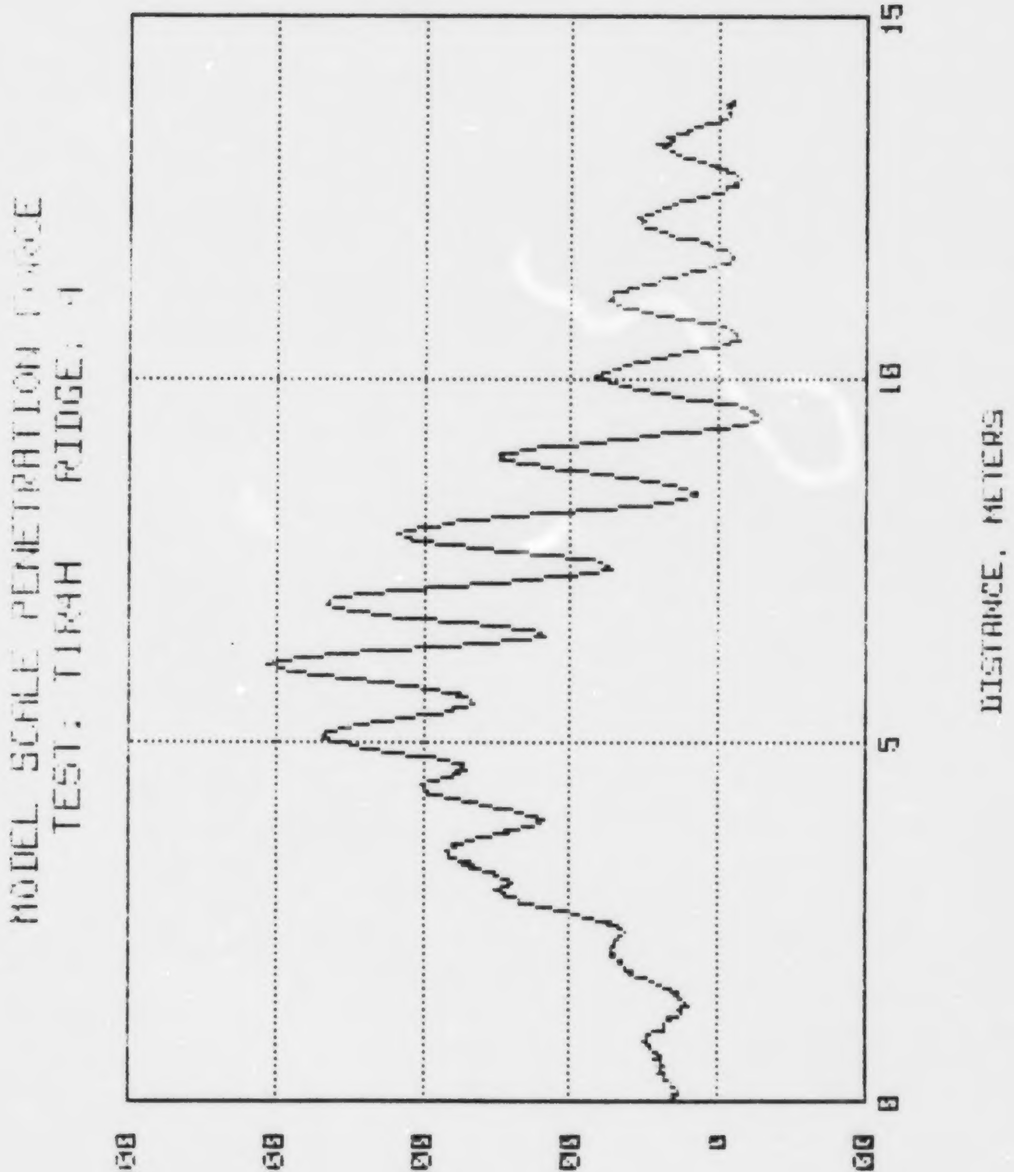
MODEL SCALE PENETRATION FORCE
TEST: T1A4H RIDGE: 1
RESISTANCE, NEWTONS
2000
1500
1000
500
0
-500
DISTANCE, METERS
0
5
10
15

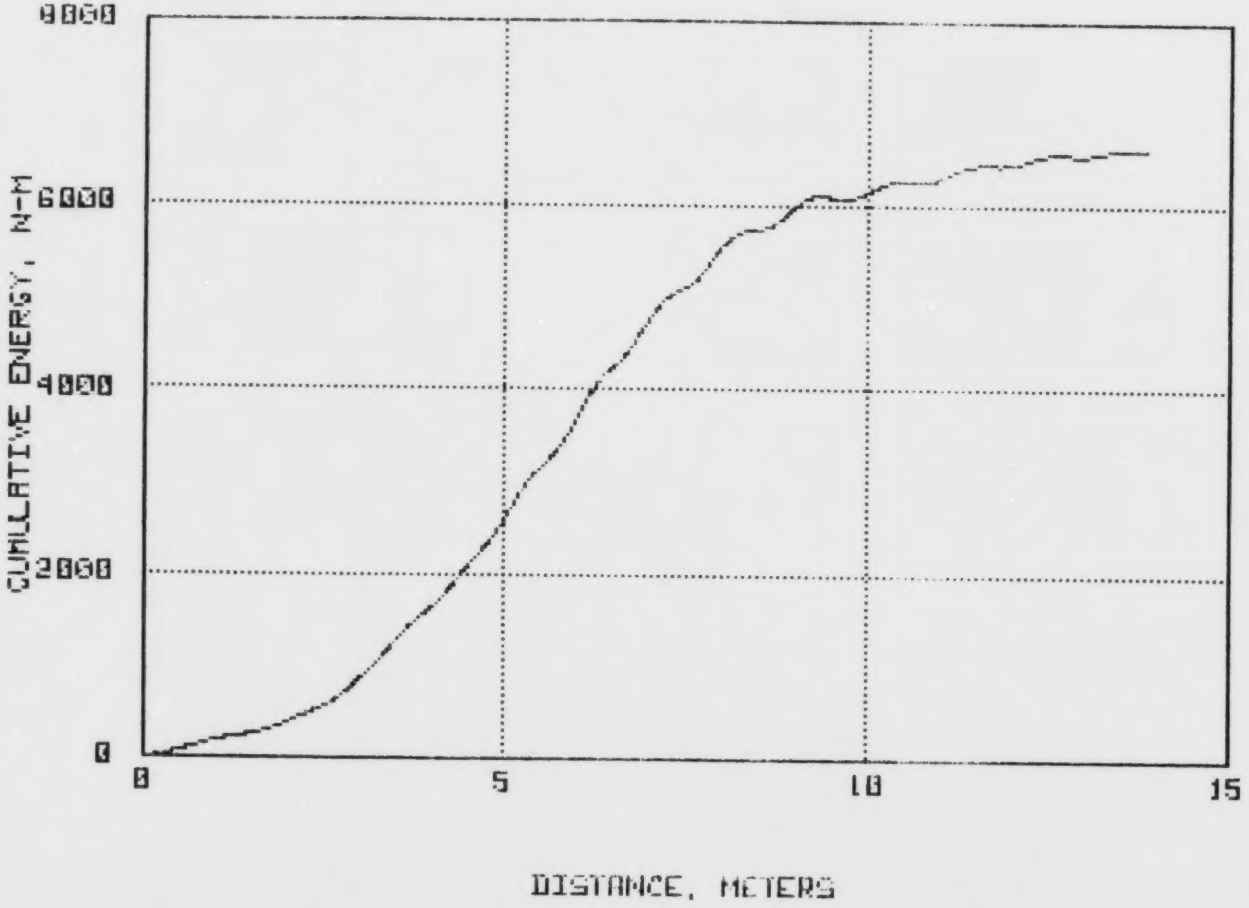

MODEL SCALE PENETRATION ENERGY
TEST: T1R4H   RIDGE. 4

APPENDIX C.4

ICE AND RIDGE PROPERTIES

Engineering Design Calculations

JOB No. 3208
SHEET 1 OF 2
DATE May 11/86
BY
CH'K BY

PROJECT: RIDGE MODELLING
SUBJECT: RIDGE MECHANICAL PROPERTIES

[illegible] STRENGTH OF RIDGE CONSOLIDATED LAYER

MEAS. TIME	RIDGE #	CRUST THICK (mm)	TOTAL THICK (mm)	WIDTH (mm)	LENGTH (mm)	FAILURE LOAD (Kg)	FLEX. STR. (Kpa)
1330	1-1	100	no data	125	250	0.7	10.3
		65	300	130	330	1.4	49.5
		75	204	110	310	0.25	7.4
[illegible]	1-4	70	310	110	270	1.7	53.1
		110	no data	120	330	3.7	49.4
		90	no data	110	305	1.12	22.3
		220	no data	120	240	1.87	45.4

NOTE: FLEXURAL STRENGTH COMPUTED BASED ON CRUST THICK OF BEAM.

THICKNESS OF CONSOLIDATED LAYER

RIDGE	MEASURED VALUES (mm)	AVG. (mm)
1-1	100 ; 65 ; 75	80 ± 15
1-4	70 ; 110 ; 90 ; 220 ; 70 ; 110 ; 120 ; 80 ; 90	107 ± 43

RIDGE BULK DENSITY

TEST TYPE : SUBMERGENCE
RIDGE : 1-4
TEST TIME : 1430

SUBMERGENCE FORCE (Kg)	ICE COLUMN SIZE		BULK DENSITY (KN/m³)
	AREA (cm × cm)	DEPTH (cm)	
6.5	33 × 30	20	6.8
1.75	22 × 23	25-30	8.6-8.9

JOB No. 2207
SHEET 2 OF 2
DATE May 1/89
BY M. Comfort
CH'K BY

PROJECT
SUBJECT RIDGE MECHANICAL PROPERTIES

VOLUME OF ICE PUT IN RIDGE PRIOR TO SECOND FREEZE

Ice thickness : 20 mm

Ridge #	Length of ice sheet put into ridge	Volume of ice (m³/m width of the basin)
1-1	15 m	0.3
1-2	15 m	0.3
1-3	15 m	0.3
1-4	30 m	0.6

Note : The broken ice sheet was redistributed when the floating boom was repositioned. Therefore the volume of ice put into the ridge is not well-known.

RIDGE CROSS - SECTIONAL AREA

RIDGE #	RIDGE WIDTH (m)	TOTAL AREA³ (m³) OF CONS. LAYER	TOTAL AREA (m²) OF KEEL
1-1	2.1	0.167	0.563
1-2	2.1	0.224¹	0.264
1-3	2.1	0.167²	0.344
1-4	4.0	0.428	0.766

NOTES :

1. INFERRED FROM MEASUREMENTS OF CONS. LAYER THICKNESS FOR RIDGE 1-4 (AS THIS RIDGE WAS ALSO NOT INSULATED).
2. INFERRED FROM MEASUREMENT OF CONS. LAYER THICKNESS FOR RIDGE 1-1 (AS THIS RIDGE WAS ALSO INSULATED).
3. AREA OF CONS. LAYER COMPUTED AS: MEAN THICKNESS x RIDGE WIDTH

JOB No. 3208
SHEET 1 OF 3
DATE MAY 1 /'83
BY [illegible]
CHK BY

PROJECT RIDGE MODELLING
SUBJECT CROSS-SECTIONAL PROFILE DATA FOR RIDGES IN SHEET #1

RIDGE 1-1		RIDGE 1-2		RIDGE 1-3		RIDGE 1-4			
X (cm)	Y (cm)	X (cm)	Y (cm)	X (cm)	Y (cm)	X (cm)	Y (cm)	X (cm)	Y (cm)
0	3	0	5	0	3	0	3	220	25
10	33	12	6 (1-9)	20	10	20	15	240	[illegible]
24	27	34	8 (3-16)	40	15	40	20	260	15
38	27 (23-36)	50	11 (6-20)	60	20	60	15	280	[illegible]
47	27 (19-31)	75	20 (15-24)	80	15	80	20	300	[illegible]
62	31 (22-36)	95	17 (11-22)	100	25	100	18	320	[illegible]
[illegible]	36 (32-41)	114	22 (19-26)	120	25	120	22	340	15
[illegible]	37 (31-37)	125	16 (11-23)	140	15	140	18	360	15
114	37	139	20 (19-20)	160	20	160	15	[illegible]	3
127	35	155	17 (13-24)	180	15	180	30		
141	35	167	13 (10-14)	200	15	200	33		
154	35	184	4 (3-5)						
168	[illegible]	197	3						
[illegible]	[illegible]	209	3						
175	15 ([illegible])								
209	3								

PLAN LAYOUT OF BASIN:

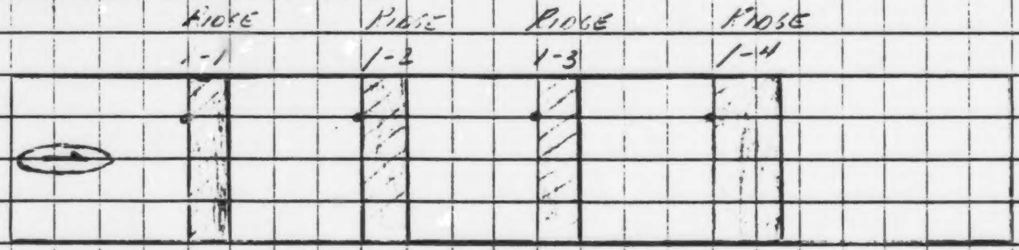

NOTES: 1. • ORIGIN OF COORDINATE SYSTEM FOR EACH RIDGE.

2. THE ABOVE MEASUREMENTS IN THE Z DIRECTION APPLY TO THE DEPTH OF THE RIDGE BELOW WATERLINE.

3. SEVERAL KEEL DEPTH MEASUREMENTS WERE TAKEN AT SOME STATIONS BY MOVING THE PROFILING STICK RADIALLY. THE RANGE OF MEASUREMENTS IS SHOWN IN BRACKETS, ALONG WITH THE AVERAGE VALUE.

FLEET TECHNOLOGY LIMITED (FTL)

Engineering Design Calculations

JOB No. 3209
SHEET 2 OF 3
DATE May 1 /88
BY
CH'K BY

PROJECT: RIDGE MODELLING
SUBJECT: CROSS-SECTIONAL PROFILES OF RIDGES IN SHEET #1

RIDGE 1-1:

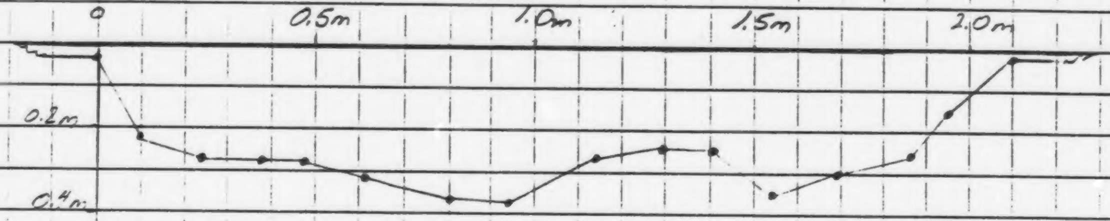

RIDGE 1-2:

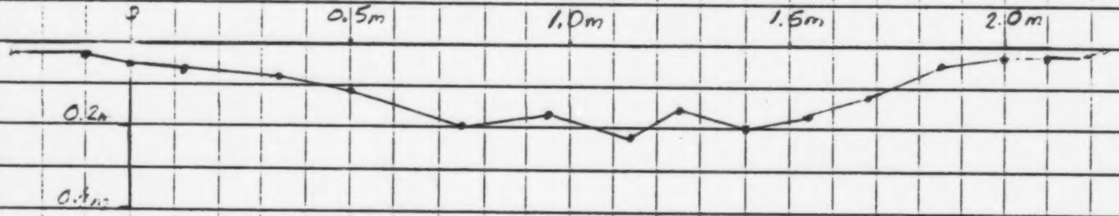

RIDGE 1-3:

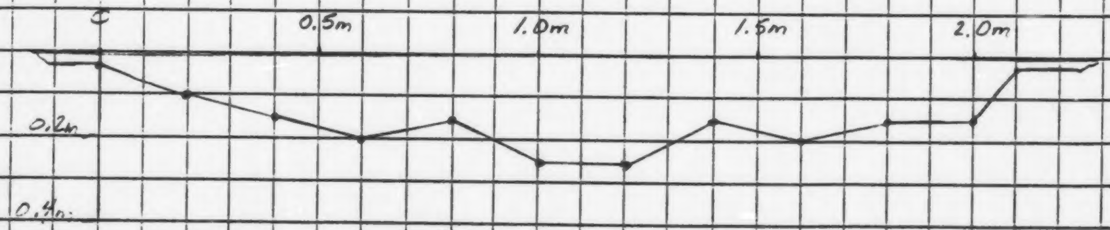

FLEET TECHNOLOGY LIMITED (FTL)

Engineering Design Calculations

JOB No. 3229
SHEET 3 OF 8
DATE May 1/85
BY A. Comfort
CH'K BY

PROJECT RIDGE MODELLING
SUBJECT CROSS-SECTIONAL PROFILES OF RIDGES IN SHEET #1

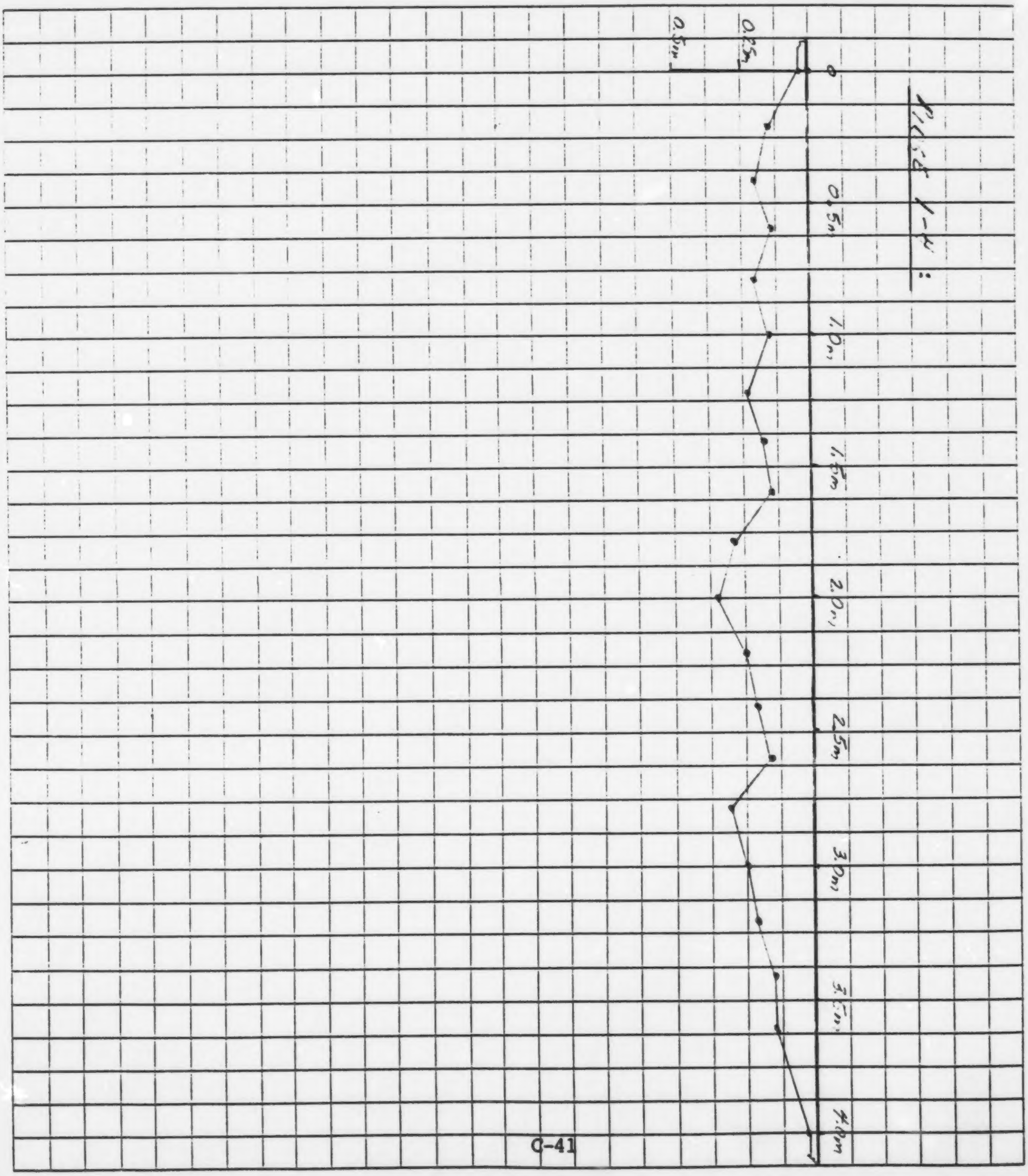

NRC - INSTITUTE FOR MARINE DYNAMICS

ARCTIC VESSEL RESEARCH SECTION

ICE SHEET SUMMARY

Test Name: RIDGE1

Project Number: 88112

Target ice thickness: (mm) 24.0

EG/AD/S: (%) .39/.027/0

Target ice strength: (kPa) 18.0

SEEDING:

Air temp.(max/min) C: -18.7/-13.4
Seeding completed at 2310 28-APR-1988
Seed volume: l 0.0
Humidity: tank(%) 0
room(%) 0

Tank water temp. C: 0.11
Seed duration: (min) 35.
Seed water temp.: C 55.0

GROWTH:

Target temp.: C -20.0
Avg temp. at plateau: C -20.3
Avg temp. of freeze cycle C -19.8
Total negative deg. hours 109.2
Avg growth rate: (mm/hr) 2.960

Time to target temp. hrs: 0.6
Duration of plateau hrs: 4.9
Duration of freeze cycle hrs: 5.5
Thickness at end of freeze:(mm) 16.3
Avg growth rate: (mm/fdh) .149

WARM-UP:

Warm-up commenced at 0440 29-APR-1988
Time to tempering temp: (hrs) 3.3
Final ice thickness: (mm) 23.0
Total growth rate: (mm/hr) 4.179

Length of warm-up: (hrs) 8.
Avg tempering temperature: (C) 0.8
Ice growth during warm-up: (mm) 6.7
Total growth rate: (mm/fdh) .211

* thickness at end of freeze was estimated
** final ice thickness was estimated

Ridges made from previous 20mm ice sheet (145fdh)

NRC - INSTITUTE FOR MARINE DYNAMICS

ARCTIC VESSEL RESEARCH SECTION

ICE MECHANICAL PROPERTIES SUMMARY

Test Name: RIDGE1 Project Number: 88112

Warm up commenced: 04:40 29-APR-1988

Time	Warm-up hrs	Loc	hi mm	Sf kPa	Lc cm	E MPa	E/Sf	Lc/hi	K1c N/m	Sf/K1c m-.5	Sc/s kPa	Rhoi Mg/m3
0900	4.33	N	22.7± 1.3 n= 3									
		S	22.1± 0.4 n= 3									
0918	4.63	48N	22.5	31.± 2.9								
			22.4	10.(u/d 33%)								
0921	4.68	48S	22.5	36.± 2.9								
			22.5	12.(u/d 31%)								
0927	4.78	48N	22.5							s	15.9± 3.0	
0929	4.81	48S	22.5							s	14.5± 4.8	
1019	5.65	47S	22.5	29.± 3.8								
			22.5	17.(u/d 57%)								
1023	5.71	47N	22.9	19.± 1.7								
			22.8	9.(u/d 48%)								
1027	5.78	47N	22.8							c	28.5± 3.6	
1030	5.83	47S	22.5							c	26.4± 3.5	
1110	6.50	45S	22.2		19.	13.4	831	8.7				
1125	6.75	45N	23.1	14.± 2.4								
			22.7	10.(u/d 73%)								
1130	6.83	45S	22.9	15.± 1.6								
			23.0	7.(u/d 45%)								
1306	8.43	44N	23.1	12.± 2.8								
			23.2	8.(u/d 68%)								
1309	8.48	44S	23.0	13.± 2.0								
			22.9	4.(u/d 34%)								
1318	8.63	44S	22.2									.951

Run #	Date	Time	Hours from Warm-up	Flexural Strength north	Flexural Strength south	Flexural Strength mean

FROM	1	04/29/88	1201	7.35		11.8	12.6	12.2
TO	2	04/29/88	1255	8.25		12.4	13.7	13.0

RIDGE 1

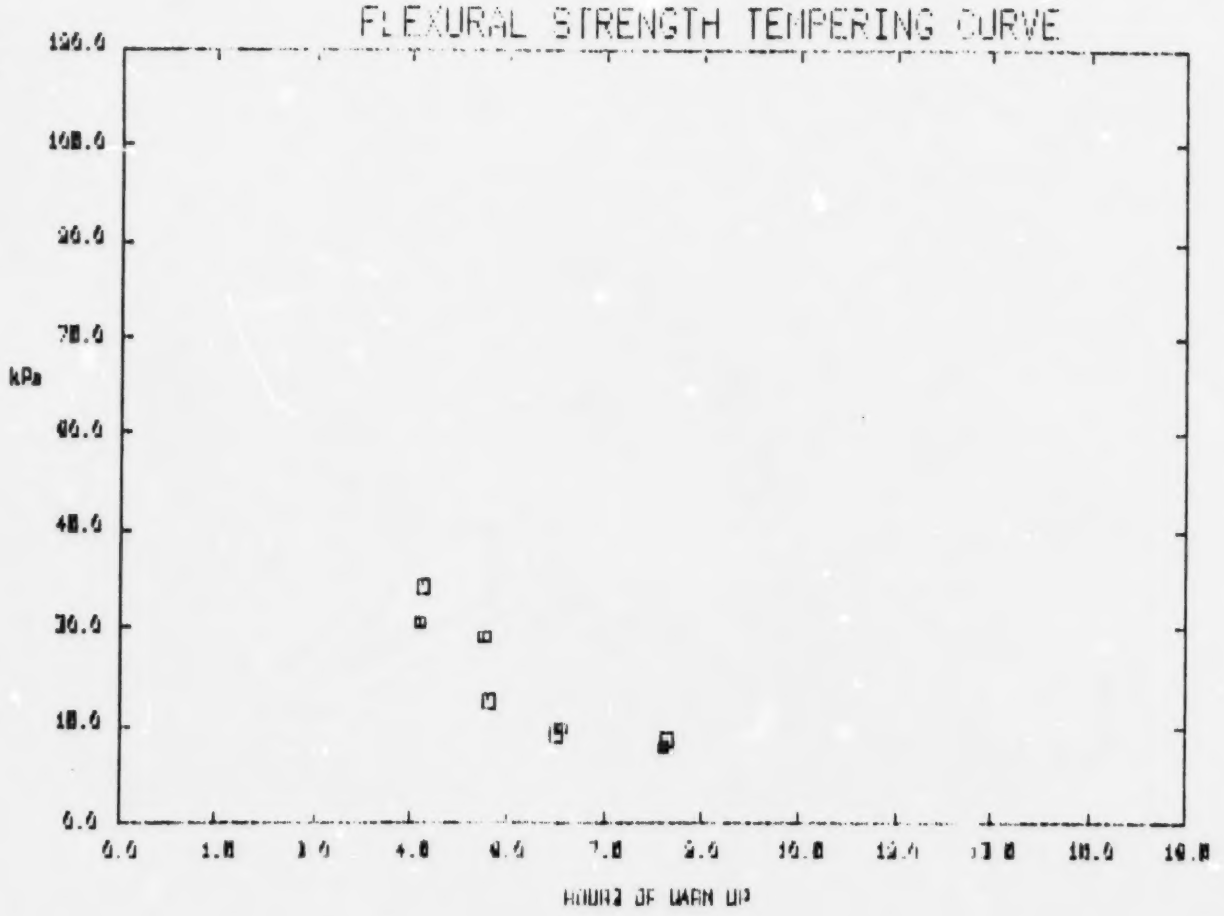
FLEXURAL STRENGTH TEMPERING CURVE
kPa
120.0
105.0
90.0
75.0
60.0
45.0
30.0
15.0
0.0
0.0
1.5
3.0
4.5
6.0
7.5
9.0
10.5
12.0
13.5
15.0
16.5
HOURS OF WARM UP

APPENDIX C.5

TEMPERATURE DATA

FLEET TECHNOLOGY LIMITED (FTL)

Engineering Design Calculations

JOB No. 3209
SHEET 1 OF 2
DATE April 30/89
BY
CH'K BY

PROJECT Ridge Modelling
SUBJECT Ridge Temperatures (°C)

Thermocouple Location	23^{30} April 28	09^{30} April 29	10^{15} April 29	11^{15} April 29
1	-17.7	+2.4	+1.7	-1.1
2	-13.8	+0.4	+0.2	+0.7
3	+0.2	-0.8	-0.5	-1.4
4	+0.8	-0.5	-0.3	+1.1
5	-12.3	+1.4	+0.8	-0.2
6	-2.8	+0.2	-0.2	+0.4
7	+0.7	-0.9	-0.4	+0.3
8	-0.7	-0.6	-0.6	-0.8
9	-0.8	-0.2	0.0	+0.7
10	-17.9	+4.0	+2.0	0.0
11	-1.3	-0.2	+0.1	-1.0
12	0.0	0.0	+0.5	-0.6
13	0.0	0.0	+0.6	+3.5
14	0.0	+0.2	+0.6	-0.3
15	+17.6	+4.2	+2.1	+0.3
16	-4.2	0.0	+0.2	+0.7
17	0.0	0.0	+0.2	+0.6
18	0.0	0.0	0.0	-0.7

Event Log:

23^{30} April 28 - Ridges Formed And Freeze #2 Commenced.
04^{40} April 29 - Warmup Commenced.
09^{40} April 29 - Insulation Removed From Ridge Surface.

FLEET TECHNOLOGY LIMITED (FTL)

Engineering Design Calculations

JOB No. 3203
SHEET 2 OF 2
DATE APRIL 30/83
BY
CH'K BY

PROJECT RIDGE MODELLING
SUBJECT THERMOCOUPLE LOCATIONS

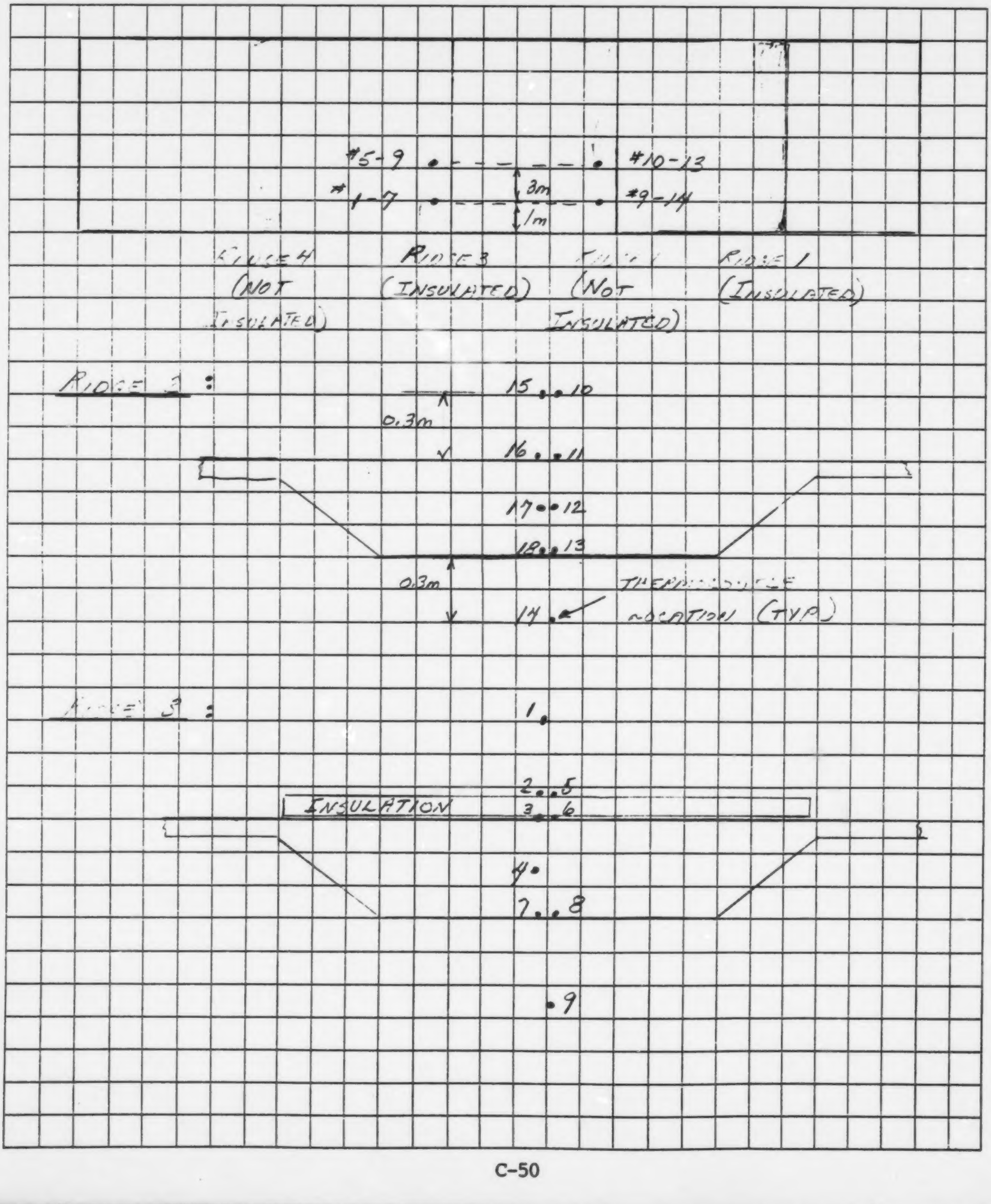
#5-9
#10-13
3m
#1-7
#9-14
1m
RIDGE 4
(NOT
INSULATED)
RIDGE 3
(INSULATED)
RIDGE 2
(NOT
INSULATED)
RIDGE 1
(INSULATED)
RIDGE 2 :
15 10
0.3m
16 11
17 12
18 13
0.3m
14
THERMOCOUPLE
LOCATION (TYP)
RIDGE 3 :
1
2 5
INSULATION
3 6
4
7 8
9

APPENDIX D

RAW DATA FROM SHEET #2 TESTS AT THE IMD

CONTENTS:

D.1 Raw Time Histories For All Data Channels

D.2 Reduced Plots of Force vs. Displacement and Cumulative Penetration Energy - Test Data Filtered at 2 Hz

D.3 Reduced Plots of Force Vs. Displacement and Cumulative Penetration Energy - Test Data Filtered at 100 Hz

D.4 Ice and Ridge Properties

D.5 Temperature Data

APPENDIX D.1

SHEET #2 TESTS AT THE IMD:
RAW TIME HISTORIES FOR ALL DATA CHANNELS

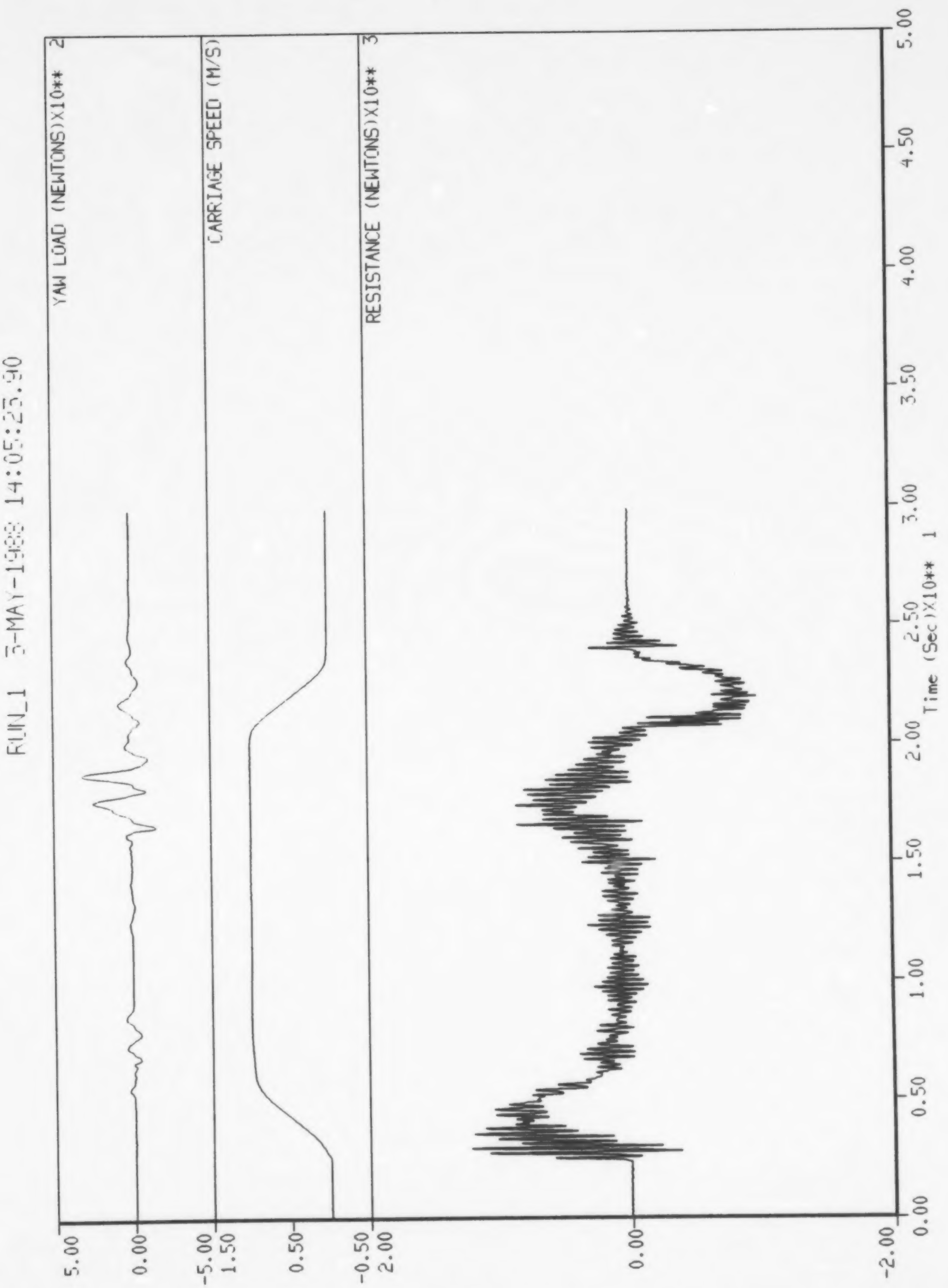
RUN_1 3-MAY-1988 14:05:23.90
YAW LOAD (NEWTONS)X10** 2
CARRIAGE SPEED (M/S)
RESISTANCE (NEWTONS)X10** 3
5.00
0.00
-5.00
1.50
0.50
-0.50
2.00
0.00
-2.00
0.00
0.50
1.00
1.50
2.00
2.50
3.00
3.50
4.00
4.50
5.00
Time (Sec)X10** 1

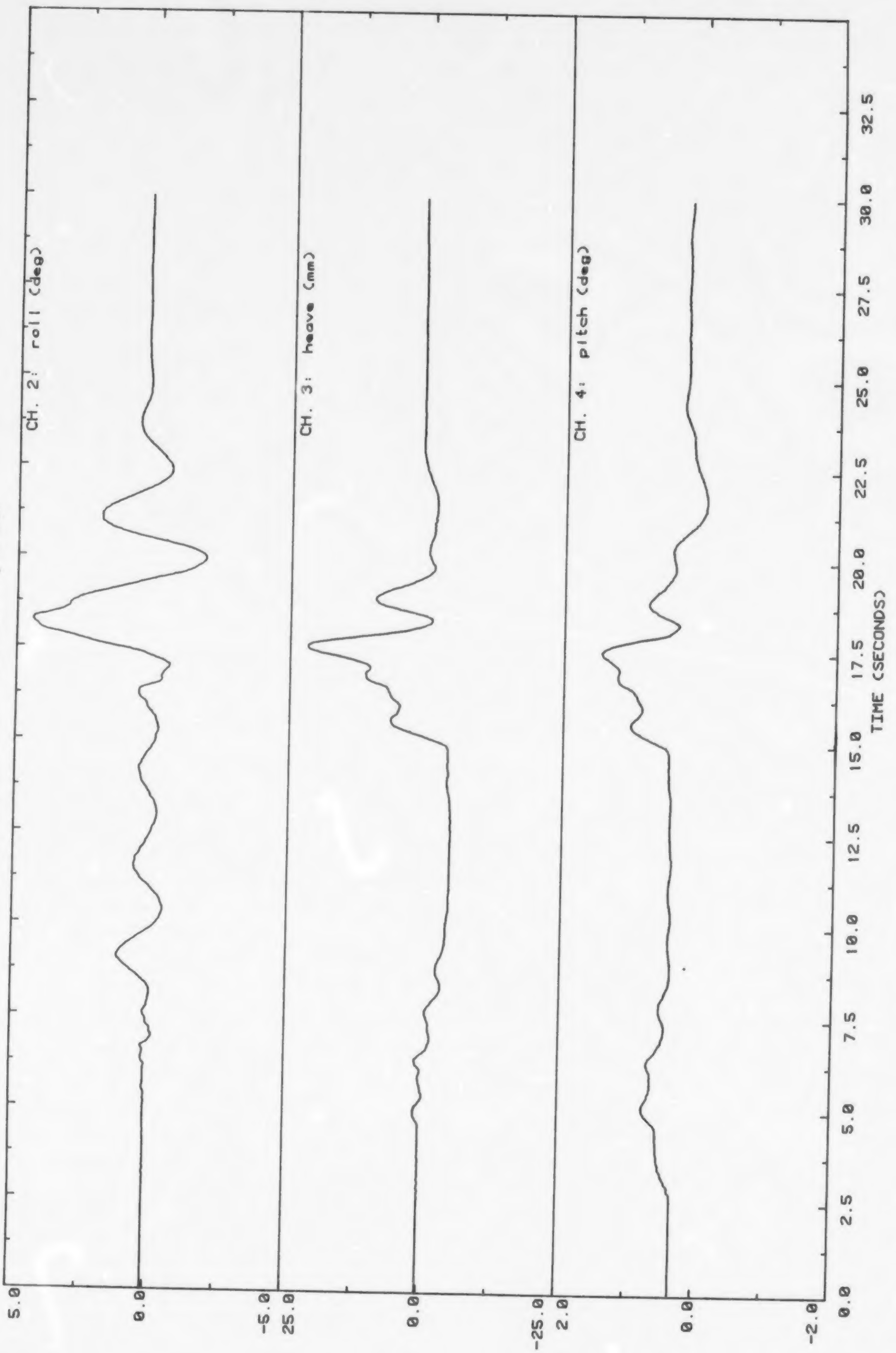

TEST: T2 R1 RIDGE: 2-1 N TEST DATE: May 3, 1988

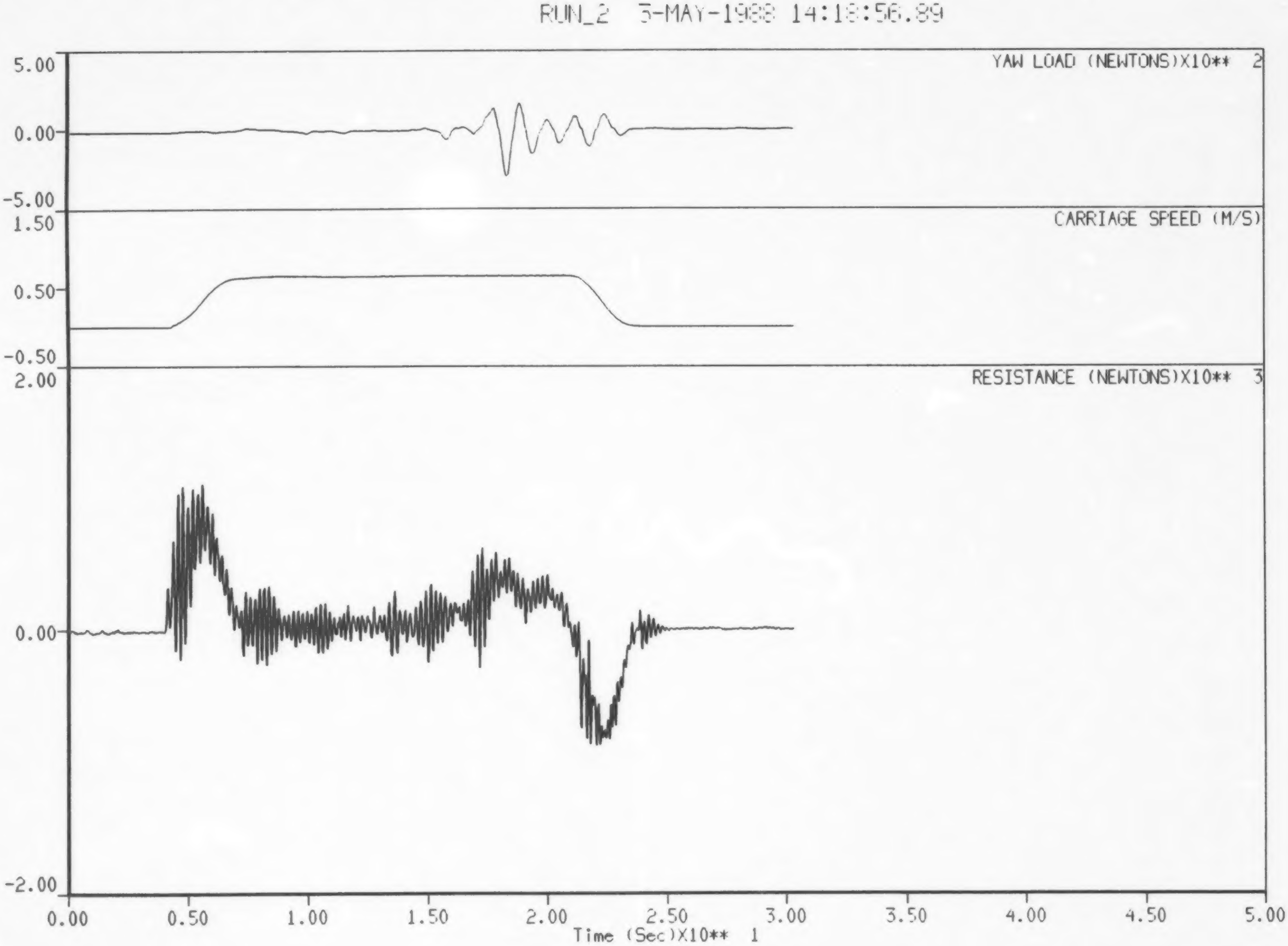
RUN_2 3-MAY-1988 14:18:56.89

RUN_2 3-MAY-1988 14:18:56.89

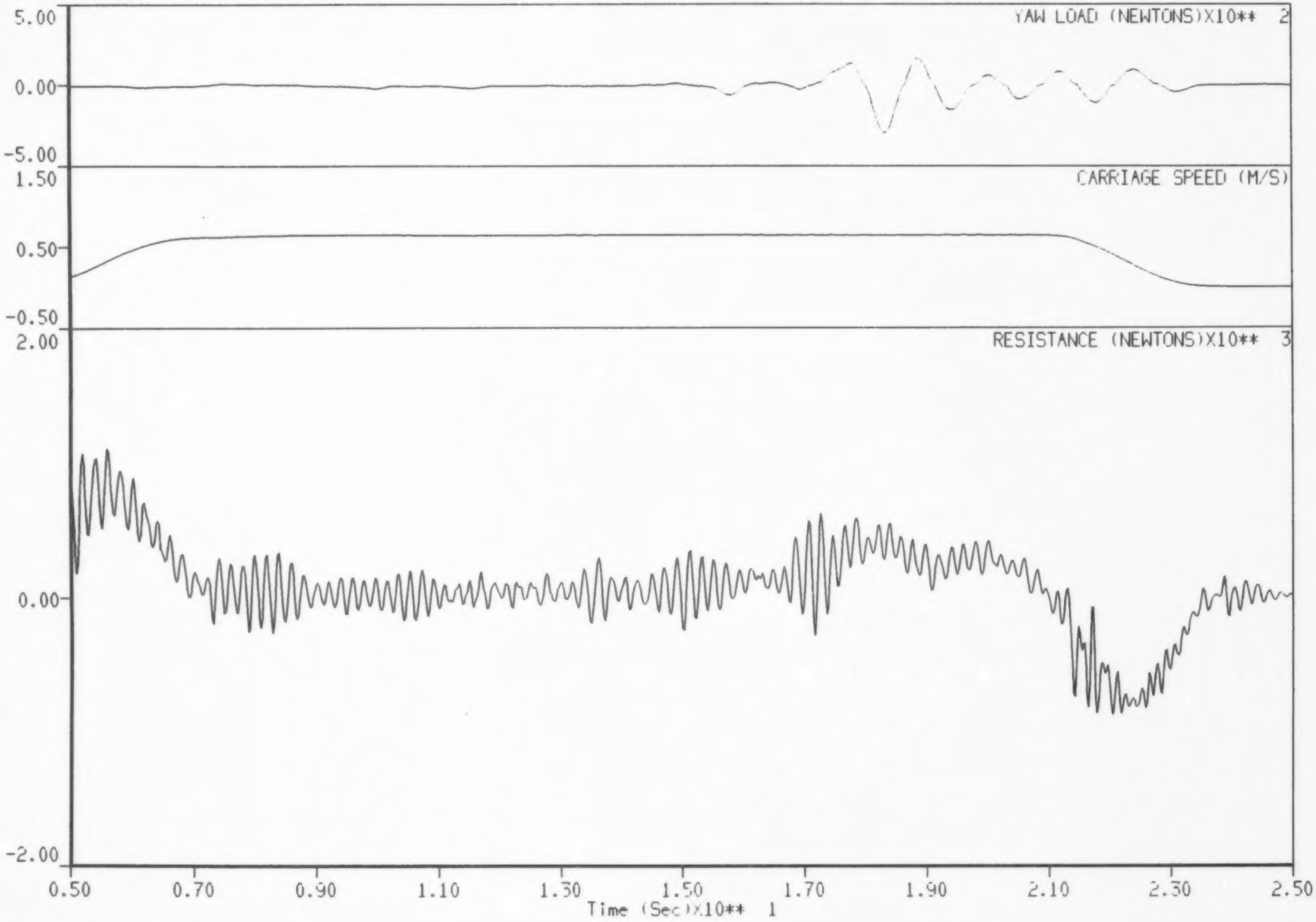

TEST: T2 R2 RIDGE: 2-2 N TEST DATE: May 3, 1988

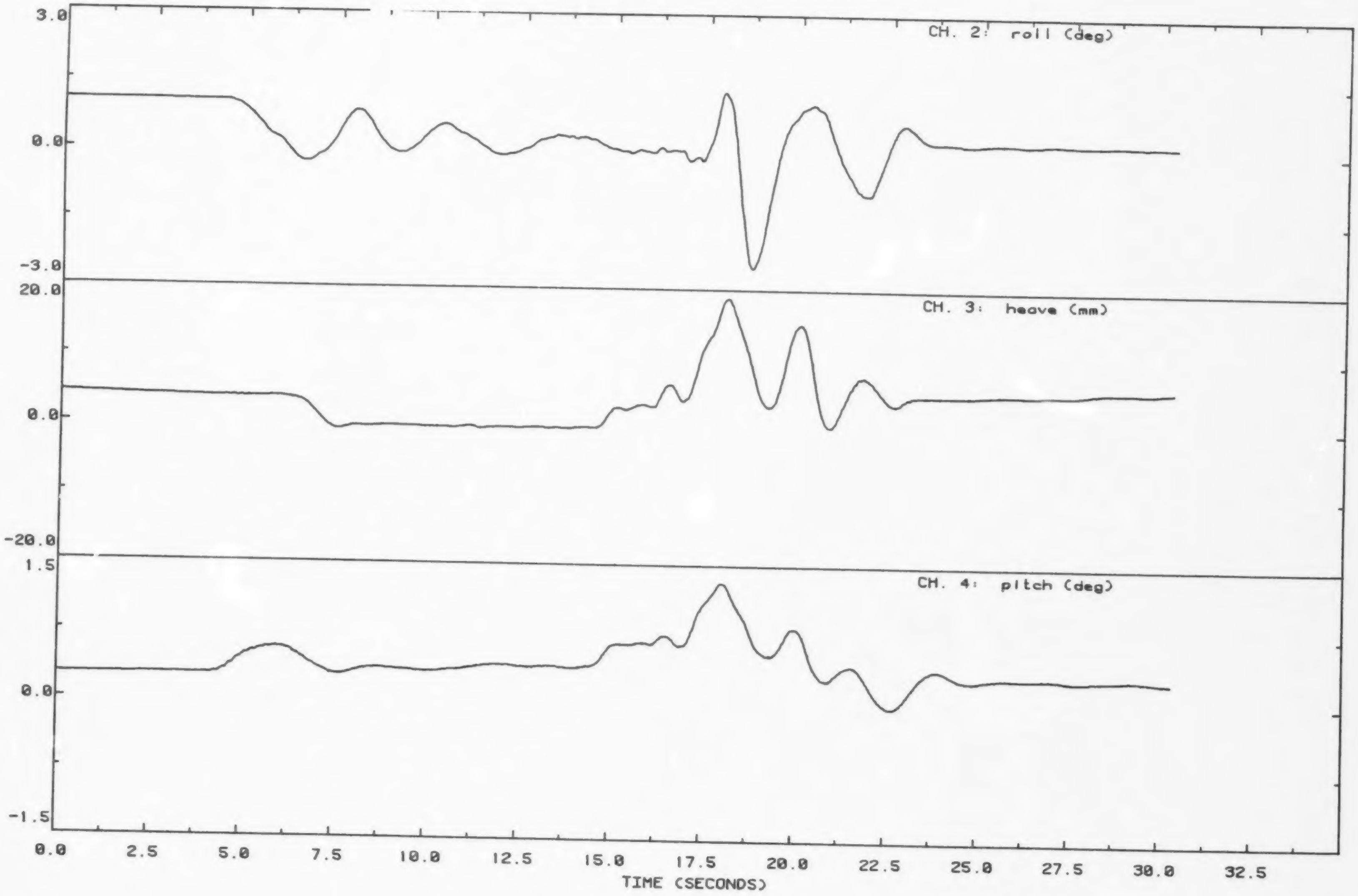

RUN_3 3-MAY-1988 14:36:29.87

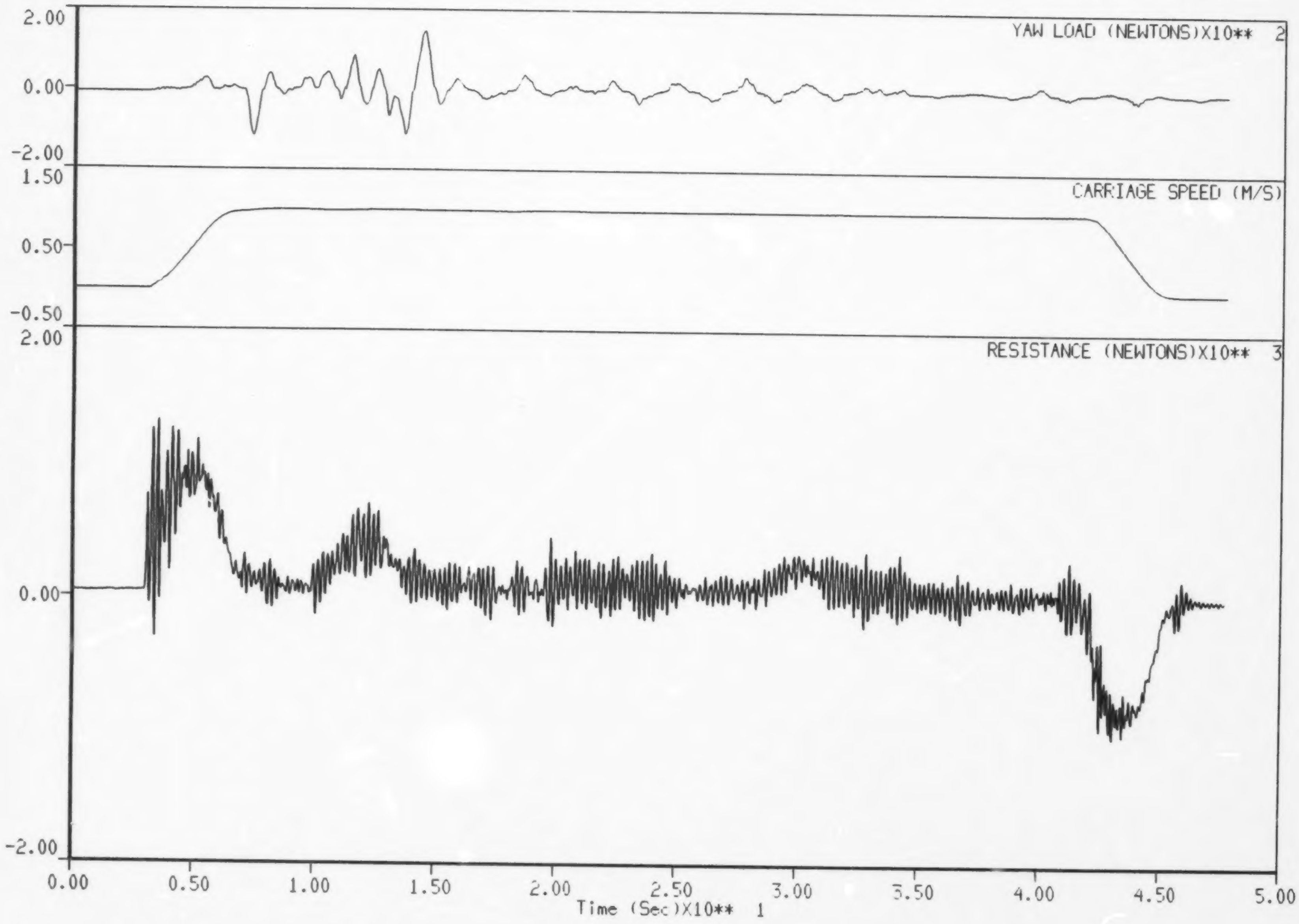

RUN_3 3-MAY-1988 14:36:29.87

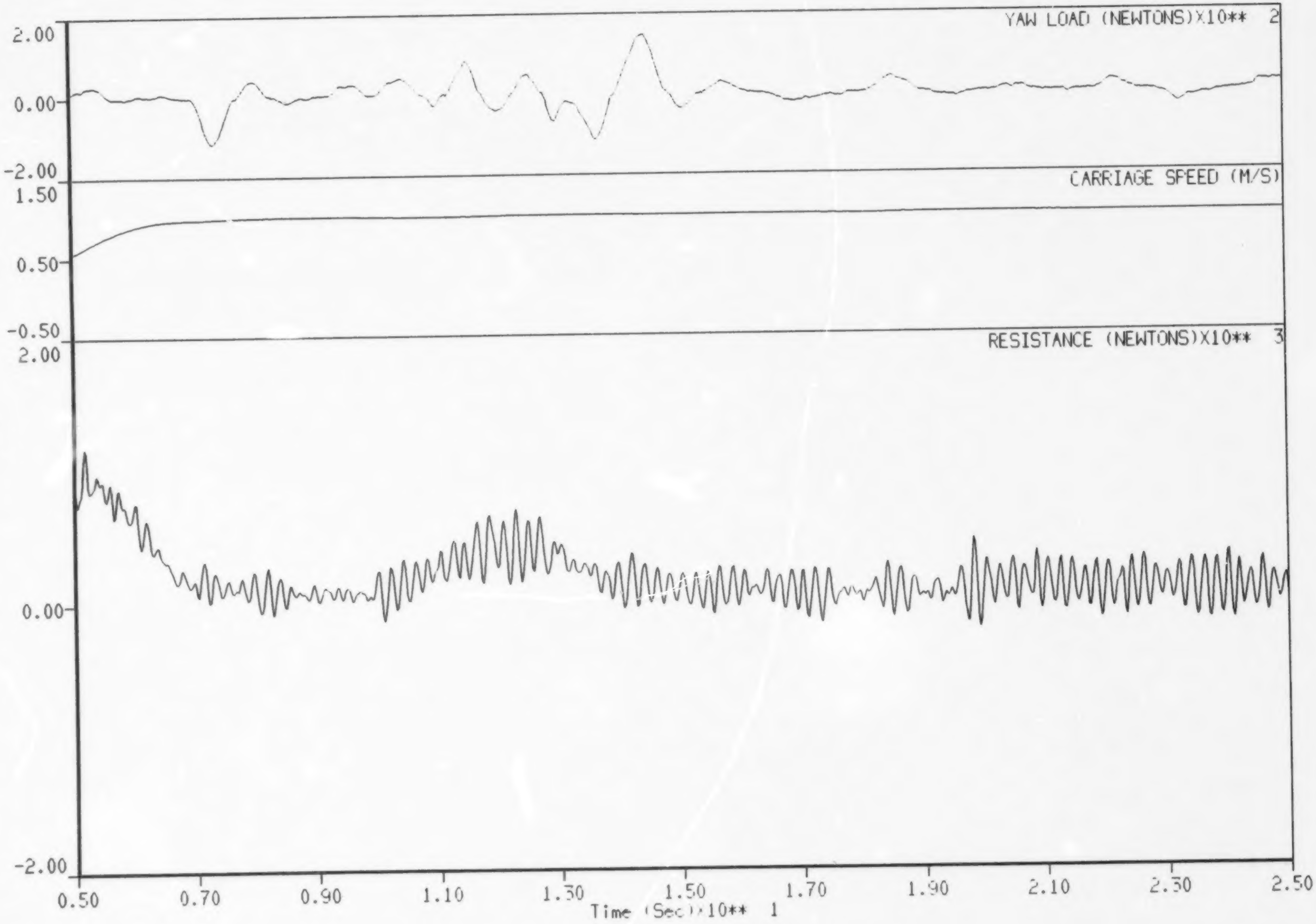

RUN_3 3-MAY-1988 14:36:29.87

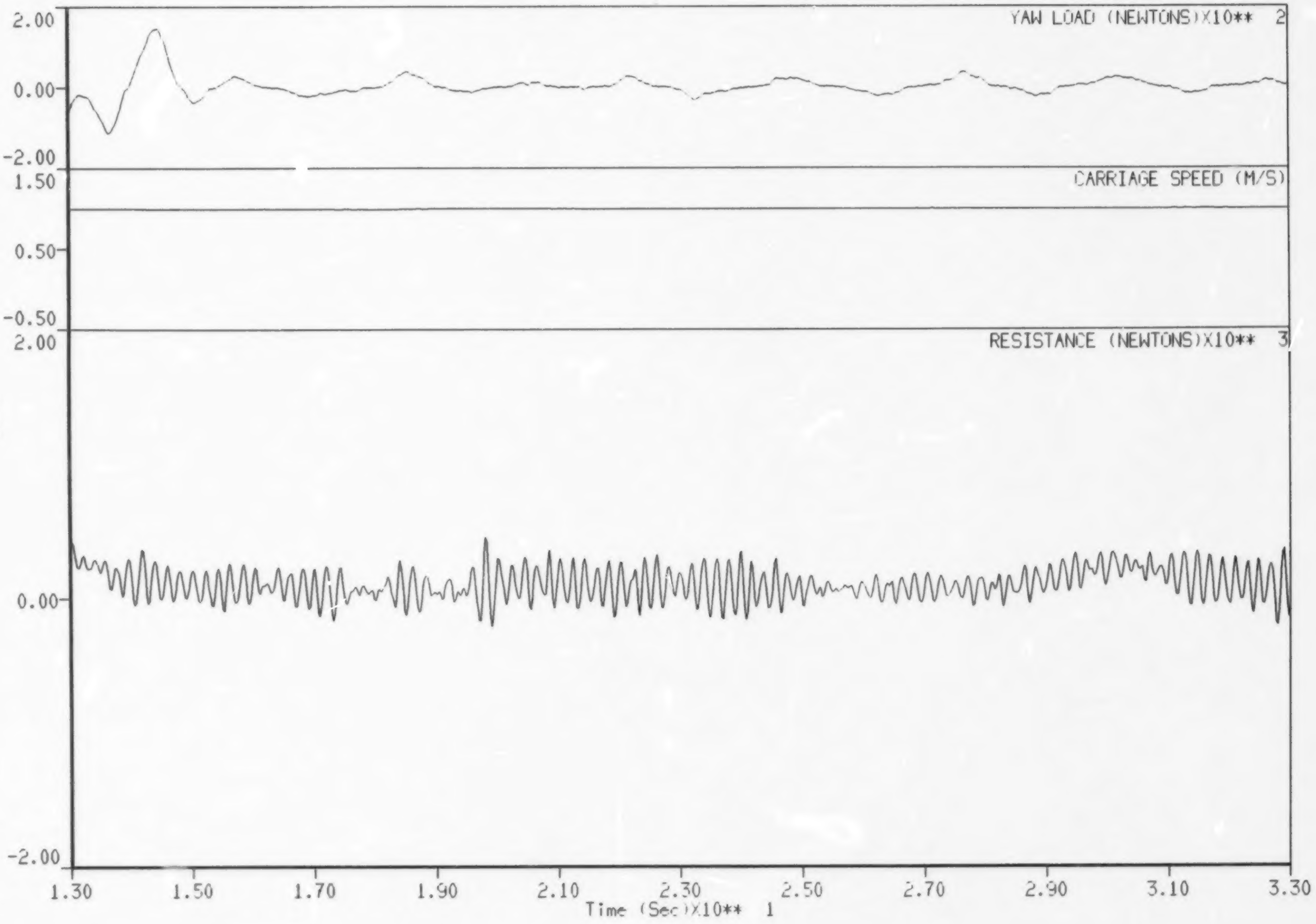

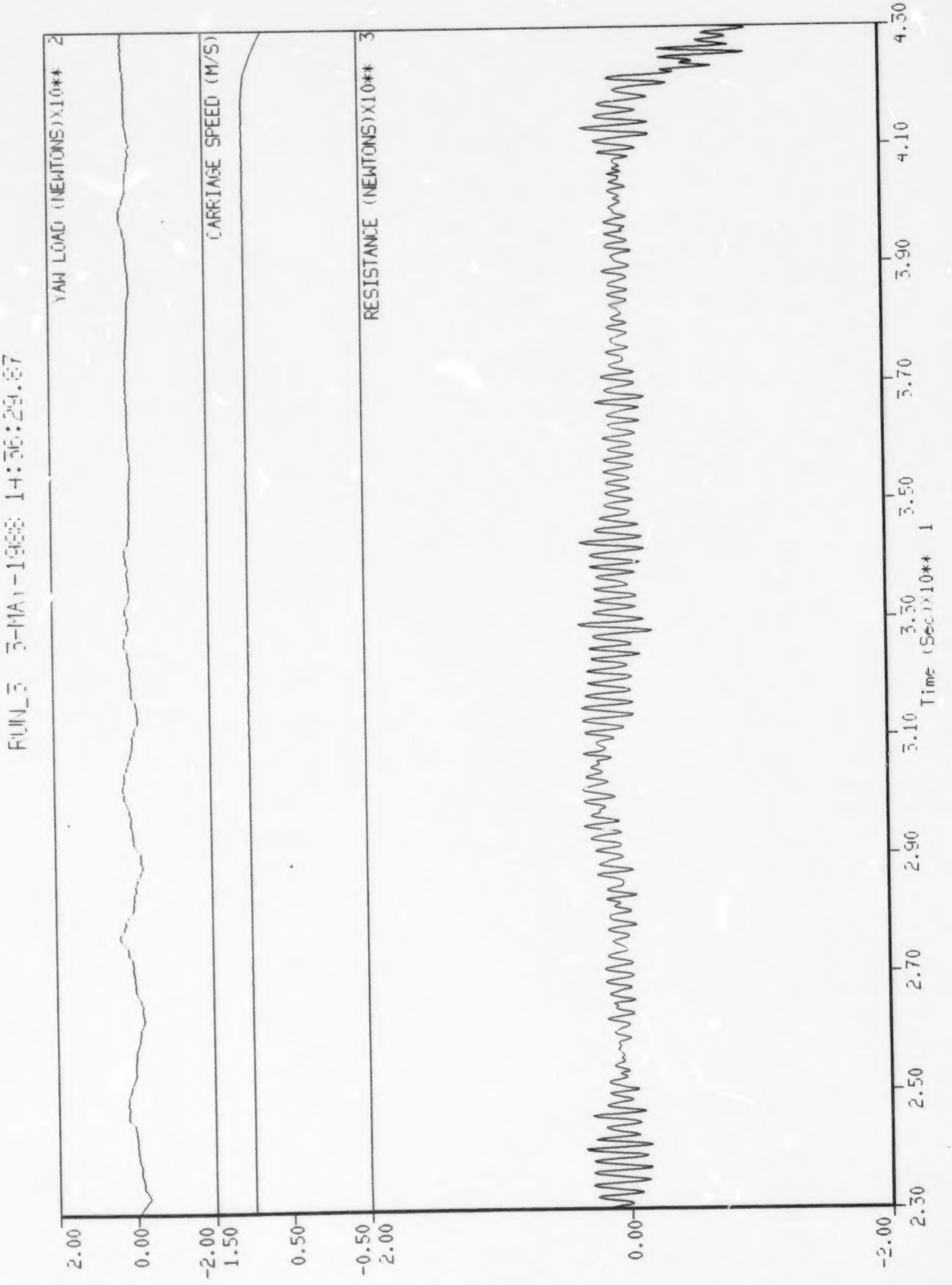
RUN_3 3-MAY-1988 14:36:29.87
YAW LOAD (NEWTONS)X10** 2
CARRIAGE SPEED (M/S)
RESISTANCE (NEWTONS)X10** 3
2.00
0.00
-2.00
1.50
0.50
-0.50
2.00
0.00
-2.00
2.30
2.50
2.70
2.90
3.10
3.30
3.50
3.70
3.90
4.10
4.30
Time (Sec)X10** 1

TEST: T2 R3 RIDGES: 2-3 N, 2-4 N and 2-5 N TEST DATE: May 3, 1988

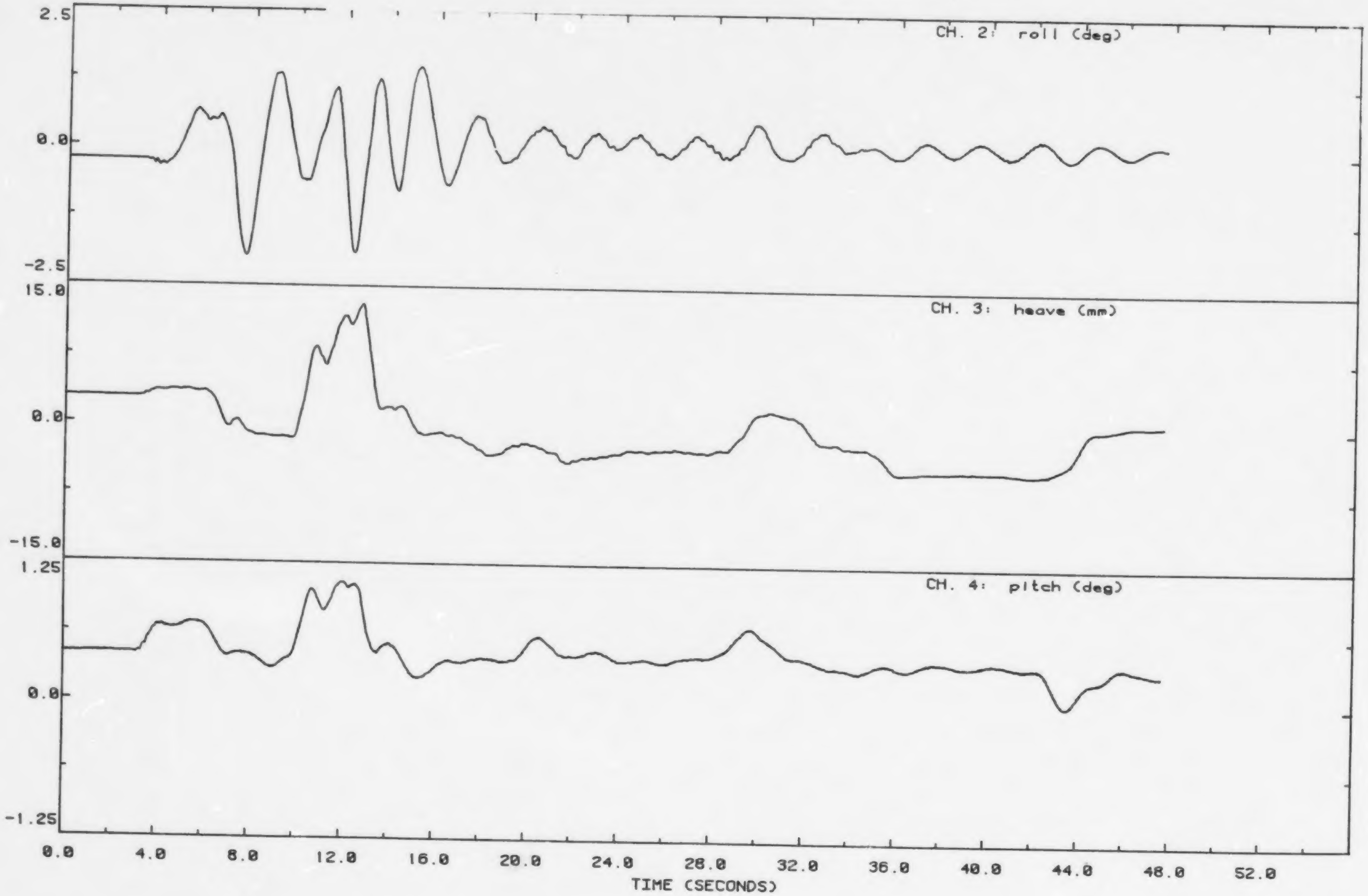

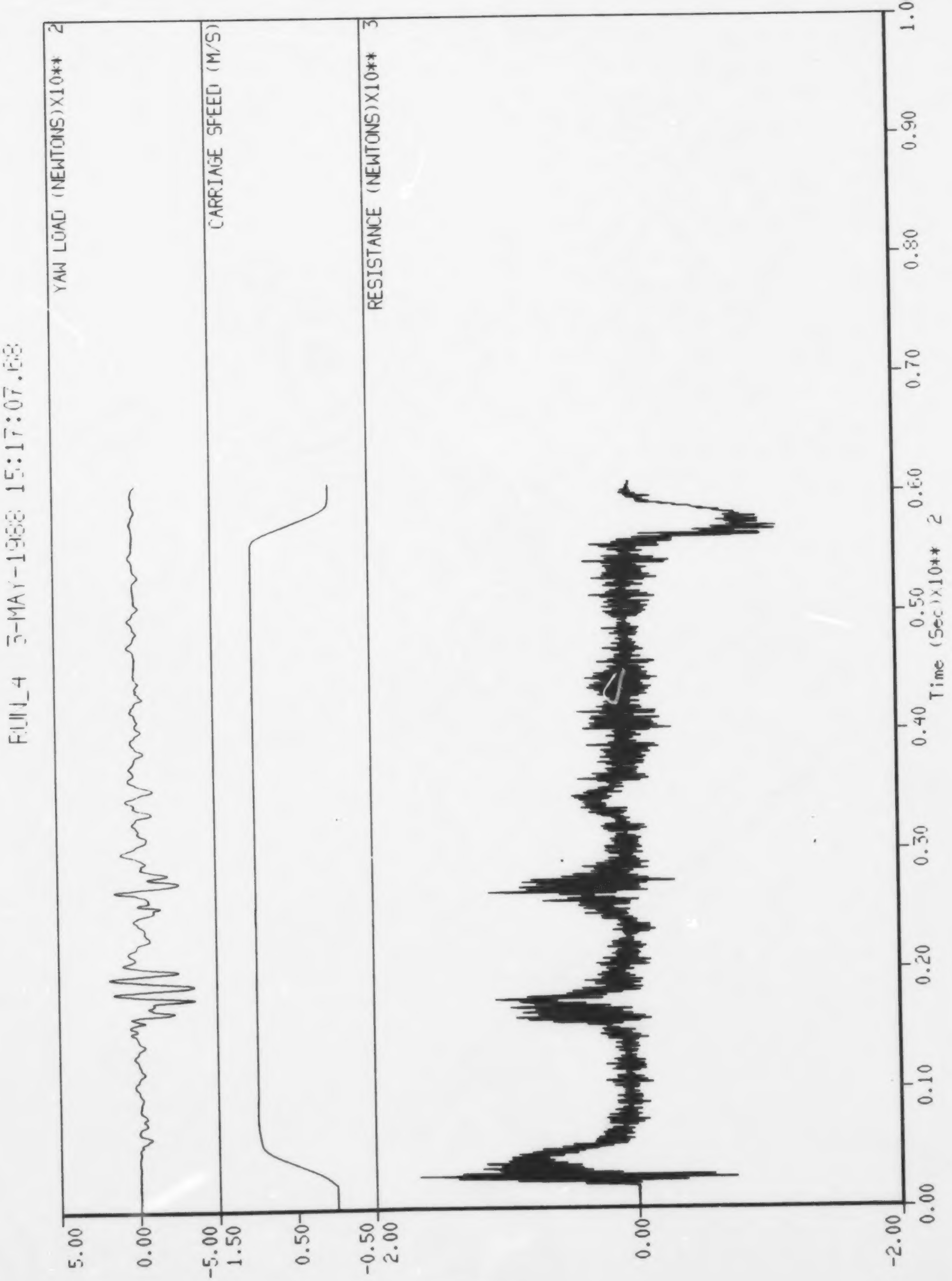
RUN_4 3-MAY-1988 15:17:07.68
YAW LOAD (NEWTONS)X10** 2
CARRIAGE SPEED (M/S)
RESISTANCE (NEWTONS)X10** 3
5.00
0.00
-5.00
1.50
0.50
-0.50
2.00
0.00
-2.00
0.00
0.10
0.20
0.30
0.40
0.50
0.60
0.70
0.80
0.90
1.00
Time (Sec)X10** 2

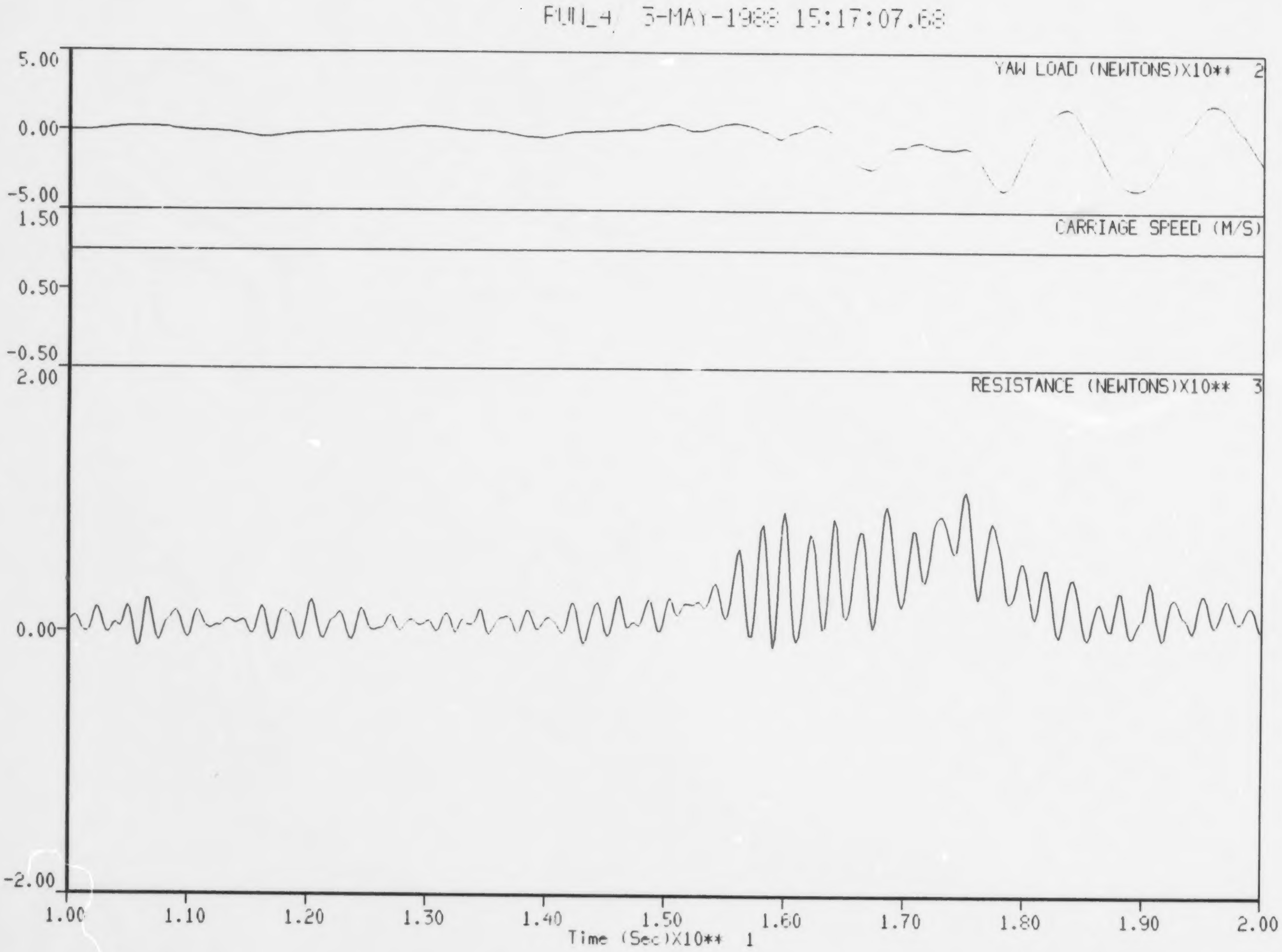
RUN_4 3-MAY-1988 15:17:07.68
YAW LOAD (NEWTONS)X10** 2
5.00
0.00
-5.00
CARRIAGE SPEED (M/S)
1.50
0.50
-0.50
RESISTANCE (NEWTONS)X10** 3
2.00
0.00
-2.00
1.00
1.10
1.20
1.30
1.40
1.50
1.60
1.70
1.80
1.90
2.00
Time (Sec)X10** 1

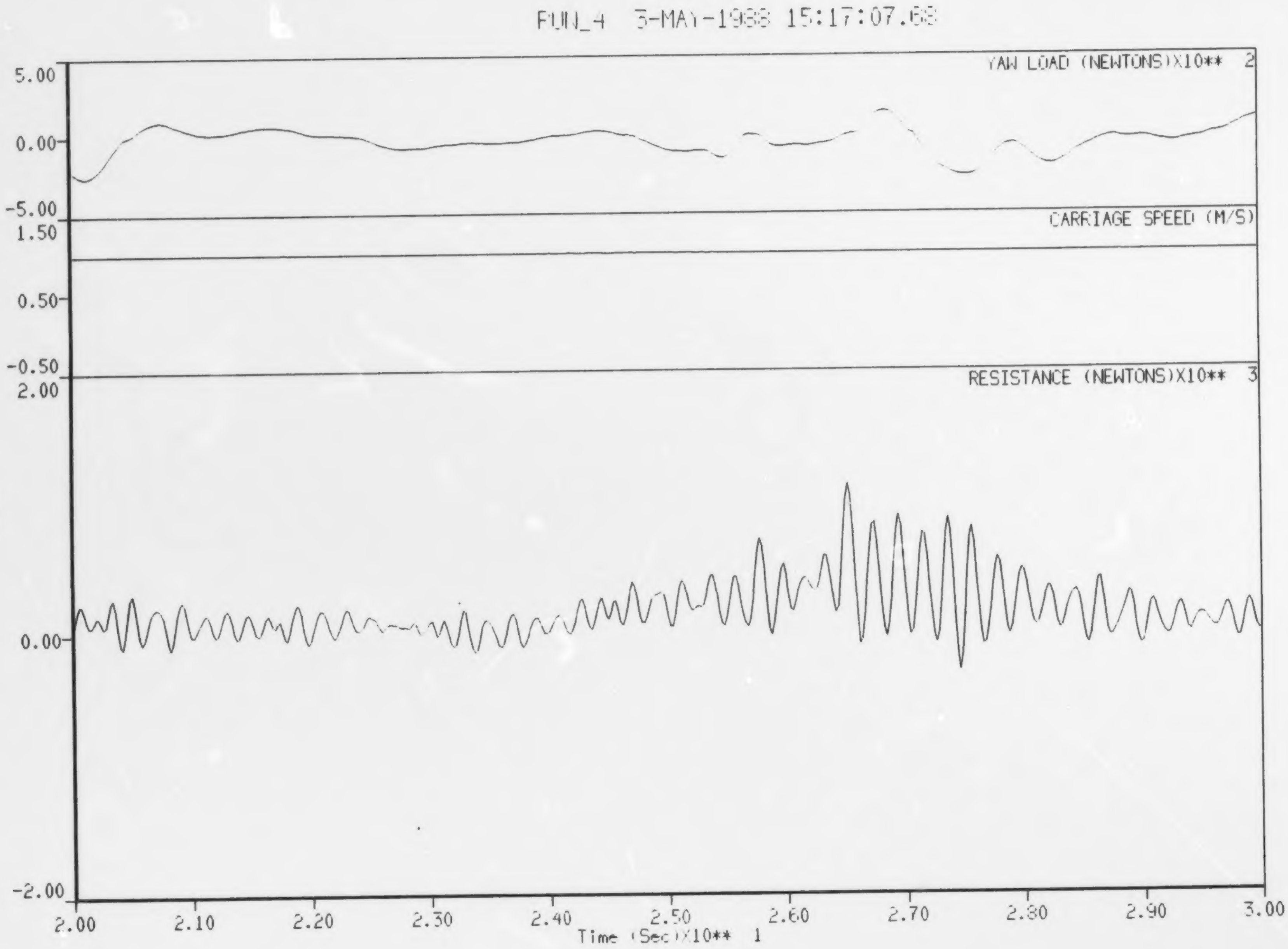
RUN_4 3-MAY-1988 15:17:07.68
YAW LOAD (NEWTONS)X10** 2
CARRIAGE SPEED (M/S)
RESISTANCE (NEWTONS)X10** 3
5.00
0.00
-5.00
1.50
0.50
-0.50
2.00
0.00
-2.00
2.00
2.10
2.20
2.30
2.40
2.50
2.60
2.70
2.80
2.90
3.00
Time (Sec)X10** 1

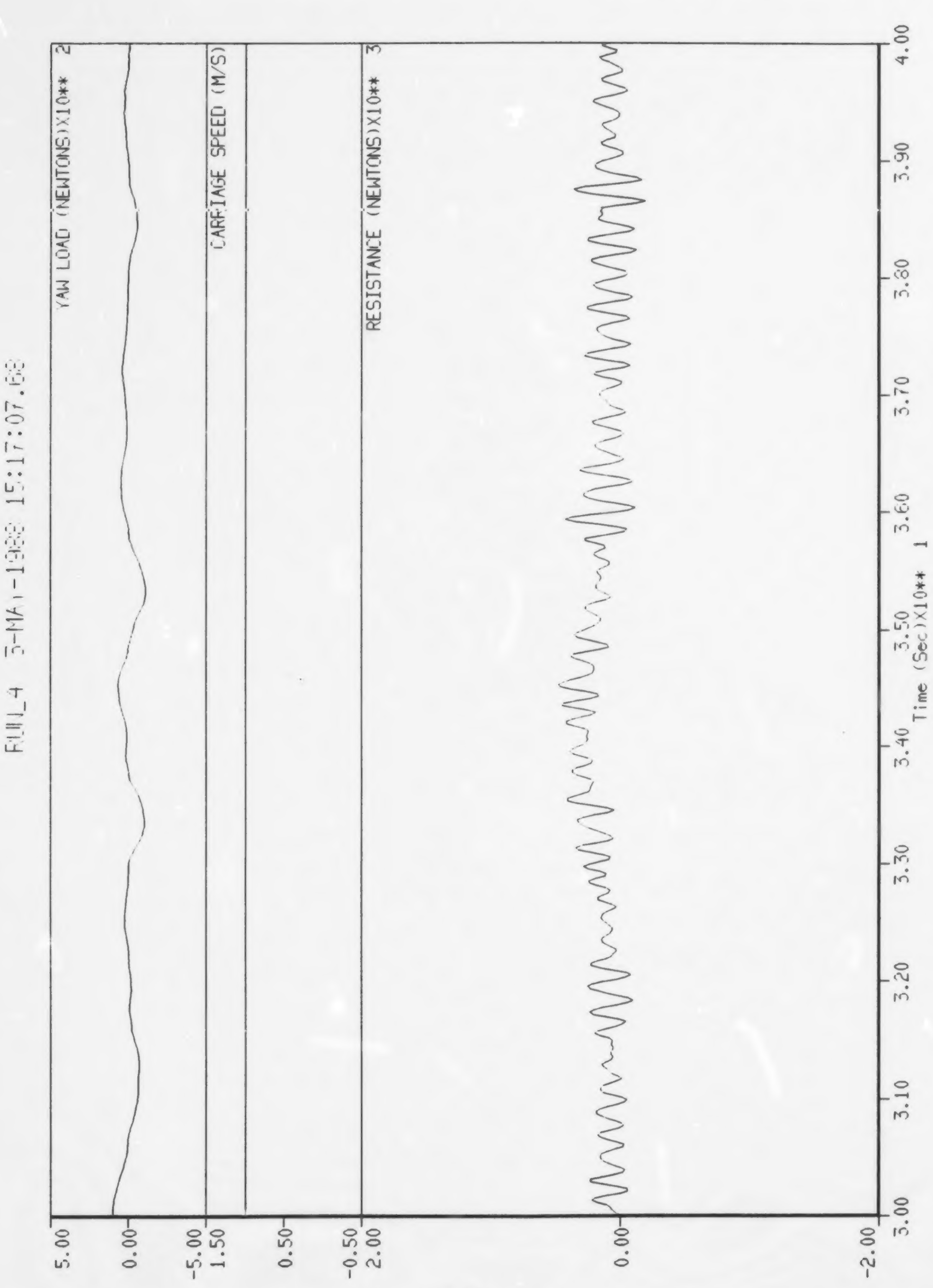
RUN_4 5-MAY-1988 15:17:07.68
YAW LOAD (NEWTONS)X10** 2
CARRIAGE SPEED (M/S)
RESISTANCE (NEWTONS)X10** 3
5.00
0.00
-5.00
1.50
0.50
-0.50
2.00
0.00
-2.00
3.00
3.10
3.20
3.30
3.40
3.50
3.60
3.70
3.80
3.90
4.00
Time (Sec)X10** 1

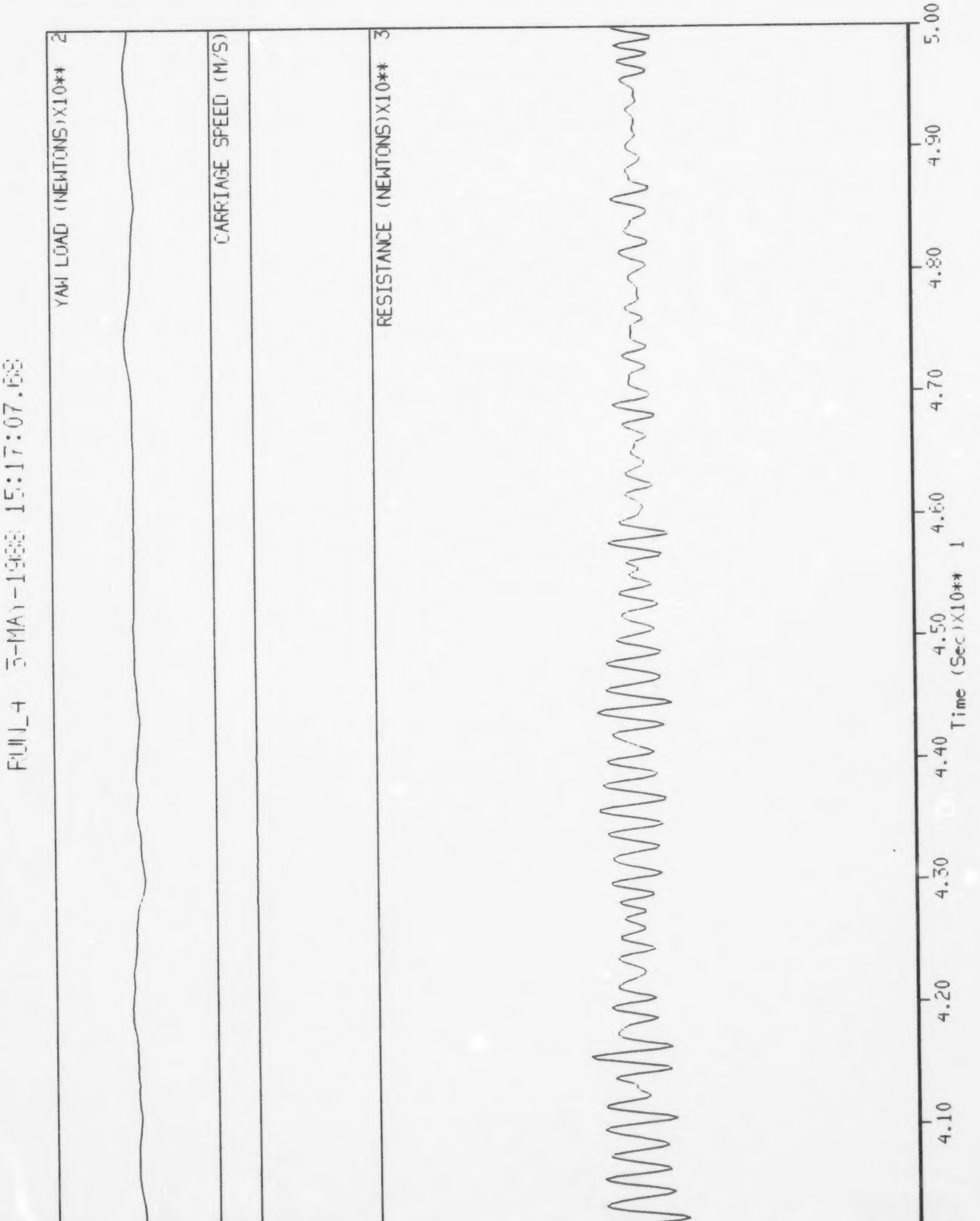
RUN_4 5-MAY-1988 15:17:07.68
YAW LOAD (NEWTONS)X10** 2
CARRIAGE SPEED (M/S)
RESISTANCE (NEWTONS)X10** 3
5.00
0.00
-5.00
1.50
0.50
-0.50
2.00
0.00
-2.00
4.00
4.10
4.20
4.30
4.40
4.50
4.60
4.70
4.80
4.90
5.00
Time (Sec)X10** 1

TEST: T2 R4 RIDGES: 2-1 S, 2-2 S, 2-3 S and 2-4 S TEST DATE: May 3, 1988

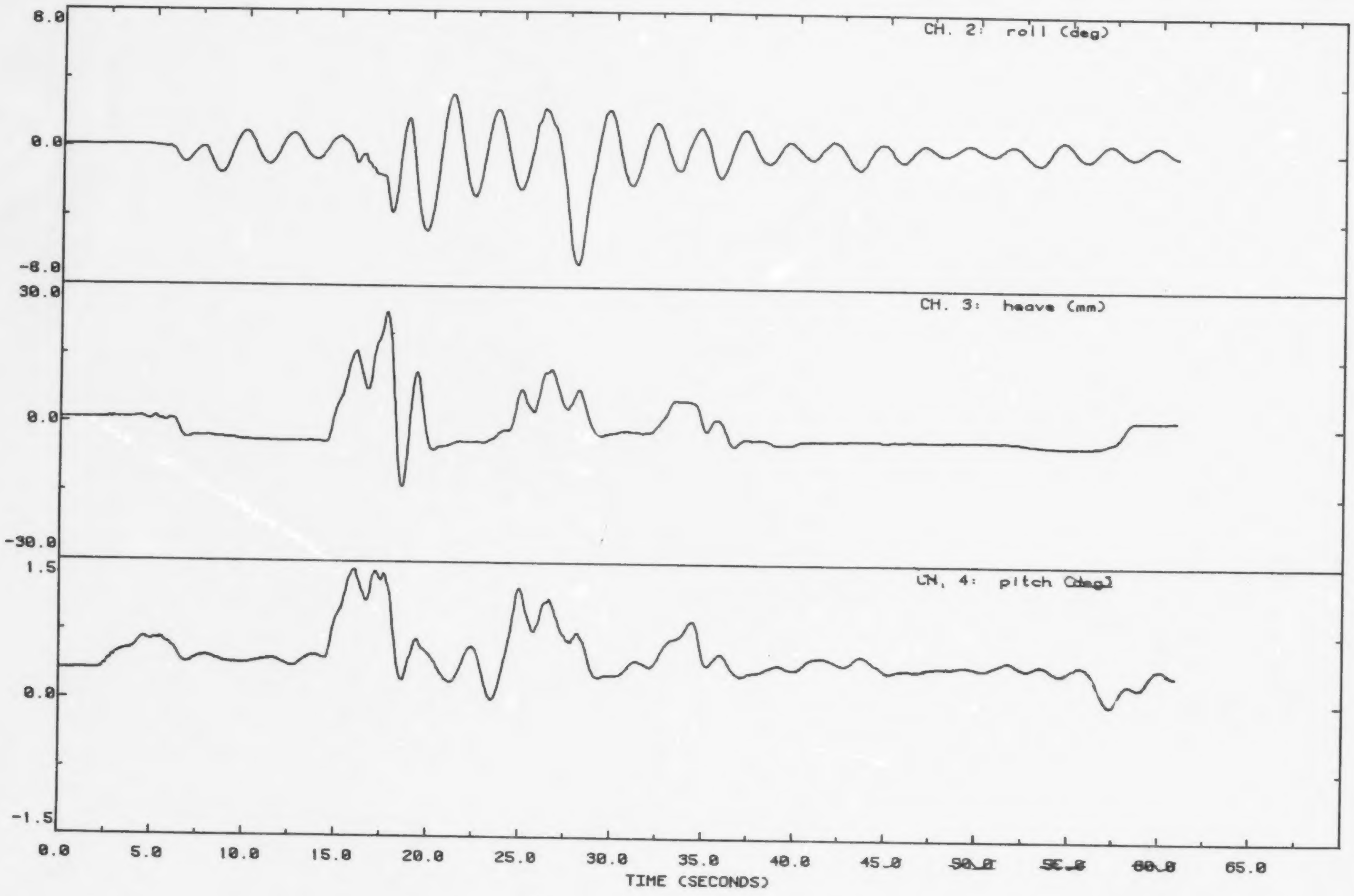

APPENDIX D.2

SHEET #2 TESTS AT THE IMD:

REDUCED PLOTS OF FORCE VS. DISPLACEMENT AND CUMULATIVE PENETRATION ENERGY - TEST DATA FILTERED AT 2 HZ

MODEL SCALE RIDGE START POINT PENETRATION DISTANCES USED FOR REDUCTION OF PLOTS OF CUMULATIVE PENETRATION ENERGY VS. PENETRATION DISTANCE

RIDGE	PENETRATION (m) AT WHICH THE BOW WAS CONSIDERED TO FIRST CONTACT THE RIDGE
1-1	1.7
1-4	0.7
2-1 N	3.4
2-2 N	2.4
2-3 N	1.4
2-4 N	2.2
2-5 N	3.3
2-1 S	2.1
2-2 S	2.0
2-3 S	2.0
2-4 S	2.0
3-1 N	2.0
3-2 N	3.8
3-3 N	1.3
3-4 N	3.4
3-5 N	2.8
3-1 S	2.0
3-2 S	2.0
3-3 S	2.0
3-4 S	0

```
TEST:      T2R1             RIDGE:2-1N

DISTANCE,M                  FORCE,N      CUM. ENERGY,N-M
    0.00                       67                 0
     .91                       75                54
    1.81                       63               111
    2.72                       75               175
    3.63                      125               252
    4.53                      256               414
    5.44                      325               693
    6.35                      467              1162
    7.25                      325              1527
    8.16                      160              1743

PENETRATION OF   5.94 M AT MAX FORCE OF   596 N
PENETRATION OF   8.96 M AT MAX ENERGY OF  1844 N-M
```

```
TEST:      T2R2             RIDGE:2-2N

DISTANCE,M                  FORCE,N      CUM. ENERGY,N-M
    0.00                       44                 0
     .65                       58                30
    1.30                       67                70
    1.95                       69               110
    2.61                       87               155
    3.27                      112               222
    3.92                      204               318
    4.57                      452               493
    5.23                      290               754
    5.88                      315               935
    6.53                      117              1097

PENETRATION OF   4.57 M AT MAX FORCE OF   452 N
PENETRATION OF   6.53 M AT MAX ENERGY OF  1097 N-M
```

```
TEST:     T2R3          RIDGE:2-3N

DISTANCE,M              FORCE,N      CUM. ENERGY,N-M
    0.00                  38               0
     .91                  35              36
    1.81                 125              87
    2.71                 314             282
    3.61                 375             615
    4.52                 273             942
    5.42                 100            1093
    6.33                  71            1176
    7.23                  67            1223
    8.14                  48            1281

PENETRATION OF   3.21 M AT MAX FORCE OF   431 N
PENETRATION OF   8.44 M AT MAX ENERGY OF  1293 N-M


TEST:     T2R3          RIDGE:2-4N

DISTANCE,M              FORCE,N      CUM. ENERGY,N-M
    0.00                  13               0
     .90                  10              18
    1.80                  35              49
    2.71                  62              76
    3.62                  92             148
    4.52                  71             225
    5.43                  60             275
    6.33                  75             339
    7.23                  35             384
    8.13                  42             417

PENETRATION OF   3.92 M AT MAX FORCE OF   102 N
PENETRATION OF   8.44 M AT MAX ENERGY OF   428 N-M


TEST:     T2R3          RIDGE:2-5N

DISTANCE,M              FORCE,N      CUM. ENERGY,N-M
    0.00                  42               0
    1.10                  29              36
    2.21                  37              74
    3.31                  38             114
    4.42                 160             226
    5.52                 179             435
    6.63                  85             584
    7.73                  44             653
    8.84                  42             702
    9.94                  10             732

PENETRATION OF   5.02 M AT MAX FORCE OF   210 N
PENETRATION OF  10.44 M AT MAX ENERGY OF   735 N-M
```

```
TEST:      T2R3            RIDGE:2-345N

DISTANCE,M              FORCE,N       CUM. ENERGY,N-M
    0.00                  38                 0
    2.70                 362               368
    5.42                 121              1118
    8.13                  13              1282
   10.84                  62              1358
   13.56                  60              1558
   16.27                  42              1700
   18.98                  35              1790
   21.69                 181              2117
   24.40                  46              2371

PENETRATION OF    2.90 M AT MAX FORCE OF    431 N
PENETRATION OF   26.71 M AT MAX ENERGY OF  2434 N-M
```

```
TEST:      T2R4            RIDGE:2-1S

DISTANCE,M              FORCE,N       CUM. ENERGY,N-M
    0.00                  60                 0
     .91                  67                57
    1.81                  67               124
    2.72                 146               217
    3.63                 406               466
    4.53                 514               846
    5.44                 600              1433
    6.35                 121              1722
    7.25                 154              1845
    8.16                 108              1972
    9.07                  75              2050

PENETRATION OF    5.24 M AT MAX FORCE OF    818 N
PENETRATION OF    9.27 M AT MAX ENERGY OF  2064 N-M
```

```
TEST:      T2R4            RIDGE:2-2S

DISTANCE,M              FORCE,N       CUM. ENERGY,N-M
    0.00                  63                 0
     .91                  83                64
    1.81                   2               107
    2.72                  94               130
    3.63                 229               293
    4.54                 302               542
    5.44                 398               922
    6.35                 244              1215
    7.26                 119              1389
    8.16                  77              1467

PENETRATION OF    5.04 M AT MAX FORCE OF    573 N
PENETRATION OF    8.67 M AT MAX ENERGY OF  1[illegible]08 N-M
```

```
TEST:     T2R4          RIDGE:2-3S

DISTANCE,M              FORCE,N      CUM. ENERGY,N-M
    0.00                  87                 0
     .81                  83                65
    1.61                  92               129
    2.42                 102               204
    3.22                 204               333
    4.03                 300               553
    4.83                 237               797
    5.64                 164               946
    6.45                 110              1053
    7.25                  94              1126

PENETRATION OF   4.43 M AT MAX FORCE OF   337 N
PENETRATION OF   7.96 M AT MAX ENERGY OF  1185 N-M


TEST:     T2R4          RIDGE:2-4S

DISTANCE,M              FORCE,N      CUM. ENERGY,N-M
    0.00                  71                 0
     .91                  77                69
    1.81                  52               134
    2.72                  87               197
    3.63                 104               284
    4.53                  92               382
    5.44                  94               470
    6.35                 112               565
    7.26                  56               634
    8.16                  63               684

PENETRATION OF   4.13 M AT MAX FORCE OF   115 N
PENETRATION OF   8.97 M AT MAX ENERGY OF   725 N-M


TEST:     T2R4          RIDGE:2-1234S

DISTANCE,M              FORCE,N      CUM. ENERGY,N-M
    0.00                  60                 0
    3.43                 335               391
    6.85                 150              1785
   10.28                  83              2137
   13.71                 329              2574
   17.13                  75              3508
   20.56                 117              3798
   23.98                 133              4579
   27.41                  85              4873
   30.84                 100              5178
   34.26                  48              5452

PENETRATION OF   5.24 M AT MAX FORCE OF   818 N
PENETRATION OF  34.56 M AT MAX ENERGY OF  5467 N-M
```

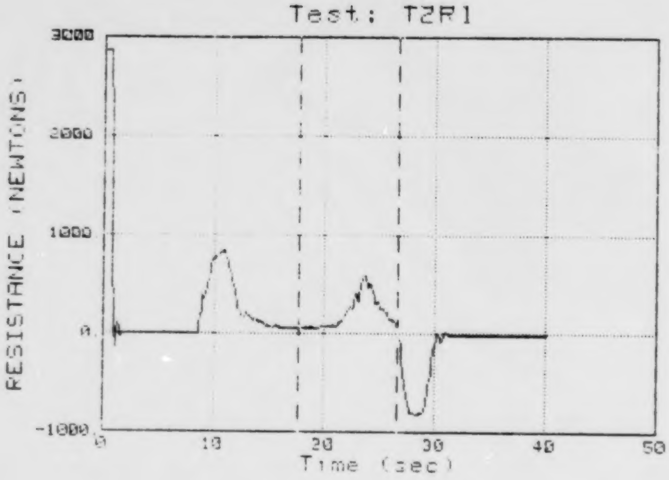
Test: T2R1

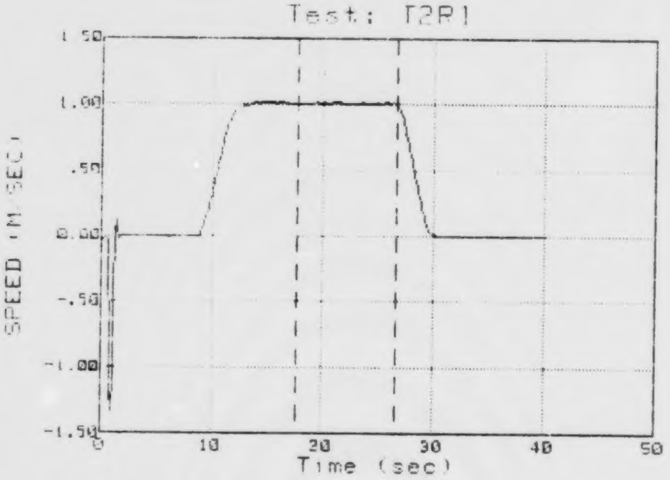
Test: T2R1

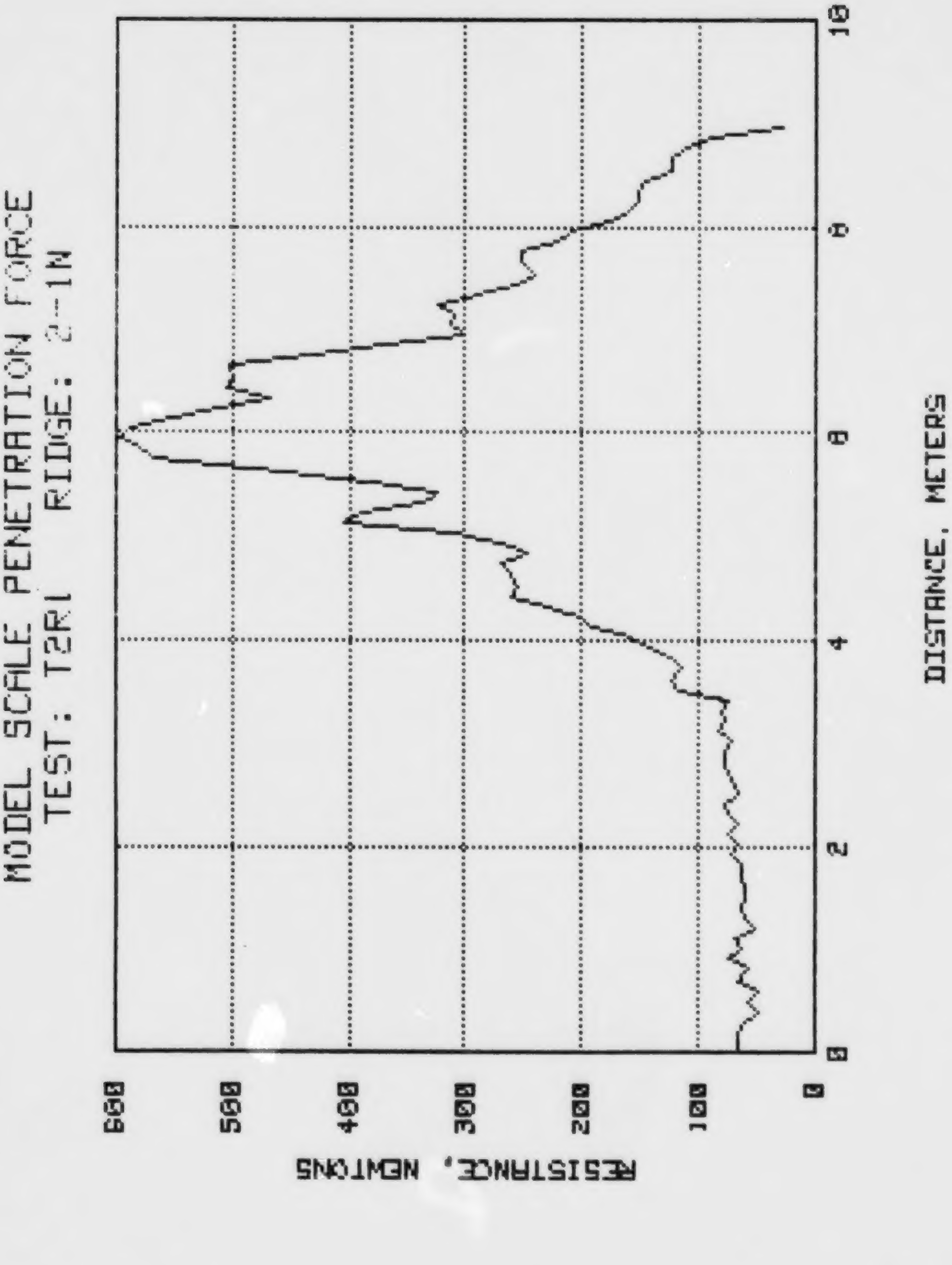
MODEL SCALE PENETRATION FORCE
TEST: T2R1   RIDGE: 2-1N
RESISTANCE, NEWTONS
0
100
200
300
400
500
600
DISTANCE, METERS
0
2
4
6
8
10

MODEL SCALE PENETRATION ENERGY
TEST: T2R1 RIDGE: 2-1N

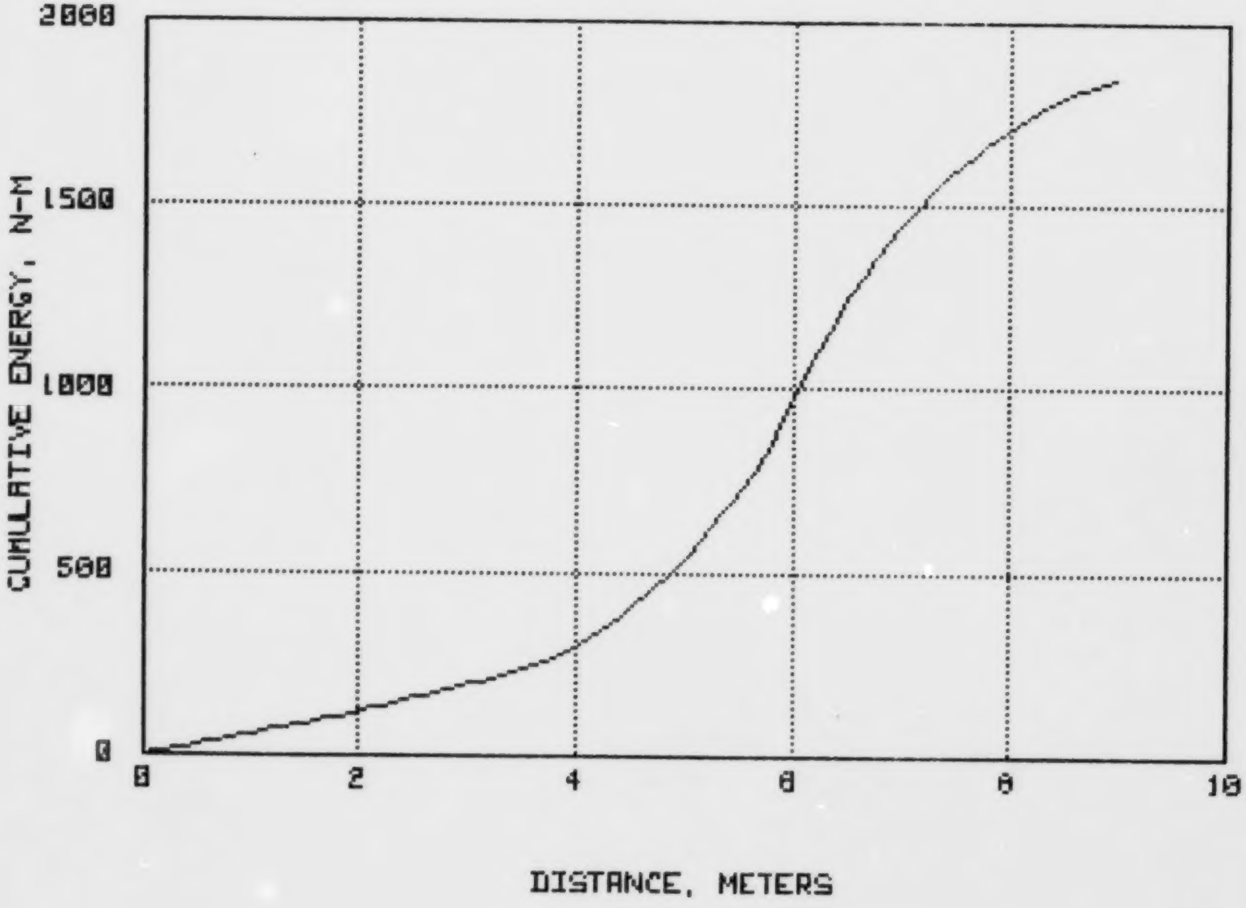

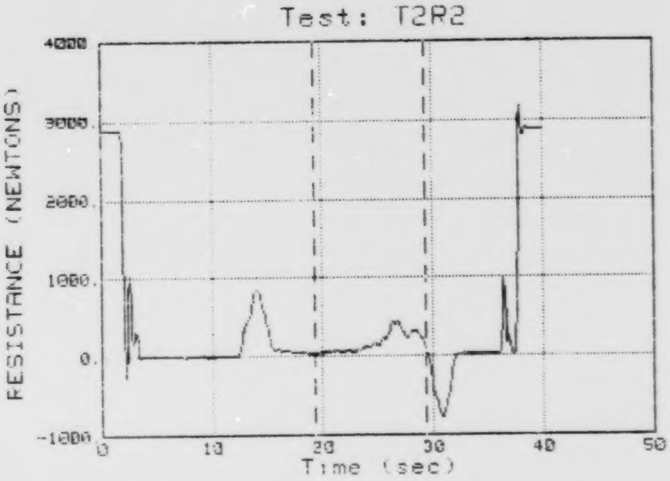
Test: T2R2
RESISTANCE (NEWTONS)
4000
3000.
2000.
1000.
0.
-1000
0
10
20
30
40
50
Time (sec)

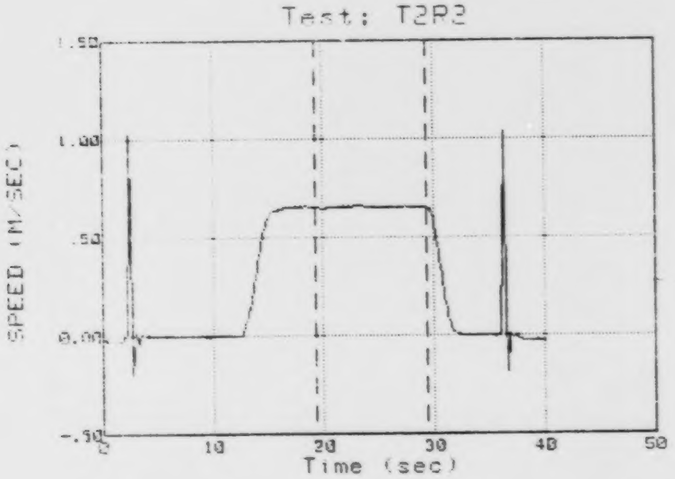
Test: T2R2
SPEED (M/SEC)
1.50
1.00
.50
0.00
-.50
0
10
20
30
40
50
Time (sec)

MODEL SCALE PENETRATION FORCE
TEST: T2R2   RIDGE: 2-2N

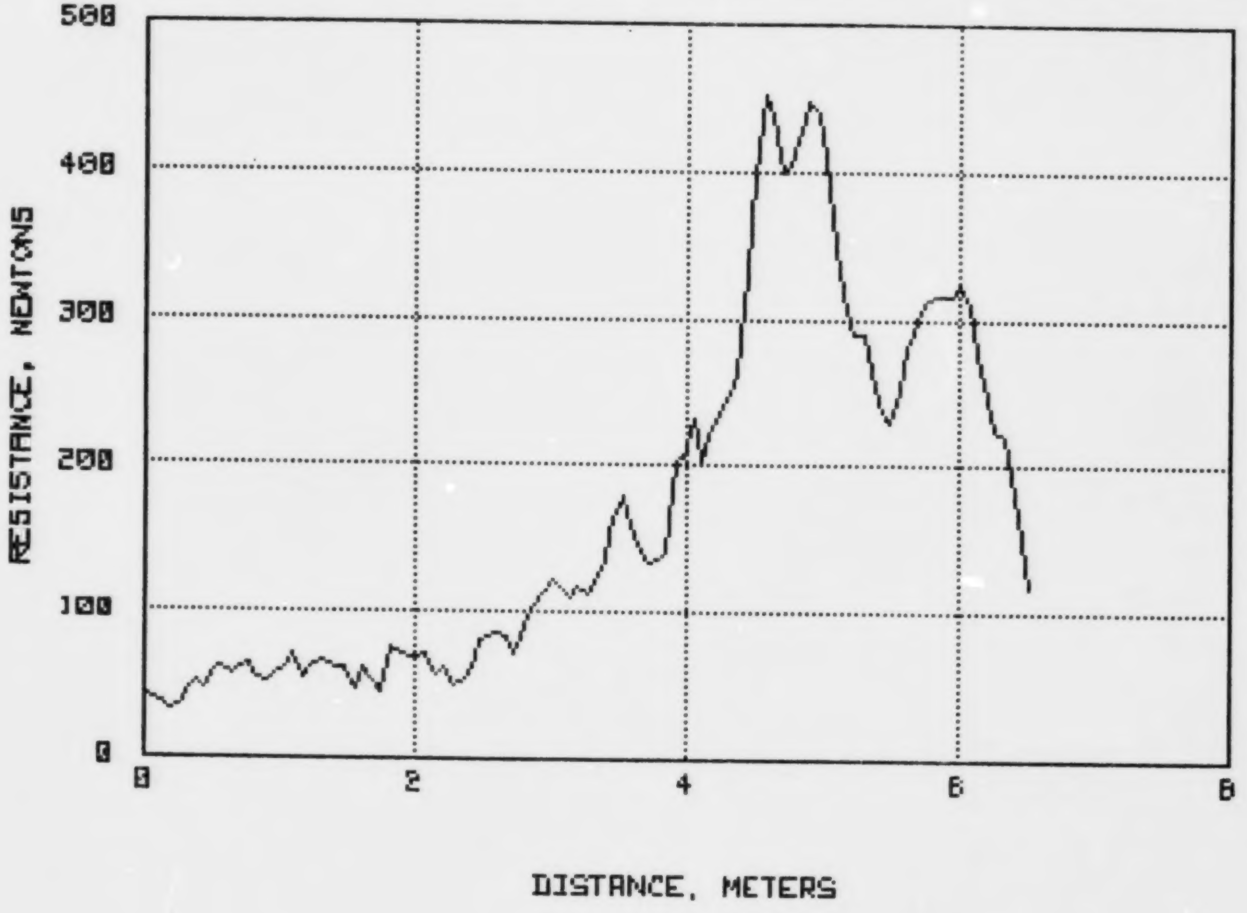

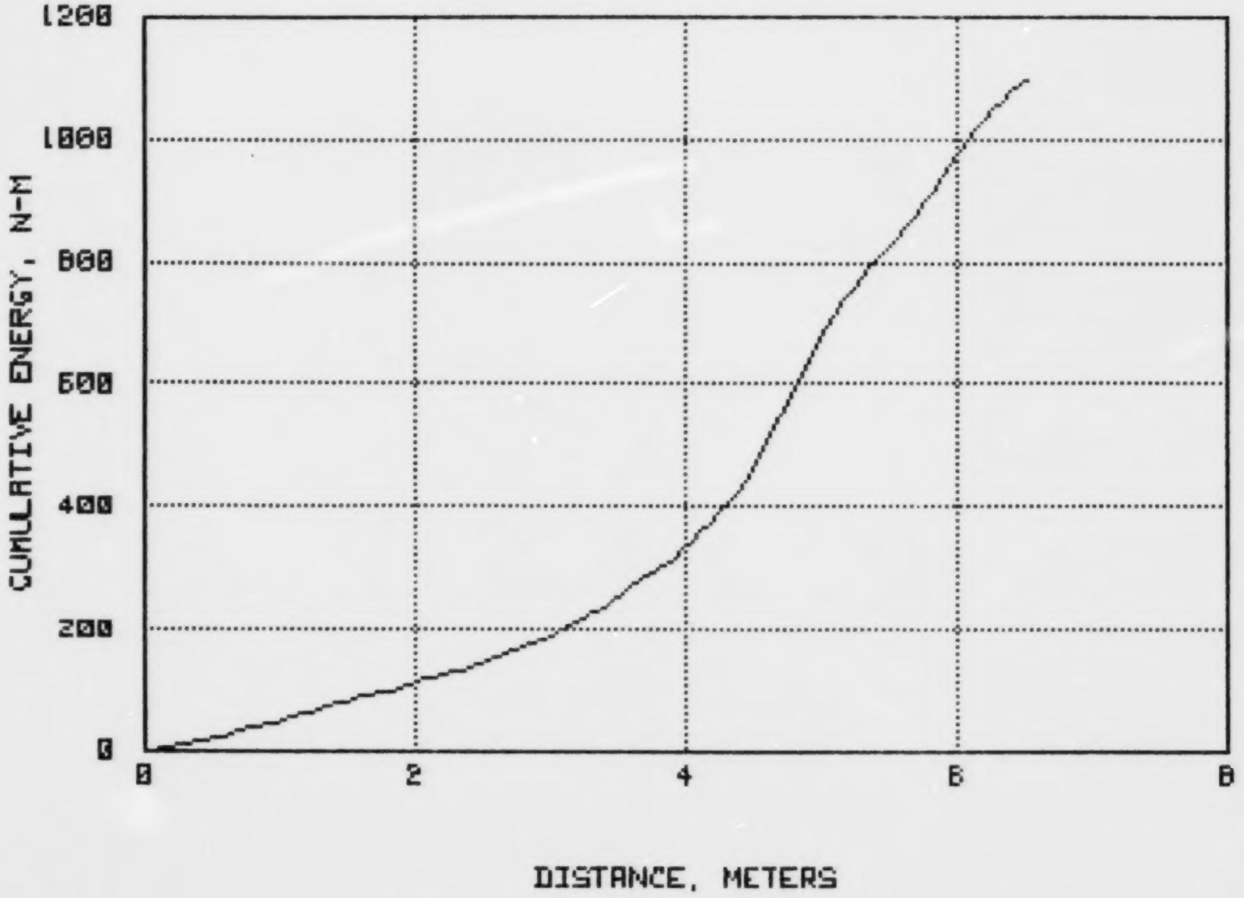

MODEL SCALE PENETRATION ENERGY
TEST: T2R2   RIDGE: 2-2N

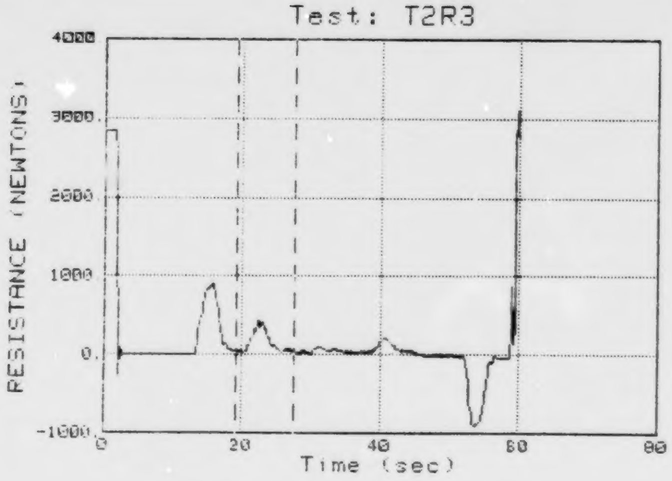
Test: T2R3
RESISTANCE (NEWTONS)
4000
3000.
2000.
1000.
0.
-1000.
0
20
40
60
80
Time (sec)

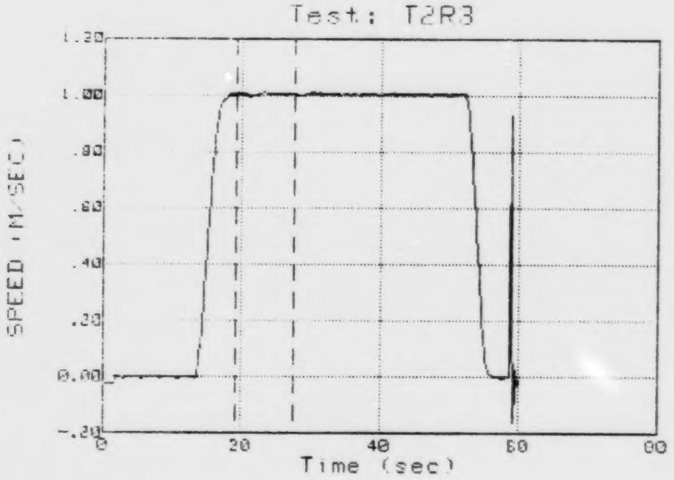
Test: T2R3
SPEED (M/SEC)
1.20
1.00
.80
.60
.40
.20
0.00
-.20
0
20
40
60
80
Time (sec)

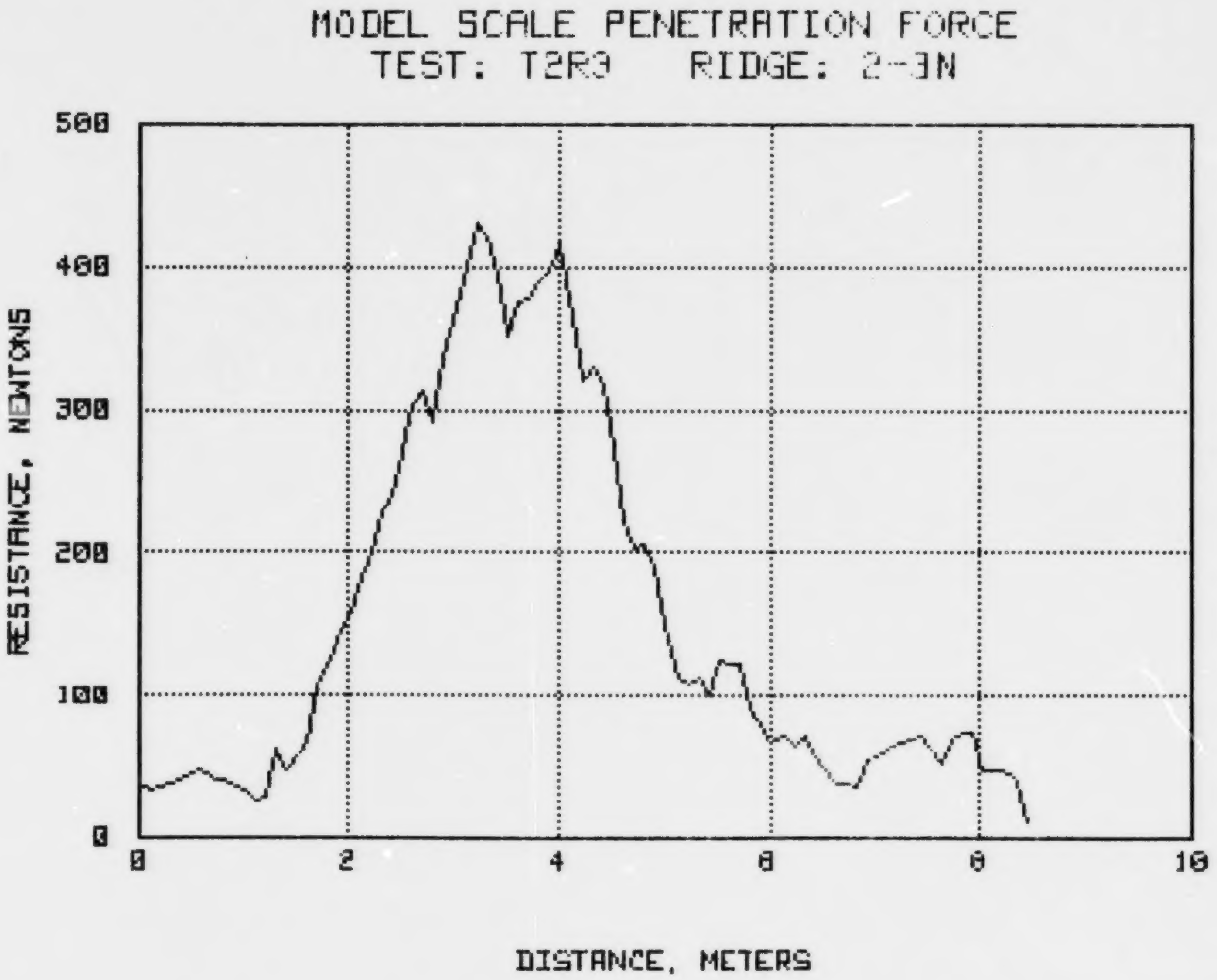

MODEL SCALE PENETRATION FORCE
TEST: T2R3 RIDGE: 2-3N

MODEL SCALE PENETRATION ENERGY
TEST: T2R3   RIDGE: 2--3N

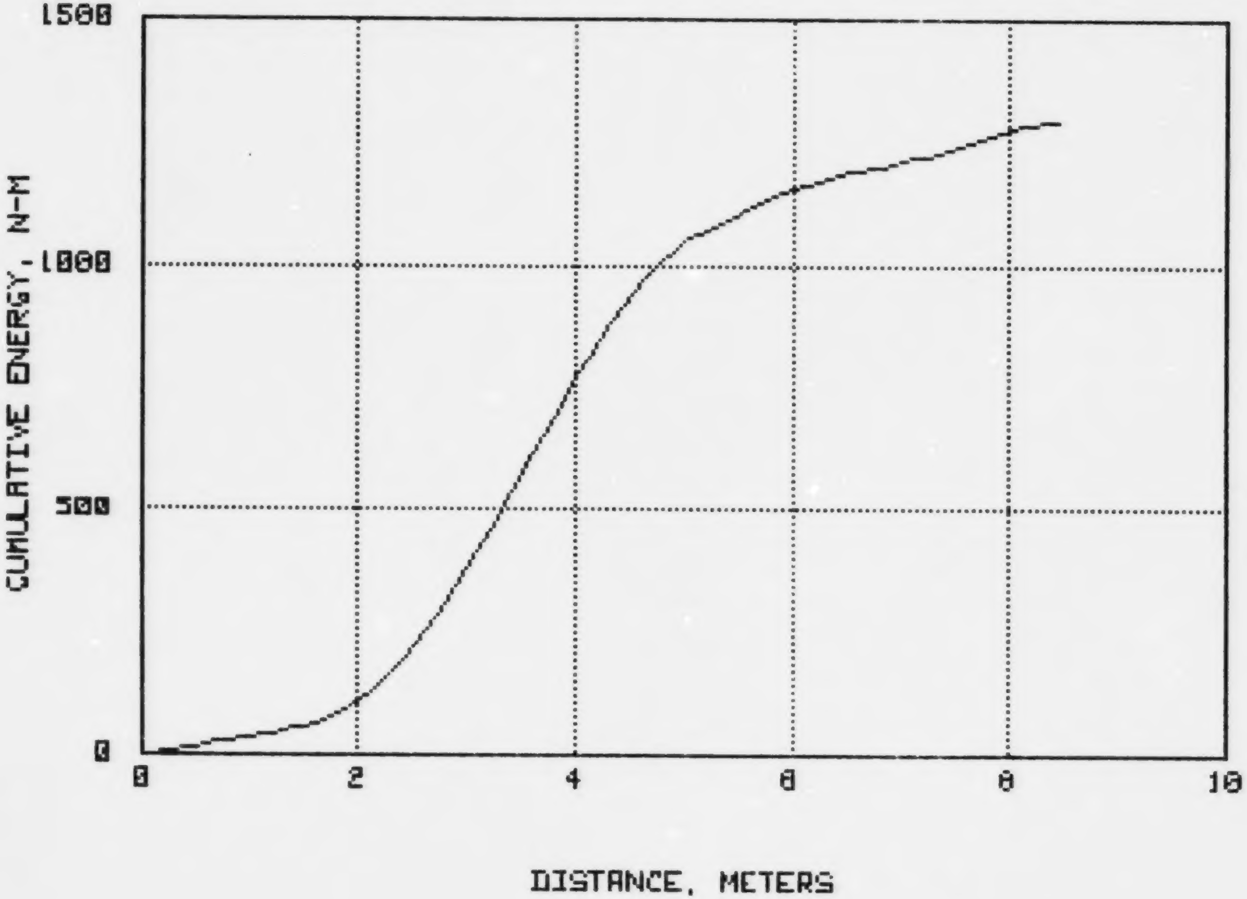

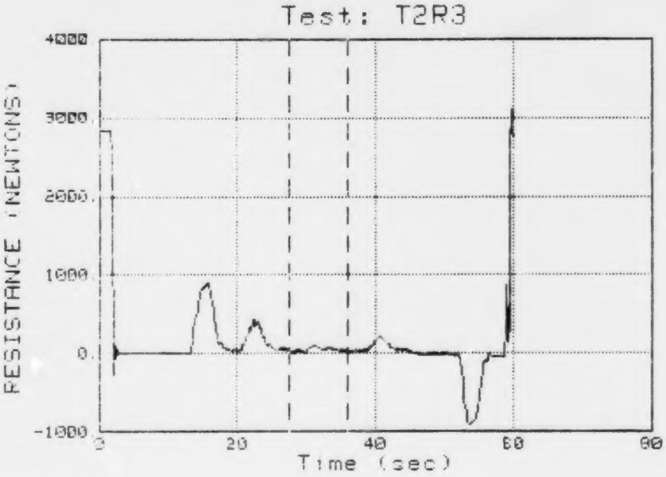
Test: T2R3
4000
3000.
2000.
1000.
0.
-1000.
RESISTANCE (NEWTONS)
0
20
40
60
80
Time (sec)

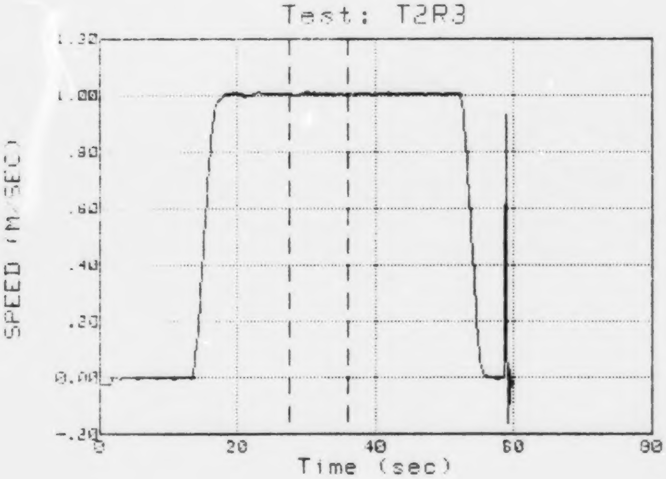
Test: T2R3
1.20
1.00
.80
.60
.40
.20
0.00
-.20
SPEED (M/SEC)
0
20
40
60
80
Time (sec)

MODEL SCALE PENETRATION FORCE
TEST: T2R3 RIDGE: 2-4N

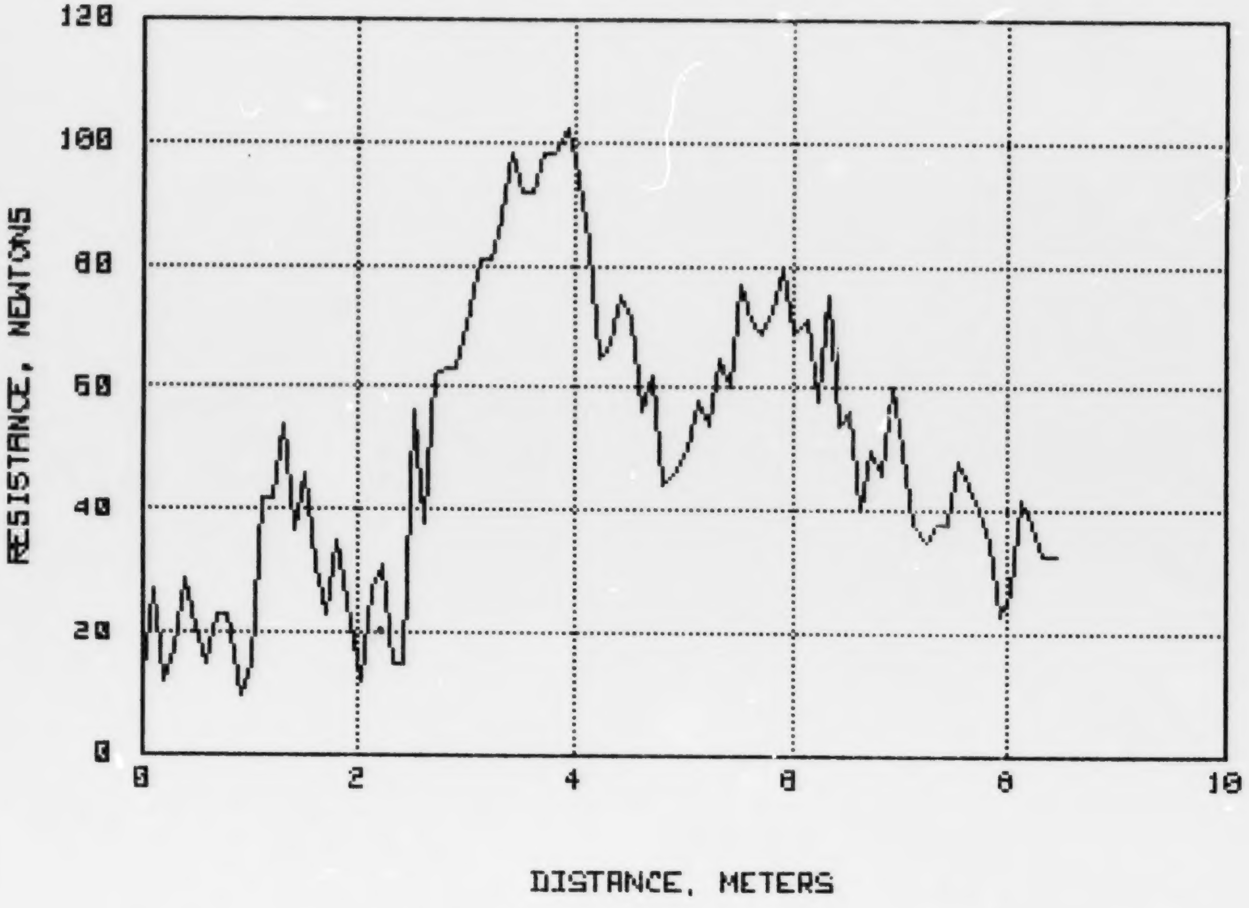

MODEL SCALE PENETRATION ENERGY
TEST: T2R3   RIDGE: 2-4N

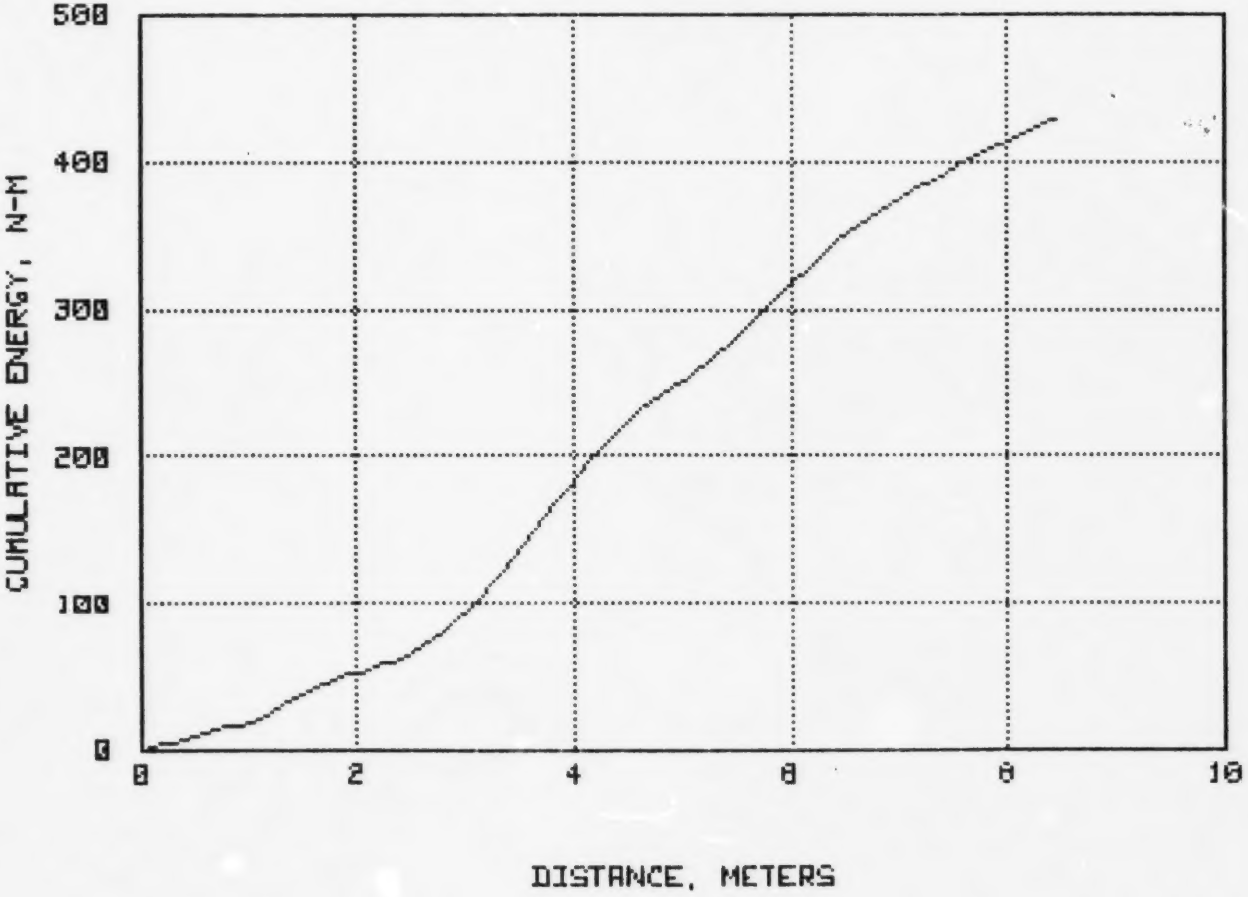

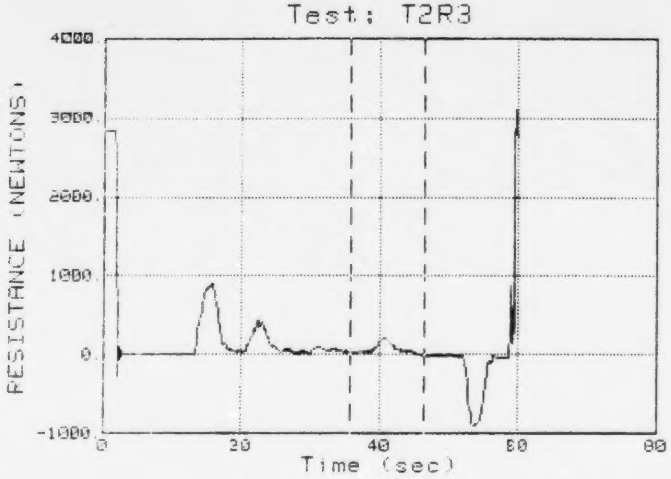
Test: T2R3
RESISTANCE (NEWTONS)
4000
3000
2000
1000
0
-1000
0
20
40
60
80
Time (sec)

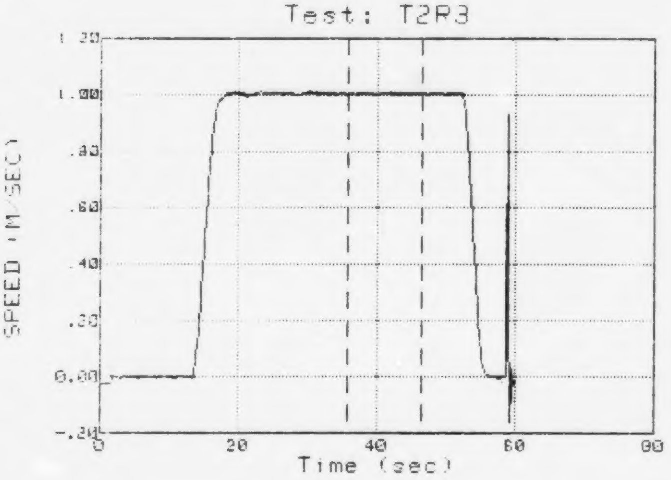
Test: T2R3
SPEED (M/SEC)
1.20
1.00
.80
.60
.40
.20
0.00
-.20
0
20
40
60
80
Time (sec)

MODEL SCALE PENETRATION FORCE
TEST: T2R3 RIDGE: 2-5N

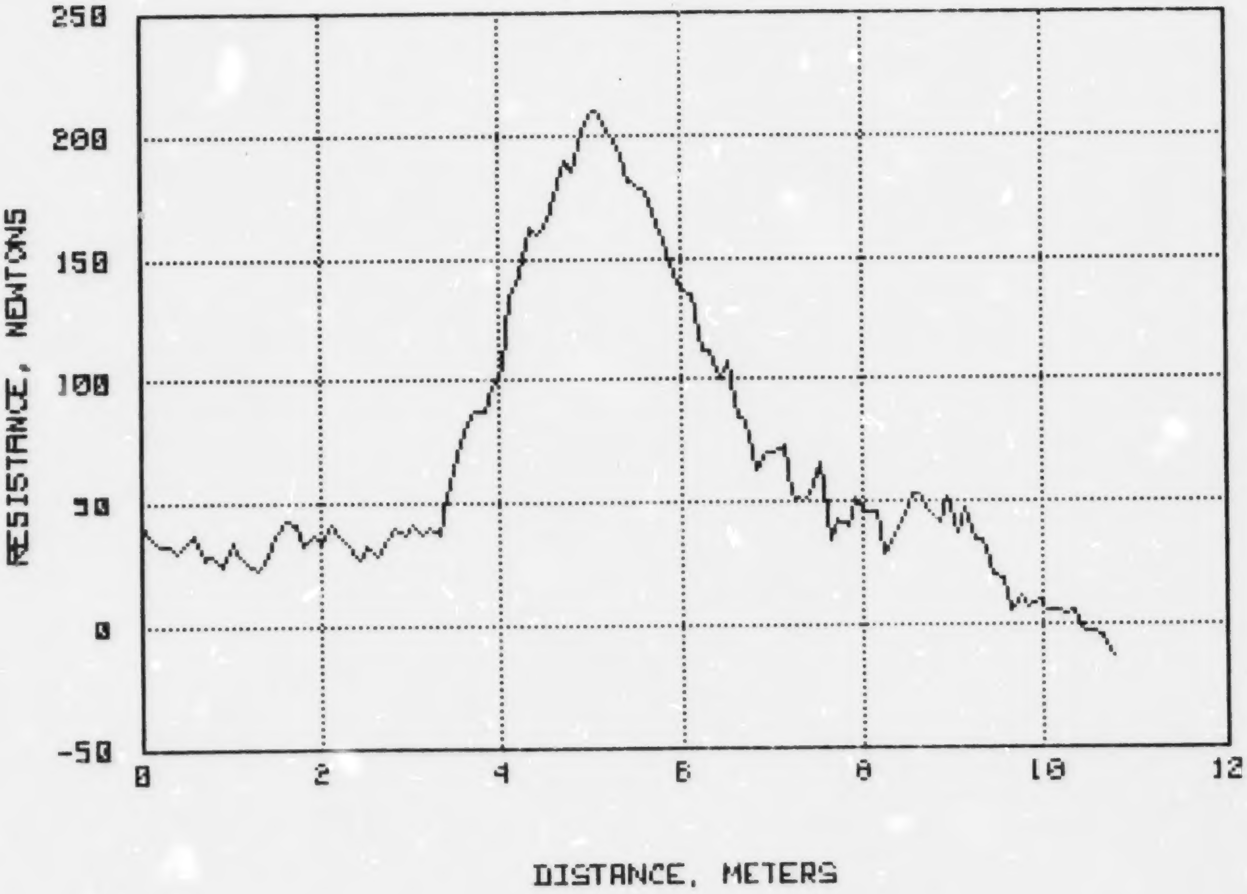

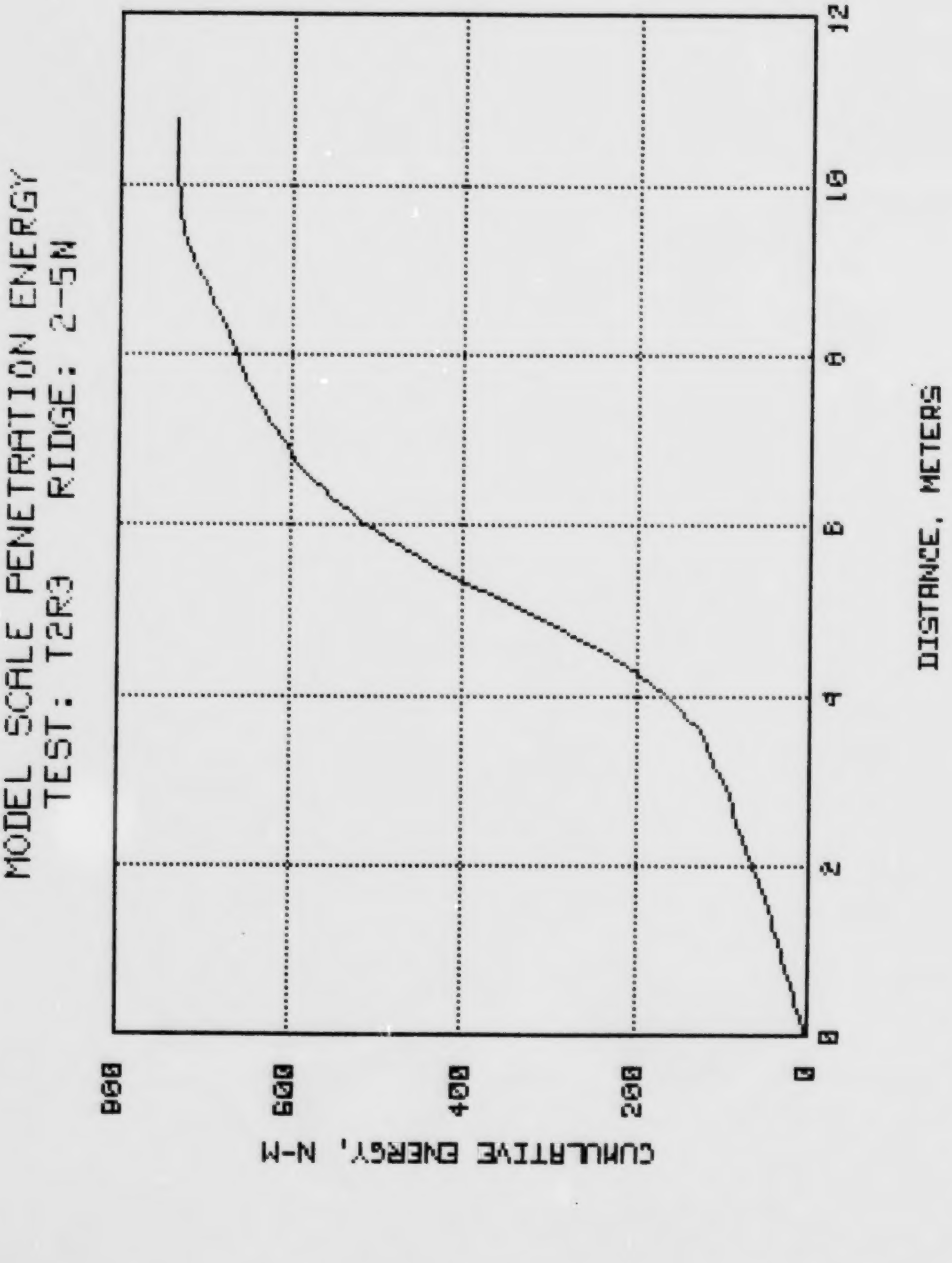
MODEL SCALE PENETRATION ENERGY
TEST: T2R3 RIDGE: 2-5N
CUMULATIVE ENERGY, N-M
0
200
400
600
800
DISTANCE, METERS
0
2
4
6
8
10
12

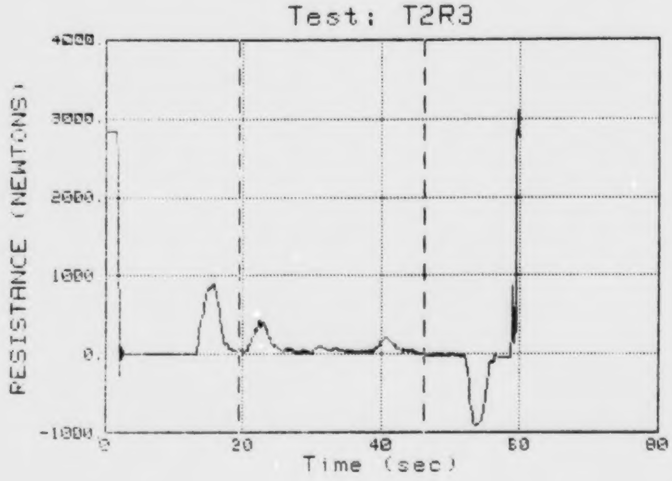
Test: T2R3
RESISTANCE (NEWTONS)
4000.
3000.
2000.
1000
0.
-1000
0
20
40
60
80
Time (sec)

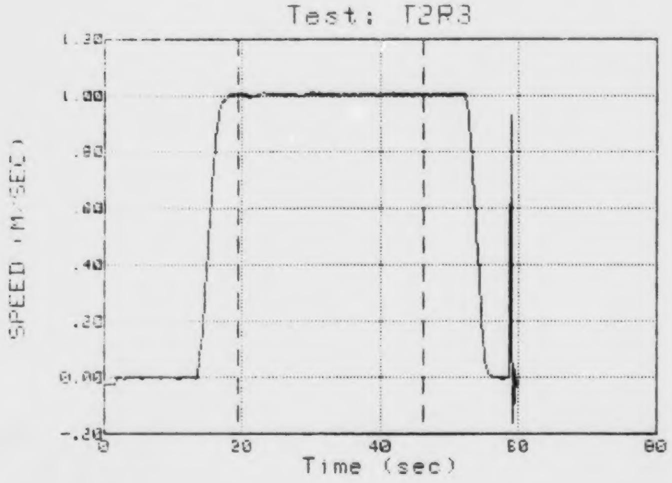
Test: T2R3
SPEED (M/SEC)
1.20
1.00
.80
.60
.40
.20
0.00
-.20
0
20
40
60
80
Time (sec)

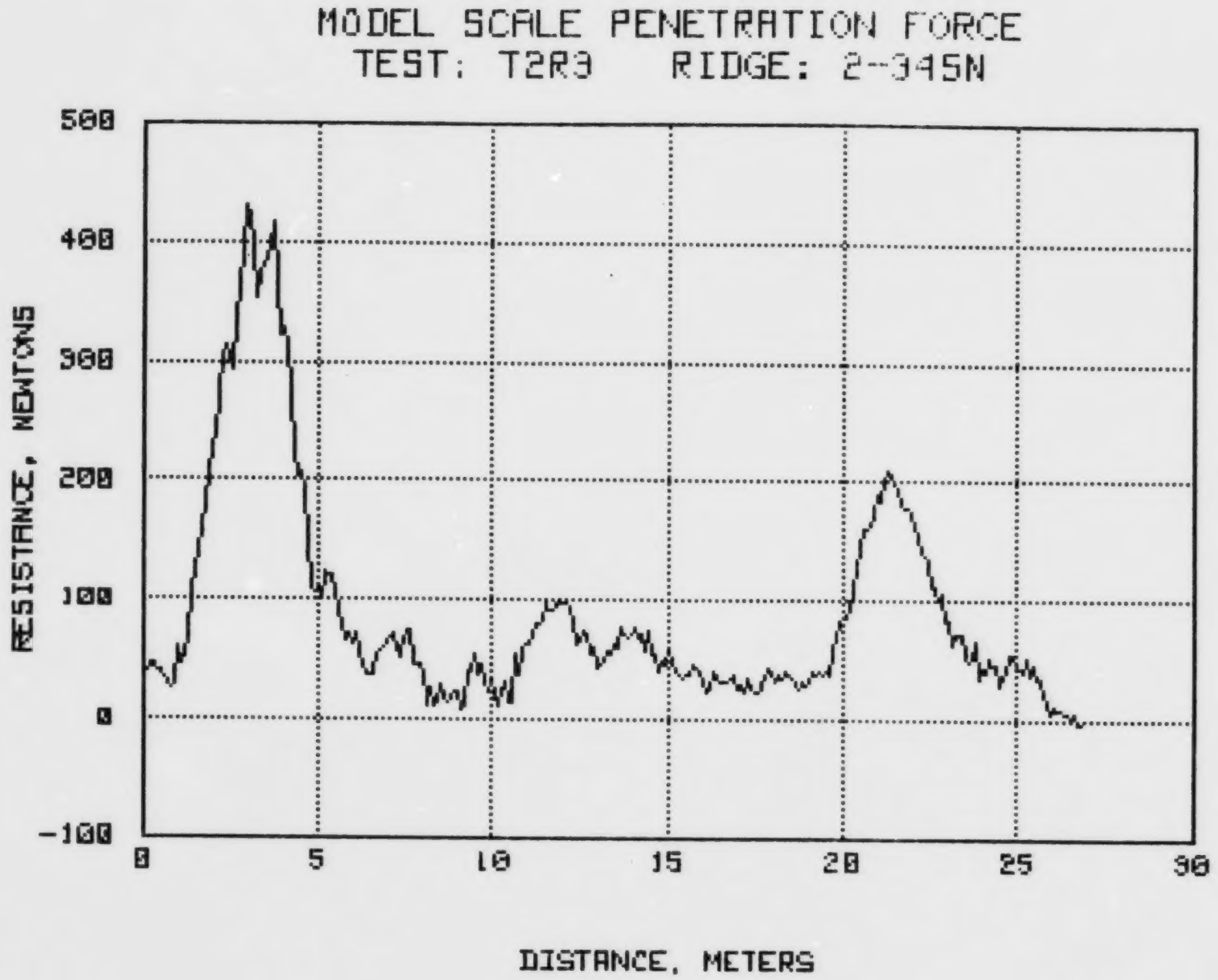
MODEL SCALE PENETRATION FORCE
TEST: T2R3 RIDGE: 2-345N
RESISTANCE, NEWTONS
500
400
300
200
100
0
-100
0
5
10
15
20
25
30
DISTANCE, METERS

MODEL SCALE PENETRATION ENERGY
TEST: T2R3 RIDGE: 2-345N

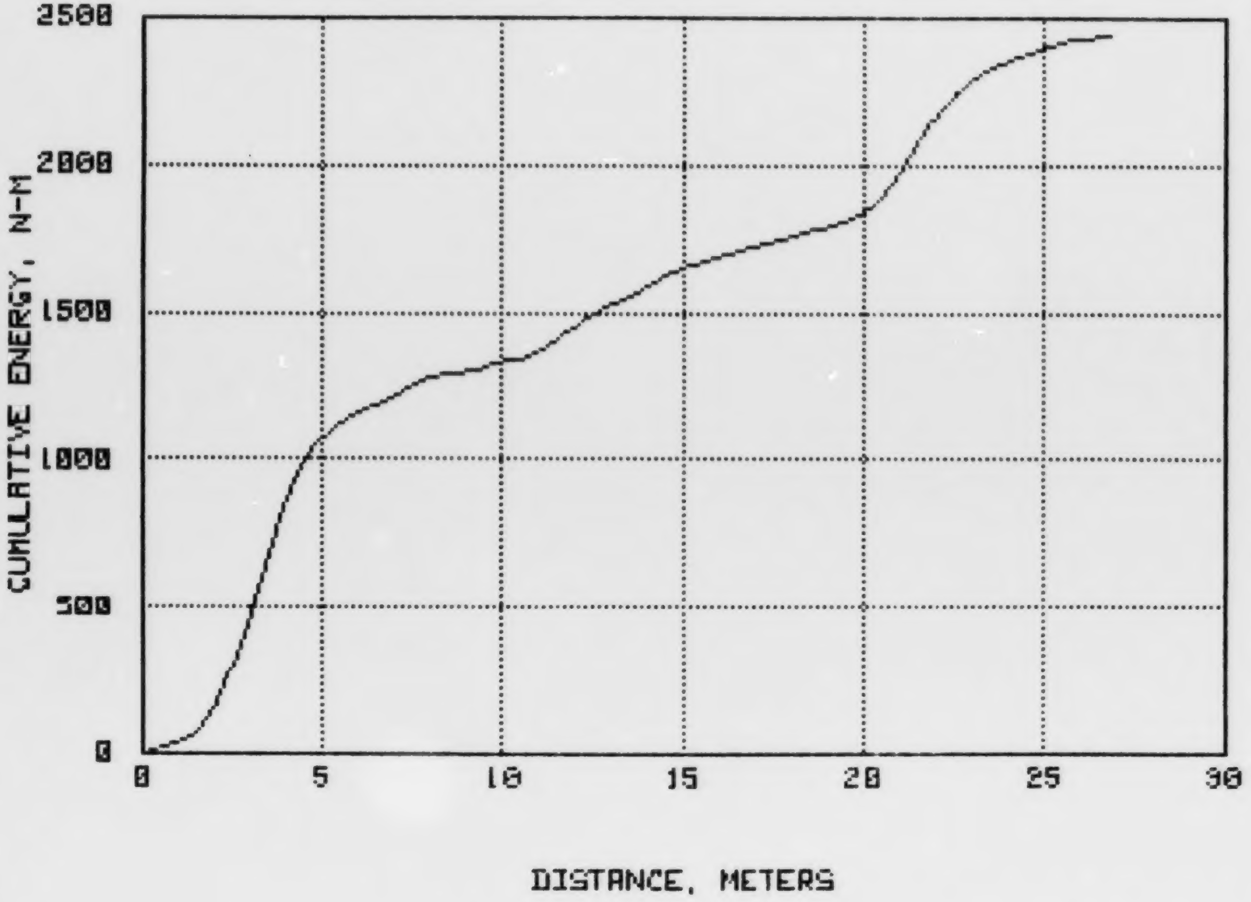

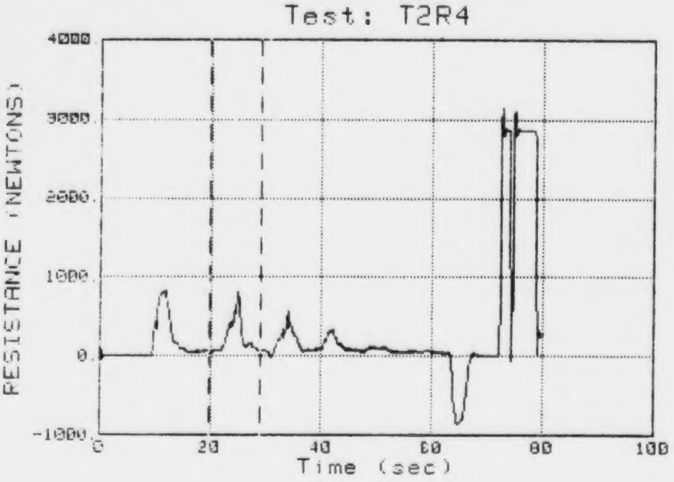
Test: T2R4
RESISTANCE (NEWTONS)
4000.
3000.
2000.
1000.
0.
-1000.
0
20
40
60
80
100
Time (sec)

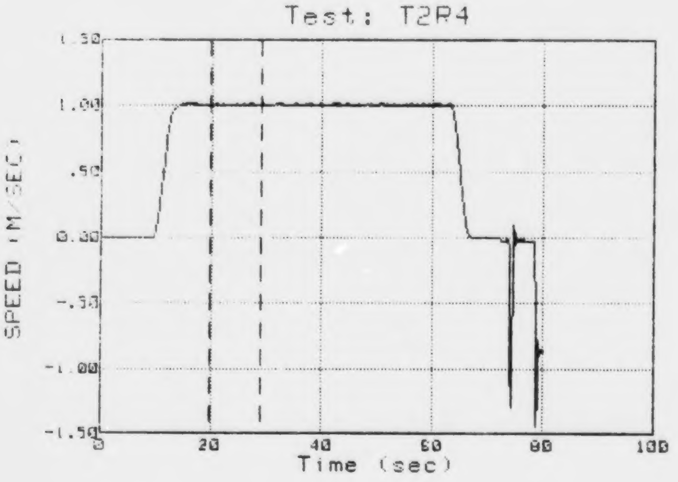
Test: T2R4
SPEED (M/SEC)
1.50
1.00
.50
0.00
-.50
-1.00
-1.50
0
20
40
60
80
100
Time (sec)

MODEL SCALE PENETRATION FORCE
TEST: T2R4 RIDGE: 2-15

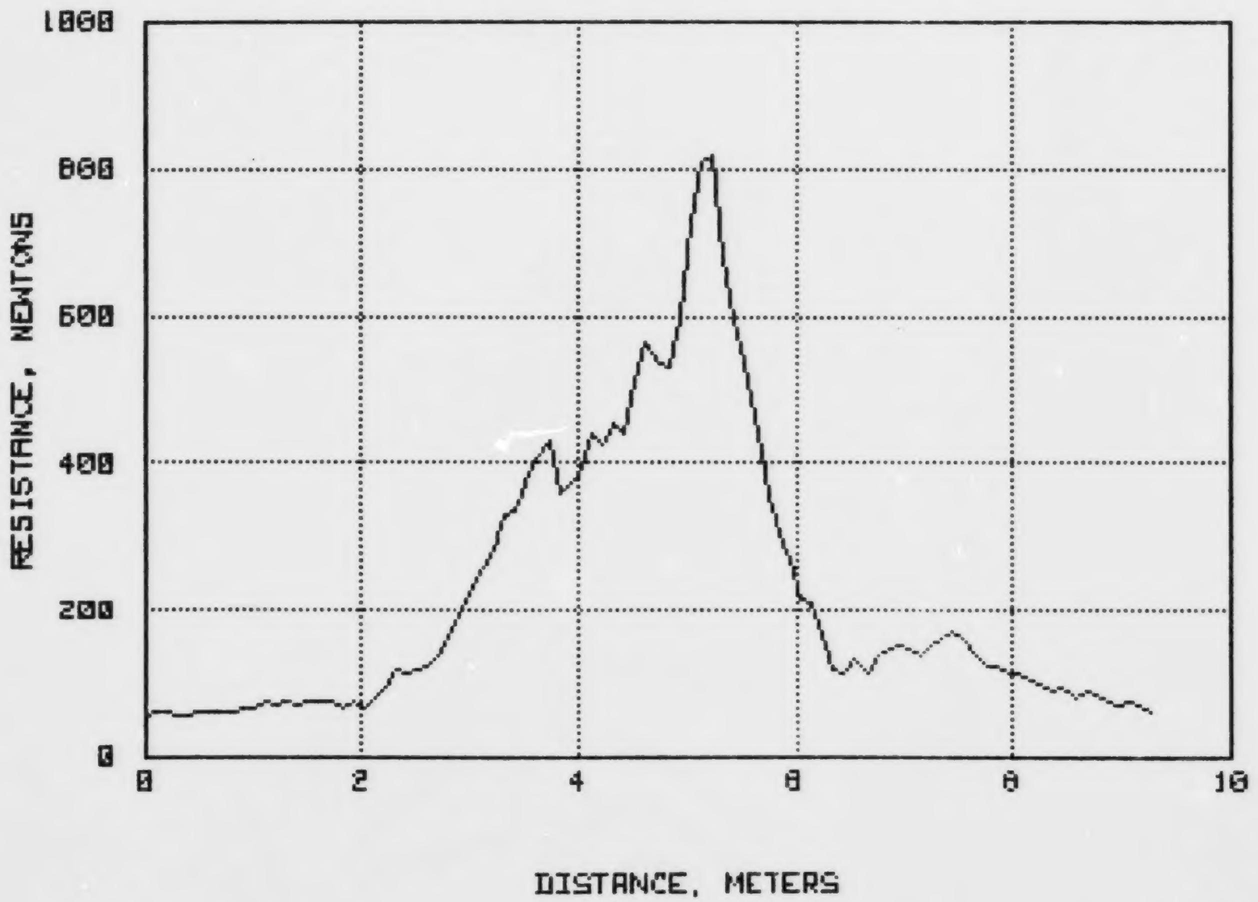

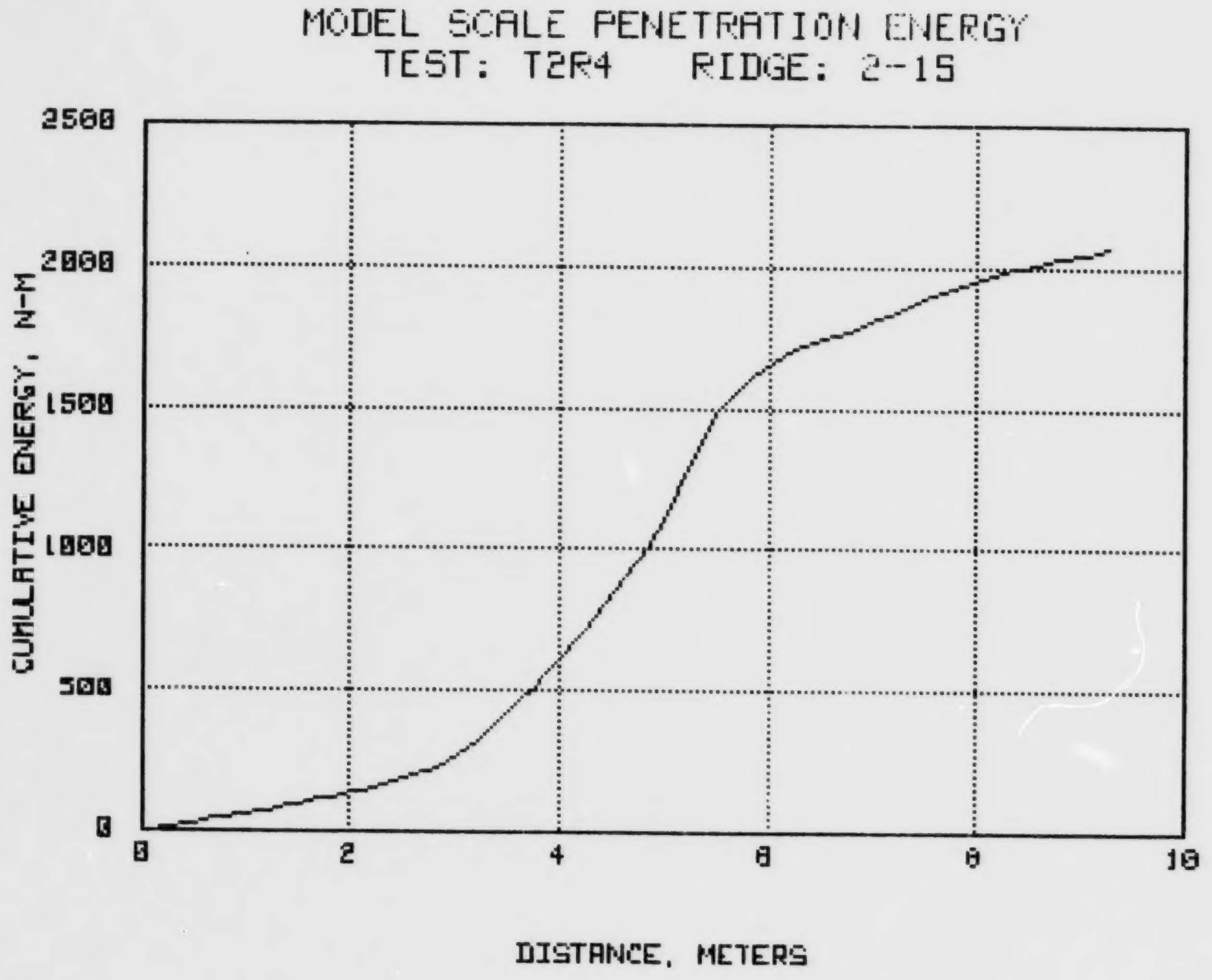

MODEL SCALE PENETRATION ENERGY
TEST: T2R4 RIDGE: 2-15

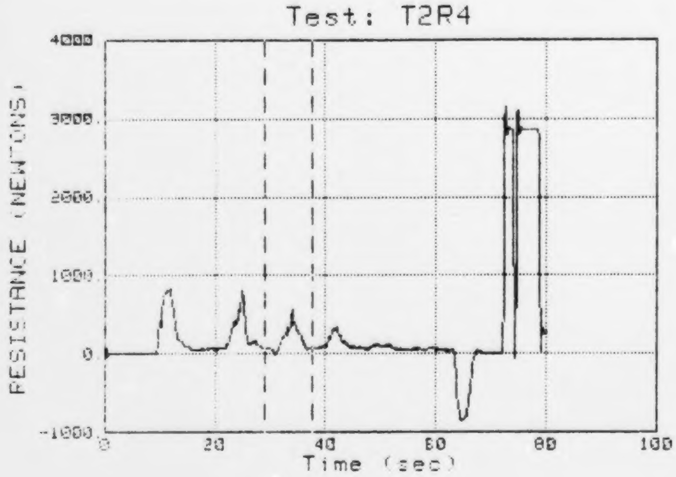
Test: T2R4
RESISTANCE (NEWTONS)
4000
3000.
2000.
1000.
0.
-1000.
0
20
40
60
80
100
Time (sec)

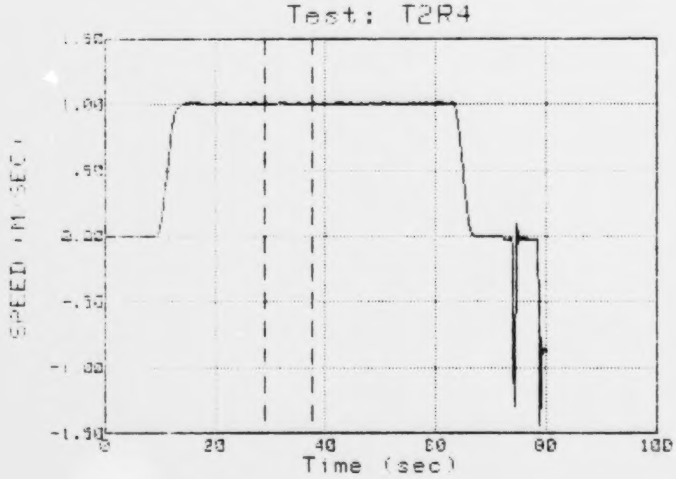
Test: T2R4
SPEED (M/SEC)
1.50
1.00
.50
0.00
-.50
-1.00
-1.50
0
20
40
60
80
100
Time (sec)

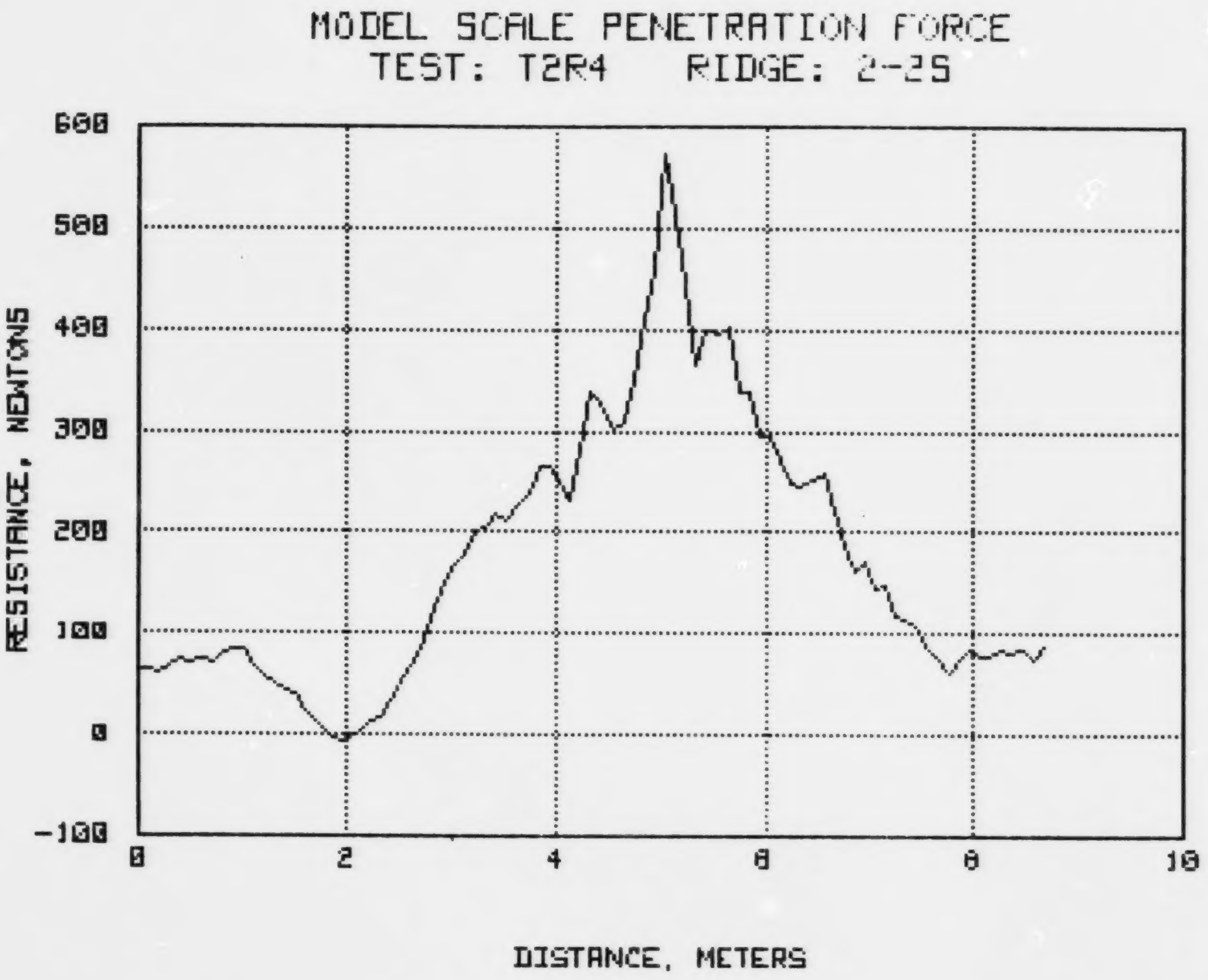
MODEL SCALE PENETRATION FORCE
TEST: T2R4 RIDGE: 2-25
RESISTANCE, NEWTONS
600
500
400
300
200
100
0
-100
0
2
4
6
8
10
DISTANCE, METERS

MODEL SCALE PENETRATION ENERGY
TEST: T2R4 RIDGE: 2-25

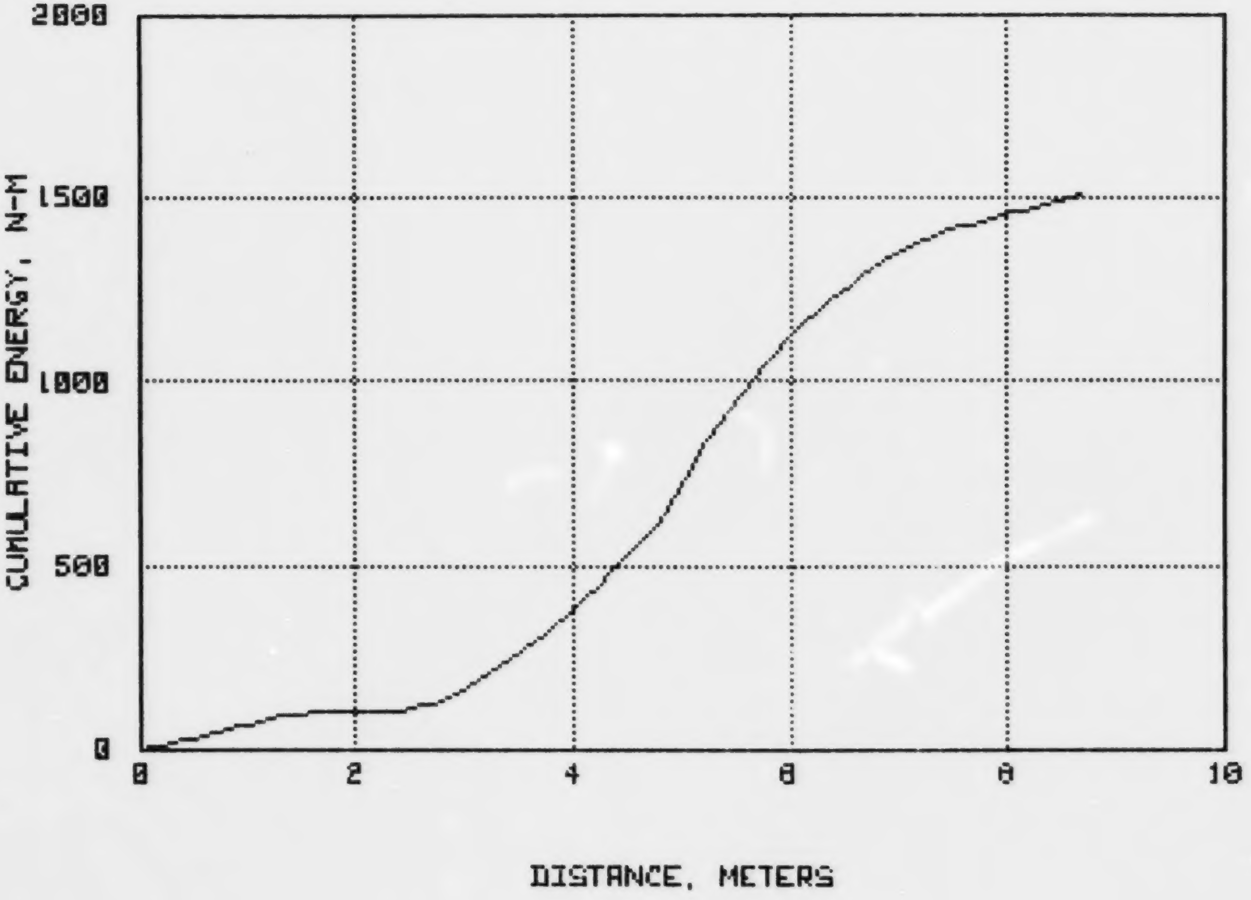

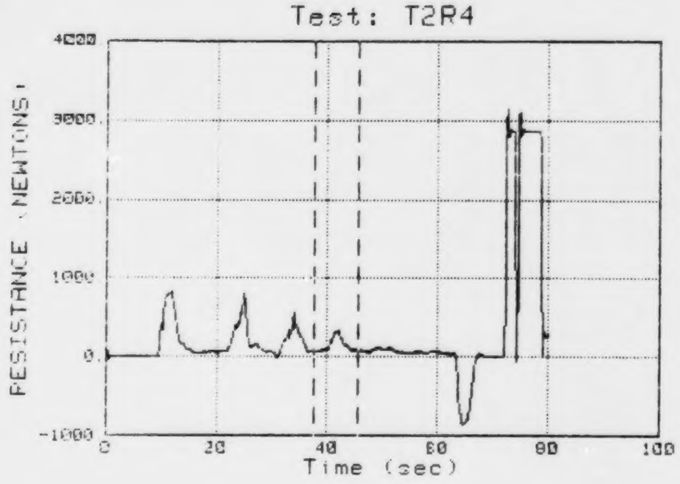
Test: T2R4

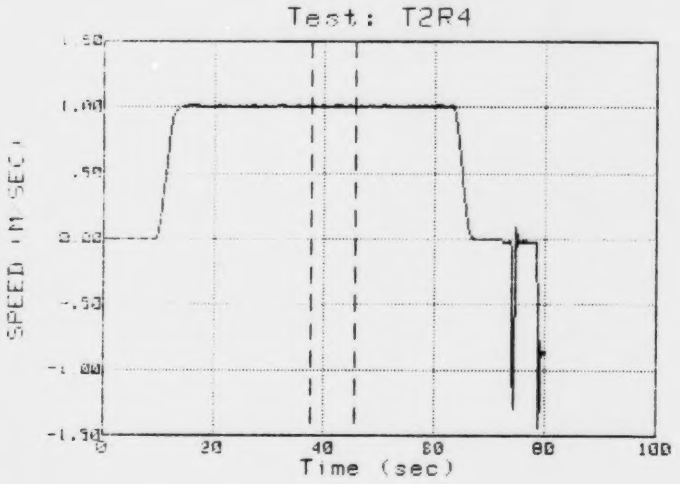
Test: T2R4

MODEL SCALE PENETRATION FORCE
TEST: T2R4   RIDGE: 2-35

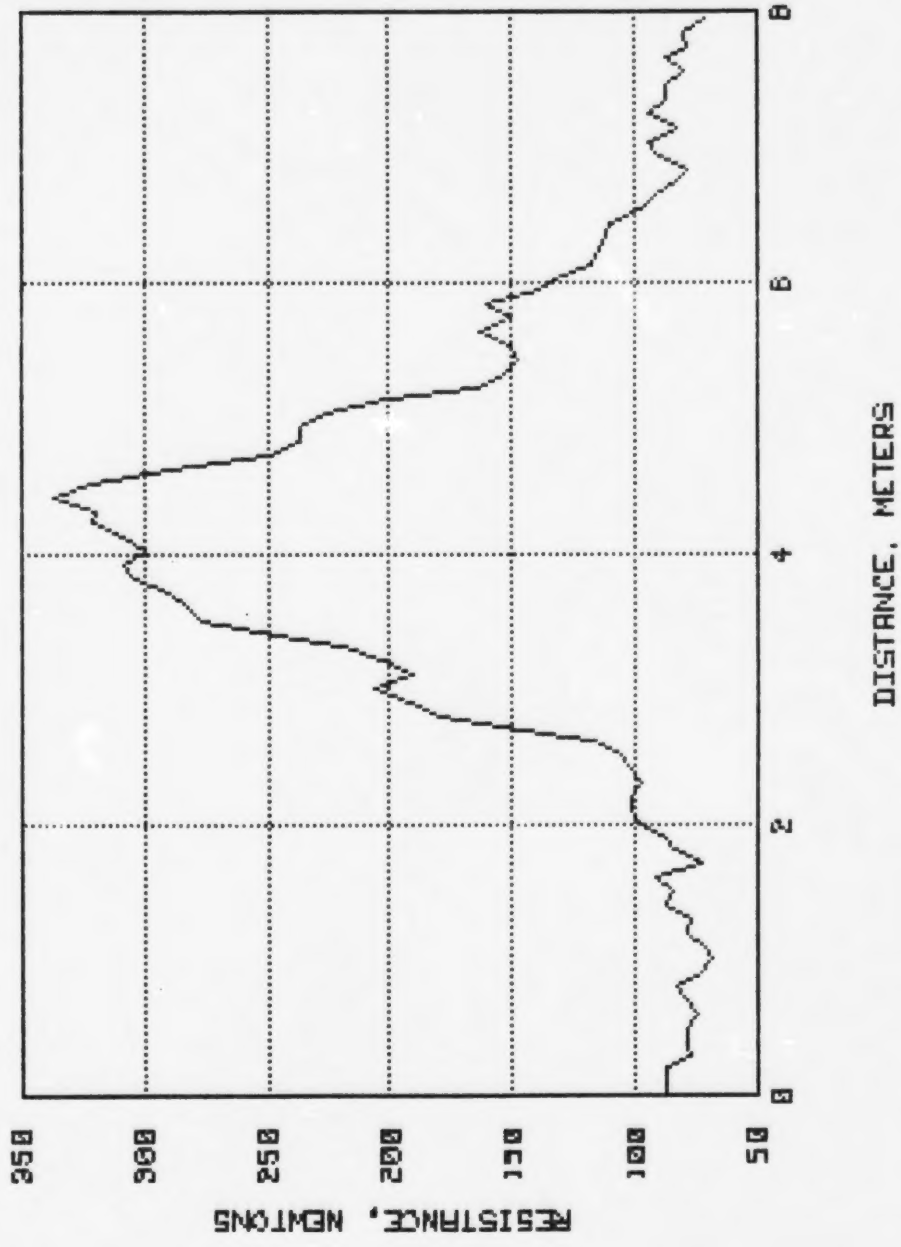

MODEL SCALE PENETRATION ENERGY
TEST: T2R4   RIDGE: 2-35

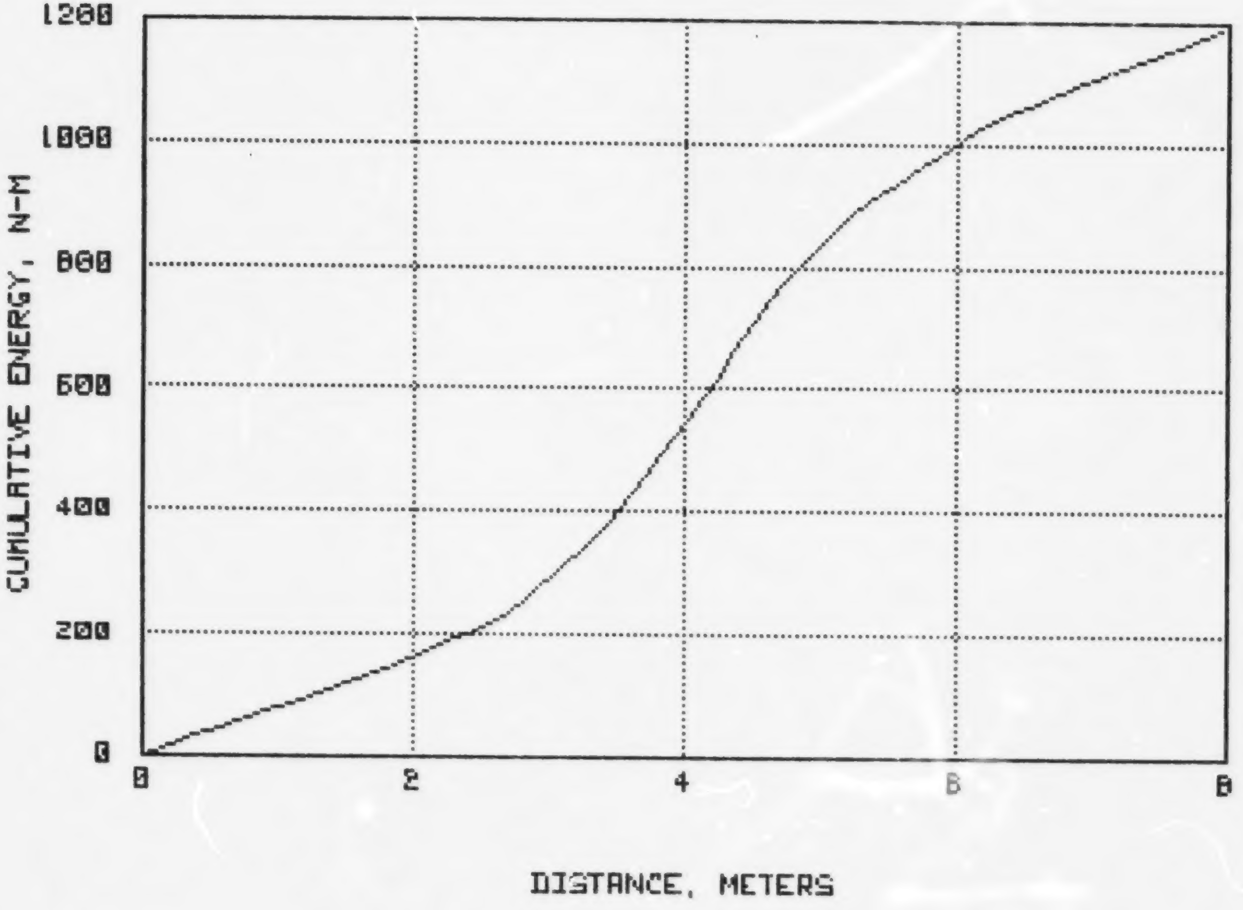

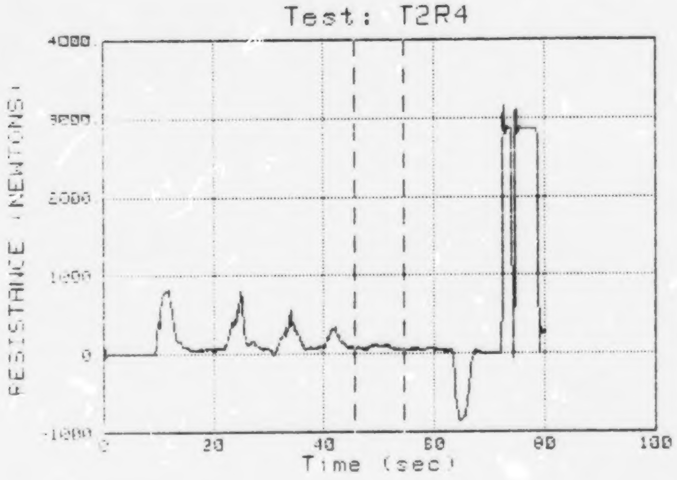
Test: T2R4

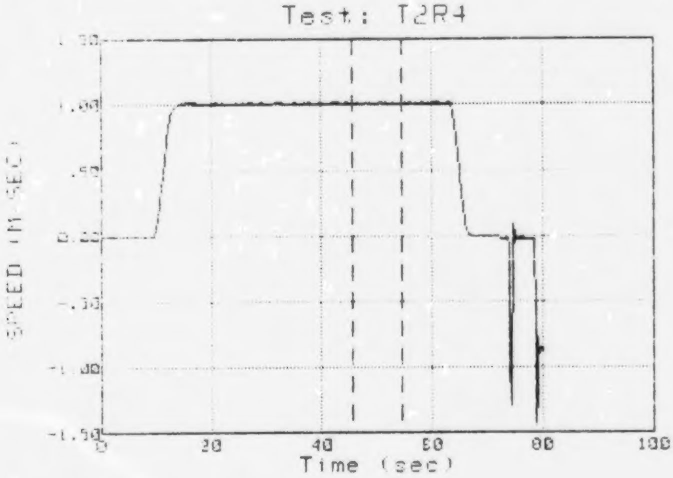
Test: T2R4

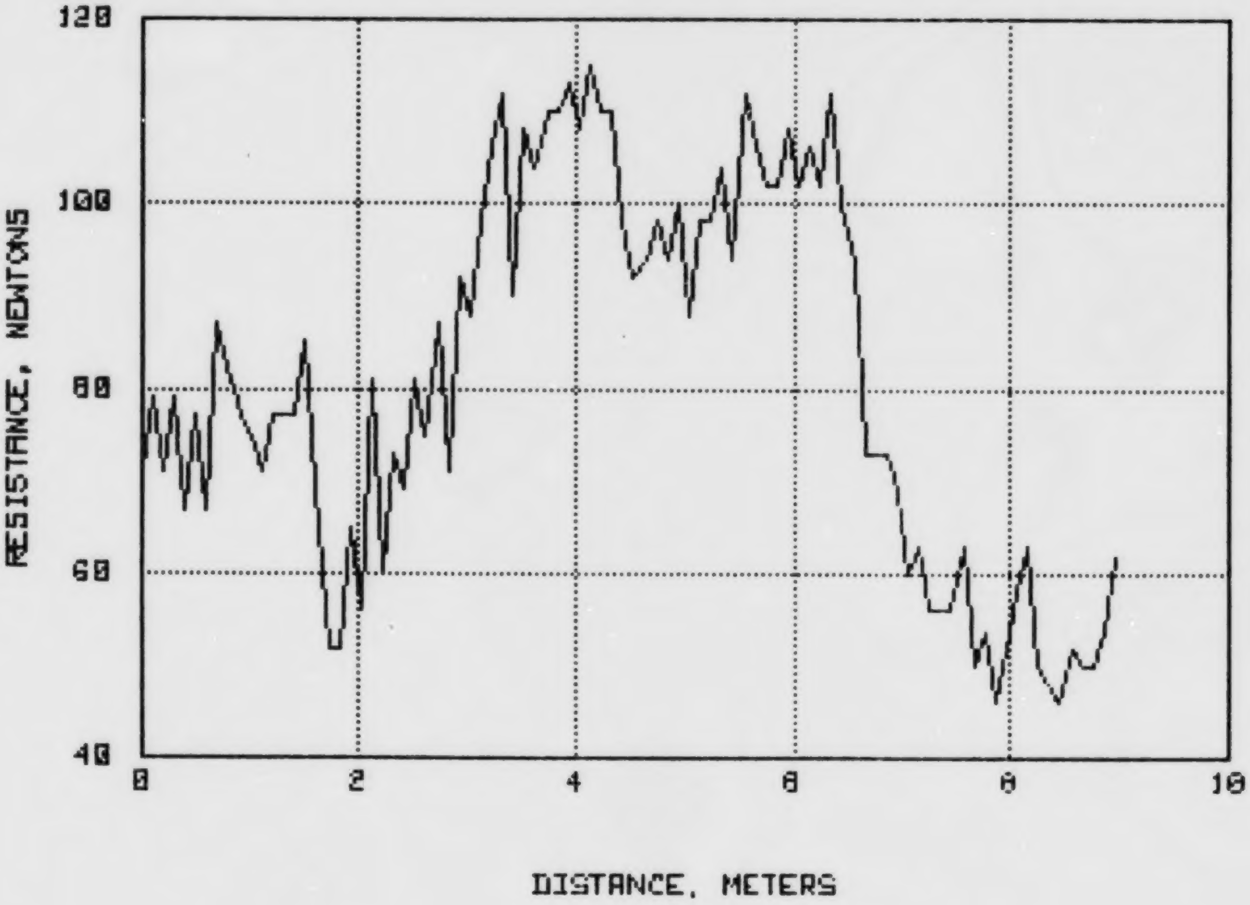

MODEL SCALE PENETRATION FORCE
TEST: T2R4 RIDGE: 2-45

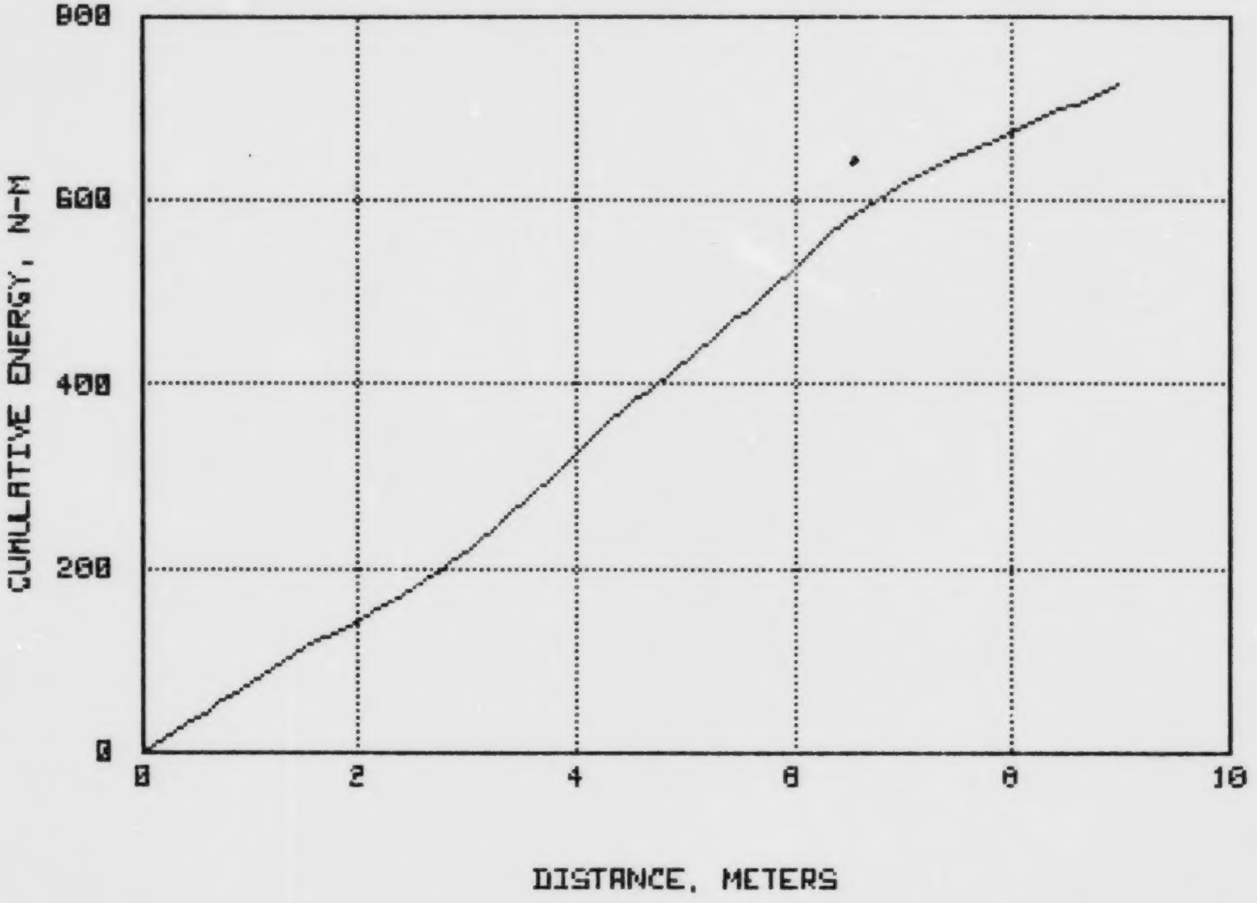

MODEL SCALE PENETRATION ENERGY
TEST: T2R4 RIDGE: 2-45

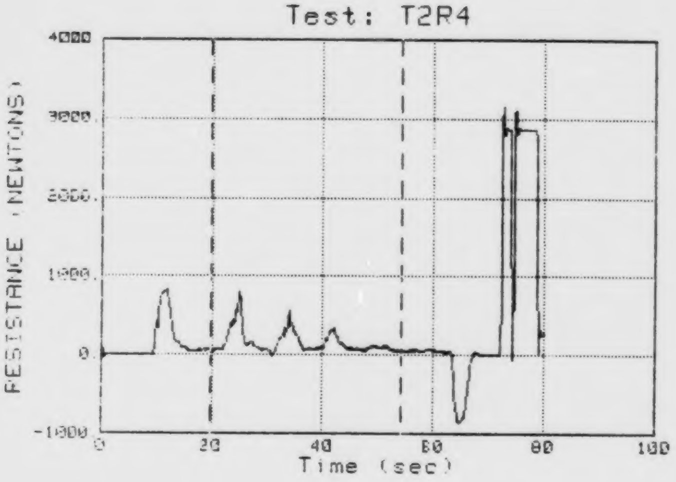
Test: T2R4

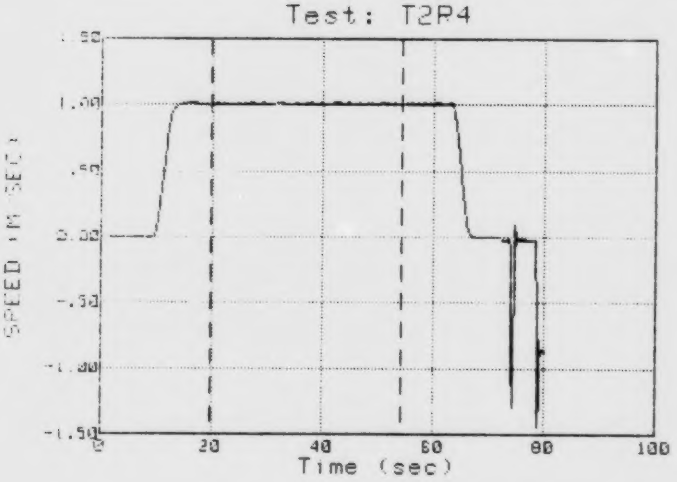
Test: T2R4

MODEL SCALE PENETRATION FORCE
TEST: T2R4 RIDGE: 2-12345

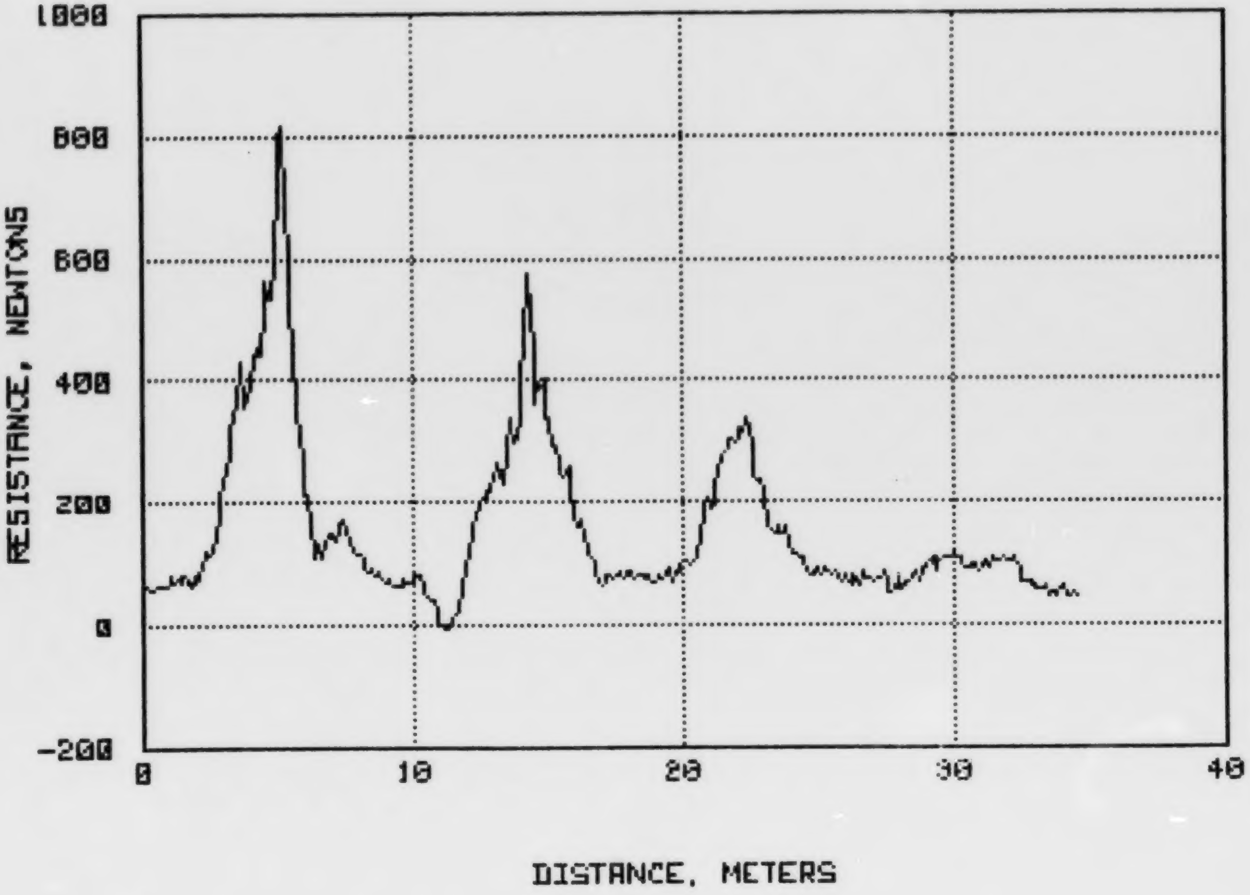

MODEL SCALE PENETRATION ENERGY
TEST: T2R4 RIDGE: 2-12345

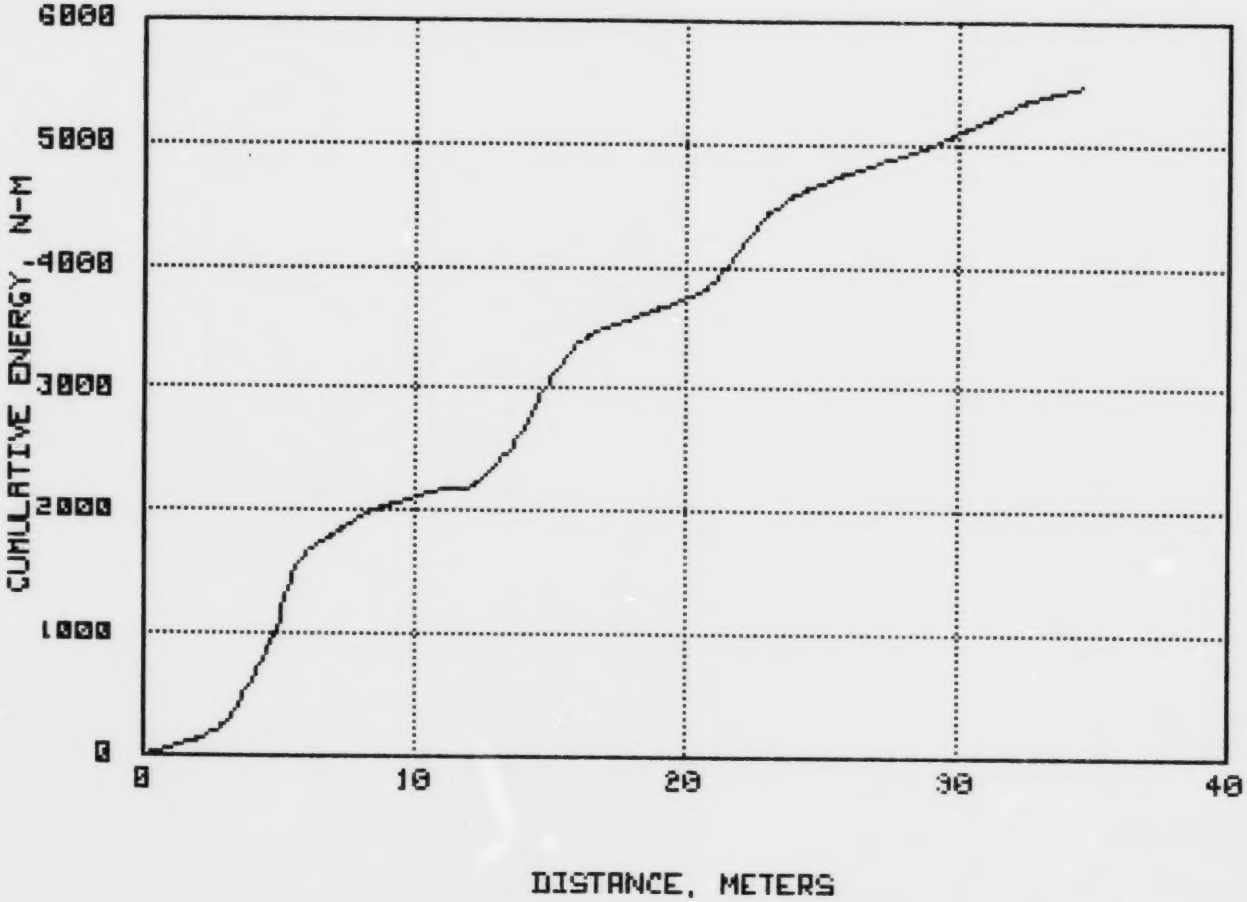

APPENDIX D.3

SHEET #2 TESTS AT THE IMD:

REDUCED PLOTS OF FORCE VS. DISPLACEMENT AND CUMULATIVE PENETRATION ENERGY - TEST DATA FILTERED AT 100 HZ

```
TEST:     T2R1H          RIDGE:2-1N

DISTANCE,M             FORCE,N      CUM. ENERGY,N-M
    0.00                  58                 0
     .94                  83                66
    1.88                  58               121
    2.82                  83               188
    3.76                  17               257
    4.70                 417               418
    5.63                  23               690
    6.57                 752              1169
    7.51                 448              1582
    8.46                  96              1819

PENETRATION OF   6.34 M AT MAX FORCE OF   896 N
PENETRATION OF   9.29 M AT MAX ENERGY OF  1928 N-M
```

```
TEST:     T2R2           RIDGE:2-2N

DISTANCE,M             FORCE,N      CUM. ENERGY,N-M
    0.00                  71                 0
     .68                 106                33
    1.35                 -21                75
    2.03                 171               115
    2.72                -171               153
    3.40                  50               232
    4.08                  69               334
    4.75                 321               546
    5.44                 391               800
    6.12                 271               987
    6.80                  63              1141

PENETRATION OF   4.26 M AT MAX FORCE OF   654 N
PENETRATION OF   6.84 M AT MAX ENERGY OF  1144 N-M
```

```
TEST:     T2R3H          RIDGE:2-3N

DISTANCE,M               FORCE,N       CUM. ENERGY,N-M
    0.00                   58                 0
     .90                  -60                40
    1.79                  196               146
    2.69                  394               410
    3.59                  556               764
    4.49                  160              1031
    5.39                  217              1143
    6.29                  173              1211
    7.19                   67              1260
    8.09                  -71              1309
    8.98                   58              1331

PENETRATION OF   3.21 M AT MAX FORCE OF   658 N
PENETRATION OF   9.02 M AT MAX ENERGY OF  1333 N-M


TEST:     T2R3H          RIDGE:2-4N

DISTANCE,M               FORCE,N       CUM. ENERGY,N-M
    0.00                   17                 0
     .85                  154                29
    1.71                  108                50
    2.57                  162                90
    3.43                  177               168
    4.29                  -48               230
    5.14                 -100               271
    6.00                  112               327
    6.85                  198               372
    7.71                   46               411

PENETRATION OF   2.32 M AT MAX FORCE OF   439 N
PENETRATION OF   8.50 M AT MAX ENERGY OF   434 N-M


TEST:     T2R3H          RIDGE:2-5N

DISTANCE,M               FORCE,N       CUM. ENERGY,N-M
    0.00                   12                 0
    1.29                  -19                38
    2.59                  127                84
    3.89                   73               161
    5.18                  217               396
    6.48                  287               586
    7.77                  154               670
    9.07                 -214               718
   10.36                   -6               740
   11.66                  189               728
   12.95                   44               718

PENETRATION OF   7.73 M AT MAX FORCE OF   321 N
PENETRATION OF  10.47 M AT MAX ENERGY OF   747 N-M
```

```
TEST:     T2R3H          RIDGE:2-345N

DISTANCE,M               FORCE,N      CUM. ENERGY,N-M
    0.00                    94                 0
    3.02                   623               457
    6.05                    71              1188
    9.09                    23              1339
   12.12                  -156              1470
   15.15                    98              1687
   18.17                   -17              1787
   21.20                   225              1931
   24.23                    87              2390
   27.26                   -21              2501
   30.29                    13              2485

PENETRATION OF   3.48 M AT MAX FORCE OF   658 N
PENETRATION OF  27.74 M AT MAX ENERGY OF  2511 N-M


TEST:     T2R4H          RIDGE:2-1S

DISTANCE,M               FORCE,N      CUM. ENERGY,N-M
    0.00                    75                 0
    1.33                    17                89
    2.66                   187               177
    4.01                    35               274
    5.34                   219               403
    6.68                   189               839
    8.02                   619              1607
    9.36                   106              2015
   10.70                    46              2209
   12.03                    21              2331

PENETRATION OF   7.95 M AT MAX FORCE OF  1096 N
PENETRATION OF  13.29 M AT MAX ENERGY OF  2425 N-M


TEST:     T2R4H          RIDGE:2-2S

DISTANCE,M               FORCE,N      CUM. ENERGY,N-M
    0.00                    33                 0
     .83                   -56                23
    1.67                    75                51
    2.51                    56               208
    3.34                   479               437
    4.18                  -117               769
    5.01                   115              1099
    5.85                   346              1292
    6.68                    10              1400
    7.51                   -54              1472

PENETRATION OF   4.07 M AT MAX FORCE OF  1152 N
PENETRATION OF   8.31 M AT MAX ENERGY OF  1547 N-M
```

```
TEST:     T2R4H          RIDGE:2-3S

DISTANCE,M               FORCE,N      CUM. ENERGY,N-M
    0.00                    33                0
     .83                    71               61
    1.67                   167              140
    2.50                   300              247
    3.34                   387              440
    4.18                   412              709
    5.01                   165              899
    5.85                   256             1030
    6.69                   131             1113
    7.52                   167             1190

PENETRATION OF   4.14 M AT MAX FORCE OF   492 N
PENETRATION OF   8.30 M AT MAX ENERGY OF  1244 N-M
```

```
TEST:     T2R4H          RIDGE:2-4S

DISTANCE,M               FORCE,N      CUM. ENERGY,N-M
    0.00                  -187                0
    1.02                    48               68
    2.04                     2              154
    3.07                   202              260
    4.09                    27              365
    5.12                   214              463
    6.14                    75              572
    7.17                   -21              636
    8.20                    46              695
    9.22                   102              758
   10.24                   -10              827

PENETRATION OF   2.84 M AT MAX FORCE OF   435 N
PENETRATION OF  10.24 M AT MAX ENERGY OF   827 N-M
```

```
TEST:     T2R4H          RIDGE:2-1234S

DISTANCE,M               FORCE,N      CUM. ENERGY,N-M
    0.00                    75                0
    4.09                   113              278
    8.18                   860             1693
   12.29                   129             2352
   16.38                   437             2778
   20.47                   125             3871
   24.56                   181             4317
   28.66                   250             5118
   32.75                    50             5445
   36.86                   164             5862

PENETRATION OF  17.36 M AT MAX FORCE OF  1152 N
PENETRATION OF  40.87 M AT MAX ENERGY OF  6098 N-M
```

Test: T2R1H

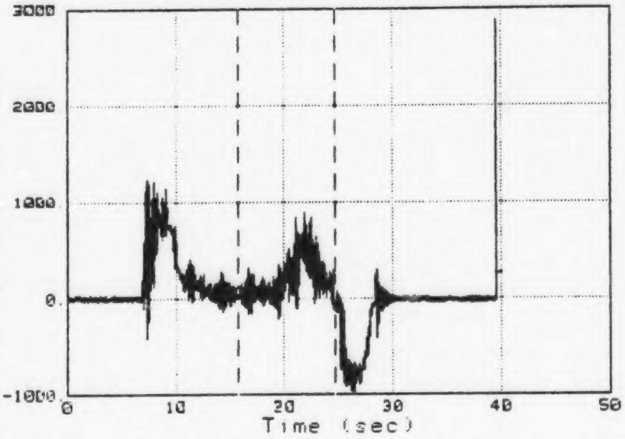

Test: T2P1H

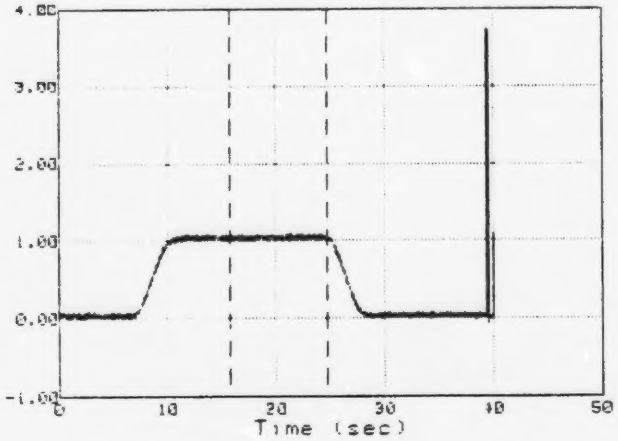

MODEL SCALE PENETRATION FORCE
TEST: T2R1H RIDGE: 2-IN

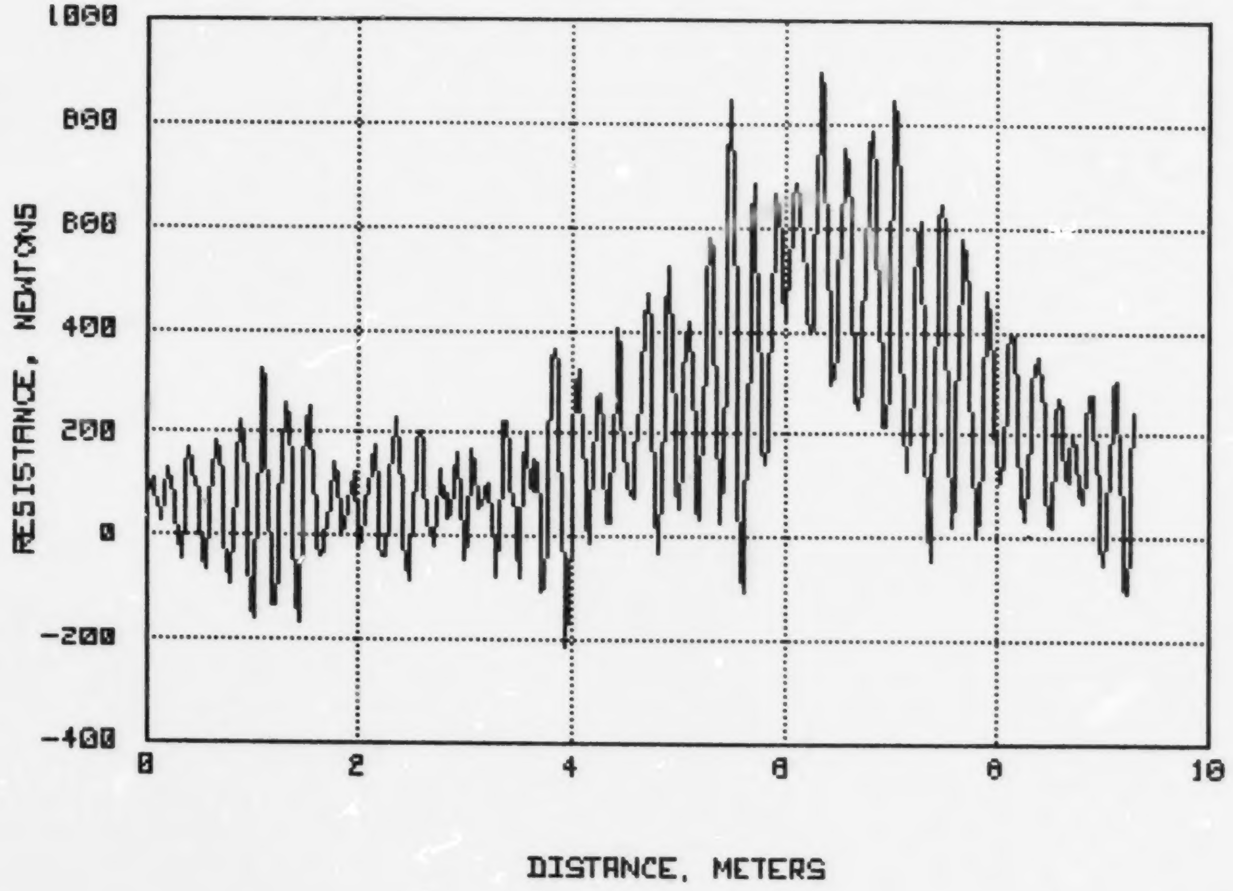

MODEL SCALE PENETRATION ENERGY
TEST: T2R1H   RIDGE: 2-1N

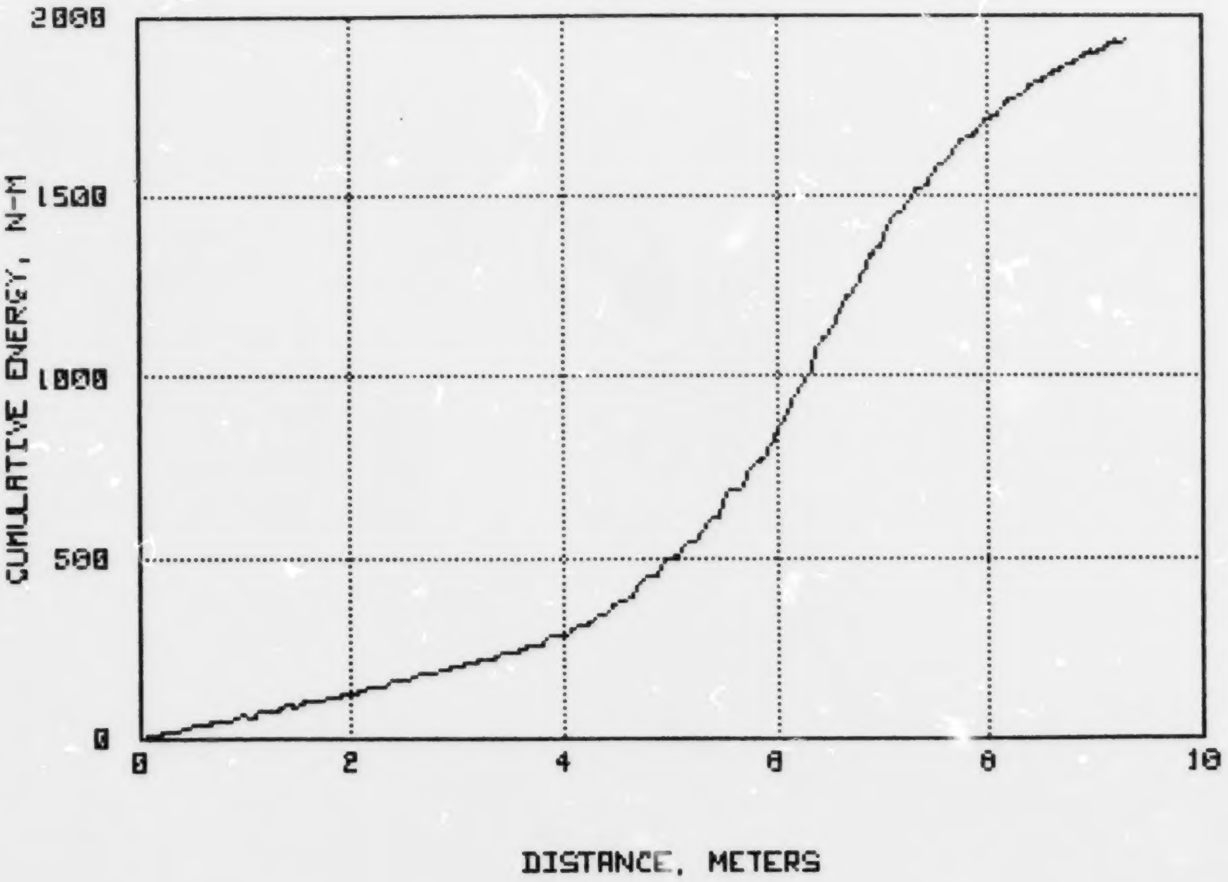

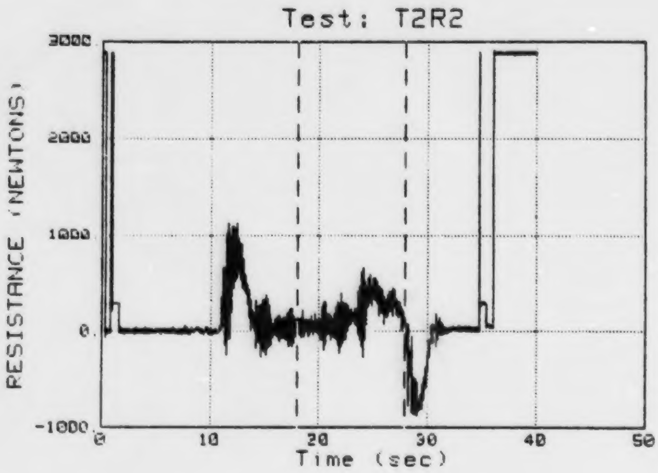
Test: T2R2
RESISTANCE (NEWTONS)
3000
2000
1000
0.
-1000
0
10
20
30
40
50
Time (sec)

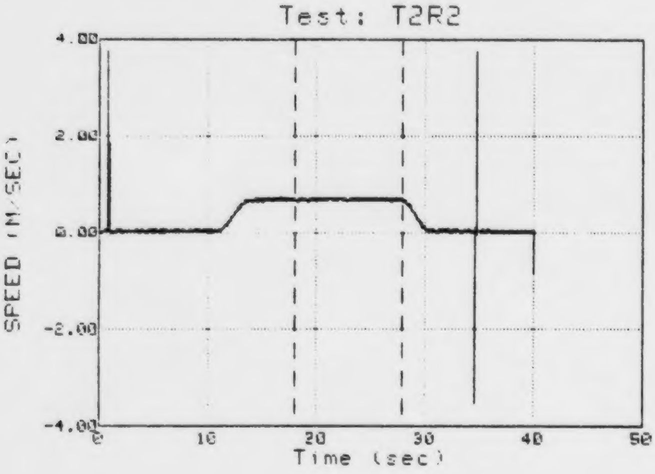
Test: T2R2
SPEED (M/SEC)
4.00
2.00
0.00
-2.00
-4.00
0
10
20
30
40
50
Time (sec)

MODEL SCALE PENETRATION FORCE
TEST: T2R2   RIDGE: 2-2N

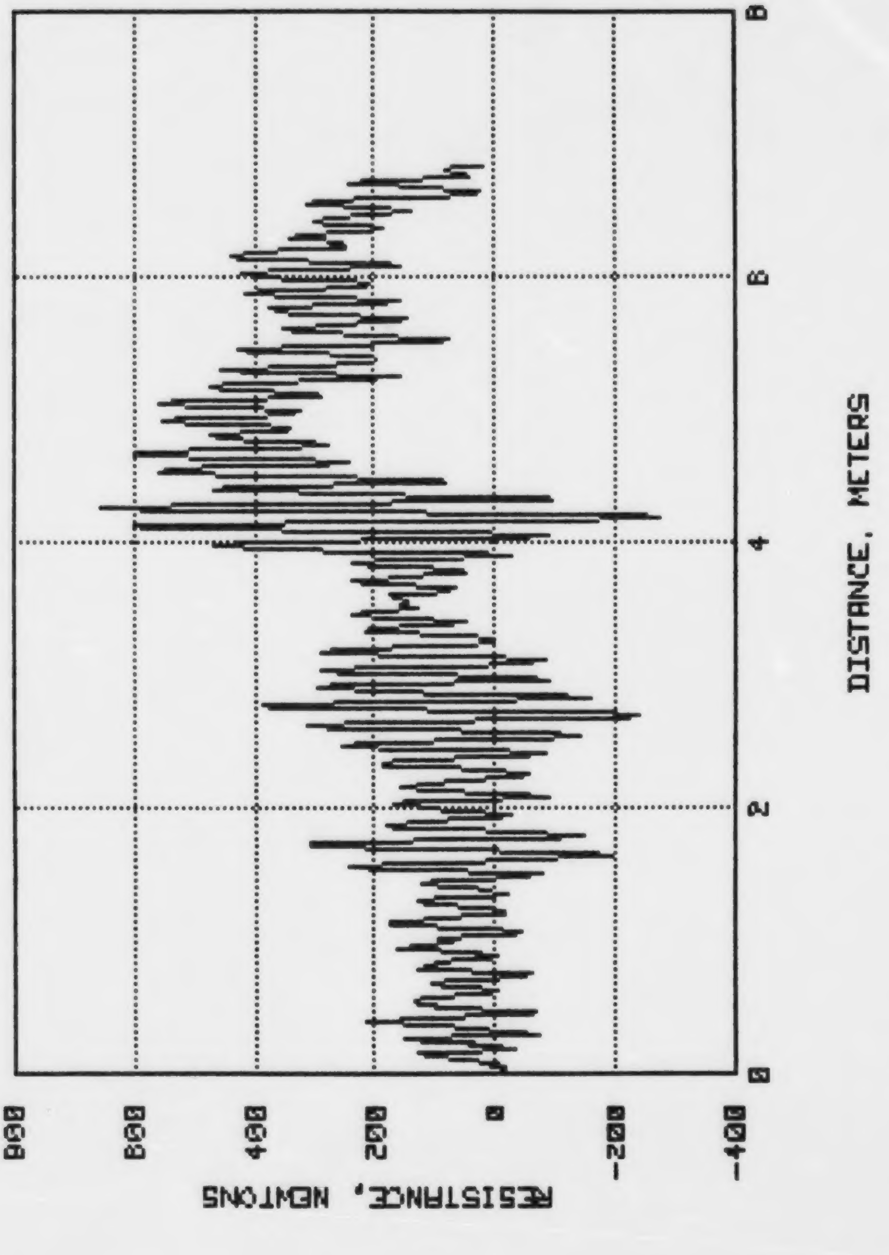

MODEL SCALE PENETRATION ENERGY
TEST: T2R2   RIDGE: 2-2N

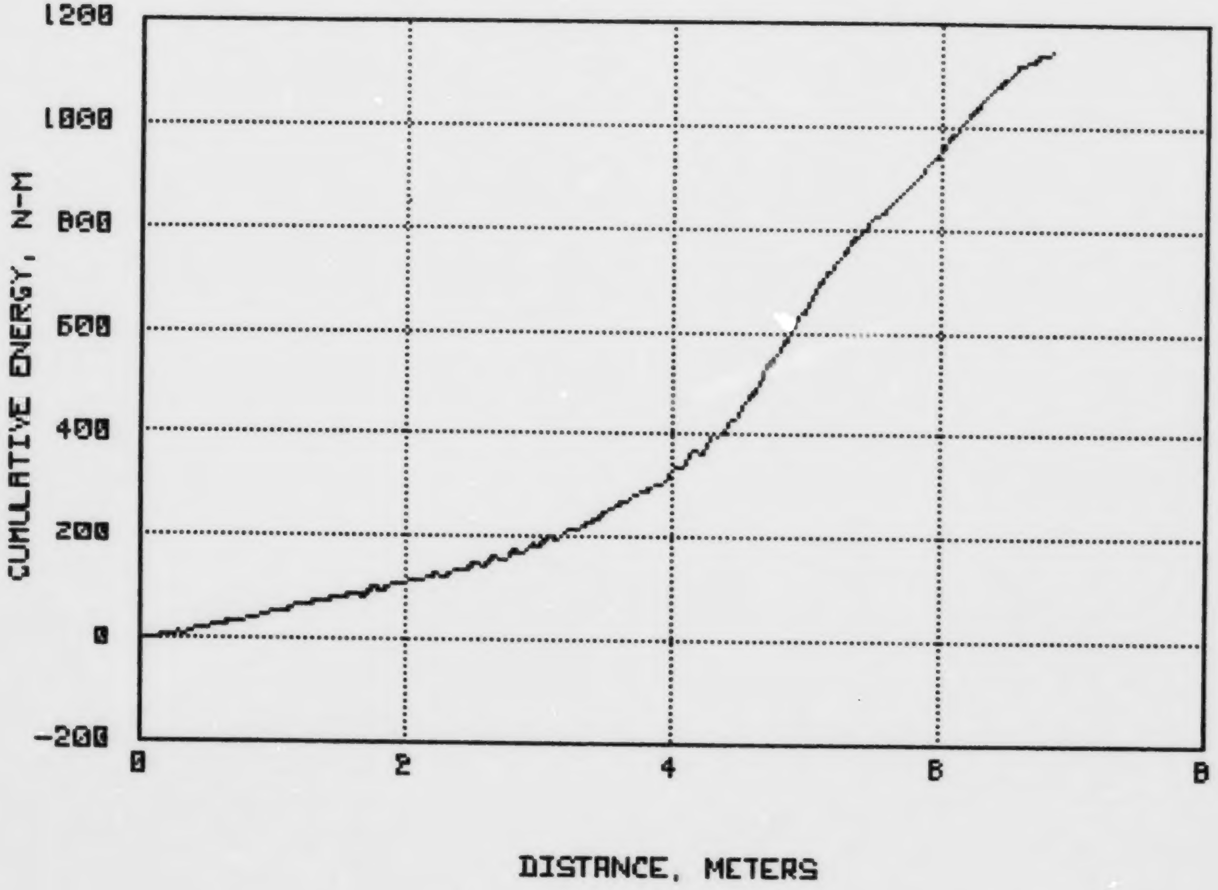

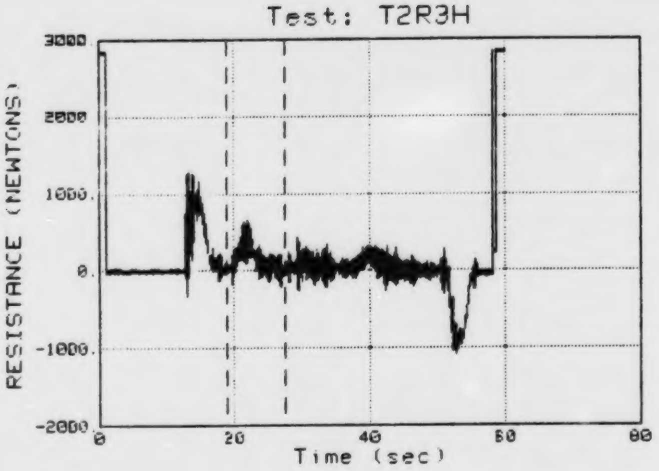
Test: T2R3H
RESISTANCE (NEWTONS)
3000
2000
1000.
0.
-1000.
-2000
0
20
40
60
80
Time (sec)

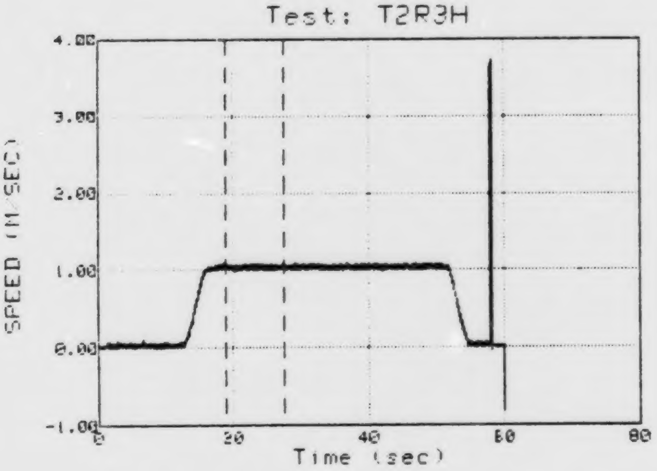
Test: T2R3H
SPEED (M/SEC)
4.00
3.00
2.00
1.00
0.00
-1.00
0
20
40
60
80
Time (sec)

MODEL SCALE PENETRATION FORCE
TEST: T2R3H RIDGE: 2-3N

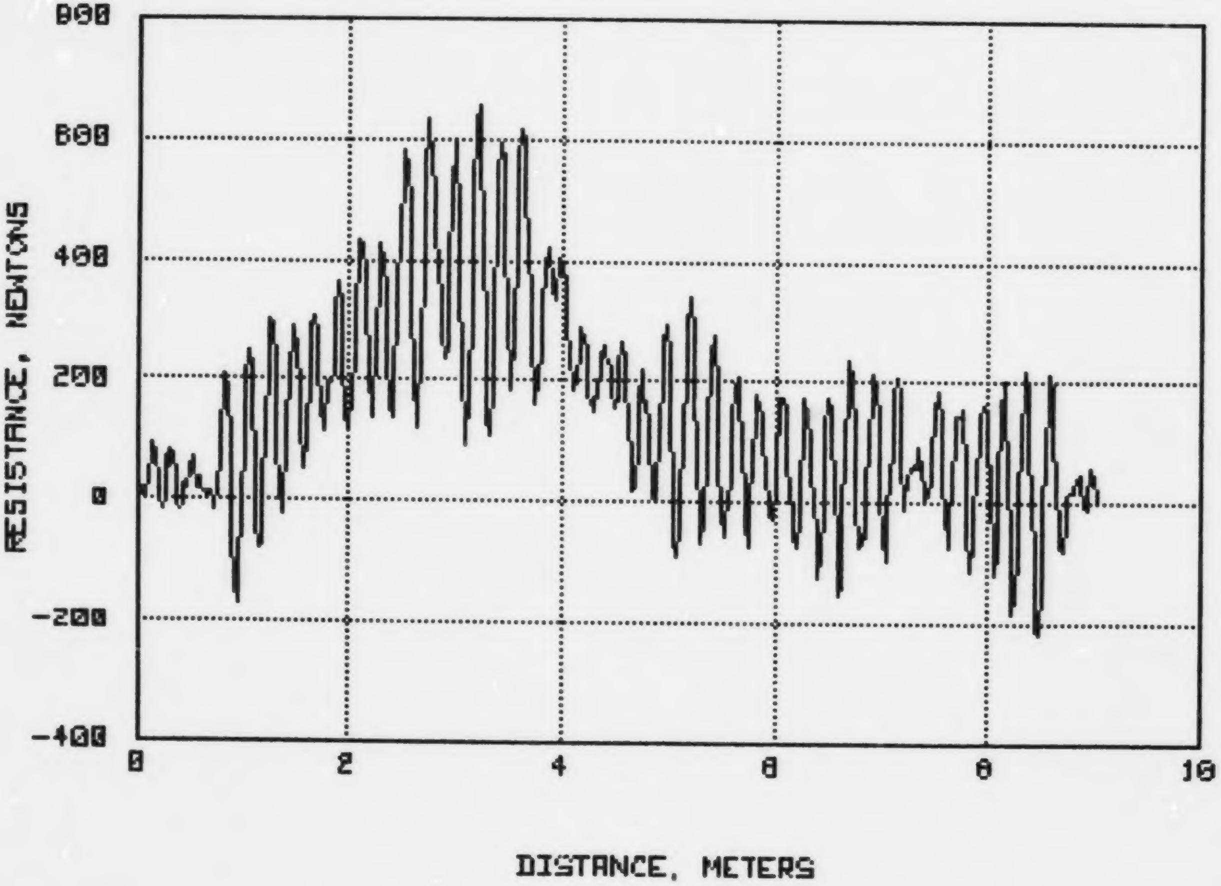

MODEL SCALE PENETRATION ENERGY
TEST: T2R3H   RIDGE: 2-3N

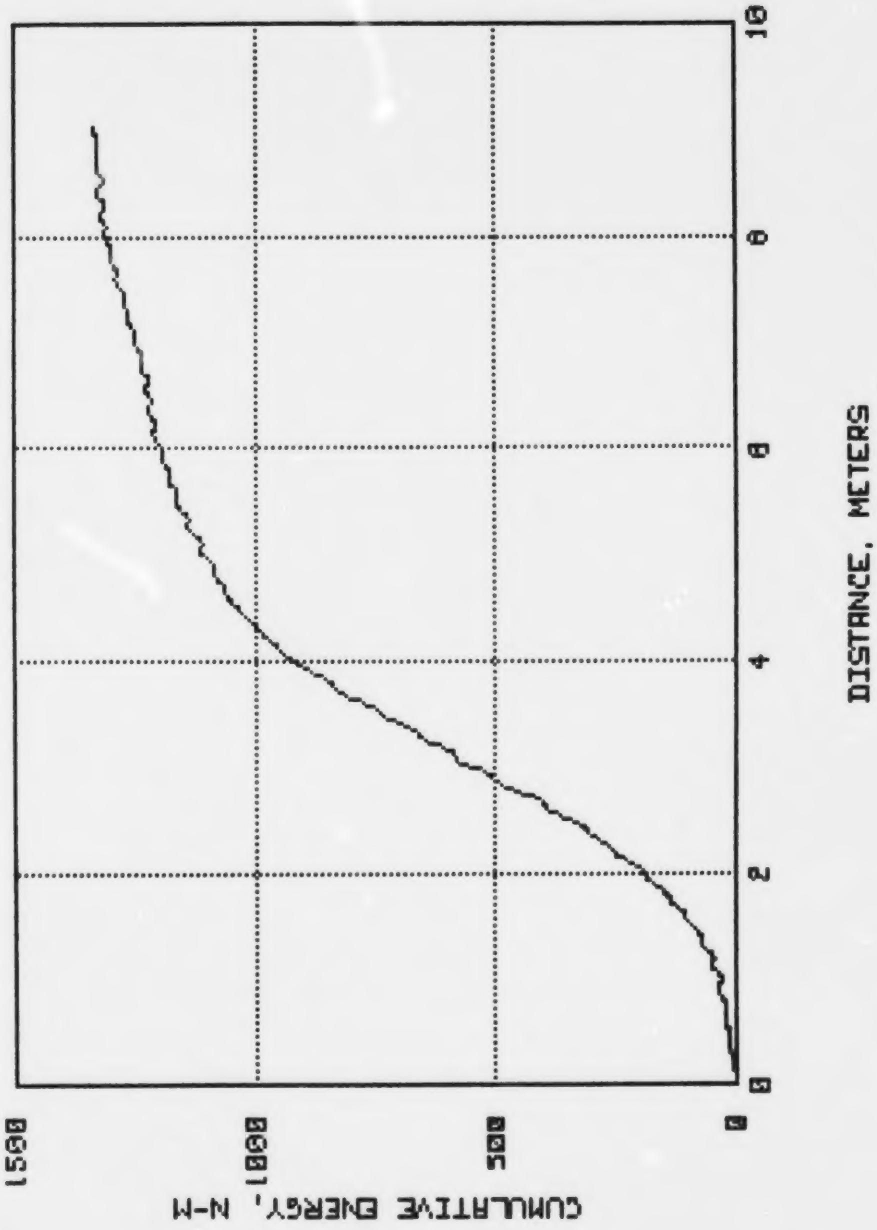

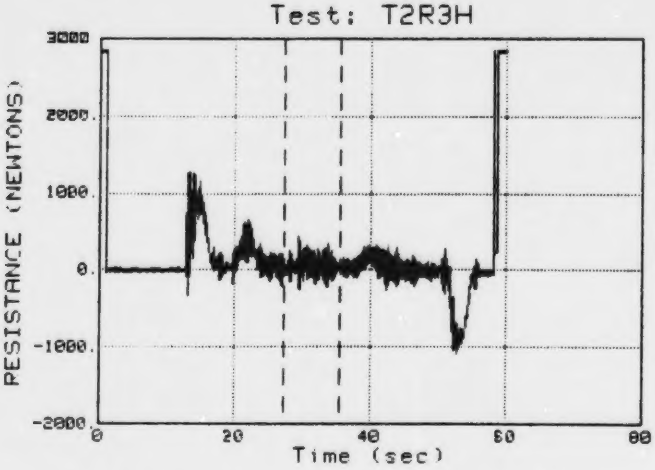
Test: T2R3H
RESISTANCE (NEWTONS)
3000
2000.
1000.
0.
-1000.
-2000.
0
20
40
60
80
Time (sec)

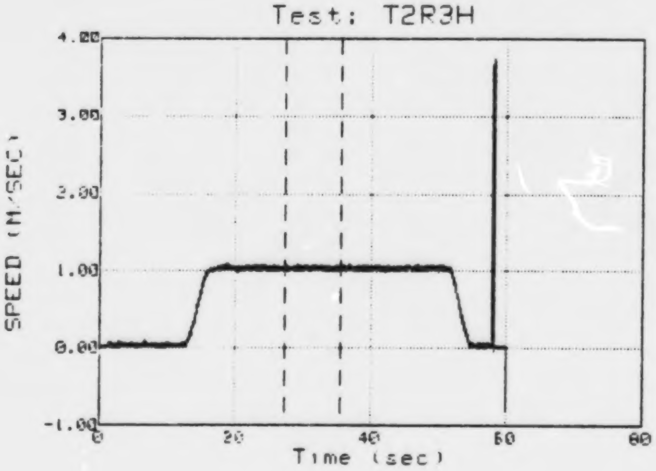
Test: T2R3H
SPEED (M/SEC)
4.00
3.00
2.00
1.00
0.00
-1.00
0
20
40
60
80
Time (sec)

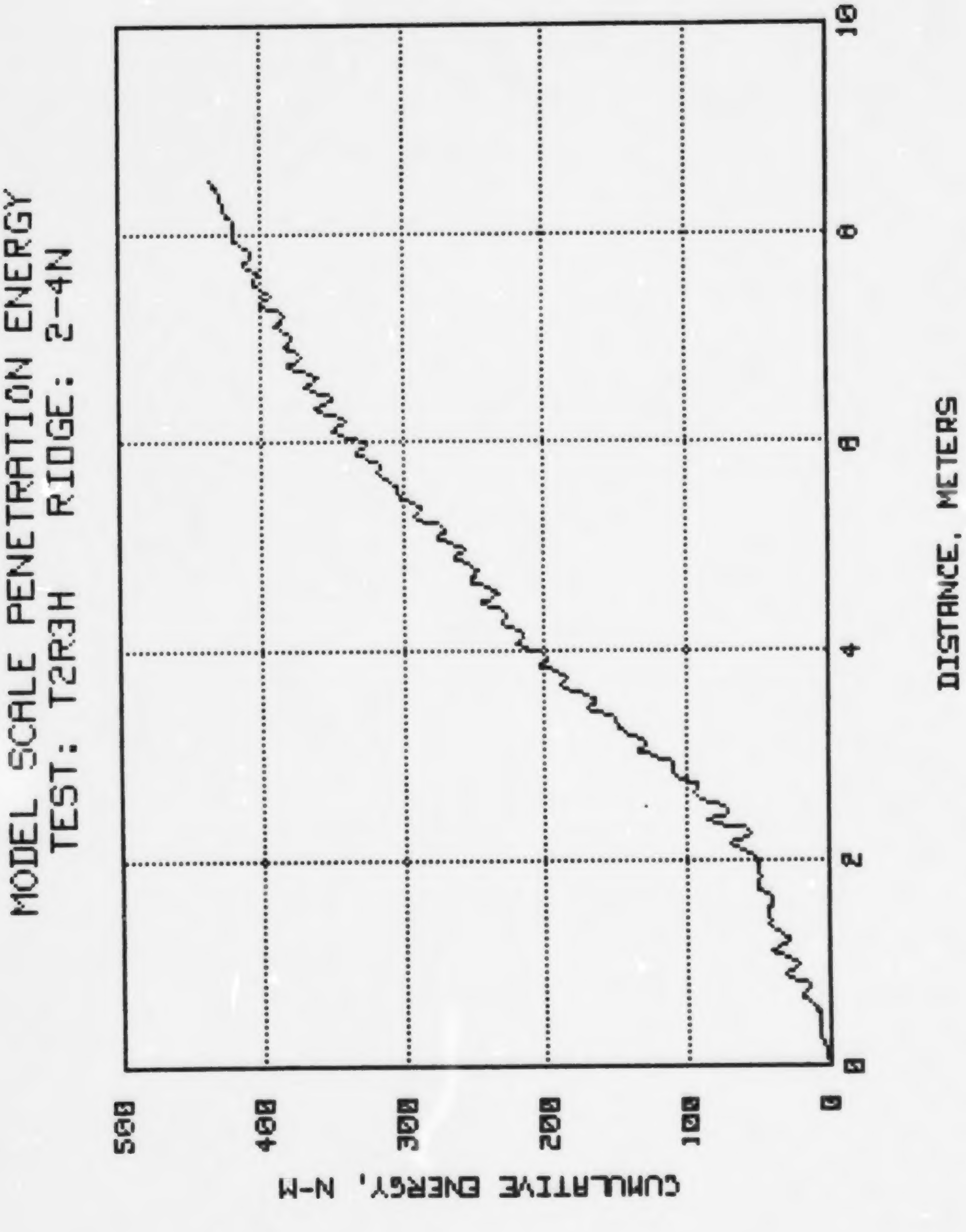
MODEL SCALE PENETRATION ENERGY
TEST: T2R3H RIDGE: 2-4N
CUMULATIVE ENERGY, N-M
0
100
200
300
400
500
DISTANCE, METERS
0
2
4
6
8
10

MODEL SCALE PENETRATION FORCE
TEST: T2R3H RIDGE: 2-4N

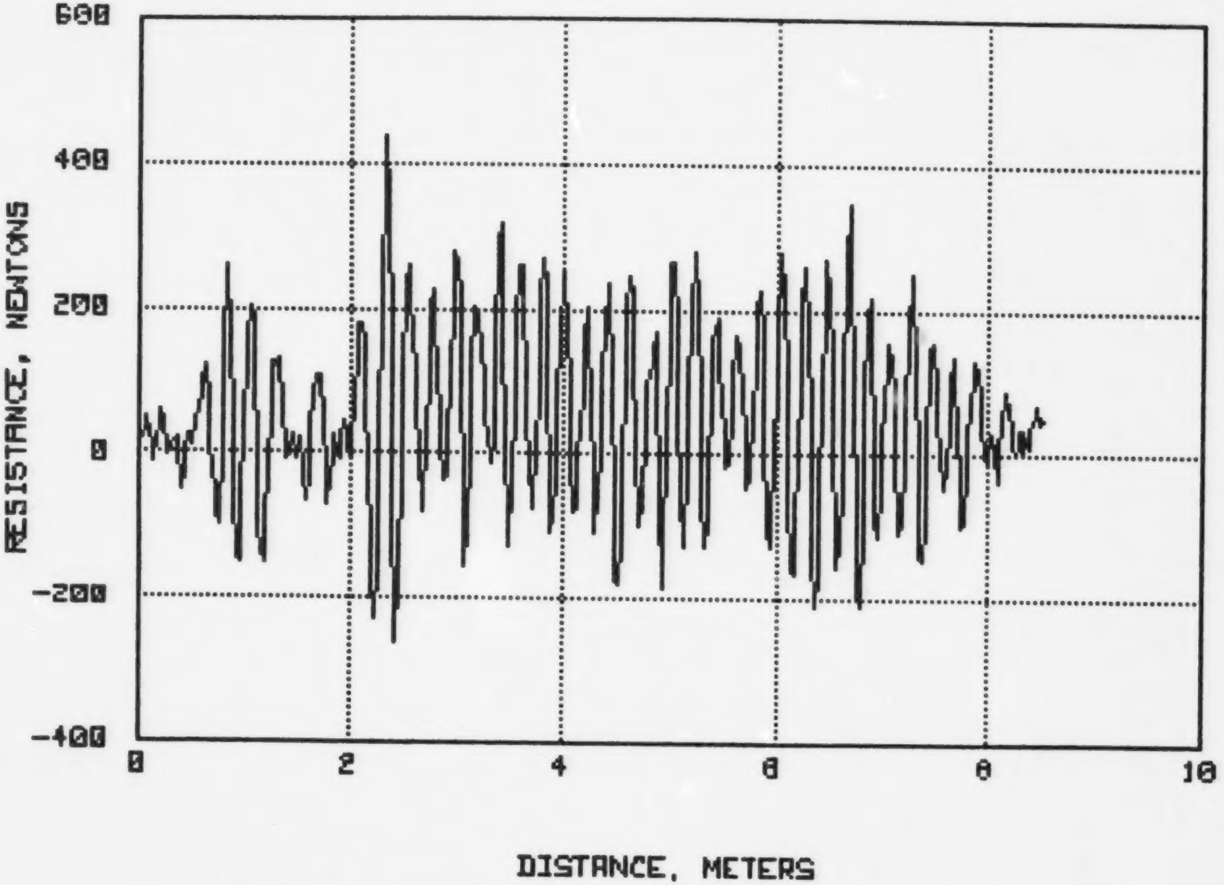

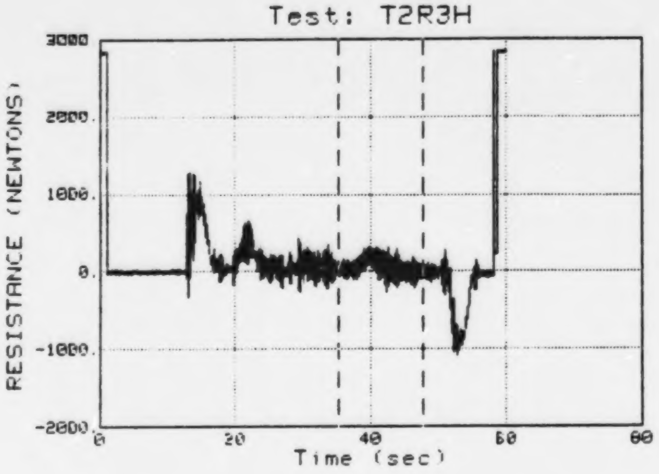
Test: T2R3H
RESISTANCE (NEWTONS)
3000
2000.
1000.
0.
-1000.
-2000.
0
20
40
60
80
Time (sec)

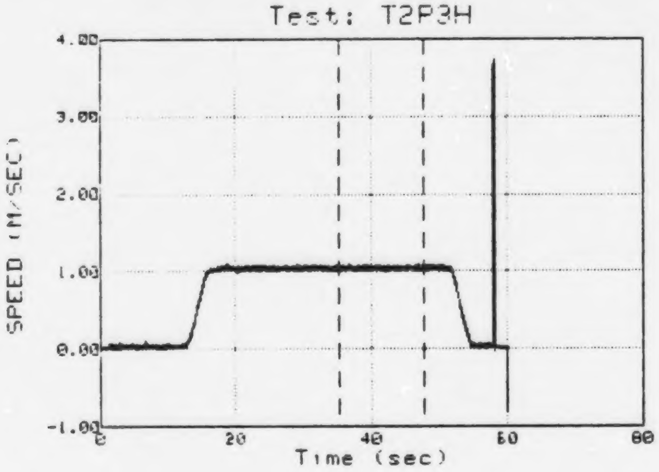
Test: T2P3H
SPEED (M/SEC)
4.00
3.00
2.00
1.00
0.00
-1.00
0
20
40
60
80
Time (sec)

MODEL SCALE PENETRATION FORCE
TEST: T2R3H RIDGE: 2-5N

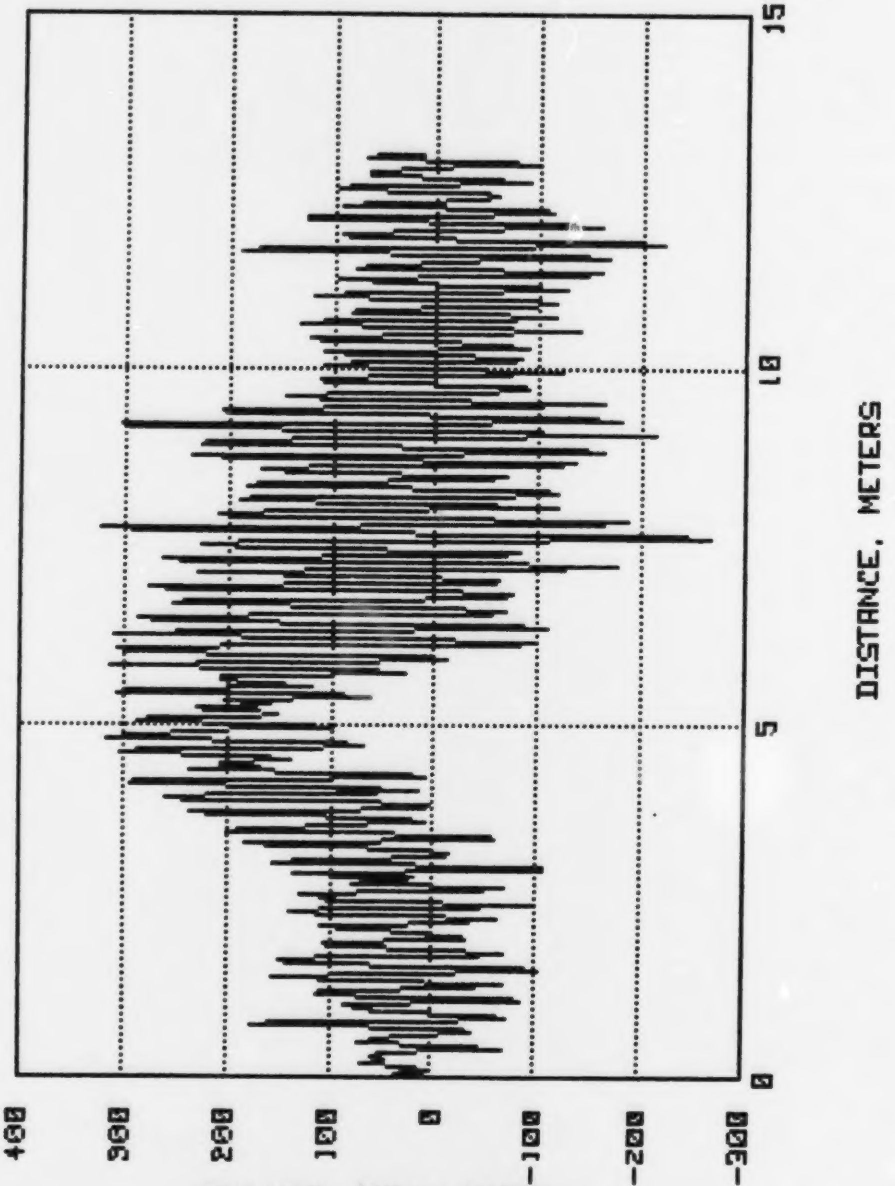

MODEL SCALE PENETRATION ENERGY
TEST: T2R3H   RIDGE: 2-5N

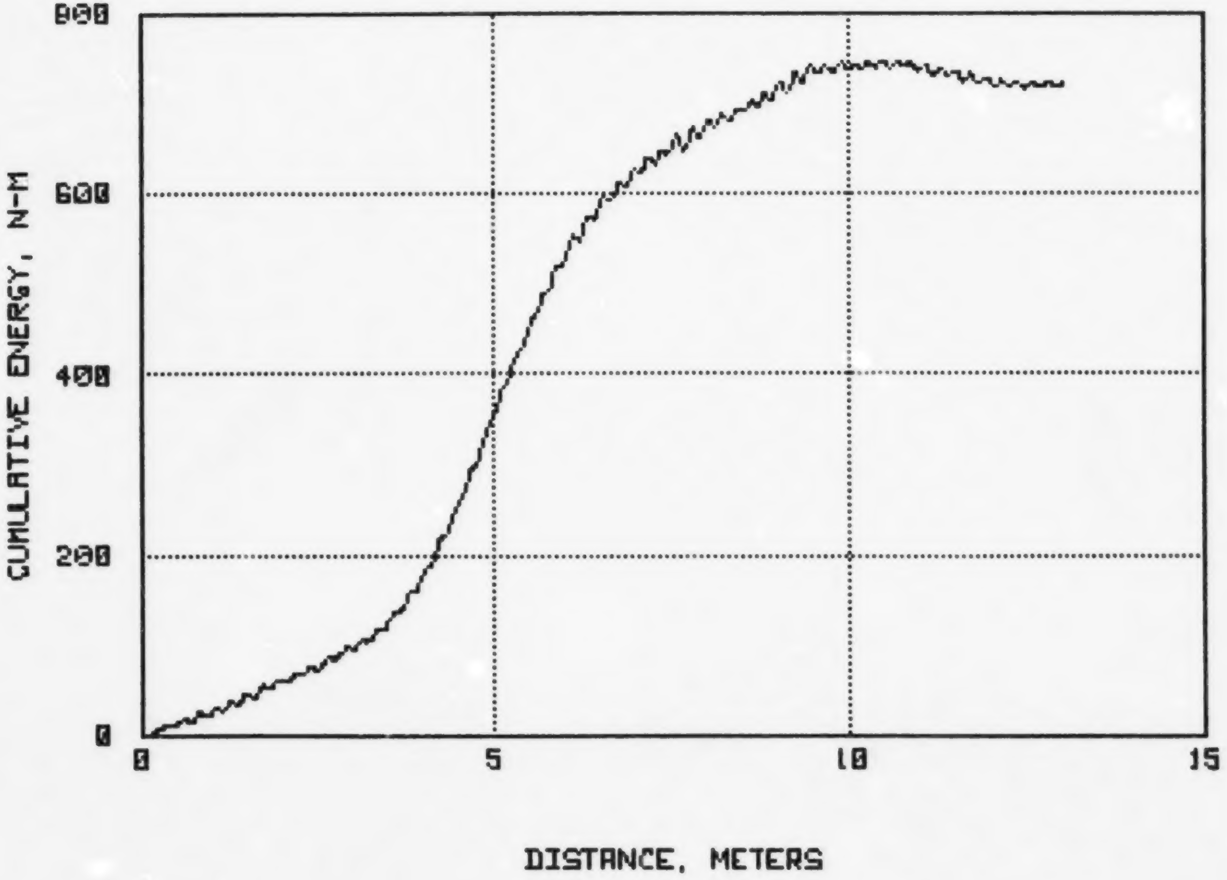

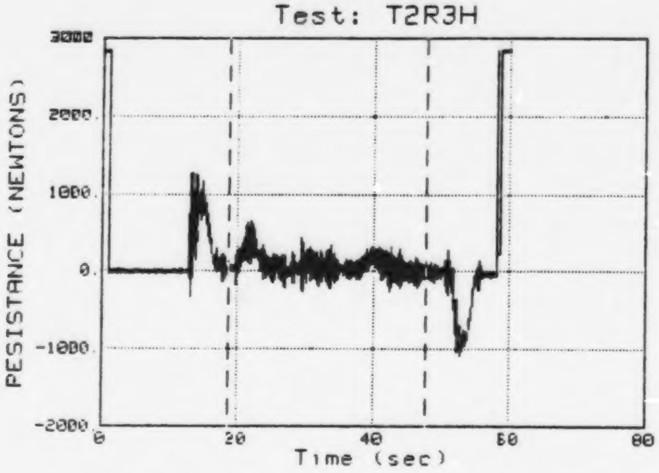
Test: T2R3H
RESISTANCE (NEWTONS)
3000
2000.
1000.
0.
-1000.
-2000.
0
20
40
60
80
Time (sec)

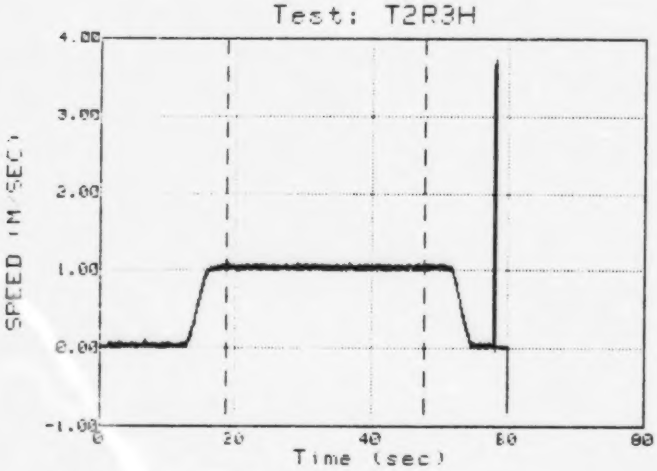
Test: T2R3H
SPEED (M/SEC)
4.00
3.00
2.00
1.00
0.00
-1.00
0
20
40
60
80
Time (sec)

MODEL SCALE PENETRATION FORCE
TEST: T2R3H   RIDGE: 2-345N

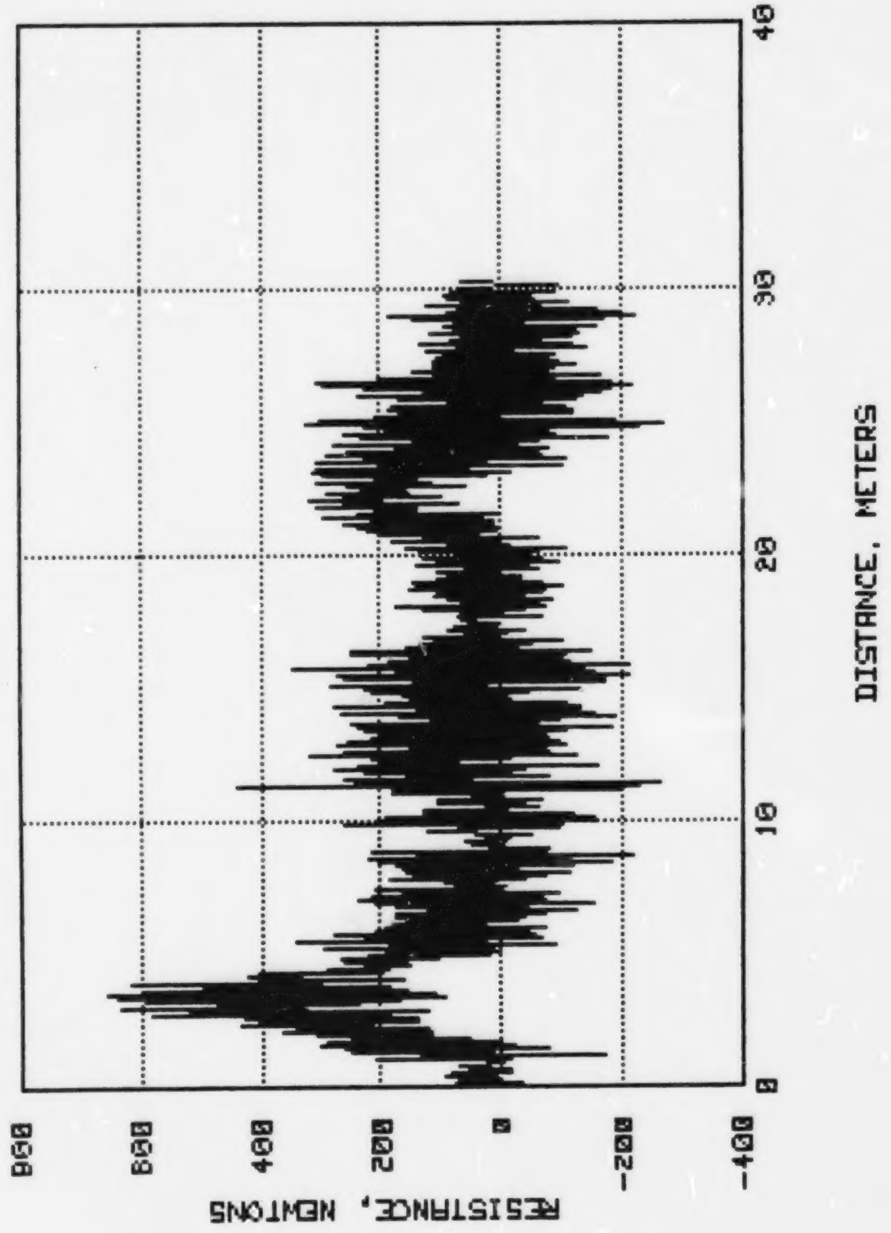

MODEL SCALE PENETRATION ENERGY
TEST: T2R3H RIDGE: 2-345N

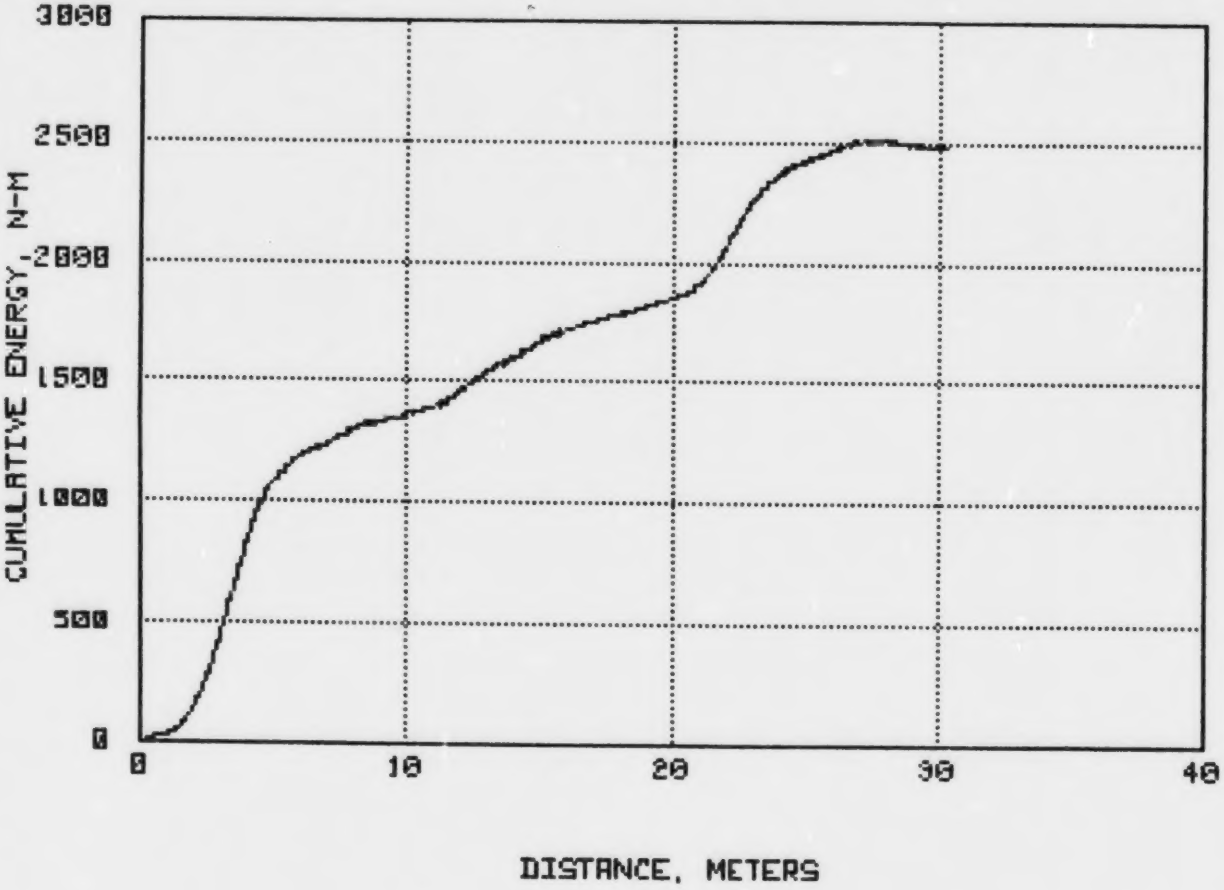

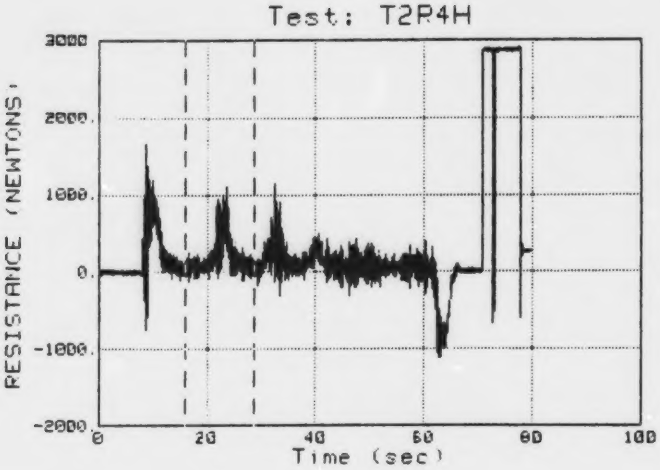
Test: T2R4H
RESISTANCE (NEWTONS)
3000
2000.
1000.
0.
-1000.
-2000.
0
20
40
60
80
100
Time (sec)

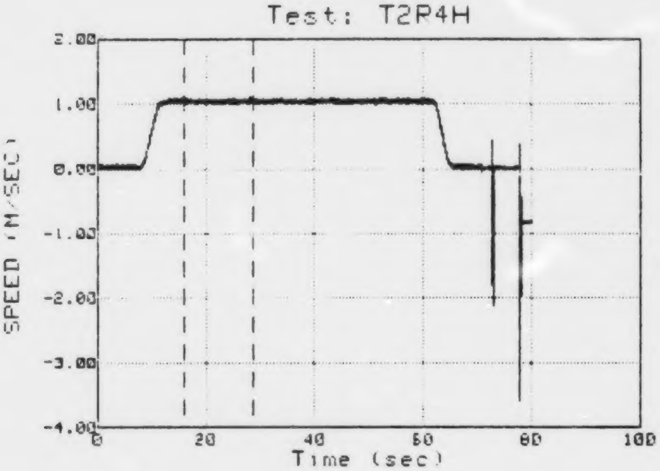
Test: T2R4H
SPEED (M/SEC)
2.00
1.00
0.00
-1.00
-2.00
-3.00
-4.00
0
20
40
60
80
100
Time (sec)

MODEL SCALE PENETRATION FORCE
TEST: T2R4H   RIDGE: 2-1S

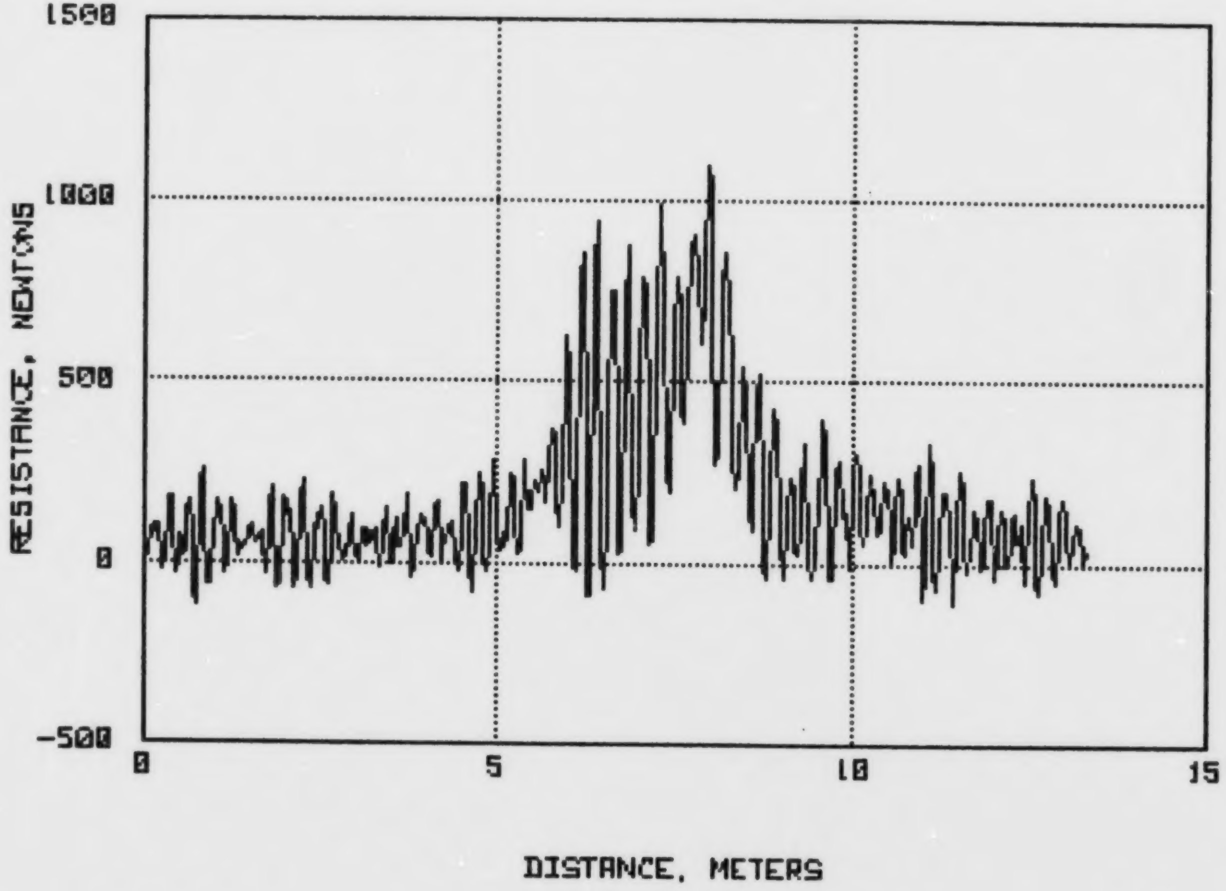

MODEL SCALE PENETRATION ENERGY
TEST: T2R4H   RIDGE: 2-1S

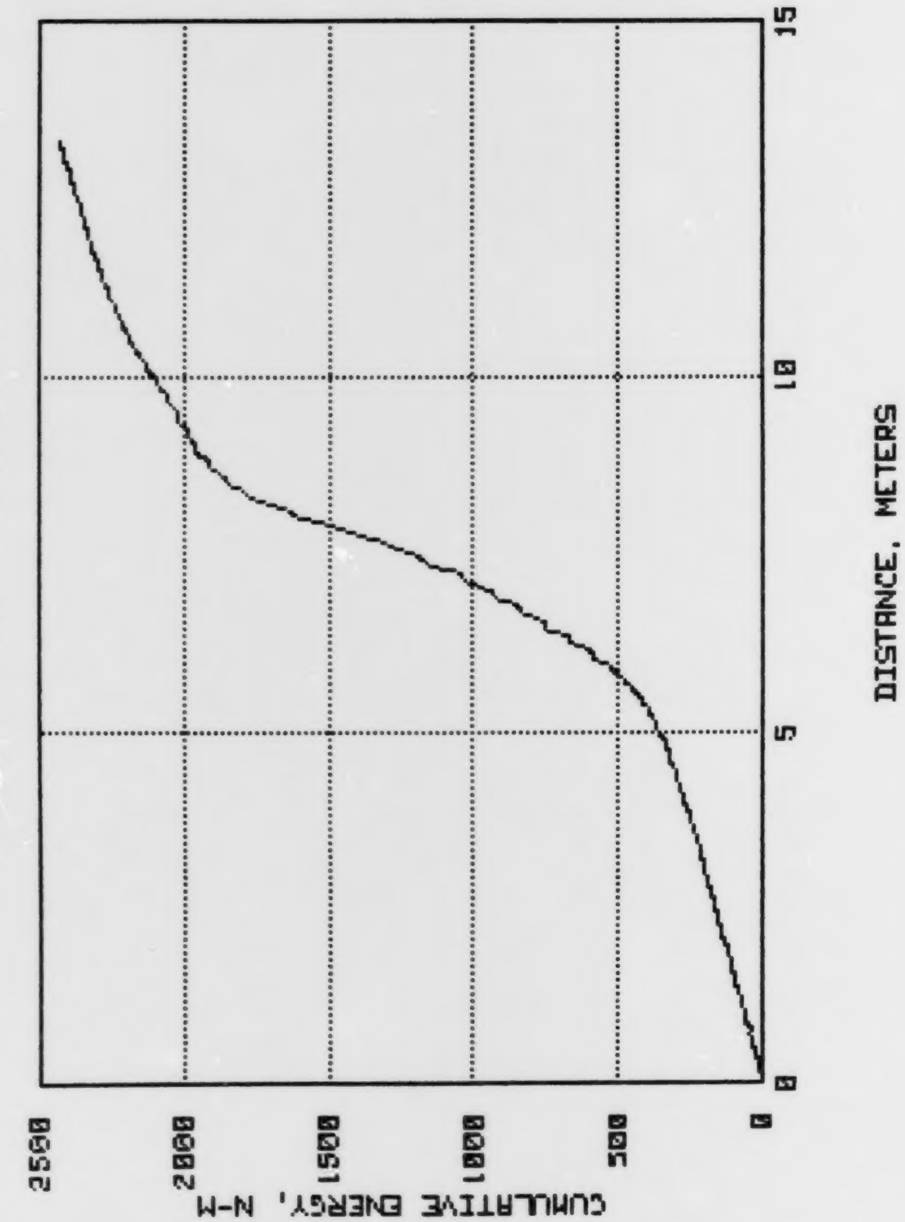

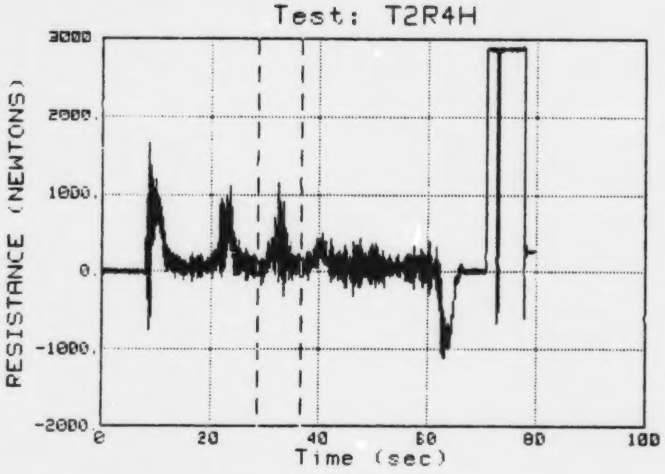
Test: T2R4H
RESISTANCE (NEWTONS)
3000
2000.
1000.
0.
-1000.
-2000
0
20
40
60
80
100
Time (sec)

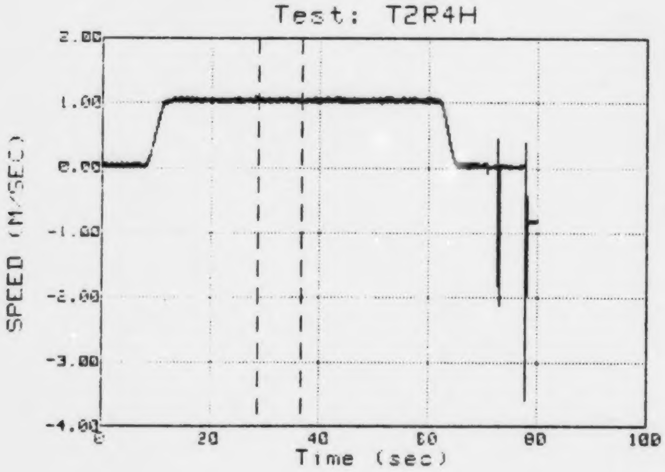
Test: T2R4H
SPEED (M/SEC)
2.00
1.00
0.00
-1.00
-2.00
-3.00
-4.00
0
20
40
60
80
100
Time (sec)

MODEL SCALE PENETRATION FORCE
TEST: T2R4H   RIDGE: 2-2S

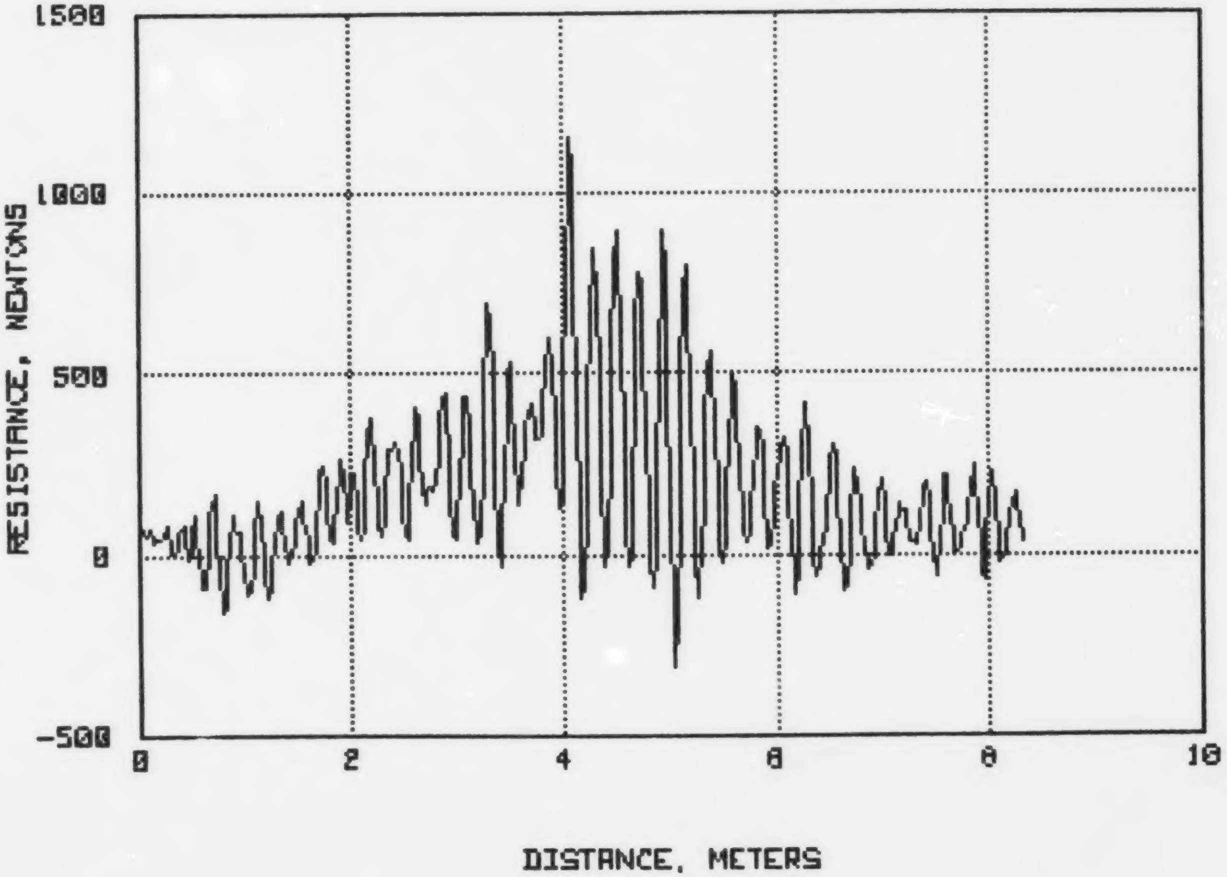

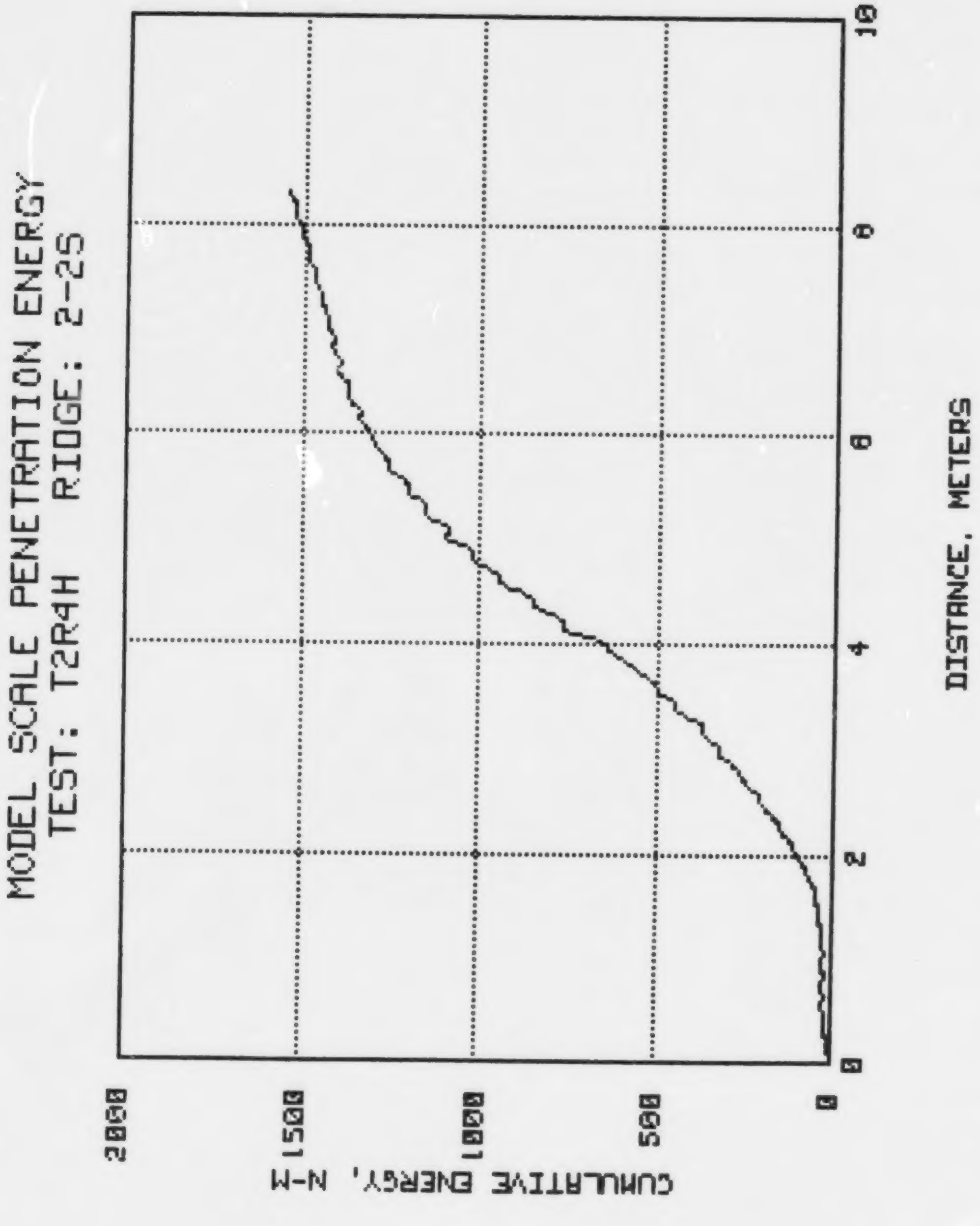
MODEL SCALE PENETRATION ENERGY
TEST: T2R4H RIDGE: 2-25
CUMULATIVE ENERGY, N-M
2000
1500
1000
500
0
DISTANCE, METERS
0
2
4
6
8
10

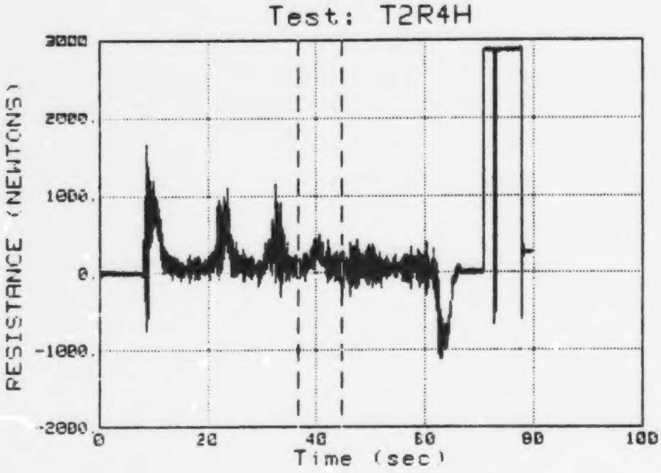
Test: T2R4H
3000
2000.
1000.
0.
-1000.
-2000.
RESISTANCE (NEWTONS)
0
20
40
60
80
100
Time (sec)

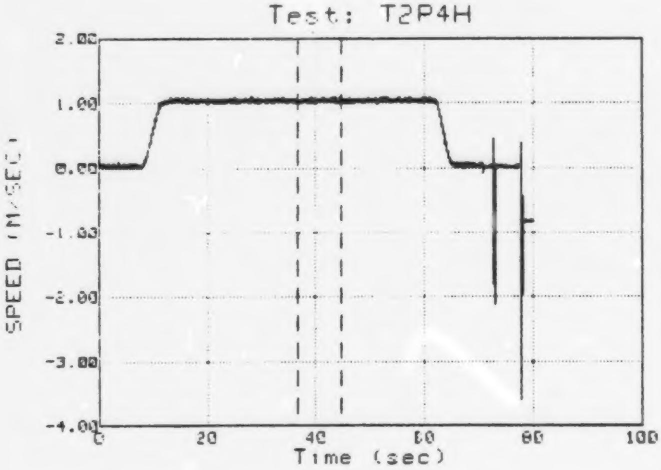
Test: T2P4H
2.00
1.00
0.00
-1.00
-2.00
-3.00
-4.00
SPEED (M/SEC)
0
20
40
60
80
100
Time (sec)

MODEL SCALE PENETRATION FORCE
TEST: T2R4H RIDGE: 2-3S

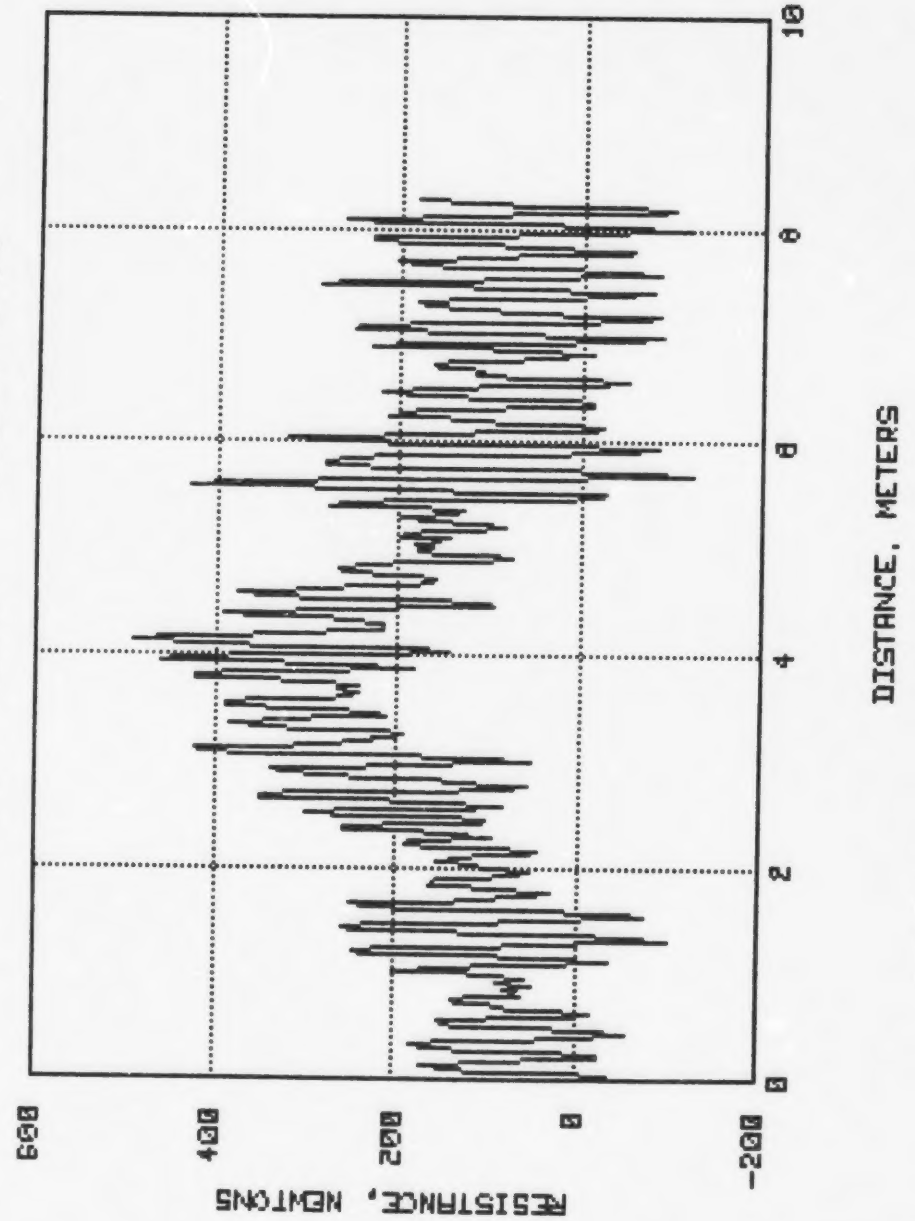

MODEL SCALE PENETRATION ENERGY
TEST: T2R4H RIDGE: 2-3S

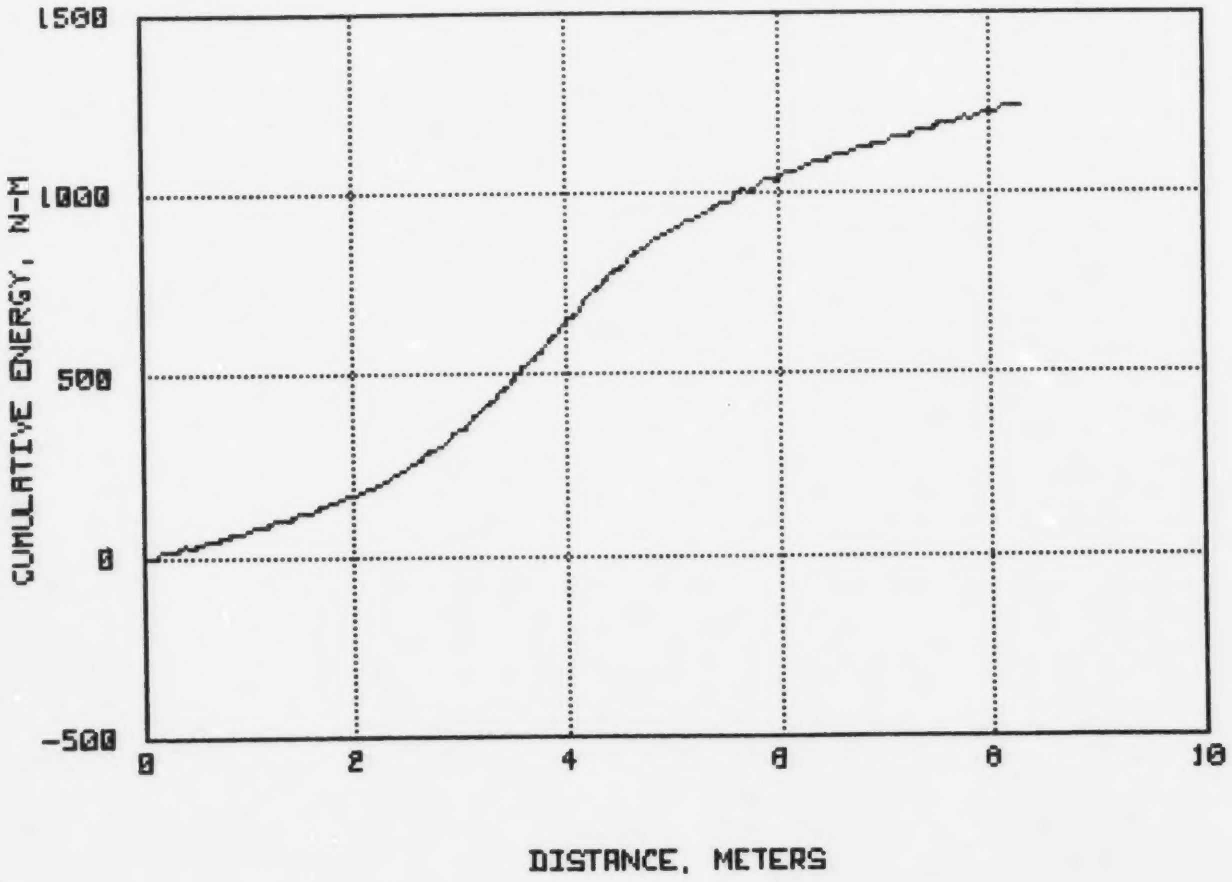

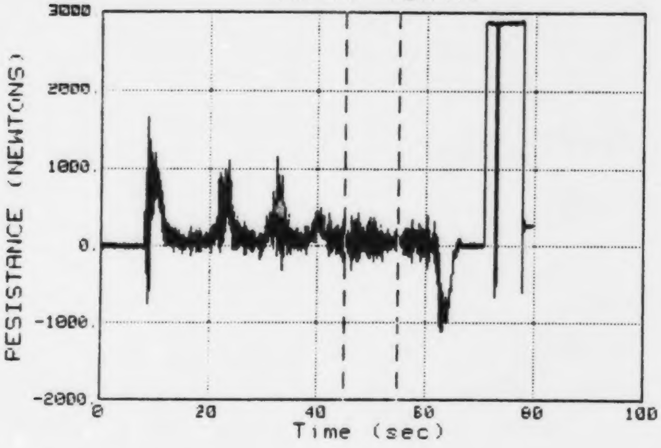

Test: T2R4H

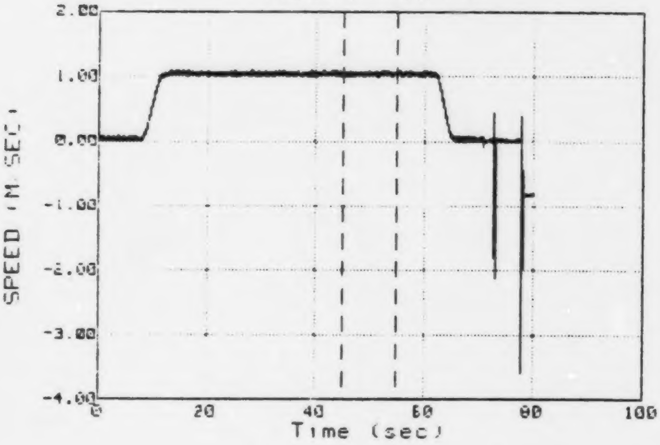

Test: T2P4H

MODEL SCALE PENETRATION FORCE
TEST: T2R4H RIDGE: 2-4S

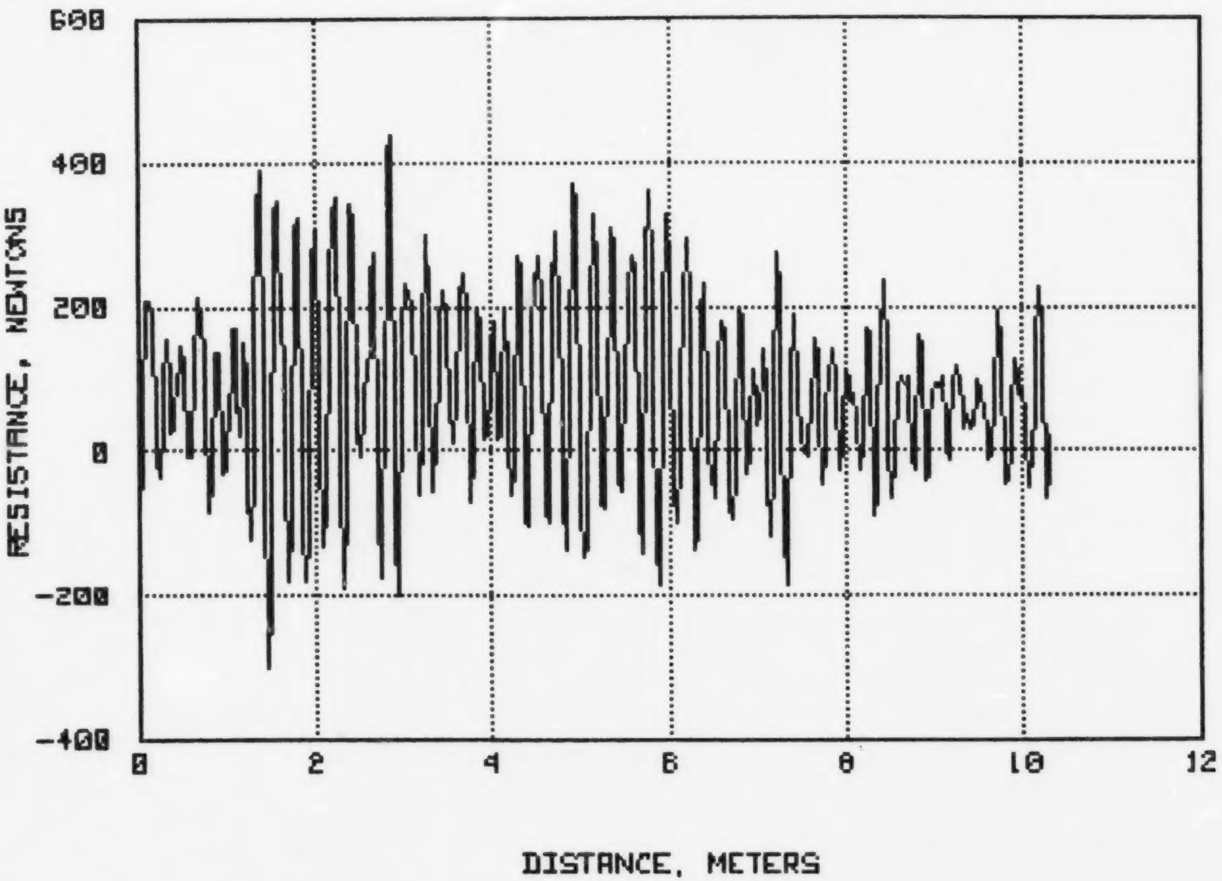

MODEL SCALE PENETRATION ENERGY
TEST: T2R4H RIDGE: 2-45

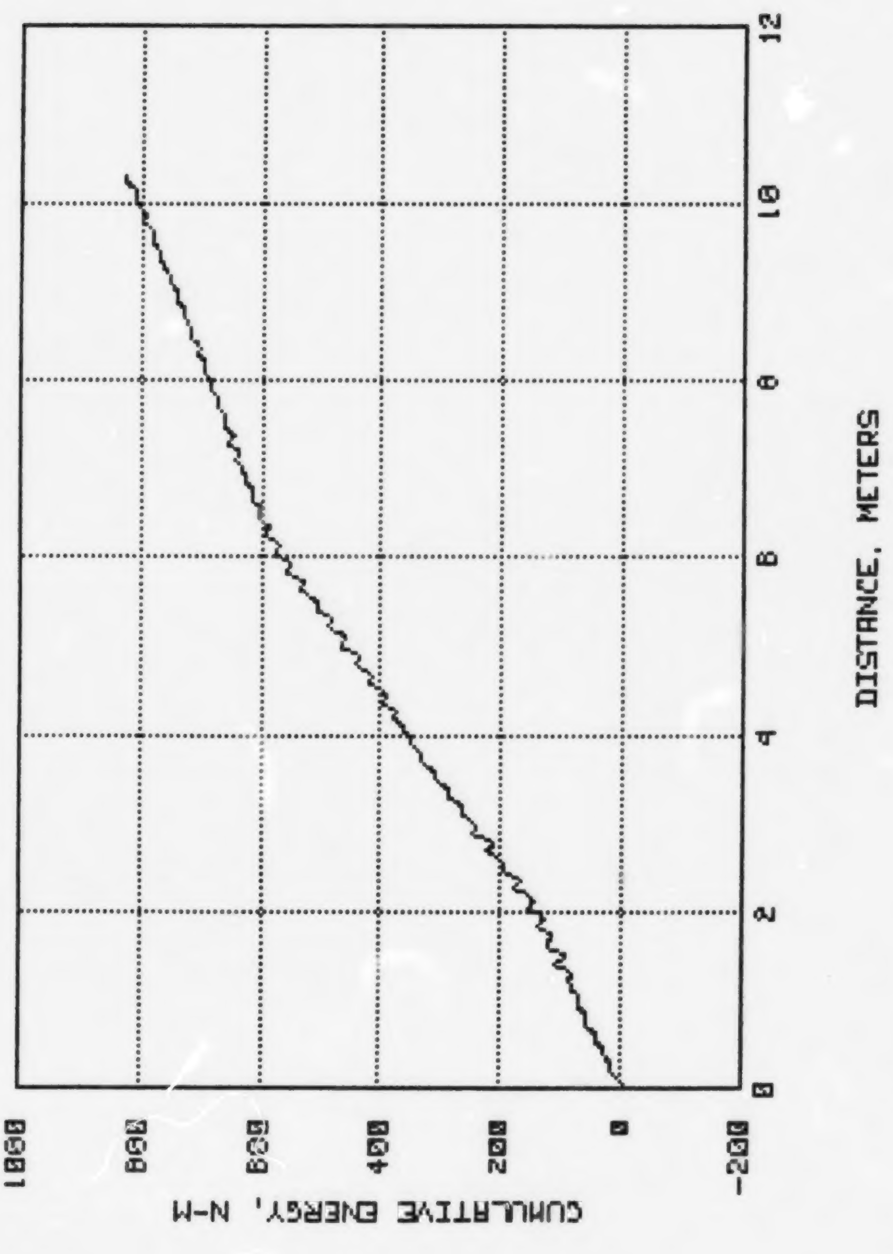

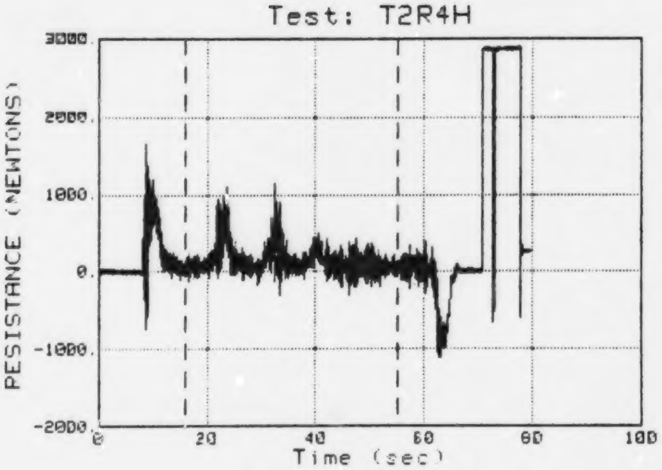
Test: T2R4H
RESISTANCE (NEWTONS)
3000.
2000.
1000.
0.
-1000.
-2000.
0
20
40
60
80
100
Time (sec)

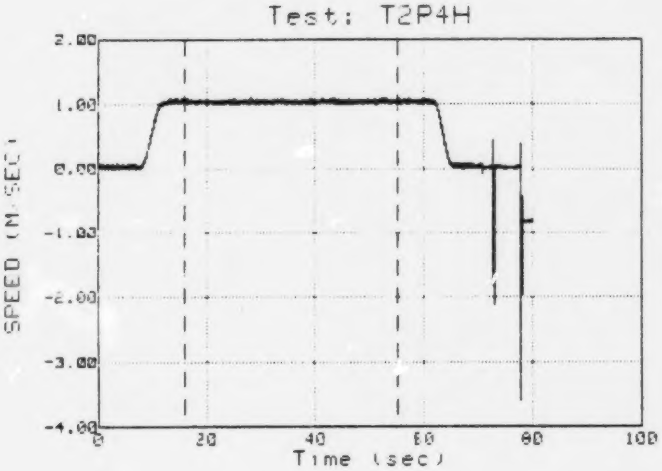
Test: T2P4H
SPEED (M/SEC)
2.00
1.00
0.00
-1.00
-2.00
-3.00
-4.00
0
20
40
60
80
100
Time (sec)

MODEL SCALE PENETRATION ENERGY
TEST: T2R4H   RIDGE: 2-12345

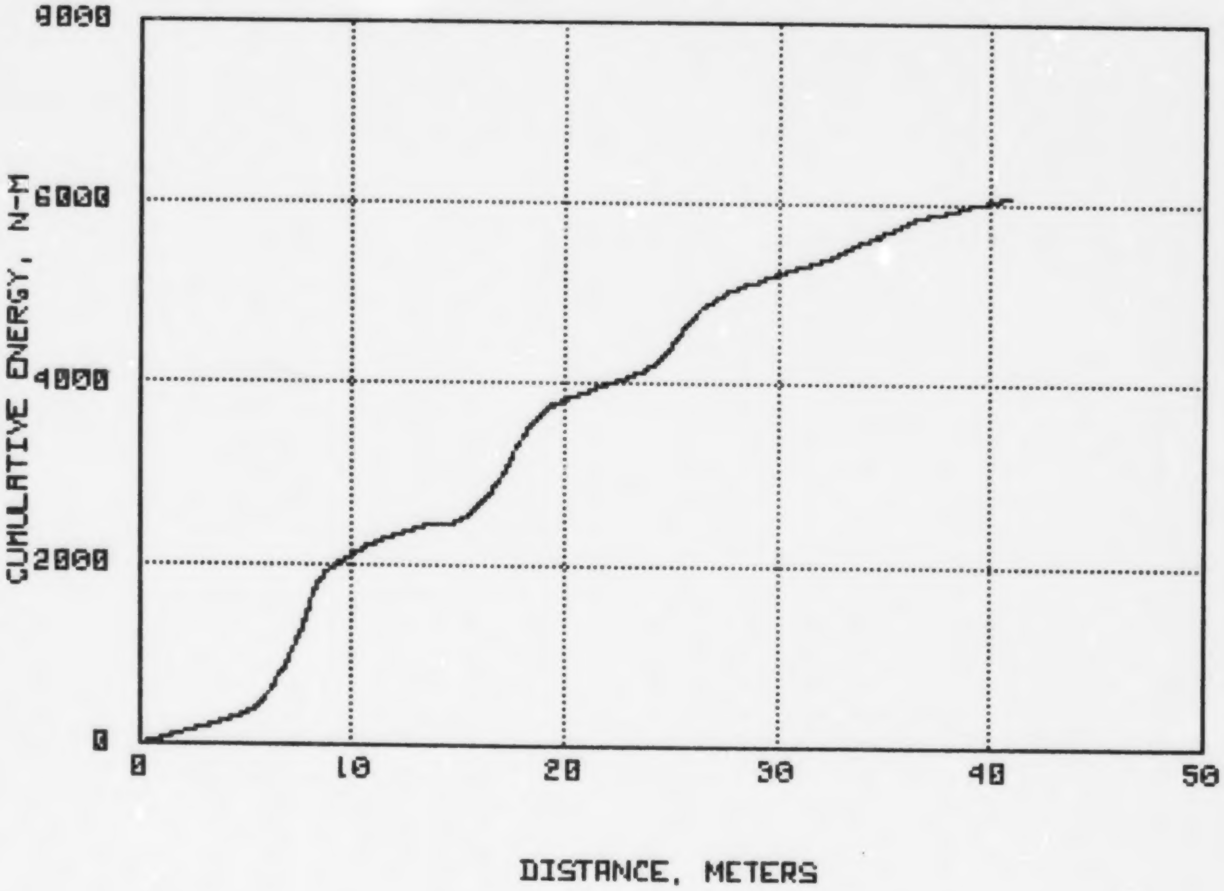

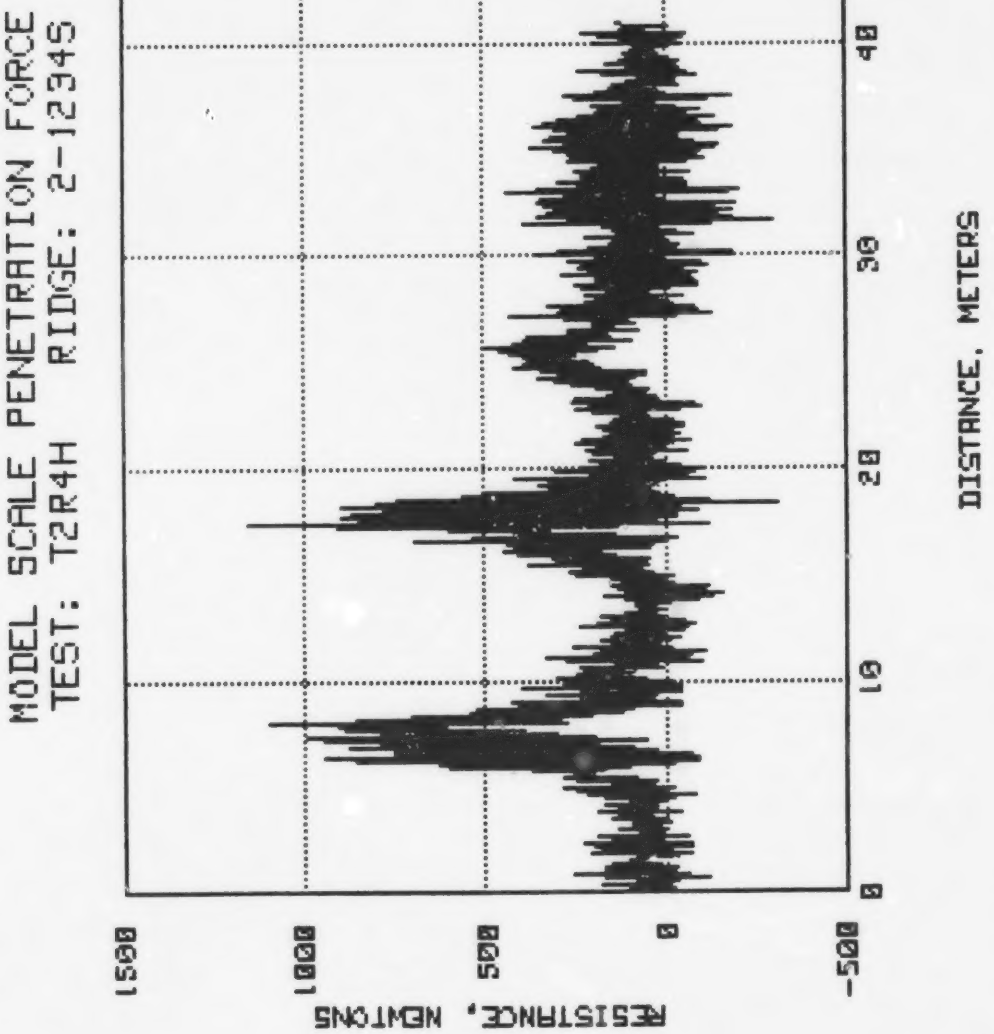
MODEL SCALE PENETRATION FORCE
TEST: T2R4H RIDGE: 2-12345
RESISTANCE, NEWTONS
1500
1000
500
0
-500
DISTANCE, METERS
0
10
20
30
40
50

APPENDIX D.4

ICE AND RIDGE PROPERTIES

FLEET TECHNOLOGY LIMITED (FTL)

Engineering Design Calculations

JOB No. 3229
SHEET 1 OF 5
DATE May 4/88
BY G. Comfort
CH'K BY

PROJECT RIDGE MODELLING
SUBJECT RIDGE MECHANICAL PROPERTIES

FLEXURAL STRENGTH OF CONSOLIDATED LAYER

MEAS. TIME	RIDGE #	CRUST THICK. (mm)	BEAM WIDTH (mm)	BEAM LENGTH (mm)	FAILURE LOAD (kg)	FLEX. STR (kPa)
0930	2-1N	70.9	[illegible]	260	3.5	93.1
		33.2	104.2	382	3.2	99.8
1000	2-1N	39	139	370	1.3	134
		37.5	147	[illegible]	1.3	147
1200	2-2N	57.9	103	310	1.8	77
		60.9	101	300	1.85	87
1400	2-3N	52.9	105.5	255	1.1	56
		53.2	106.5	260	1.45	74
1420	2-1N	67.0	108.5	253	2.65	81
	2-1N	65.3	106.1	260	1.23	42
1430	2-1S	72.5	120	315	3.02	78
	2-1S	69.6	123	300	2.5	74

SHEAR STRENGTH OF RIDGE CONSOLIDATED LAYER

TIME OF MEASUREMENT: 1030

RIDGE #	BLOCK WIDTH (mm)	BLOCK THICK (mm)	FAILURE LOAD (kg)	SHEAR STRENGTH (kPa)
2-1N	86.5	59.2	5.0	28
2-1N	81	58.8	5.7	34
2-2N	92.2	58.3	7.1	38

JOB No. 3208
SHEET 2 OF 3
DATE May 4/83
BY M. Comfort
CH'K BY

PROJECT RIDGE MODELLING
SUBJECT
RIDGE MECHANICAL PROPERTIES

THICKNESS OF CONSOLIDATED LAYER

RIDGE	MEASURED VALUES (mm)	AVE (mm)
2-1N	67, 65, 64	65 ± 1
2-2N	58, 61	59
2-3N	63, 76, 85, 68, 60, 61	69 ± 9
2-1S	59, 67, 44, 78, 76, 76, 69, 71, 72, 74, 66, 70, 71, 70, 74, 65, 68, 67, 65	69 ± 7
2-2S	44, 43, 44, 54, 56, 55, 58, 56, 52, 58, 53, 55, 48, 46, 44, 48, 41, 53	50 ± 6
2-3S	53, 53	53

COMPRESSIVE STRENGTH OF CONSOLIDATED LAYER

TIME OF MEASUREMENT : 1030

[illegible]	[illegible] Thick (mm)	Block Thick (mm)	[illegible]	[illegible]
2-1	71	62	2.9	[illegible]
2-1	[illegible]	64	7.5	[illegible]
2-1	75	51	[illegible]	[illegible]
[illegible]	77	56	2.8	[illegible]
2-1	67	57	7.1	[illegible]
[illegible]	51	57	6.0	[illegible]
[illegible]	77	60	6.7	58
2-2	85	58	7.1	45
2-2	75	54	6.7	[illegible]
[illegible]	71	58	8.9	86
[illegible]	77	58	5.6	42
[illegible]	75	57	N	145

FLEET TECHNOLOGY LIMITED (FTL)

Engineering Design Calculations

JOB No. [illegible]
SHEET [illegible] OF 3
DATE [illegible]
BY
CH'K BY

PROJECT [illegible]
SUBJECT [illegible]

[illegible]

	Ridge Width	[illegible]	[illegible]
[illegible]	1.7?m	0.114	[illegible]
3-2N	2.0m	0.115	[illegible]
[illegible]	2.5m	0.173	[illegible]
[illegible]	0.2m	Nil	[illegible]

[illegible] Ave. [illegible]

[illegible] BULK DENSITY

R[illegible]	[illegible]	[illegible] (cm×cm)	[illegible] (cm)	[illegible]	BULK DENSITY (kN/m³)
2-3N	1.20	26 x 33	Not used	9.5	5.4[1]
2-3N	1.20	26 x 33	30[3]	[illegible]	9.5[2]
3-1N	0.73	23 x 21	30[3]	Not Meas.	9.5[2]

Notes: 1. [illegible] ...ated [illegible]
[illegible]
2. [illegible] measurements
of submergence force and volume of ice column.
3. Depth of ice column taken as average
of mid-portion of ridge profile.

VOL. OF ICE USED TO BUILD THE RIDGE

ICE SHEET THICKNESS : 20 mm
LENGTH OF SHEET PUSHED INTO EACH RIDGE : 15 m
VOLUME OF ICE USED FOR EACH RIDGE : 0.3 m³/m WIDTH OF BASIN

FLEET TECHNOLOGY LIMITED (FTL)

Engineering Design Calculations

JOB No. 3208
SHEET 1 OF 2
DATE MAY 4/88
BY M Comfort
CH'K BY

PROJECT RIDGE MODELLING
SUBJECT CROSS - SECTIONAL PROFILE DATA FOR RIDGES IN SHEET #2

RIDGE 2-1 N		RIDGE 2-2 N		RIDGE 2-3 N		RIDGE 2-5 N	
X (cm)	Z (cm)	X (cm)	Z (cm)	X (cm)	Z (cm)	X (cm)	Z (cm)
0	2.5	0	2.5	0	2.5	0	2.5
25	2.5	25	17.5	25	17.5	25	17.5
50	2.5	50	27.5	50	17.5	50	22.5
75	27.5	75	32.5	75	27.5	75	27.5
100	32.5	100	37.5	100	32.5	100	32.5
125	27.5	125	27.5	125	32.5	125	32.5
150	27.5	150	32.5	150	27.5	150	32.5
175	32.5	175	no data	175	27.5	175	17.5
200	17.5	200	2.5	200	32.5	200	17.5
225	2.5			225	27.5	225	2.5
				250	2.5		

PLAN LAYOUT OF BASIN : RIDGE 2-1N RIDGE 2-2N RIDGE 2-3N RIDGE 2-4N RIDGE 2-5N

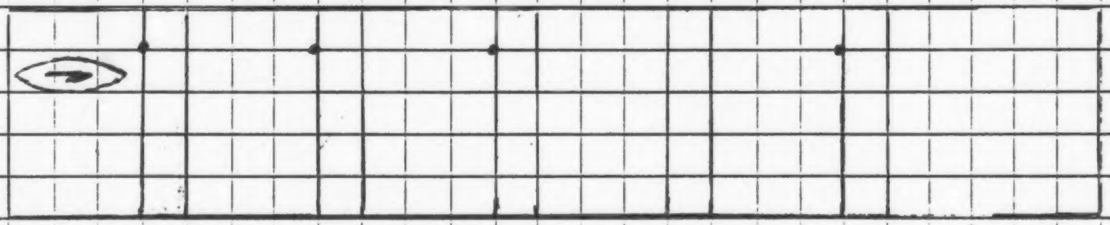

• ORIGIN OF COORDINATE SYSTEM USED FOR EACH RIDGE

NOTE : ALL MEASUREMENTS IN THE Z DIRECTION APPLY TO THE TOTAL DEPTH (i.e. SAIL AND KEEL) OF THE RIDGE.

FLEET TECHNOLOGY LIMITED [FTL]

Engineering Design Calculations

JOB No. 3208
SHEET 2 OF 2
DATE MAY 4/88
BY M. C[illegible]
CH'K BY

PROJECT RIDGE MODELLING
SUBJECT CROSS SECTIONAL PROFILES FOR RIDGES IN SHEET #2

RIDGE 2-1 N:

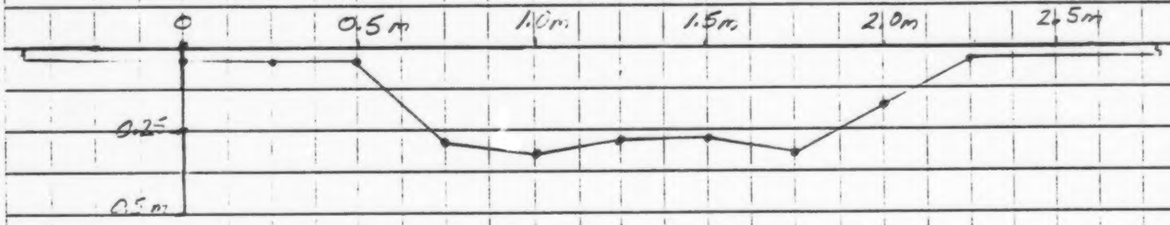

RIDGE 2-2 N:

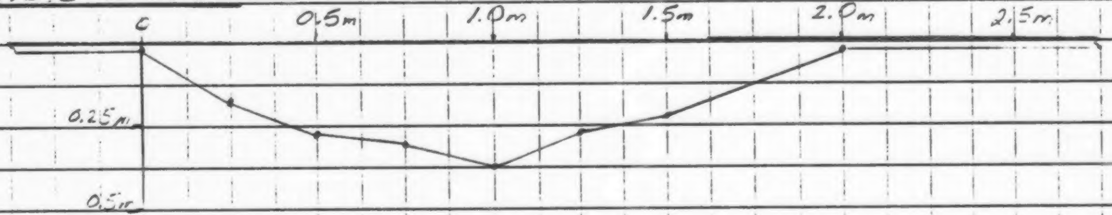

RIDGE 2-3 N:

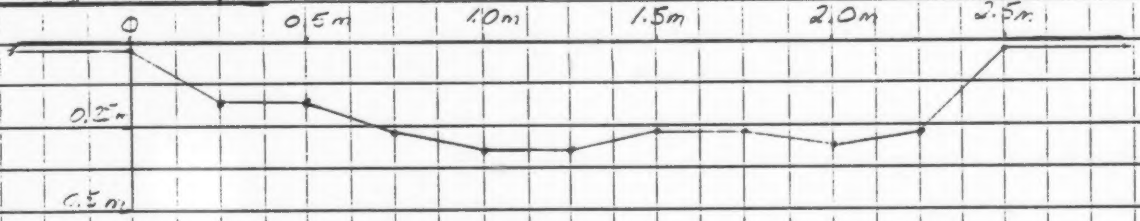

RIDGE 2-5 N:

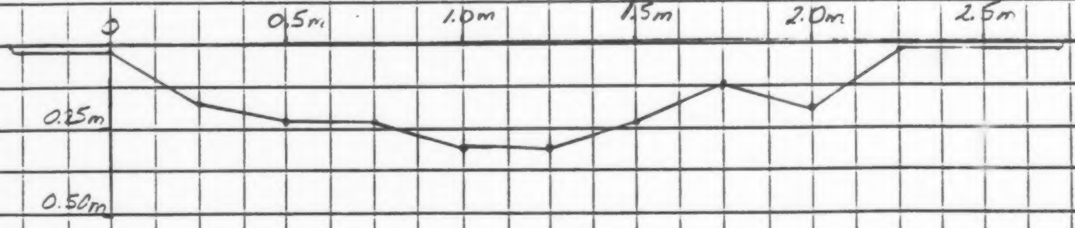

```
                 NRC - INSTITUTE FOR MARINE DYNAMICS

                    ARCTIC VESSEL RESEARCH SECTION


                          ICE SHEET SUMMARY

Test Name:  RIDGE2                         Project Number: 88112

Target ice thickness: (mm)  24.0           EG/AD/S: (%) .39/.027/0

Target ice strength: (kPa)  18.0

SEEDING:
-------
Air temp.(max/min) C: -19.9/-14.7          Tank water temp. C: 0.06
Seeding completed at 2035  2-MAY-1988      Seed duration: (min)  35.
Seed volume: l 28.6                        Seed water temp.: C  55.0
Humidity: tank(%) 80
          room(%) 39

GROWTH:
------
Target temp.: C -15.0                      Time to target temp. hrs:  0.0
Avg temp. at plateau: C -15.5              Duration of plateau hrs:  6.9
Avg temp. of freeze cycle C -15.5          Duration of freeze cycle hrs:  6.9
Total negative deg. hours  107.5           Thickness at end of freeze:(mm) 14.4
Avg growth rate: (mm/hr) 2.078             Avg growth rate: (mm/fdh) .134

WARM-UP:
-------
Warm-up commenced at 0330  3-MAY-1988      Length of warm-up: (hrs)  10.
Time to tempering temp: (hrs)  3.2         Avg tempering temperature: (C)  0.4
Final ice thickness: (mm)  21.5            Ice growth during warm-up: (mm)   7.1
Total growth rate: (mm/hr) 3.108           Total growth rate: (mm/fdh) .200


* thickness at end of freeze  was estimated
** final ice thickness was estimated
```

NRC - INSTITUTE FOR MARINE DYNAMICS

ARCTIC VESSEL RESEARCH SECTION

ICE MECHANICAL PROPERTIES SUMMARY

Test Name: RIDGE2 Project Number: 88112

Warm up commenced: 03:30 3-MAY-1988

Time	Warm-up hrs	Loc	hi mm	Sf kPa	Lc cm	E MPa	E/Sf	Lc/hi	Klc N/m	Sf/Klc m-.5	Sc/s kPa	Rhoi Mg/m3
0835	5.08	N	21.1± 1.0 n= 3									
		S	20.5± 0.6 n= 3									
0843	5.22	41N	20.6	37.± 5.0								
			20.5	11.(u/d 28%)								
0847	5.28	41S	20.4	32.± 2.9								
			20.3	9.(u/d 29%)								
0958	6.47	40S	20.8	27.± 4.3								
			20.8	8.(u/d 31%)								
1005	6.58	40N	21.1	24.± 2.3								
			21.0	5.(u/d 20%)								
1239	9.15	49S	20.9									.953
1411	10.68	31S	21.5	12.± 1.1								
			21.3	12.(u/d 93%)								

	Run #	Date	Time	Hours from Warm-up	Flexural Strength north	south	mean
FROM	1	05/03/88	1230	9.00	11.4	16.7	14.0
TO	2	05/03/88	1348	10.30	7.6	13.3	10.4

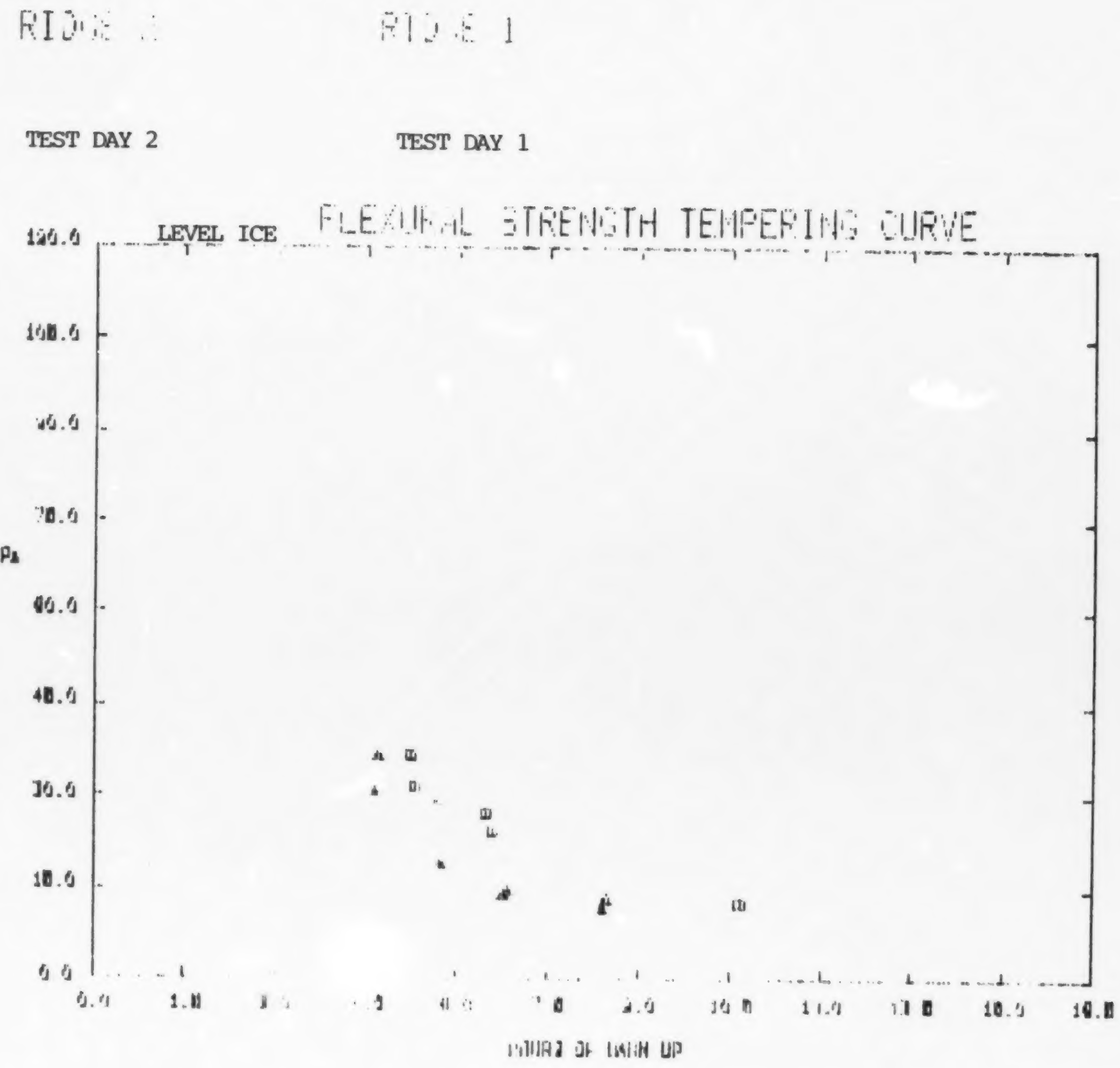RIDGE 2
RIDGE 1
TEST DAY 2
TEST DAY 1
LEVEL ICE
FLEXURAL STRENGTH TEMPERING CURVE
kPa
120.0
100.0
90.0
70.0
60.0
40.0
30.0
10.0
0.0
0.0
1.0
10.0
11.0
18.0
HOURS OF WARM UP

APPENDIX D.5

TEMPERATURE DATA

FLEET TECHNOLOGY LIMITED [FTL]

Engineering Design Calculations

JOB No. 3208
SHEET 1 OF 2
DATE MAY 4/93
BY A Comfort
CH'K BY

PROJECT RIDGE MODELLING
SUBJECT RIDGE TEMPERATURES (°C)

THERMOCOUPLE LOCATION	2130 MAY 2	0845 MAY 3	0945 MAY 3	11.35 MAY 3
1	-15.3	+0.9	0.0	-1.2
2	-7.4	+0.3	-0.5	-1.3
3	-1.1	0.0	-0.7	-1.4
4	-0.3	-0.2	-1.0	-1.2
5	-12.8	+0.2	-0.3	-1.3
6	-3.6	+0.4	-0.2	-1.3
7	-0.2	-0.3	-1.0	-1.2
8	-0.5	-0.5	-1.1	-1.3
9	-0.8	-0.3	-1.0	-1.2
10	-13.4	+1.4	+0.8	-2.7
11	-3.8	0.0	-0.7	-1.1
12	+0.4	+0.3	-0.6	-1.0
13	-0.2	+0.4	-0.3	-0.9
14	+0.2	+0.4	-0.3	-0.8
15	-13.0	+1.4	+0.7	-0.8
16	-0.6	-0.2	-1.0	-1.4
17	0.0	+0.2	-0.5	-1.1
18	0.0	+0.2	-0.5	-1.1

EVENT LOG:

2130 MAY 2 - RIDGES FORMED AND FREEZE #2 COMMENCED.
0330 MAY 3 - WARMUP COMMENCED
- INSULATION REMOVED FROM RIDGE SURFACE.
0930-1000 MAY 3 - RIDGES 2-4 AND 2-5 FORMED.

FLEET TECHNOLOGY LIMITED (FTL)

Engineering Design Calculations

JOB No. 3208
SHEET 2 OF 2
DATE May 4/88
BY R. Campbell
CH'K BY

PROJECT Ridge Modelling
SUBJECT Thermocouple Locations

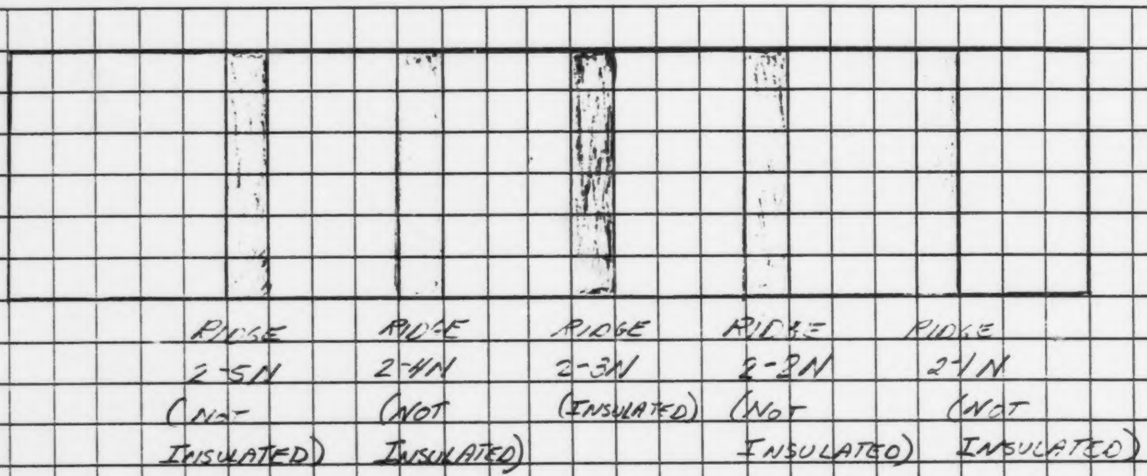
RIDGE 2-5N (NOT INSULATED)
RIDGE 2-4N (NOT INSULATED)
RIDGE 2-3N (INSULATED)
RIDGE 2-2N (NOT INSULATED)
RIDGE 2-1N (NOT INSULATED)

RIDGE 2-3N :

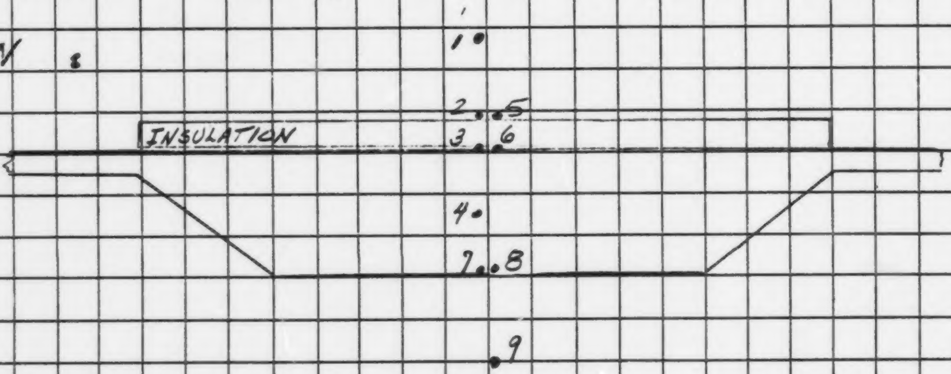
1
2 5
INSULATION
3 6
4
7 8
9

RIDGE 2-2N :

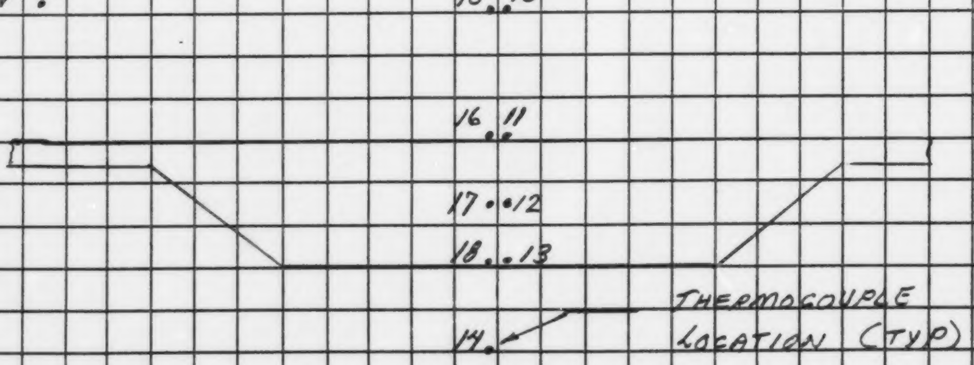
15 10
16 11
17 12
18 13
14
THERMOCOUPLE LOCATION (TYP)

APPENDIX E

RAW DATA FROM SHEET #3 TESTS AT THE IMD

CONTENTS:

E.1 Raw Time Histories For All Data Channels

E.2 Reduced Plots of Force vs. Penetration and Cumulative Penetration Energy - Test Data Filtered at 2 Hz

E.3 Reduced Plots of Force Vs. Penetration and Cumulative Penetration Energy - Test Data Filtered at 100 Hz

E.4 Ice and Ridge Properties

E.5 Temperature Data

APPENDIX E.1

SHEET #3 TESTS AT THE IMD: RAW TIME HISTORIES FOR ALL DATA CHANNELS

RUN_1 5-MAY-1988 14:10:54.28

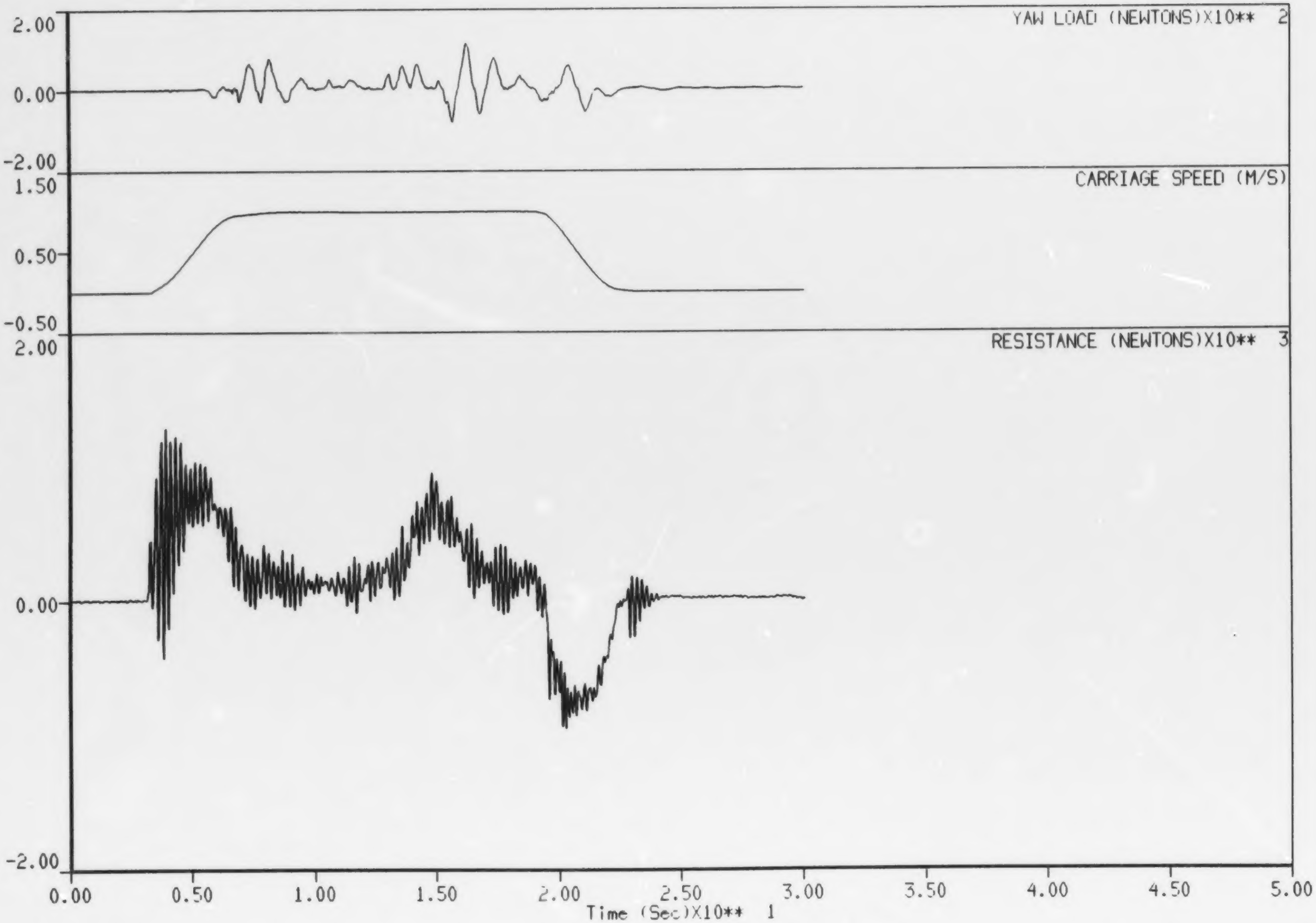

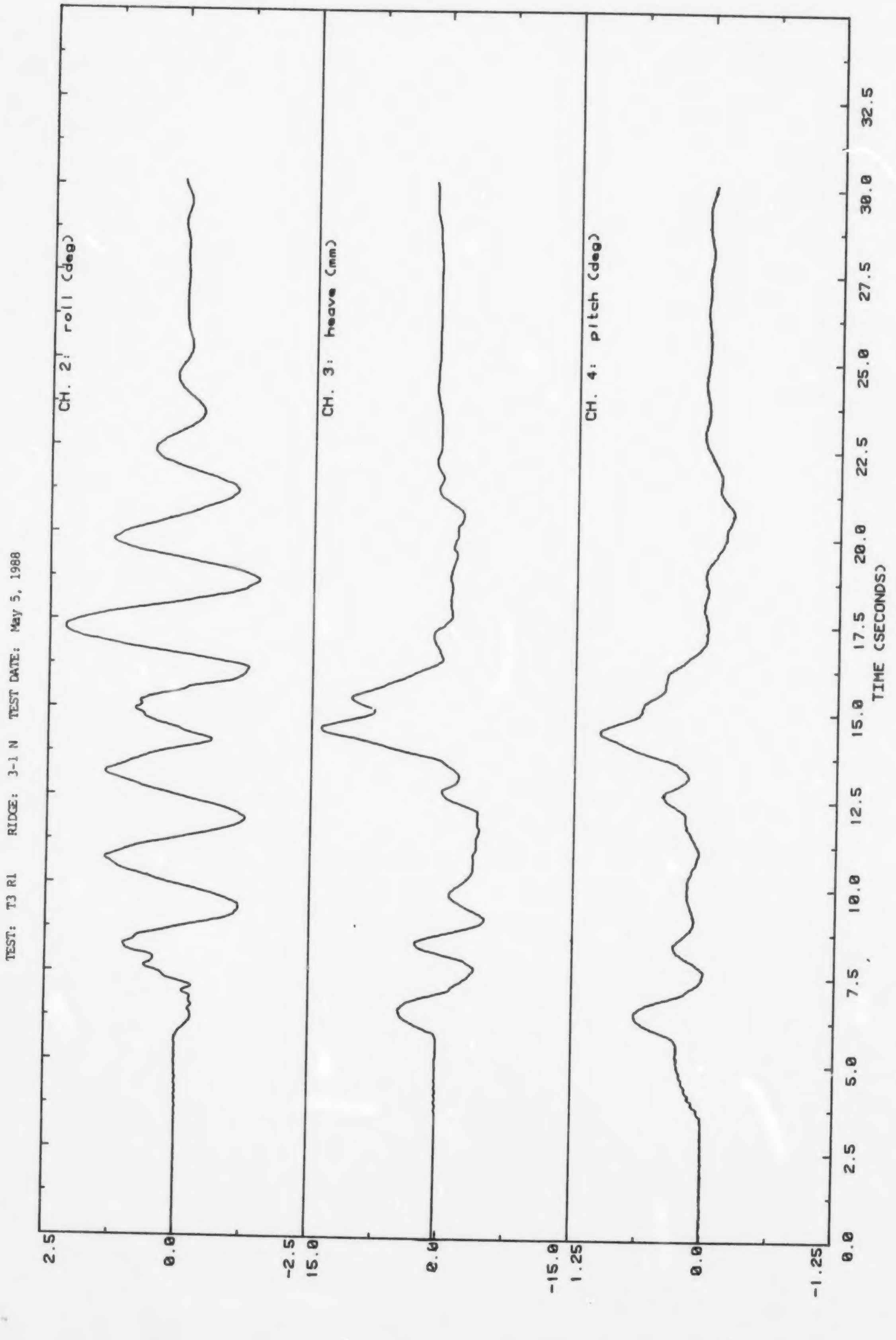
TEST: T3 R1   RIDGE: 3-1 N   TEST DATE: May 5, 1988
CH. 2: roll (deg)
CH. 3: heave (mm)
CH. 4: pitch (deg)
2.5
0.0
-2.5
15.0
0.0
-15.0
1.25
0.0
-1.25
0.0
2.5
5.0
7.5
10.0
12.5
15.0
17.5
20.0
22.5
25.0
27.5
30.0
32.5
TIME (SECONDS)

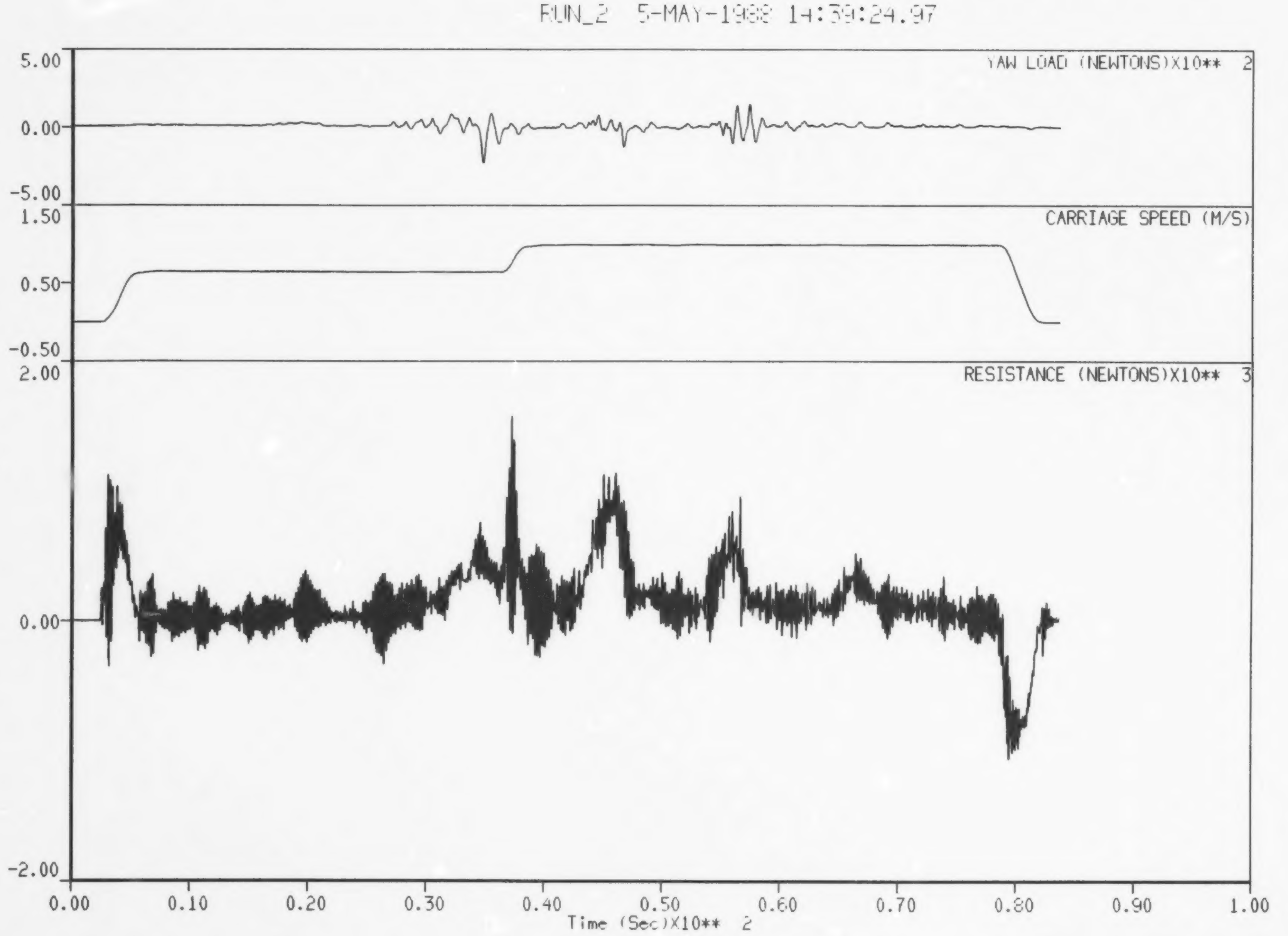
RUN_2 5-MAY-1988 14:39:24.97
YAW LOAD (NEWTONS)X10** 2
5.00
0.00
-5.00
CARRIAGE SPEED (M/S)
1.50
0.50
-0.50
RESISTANCE (NEWTONS)X10** 3
2.00
0.00
-2.00
0.00
0.10
0.20
0.30
0.40
0.50
0.60
0.70
0.80
0.90
1.00
Time (Sec)X10** 2

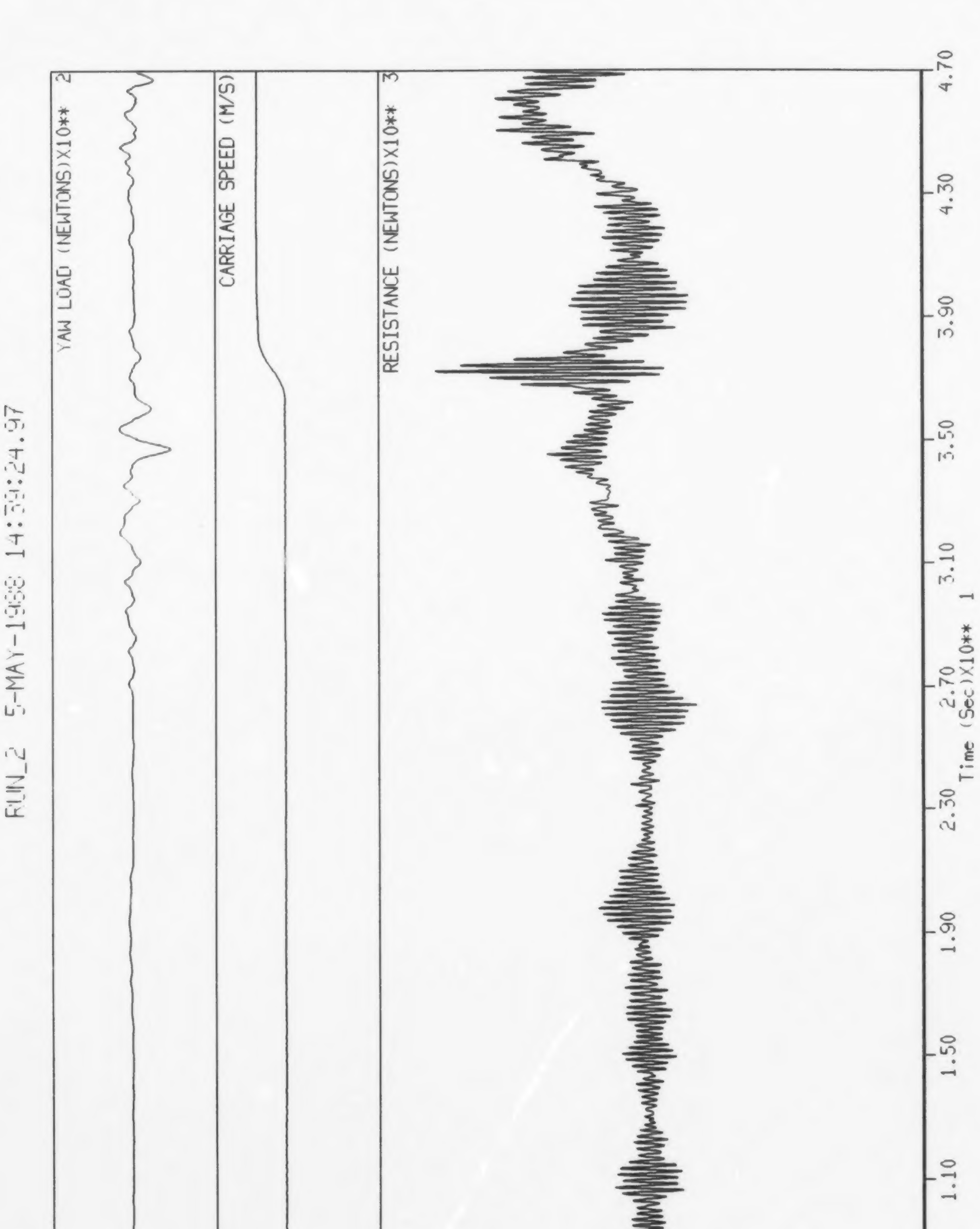
RUN_2 5-MAY-1988 14:39:24.97
YAW LOAD (NEWTONS)X10** 2
CARRIAGE SPEED (M/S)
RESISTANCE (NEWTONS)X10** 3
5.00
0.00
-5.00
1.50
0.50
-0.50
2.00
0.00
-2.00
0.70
1.10
1.50
1.90
2.30
2.70
3.10
3.50
3.90
4.30
4.70
Time (Sec)X10** 1

RUN_2 5-MAY-1988 14:39:24.97

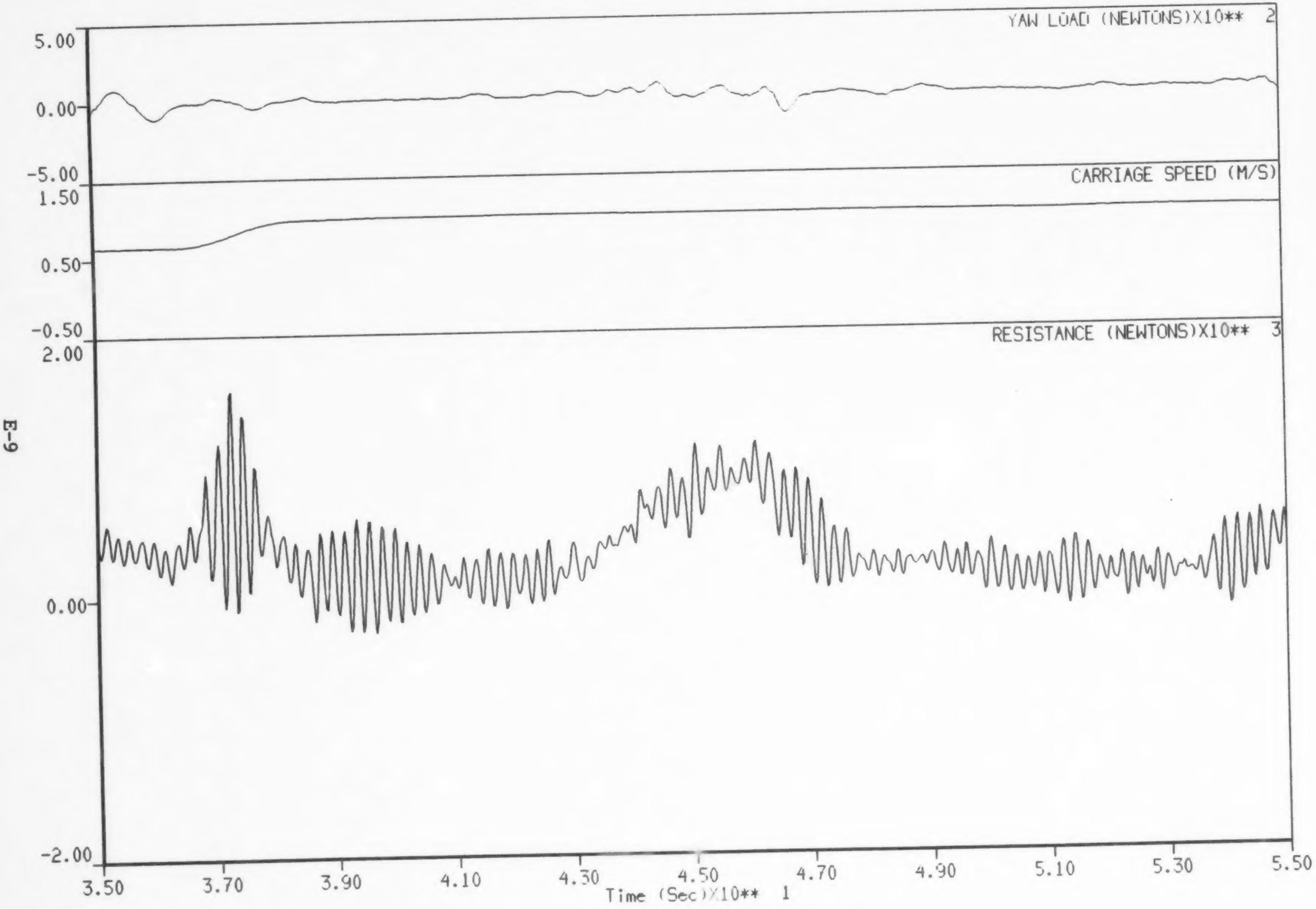

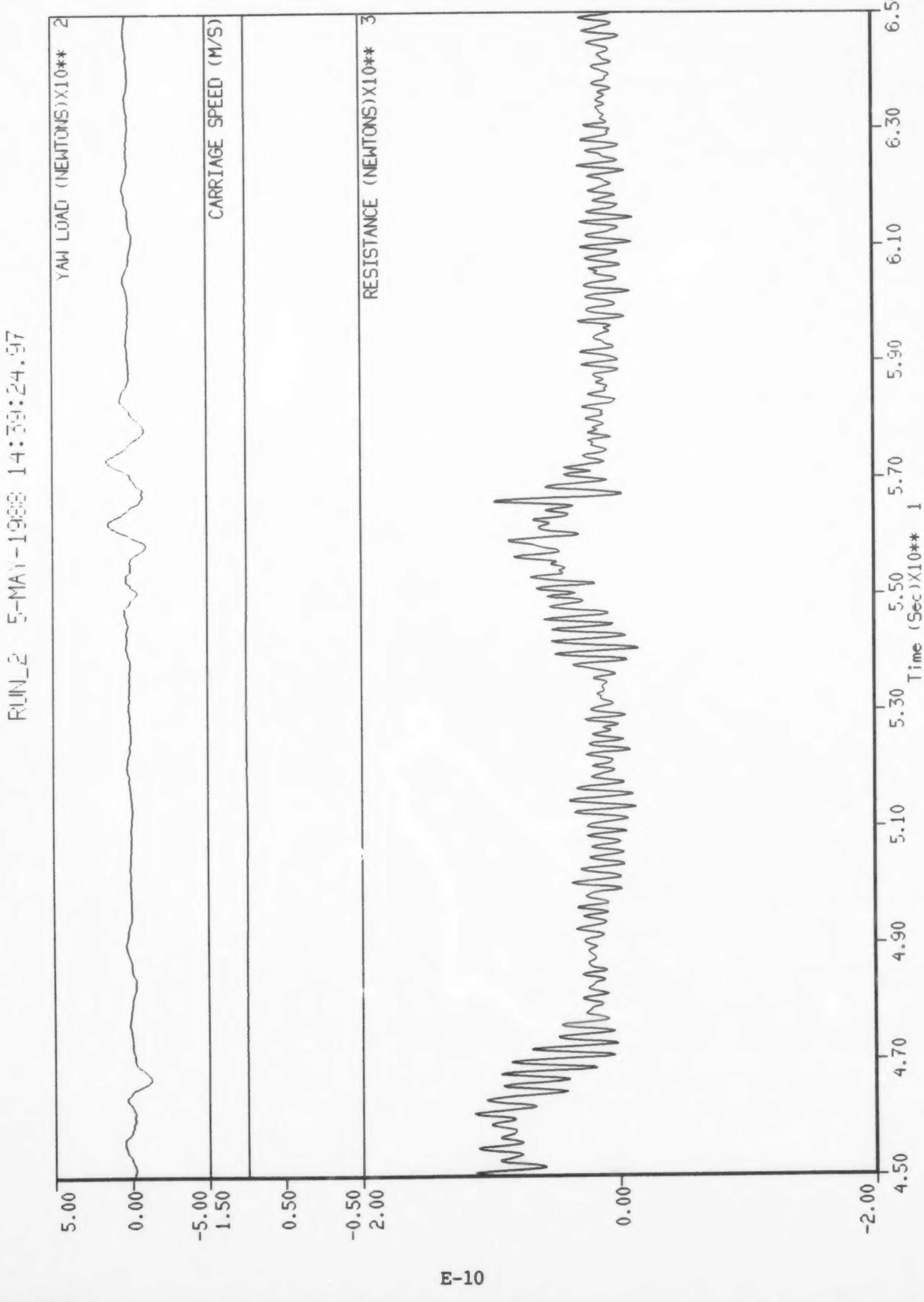
RUN_2 5-MAY-1988 14:39:24.97
YAW LOAD (NEWTONS)X10** 2
CARRIAGE SPEED (M/S)
RESISTANCE (NEWTONS)X10** 3
5.00
0.00
-5.00
1.50
0.50
-0.50
2.00
0.00
-2.00
4.50
4.70
4.90
5.10
5.30
5.50
5.70
5.90
6.10
6.30
6.50
Time (Sec)X10** 1

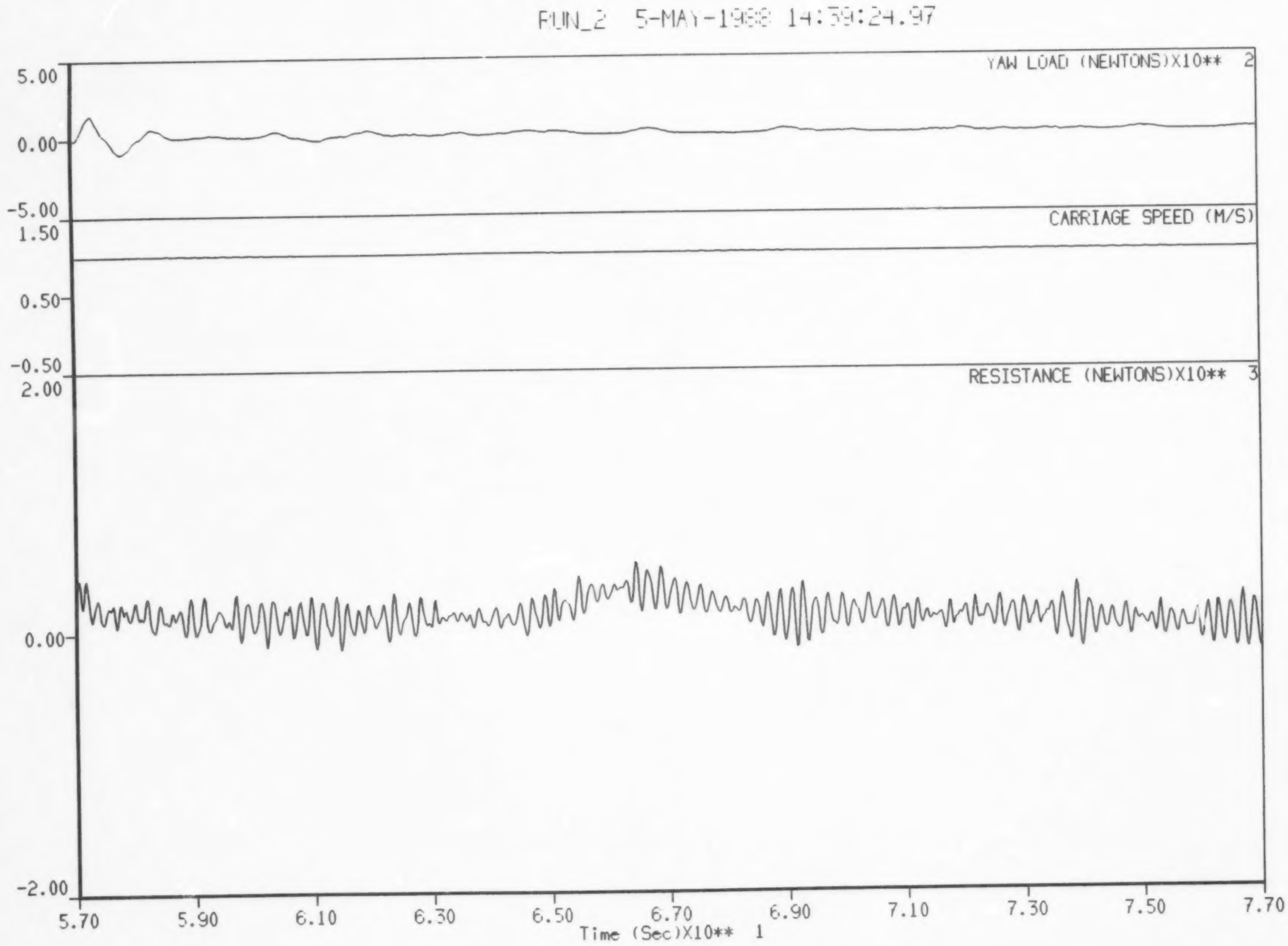
RUN_2 5-MAY-1988 14:59:24.97
YAW LOAD (NEWTONS)X10** 2
CARRIAGE SPEED (M/S)
RESISTANCE (NEWTONS)X10** 3
5.00
0.00
-5.00
1.50
0.50
-0.50
2.00
0.00
-2.00
5.70
5.90
6.10
6.30
6.50
6.70
6.90
7.10
7.30
7.50
7.70
Time (Sec)X10** 1

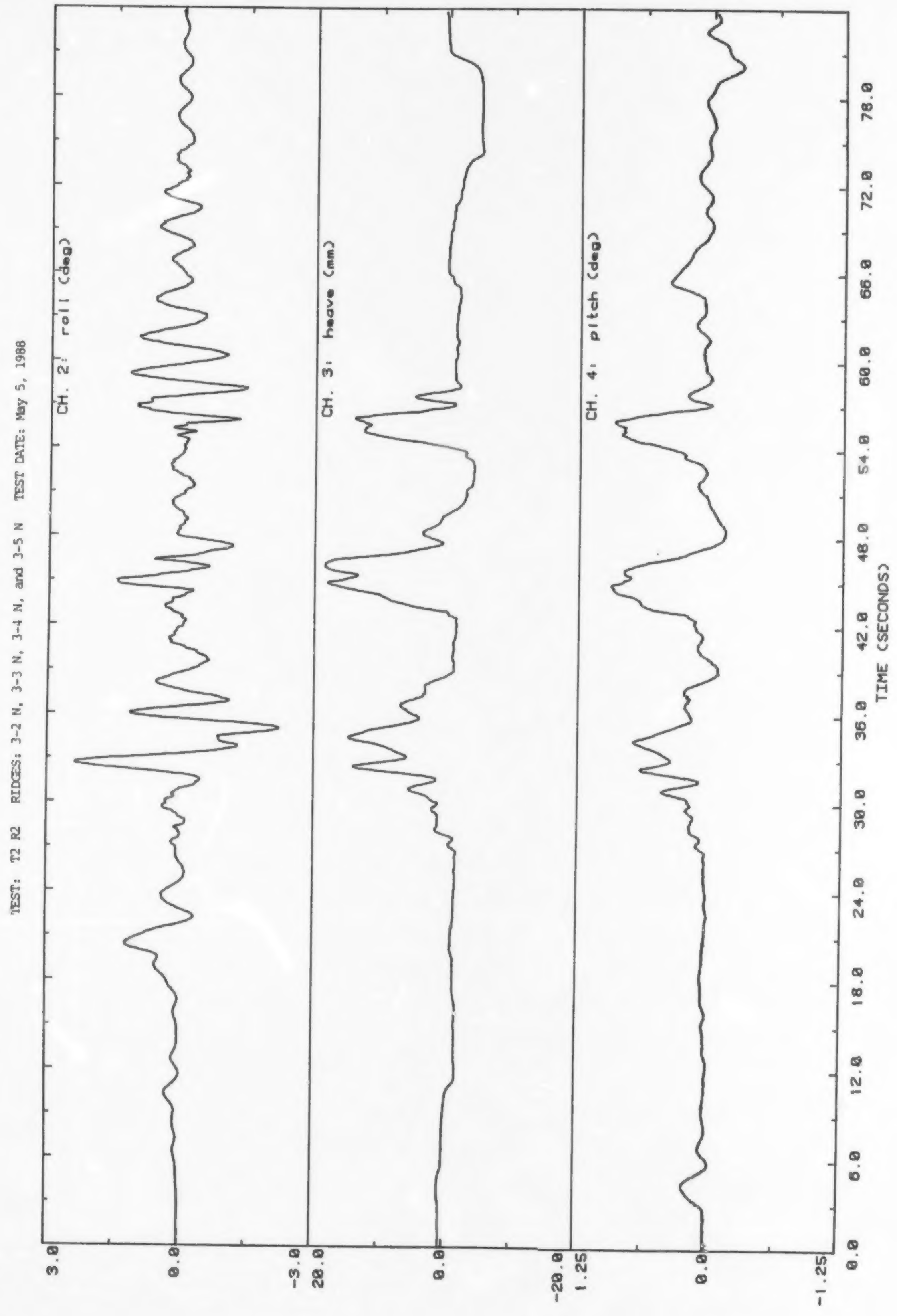
TEST: T2 R2 RIDGES: 3-2 N, 3-3 N, 3-4 N, and 3-5 N TEST DATE: May 5, 1988

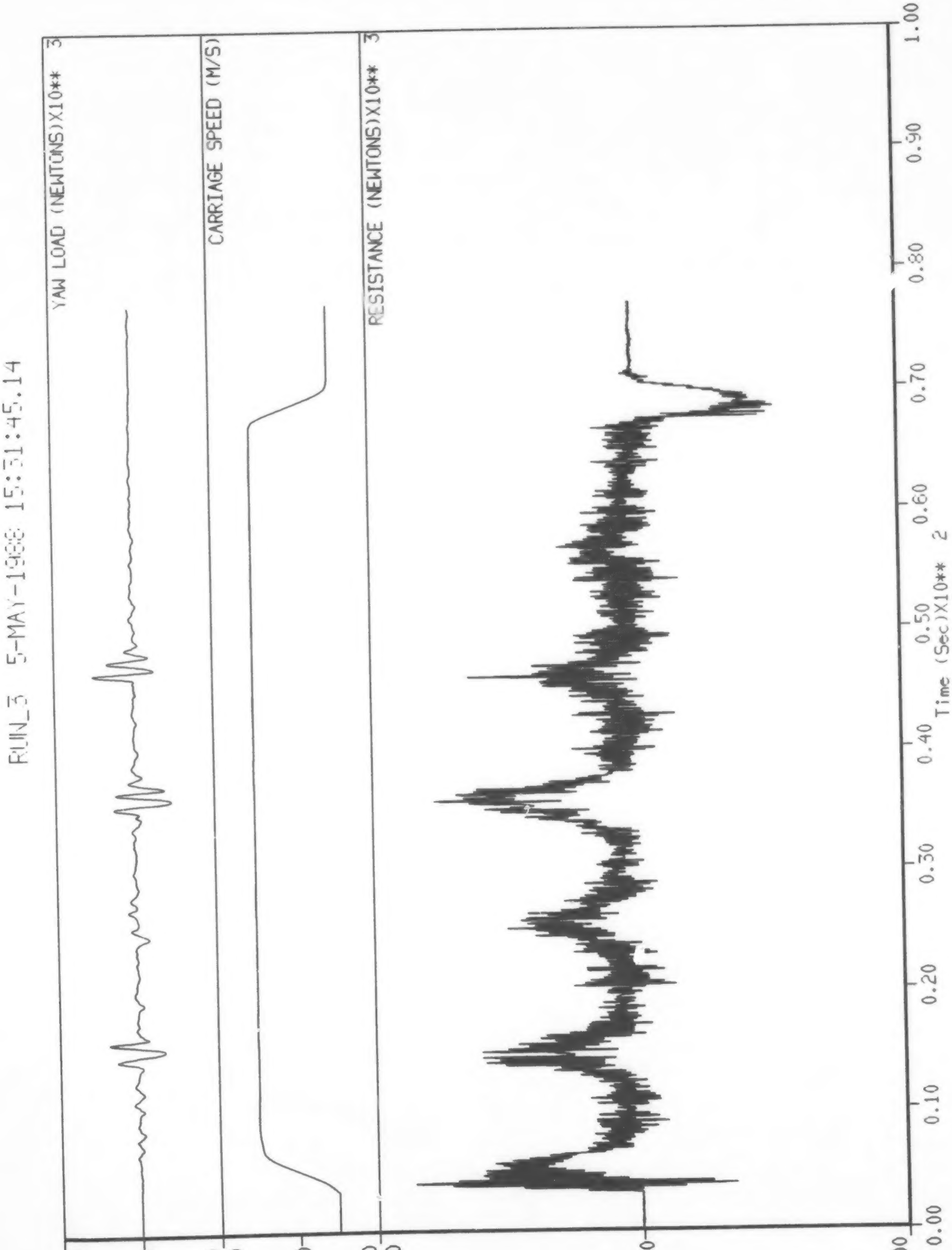
RUN_3 5-MAY-1988 15:31:45.14
YAW LOAD (NEWTONS)X10** 3
CARRIAGE SPEED (M/S)
RESISTANCE (NEWTONS)X10** 3
1.00
0.00
-1.00
1.50
0.50
-0.50
2.00
0.00
-2.00
0.00
0.10
0.20
0.30
0.40
0.50
0.60
0.70
0.80
0.90
1.00
Time (Sec)X10** 2

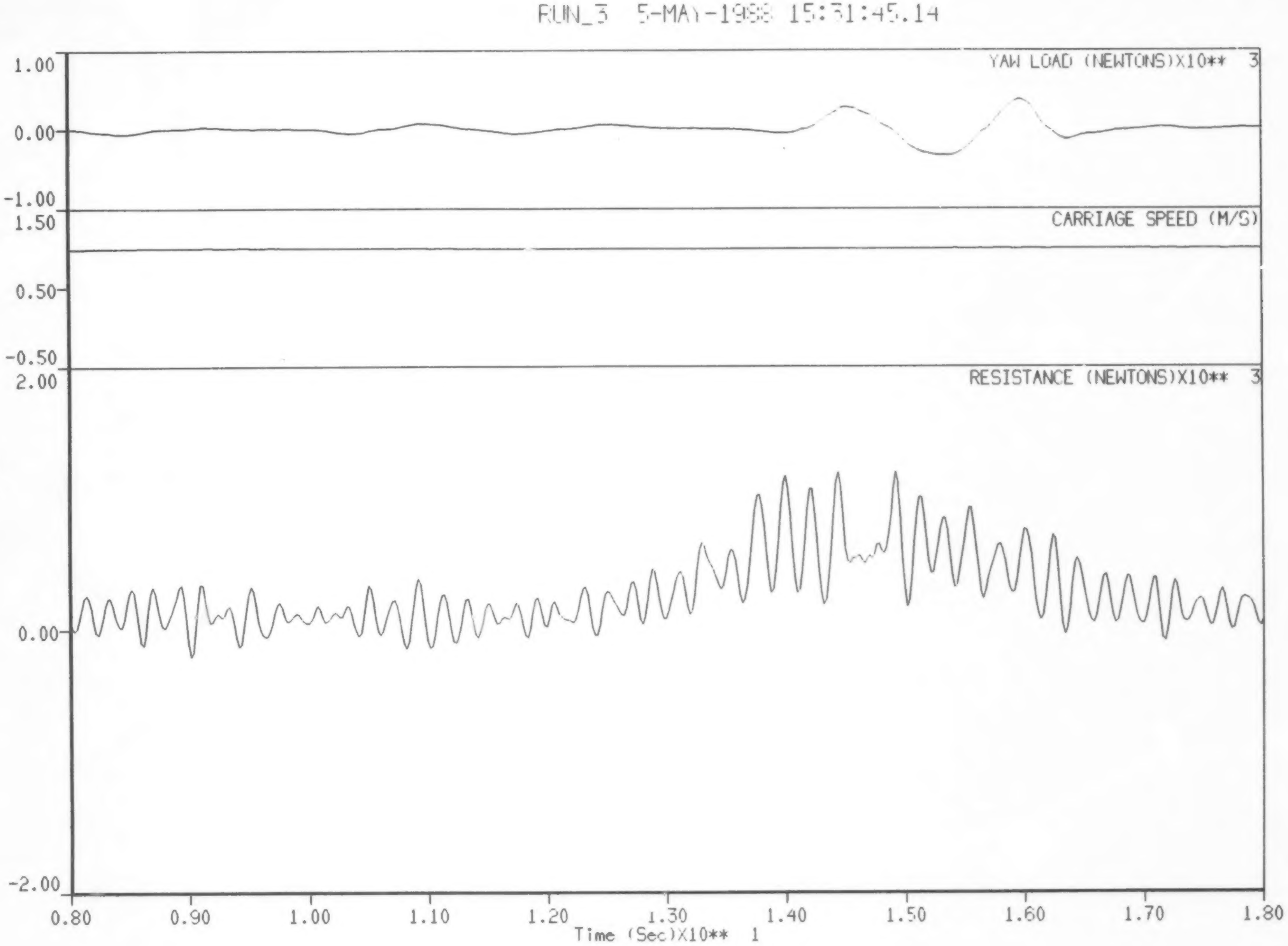
RUN_3 5-MAY-1988 15:31:45.14
YAW LOAD (NEWTONS)X10** 3
CARRIAGE SPEED (M/S)
RESISTANCE (NEWTONS)X10** 3
1.00
0.00
-1.00
1.50
0.50
-0.50
2.00
0.00
-2.00
0.80
0.90
1.00
1.10
1.20
1.30
1.40
1.50
1.60
1.70
1.80
Time (Sec)X10** 1

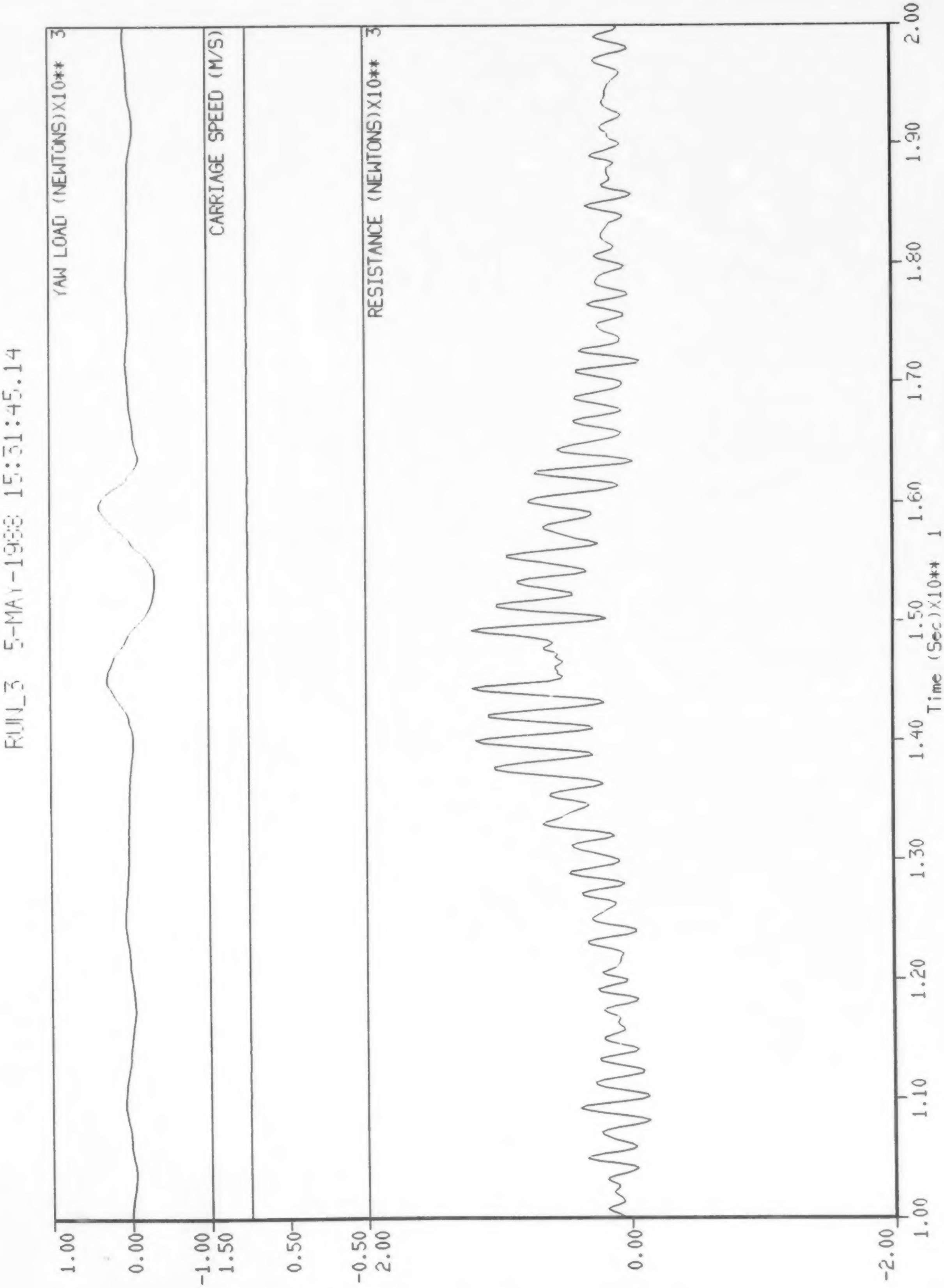
RUN_3 5-MAY-1988 15:31:45.14
YAW LOAD (NEWTONS)X10** 3
CARRIAGE SPEED (M/S)
RESISTANCE (NEWTONS)X10** 3
1.00
0.00
-1.00
1.50
0.50
-0.50
2.00
0.00
-2.00
1.00
1.10
1.20
1.30
1.40
1.50
1.60
1.70
1.80
1.90
2.00
Time (Sec)X10** 1

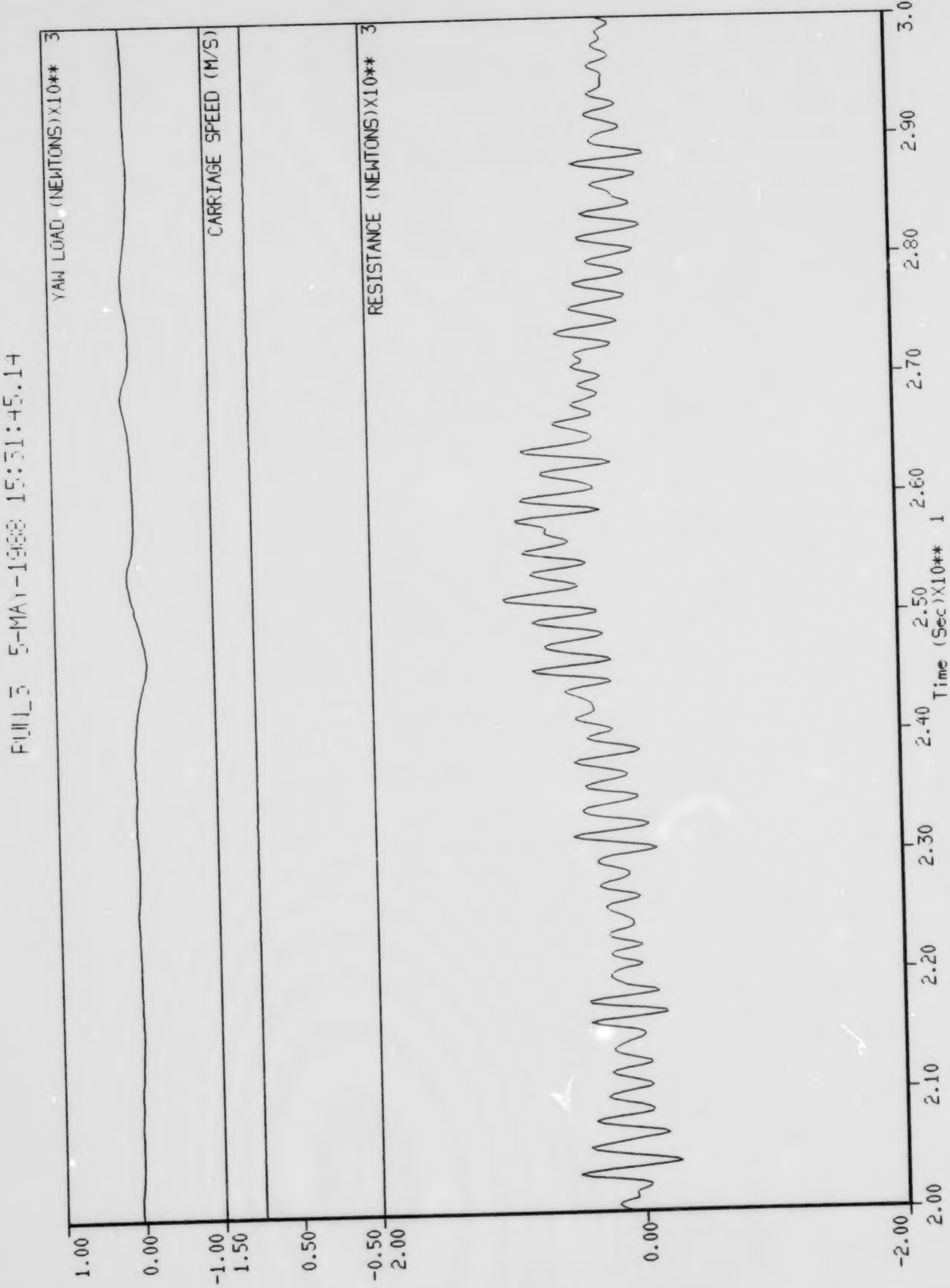
RUN_5 5-MAY-1988 15:31:45.14
YAW LOAD (NEWTONS)X10** 3
CARRIAGE SPEED (M/S)
RESISTANCE (NEWTONS)X10** 3
1.00
0.00
-1.00
1.50
0.50
-0.50
2.00
0.00
-2.00
2.00
2.10
2.20
2.30
2.40
2.50
2.60
2.70
2.80
2.90
3.00
Time (Sec)X10** 1

RUN_3 5-MAY-1988 15:31:45.14

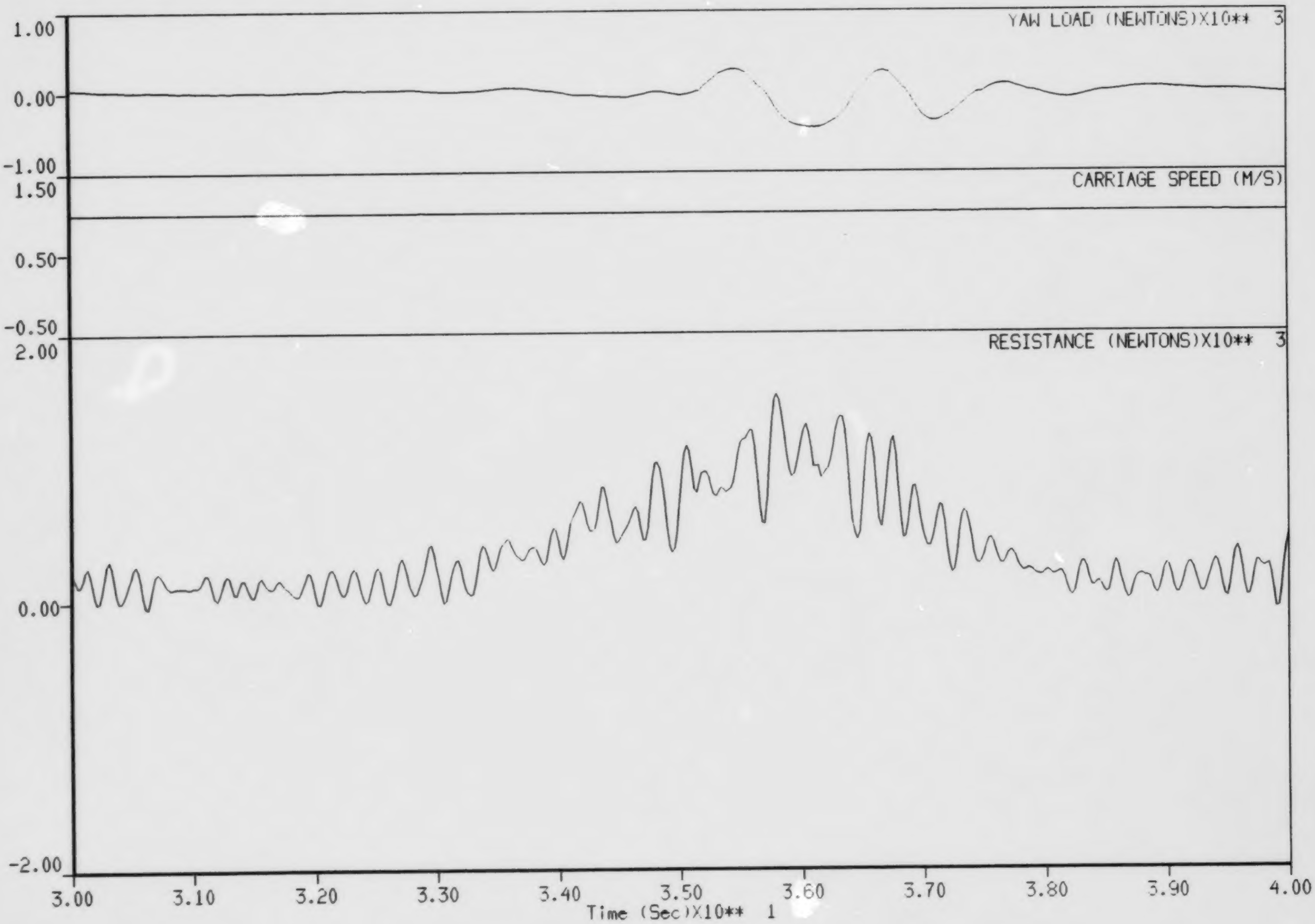

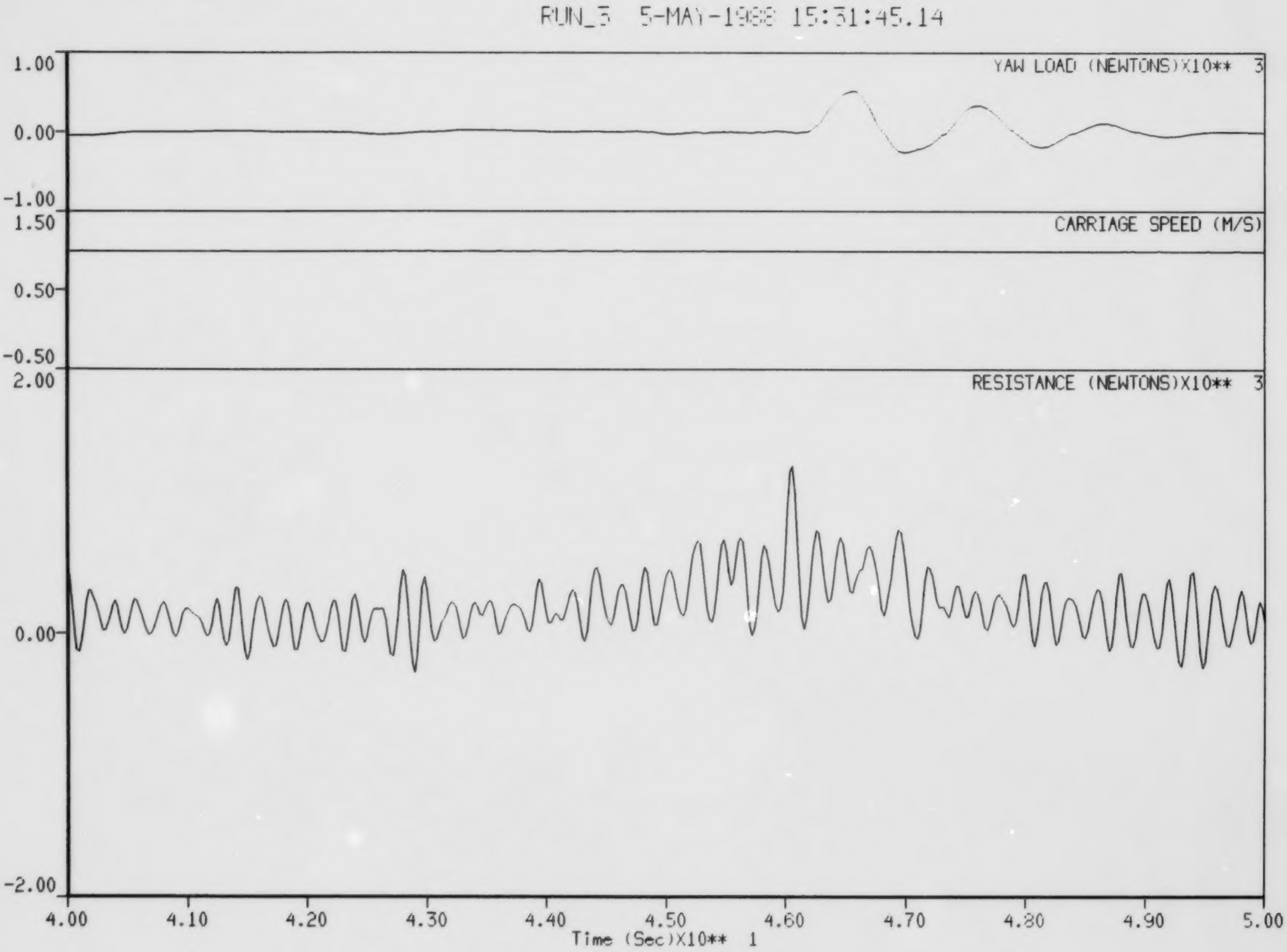
RUN_3 5-MAY-1988 15:31:45.14
YAW LOAD (NEWTONS)X10** 3
1.00
0.00
-1.00
CARRIAGE SPEED (M/S)
1.50
0.50
-0.50
RESISTANCE (NEWTONS)X10** 3
2.00
0.00
-2.00
4.00
4.10
4.20
4.30
4.40
4.50
4.60
4.70
4.80
4.90
5.00
Time (Sec)X10** 1

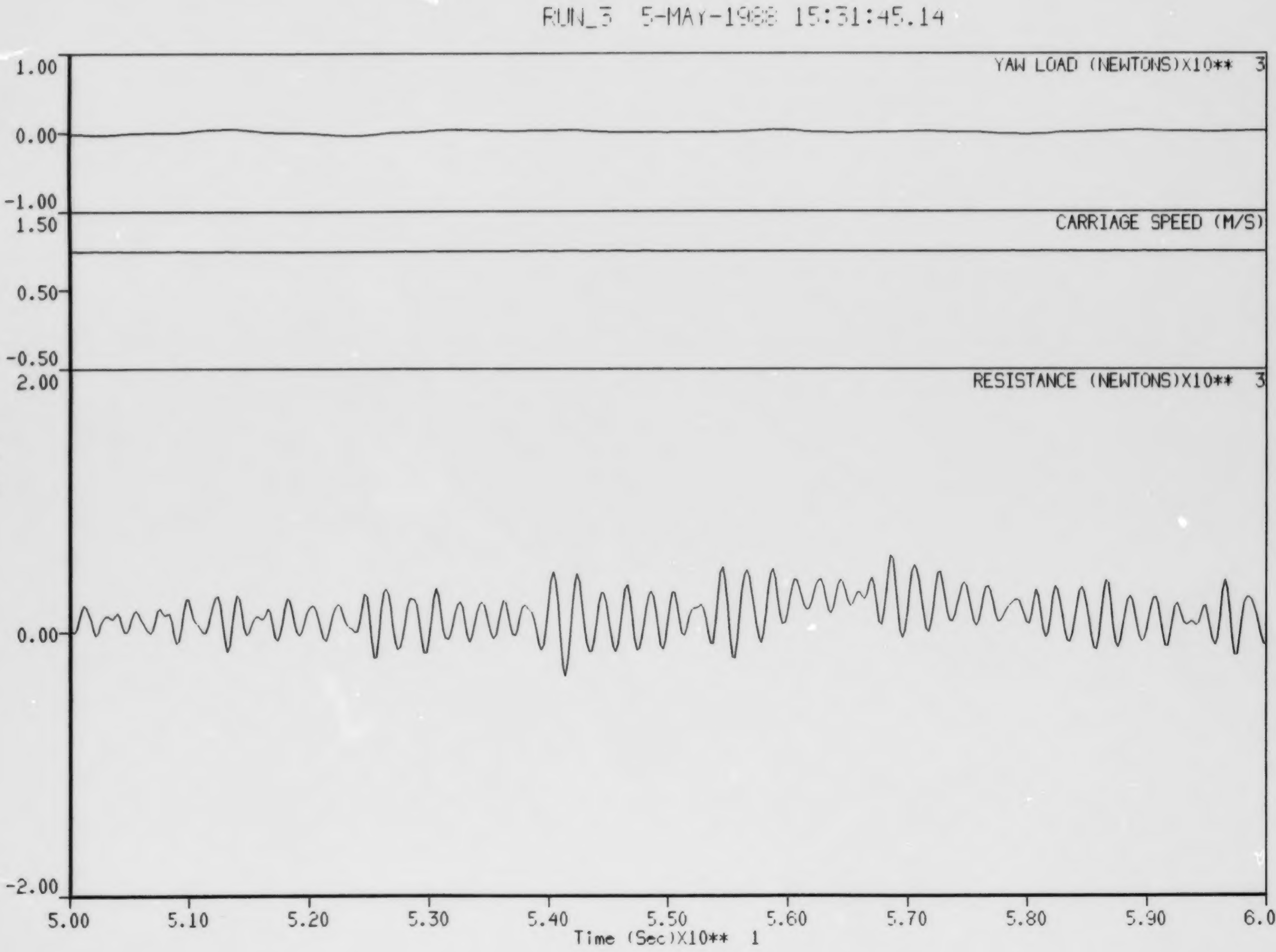
RUN_3 5-MAY-1988 15:31:45.14
YAW LOAD (NEWTONS)X10** 3
CARRIAGE SPEED (M/S)
RESISTANCE (NEWTONS)X10** 3
1.00
0.00
-1.00
1.50
0.50
-0.50
2.00
0.00
-2.00
5.00
5.10
5.20
5.30
5.40
5.50
5.60
5.70
5.80
5.90
6.00
Time (Sec)X10** 1

TEST: T3 R3 RIDGES: 3-1 S, 3-2 S, 3-3 S, and 3-4 S TEST DATE: May 5, 1988

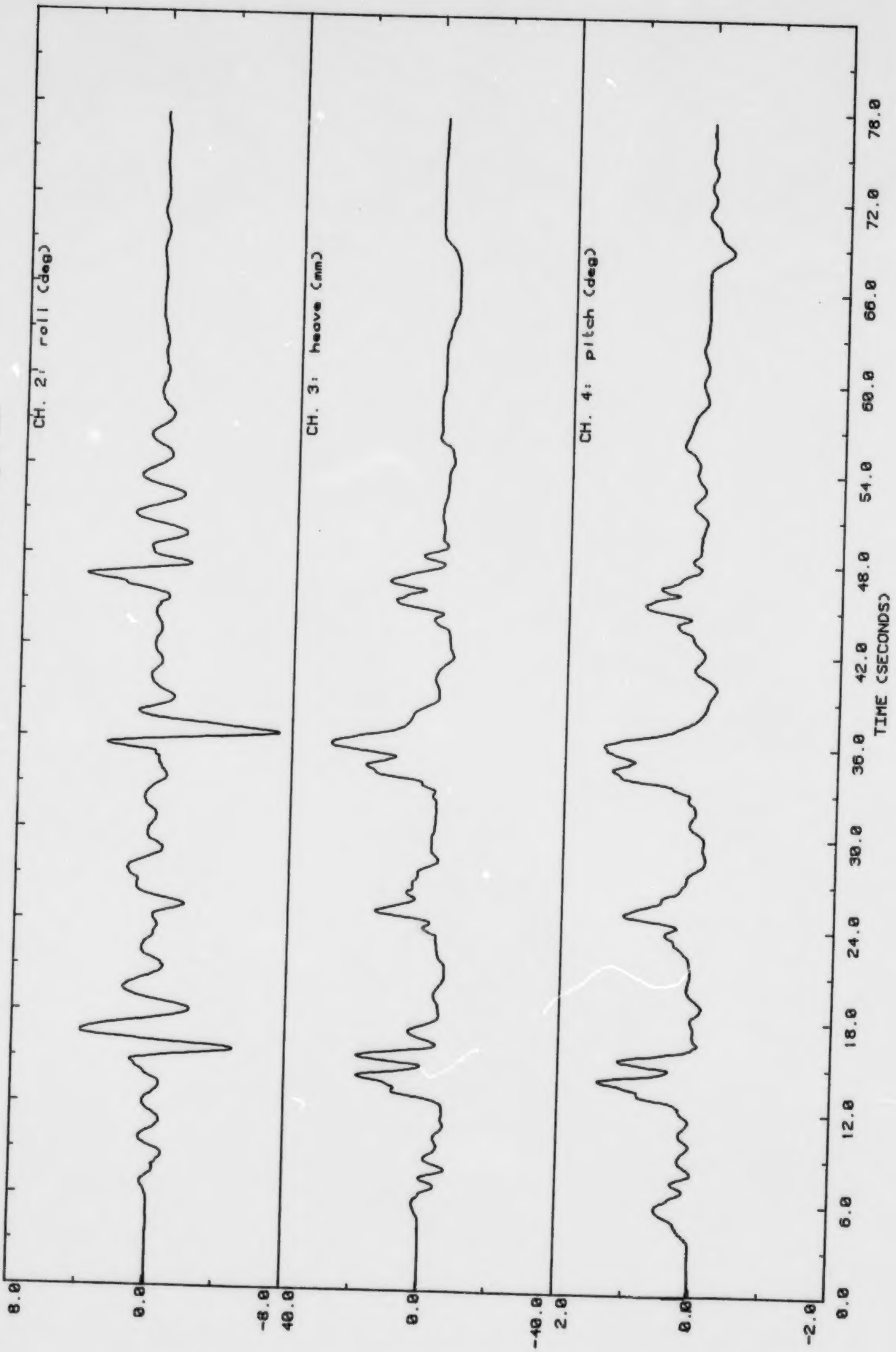

RUN_4 5-MAY-1988 18:42:53.97

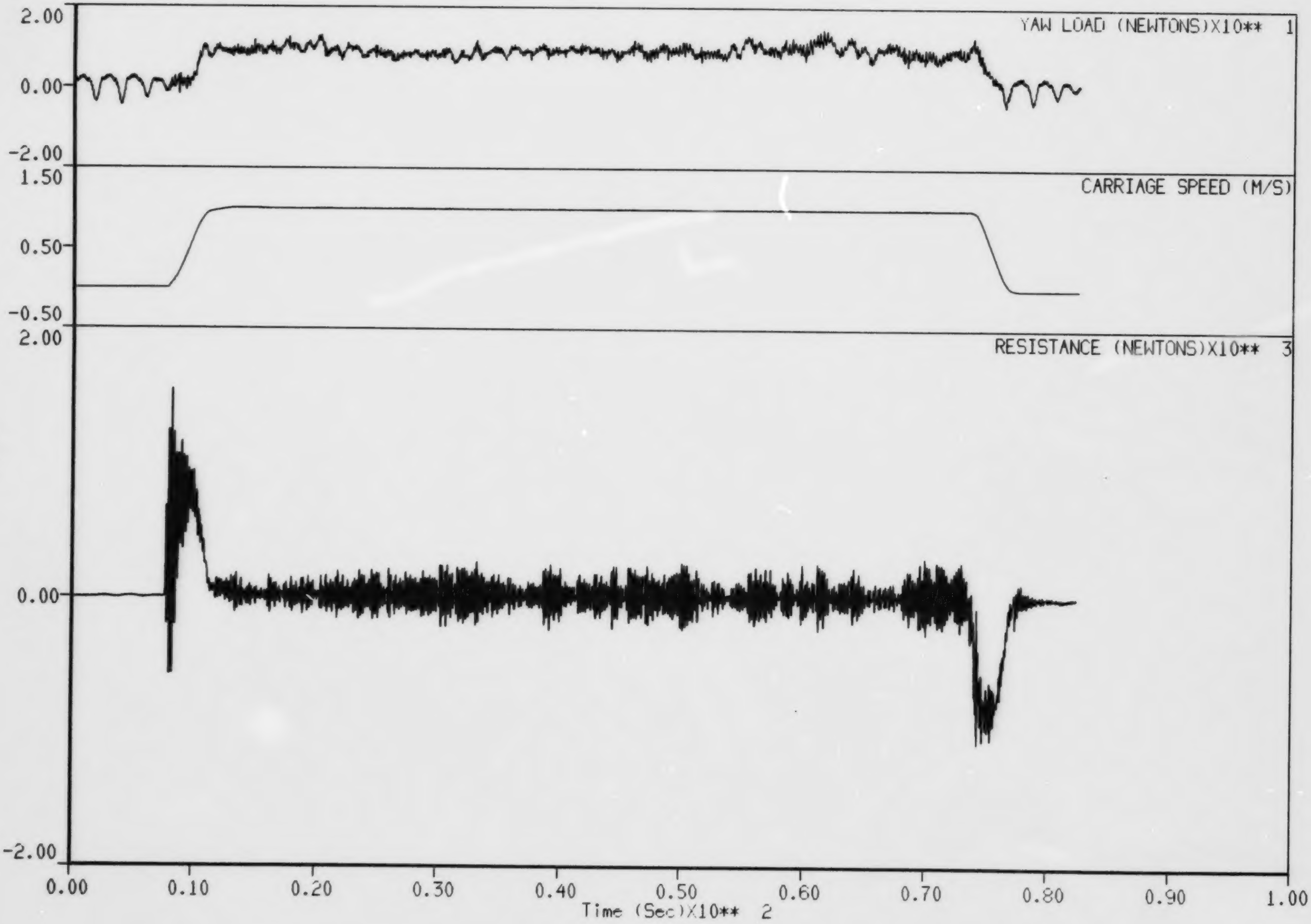

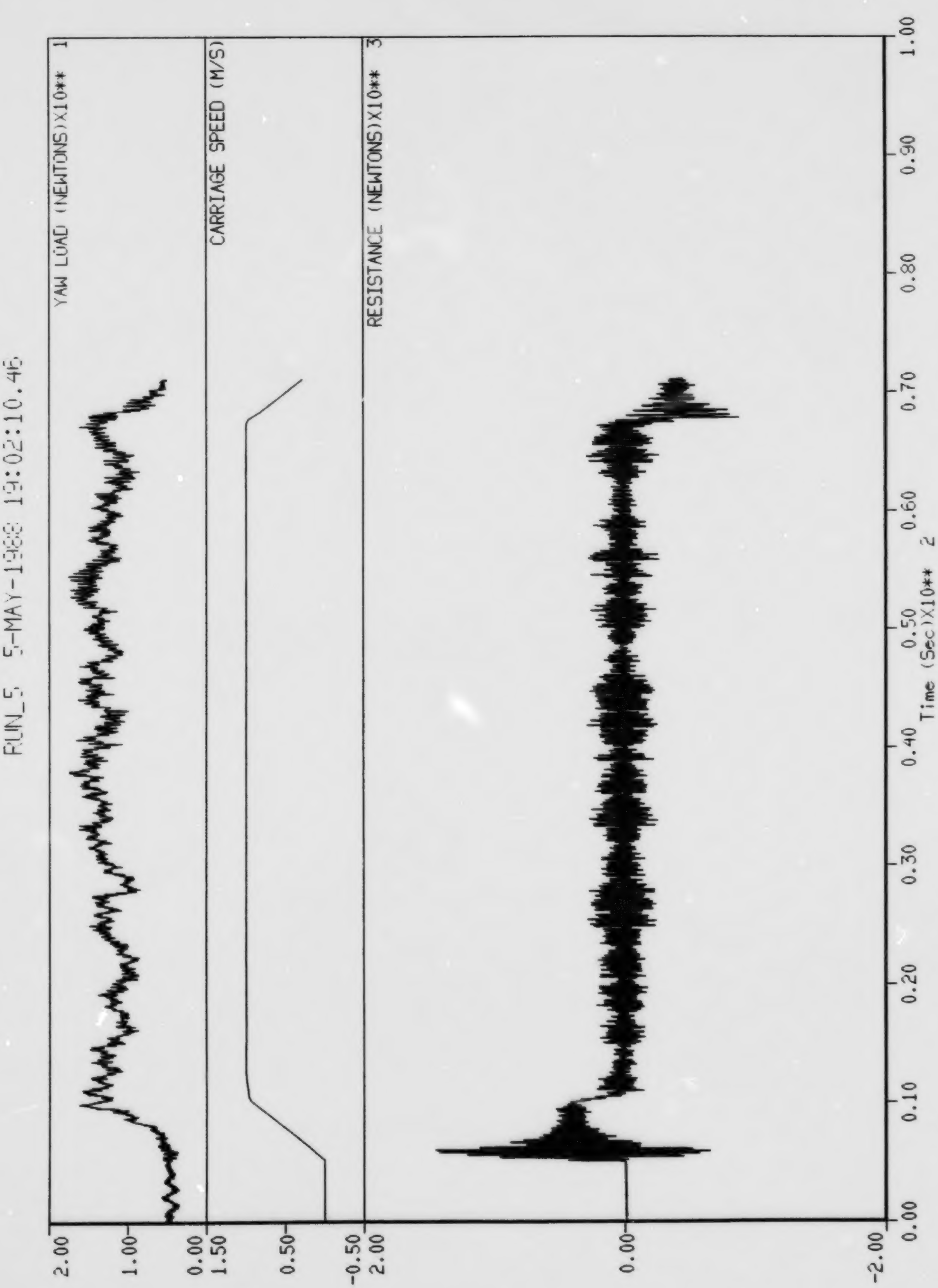
RUN_5 5-MAY-1988 19:02:10.46
YAW LOAD (NEWTONS)X10** 1
2.00
1.00
0.00
CARRIAGE SPEED (M/S)
1.50
0.50
-0.50
RESISTANCE (NEWTONS)X10** 3
2.00
0.00
-2.00
0.00
0.10
0.20
0.30
0.40
0.50
0.60
0.70
0.80
0.90
1.00
Time (Sec)X10** 2

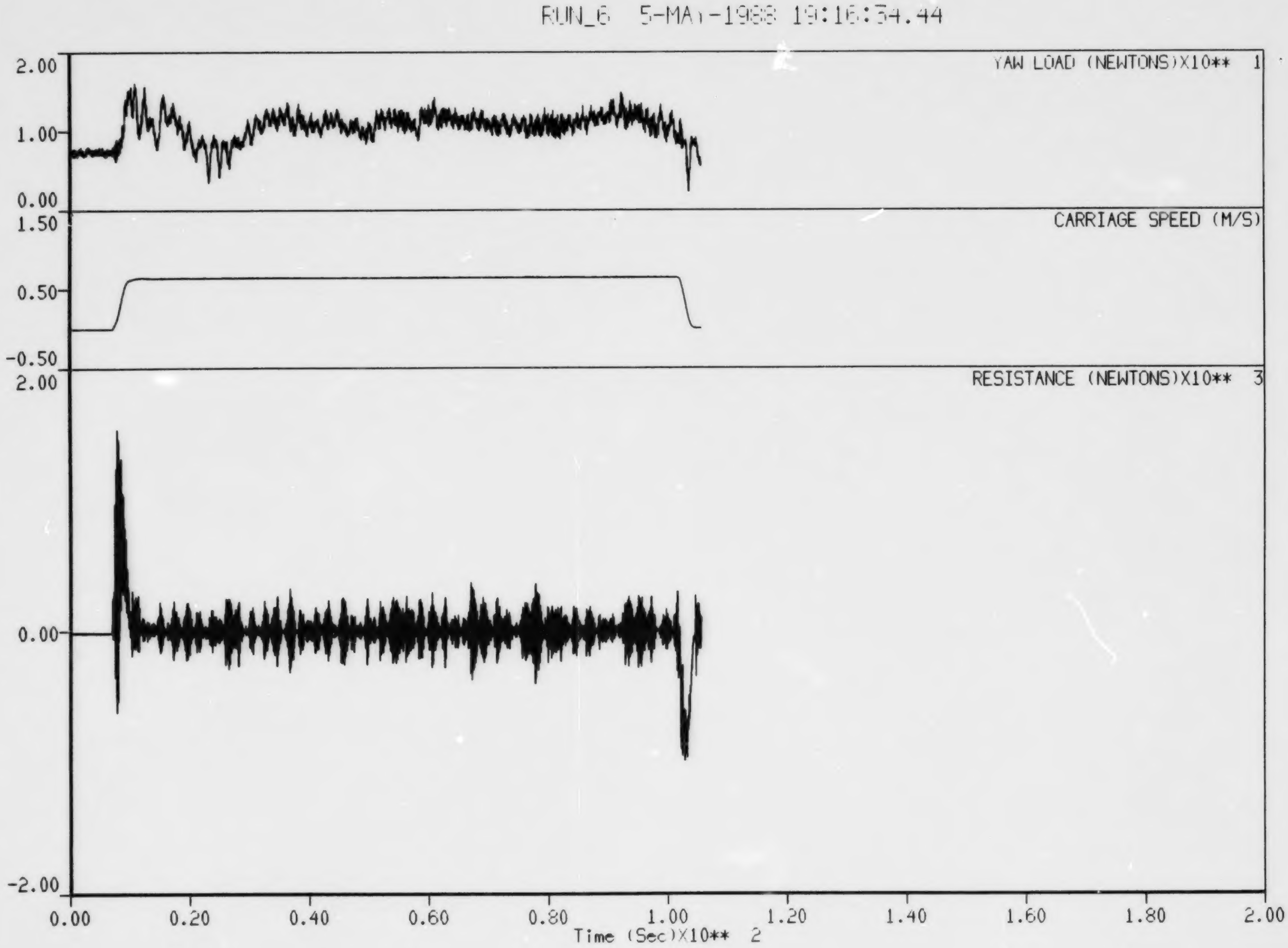
RUN_6 5-MAY-1988 19:16:34.44
YAW LOAD (NEWTONS)X10** 1
2.00
1.00
0.00
CARRIAGE SPEED (M/S)
1.50
0.50
-0.50
RESISTANCE (NEWTONS)X10** 3
2.00
0.00
-2.00
0.00
0.20
0.40
0.60
0.80
1.00
1.20
1.40
1.60
1.80
2.00
Time (Sec)X10** 2

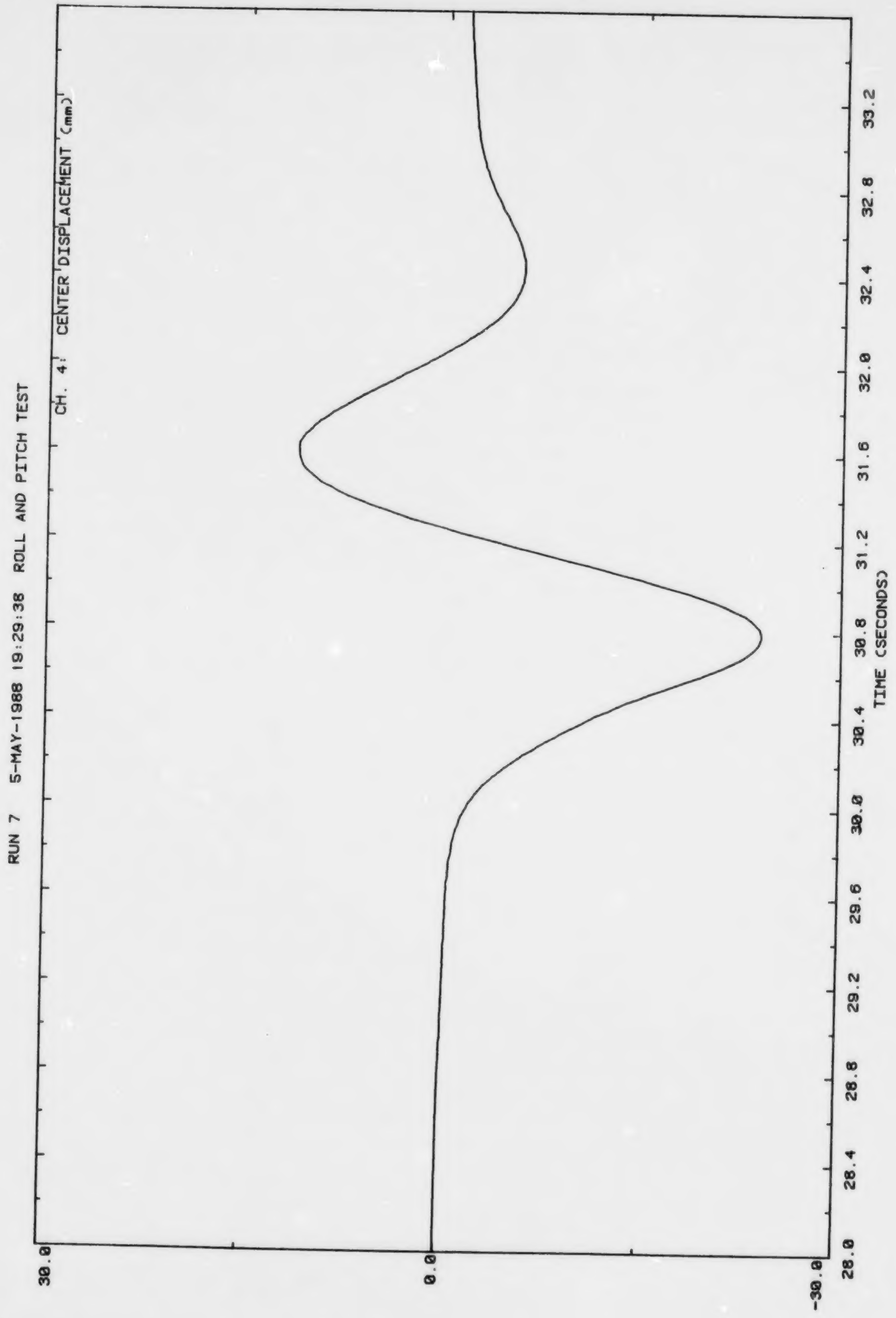
RUN 7 5-MAY-1988 19:29:38 ROLL AND PITCH TEST
CH. 4: CENTER DISPLACEMENT (mm)
30.0
0.0
-30.0
28.0
28.4
28.8
29.2
29.6
30.0
30.4
30.8
31.2
31.6
32.0
32.4
32.8
33.2
TIME (SECONDS)

RUN 7 5-MAY-1988 19:29:38 ROLL AND PITCH TEST

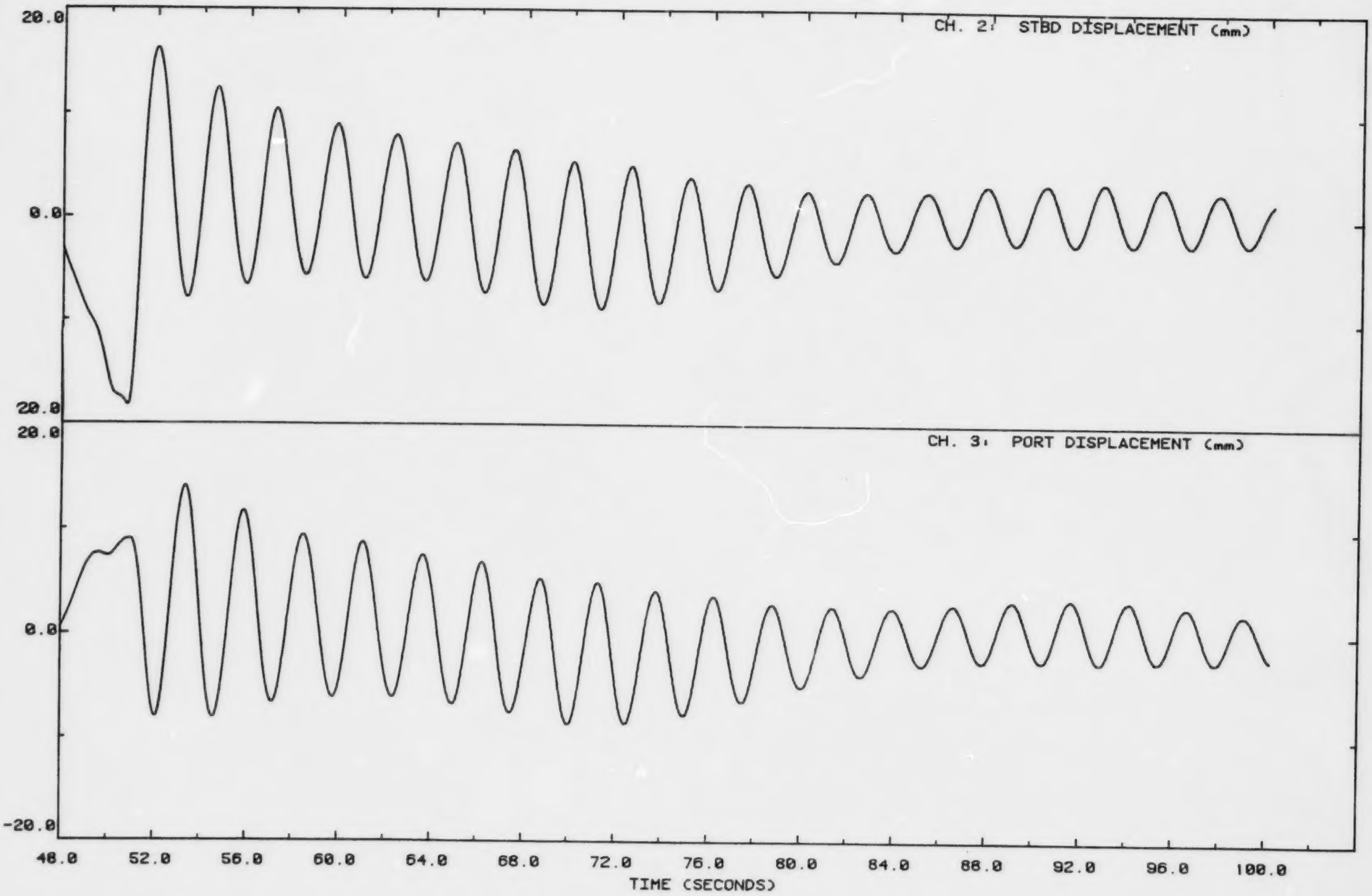

APPENDIX E.2

SHEET #3 TESTS AT THE IMD: REDUCED PLOTS OF FORCE VS. PENETRATION AND CUMULATIVE PENETRATION ENERGY - TEST DATA FILTERED AT 2 HZ

MODEL SCALE RIDGE START POINT PENETRATION DISTANCES USED FOR REDUCTION OF PLOTS OF CUMULATIVE PENETRATION ENERGY VS. PENETRATION DISTANCE

RIDGE	PENETRATION (m) AT WHICH THE BOW WAS CONSIDERED TO FIRST CONTACT THE RIDGE
1-1	1.7
1-4	0.7
2-1 N	3.4
2-2 N	2.4
2-3 N	1.4
2-4 N	2.2
2-5 N	3.3
2-1 S	2.1
2-2 S	2.0
2-3 S	2.0
2-4 S	2.0
3-1 N	2.0
3-2 N	3.8
3-3 N	1.3
3-4 N	3.4
3-5 N	2.8
3-1 S	2.0
3-2 S	2.0
3-3 S	2.0
3-4 S	0

```
TEST:     T3R1            RIDGE:3-1N

DISTANCE,M                 FORCE,N      CUM. ENERGY,N-M
   0.00                      112              0
    .91                      110            113
   1.82                      117            216
   2.72                      169            349
   3.63                      283            543
   4.53                      541            944
   5.44                      541           1538
   6.35                      365           2005
   7.26                      196           2243
   8.17                      150           2384
   9.07                      171           2532

PENETRATION OF   5.04 M AT MAX FORCE OF    752 N
PENETRATION OF   9.17 M AT MAX ENERGY OF  2547 N-M
```

```
TEST:     T3R2            RIDGE:3-2N

DISTANCE,M                 FORCE,N      CUM. ENERGY,N-M
   0.00                       33              0
    .65                       56             26
   1.30                       96             76
   1.95                      117            153
   2.61                      127            237
   3.26                      158            336
   3.91                      198            443
   4.57                      371            652
   5.22                      425            877
   5.87                      514           1210
   6.53                      371           1486

PENETRATION OF   5.68 M AT MAX FORCE OF    542 N
PENETRATION OF   6.72 M AT MAX ENERGY OF  1552 N-M
```

```
TEST:     T3R2            RIDGE:3-3N

DISTANCE,M                 FORCE,N      CUM. ENERGY,N-M
   0.00                      125              0
    .90                      121            111
   1.81                      208            274
   2.72                      594            626
   3.62                      739           1247
   4.52                      910           2023
   5.42                      581           2734
   6.32                      223           3055
   7.23                      204           3232
   8.14                      189           3422
   9.04                      106           3565

PENETRATION OF   4.62 M AT MAX FORCE OF    962 N
PENETRATION OF   9.24 M AT MAX ENERGY OF  3583 N-M
```

```
TEST:      T3R2            RIDGE:3-4N

DISTANCE,M              FORCE,N      CUM. ENERGY,N-M
    0.00                  144                 0
    1.10                  113               119
    2.20                   92               249
    3.31                  121               373
    4.42                  300               593
    5.52                  610              1090
    6.62                  289              1675
    7.73                  162              1913
    8.83                  104              2055
    9.93                  112              2184
   11.04                   94              2300

PENETRATION OF   5.72 M AT MAX FORCE OF    652 N
PENETRATION OF  11.14 M AT MAX ENERGY OF  2310 N-M


TEST:      T3R2            RIDGE:3-5N

DISTANCE,M              FORCE,N      CUM. ENERGY,N-M
    0.00                   81                 0
    1.40                  113               148
    2.81                  108               298
    4.22                  296               560
    5.62                  264              1001
    7.03                  144              1273
    8.43                  131              1438
    9.83                   96              1610
   11.24                  102              1758
   12.65                   67              1882

PENETRATION OF   4.82 M AT MAX FORCE OF    344 N
PENETRATION OF  13.85 M AT MAX ENERGY OF  1944 N-M


TEST:      T3R2            RIDGE:3-2345N

DISTANCE,M              FORCE,N      CUM. ENERGY,N-M
    0.00                   13                 0
    4.18                   69               124
    8.35                   35               389
   12.53                  179               795
   16.84                  616              2575
   23.21                  512              3911
   29.63                  106              6905
   36.06                  289              8555
   42.47                  110              9387
   48.90                  115             10606

PENETRATION OF  25.21 M AT MAX FORCE OF    962 N
PENETRATION OF  55.12 M AT MAX ENERGY OF 11174 N-M
```

```
TEST:     T3R3           RIDGE:3-1S

DISTANCE,M                FORCE,N      CUM. ENERGY,N-M
   0.00                      98                 0
   1.11                      75               112
   2.21                     144               222
   3.31                     483               495
   4.42                     721              1178
   5.52                     596              1895
   6.63                     219              2334
   7.73                     144              2523
   8.84                     162              2682
   9.94                     129              2827

PENETRATION OF    3.91 M AT MAX FORCE OF    756 N
PENETRATION OF   10.54 M AT MAX ENERGY OF  2896 N-M
```

```
TEST:     T3R3           RIDGE:3-2S

DISTANCE,M                FORCE,N      CUM. ENERGY,N-M
   0.00                     112                 0
   1.00                     117               104
   2.01                     150               229
   3.01                     219               417
   4.01                     464               740
   5.02                     612              1311
   6.02                     446              1862
   7.03                     258              2202
   8.03                     113              2360
   9.04                     185              2508

PENETRATION OF    4.62 M AT MAX FORCE OF    694 N
PENETRATION OF    9.54 M AT MAX ENERGY OF  2592 N-M
```

```
TEST:     T3R3           RIDGE:3-3S

DISTANCE,M                FORCE,N      CUM. ENERGY,N-M
   0.00                     117                 0
   1.10                     102               127
   2.21                     204               269
   3.31                     412               585
   4.41                     850              1295
   5.52                    1054              2437
   6.62                     452              3311
   7.73                     150              3617
   8.84                     179              3780
   9.94                     121              3958
  11.04                      79              4067

PENETRATION OF    5.22 M AT MAX FORCE OF   1179 N
PENETRATION OF   11.24 M AT MAX ENERGY OF  4081 N-M
```

```
TEST:      T3R3            RIDGE:3-4S

DISTANCE,M              FORCE,N      CUM. ENERGY,N-M
    0.00                    73                  0
     .90                   104                 82
    1.81                   200                210
    2.71                   250                404
    3.61                   369                757
    4.52                   508               1207
    5.42                   208               1503
    6.32                   131               1658
    7.23                    94               1766
    8.13                    87               1851

PENETRATION OF    3.91 M AT MAX FORCE OF    648 N
PENETRATION OF    8.93 M AT MAX ENERGY OF  1919 N-M


TEST:      T3R3            RIDGE:3-5S

DISTANCE,M              FORCE,N      CUM. ENERGY,N-M
    0.00                    92                  0
    1.20                    85                105
    2.41                   106                210
    3.61                   102                319
    4.82                   283                532
    6.02                   235                857
    7.23                   115               1062
    8.43                   100               1176
    9.63                    85               1295
   10.84                    85               1390

PENETRATION OF    4.92 M AT MAX FORCE OF    289 N
PENETRATION OF   11.54 M AT MAX ENERGY OF  1445 N-M


TEST:      T3R3            RIDGE:3-12345S

DISTANCE,M              FORCE,N      CUM. ENERGY,N-M
    0.00                    77                  0
    5.32                   729               1546
   10.65                   131               2898
   15.96                   612               4245
   21.29                   117               5629
   26.61                  1054               8042
   31.93                    83               9654
   37.25                   439              10961
   42.57                    85              11718
   47.89                   235              12512

PENETRATION OF   26.31 M AT MAX FORCE OF   1179 N
PENETRATION OF   53.01 M AT MAX ENERGY OF 13070 N-M
```

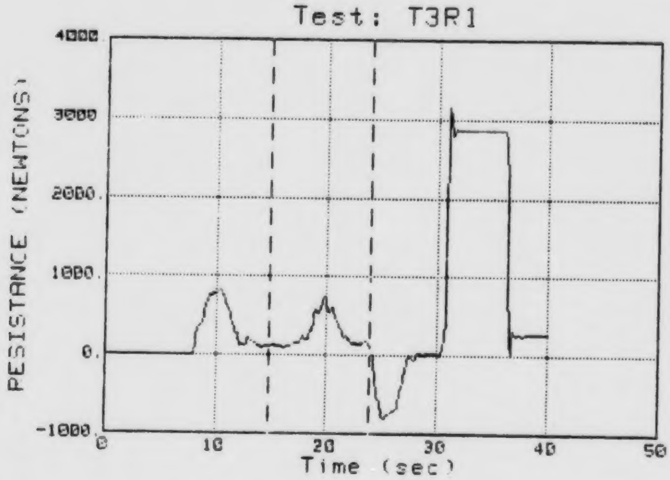
Test: T3R1
RESISTANCE (NEWTONS)
4000
3000
2000.
1000.
0.
-1000.
0
10
20
30
40
50
Time (sec)

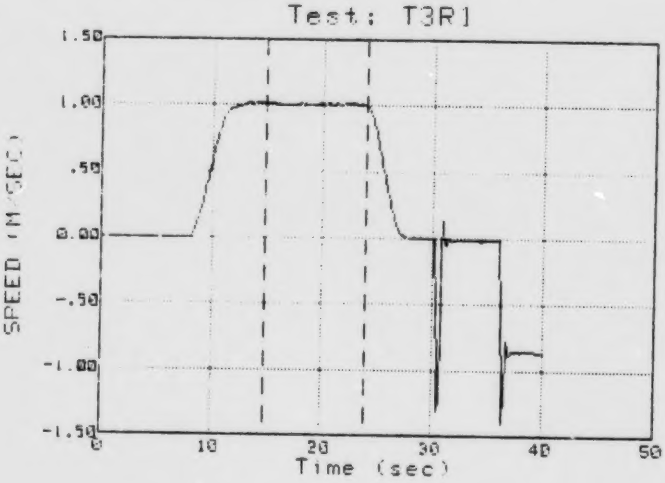
Test: T3R1
SPEED (M/SEC)
1.50
1.00
.50
0.00
-.50
-1.00
-1.50
0
10
20
30
40
50
Time (sec)

MODEL SCALE PENETRATION FORCE
TEST: T3R1 RIDGE: 3-1N

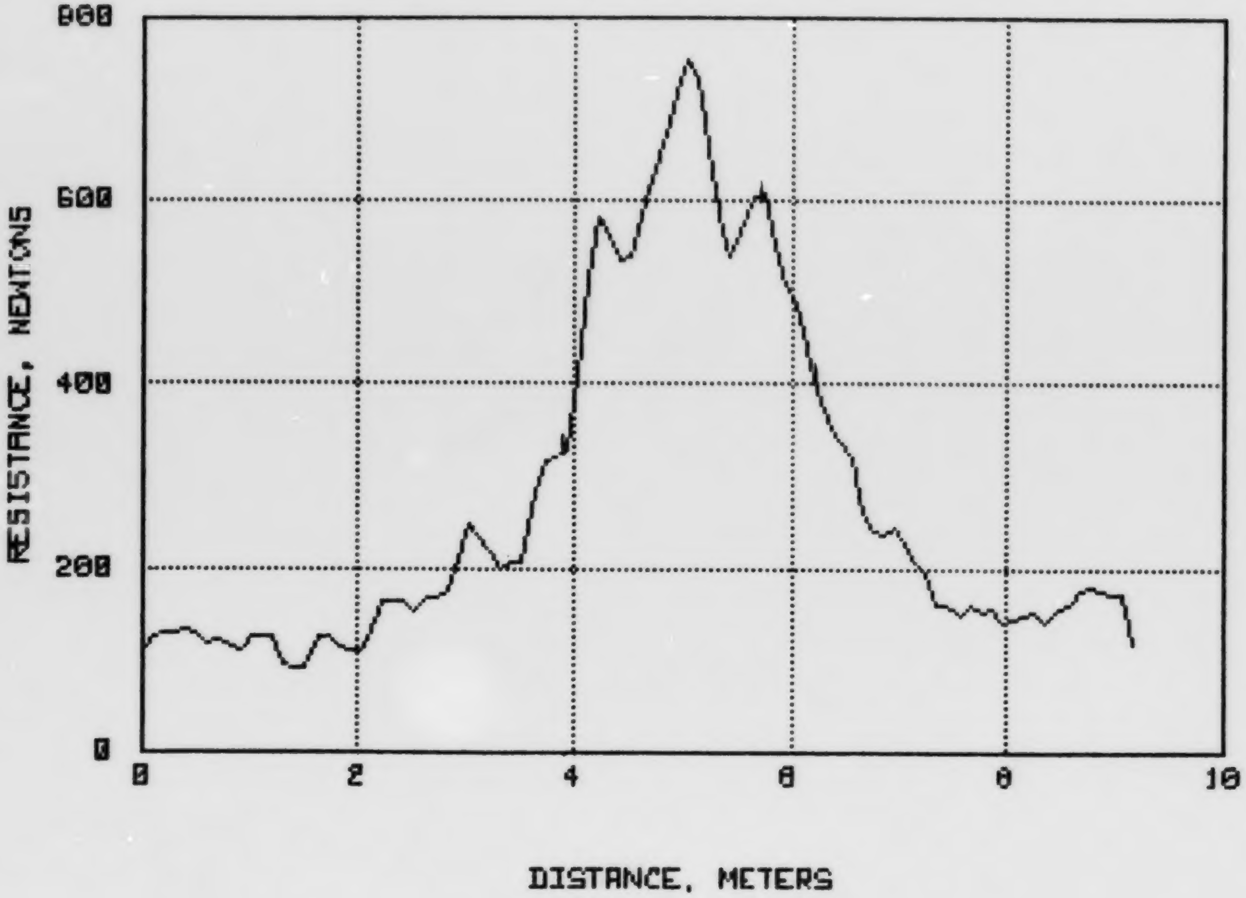

MODEL SCALE PENETRATION ENERGY
TEST: T3R1 RIDGE: 3-1N

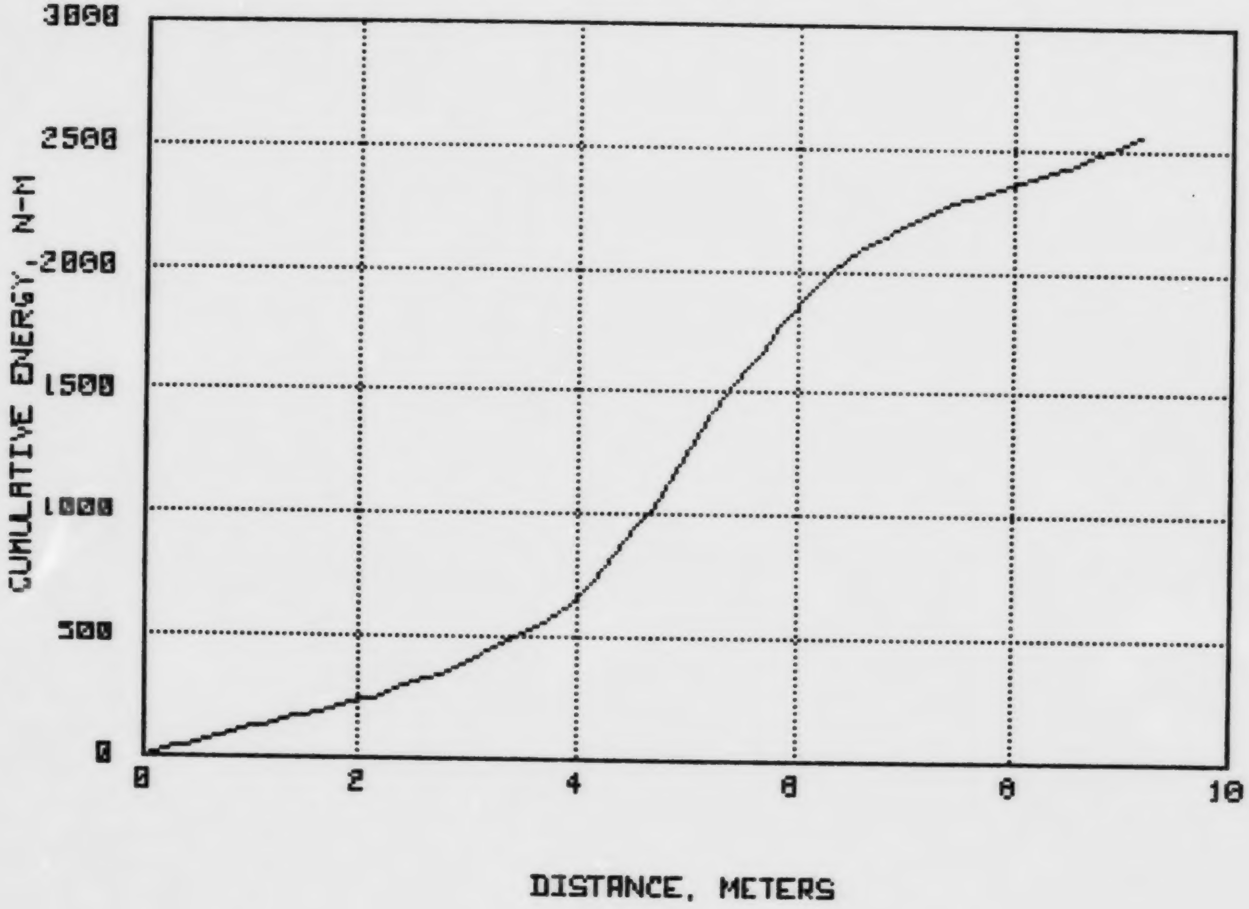

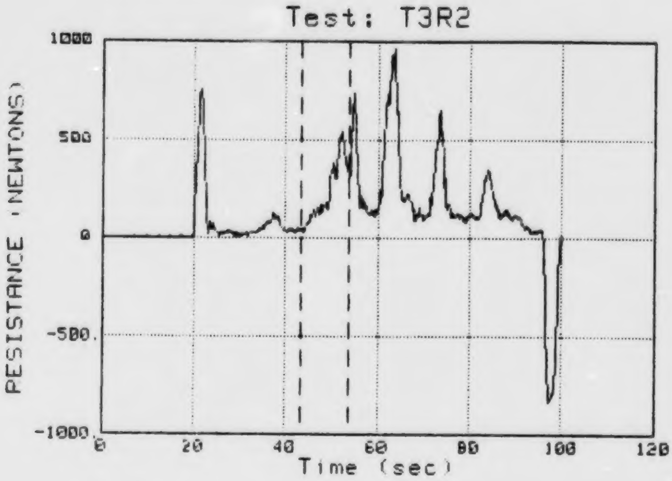
Test: T3R2
RESISTANCE (NEWTONS)
1000
500
0
-500.
-1000.
0
20
40
60
80
100
120
Time (sec)

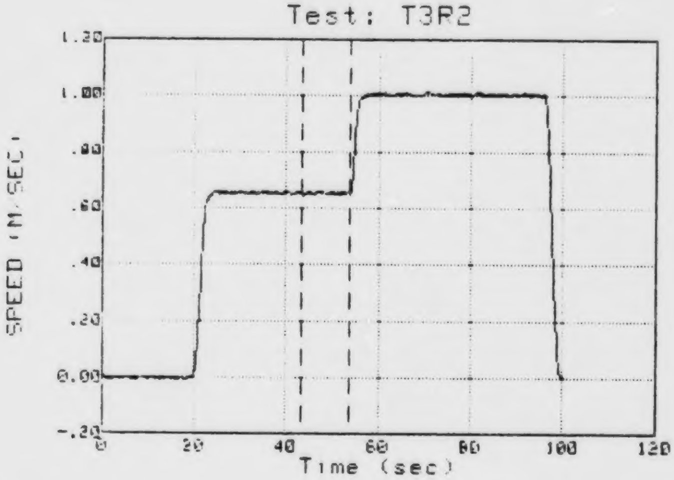
Test: T3R2
SPEED (M/SEC)
1.20
1.00
.80
.60
.40
.20
0.00
-.20
0
20
40
60
80
100
120
Time (sec)

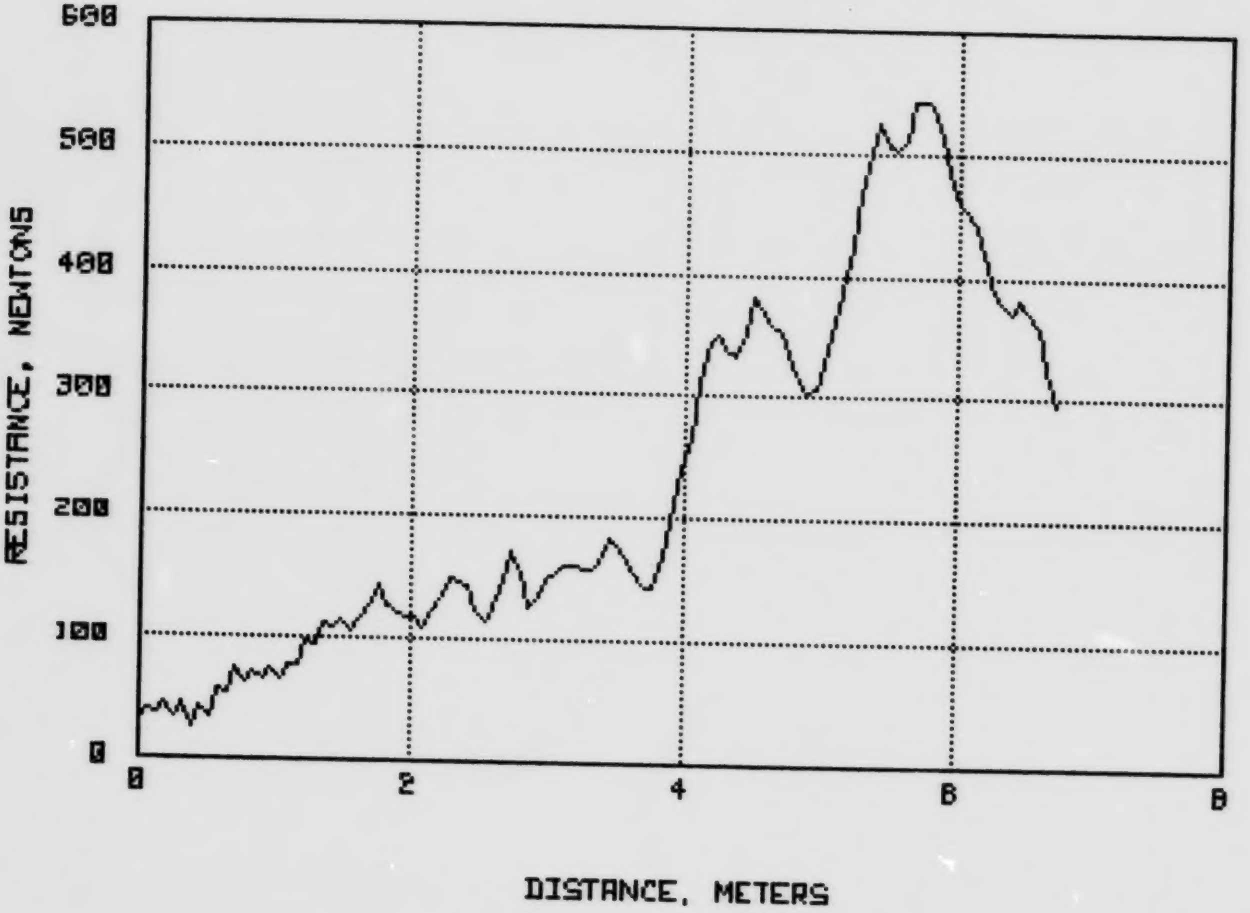

MODEL SCALE PENETRATION FORCE
TEST: T3R2 RIDGE: 3-2N

MODEL SCALE PENETRATION ENERGY
TEST: T3R2   RIDGE: 3-2N

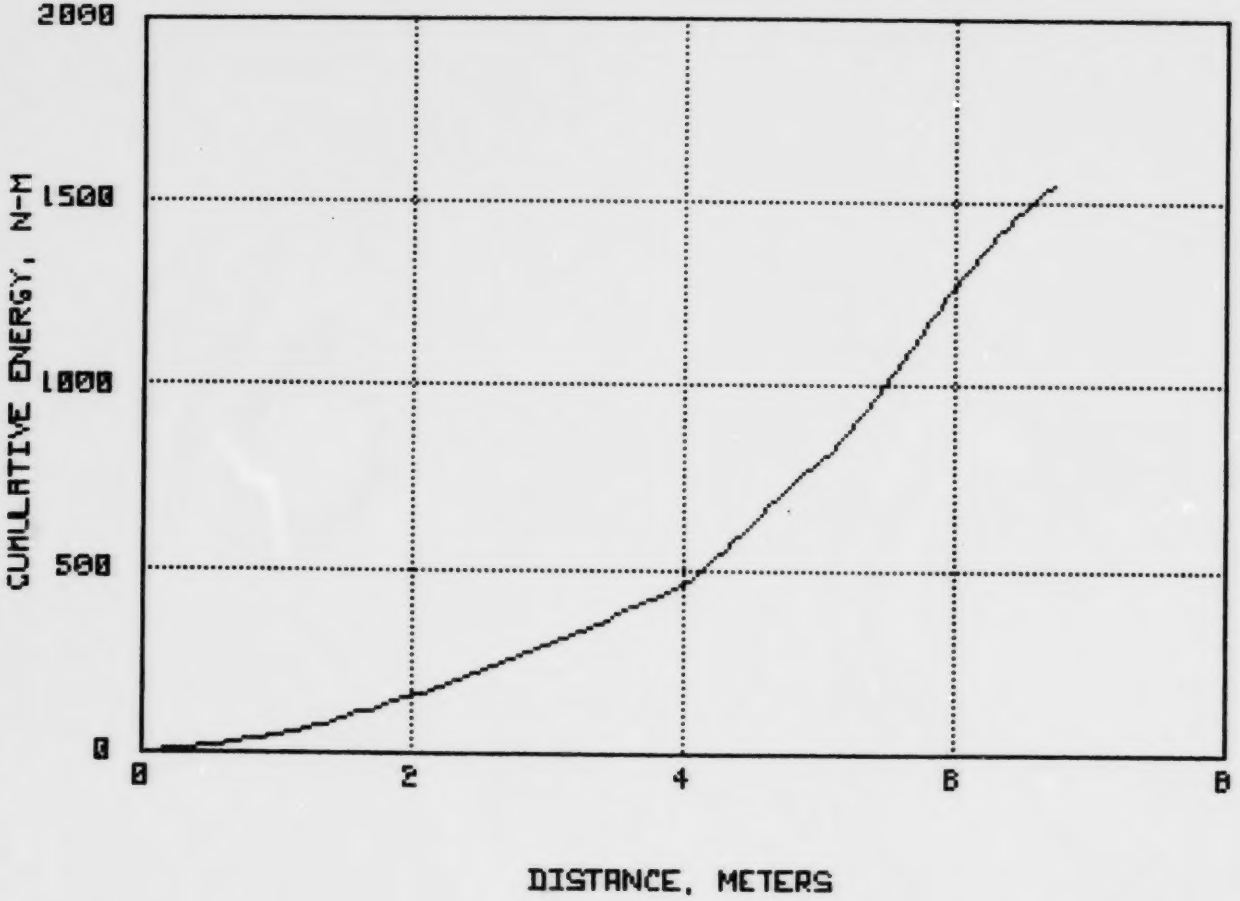

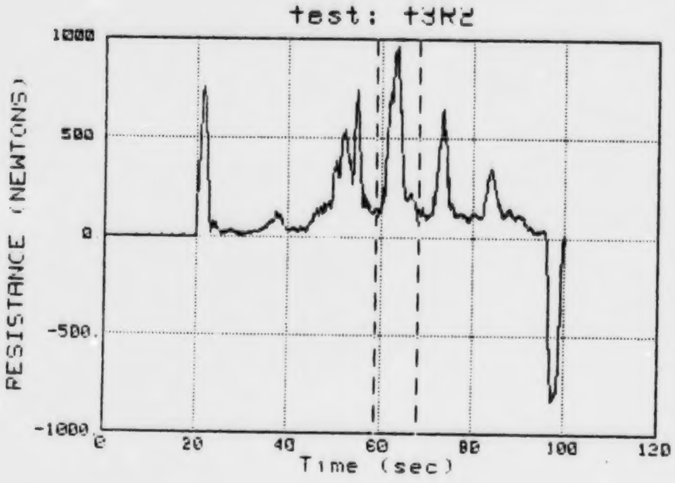
test: t3R2
RESISTANCE (NEWTONS)
1000
500
0
-500.
-1000
0
20
40
60
80
100
120
Time (sec)

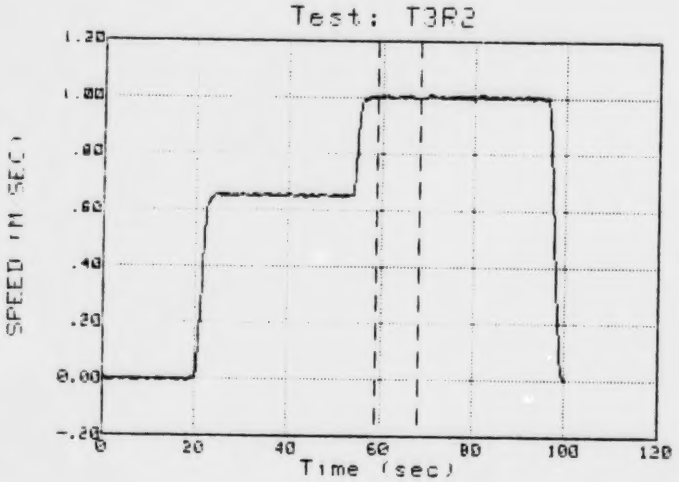
Test: T3R2
SPEED (M SEC)
1.20
1.00
.80
.60
.40
.20
0.00
-.20
0
20
40
60
80
100
120
Time (sec)

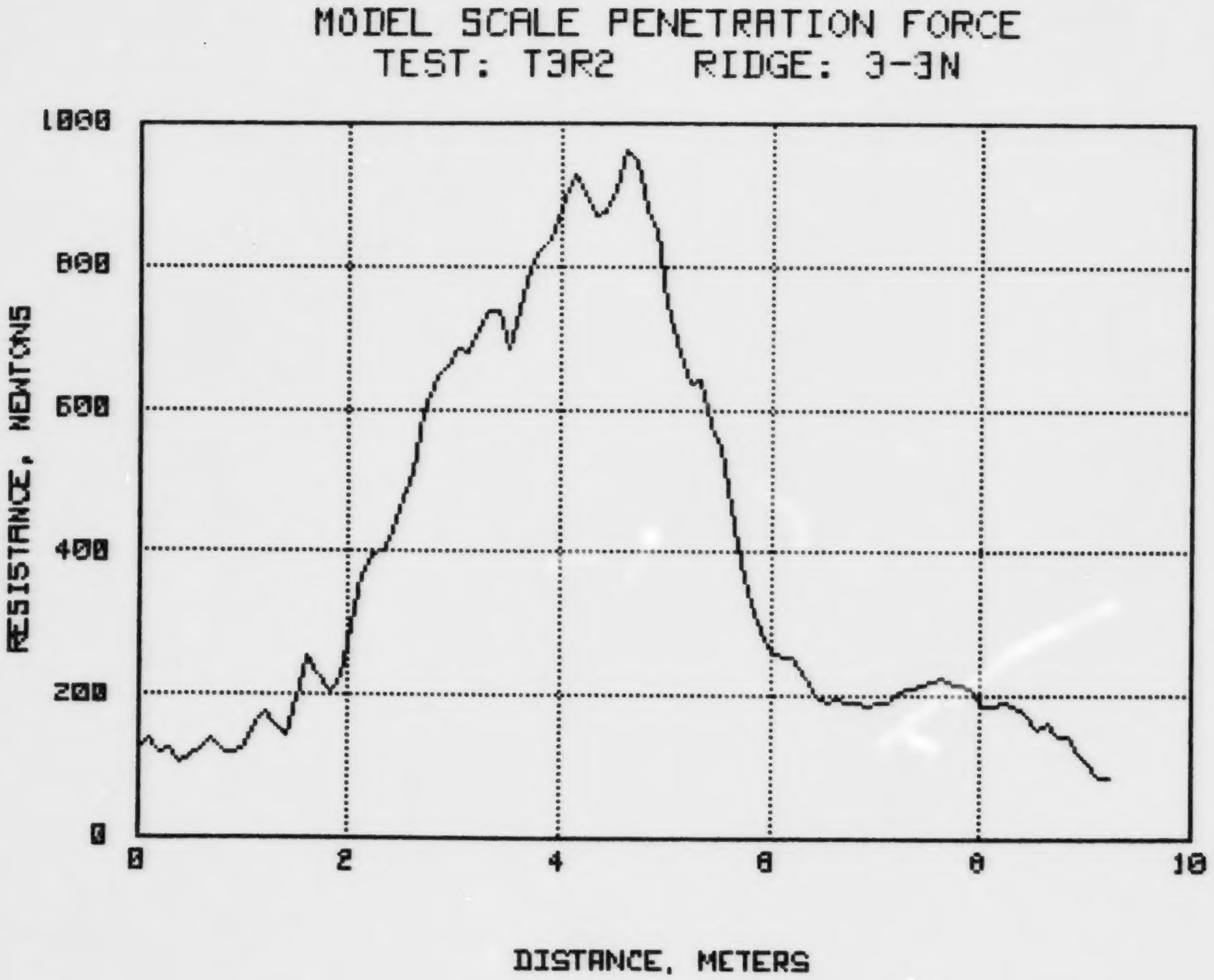
MODEL SCALE PENETRATION FORCE
TEST: T3R2 RIDGE: 3-3N
1000
800
600
400
200
0
RESISTANCE, NEWTONS
0
2
4
6
8
10
DISTANCE, METERS

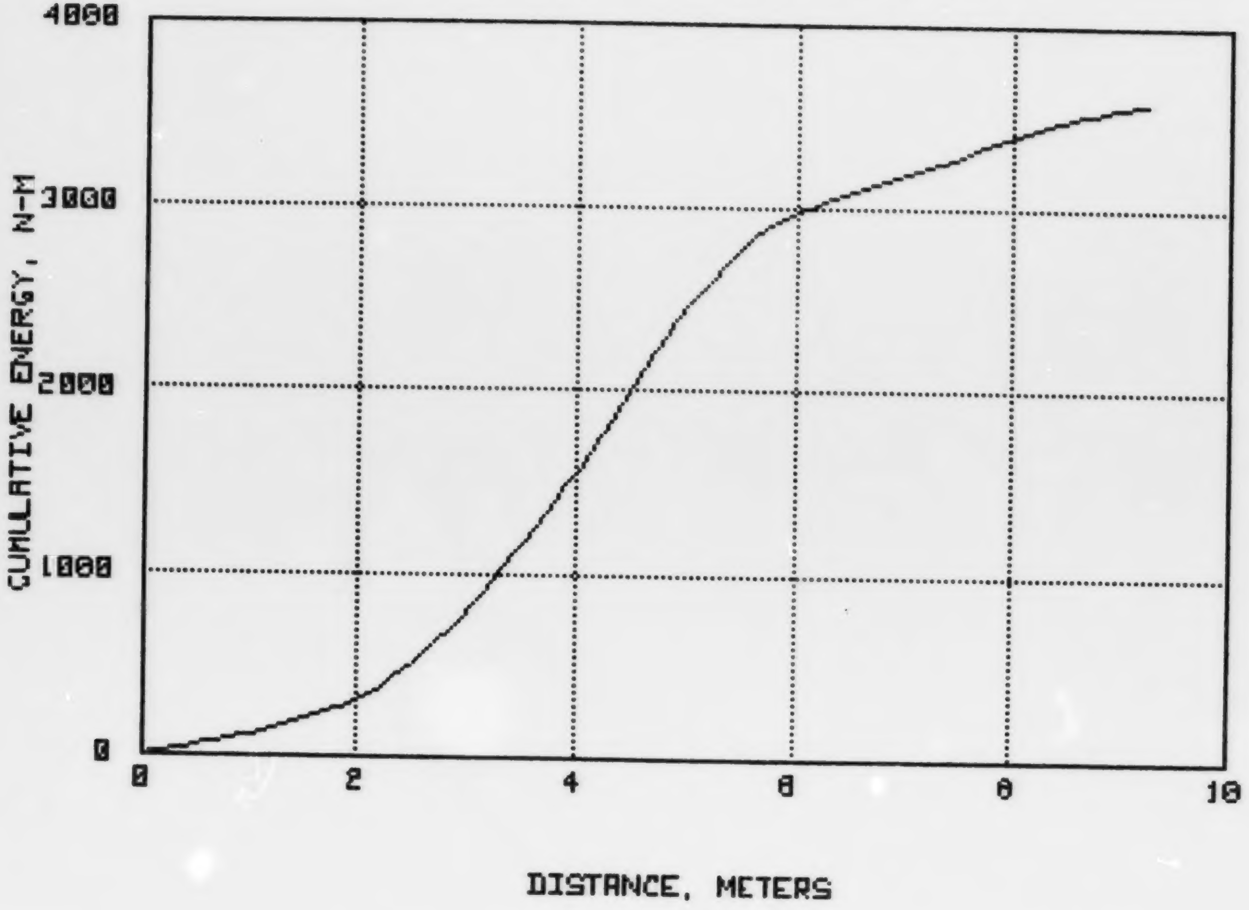

MODEL SCALE PENETRATION ENERGY
TEST: T3R2 RIDGE: 3-3N

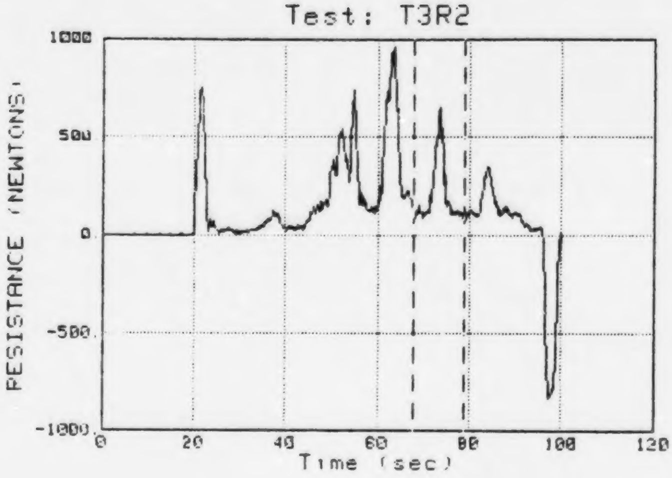
Test: T3R2

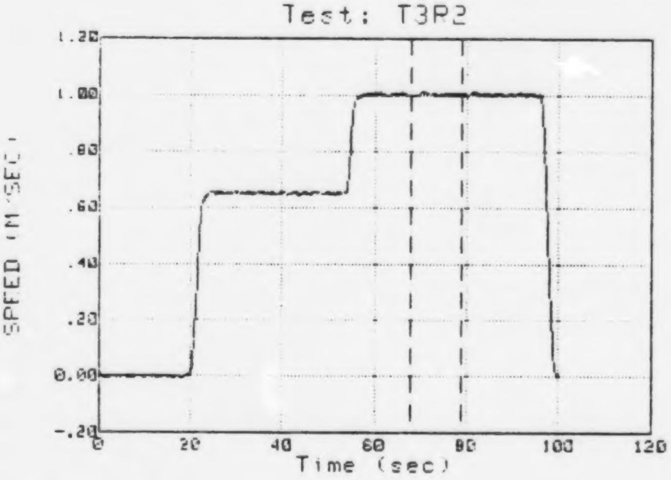
Test: T3R2

MODEL SCALE PENETRATION FORCE
TEST: T3R2 RIDGE: 3-4N

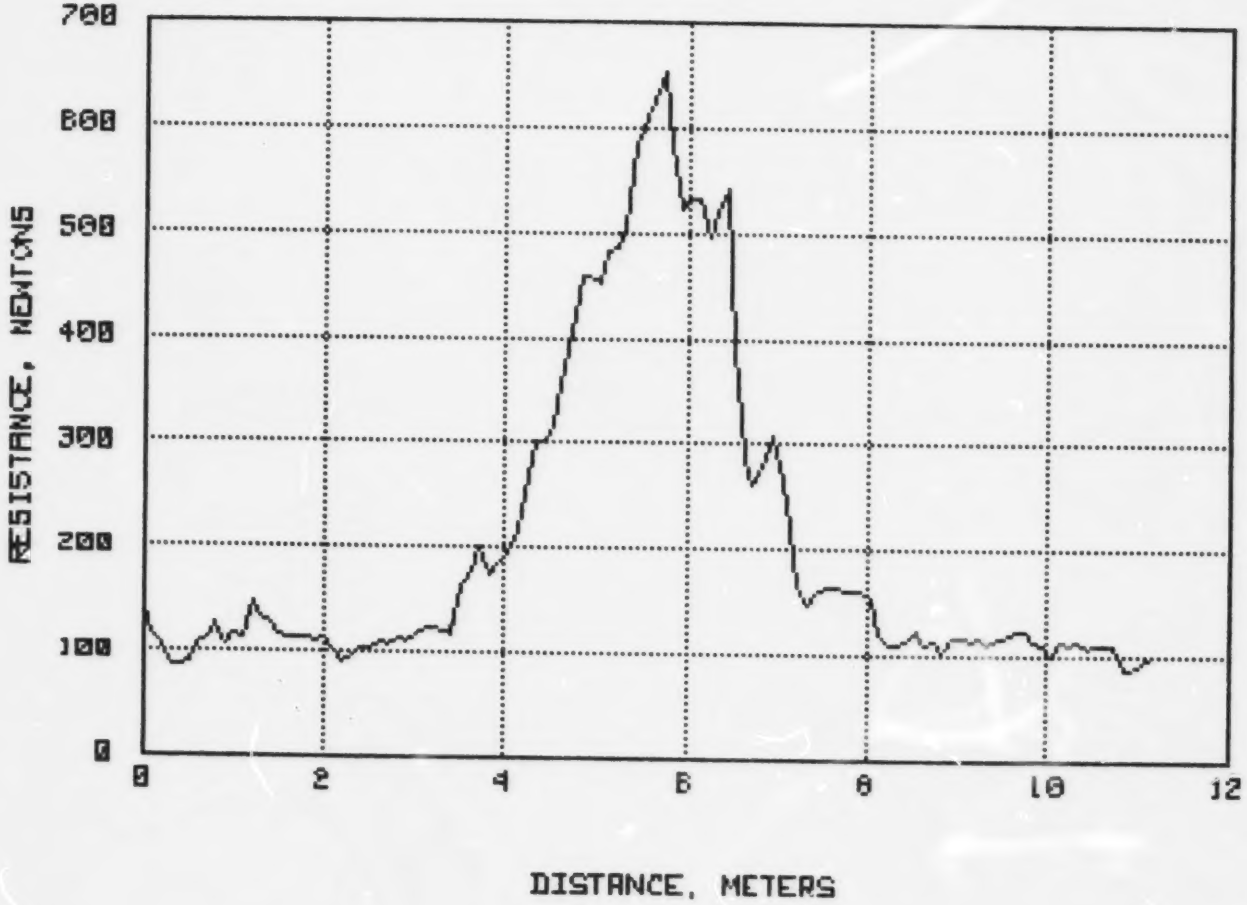

MODEL SCALE PENETRATION ENERGY
TEST: T3R2 RIDGE: 3-4N

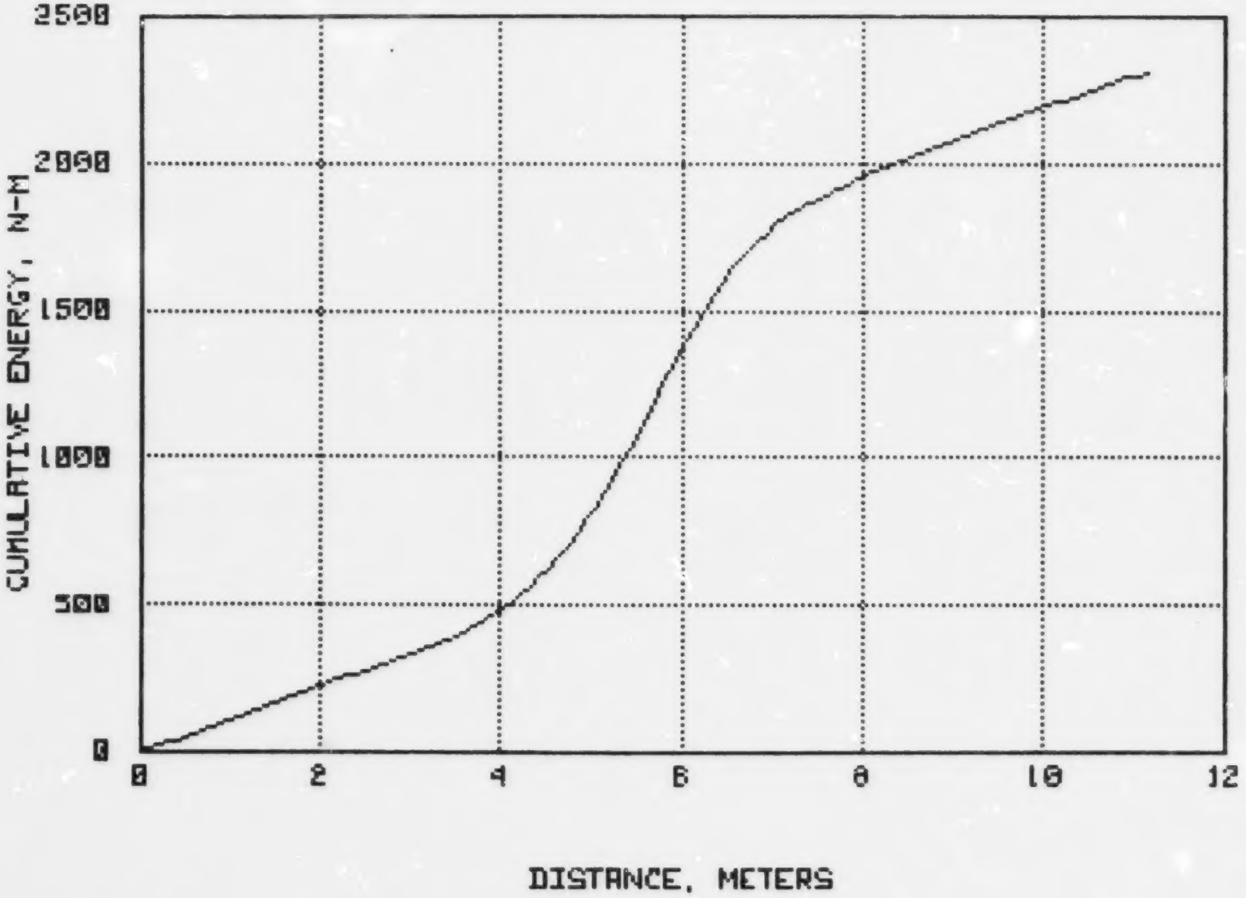

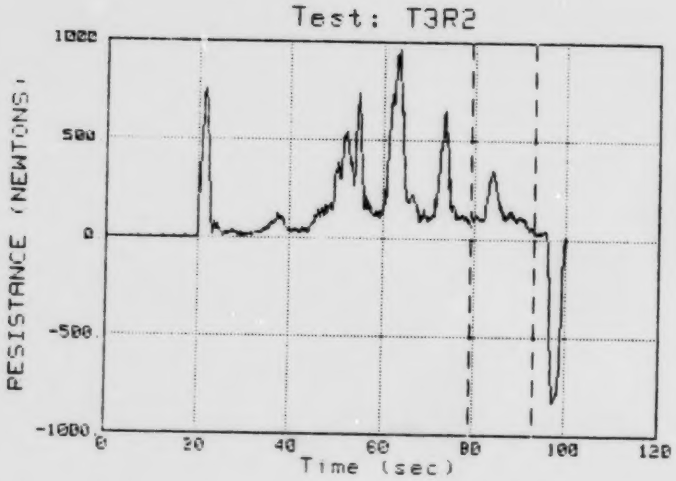
Test: T3R2
RESISTANCE (NEWTONS)
1000
500
0
-500
-1000
0
20
40
60
80
100
120
Time (sec)

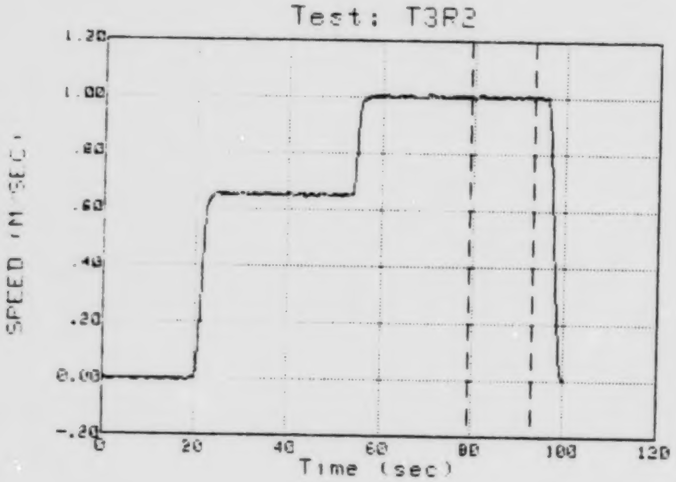
Test: T3R2
SPEED (M/SEC)
1.20
1.00
.80
.60
.40
.20
0.00
-.20
0
20
40
60
80
100
120
Time (sec)

MODEL SCALE PENETRATION FORCE
TEST: T3R2   RIDGE: 3-5N

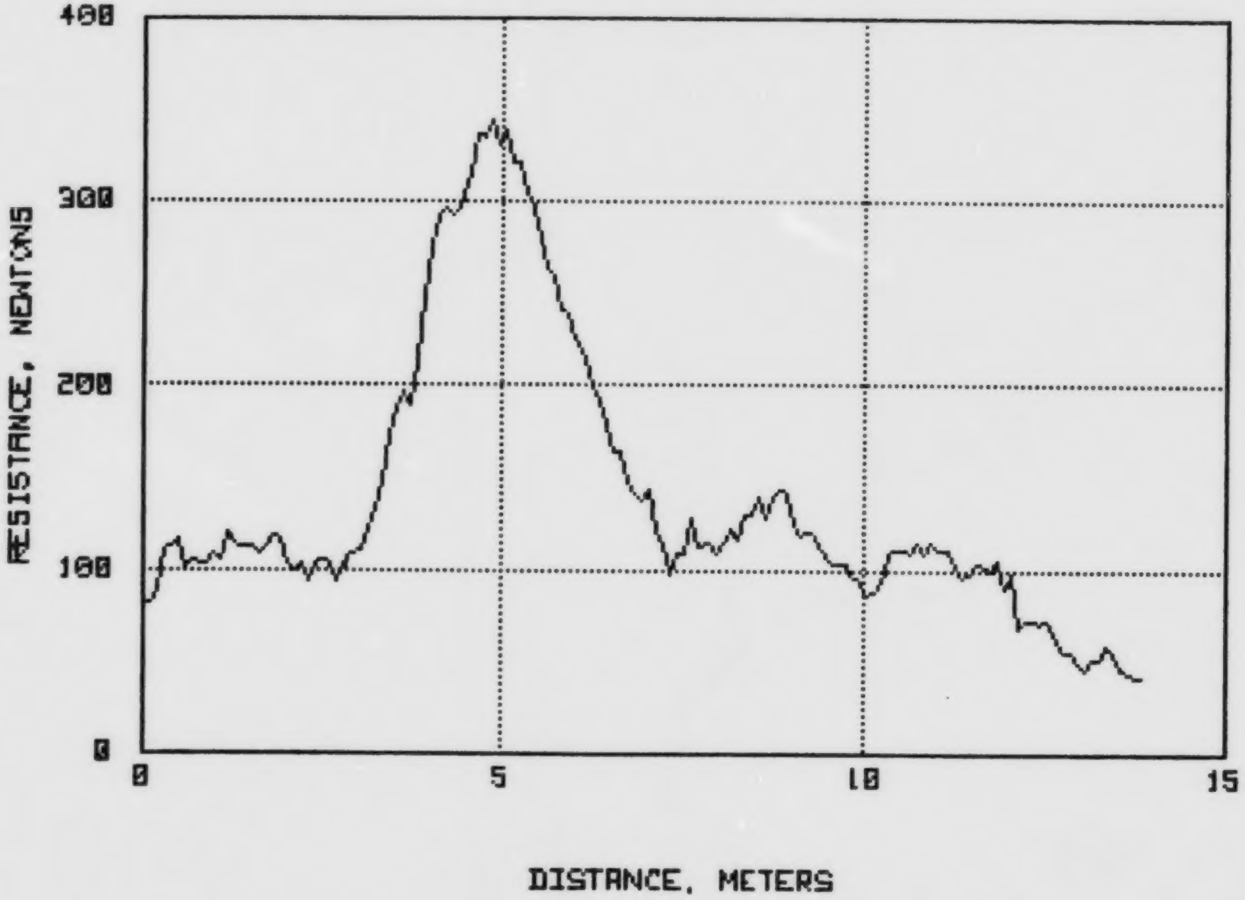

MODEL SCALE PENETRATION ENERGY
TEST: T3R2 RIDGE: 3-5N

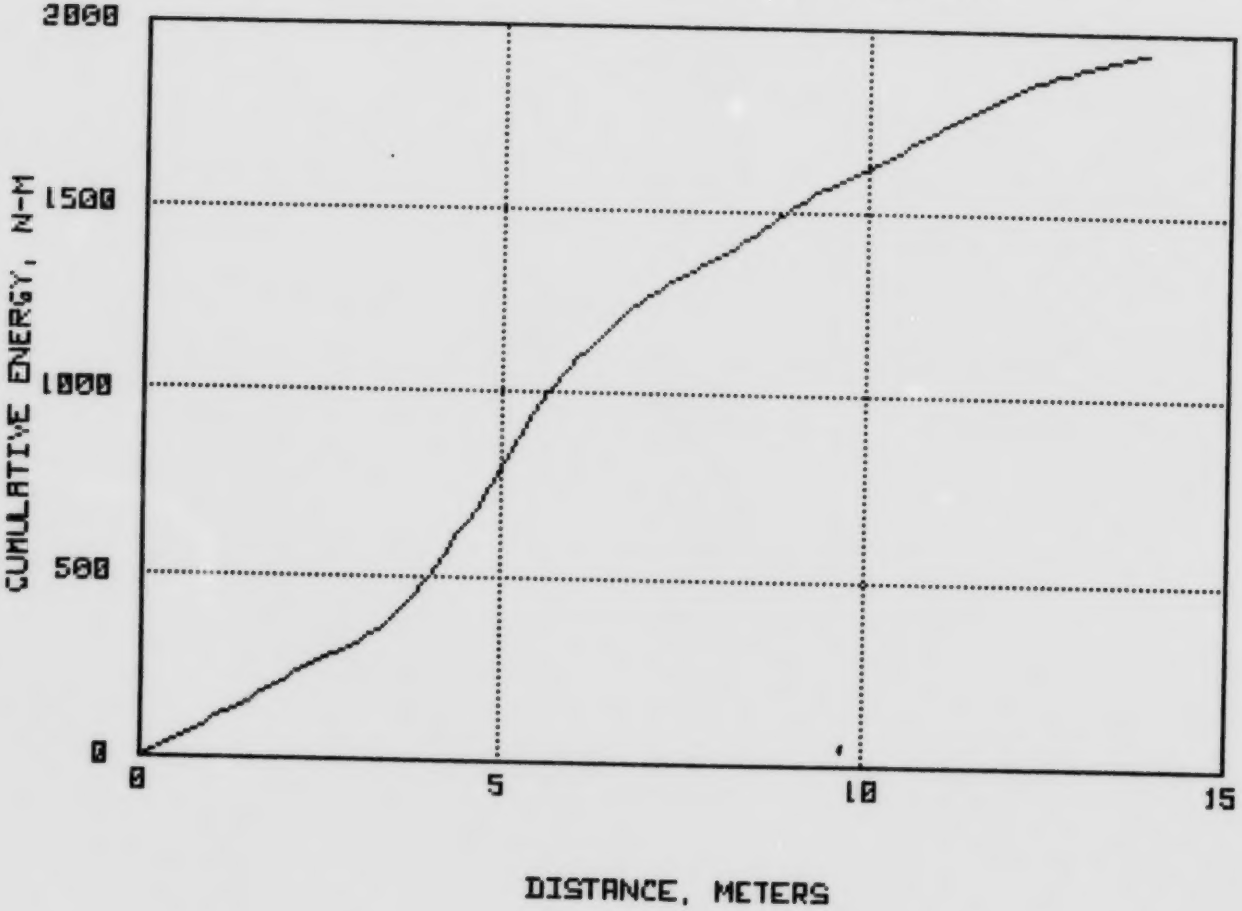

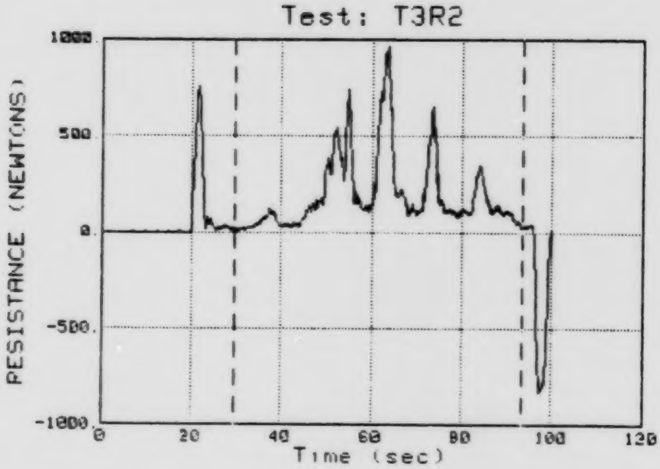

Test: T3R2

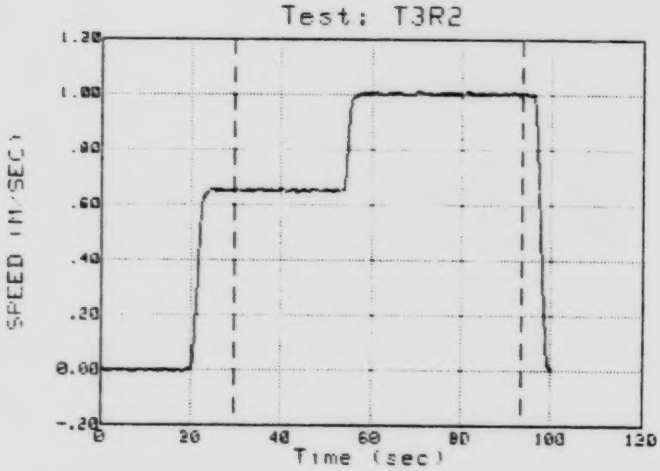

Test: T3R2

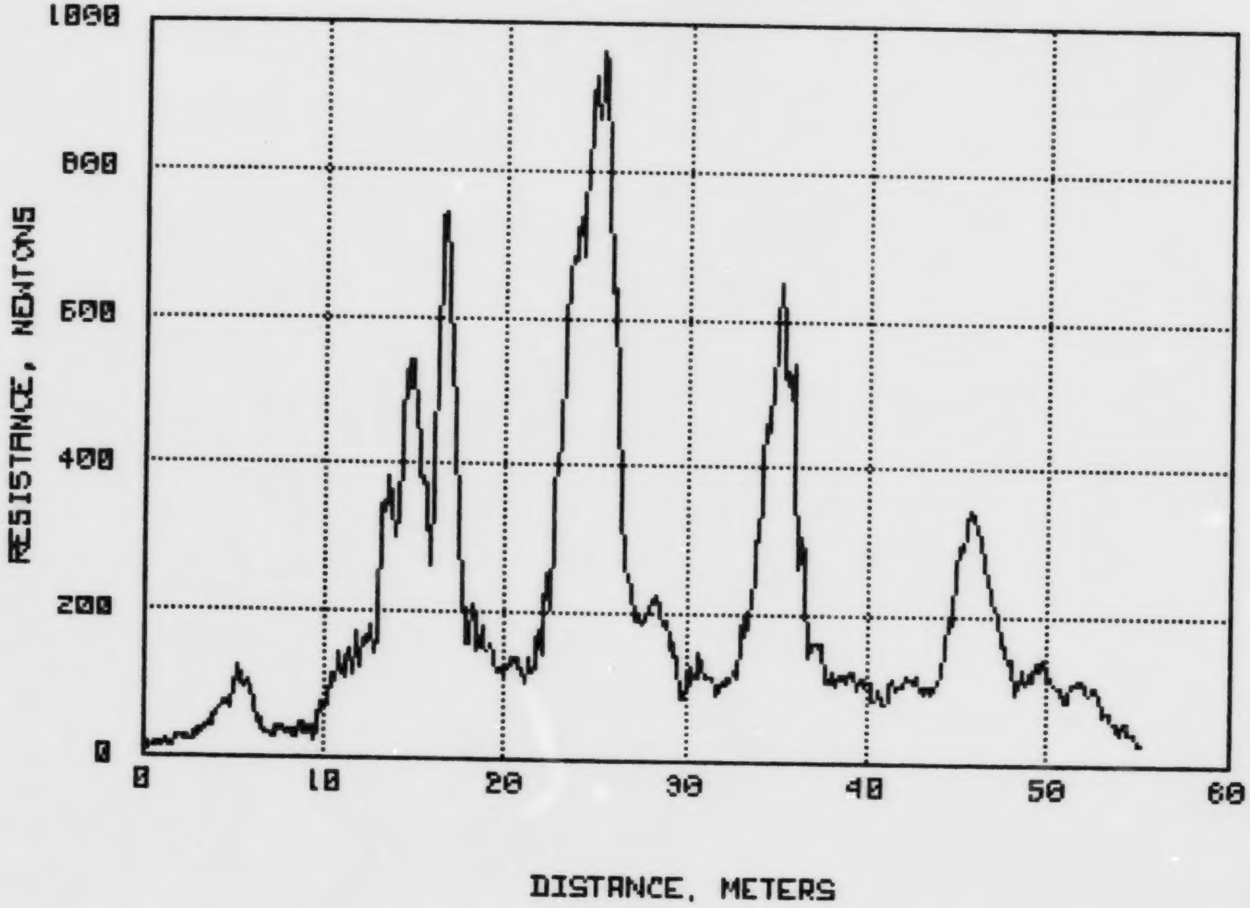

MODEL SCALE PENETRATION FORCE
TEST: T3R2 RIDGE: 3-2345N

MODEL SCALE PENETRATION ENERGY
TEST: T3R2 RIDGE: 3-2345N

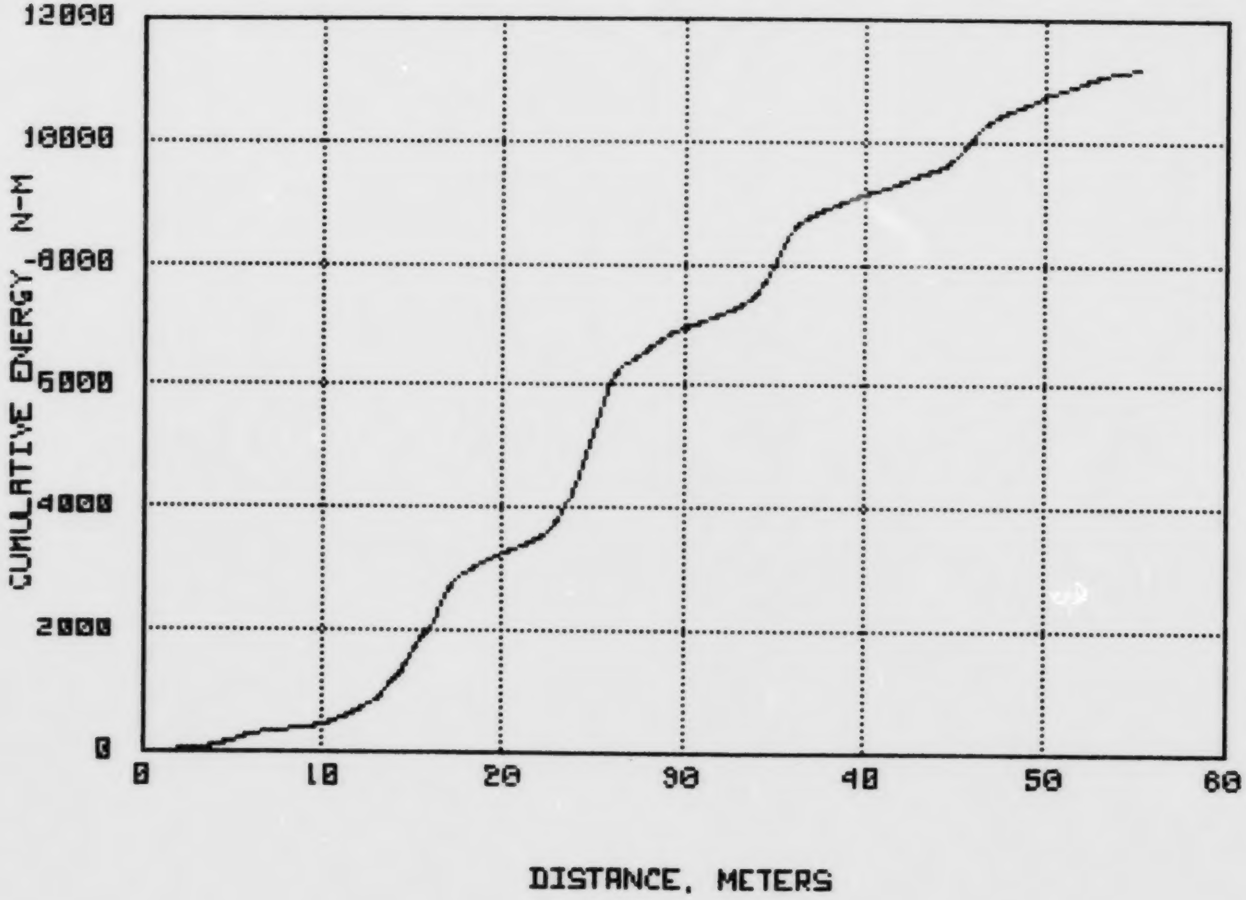

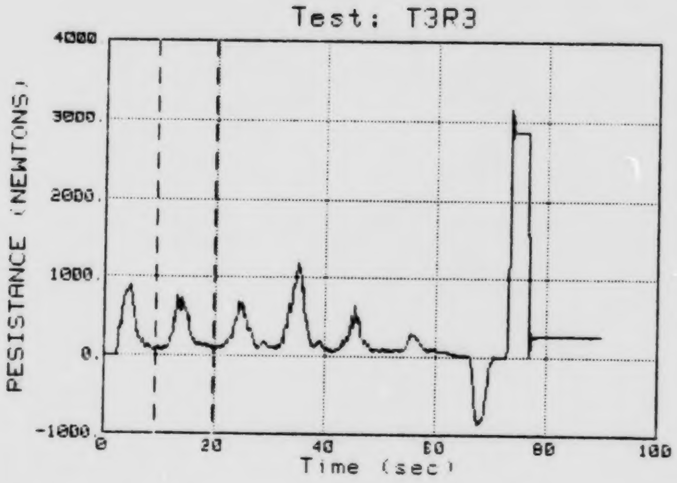
Test: T3R3
RESISTANCE (NEWTONS)
4000
3000.
2000.
1000.
0.
-1000.
0
20
40
60
80
100
Time (sec)

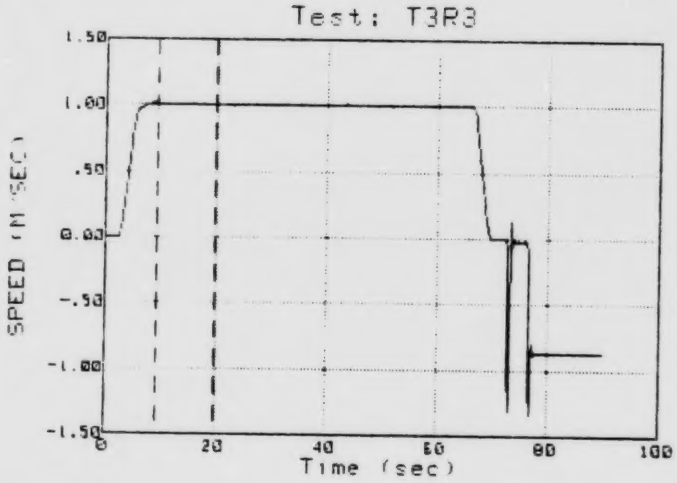
Test: T3R3
SPEED (M/SEC)
1.50
1.00
.50
0.00
-.50
-1.00
-1.50
0
20
40
60
80
100
Time (sec)

MODEL SCALE PENETRATION FORCE
TEST: T3R3   RIDGE: 3-15

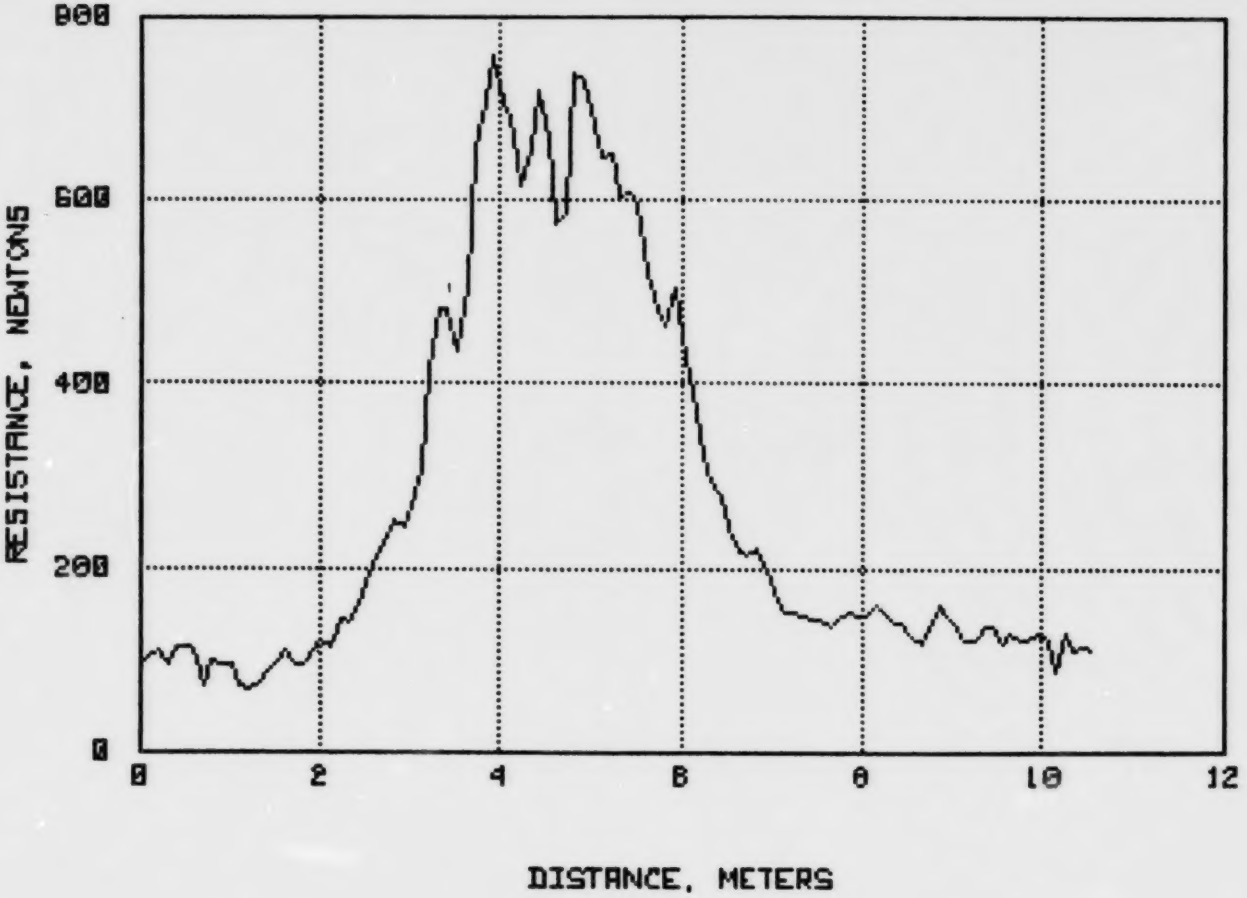

MODEL SCALE PENETRATION ENERGY
TEST: T3R3 RIDGE: 3-15

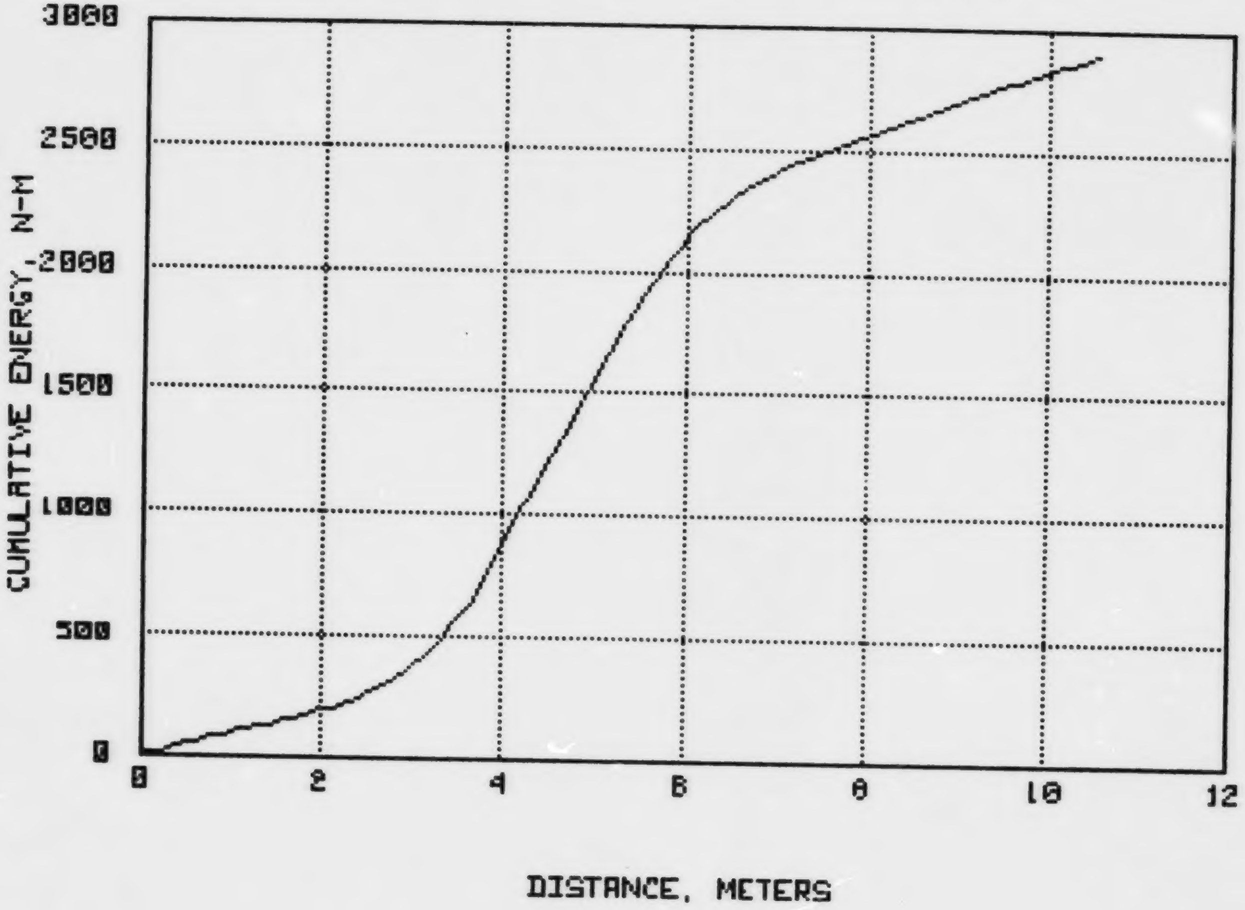

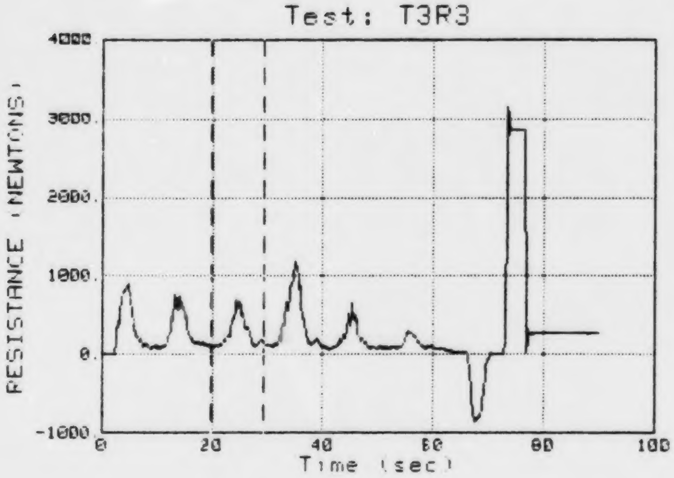
Test: T3R3
RESISTANCE (NEWTONS)
4000
3000.
2000.
1000.
0.
-1000
0
20
40
60
80
100
Time (sec)

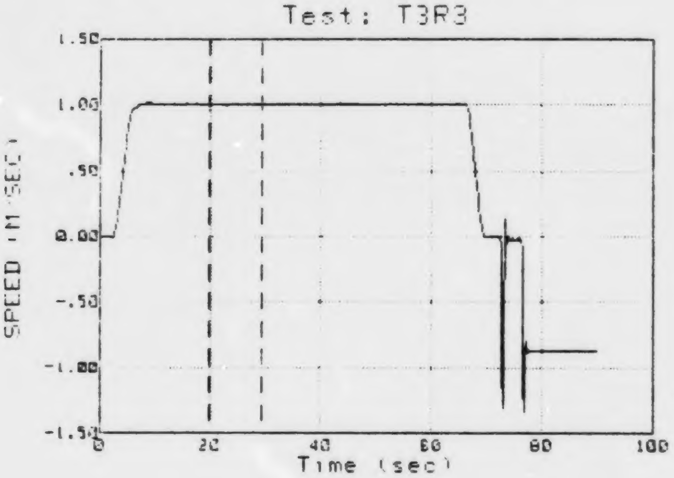
Test: T3R3
SPEED (M/SEC)
1.50
1.00
.50
0.00
-.50
-1.00
-1.50
0
20
40
60
80
100
Time (sec)

MODEL SCALE PENETRATION FORCE
TEST: T3R3   RIDGE: 3-25

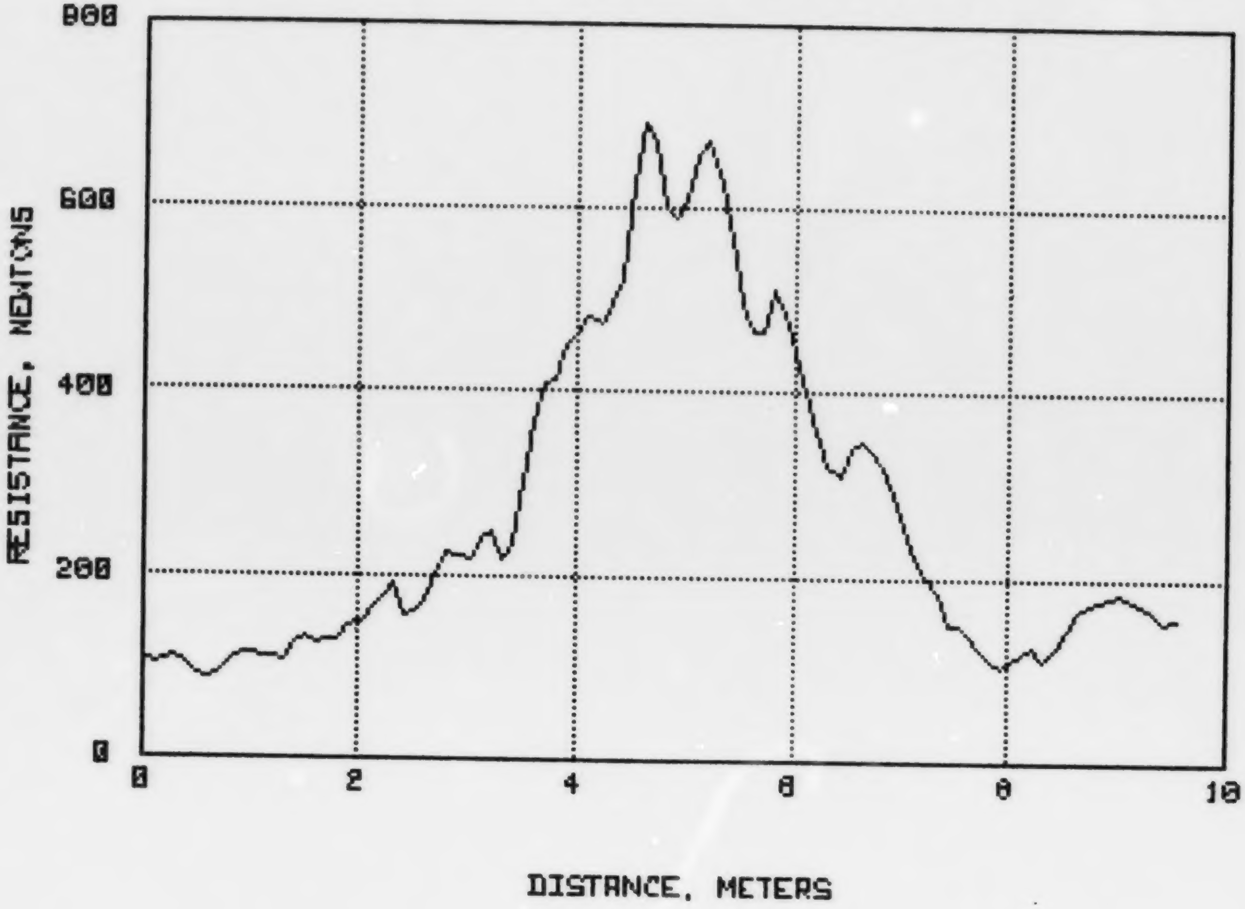

MODEL SCALE PENETRATION ENERGY
TEST: T3R3   RIDGE: 3-25

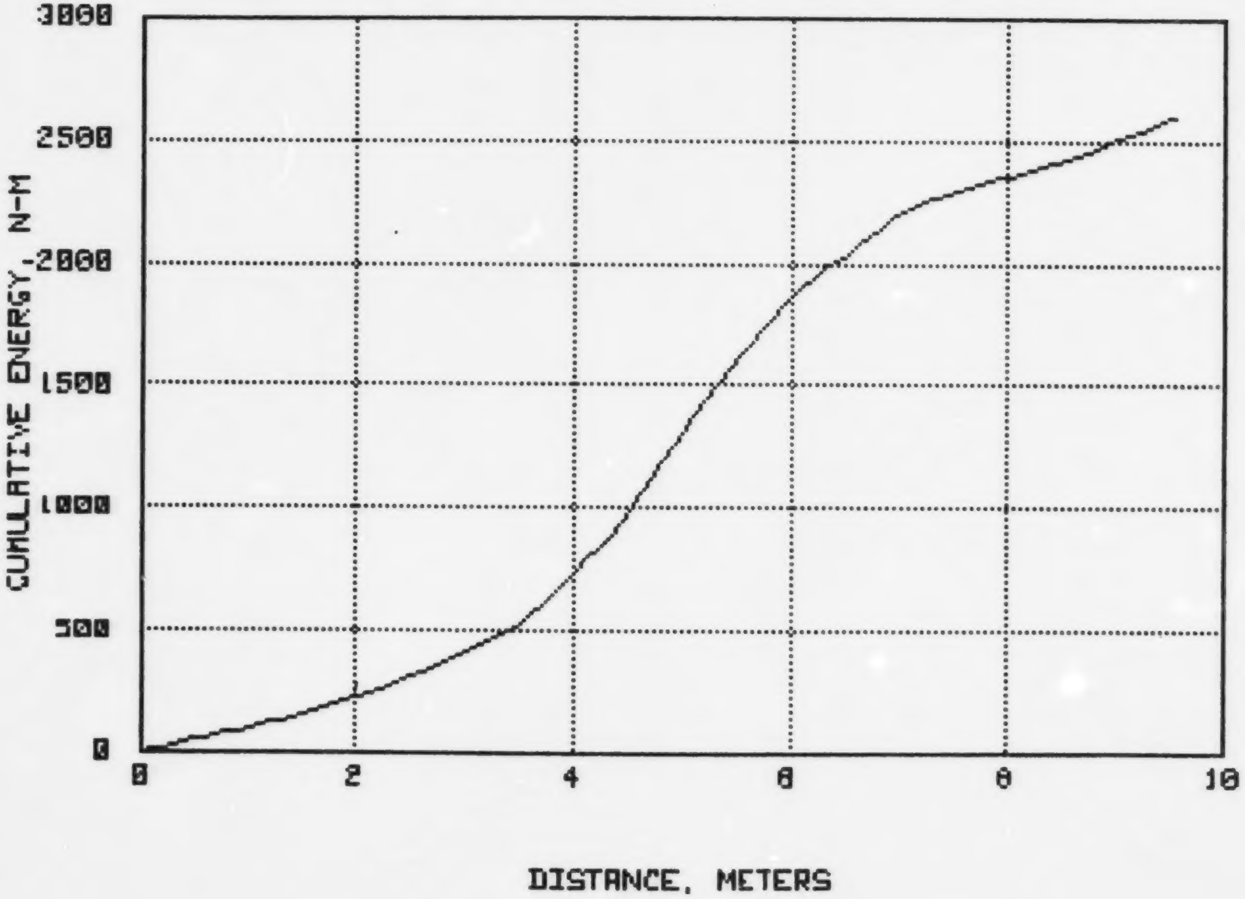

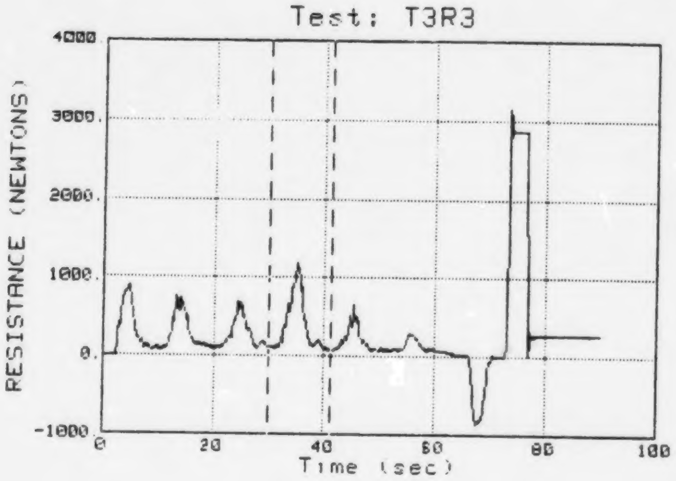
Test: T3R3
RESISTANCE (NEWTONS)
4000
3000.
2000.
1000.
0.
-1000
0
20
40
60
80
100
Time (sec)

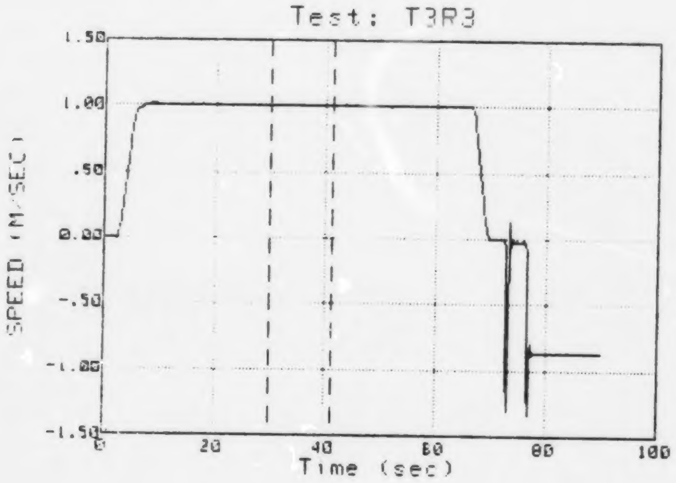
Test: T3R3
SPEED (M/SEC)
1.50
1.00
.50
0.00
-.50
-1.00
-1.50
0
20
40
60
80
100
Time (sec)

MODEL SCALE PENETRATION FORCE
TEST: T3R3 RIDGE: 3-35

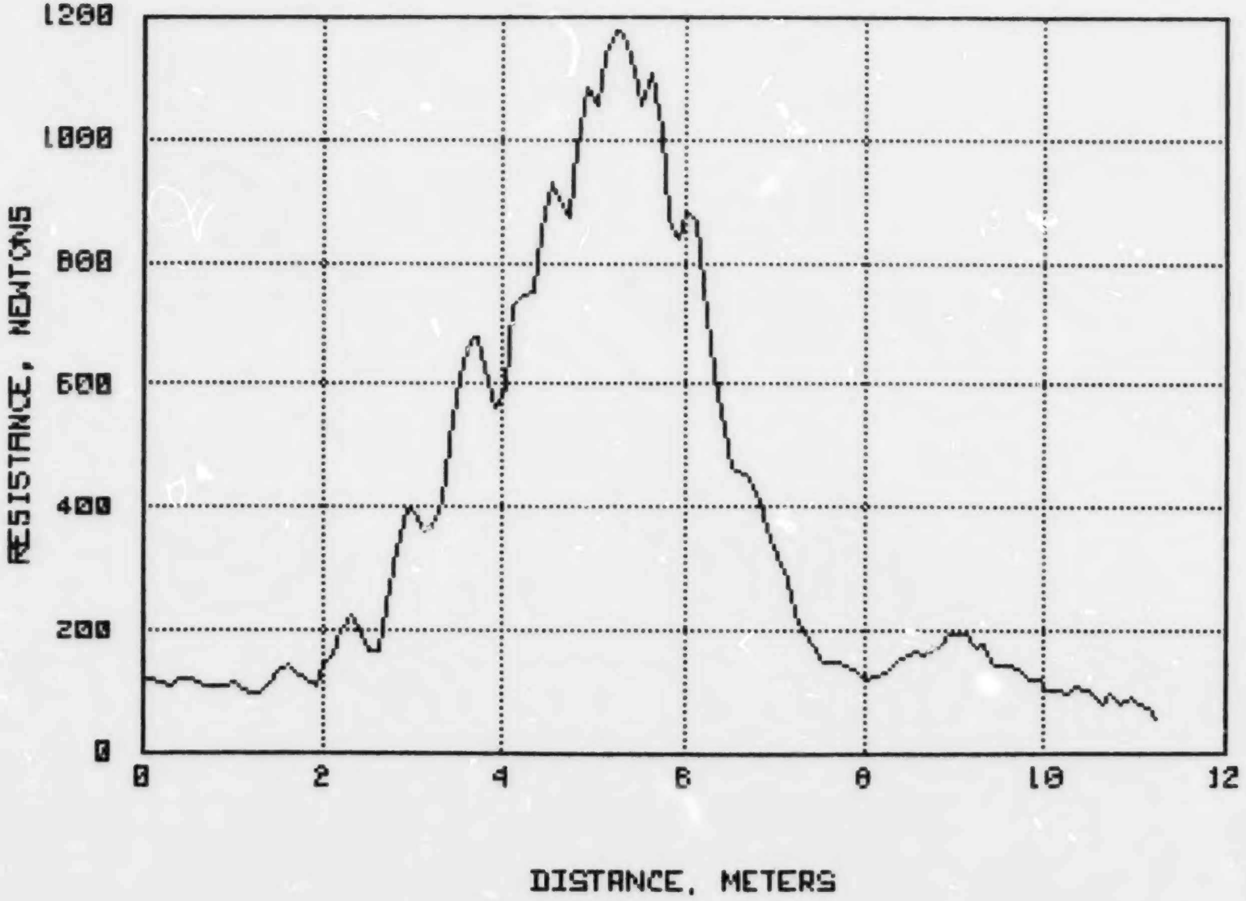

MODEL SCALE PENETRATION ENERGY
TEST: T3R3   RIDGE: 3-35

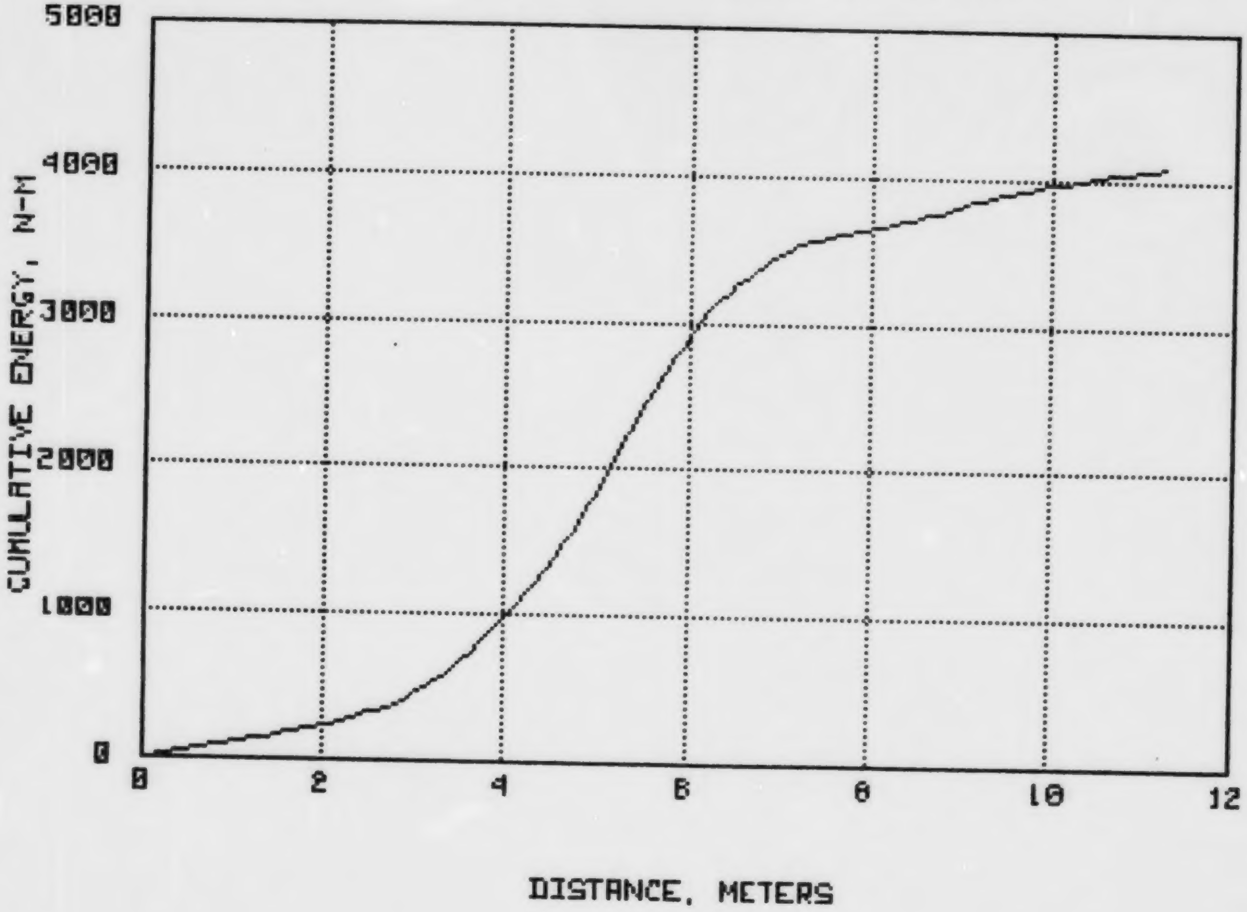

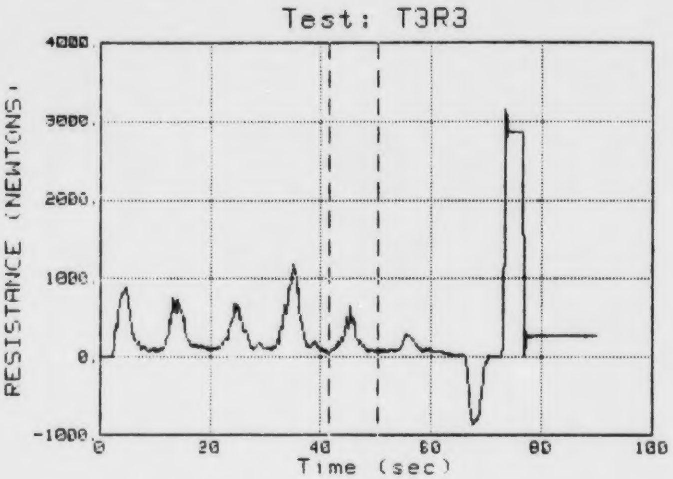
Test: T3R3
RESISTANCE (NEWTONS)
4000.
3000.
2000.
1000.
0.
-1000.
0
20
40
60
80
100
Time (sec)

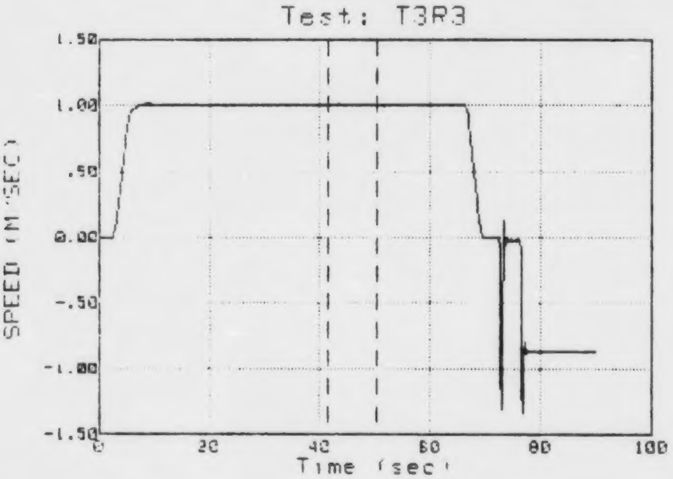
Test: T3R3
SPEED (M/SEC)
1.50
1.00
.50
0.00
-.50
-1.00
-1.50
0
20
40
60
80
100
Time (sec)

MODEL SCALE PENETRATION FORCE
TEST: T3R3   RIDGE: 3-45

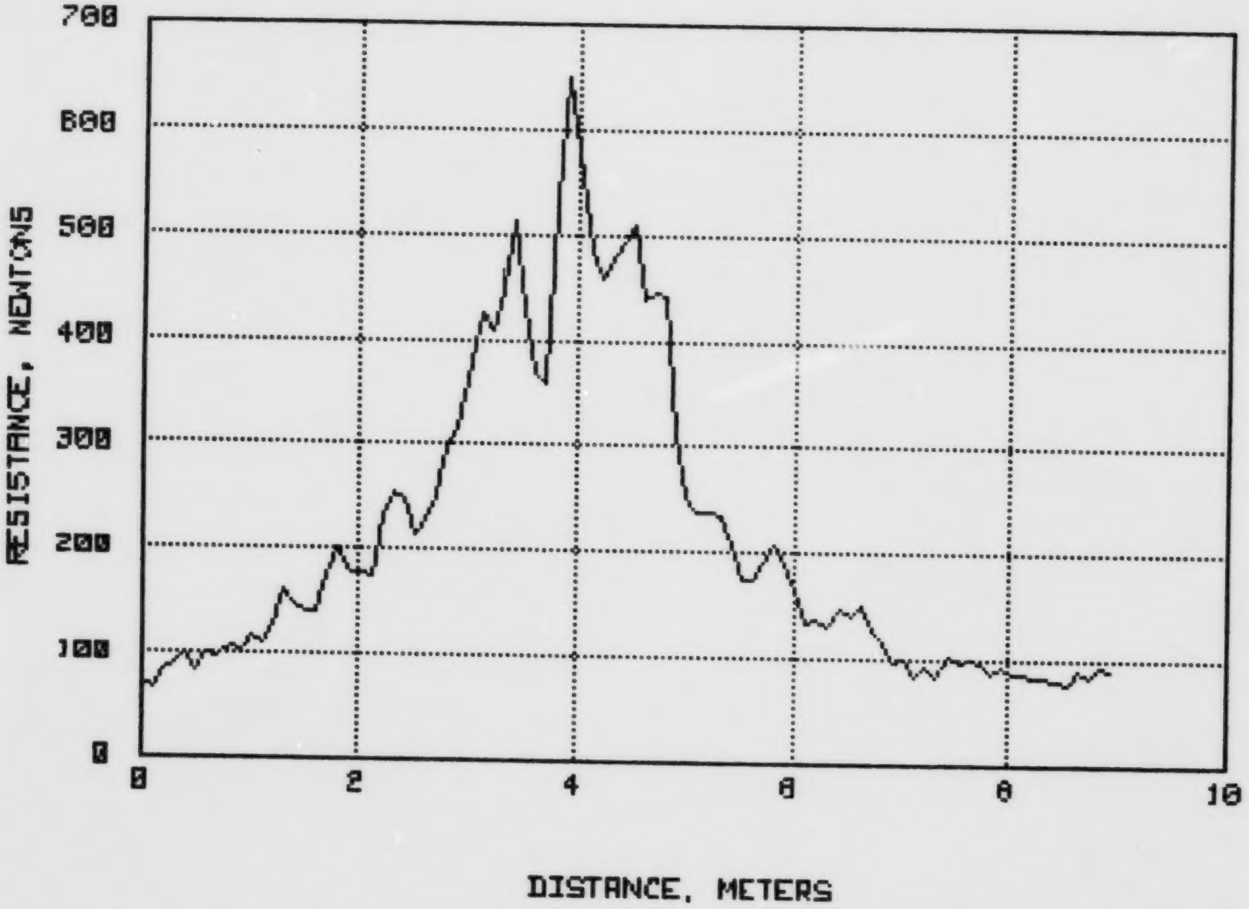

MODEL SCALE PENETRATION ENERGY
TEST: T3R3 RIDGE: 3-45

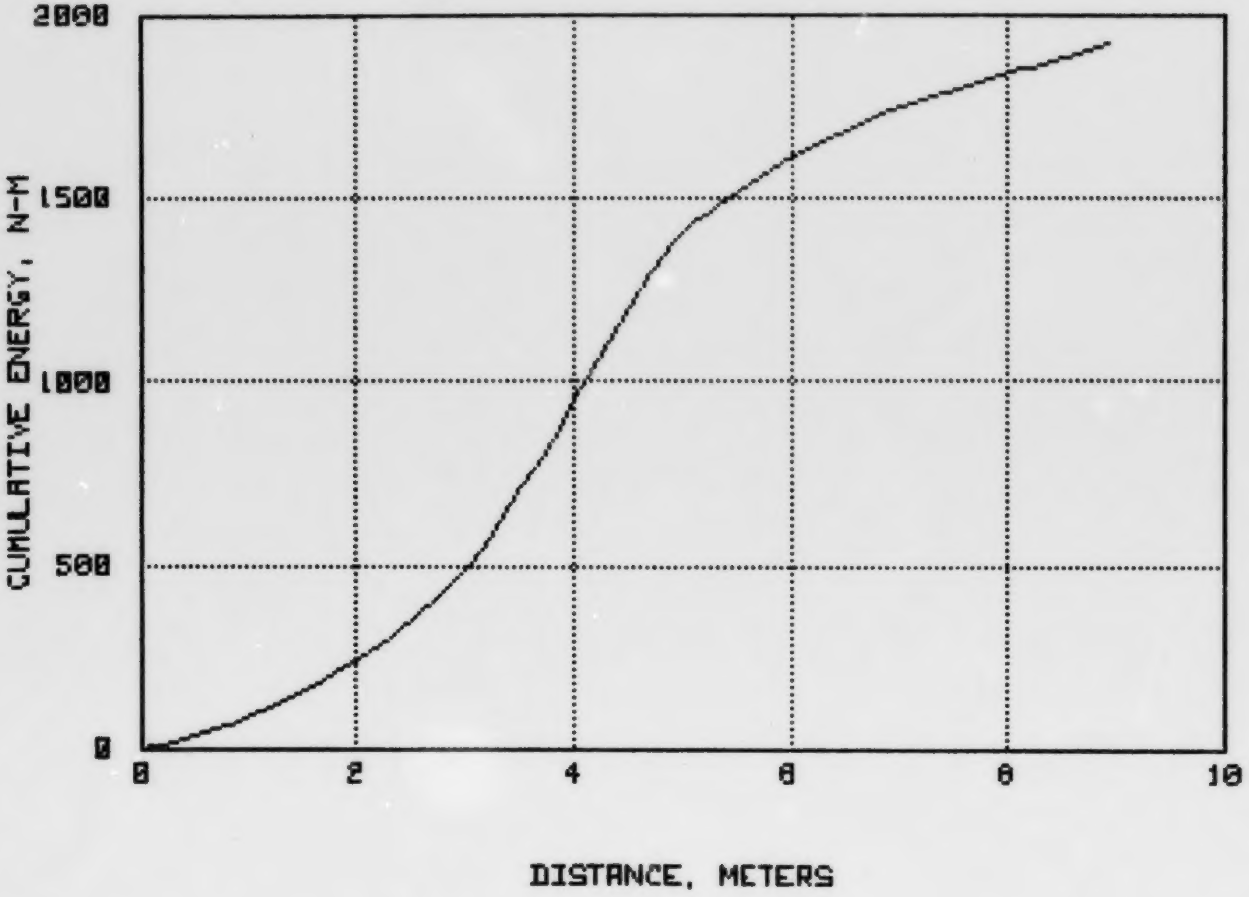

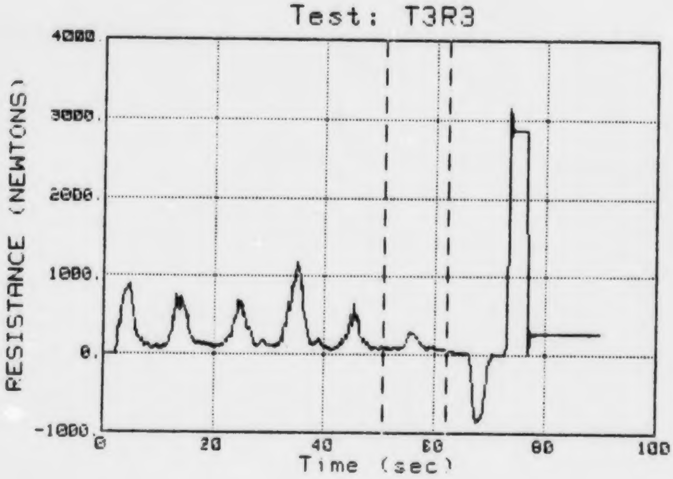
Test: T3R3
RESISTANCE (NEWTONS)
4000.
3000.
2000.
1000.
0.
-1000.
0
20
40
60
80
100
Time (sec)

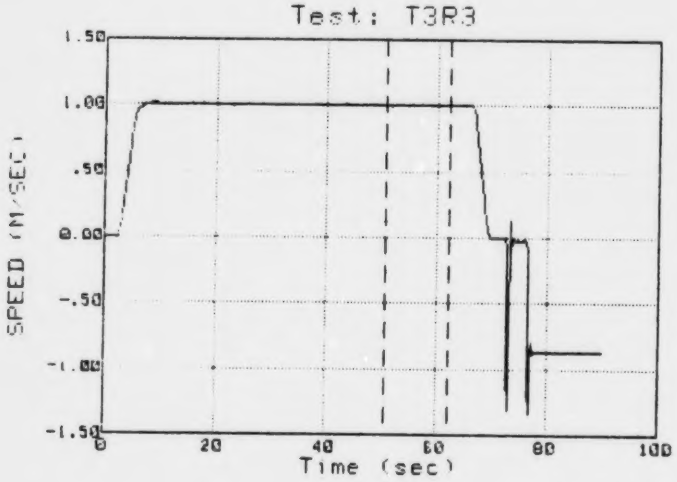
Test: T3R3
SPEED (M/SEC)
1.50
1.00
.50
0.00
-.50
-1.00
-1.50
0
20
40
60
80
100
Time (sec)

MODEL SCALE PENETRATION FORCE
TEST: T3R3 RIDGE: 3-55

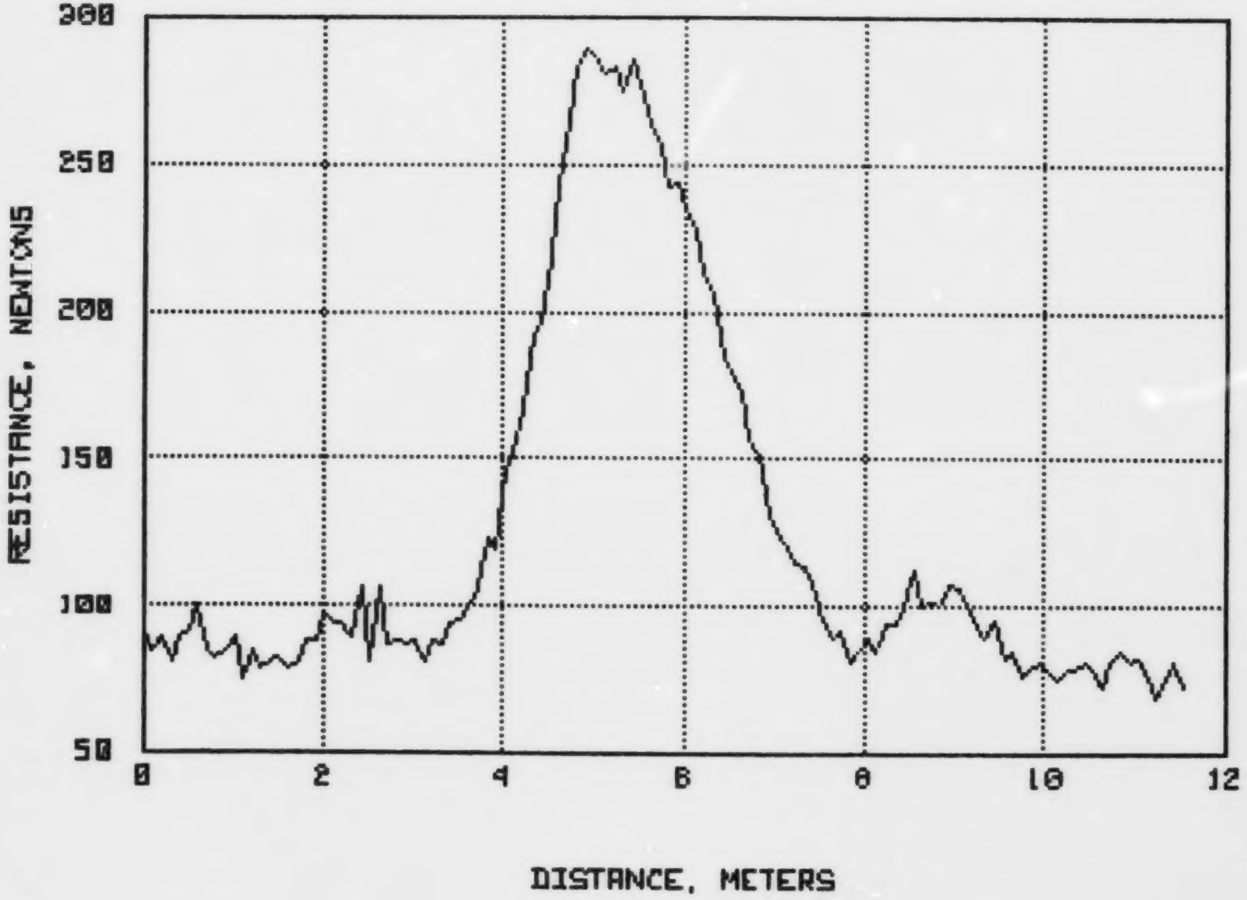

MODEL SCALE PENETRATION ENERGY
TEST: T3R3   RIDGE: 3-55

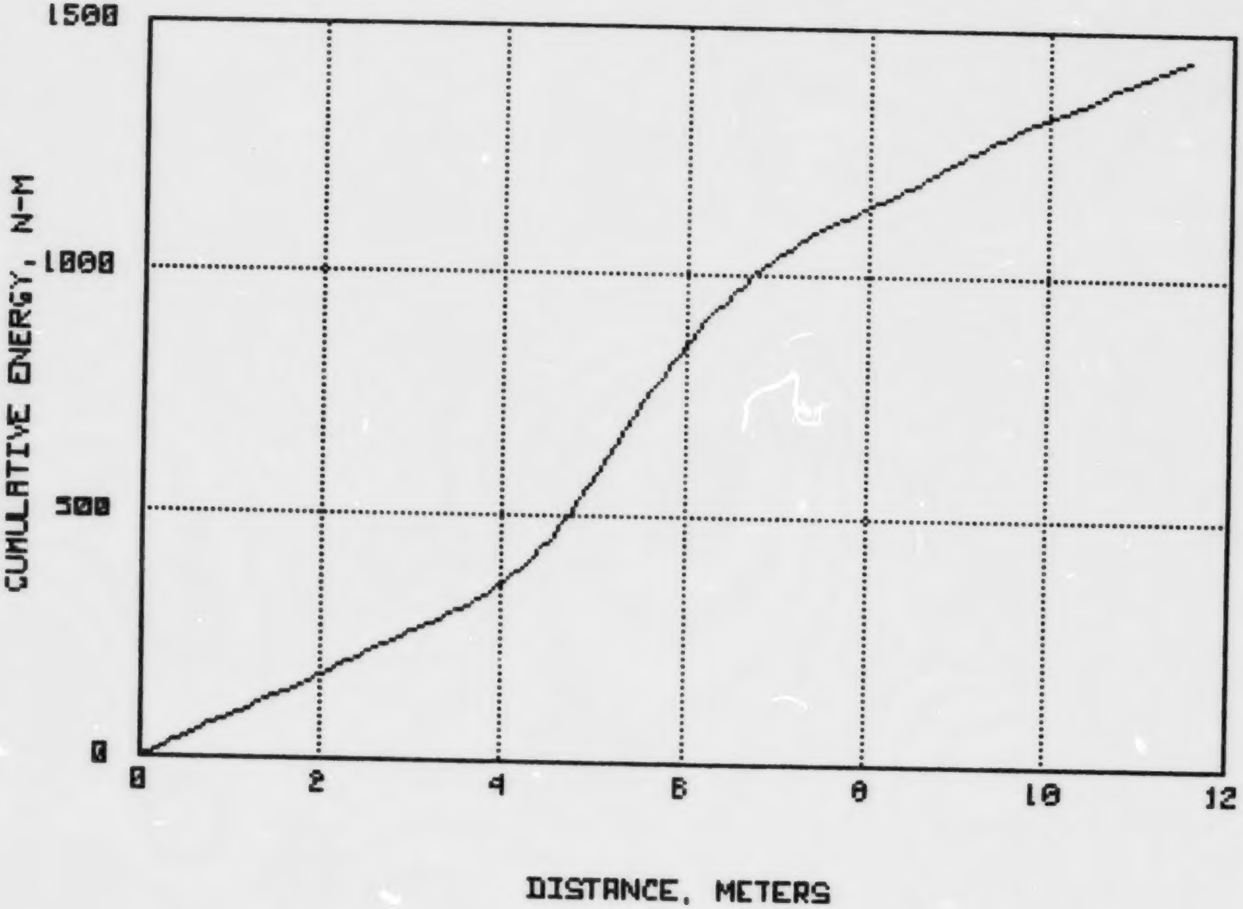

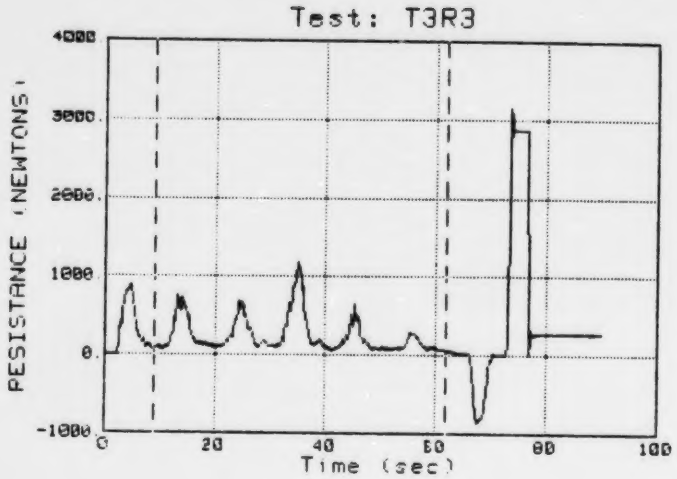
Test: T3R3
RESISTANCE (NEWTONS)
4000
3000.
2000.
1000
0.
-1000
0
20
40
60
80
100
Time (sec)

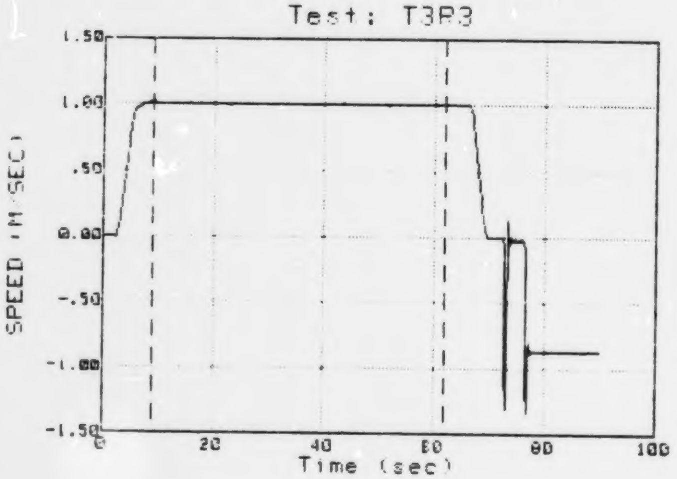
Test: T3R3
SPEED (M/SEC)
1.50
1.00
.50
0.00
-.50
-1.00
-1.50
0
20
40
60
80
100
Time (sec)

MODEL SCALE PENETRATION FORCE
TEST: T3R3 RIDGE: 3-123455

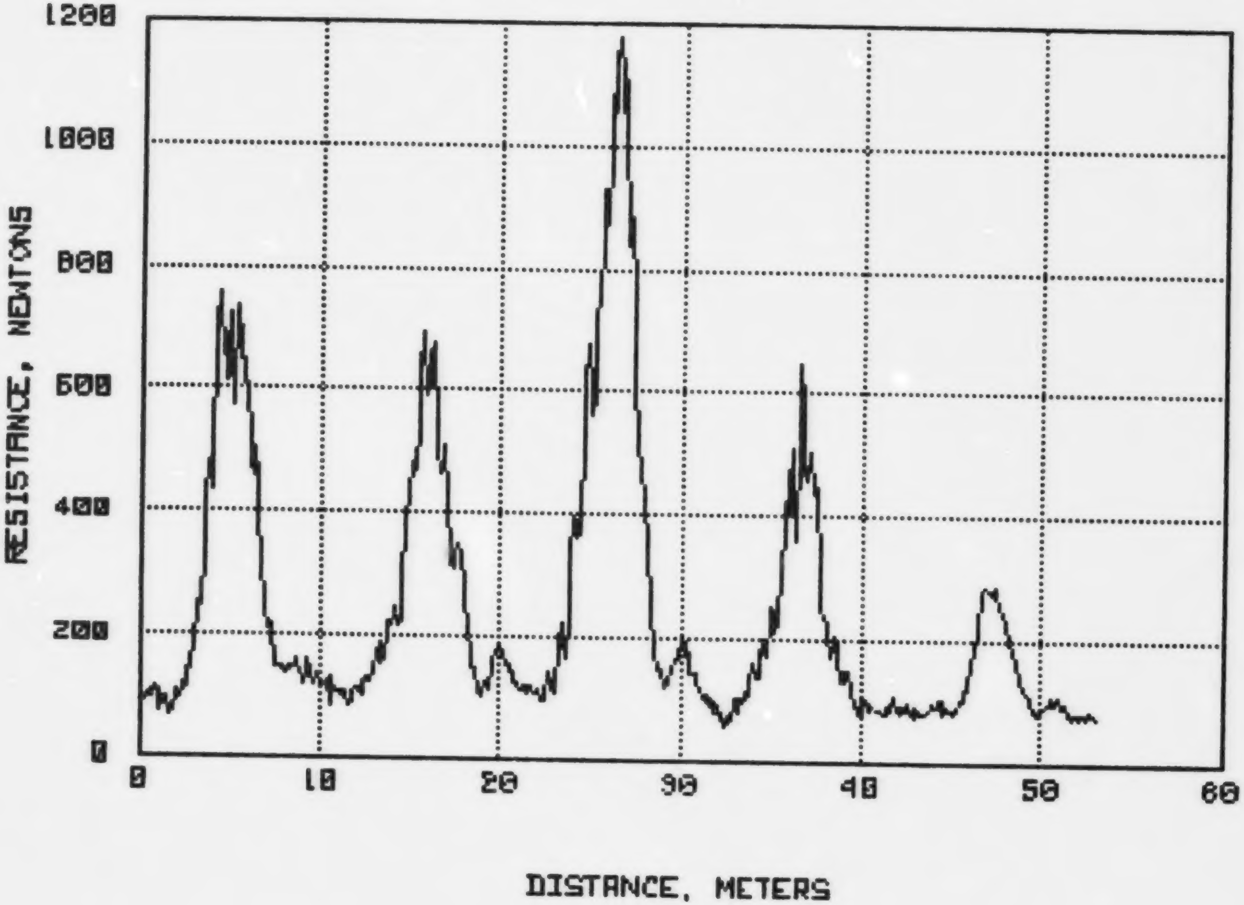

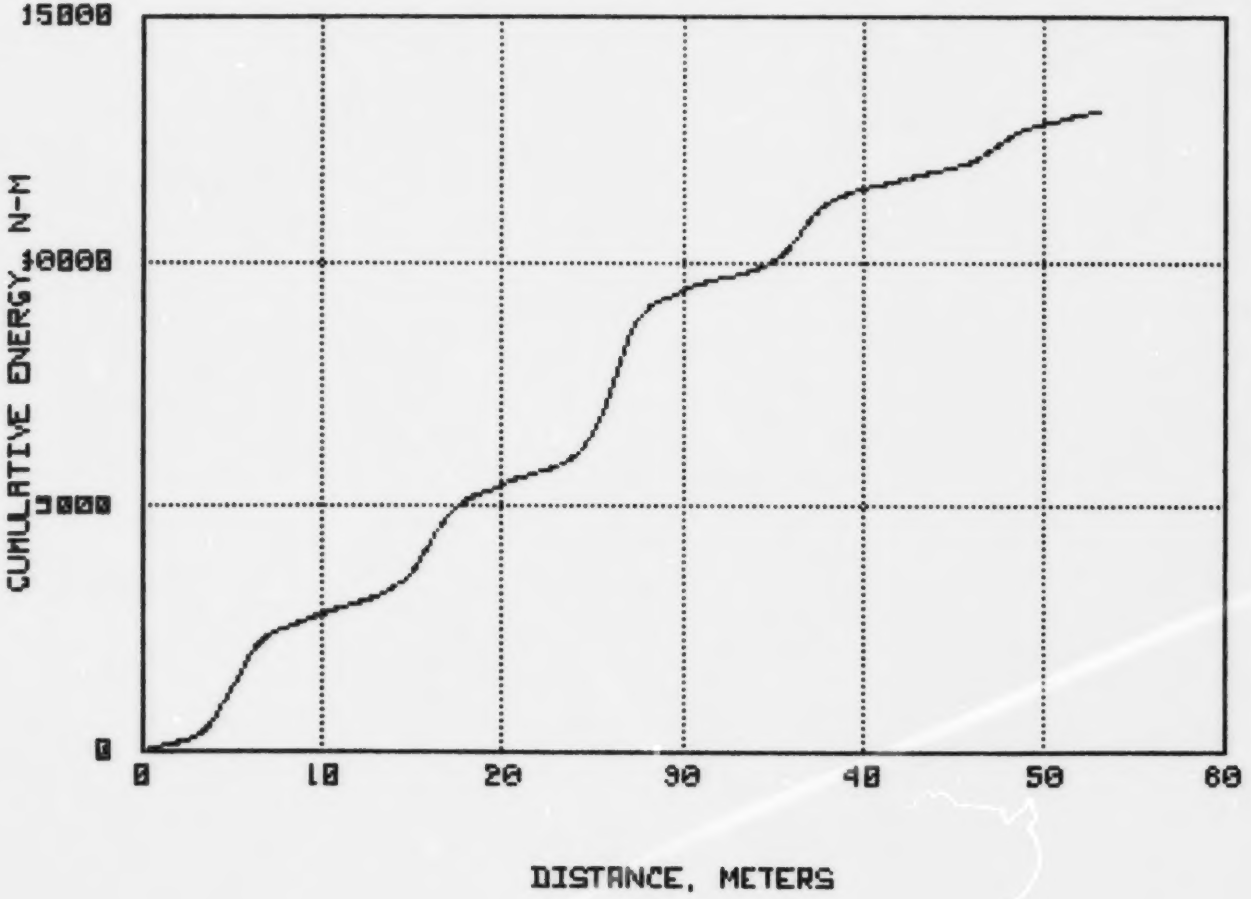

MODEL SCALE PENETRATION ENERGY
TEST: T3R3   RIDGE: 3-123455

APPENDIX E.3

SHEET #3 TESTS AT THE IMD: REDUCED PLOTS OF FORCE VS. PENETRATION AND CUMULATIVE PENETRATION ENERGY - TEST DATA FILTERED AT 100 HZ

```
TEST:     T3R1H         RIDGE:3-1N

DISTANCE,M            FORCE,N      CUM. ENERGY,N-M
    0.00                131                0
     .98                173              124
    1.95                190              238
    2.94                281              372
    3.92                331              567
    4.90                460             1015
    5.88                602             1644
    6.85                 85             2125
    7.84                -12             2362
    8.82                164             2512

PENETRATION OF   5.25 M AT MAX FORCE OF   970 N
PENETRATION OF   9.69 M AT MAX ENERGY OF  2653 N-M
```

```
TEST:     T3R3H         RIDGE:3-1S

DISTANCE,M            FORCE,N      CUM. ENERGY,N-M
    0.00                260                0
    1.03                169               99
    2.05               -113              200
    3.07                113              293
    4.09                113              474
    5.11               1166              967
    6.13                731             1676
    7.15                423             2240
    8.17                165             2569
    9.20                187             2725
   10.22                256             2862

PENETRATION OF   6.09 M AT MAX FORCE OF  1202 N
PENETRATION OF  10.28 M AT MAX ENERGY OF  2877 N-M
```

```
TEST:     T3R3H         RIDGE:3-2S

DISTANCE,M            FORCE,N      CUM. ENERGY,N-M
    0.00                140                0
    1.27                 79              165
    2.54                -60              305
    3.81                177              440
    5.08                185              652
    6.35                706             1080
    7.63                821             1842
    8.90                404             2387
   10.17                221             2658
   11.44                258             2832

PENETRATION OF   6.77 M AT MAX FORCE OF  1033 N
PENETRATION OF  12.58 M AT MAX ENERGY OF  2993 N-M
```

```
TEST:      T3P3H           RIDGE:3-3S

DISTANCE,M                FORCE,N       CUM. ENERGY,N-M
   0.00                     15                  0
   1.02                    100                113
   2.04                    189                229
   3.06                    217                383
   4.08                    591                819
   5.10                    769               1563
   6.12                   1225               2644
   7.14                    204               3429
   8.16                     19               3729
   9.19                    256               3876
  10.21                    327               4046

PENETRATION OF    5.62 M AT MAX FORCE OF   1552 N
PENETRATION OF   10.27 M AT MAX ENERGY OF  4061 N-M
```

```
TEST:      T3R3H           RIDGE:3-4S

DISTANCE,M                FORCE,N       CUM. ENERGY,N-M
   0.00                    131                  0
   1.10                      0                156
   2.21                    -60                256
   3.31                    467                352
   4.42                     73                483
   5.53                    113                720
   6.63                    514               1146
   7.74                     79               1714
   8.83                    104               1934
   9.94                    333               2084

PENETRATION OF    6.69 M AT MAX FORCE OF   1308 N
PENETRATION OF   10.93 M AT MAX ENERGY OF  2176 N-M
```

```
TEST:      T3R3H           RIDGE:3-5S

DISTANCE,M                FORCE,N       CUM. ENERGY,N-M
   0.00                     67                  0
   1.23                    108                103
   2.46                     25                196
   3.68                     -6                300
   4.92                     38                419
   6.14                    169                671
   7.37                    285                994
   8.60                    215               1187
   9.83                    237               1294
  11.05                    279               1408

PENETRATION OF    6.68 M AT MAX FORCE OF    573 N
PENETRATION OF   12.26 M AT MAX ENERGY OF  1499 N-M
```

```
TEST:      T3R3H          RIDGE:3-123455

DISTANCE,M               FORCE,N      CUM. ENERGY,N-M
    0.00                  -100                  0
    5.55                   556               1433
   11.10                   194               2972
   16.64                   733               4254
   22.18                   167               5766
   27.72                  1262               8092
   33.26                   -85               9915
   38.82                   548              11213
   44.35                   119              12034
   49.89                   385              12843

PENETRATION OF  27.49 M AT MAX FORCE OF  1552 N
PENETRATION OF  55.34 M AT MAX ENERGY OF 13423 N-M
```

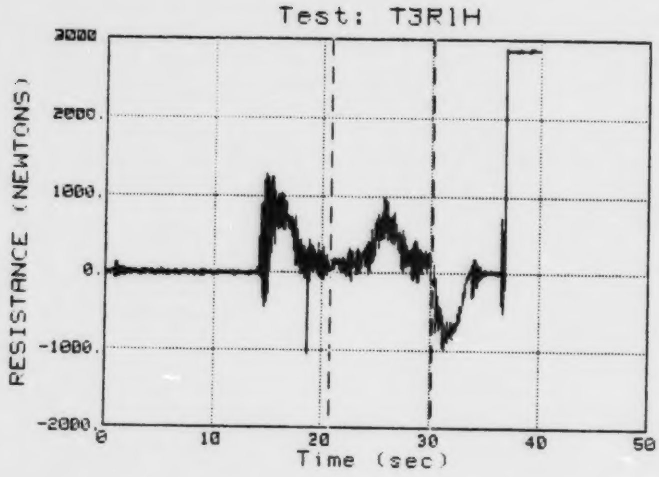
Test: T3R1H
RESISTANCE (NEWTONS)
3000
2000.
1000.
0.
-1000.
-2000.
0
10
20
30
40
50
Time (sec)

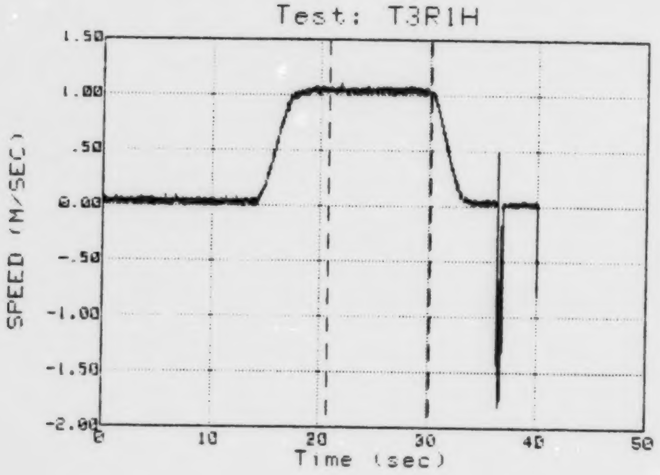
Test: T3R1H
SPEED (M/SEC)
1.50
1.00
.50
0.00
-.50
-1.00
-1.50
-2.00
0
10
20
30
40
50
Time (sec)

MODEL SCALE PENETRATION FORCE
TEST: T3R1H RIDGE: 3-1N

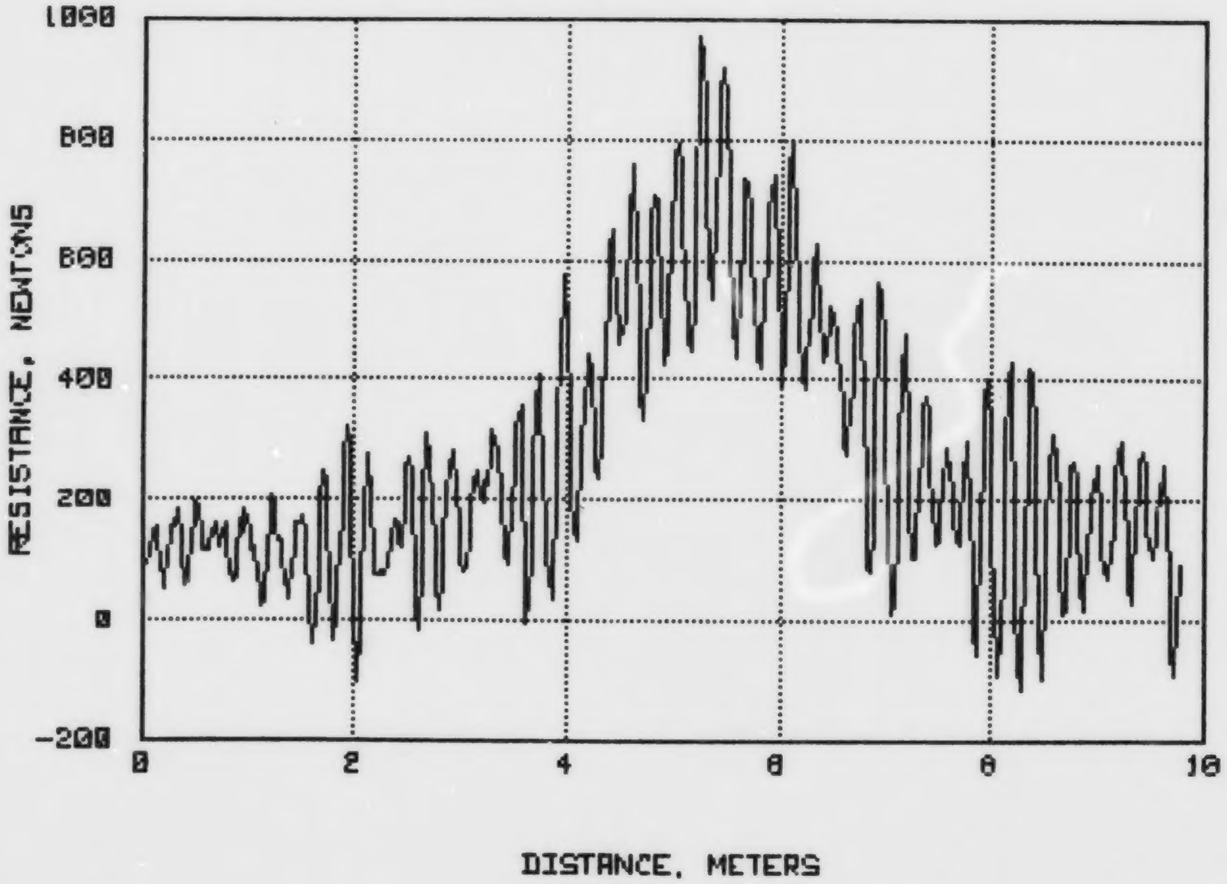

MODEL SCALE PENETRATION ENERGY
TEST: T3R1H   RIDGE: 3-1N

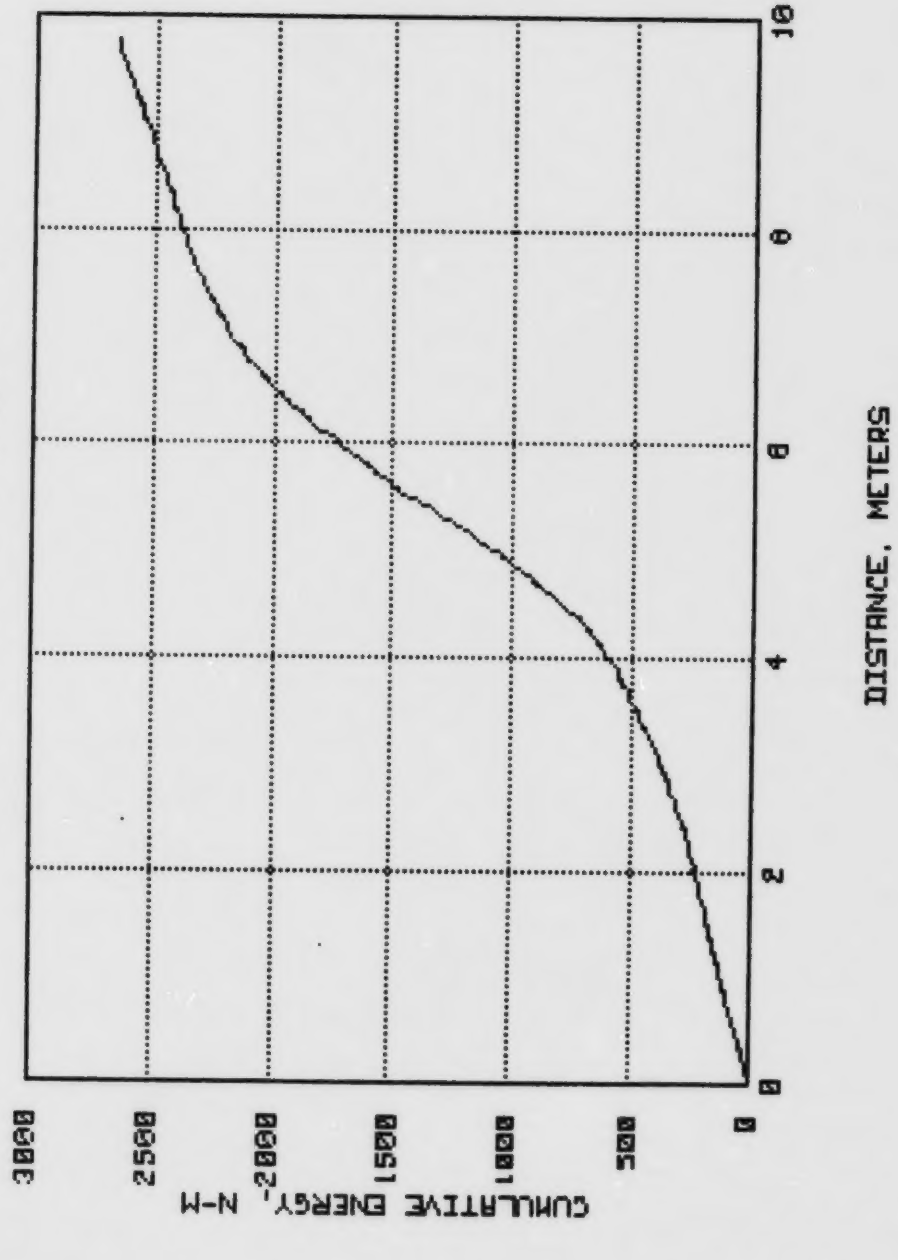

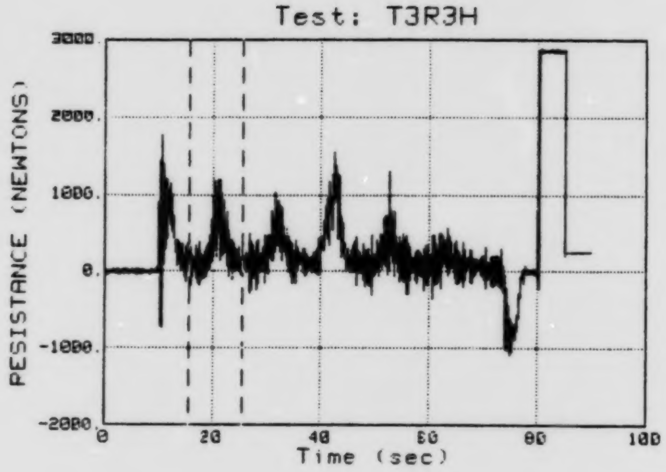
Test: T3R3H
RESISTANCE (NEWTONS)
3000.
2000.
1000.
0.
-1000.
-2000.
0
20
40
60
80
100
Time (sec)

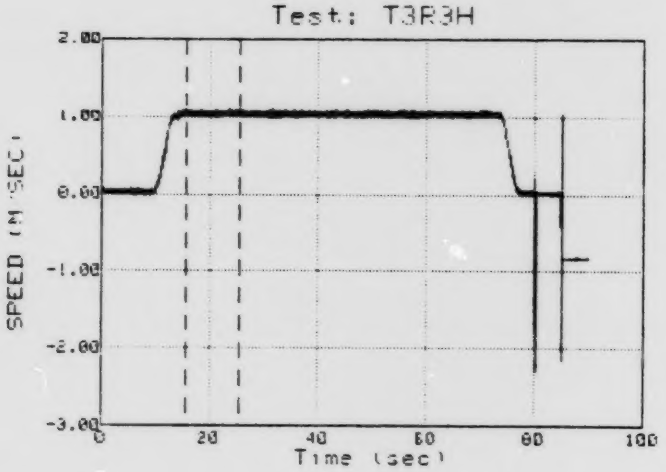
Test: T3R3H
SPEED (M/SEC)
2.00
1.00
0.00
-1.00
-2.00
-3.00
0
20
40
60
80
100
Time (sec)

MODEL SCALE PENETRATION FORCE
TEST: T3R3H RIDGE: 3-1S

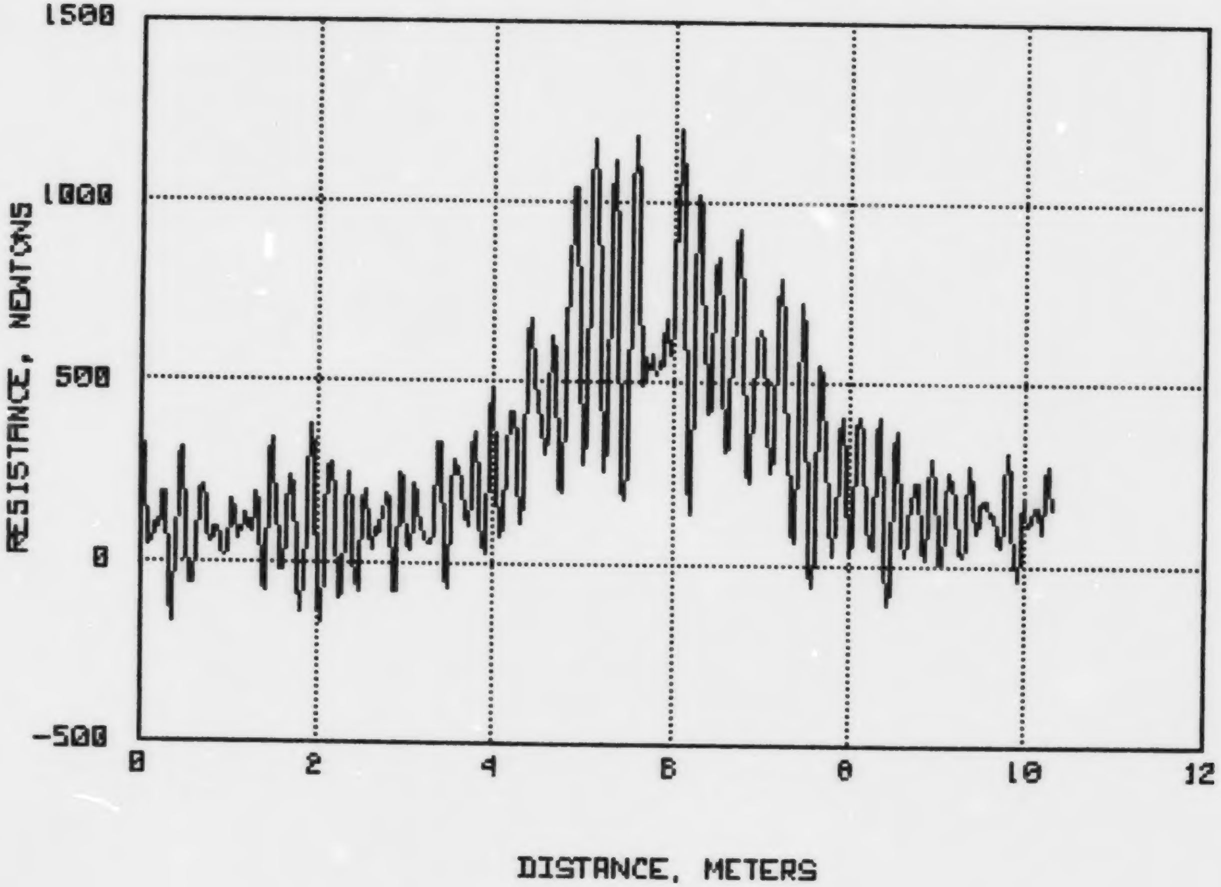

MODEL SCALE PENETRATION ENERGY
TEST: T3R3H RIDGE: 3-1S

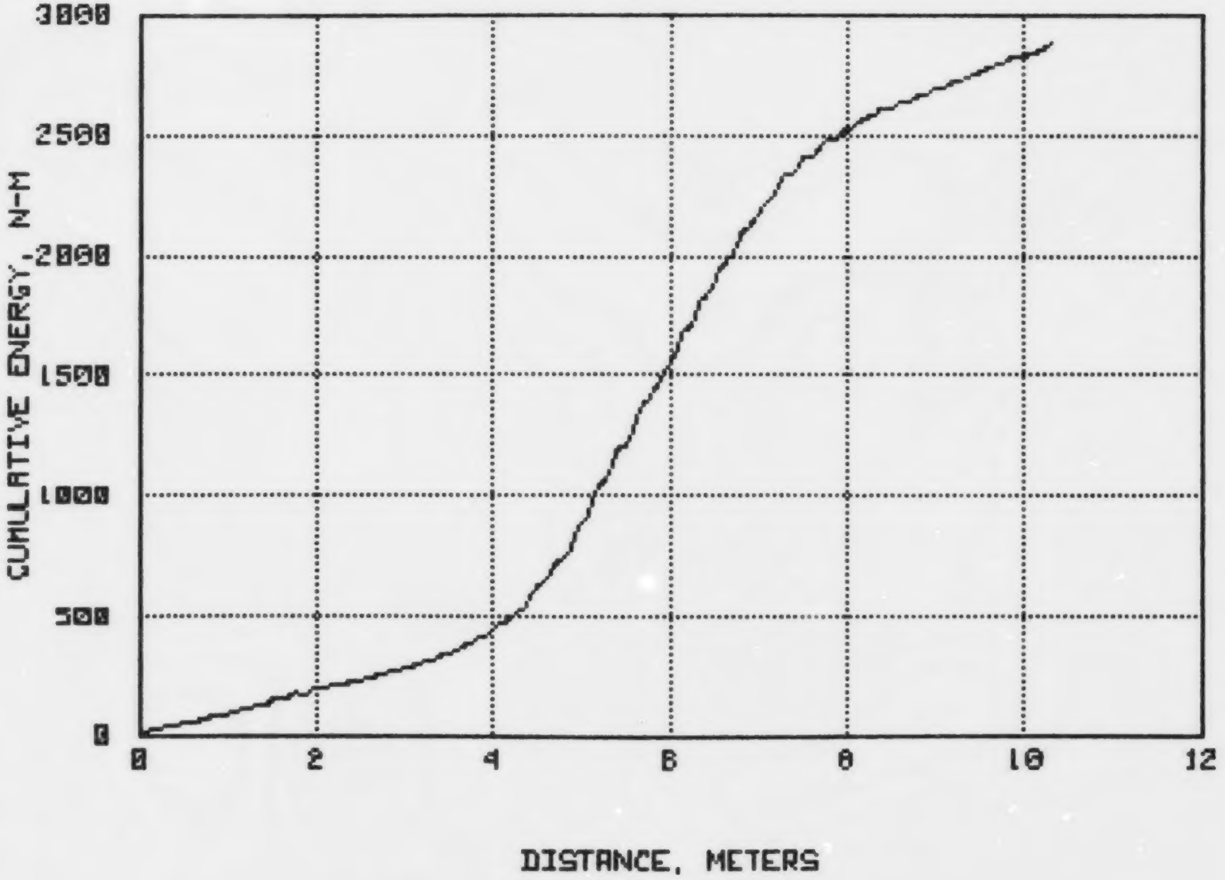

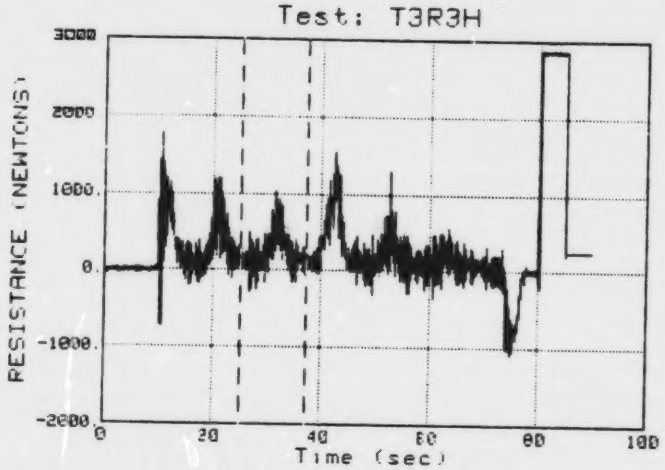
Test: T3R3H
RESISTANCE (NEWTONS)
3000
2000
1000.
0.
-1000.
-2000.
0
20
40
60
80
100
Time (sec)

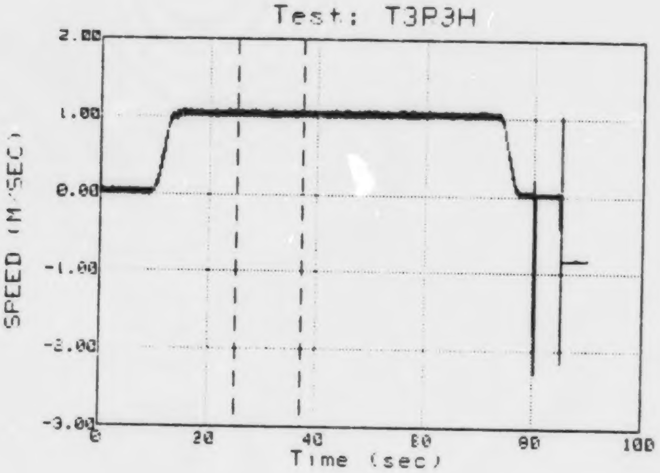
Test: T3P3H
SPEED (M/SEC)
2.00
1.00
0.00
-1.00
-2.00
-3.00
0
20
40
60
80
100
Time (sec)

MODEL SCALE PENETRATION FORCE
TEST: T3R3H RIDGE: 3-2S

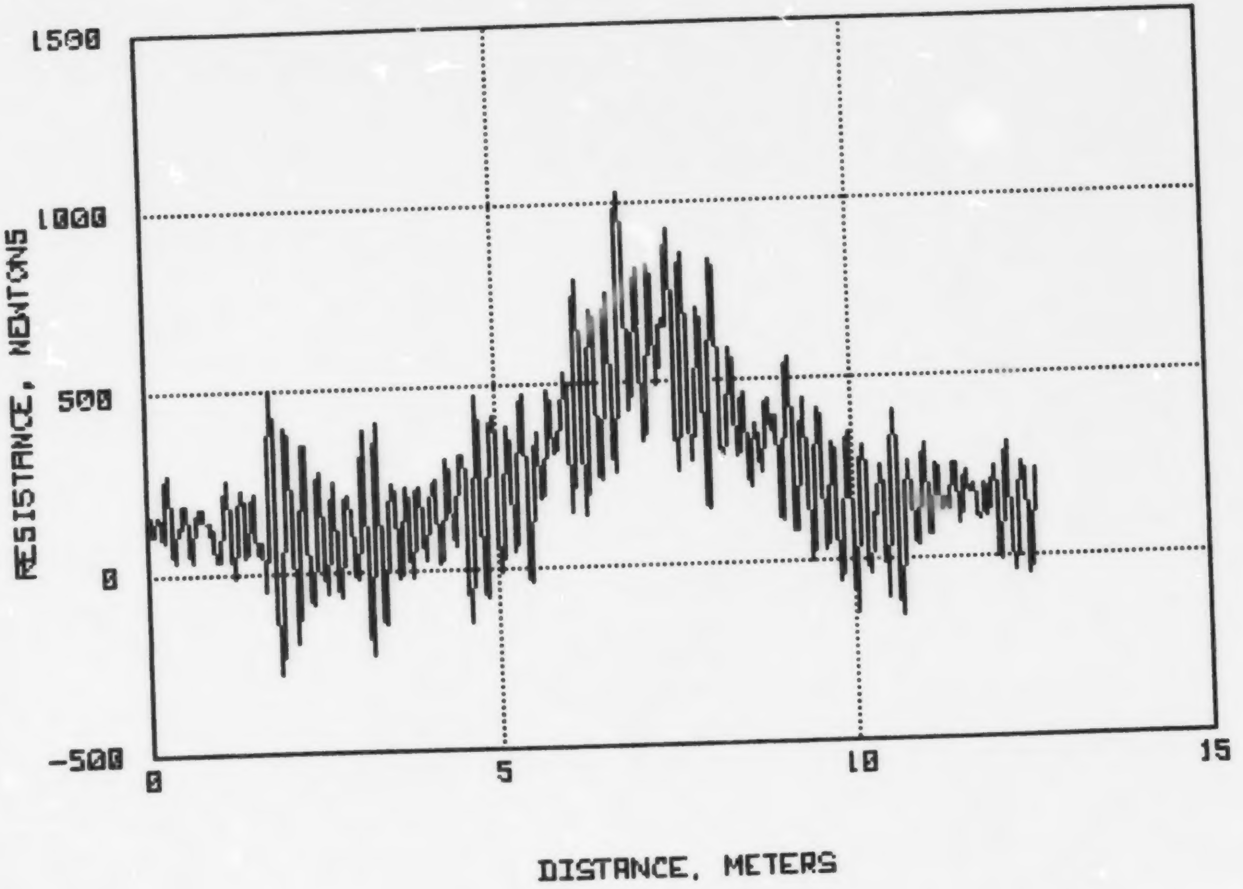

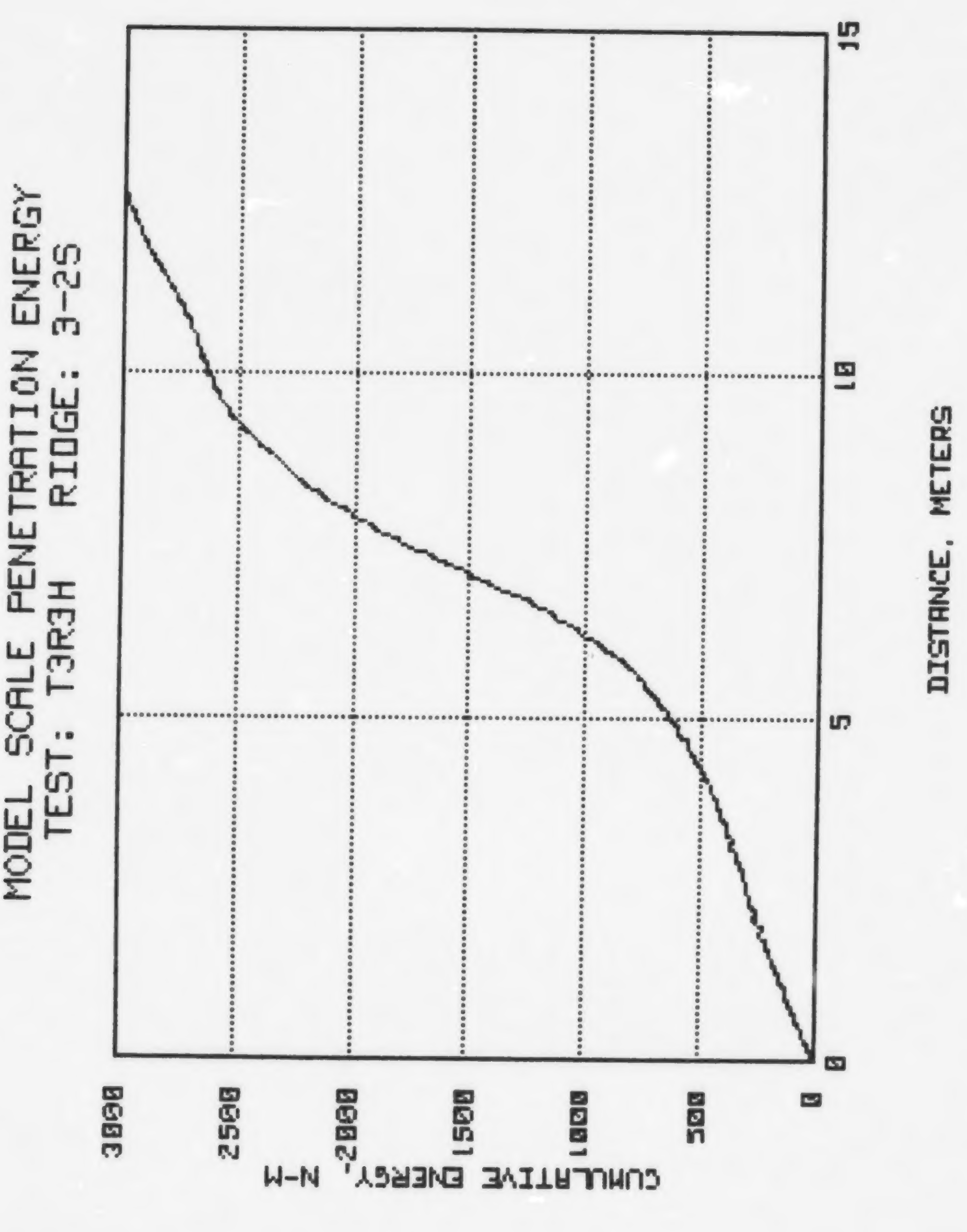
MODEL SCALE PENETRATION ENERGY
TEST: T3R3H RIDGE: 3-2S
CUMULATIVE ENERGY, N-M
3000
2500
2000
1500
1000
500
0
0
5
10
15
DISTANCE, METERS

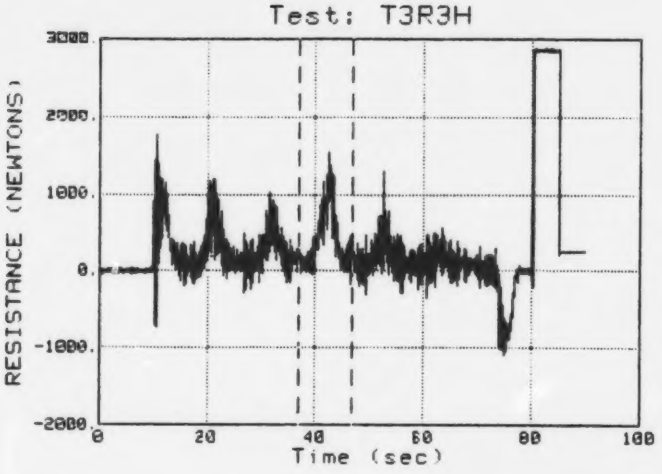
Test: T3R3H
RESISTANCE (NEWTONS)
3000.
2000.
1000.
0.
-1000.
-2000.
0
20
40
60
80
100
Time (sec)

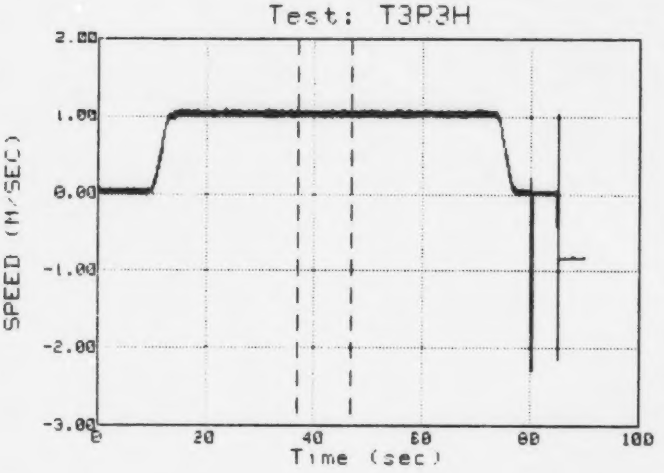
Test: T3R3H
SPEED (M/SEC)
2.00
1.00
0.00
-1.00
-2.00
-3.00
0
20
40
60
80
100
Time (sec)

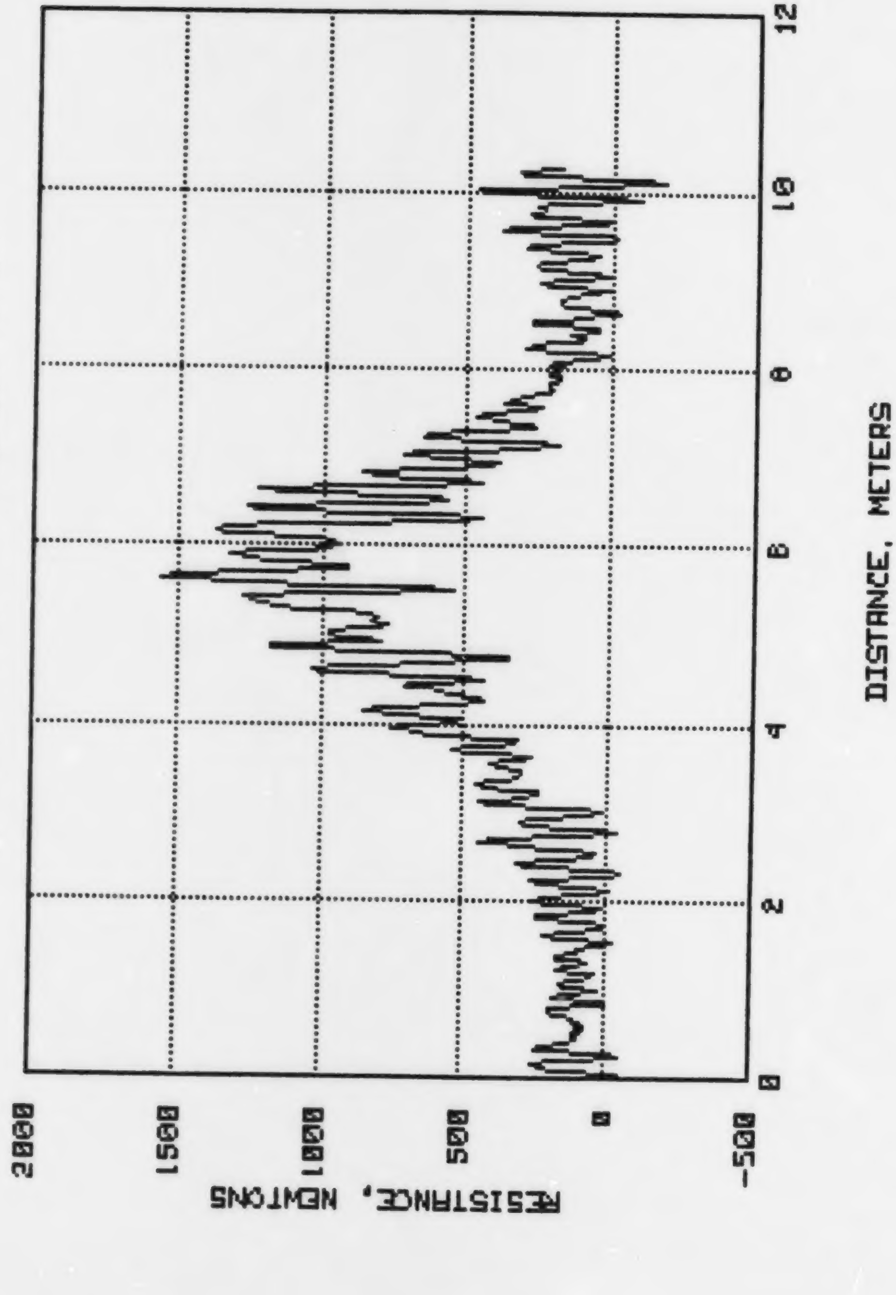

MODEL SCALE PENETRATION FORCE
TEST: T3R3H RIDGE: 3-3S

MODEL SCALE PENETRATION ENERGY
TEST: T3R3H RIDGE: 3-3S

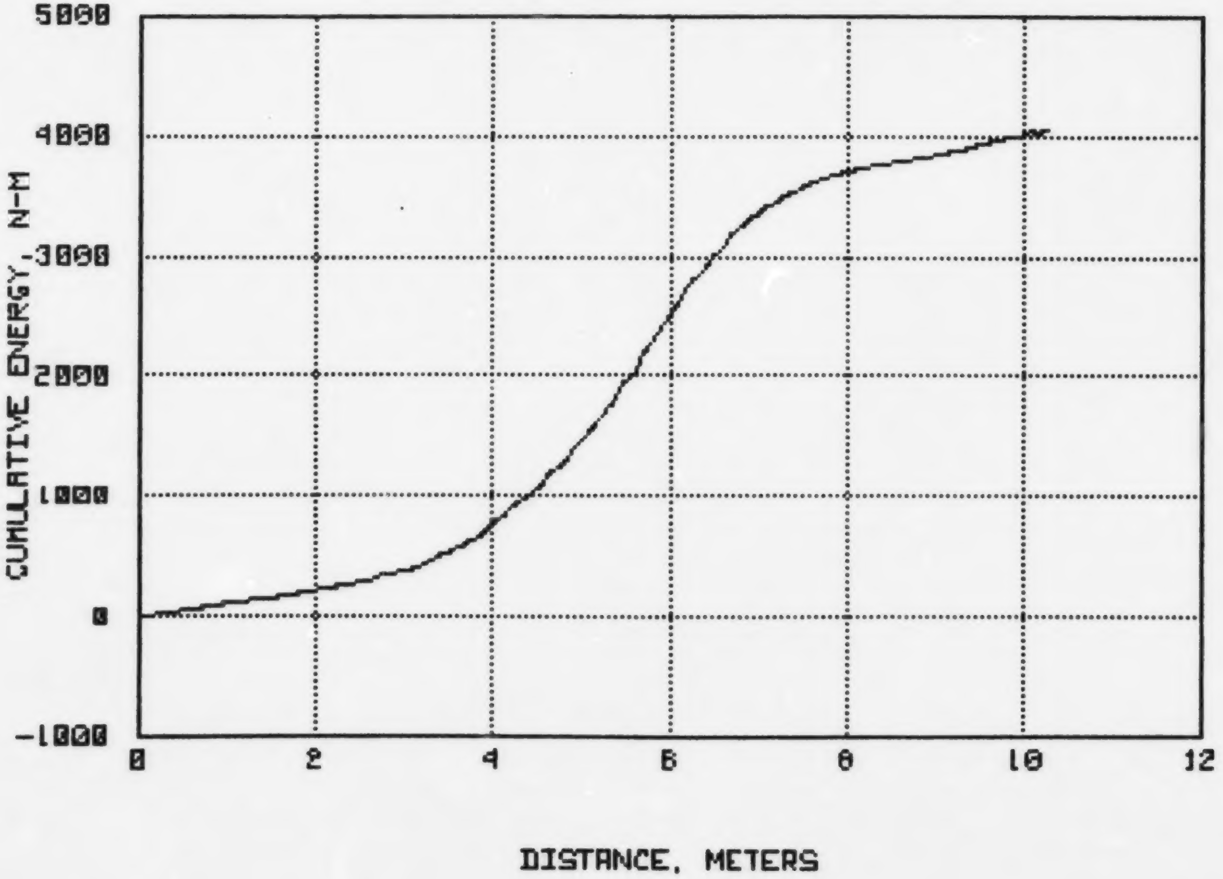

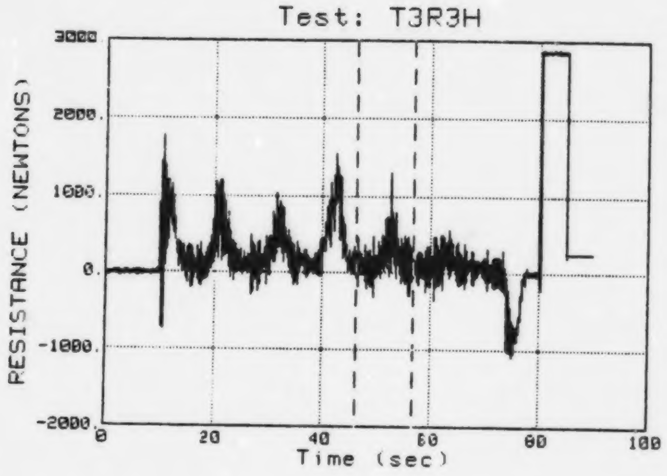
Test: T3R3H
RESISTANCE (NEWTONS)
3000
2000.
1000.
0.
-1000.
-2000.
0
20
40
60
80
100
Time (sec)

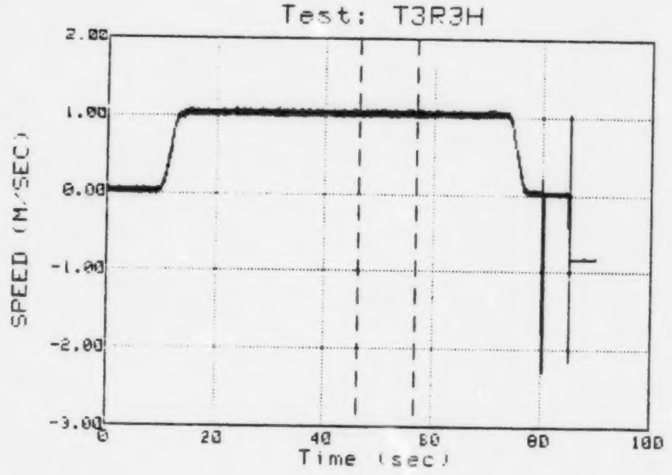
Test: T3R3H
SPEED (M/SEC)
2.00
1.00
0.00
-1.00
-2.00
-3.00
0
20
40
60
80
100
Time (sec)

MODEL SCALE PENETRATION FORCE
TEST: T3R3H RIDGE: 3-4S

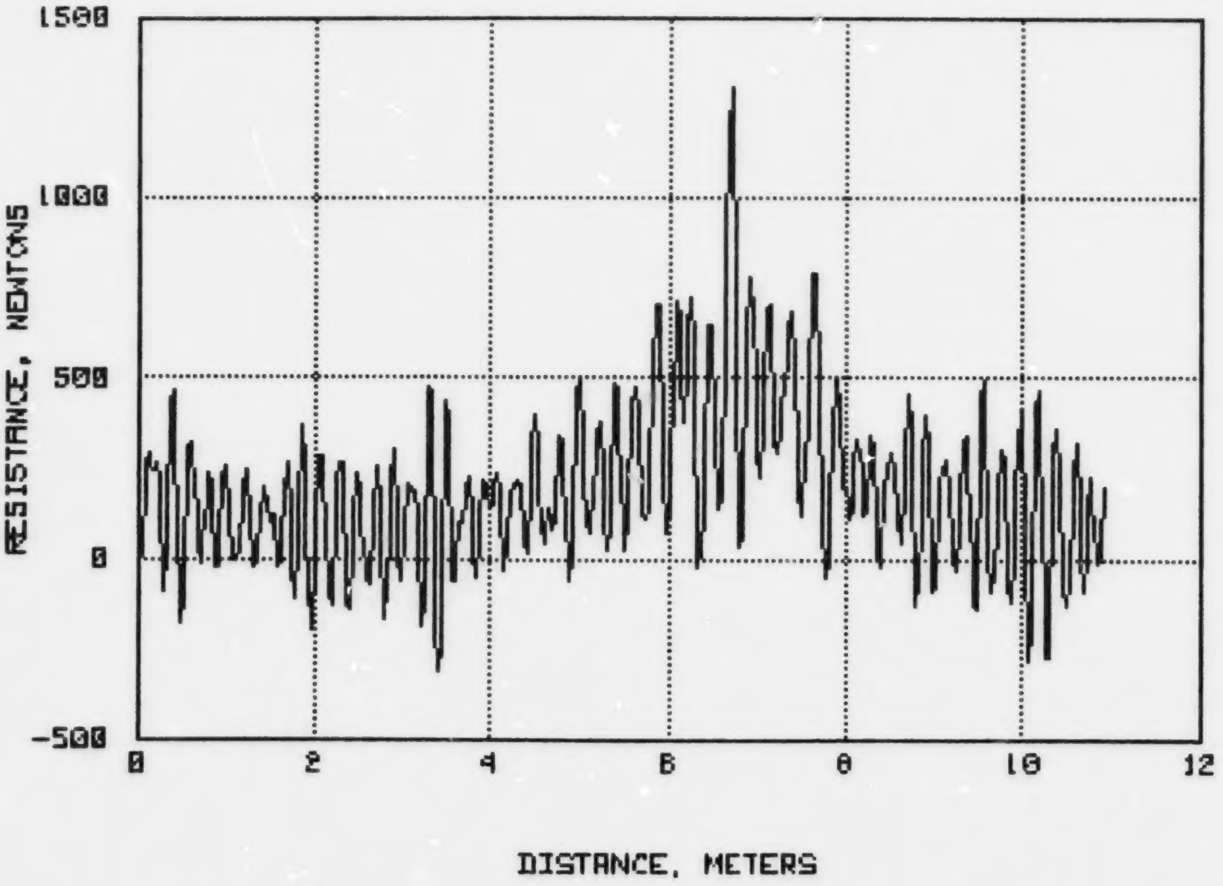

MODEL SCALE PENETRATION ENERGY
TEST: T3R3H RIDGE: 3-4S

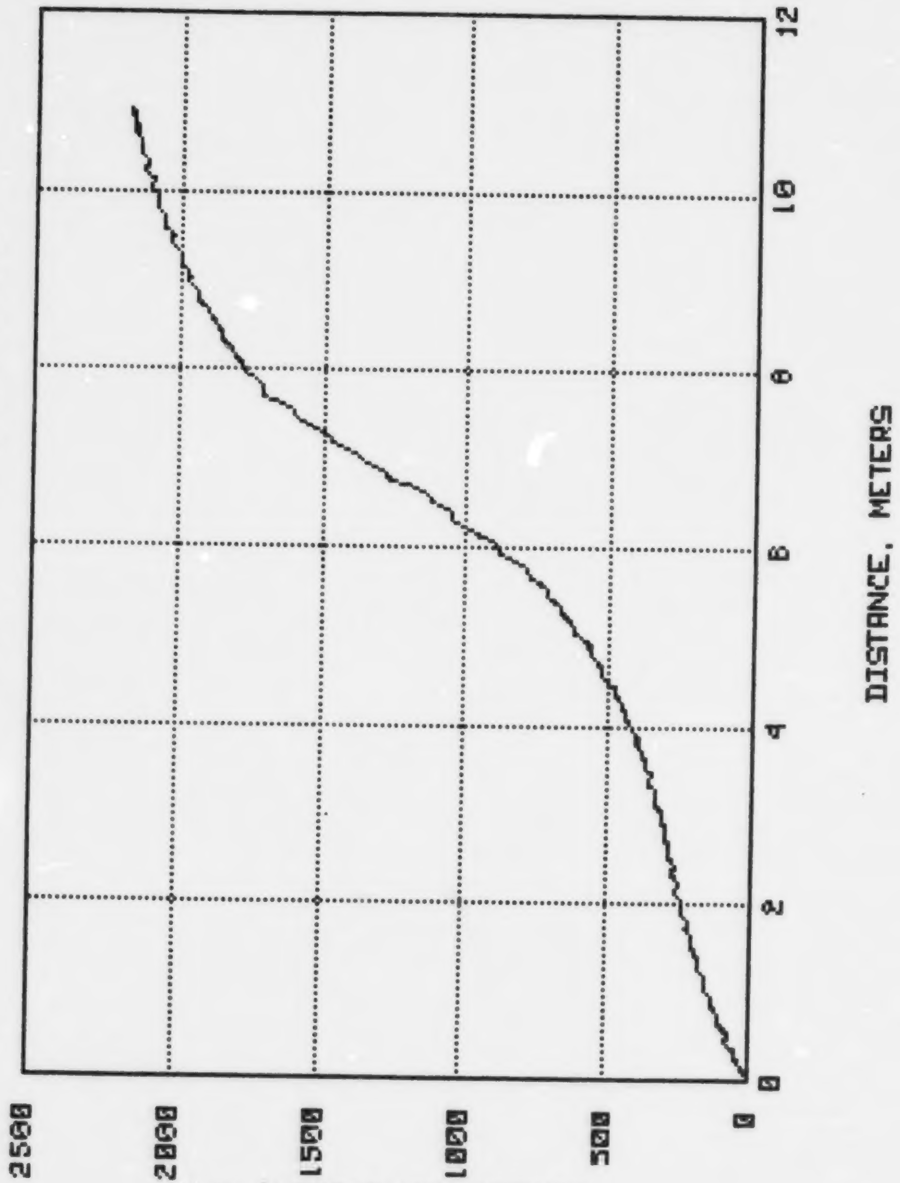

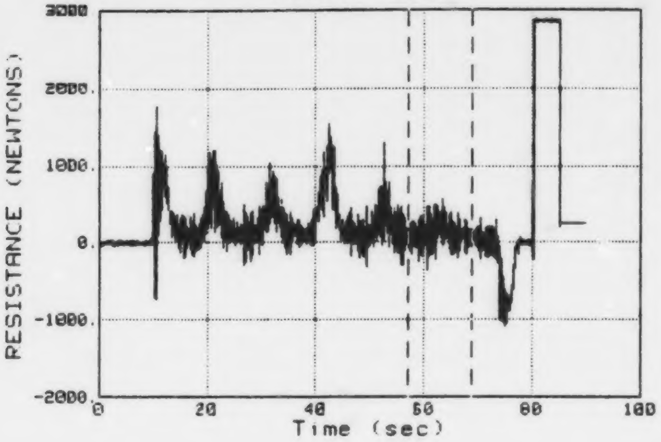

Test: T3R3H

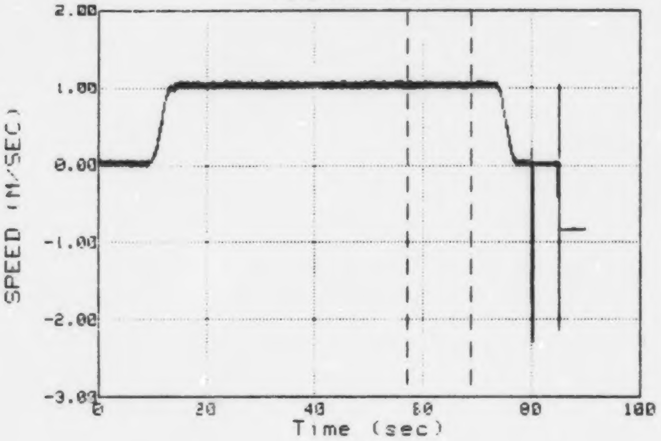

Test: T3R3H

MODEL SCALE PENETRATION FORCE
TEST: T3R3H   RIDGE: 3-5S

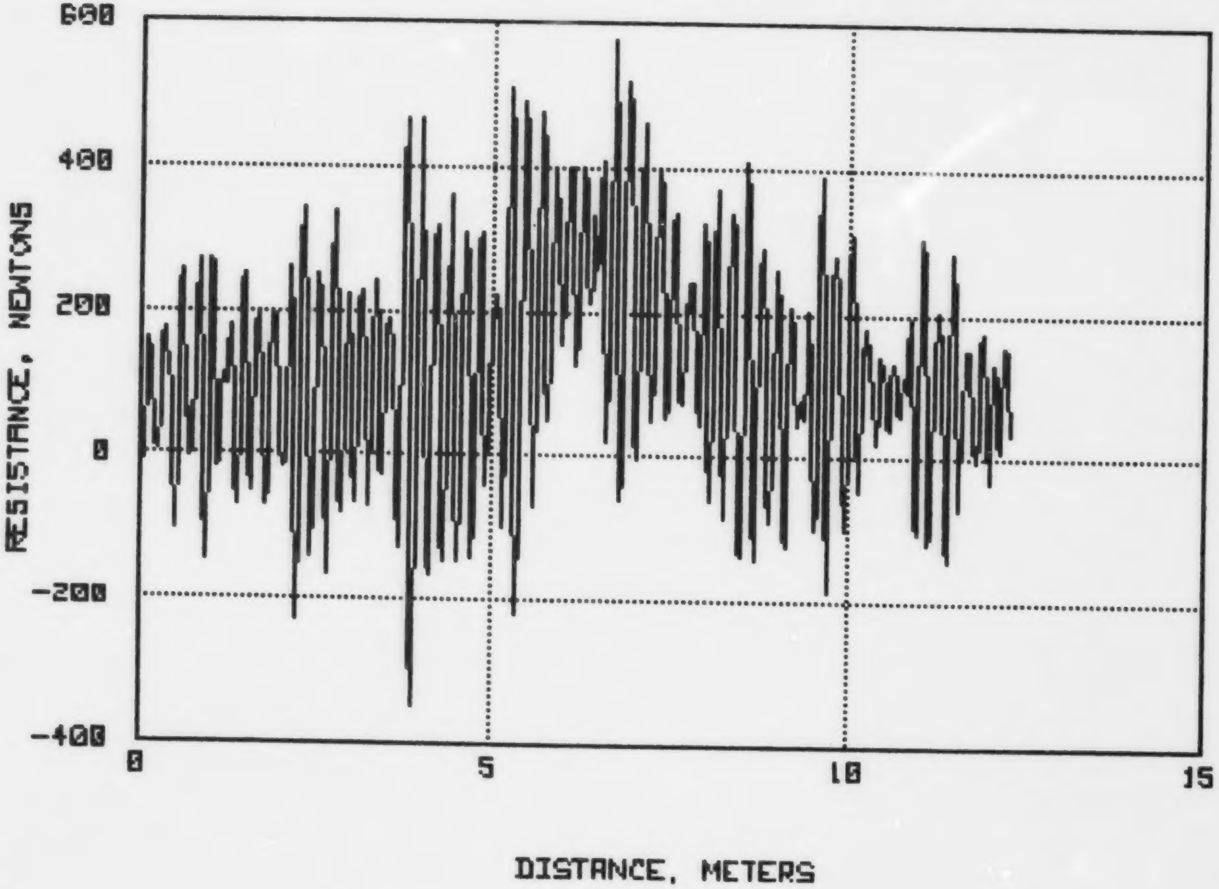

MODEL SCALE PENETRATION ENERGY
TEST: T3R3H RIDGE: 3-55

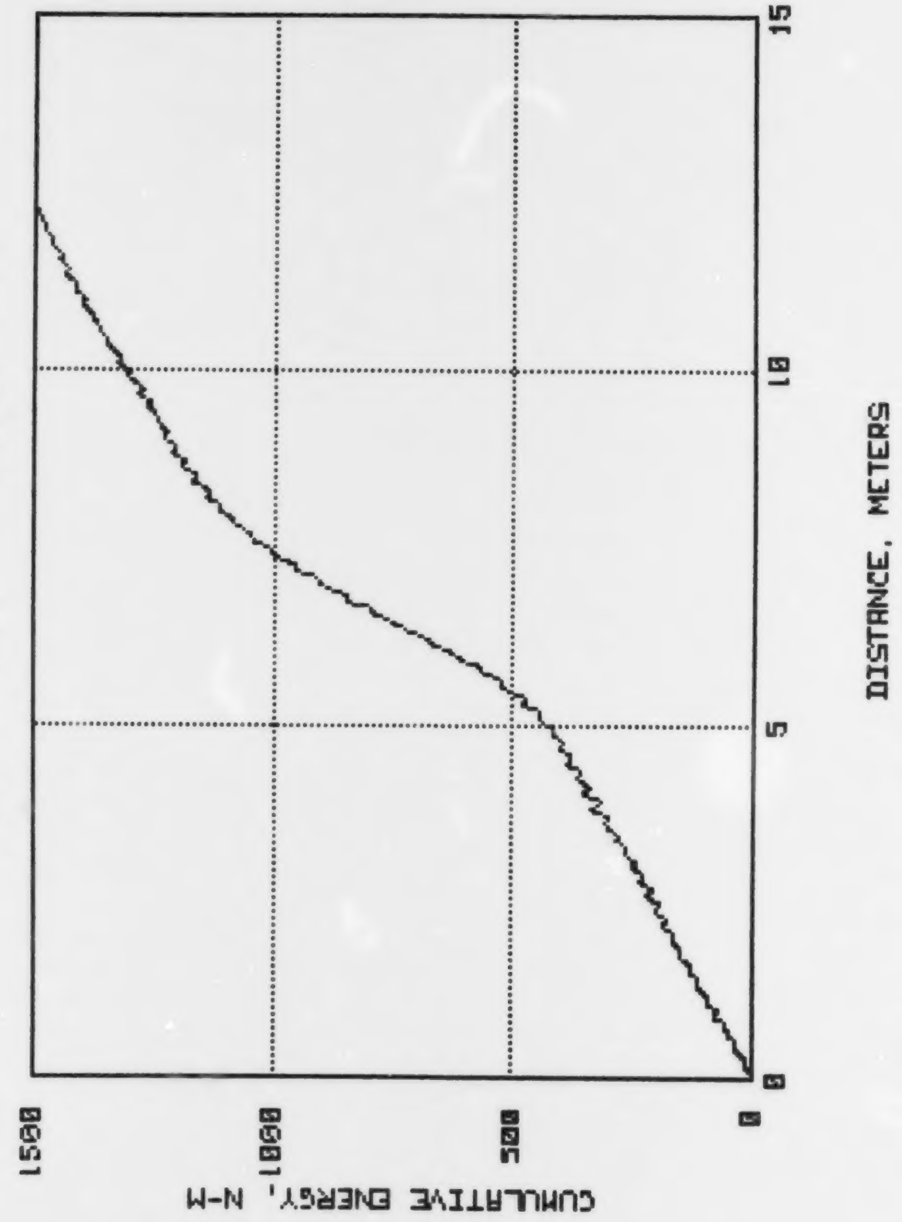

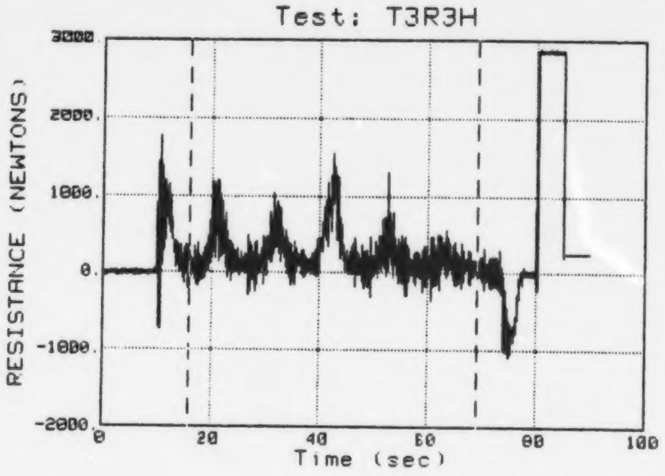
Test: T3R3H
RESISTANCE (NEWTONS)
3000
2000.
1000.
0.
-1000.
-2000
0
20
40
60
80
100
Time (sec)

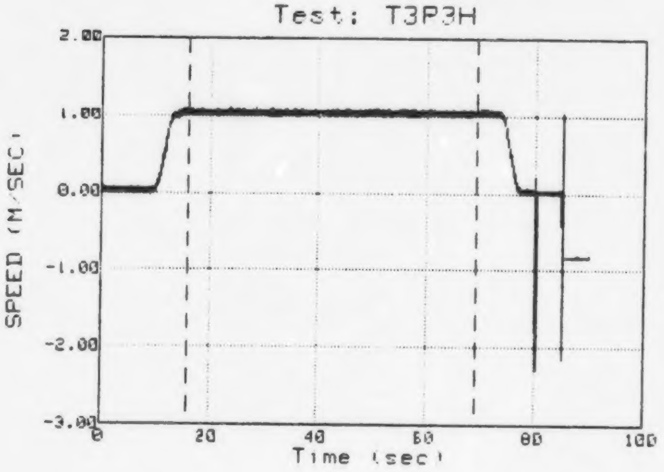
Test: T3P3H
SPEED (M/SEC)
2.00
1.00
0.00
-1.00
-2.00
-3.00
0
20
40
60
80
100
Time (sec)

MODEL SCALE PENETRATION FORCE
TEST: T3R3H   RIDGE: 3-12345S

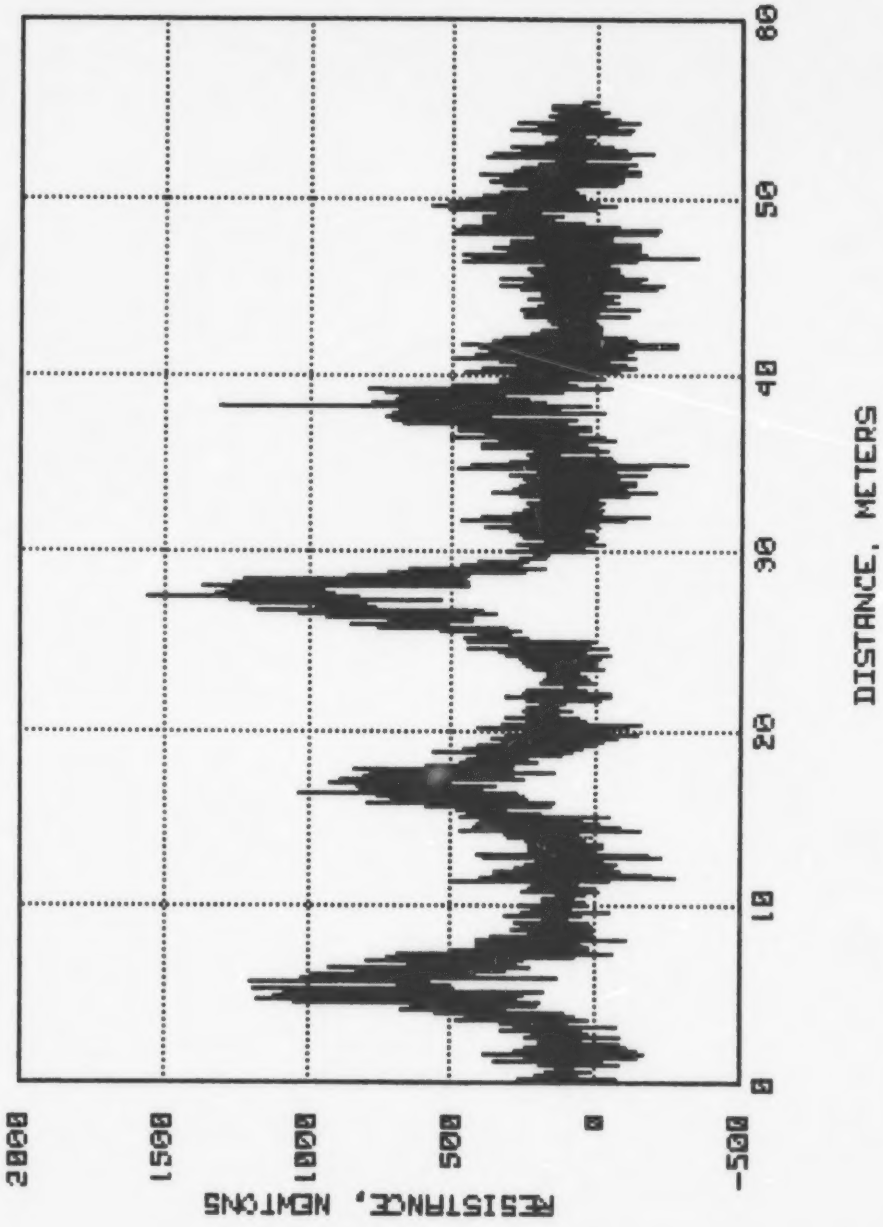

MODEL SCALE PENETRATION ENERGY
TEST: T3R3H   RIDGE: 3-12345S

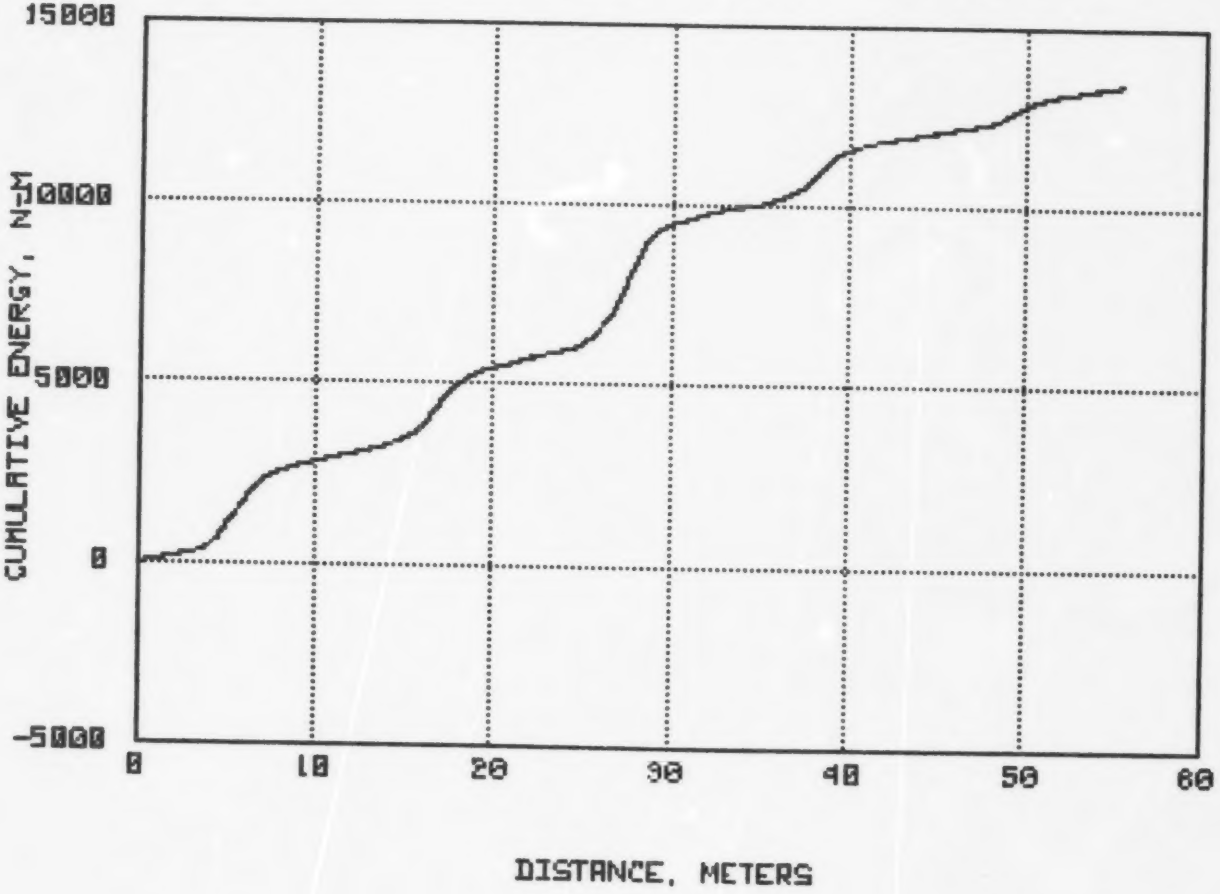

APPENDIX E.4

ICE AND RIDGE PROPERTIES

FLEET TECHNOLOGY LIMITED (FTL)

Engineering Design Calculations

JOB No. 3208
SHEET 1 OF 2
DATE May 6/87
BY
CH'K BY

PROJECT RIDGE MODELLING
SUBJECT RIDGE MECHANICAL PROPERTIES

FLEXURAL STRENGTH OF CONSOLIDATED LAYER

MEAS. TIME	RIDGE #	BEAM THICK (mm)	BEAM WIDTH (mm)	BEAM LENGTH (mm)	FAILURE LOAD (kg)	FLEX. STR. (kpa)	COMMENTS
1450	3-3S	66	108	203	5.5	138	BROKE SHORT
	3-3S	105	132	218	1.8	16	
1500	3-3N	74	114	235	1.3	28	
	3-3N	69	108	265	2.0	61	
	3-3N	69	102	220	1.5	40	
1520	3-2S	62	126	270	1.1	79	

THICKNESS OF CONSOLIDATED LAYER

RIDGE	MEASURED VALUES (mm)	AVG (mm)
3-1N	40, 52, 39, 28, 60, 65, 64, 33, 45	47 ± 13
3-2N	50, 50, 45, 40, 30, 45, 50	44 ± 7
3-3N	65, 70, 60, 75, 60, 55, 55, 60, 65, 60	63 ± 6
3-1S	80, 55, 60, 65, 90, 105, 105, 80, 110, 92	84 ± 19
3-2S	34, 33, 72, 74, 77, 45, 43, 40, 67, 68, 64	56 ± 16
3-3S	90, 80, 80, 80, 90, 75, 105, 95, 77, 101, 103	93 ± 9

VOLUME OF ICE USED TO BUILD THE RIDGES

ICE THICKNESS = 20 mm
LENGTH OF ICE SHEET USED PER RIDGE = 15m
INITIAL VOLUME OF ICE PER RIDGE = 0.30 m^3/m WIDTH OF THE BASIN

ARCTEC CANADA LIMITED
Engineering Design Calculations

JOB No. 3208
SHEET 2 OF 2
DATE May 6/81
BY
CH'K BY

PROJECT RIDGE MODELLING
SUBJECT RIDGE MECHANICAL PROPERTIES

RIDGE CROSS-SECTIONAL AREA

RIDGE #	RIDGE WIDTH (m)	TOTAL AREA OF CONS. LAYER (m^2)	TOTAL AREA OF RIDGE (m^2)
3-1N	2.2	0.103	0.560
3-2N	2.5	0.110	0.740
3-3N	2.0	0.126	0.695
3-1S	2.5	0.210	0.845
3-2S	3.0	0.168	0.870
3-3S	2.5	0.233	0.870

RIDGE BULK DENSITY

TIME : 1530

RIDGE #	SUBMERGENCE FORCE (kg)	ICE COLUMN SIZE AREA (cm x cm)	ICE COLUMN SIZE DEPTH (cm)	WT. IN AIR (kg)	BULK DENSITY (kN/m^3)
3-1S	1.5	23 x 22	40[1]	Not Meas.	9.3[2]
3-1S	0.90	30 x 20	40[1]	Not Meas.	9.6[2]
3-1N	1.15	21 x 22	35[1]	Not Meas.	9.3[2]
3-2N	1.5	26 cm Ø	Not Used	9.5	8.6[3]
3-2N	1.5	26 cm Ø	31	Not Used	9.1[2]

Notes: 1. Average ridge depth (approx) in centre area of ridge profile.
2. Bulk density computed from measurements of ice column size and submergence force.
3. Bulk density computed from measurement of submergence force and wt. of ice in air.

FLEET TECHNOLOGY LIMITED (FTL)

Engineering Design Calculations

JOB No. 3208
SHEET 1 OF 3
DATE MAY 6/93
BY
CH'K BY

PROJECT RIDGE MODELLING
SUBJECT CROSS-SECTIONAL PROFILE DATA FOR RIDGES 111
SHEET #3

RIDGE 3-1N		RIDGE 3-2N		RIDGE 3-3N		RIDGE 3-1S		RIDGE 3-2S		RIDGE 3-3S	
X(cm)	Z(cm)	X(cm)	Z(cm)	X(cm)	Z(cm)	X(cm)	Z(cm)	X(cm)	Z(cm)	X(cm)	Z(cm)
0	2.5	0	2.5	0	2.5	0	2.5	0	2.5	0	2.5
25	17.5	25	27.5	25	45	50	37.5	50	17.5	50	45
50	22.5	50	37.5	50	37.5	100	45	100	32.5	100	45
75	37.5	75	42.5	75	37.5	150	45	150	45	150	45
100	[illegible]	100	42.5	100	45	200	2.5	200	45	200	2.5
125	[illegible]	125	37.5	125	45			250	2.5		
150	[illegible]	150	32.5	150	37.5						
175	[illegible]	175	32.5	175	12.5						
200	[illegible]	200	22.5	200	2.5						
[illegible]	2.5	225	17.5								
		250	2.5								

PLAN LAYOUT OF BASIN :

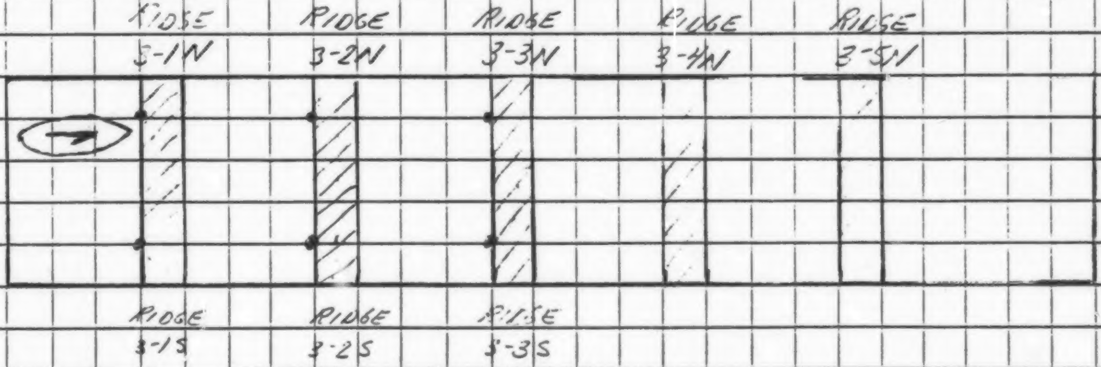

- ORIGIN OF COORDINATE SYSTEM USED FOR EACH RIDGE.

NOTE: ALL MEASUREMENTS IN THE Z DIRECTION APPLY TO THE TOTAL DEPTH (i.e. SAIL AND KEEL) OF THE RIDGE.

FLEET TECHNOLOGY LIMITED (FTL)

Engineering Design Calculations

JOB No. 3208
SHEET 2 OF 3
DATE May 6/83
BY
CH'K BY

PROJECT: RIDGE MODELLING
SUBJECT: CROSS-SECTIONAL PROFILES OF RIDGES IN SHEET #3

RIDGE 3-1 N:

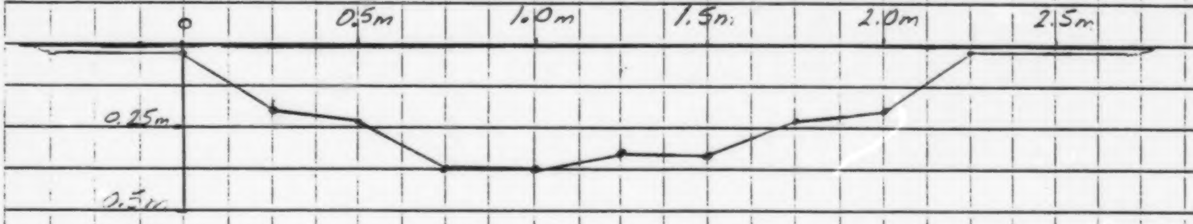

RIDGE 3-2 N:

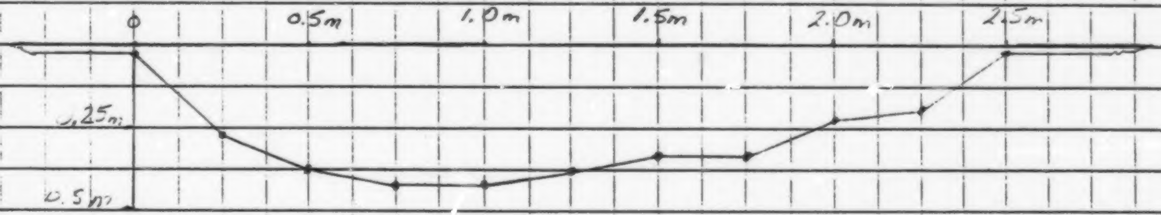

RIDGE 3-1 S:

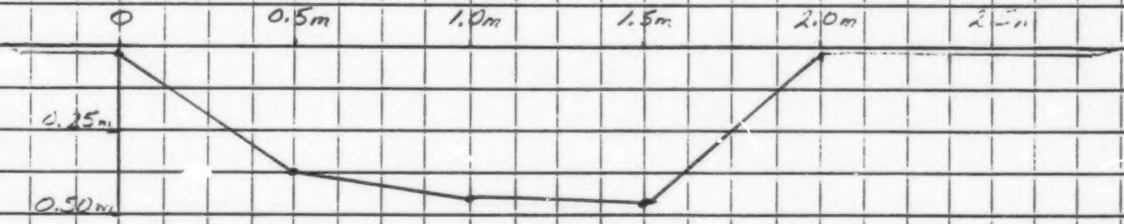

RIDGE 3-2 S:

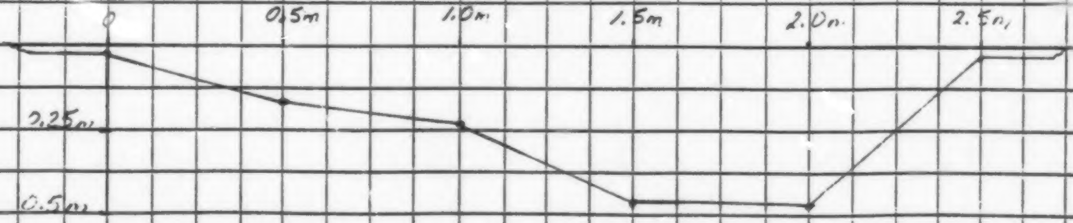

FLEET TECHNOLOGY LIMITED (FTL)

Engineering Design Calculations

JOB No. 3203
SHEET 3 OF 3
DATE May 6/83
BY
CH'K BY

PROJECT ICE MODELLING
SUBJECT CROSS-SECTIONAL PROFILES OF RIDGES IN SHEET #3

RIDGE 3-3N:

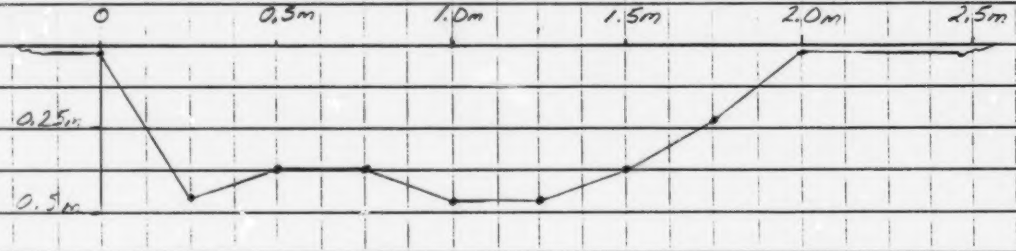

RIDGE 3-3S:

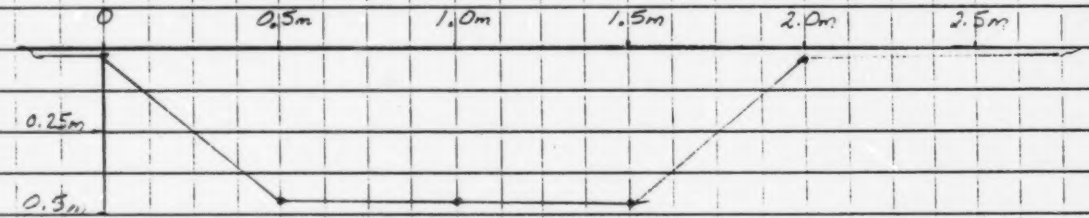

NRC - INSTITUTE FOR MARINE DYNAMICS

ARCTIC VESSEL RESEARCH SECTION

ICE SHEET SUMMARY

```
Test Name:  RIDGE3                              Project Number: 88112

Target ice thickness: (mm)  24.0                EG/AD/S: (%) .39/.027/0

Target ice strength: (kPa)  18.0

SEEDING:
-------
Air temp.(max/min) C: -15.0/-15.0               Tank water temp. C: -.06
Seeding completed at 2050  4-MAY-1988           Seed duration: (min)   5.
Seed volume: 1  0.0                             Seed water temp.: C   0.0
Humidity: tank(%) 80
          room(%) 40

GROWTH:
------
Target temp.: C -15.0                           Time to target temp. hrs:  0.0
Avg temp. at plateau: C -15.0                   Duration of plateau hrs:  8.1
Avg temp. of freeze cycle C -15.0               Duration of freeze cycle hrs:  8.1
Total negative deg. hours  121.3                Thickness at end of freeze:(mm) 16.0*
Avg growth rate: (mm/hr) 1.977                  Avg growth rate: (mm/fdh) .132

WARM-UP:
-------
Warm-up commenced at 0455  5-MAY-1988           Length of warm-up: (hrs)  10.
Time to tempering temp: (hrs)  3.2              Avg tempering temperature: (C)  0.3
Final ice thickness: (mm)  23.0                 Ice growth during warm-up: (mm)   7.0
Total growth rate: (mm/hr) 2.844                Total growth rate: (mm/fdh) .190

* thickness at end of freeze  was estimated

** seeding occurred naturally with ice crystals already prsent in the air.
```

NRC - INSTITUTE FOR MARINE DYNAMICS

ARCTIC VESSEL RESEARCH SECTION

ICE MECHANICAL PROPERTIES SUMMARY

Test Name: RIDGE3 Project Number: 88112

Warm up commenced: 04:55 5-MAY-1988

Time	Warm-up hrs	Loc	hi mm	Sf kPa	Lc cm	E MPa	E/Sf	Lc/hi	Klc N/m	Sf/Klc m-.5	Sc/s kPa	Rhoi Mg/m3
0905	4.16	N	22.6± 1.2 n= 3									
		S	21.5± 2.0 n= 3									
0930	4.58	11S	24.9	46.± 3.4								
			25.0	18.(u/d 38%)								
0941	4.76	43N	21.4	36.± 1.5								
			21.3	9.(u/d 26%)								
0947	4.86	43S	21.5	32.± 7.4								
			22.1	22.(u/d 70%)								
1110	6.25	45S	21.6		20.	16.6	872	9.3				
1133	6.63	45N	22.1	18.± 2.0								
			21.9	14.(u/d 77%)								
1135	6.66	45S	23.3	17.±****								
			21.9	14.(u/d 82%)								
1432	9.61	36S	22.4	8.± 1.5								
			22.5	6.(u/d 76%)								
1438	9.71	36N	22.8	8.± 2.0								
			22.7	13.(u/d153%)								

Run #	Date	Time	Hours from Warm-up	Flexural Strength north	south	mean
1	05/05/88	1240	7.75	12.8	11.8	12.3
2	05/05/88	1310	8.25	12.7	12.7	12.7
3	05/05/88	1400	9.08	10.0	9.7	9.8

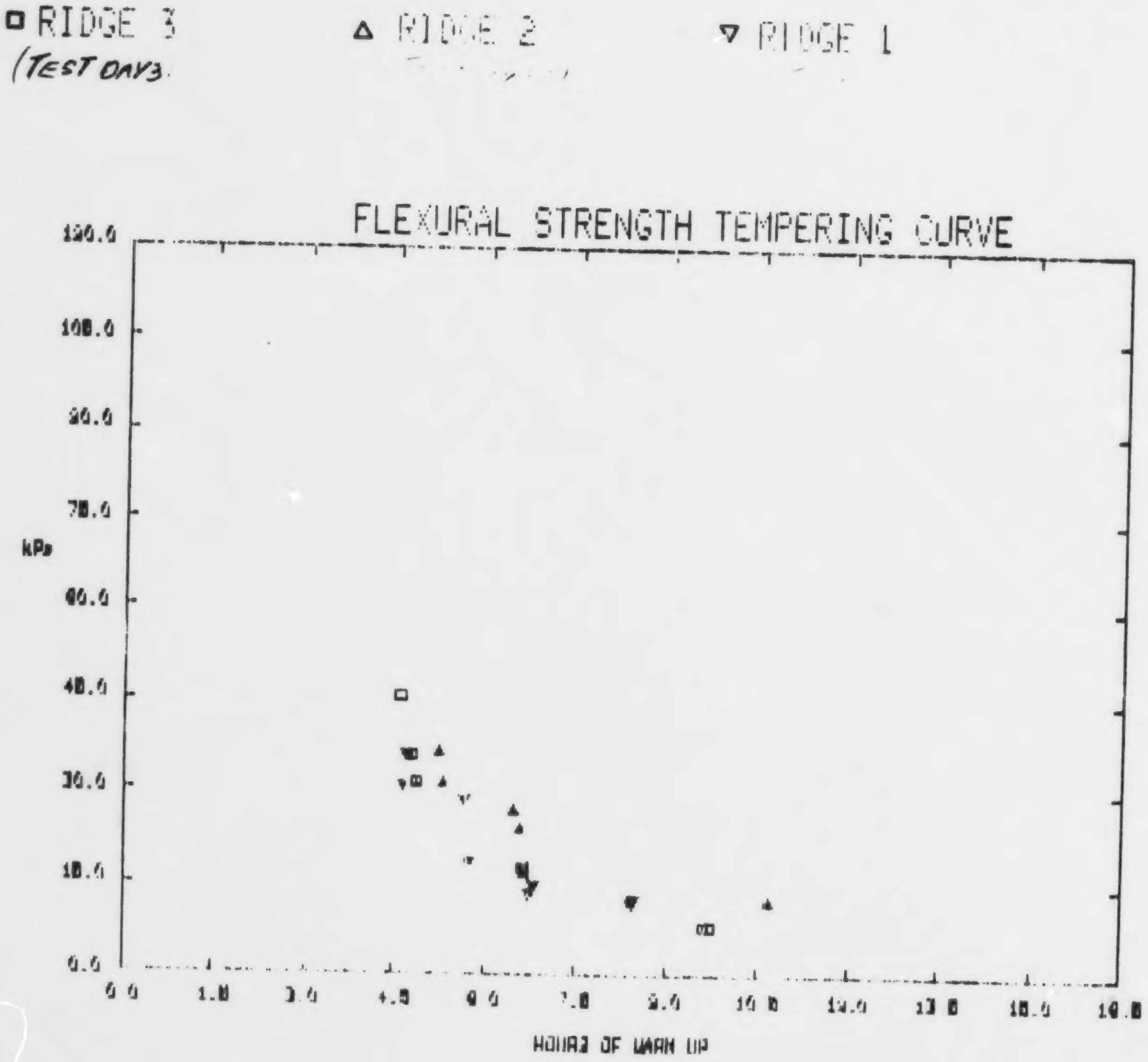□ RIDGE 3
(TEST DAY3
△ RIDGE 2
▽ RIDGE 1
FLEXURAL STRENGTH TEMPERING CURVE
kPa
120.0
105.0
90.0
75.0
60.0
45.0
30.0
15.0
0.0
0.0
1.5
3.0
4.5
6.0
7.5
9.0
10.5
12.0
13.5
15.0
16.5
HOURS OF WARM UP

APPENDIX E.5

TEMPERATURE DATA

FLEET TECHNOLOGY LIMITED [FTL]

Engineering Design Calculations

JOB No. 3223
SHEET 1 OF 2
DATE May 5 '83
BY
CH'K BY

PROJECT RIDGE MODELLING
SUBJECT RIDGE TEMPERATURE (°C)

THERMO- COUPLE #	2030 MAY 4	0845 MAY 5	0945 MAY 5	1100 MAY 5	1230 MAY 5
1	-12.8	+0.7	+0.6	-0.9	-0.9
2	-12.2	-0.4	-0.5	-1.5	-1.6
3	-2.5	-0.8	-2.0	-2.0	-2.2
4	-2.5	-0.5	-1.6	-1.6	-1.9
5	-17.0	0.0	-0.9	-1.[illegible]	-1.3
6	-2.5	-0.8	-1.7	-1.4	-1.4
[illegible]	-2.8	-0.3	-1.2	-1.0	-1.1
[illegible]	-2.6	-0.2	-1.1	-1.1	-1.1
[illegible]	-2.5	-0.1	-1.1	-1.1	-1.2
[illegible]	-18.3	+2.0	+1.2	0.0	-0.6
[illegible]	-6.8	+0.2	-0.6	-0.8	-1.0
[illegible]	-2.5	+0.2	-0.4	-0.7	-0.8
13	-2.4	+0.2	-0.5	-0.5	-0.7
14	-2.4	+0.2	-0.6	-0.6	-0.8
15	-18.2	+1.5	+1.3	0.0	-2.4
16	-4.9	-0.5	-1.0	-1.1	-1.3
[illegible]	-2.5	0.0	-0.7	-0.8	-1.0
[illegible]	-2.6	+0.2	-0.8	-1.0	-1.0

EVENT LOG:

2015 MAY 4 - RIDGES FORMED AND FREEZE #2 COMMENCED.
0455 MAY 5 - TEMPERING OF SHEET COMMENCED.
0915 MAY 5 - INSULATION REMOVED FROM RIDGE SURFACE.

FLEET TECHNOLOGY LIMITED [FTL]

Engineering Design Calculations

JOB No. 3208
SHEET 2 OF 2
DATE May 5/83
BY
CH'K BY

PROJECT Ridge Modelling
SUBJECT Thermocouple Locations

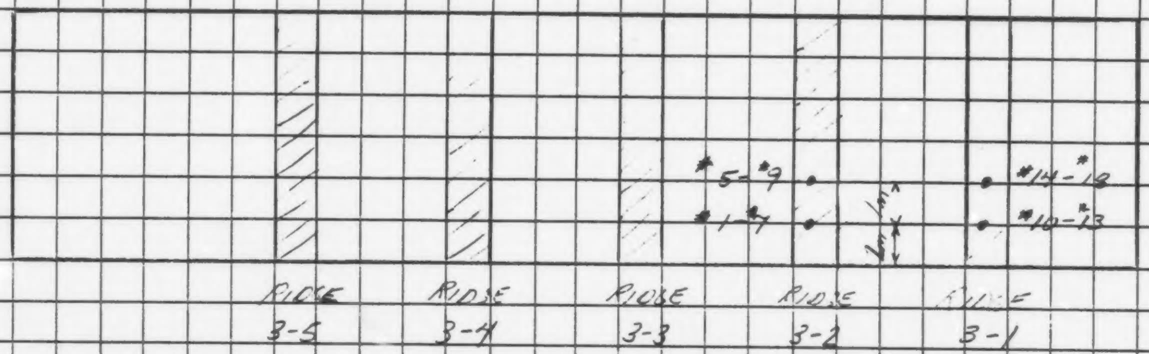
#5-#9
#1-#4
#14-#18
#10-#13
1m
1m
Ridge 3-5
Ridge 3-4
Ridge 3-3
Ridge 3-2
Ridge 3-1

Ridge 3-1 N:

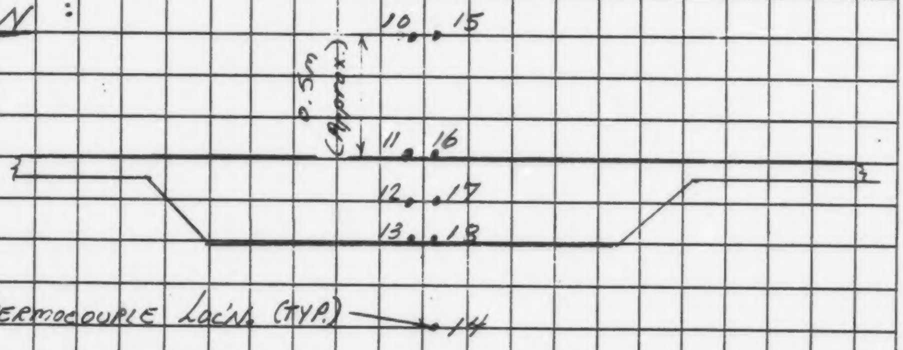
10 15
0.5m (Approx.)
11 16
12 17
13 18
Thermocouple Loc'n. (typ.)
14

Ridge 3-2 N:

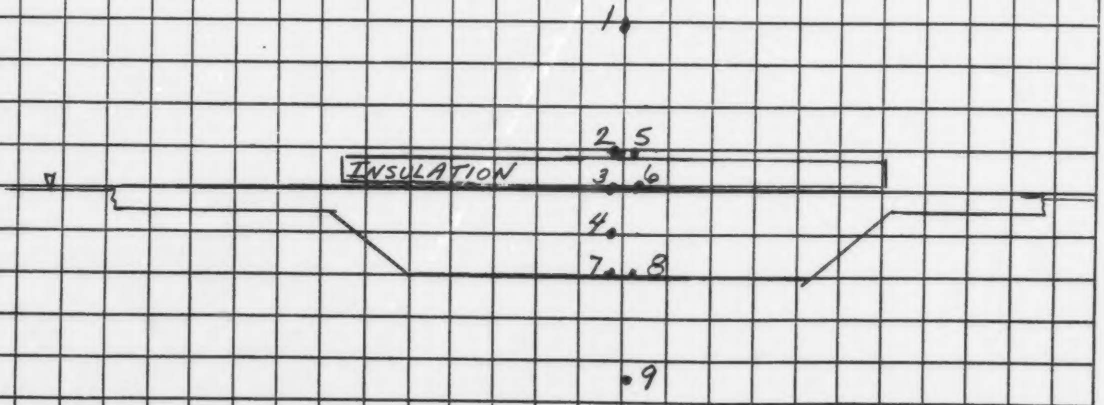
1
2 5
Insulation
3 6
4
7 8
9

APPENDIX F

RAW DATA PLOTS FOR TEST T2R1 FOR A RANGE OF FILTERING RATES

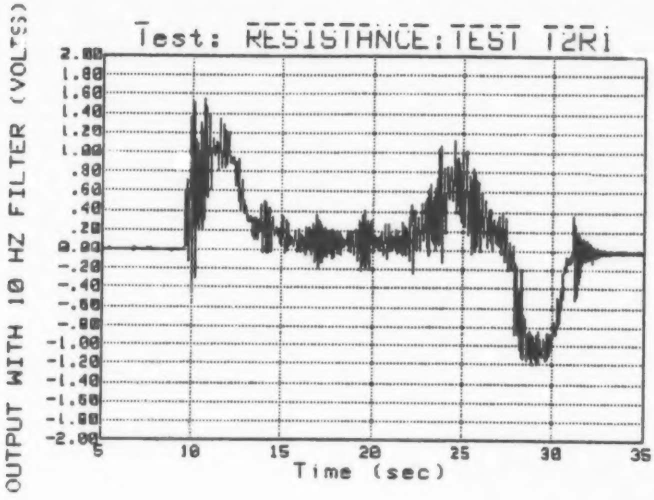

```
                         STATISTICS SUMMARY

                       Project Number 3208C
                       RIDGE MODELING IMD

              Test Name:               RESISTANCE:TEST T2R1
              Date:                             21 Jun 1988
              Start Time:                          03:55:15
              Scanning Rate                           40 Hz
              Test Duration                 60.0000 seconds

          Interval  1 beginning at:       22.0000 seconds
          Interval  1 ending at:          27.6750 seconds

CHANNEL    NAME         UNITS      MAXIMUM    MINIMUM       MEAN  STD DEVIATION
   1
  OUTPUT WITH 4 HZ FILTER
                        VOLTS       .92773    -.09033     .35773      .22158
   2
  OUTPUT WITH 5 HZ FILTER
                        VOLTS       .98145    -.11963     .35813      .23963
   3
  OUTPUT WITH 6HZ FILTER
                        VOLTS       1.0620     -.1931      .3562       .2809
   4
 OUTPUT WITH 10 HZ FILTER
                        VOLTS       1.1157     -.2393      .3559       .2955
```

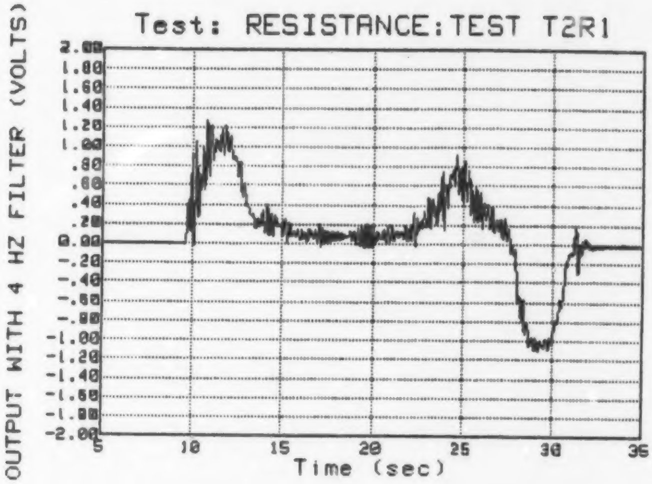
Test: RESISTANCE:TEST T2R1
OUTPUT WITH 4 HZ FILTER (VOLTS)
2.00
1.80
1.60
1.40
1.20
1.00
.80
.60
.40
.20
0.00
-.20
-.40
-.60
-.80
-1.00
-1.20
-1.40
-1.60
-1.80
-2.00
5
10
15
20
25
30
35
Time (sec)

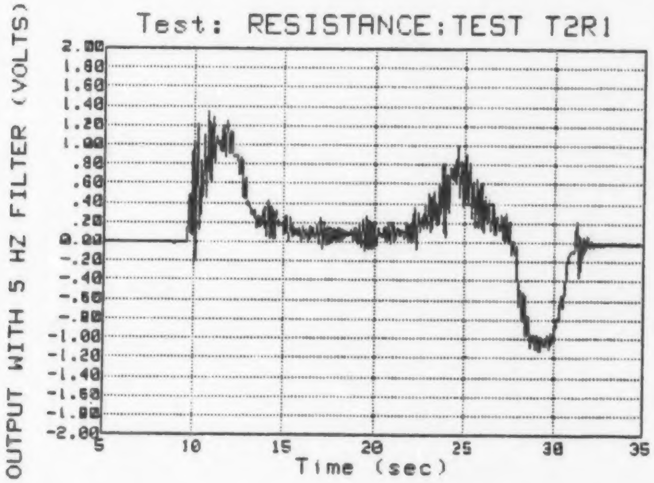
Test: RESISTANCE:TEST T2R1
OUTPUT WITH 5 HZ FILTER (VOLTS)
2.00
1.80
1.60
1.40
1.20
1.00
.80
.60
.40
.20
0.00
-.20
-.40
-.60
-.80
-1.00
-1.20
-1.40
-1.60
-1.80
-2.00
5
10
15
20
25
30
35
Time (sec)

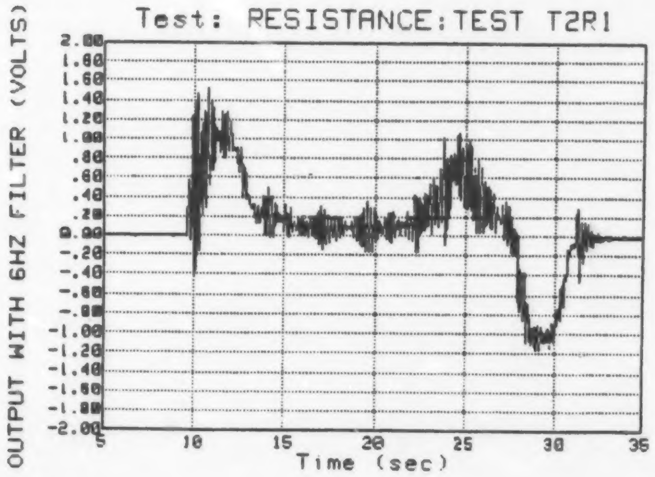
Test: RESISTANCE:TEST T2R1
OUTPUT WITH 6HZ FILTER (VOLTS)
2.00
1.80
1.60
1.40
1.20
1.00
.80
.60
.40
.20
0.00
-.20
-.40
-.60
-.80
-1.00
-1.20
-1.40
-1.60
-1.80
-2.00
5
10
15
20
25
30
35
Time (sec)

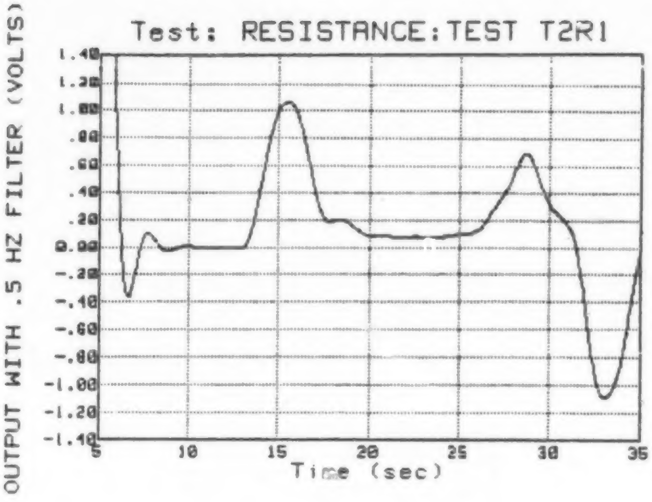

```
                              STATISTICS SUMMARY


                              Project Number 3208C
                              RIDGE MODELING IMD

                       Test Name:           RESISTANCE:TEST T2R1
                       Date:                         21 Jun 1988
                       Start Time:                      04:15:03
                       Scanning Rate                       40 Hz
                       Test Duration             60.0000 seconds


                 Interval  1 beginning at:       22.0000 seconds
                 Interval  1 ending at:          29.8500 seconds

CHANNEL      NAME        UNITS       MAXIMUM      MINIMUM        MEAN  STD DEVIATION
   1
 OUTPUT WITH .5 HZ FILTER
                         VOLTS        .69092       .07813      .26044       .21348
   2
 OUTPUT WITH 1 HZ FILTER
                         VOLTS        .74707       .07080      .27172       .21082
   3
 OUTPUT WITH 2 HZ FILTER
                         VOLTS        .76660       .06348      .27606       .21066
   4
 OUTPUT WITH 3 HZ FILTER
                         VOLTS        .83496       .03418      .27696       .21327
```

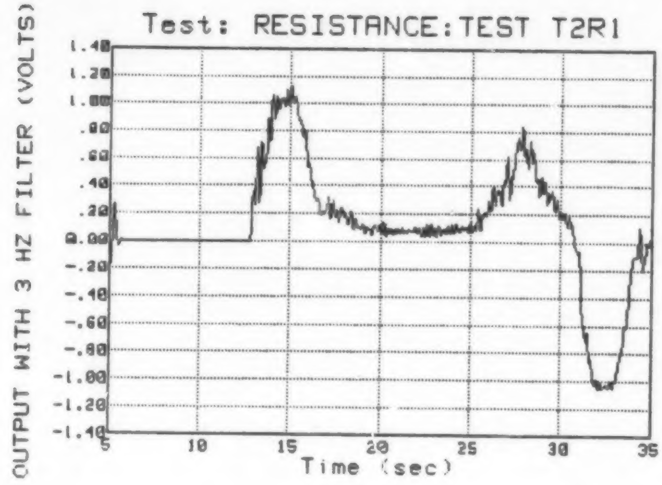
Test: RESISTANCE:TEST T2R1
OUTPUT WITH 3 HZ FILTER (VOLTS)
1.40
1.20
1.00
.80
.60
.40
.20
0.00
-.20
-.40
-.60
-.80
-1.00
-1.20
-1.40
5
10
15
20
25
30
35
Time (sec)

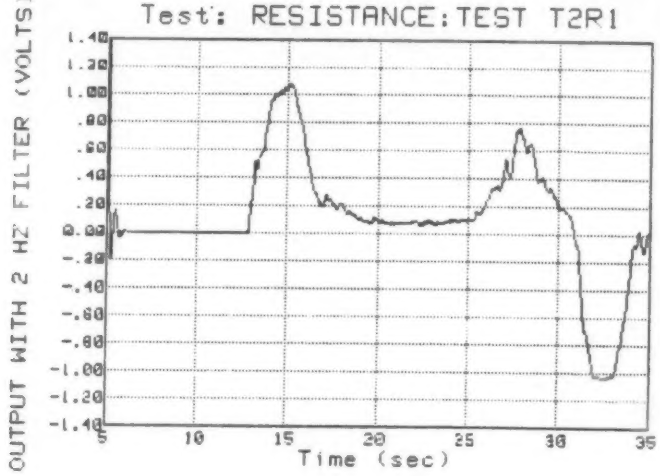
Test: RESISTANCE:TEST T2R1
OUTPUT WITH 2 HZ FILTER (VOLTS)
1.40
1.20
1.00
.80
.60
.40
.20
0.00
-.20
-.40
-.60
-.80
-1.00
-1.20
-1.40
5
10
15
20
25
30
35
Time (sec)

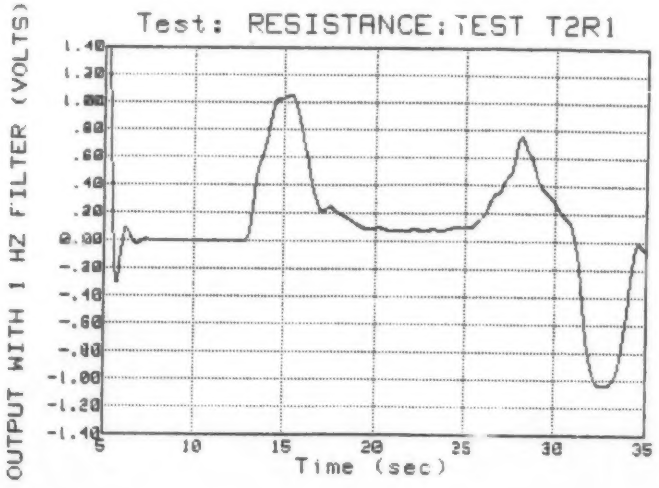
Test: RESISTANCE:TEST T2R1
OUTPUT WITH 1 HZ FILTER (VOLTS)
1.40
1.20
1.00
.80
.60
.40
.20
0.00
-.20
-.40
-.60
-.80
-1.00
-1.20
-1.40
5
10
15
20
25
30
35
Time (sec)

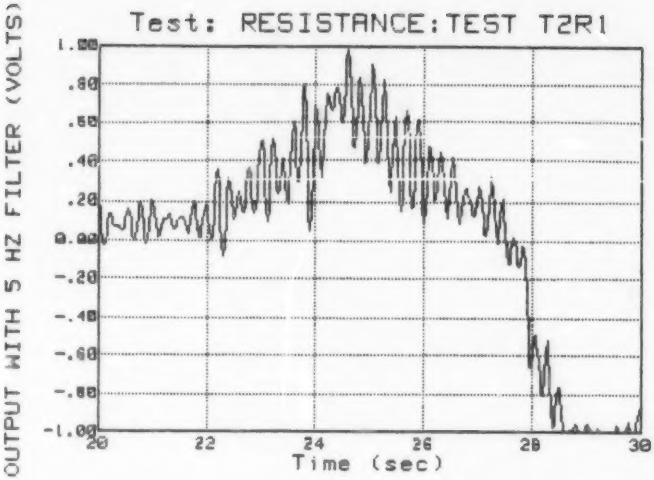
Test: RESISTANCE:TEST T2R1
OUTPUT WITH 5 HZ FILTER (VOLTS)
1.00
.80
.60
.40
.20
0.00
-.20
-.40
-.60
-.80
-1.00
20
22
24
26
28
30
Time (sec)

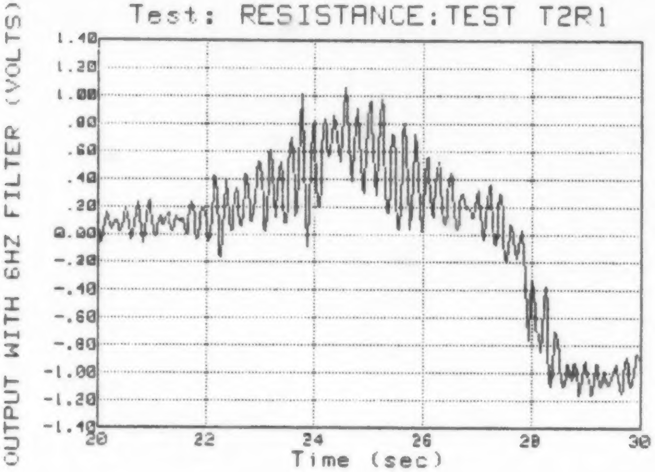
Test: RESISTANCE:TEST T2R1
OUTPUT WITH 6HZ FILTER (VOLTS)
1.40
1.20
1.00
.80
.60
.40
.20
0.00
-.20
-.40
-.60
-.80
-1.00
-1.20
-1.40
20
22
24
26
28
30
Time (sec)

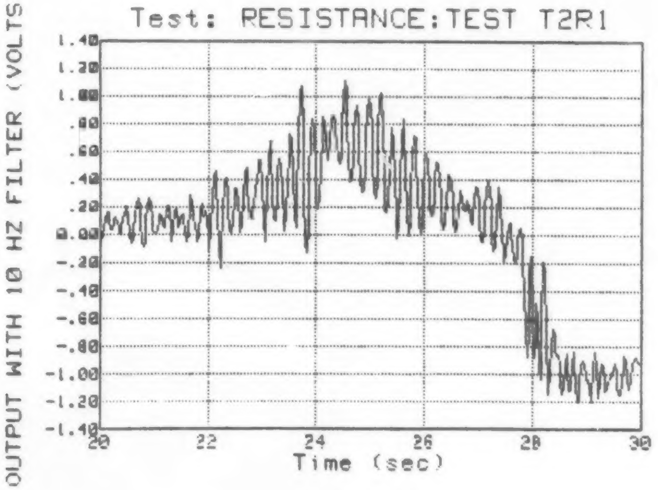
Test: RESISTANCE:TEST T2R1
OUTPUT WITH 10 HZ FILTER (VOLTS)
1.40
1.20
1.00
.80
.60
.40
.20
0.00
-.20
-.40
-.60
-.80
-1.00
-1.20
-1.40
20
22
24
26
28
30
Time (sec)

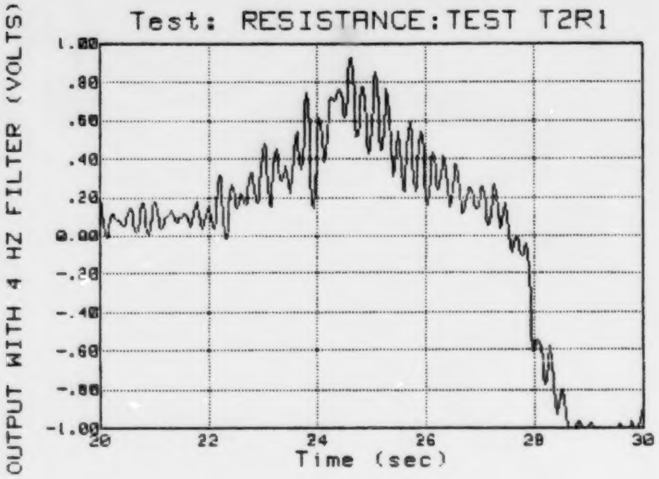
Test: RESISTANCE:TEST T2R1
OUTPUT WITH 4 HZ FILTER (VOLTS)
1.00
.80
.60
.40
.20
0.00
-.20
-.40
-.60
-.80
-1.00
20
22
24
26
28
30
Time (sec)

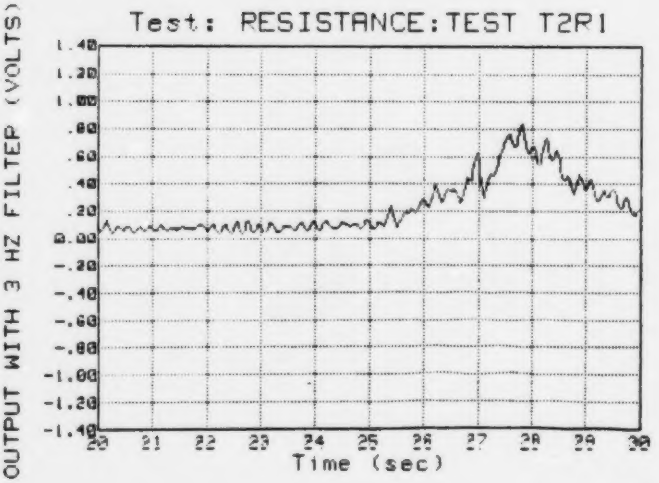
Test: RESISTANCE:TEST T2R1
OUTPUT WITH 3 HZ FILTER (VOLTS)
1.40
1.20
1.00
.80
.60
.40
.20
0.00
-.20
-.40
-.60
-.80
-1.00
-1.20
-1.40
20
21
22
23
24
25
26
27
28
29
30
Time (sec)

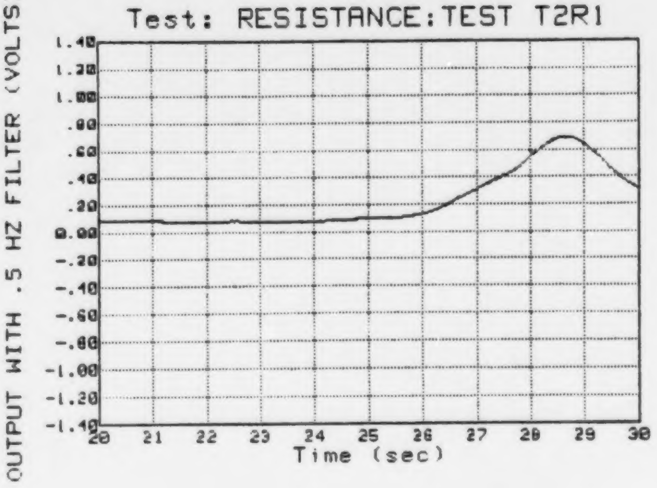
Test: RESISTANCE:TEST T2R1
OUTPUT WITH .5 HZ FILTER (VOLTS)
1.40
1.20
1.00
.80
.60
.40
.20
0.00
-.20
-.40
-.60
-.80
-1.00
-1.20
-1.40
20
21
22
23
24
25
26
27
28
29
30
Time (sec)

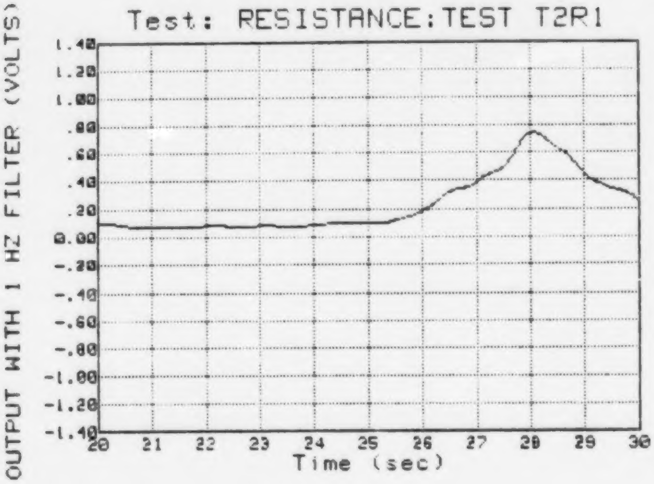
Test: RESISTANCE:TEST T2R1
OUTPUT WITH 1 HZ FILTER (VOLTS)
1.40
1.20
1.00
.80
.60
.40
.20
0.00
-.20
-.40
-.60
-.80
-1.00
-1.20
-1.40
20
21
22
23
24
25
26
27
28
29
30
Time (sec)

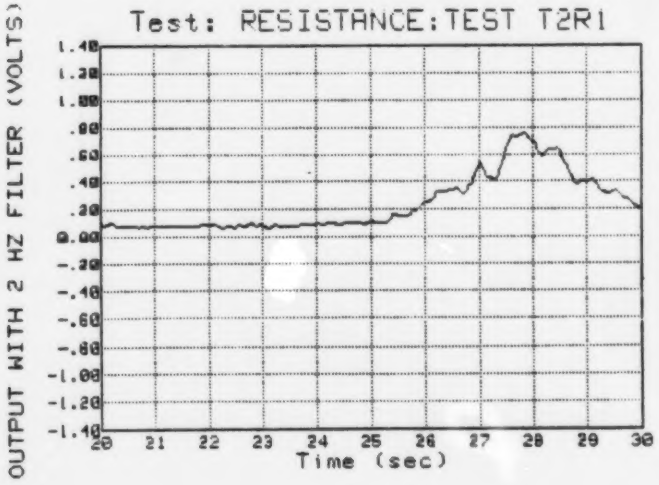
Test: RESISTANCE:TEST T2R1
OUTPUT WITH 2 HZ FILTER (VOLTS)
1.40
1.20
1.00
.80
.60
.40
.20
0.00
-.20
-.40
-.60
-.80
-1.00
-1.20
-1.40
20
21
22
23
24
25
26
27
28
29
30
Time (sec)

APPENDIX G

RAW DATA PLOTS FOR TEST T1R1 FOR A RANGE OF FILTERING RATES

```
                         STATISTICS SUMMARY

                         Project Number 3208C
                         RIDGE MODELING IMD

                 Test Name:           RESISTANCE:TEST T1R1
                 Date:                         23 Jun 1988
                 Start Time:                      22:47:29
                 Scanning Rate                       40 Hz
                 Test Duration             50.0000 seconds


               Interval  1 beginning at:        18.0000 seconds
               Interval  1 ending at:           28.0000 seconds

CHANNEL    NAME         UNITS      MAXIMUM     MINIMUM       MEAN  STD DEVIATION
    1
 OUTPUT WITH .5 HZ FILTER
                        VOLTS       .73486      .11475     .33907      .20087
    2
  OUTPUT WITH 1 HZ FILTER
                        VOLTS       .78369      .06836     .34206      .20532
    3
 OUTPUT WITH 1.5 HZ FILTER
                        VOLTS       .82520      .01221     .34356      .21597
    4
  OUTPUT WITH 2 HZ FILTER
                        VOLTS       .83252      .00732     .34597      .21602
```

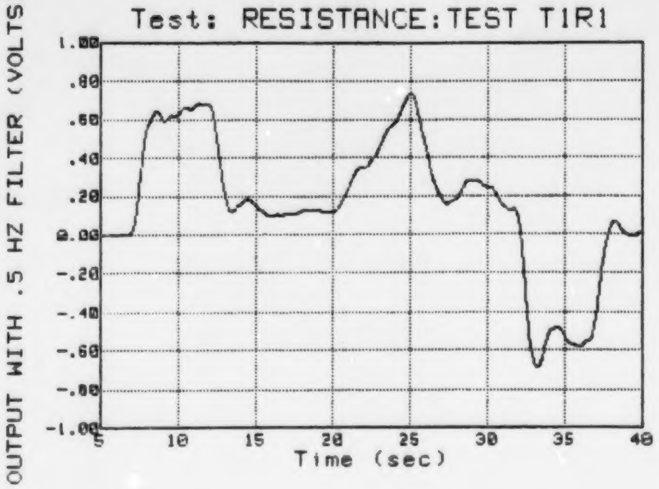
Test: RESISTANCE:TEST T1R1
OUTPUT WITH .5 HZ FILTER (VOLTS)
1.00
.80
.60
.40
.20
0.00
-.20
-.40
-.60
-.80
-1.00
5
10
15
20
25
30
35
40
Time (sec)

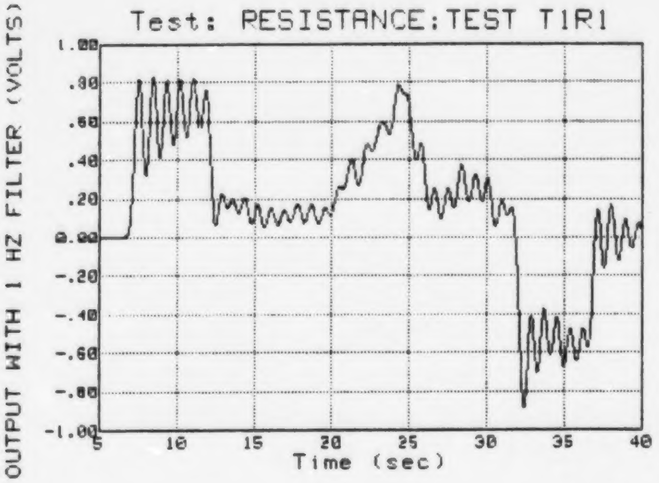
Test: RESISTANCE:TEST T1R1
OUTPUT WITH 1 HZ FILTER (VOLTS)
1.00
.80
.60
.40
.20
0.00
-.20
-.40
-.60
-.80
-1.00
5
10
15
20
25
30
35
40
Time (sec)

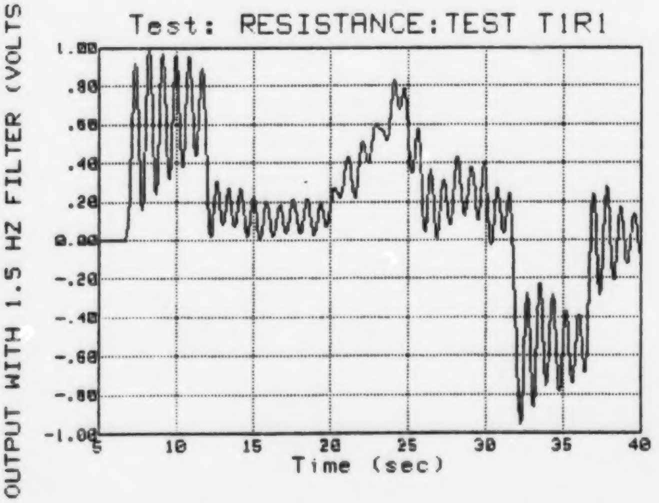
Test: RESISTANCE:TEST T1R1
OUTPUT WITH 1.5 HZ FILTER (VOLTS)
1.00
.80
.60
.40
.20
0.00
-.20
-.40
-.60
-.80
-1.00
5
10
15
20
25
30
35
40
Time (sec)

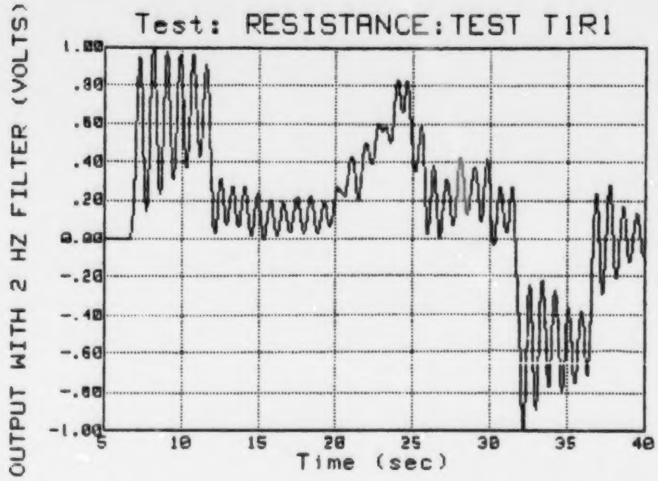
Test: RESISTANCE:TEST T1R1
OUTPUT WITH 2 HZ FILTER (VOLTS)
1.00
.80
.60
.40
.20
0.00
-.20
-.40
-.60
-.80
-1.00
5
10
15
20
25
30
35
40
Time (sec)

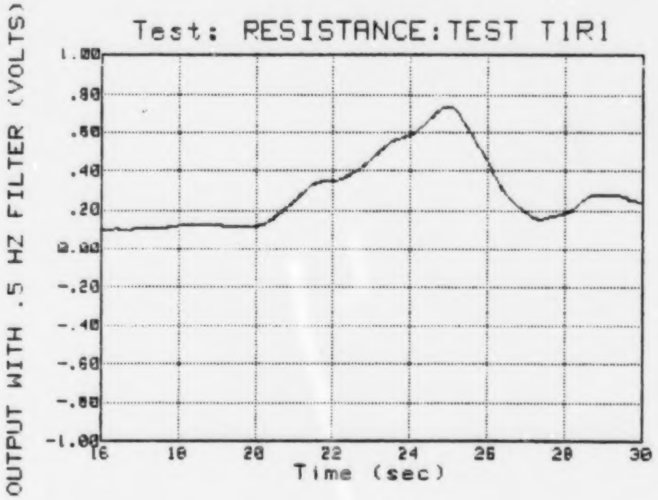
Test: RESISTANCE:TEST T1R1
OUTPUT WITH .5 HZ FILTER (VOLTS)
1.00
.80
.60
.40
.20
0.00
-.20
-.40
-.60
-.80
-1.00
16
18
20
22
24
26
28
30
Time (sec)

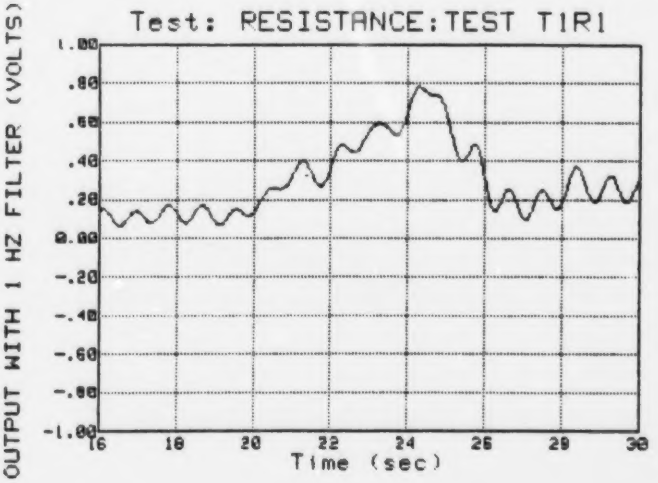
Test: RESISTANCE:TEST T1R1
OUTPUT WITH 1 HZ FILTER (VOLTS)
1.00
.80
.60
.40
.20
0.00
-.20
-.40
-.60
-.80
-1.00
16
18
20
22
24
26
28
30
Time (sec)

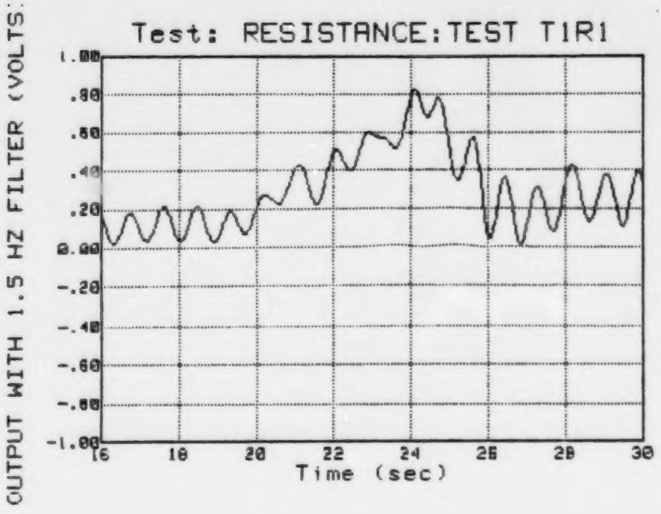
Test: RESISTANCE:TEST T1R1
OUTPUT WITH 1.5 HZ FILTER (VOLTS)
1.00
.80
.60
.40
.20
0.00
-.20
-.40
-.60
-.80
-1.00
16
18
20
22
24
26
28
30
Time (sec)

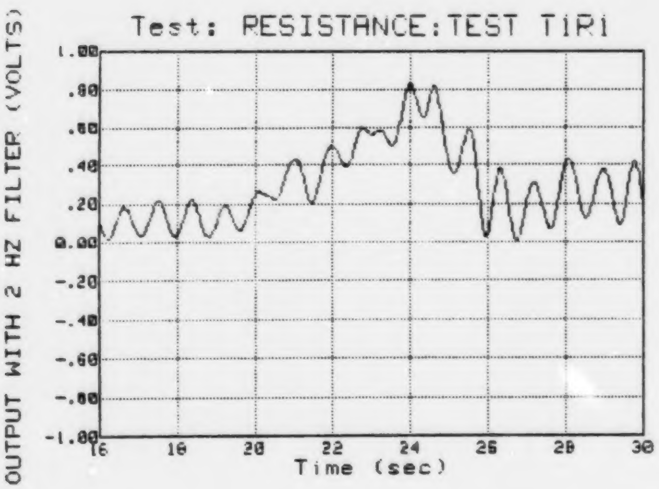
Test: RESISTANCE:TEST T1R1
OUTPUT WITH 2 HZ FILTER (VOLTS)
1.00
.80
.60
.40
.20
0.00
-.20
-.40
-.60
-.80
-1.00
16
18
20
22
24
26
28
30
Time (sec)

APPENDIX H

SUMMARY OF AVAILABLE FIELD DATA FOR RIDGES 17 AND 18

(from Geisel et al, 1982)

4.2 Results

During the 1982 deployment, ten pressure ridge resistance tests were conducted. Prior to each test, an attempt was made to completely profile the ridge or in some way define the ice conditions. During the tests 21 channels of data were recorded in both analog and digital form. Following the tests, the methods previously described were used to calculate the horizontal and vertical ice forces. To insure that the measured data was correct and accurate, computer programs were developed which (1) compared the integral of the acceleration to the measured velocity curve or (2) compared the derivative of the velocity curve to measured accelerations. These steps were critical because a sensitivity analysis of the methods used showed that the acceleration, velocity, and damping terms were predominant and therefore must be very accurate.

Analysis of a ship transit through Pressure Ridge Number 17 on the facing page illustrates an almost linear velocity decrease followed by a linear but slower velocity increase as the ship passed through the ridge. The second figure shows the calculated horizontal ice force during the ridge transit and the third figure is a profile of Ridge Number 17 included as a reference. As the ship's bow reached the 45 foot position of the ridge, ship speed began to decrease. At the point of maximum deceleration, about 115 seconds on the time-history plots, horizontal force reached a maximum of 1.9 million pounds. This corresponds to the ship's bow at the 90 foot mark and the maximum beam in the thickest consolidated portion of the ridge. At 130 seconds, when ship speed began to increase, horizontal ice force had returned to the pre-impact level of about 500,000 pounds and the ship's maximum beam was clear of the consolidated portion. Also note that while transiting level ice prior to impact, this method of analysis predicts a total resistance of about 500,000 pounds at a speed of eight knots. This is close to the resistance which would be predicted in level ice by Equation (3.3-3) for ice up to 2 feet thick, and is another indication that the rigid body analysis is accurate.

Nine additional pressure ridge transits are documented in Appendix E. Analysis was limited to calculating the horizontal force only, however, results of further testing, when combined with this data will be used to develop empirical relationships which will more accurately predict ship performance through pressure ridges.

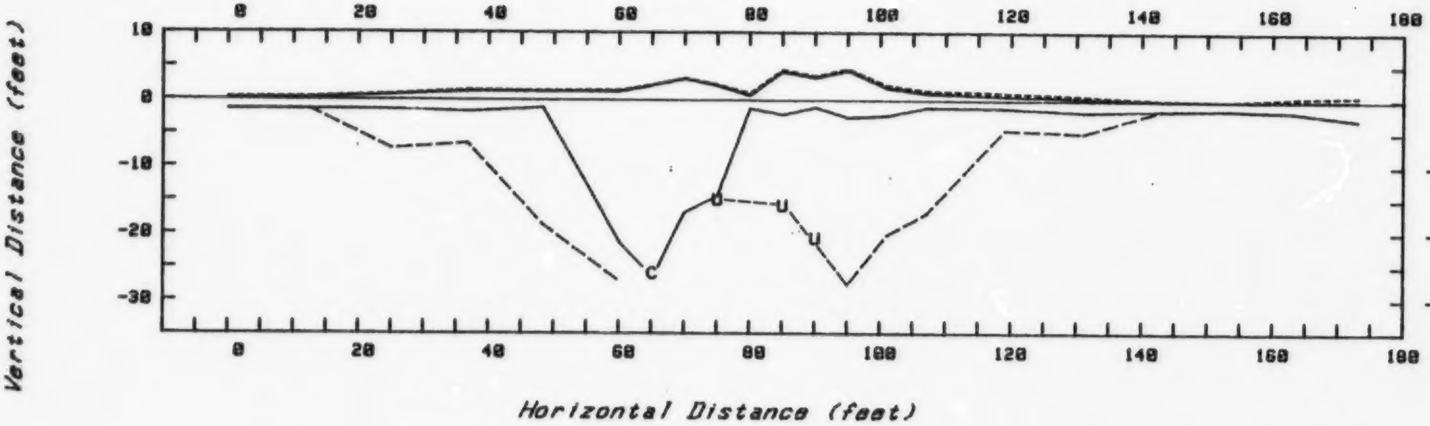

PRESSURE RIDGE NO. 17
(First-Year)

Position: Lat. 64° 16.9′ N
Long. 168° 45.1′ W

4/22/82

Floe Drift: Spd. .2 kts.
Course 241° True

Snow Cover: --
Solid Ice Surfaces: ________________________
Total Depth By Drilling: — — — — — — — — —
Sonar Depth: ——-——-——-——-——
C: Consolidated Depth, Ice Below
U: Unconsolidated Depth, Ice Below

PRESSURE RIDGE NO. 17

SUMMARY OF PHYSICAL CHARACTERISTICS

Adjacent Floe Thicknesses	1.7 ft
Maximum Sail Height	4.3 ft
Maximum Keel Depth	27.7 ft
Maximum Depth of Consolidation	26.0 ft

SUMMARY OF DIMENSIONAL RATIOS

Maximum Keel Depth/Maximum Sail Height	6.4
Maximum Consolidated Depth/Maximum Sail Height	6.0
Maximum Consolidated Depth/Adjacent Level Ice Thickness	15.3

TRANSIT THROUGH RIDGE #17

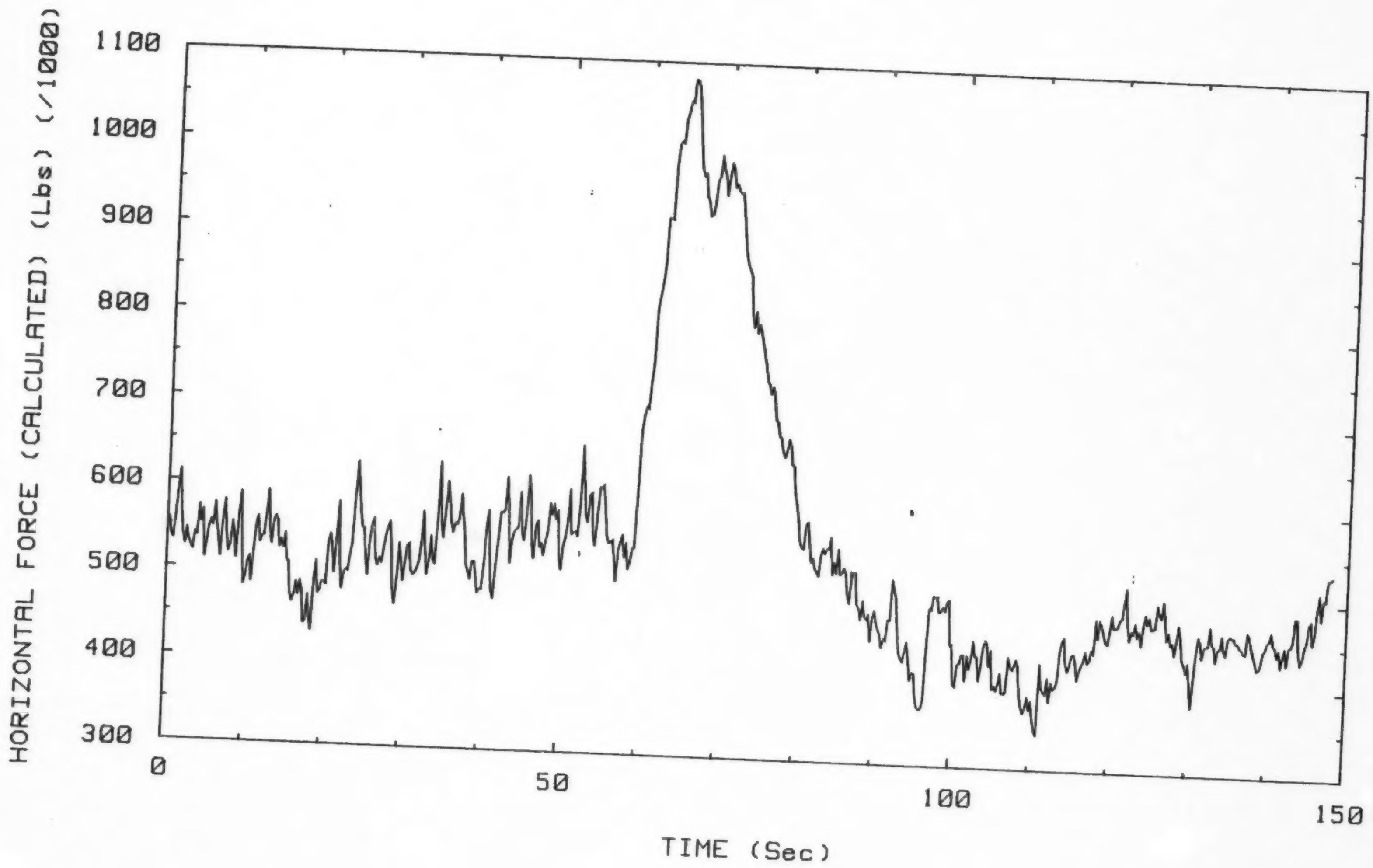

TRANSIT THROUGH RIDGE #17

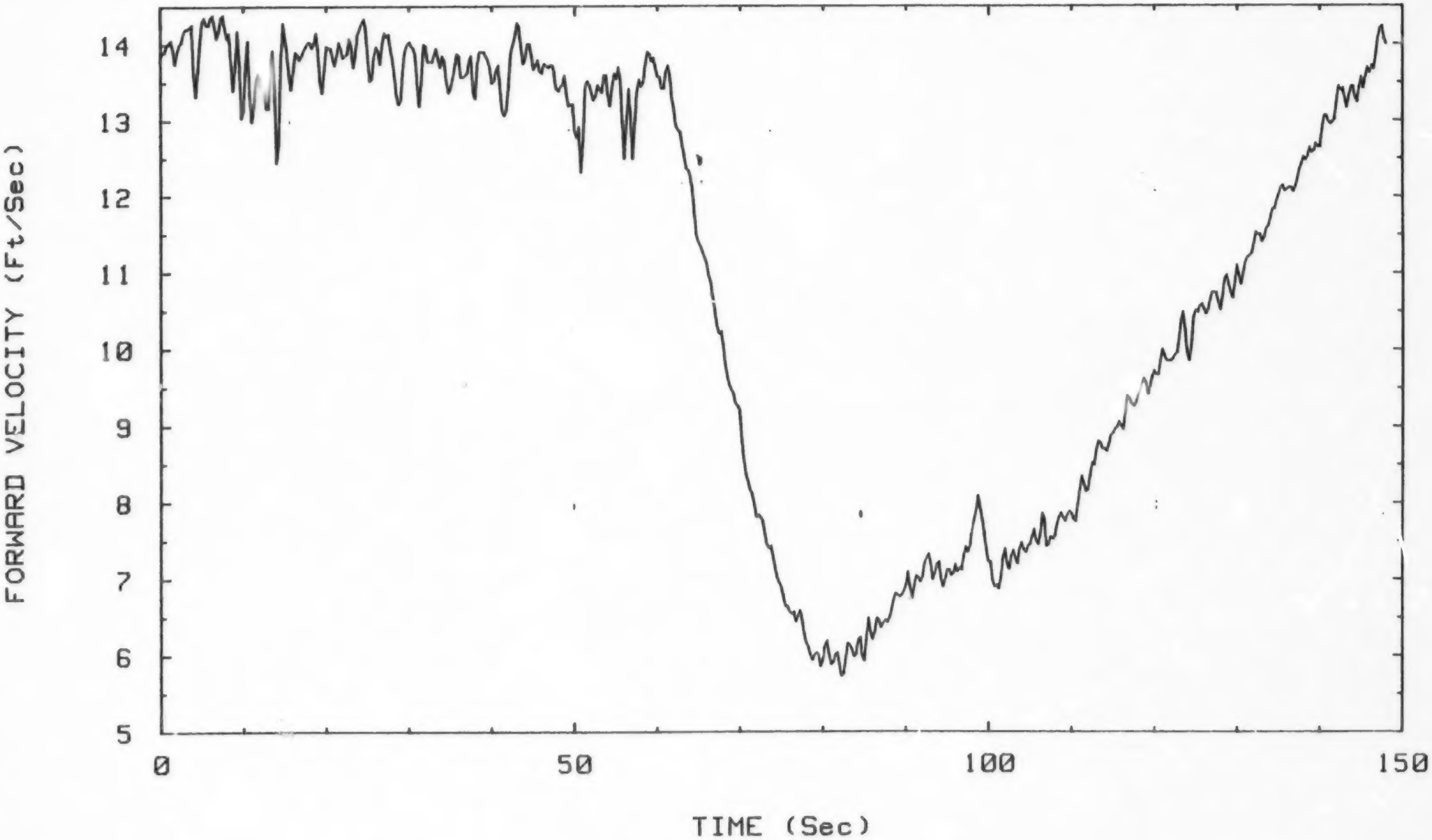

The transit of Pressure Ridge No. 18 took place on April 24, 1982. A complete profile was made the previous day, and is shown on the opposite page. During the transit, large cracks appeared in front and behind the ridge, although once through the thickest portion, there was no acceleration to pre-impact speed. Note that the velocity shown between 30 and 32 seconds is a transient, probably due to vibration of the doppler radar, and is not a real ship speed.

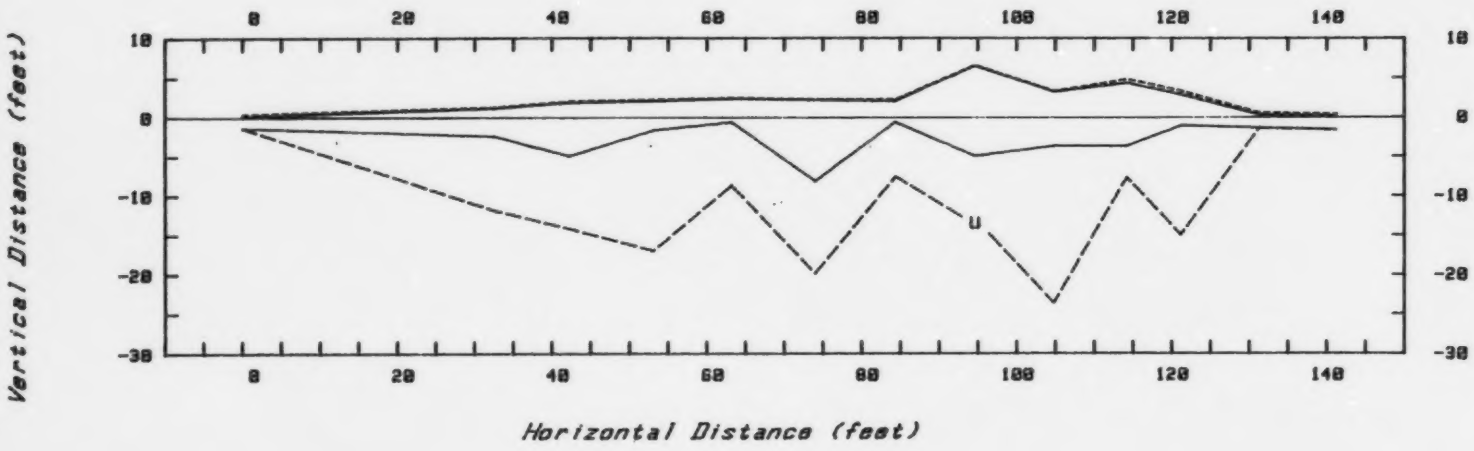

PRESSURE RIDGE NO. 18
(First-Year)

Position: Lat. 64° 16.9′ N
Long. 168° 45.1′ W

4/23/82

Floe Drift: Spd. .2 kts.
Course 241° True

Snow Cover: ------------------------
Solid Ice Surfaces: ____________
Total Depth By Drilling: — — — — —
Sonar Depth: — - — - — - — - —
C: Consolidated Depth, Ice Below
U: Unconsolidated Depth, Ice Below

PRESSURE RIDGE NO. 18

SUMMARY OF PHYSICAL CHARACTERISTICS

Adjacent Floe Thicknesses	1.5 ft
Maximum Sail Height	6.5 ft
Sail Width (83'-131')	48.0 ft
Maximum Keel Depth	23.6 ft
Keel Width (0'-131.3')	131.3 ft
Maximum Depth of Consolidation	8.2 ft

SUMMARY OF DIMENSIONAL RATIOS

Maximum Keel Depth/Maximum Sail Height	3.6
Maximum Consolidated Depth/Maximum Sail Height	1.3
Maximum Consolidated Depth/Adjacent Level Ice Thickness	5.5

TRANSIT THROUGH RIDGE #18

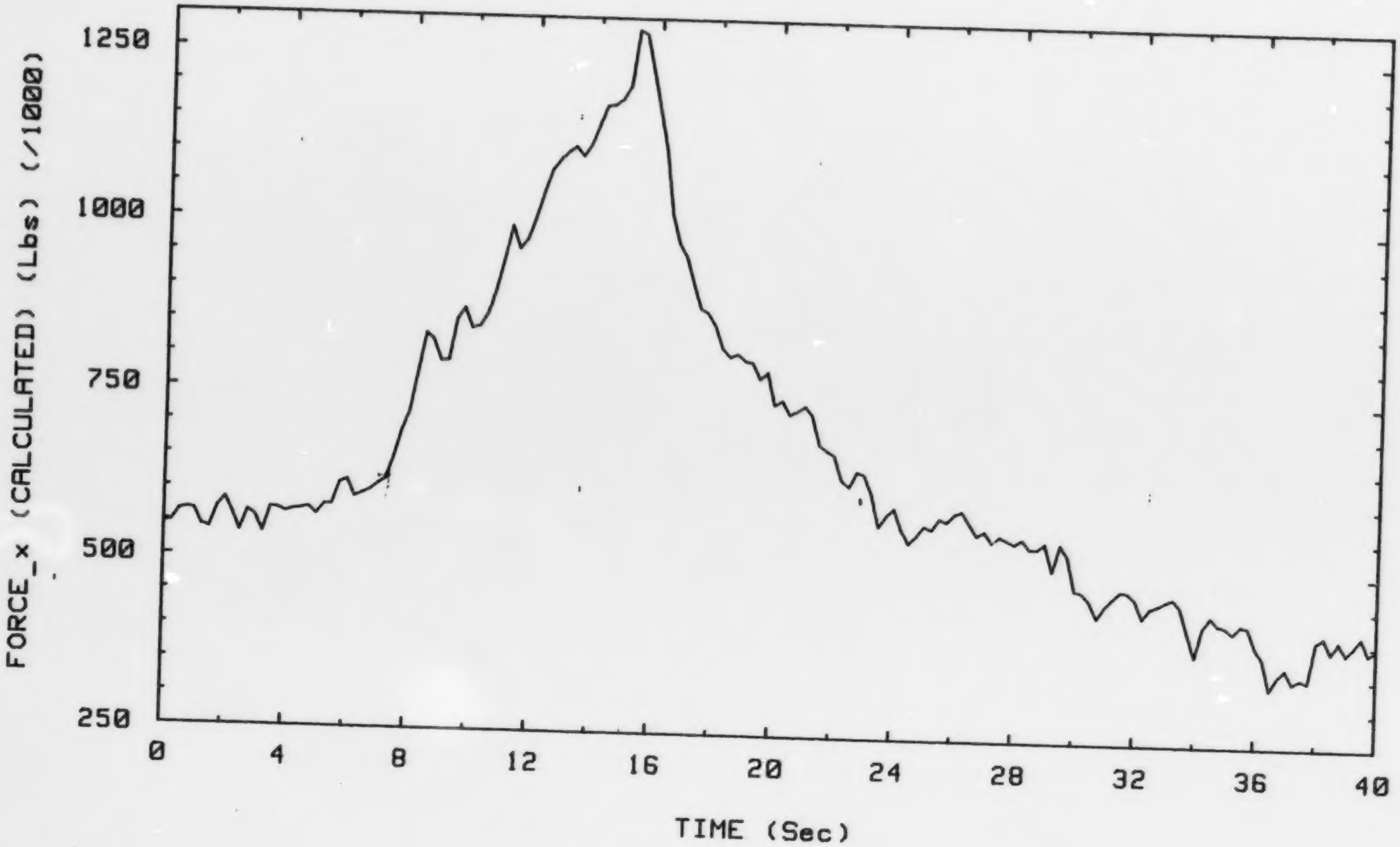

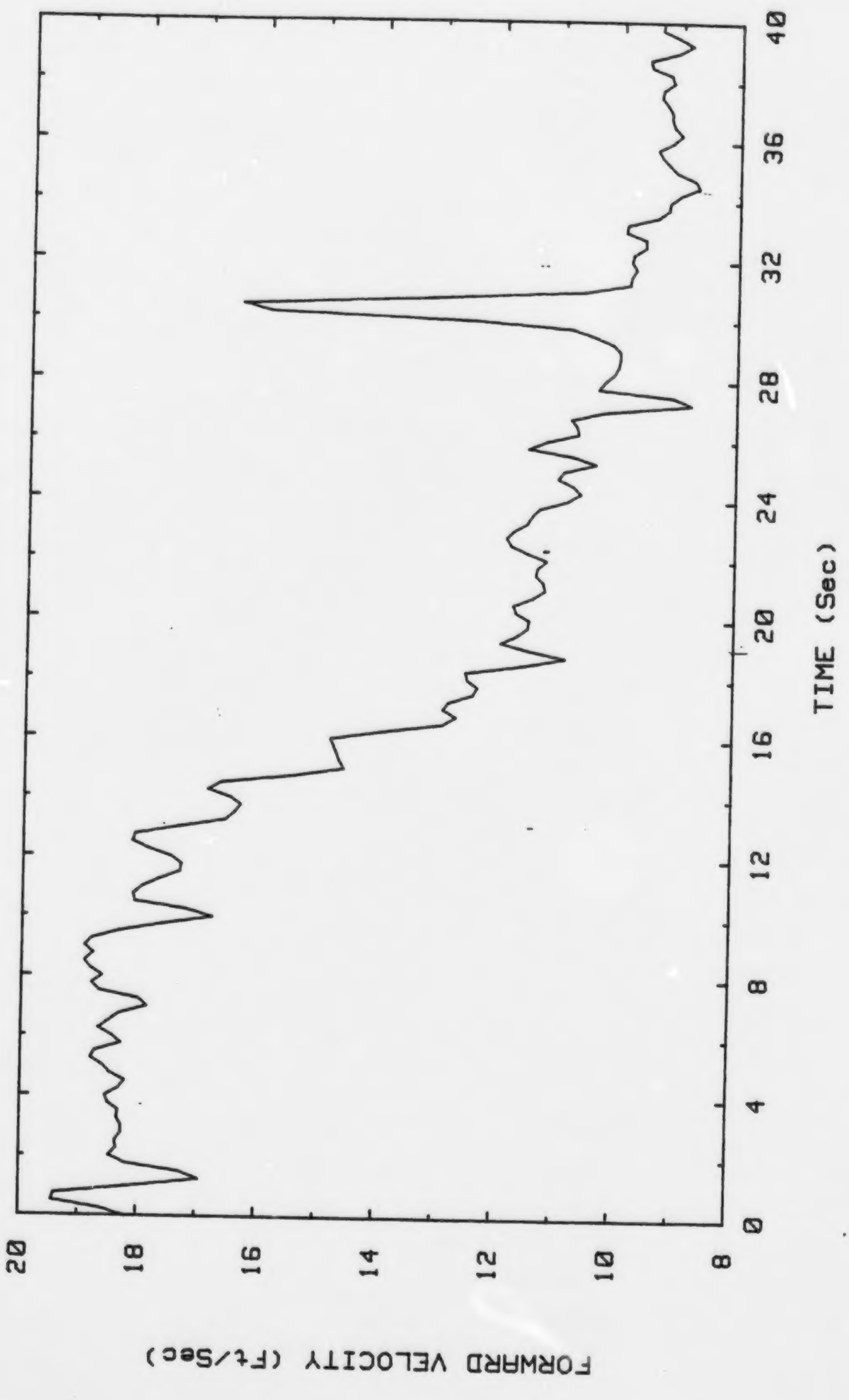
TRANSIT THROUGH RIDGE #18
FORWARD VELOCITY (Ft/Sec)
20
18
16
14
12
10
8
TIME (Sec)
0
4
8
12
16
20
24
28
32
36
40

C.2 SUMMARY OF ICE CORE DATA

DATE	CORE NO.	TOTAL DEPTH (in)	AIR TEMP °C	σ_f* VAUDREY	σ_f* LANE	σ_f* WEEKS & ASSUR	REMARKS
4/3/82	01	24	- 2.0	36.9	19.7	19.2	
4/3/82	02	30.5	- 2.0	64.5	47.7	42.8	
4/3/82	03	37	- 2.0	73.5	56.7	50.4	
4/4/82	04	11	+ 1.1	49.5	32.4	29.9	
4/4/82	05	105	+ 1.1	60.8	44.0	39.7	
4/4/82	06	145	+ 1.1	59.0	42.1	38.1	Between Pressure Ridge #0304
4/5/82	07	19	+ 2.2	46.9	29.8	27.7	
4/5/82	08	25	+ 2.2	50.2	33.2	30.6	
4/5/82	09	19	+ 2.2	49.0	31.9	29.5	
4/6/82	10	14	0.0	26.2	8.9	10.0	
4/6/82	11	19	0.0	34.2	17.0	16.9	
4/6/82	12	44	+ 1.1	41.2	24.1	22.9	
4/7/82	13	19	0.0	23.6	6.3	7.8	
4/7/82	14	20	- 5.6	32.7	15.5	15.6	
4/8/82	16	47	0.0	52.5	35.5	32.5	
4/8/82	17	21	0.0	27.2	9.9	10.9	
4/9/82	18	21	-11.7	63.9	47.0	42.3	Ridge #06
4/9/82	19	41	- 8.3	56.4	39.4	35.8	Ridge #06
4/9/82	20	14	- 7.2	28.8	11.6	12.3	
4/9/82	21	16	- 2.8	56.6	39.7	36.0	
4/9/82	22	52	- 3.3	44.8	27.8	26.0	Ridge #09
4/9/82	23	45	- 3.9	76.9	60.2	53.4	
4/10/82	24	17	-13.3	48.7	31.7	29.3	
4/10/82	25	16.5	-13.3	52.8	35.8	32.8	
4/12/82	26	21	-10.0	65.7	48.9	43.8	
4/13/82	27	26.5	-13.0	80.6	64.0	56.6	
4/14/82	28	12	-13.8	76.6	59.9	53.1	
4/14/82	29	12.5	-13.0	73.3	56.6	50.3	
4/14/82	30	13	-11.7	74.8	58.0	51.6	
4/18/82	32	69	-11.4	87.9	71.3	62.8	Rubble field, Ridge #13
4/18/82	33	60	-11.4	89.0	72.4	63.7	Rubble field, Ridge #13
4/20/82	34	38	- 6.2	51.8	34.9	32.0	Ridge #15
4/20/82	35	60	- 6.2	48.3	31.2	28.9	Ridge #15
4/20/82	36	82	- 6.2	56.0	39.0	35.5	Ridge #15
4/20/82	37	19	- 6.2	60.3	43.4	39.2	
4/23/82	38	13	- 2.0	49.5	32.5	30.0	Ridge #16
4/23/82	39	15	- 2.0	39.3	22.1	21.2	Ridge #16
4/23/82	40	15	- 2.0	40.9	23.8	22.6	Ridge #16
4/23/82	41	13	- 2.0	53.3	36.4	33.2	
4/26/82	42	35	- 8.4	48.5	31.5	29.1	
4/26/82	43	32	- 8.4	57.6	40.7	36.9	
4/27/82	44	40	- 7.0	74.3	57.5	51.1	
4/27/82	45	46	- 7.0	66.9	50.1	44.9	

* Based on top 75% of core depth. Flexural strength recorded in psi.

CORE DATA (Continued)

DATE	CORE NO.	TOTAL DEPTH (in)	AIR TEMP °C	σ_f* VAUDREY	σ_f* LANE	σ_f* WEEKS & ASSUR	REMARKS
4/28/82	46	49	- 7.2	76.2	59.5	52.8	
4/28/82	47	66	- 7.2	81.0	64.3	56.9	
4/30/82	49	42	-12.0	68.2	51.4	46.0	Ridge #22
4/30/82	50	30	-12.0	67.9	51.0	45.6	Ridge #22
4/30/82	51	24	-12.0	83.4	66.8	59.0	Ridge #22
4/30/82	52	30	-12.0	76.3	59.6	52.9	Ridge #23
4/30/82	53	15	-12.3	58.0	41.0	37.2	Ridge #23
4/30/82	54	39	-12.3	73.7	57.0	50.7	Ridge #23
5/2/82	55	60	-10.0	65.8	49.0	43.9	Ridge #25
5/2/82	56	57	-10.0	73.6	56.9	50.6	Ridge #25
σ_f AVG				58.0	41.1	37.3	
σ_f MAX				89.0	72.4	63.7	
σ_f MIN				23.6	6.3	7.8	

* Based on top 75% of core depth using Method 2 as described on page C-2.